BEILSTEIN JOURNAL OF ORGANIC CHEMISTRY

Copper-catalyzed reactions for organic synthesis

Edited by Gwilherm Evano and Olivier Riant

Imprint

Beilstein Journal of Organic Chemistry
www.bjoc.org
ISSN 1860-5397
Email: journals-support@beilstein-institut.de

The *Beilstein Journal of Organic Chemistry* is published by the Beilstein-Institut zur Förderung der Chemischen Wissenschaften.

Beilstein-Institut zur Förderung der Chemischen Wissenschaften
Trakehner Straße 7–9
60487 Frankfurt am Main
Germany
www.beilstein-institut.de

BEILSTEIN JOURNAL OF ORGANIC CHEMISTRY

Synthesis of aryl cyclopropyl sulfides through copper-promoted S-cyclopropylation of thiophenols using cyclopropylboronic acid

Emeline Benoit, Ahmed Fnaiche and Alexandre Gagnon*

Letter

Open Access

Address:
Département de chimie, Université du Québec à Montréal, C.P. 8888, Succursale Centre-Ville, Montréal, Québec, H3C 3P8, Canada

Email:
Alexandre Gagnon* - gagnon.alexandre@uqam.ca

* Corresponding author

Keywords:
aryl cyclopropyl sulfides; copper(II) acetate; copper catalysis; cyclopropylboronic acid; thiophenols

Beilstein J. Org. Chem. **2019,** *15,* 1162–1171.
doi:10.3762/bjoc.15.113

Received: 10 April 2019
Accepted: 22 May 2019
Published: 27 May 2019

This article is part of the thematic issue "Copper-catalyzed reactions for organic synthesis".

Guest Editor: G. Evano

Abstract

The copper-promoted S-cyclopropylation of thiophenols using cyclopropylboronic acid is reported. The procedure operates under simple conditions to afford the corresponding aryl cyclopropyl sulfides in moderate to excellent yields. The reaction tolerates substitution in *ortho*-, *meta*- and *para*-substitution as well as electron-donating and electron-withdrawing groups. The S-cyclopropylation of a thiophenol was also accomplished using potassium cyclopropyl trifluoroborate.

Introduction

Aryl cyclopropyl sulfides are present in many biologically active compounds, mainly in their oxidized forms. For example, aryl cyclopropyl sulfones have been used in the preparation of glucokinase (GK) activators for the treatment of type 2 diabetes [1-5] while aryl cyclopropyl sulfoximines have been utilized for the synthesis of modulators of glucokinase regulatory protein (GKRP) [6-8]. Roniciclib, also named BAY 1000394, is a pan-cyclin-dependant kinase (CDK) inhibitor that contains an aryl cyclopropyl sulfoximine and that was developed to treat patients with untreated small cell lung cancer [6,9].

Aryl cyclopropyl sulfides **1** are also remarkable synthons in organic synthesis (Scheme 1). For instance, the proton alpha to the sulfur can be removed by a strong base such as butyllithium, resulting in the cyclopropyllithium species **2**. This carbanion can then react with alkyl halides to provide the corresponding alkylated species **3** which can then be opened up by treatment with mercuric chloride to give the corresponding β-thioaryl ketone **4** [10]. Reacting **2** with epoxides results in the formation of the 1-(β-hydroxy)cyclopropyl aryl sulfides **5** [10] while reaction with formaldehydes [11] or aldehydes [12] affords

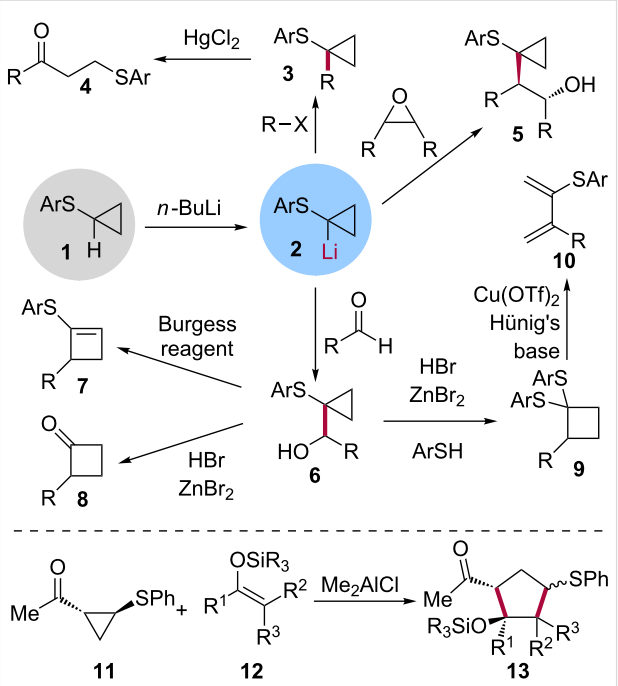

Scheme 1: Synthetic uses of aryl cyclopropyl sulfides **1**.

1-(arylthio)cyclopropylcarbinyl alcohols **6**. Treating **6** with Burgess reagent or with hydrobromic acid and zinc bromide leads to 1-arylthiocyclobutenes **7** [13] and 2-alkyl-substituted cyclobutanones **8** [11,12], respectively. Treatment of **6** with hydrobromic acid and zinc bromide in the presence of a thiophenol provides the 1,1-di(arylthio)cyclobutane **9** which, upon reaction with copper(II) triflate and Hünig's base, rearranges to give the corresponding 2-(arylthio)-3-alkyl-1,3-butadiene **10** [12]. Reacting methyl 2-phenylthiocyclopropyl ketone **11** with silyl enol ethers **12** in the presence of dimethylaluminium chloride leads to the functionalized cyclopentanes **13** via a highly diastereoselective [3 + 2] cycloaddition reaction [14,15]. The ring expansion sequence **1** → **2** → **6** → **8** has been used as a key step in the synthesis of (±)-fragranol [16], (±)-grandisol [16], (±)-α-cuparenone [17] and (±)-herbertene [17].

Aryl cycloropyl sulfides **1** are most frequently prepared by cyclopropylation of thiophenols **14** through S_N2 reaction with cyclopropyl bromide (**15**, Scheme 2a) [2,4] or by S_NAr reaction between aryl fluorides **16** and cyclopropanethiol (**17**, (Scheme 2b) [6]. Although simple and attractive, these approaches usually require harsh conditions such as the presence of a strong base and high temperatures [18]. In addition, an electron-withdrawing group (EWG) must be present on the aryl fluoride **16** for the S_NAr reaction to proceed. Aryl cyclopropyl sulfides can also be accessed by the addition of thiophenols **14** to cyclopropenes **18** (Scheme 2c) [19,20] or to *exo*-methylenecyclopropanes **20** (Scheme 2d) [21,22]. While these methods give access to highly substituted products, the requirement for a strong base could jeopardize their application in the context of synthesis of complex molecules. Furthermore, an electron-withdrawing group must be present on **18** to enable the Michael addition with thiol **14**. Treatment of 1,3-bis(phenylthio)propanes **22** with butyllithium is another way of accessing substituted aryl cyclopropyl sulfides **23** (Scheme 2e) [23]. However, in addition to requiring a very strong base, the generation of regio- and stereoisomers from a complex starting material reduces the attractiveness of this method, particularly with respect to medicinal chemistry where expedient methods from easily accessible substrates are needed.

Organobismuth compounds are organometallic reagents that possess a C–Bi bond and which can be synthesized from inexpensive and low-toxic bismuth salts [24,25]. Due to the borderline behavior of bismuth as a metal and a ligand, organobismuth species have been used as reagents and catalysts in a wide range of reactions. We reported a portfolio of methods for the construction of C–C [26-29], C–N [30] and C–O bonds [31-33] using triaryl- and trialkylbismuthines [34]. We also disclosed for the first time in 2007 the synthesis of tricyclopropylbismuth (**24**) and its use in N-cyclopropylation [35], palladium-catalyzed cross coupling [36] and carbonylative cross-coupling reactions [37]. Recently, we demonstrated that tricyclopropylbismuth (**24**) can be used to S-cyclopropylate thiophenols **14**, giving access to aryl cyclopropyl sulfides **1** (Scheme 2f) [38]. While this constituted the first example on the use of an organobismuth reagent in the construction of C(sp^3)–S bonds, synthetically, the method showed limitations such as the need for a high excess of tricyclopropylbismuth (**24**) which transfers only one cyclopropyl unit out of three to deliver the desired products in moderate yields.

Cyclopropylboronic acid has been elegantly used by Neuville and Zhu [39,40], Tsuritani [41], Taillefer [42], Hayashi [43] and Reddy [44] as a cyclopropylating reagent in N-cyclopropylation reactions, a transformation which is similar to the Chan [45], Evans [46], Lam [47] arylation reaction of N–H and O–H containing substrates. These seminal reports greatly contributed to the synthesis of cyclopropylated compounds in addition to expanding the scope of copper-catalyzed reactions in organic synthesis [48-51]. Our interest in cyclopropylation reactions led us to explore the use of cyclopropylboronic acid in the O-cyclopropylation of phenols. Unfortunately, efficient conditions could not be identified to perform this seemingly simple extension of the N-cyclopropylation reaction. Very recently, Engle and McAlpine disclosed a solution to this problem by developing a highly efficient protocol for the direct O-cyclopropylation of phenols using potassium cyclopropyl trifluoroborate [52]. Surprisingly, and to the best of our knowledge, cyclo-

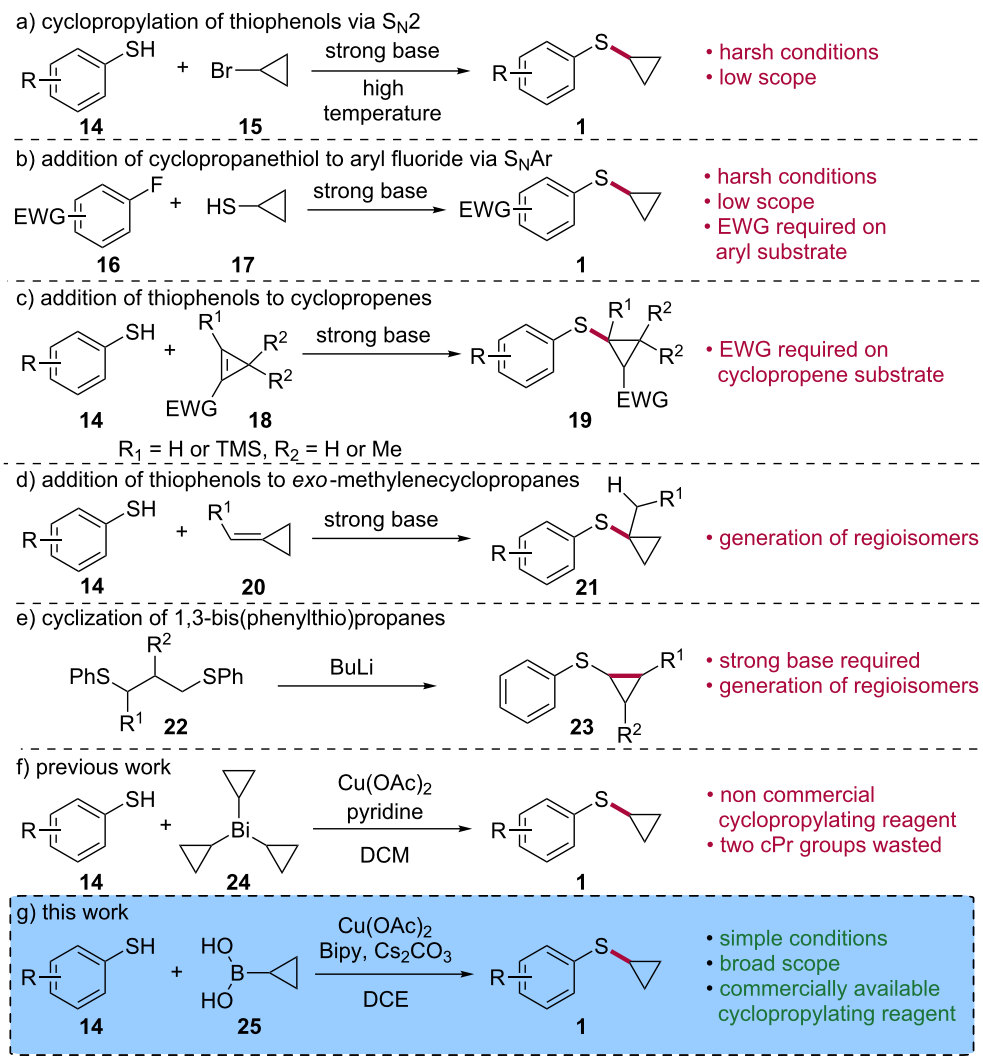

Scheme 2: Synthesis of aryl cyclopropyl sulfides.

propylboronic acid or its various ester and potassium trifluoroborate derivatives have never been used in S-cyclopropylation reactions. In light of the relevance of aryl cyclopropyl sulfides in medicinal and synthetic organic chemistry, we initiated a program to explore the use of cyclopropylboronic acid (**25**) as an S-cyclopropylating agent of thiophenols (Scheme 2g). The publication of copper-catalyzed methods by Feng and Xu to S-arylate thiophenols [53] and by Guy to S-arylate alkyl thiols [54] gave us confidence to proceed ahead with our endeavour for which we herein report our results.

Results and Discussion

We began by testing the feasibility of S-cyclopropylating 4-*tert*-butylbenzenethiol (**14a**) with cyclopropylboronic acid (**25**) using reaction conditions developed by Neuville and Zhu for the N-cyclopropylation of anilines and amines [39]. Treating thiophenol **14a** with 2.0 equivalents of cyclopropylboronic acid (**25**), 1.0 equivalent of copper(II) acetate, 1.0 equivalent of bipyridine, and 2.0 equivalents of sodium carbonate in dichloroethane at 70 °C for 16 hours provided the desired *S*-cyclopropylated compound **1a** in 86% yield accompanied by only 4% of the diaryl disulfide side-product **26a** (Table 1, entry 1, "standard conditions"). Reducing the catalyst loading by a factor of two under oxygen atmosphere led to a dramatic reduction in the yield of the reaction (Table 1, entry 2). Performing the reaction under oxygen with a stoichiometric amount of copper(II) acetate also proved unsuccessful and afforded mainly the disulfide product, suggesting a deleterious effect of oxygen (Table 1, entry 3). Yet, to our surprise, performing the reaction under argon also negatively impacted the yield of the reaction (Table 1, entry 4), showing that air is the ideal (and also most convenient) atmosphere for this reaction. Changing the solvent for toluene, dichloromethane, dimethylformamide or DMF/H_2O (4:1) led to lower yields of the desired aryl cyclopropyl sulfide

Table 1: Optimization of the reaction conditions for the copper-promoted S-cyclopropylation of thiophenol **14a** with boron-based cyclopropylating reagents.

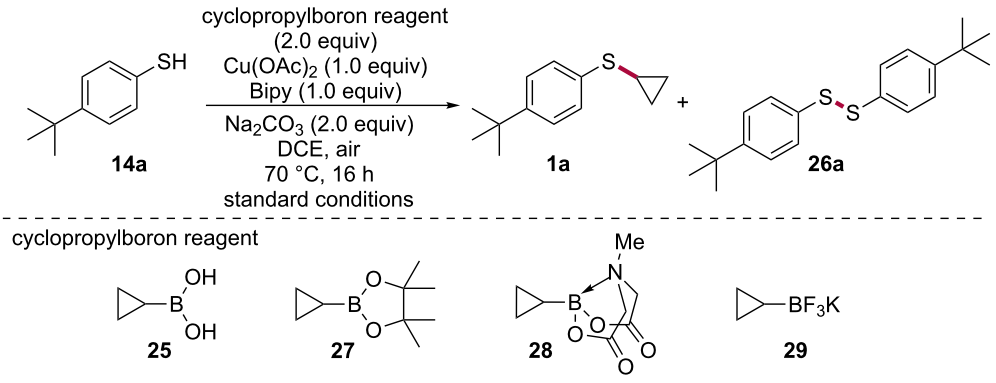

Entry	Change from "standard conditions"[a]	Yield **1a** (%)[b]	Yield **26a** (%)[b]
1	no change[a]	86	4
2	0.5 equiv of $Cu(OAc)_2$ instead of 1.0 equiv under O_2 instead of air	10	0
3	O_2 instead of air	19	62
4	argon instead of air	45	4
5	toluene, DCM, DMF or DMF/H_2O (4:1) instead of DCE	<40	0
6	50 °C instead of 70 °C	7	20
7	1,10-phenanthroline instead of bipy	81	0
8	1.5 equiv of $cPrB(OH)_2$ (**25**) instead of 2.0 and 1.0 equiv of Na_2CO_3	85	14
9	**1.5 equiv of $cPrB(OH)_2$ (25) instead of 2.0 and 1.0 equiv of Cs_2CO_3 instead of 2.0 equiv of Na_2CO_3**	**92**	**6**
10	1.5 equiv of $cPrB(OH)_2$ (**25**) instead of 2.0, 1.0 equiv of Cs_2CO_3 instead of 2.0 equiv of Na_2CO_3 and 6 h instead of 16 h	85	14
11	**27** instead of $cPrB(OH)_2$ (**25**)	0	85[c]
12	**28** instead of $cPrB(OH)_2$ (**25**)	0	96[c]
13	**29** instead of $cPrB(OH)_2$ (**25**)	23	30

[a]Standard conditions: 4-*tert*-butylbenzenethiol (**14a**, 1.0 equiv), cyclopropylboronic acid (**25**, 2.0 equiv), $Cu(OAc)_2$ (1.0 equiv), bipyridine (1.0 equiv), Na_2CO_3 (2.0 equiv), dichloroethane (0.1 M), 70 °C, 16 h, air. [b]Yields of isolated pure products. [c]Conversion calculated by NMR.

1a (Table 1, entry 5) while decreasing the temperature to 50 °C almost completely shut down the reaction (Table 1, entry 6). 1,10-Phenanthroline was found to be the only viable alternative to bipyridine (Table 1, entry 7), with other ligands commonly used in copper-catalyzed reactions such as proline and 2,2,6,6-tetramethyl-3,5-heptanedione giving yields under 15%. Reducing the number of equivalents of boronic acid **25** and sodium carbonate was found to be well tolerated, giving a comparable yield as the "standard conditions" (Table 1, entry 8). While changing the inorganic base to potassium phosphate tribasic or potassium carbonate gave yields below 75%, we found that cesium carbonate provided a net increase in the yield of the reaction (Table 1, entry 9). Attempts at reducing the reaction time led to a minor erosion in the yield of the reaction (Table 1, entry 10). Replacing cyclopropylboronic acid (**25**) with cyclopropylboronic acid pinacol ester (**27**) or cyclopropylboronic acid MIDA ester **28** afforded 85% and 96% of the corresponding diaryl disulfide **26a**, respectively, with no obsevable traces of the desired S-cyclopropylated product **1a** (Table 1, entries 11 and 12). Interestingly, however, potassium cyclopropyl trifluoroborate (**29**) provided the desired aryl cyclopropyl sulfide **1a** in 23% yield, albeit with 30% of the diaryl disulfide side-product **26a** (Table 1, entry 13). Although encouraging, it was clear that the S-cyclopropylation with $cPrBF_3K$ (**29**) would necessitate extensive optimization and therefore, we decided to pursue our work with $cPrB(OH)_2$ (**25**).

With our optimized reactions conditions in hand (i.e., Table 1, entry 9), we embarked on exploring the scope of the copper-promoted S-cyclopropylation of thiophenols using cyclopropylboronic acid (**25**, Scheme 3). Our studies showed that the reaction can be performed on unsubstituted benzenethiol as well as on *para*- and *meta*-methylbenzenethiols, affording the corresponding products **1b**–**d** in 84 to 99% yield. Substitution of the aryl ring at the *ortho*-position resulted in a considerable drop in the efficiency of the process, as indicated by compound **1e**

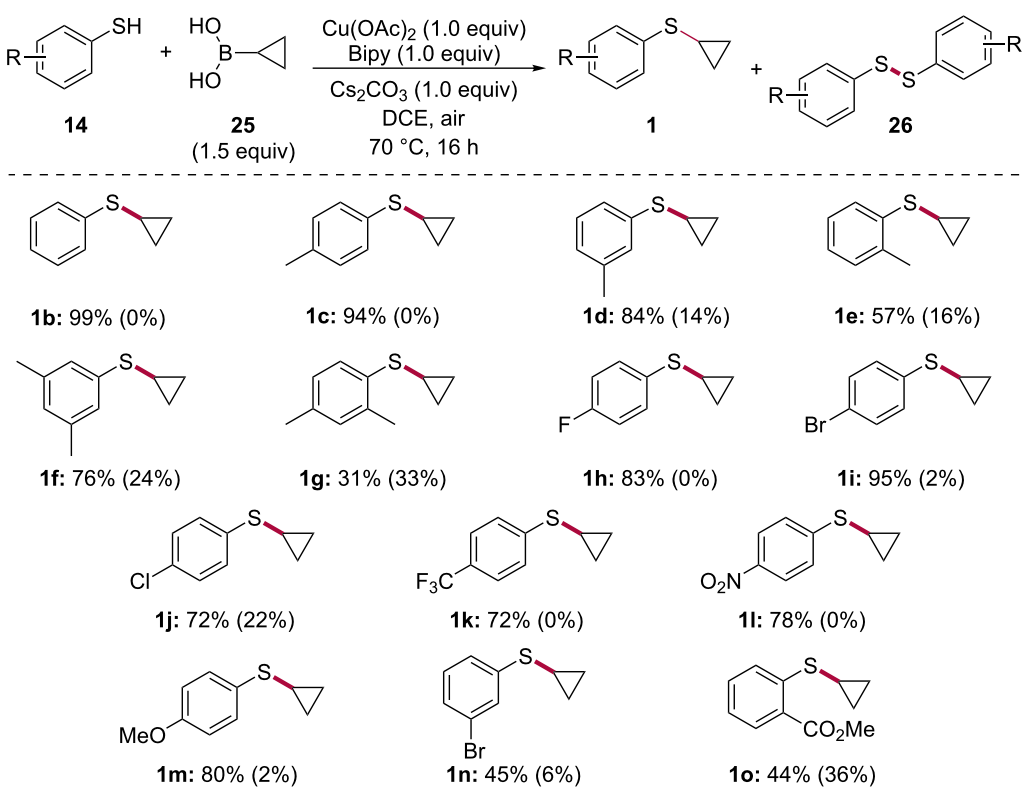

Scheme 3: Substrate scope in the copper-promoted S-cyclopropylation of thiophenols **14** using cyclopropylboronic acid (**25**). Numbers in parentheses indicate the yield of isolated pure diaryl disulfide side-products **26**.

which was obtained in a moderate 57% yield. In line with those results, cyclopropyl(3,5-dimethylphenyl)sulfane (**1f**) was obtained in 76% yield while the 2,4-isomer **1g** was produced in a low 31% yield. Electron-withdrawing groups such as a fluorine, bromine, chlorine, trifluoromethyl and a nitro group as well as electron-donating groups such as a methoxy group at the *para*-position were found to be well tolerated, as indicated by aryl cyclopropyl sulfides **1h**–**m** which were obtained in yields ranging from 72 to 95%. Moving the bromine from the *para*- to the *meta*-position resulted in a substantial reduction in the yield of the reaction, as shown by compound **1n**. Compound **1o** possessing a methyl ester at the *ortho*-position was prepared in 44%, a yield which is consistent with the one obtained for the *ortho*-methyl product **1e**. Compound **1o** indicates some level of tolerance towards functional groups that can be used à posteriori to modify the product. Diaryl disulfides **26** were isolated in yields ranging from 2 to 36%, depending on the thiophenol. Attempts at S-cyclopropylating benzyl mercaptan, an alkylthiol, failed to deliver the desired product.

Engle and McAlpine recently reported a very efficient, simple and general protocol for the O-cyclopropylation of phenols using potassium cyclopropyl trifluoroborate (**29**) that leads to the corresponding aryl cyclopropyl ethers in good to excellent yields [52]. We wanted to study the transposibility of these conditions to the S-cyclopropylation of thiophenols. In the event, treating 4-*tert*-butylbenzenethiol (**14a**) with 3.0 equivalents of potassium cyclopropyl trifluoroborate (**29**) in the presence of 0.1 equivalents of copper(II) acetate, 0.1 equivalents of 1,10-phenanthroline, 2.0 equivalents of potassium carbonate under oxygen atmosphere at 70 °C for 20 hours in a 3:1 mixture of toluene and water afforded the aryl cyclopropyl sulfide **1a** in 38% along with 8% of the corresponding side-product **26a** and 24% of recovered starting material **14a** (Scheme 4). These results are encouraging and demonstrate that the Engle/McAlpine conditions are applicable, to some extent, to the S-cyclopropylation of thiophenols. It is reasonable to believe that thorough optimization of the reaction conditions should result in a more efficient process. Efforts towards this goal are in progress in our laboratory and results will be reported in due course.

Conclusion

In conclusion, we developed a simple protocol for the S-cyclopropylation of thiophenols using cyclopropylboronic acid. The reaction is promoted by copper(II) acetate and tolerates electron-withdrawing and electron-donating groups at the *ortho*-, *meta*-, and *para*-positions of the aryl ring to afford the corre-

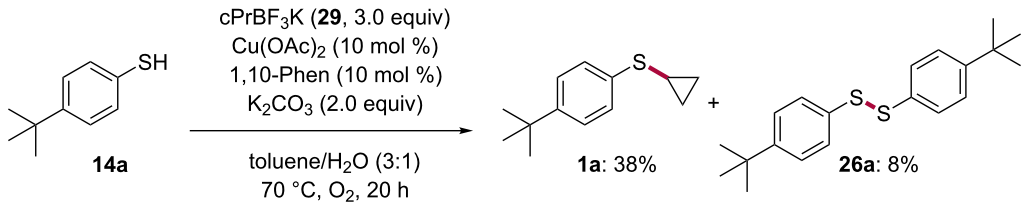

Scheme 4: Copper-catalyzed S-cyclopropylation of 4-*tert*-butylbenzenethiol (**14a**) using potassium cyclopropyl trifluoborate (**29**).

sponding aryl cyclopropyl sulfides in moderate to excellent yields. This protocol provides an efficient alternative to our previously reported method for the S-cyclopropylation of thiophenols using tricyclopropylbismuth.

Experimental

General information

Unless otherwise indicated, all reactions were run under argon in flame-dried glassware. Commercial reagents were used without further purification. $Cu(OAc)_2$ (97%) was purchased from Strem Chemicals. Anhydrous solvents were obtained using an encapsulated solvent purification system and were further dried over 4 Å molecular sieves. The evolution of reactions was monitored by analytical thin-layer chromatography using silica gel 60 F254 precoated plates. Flash chromatography was performed employing 230–400 mesh silica using the indicated solvent system according to standard techniques. Proton nuclear magnetic resonance spectra were recorded on a 300 or 600 MHz spectrometer. Chemical shifts for ^{1}H NMR spectra are recorded in parts per million from tetramethylsilane with the solvent resonance as the internal standard (chloroform, δ 7.26 ppm). Data is reported as follows: chemical shift δ, multiplicity (s = singlet, d = doublet, t = triplet, dd = doublet of doublet, ddd = doublet of doublet of doublet, td = triplet of doublet, m = multiplet), coupling constant *J* in Hz and integration. Melting points are uncorrected.

General procedure for the synthesis of aryl cyclopropyl sulfides

A sealed tube equipped with a magnetic stirring bar was charged under ambiant air with cyclopropylboronic acid (**25**, 0.6 mmol, 1.5 equiv), cesium carbonate (0.4 mmol, 1.0 equiv), $Cu(OAc)_2$ (0.4 mmol, 1.0 equiv), 2,2'-bipyridine (0.4 mmol, 1.0 equiv) and thiophenol **14** (0.4 mmol, 1.0 equiv). Dichloroethane (0.1 M) was added, the tube was sealed and heated at 70 °C for 16 hours. The reaction mixture was cooled to room temperature and aqueous NH_4OH 25% (5 mL) was added. The reaction mixture was stirred for a few minutes, transferred in a separatory funnel and extracted with DCM (3 × 5 mL). The combined organic layers were washed with brine (2 × 10 mL), dried over anhydrous Na_2SO_4 and concentrated under reduced pressure. The residue was purified by flash column chromatography using the indicated solvent system to afford the corresponding aryl cyclopropyl sulfide **1** and diaryl disulfide **26** as a side-product.

(4-(*tert*-Butyl)phenyl)(cyclopropyl)sulfane (1a) and 1,2-bis(4-(*tert*-butyl)phenyl)disulfane (26a). The general procedure was followed on 0.425 mmol scale starting from 4-(*tert*-butyl)benzenethiol (**14a**). The residue was purified on silica gel (100% Hex) to afford **1a** (80.4 mg, 92%) and **26a** (4.2 mg, 6%) as a colorless oil and a white solid, respectively. **1a**: Spectral data was identical to literature compound [38]. ^{1}H NMR (300 MHz, $CDCl_3$) δ 7.33 (s, 4H), 2.23–2.16 (m, 1H), 1.33 (s, 9H), 1.08–1.02 (m, 2H), 0.73-0.68 (m, 2H). **26a**: mp 65.0–68.5 °C. Spectral data was identical to literature compound [55]. ^{1}H NMR (300 MHz, $CDCl_3$) δ 7.44 (d, *J* = 8.7 Hz, 2H), 7.33 (d, *J* = 8.4 Hz, 2H), 1.30 (s, 9H).

Cyclopropyl(phenyl)sulfane (1b). The general procedure was followed on 0.400 mmol scale starting from benzenethiol (**14b**). The residue was purified on silica gel (100% Hex) to afford **1b** (59.2 mg, 99%) as a slightly yellow oil: Spectral data was identical to literature compound [38]. ^{1}H NMR (300 MHz, $CDCl_3$) δ 7.39–7.35 (m, 2H), 7.32–7.28 (m, 1H), 7.17–7.11 (m, 1H), 2.23–2.15 (tt, *J* = 8.4, 1.2 Hz, 1H), 1.10–1.04 (m, 2H), 0.72–0.62 (m, 2H).

Cyclopropyl(*p*-tolyl)sulfane (1c). The general procedure was followed on 0.400 mmol scale starting from 4-methylbenzenethiol (**14c**). The residue was purified on silica gel (100% Hex) to afford **1c** (61.8 mg, 94%) as a colorless oil: Spectral data was identical to literature compound [38]. ^{1}H NMR (300 MHz, $CDCl_3$) δ 7.29 (d, *J* = 3.9 Hz, 2H), 7.12 (d, *J* = 4.2 Hz, 2H), 2.33 (s, 3H), 2.22–2.18 (m, 1H), 1.06–1.03 (m, 2H), 0.71–0.68 (m, 2H).

Cyclopropyl(*m*-tolyl)sulfane (1d) and 1,2-di(*m*-tolyl)disulfane (26d). The general procedure was followed on 0.400 mmol scale starting from 3-methylbenzenethiol (**14d**). The residue was purified on silica gel (100% Hex) to afford **1d** (55.2 mg, 84%) and **26d** (6.9 mg, 14%) as a colorless and a yellow oil, re-

spectively. **1d**: Spectral data was identical to literature compound [38]. ^{1}H NMR (300 MHz, $CDCl_3$) δ 7.19–7.18 (m, 3H), 6.97–6.94 (m, 1H), 2.34 (s, 3H), 2.23–2.15 (m, 1H), 1.09–1.03 (m, 2H), 0.72–0.67 (m, 2H). **26d**: Spectral data was identical to literature compound [56]. ^{1}H NMR (300 MHz, $CDCl_3$) δ 7.32 (s, 2H), 7.30 (d, *J* = 3.9 Hz, 2H), 7.19 (t, *J* = 8.0 Hz, 2H), 7.03 (d, *J* = 7.5 Hz, 2H), 2.32 (s, 6H).

Cyclopropyl(*o*-tolyl)sulfane (1e) and 1,2-di(*o*-tolyl)disulfane (26e). The general procedure was followed on 0.400 mmol scale starting from 2-methylbenzenethiol (**14e**). The residue was purified on silica gel (100% Hex) to afford **1e** (37.5 mg, 57%) and **26e** (7.9 mg, 16%) as a slightly yellow and a yellow oil, respectively. **1e**: Spectral data was identical to literature compound [38]. ^{1}H NMR (300 MHz, $CDCl_3$) δ 7.53 (d, *J* = 7.5 Hz, 1H), 7.20 (td, *J* = 7.5, 1.8 Hz, 1H), 7.15–7.03 (m, 2H), 2.27 (s, 3H), 2.17–2.09 (m, 1H), 1.13–1.07 (m, 2H), 0.73–0.67 (m, 2H). **26e**: Spectral data was identical to literature compound [57]. ^{1}H NMR (300 MHz, $CDCl_3$) δ 7.52–7.49 (m, 2H), 7.17–7.09 (m, 6H), 2.43 (s, 6H).

Cyclopropyl(3,5-dimethylphenyl)sulfane (1f) and 1,2-bis(3,5-dimethylphenyl)disulfane (26f). The general procedure was followed on 0.400 mmol scale starting from 3,5-dimethylbenzenethiol (**14f**). The residue was purified on silica gel (100% Hex) to afford **1f** (54.2 mg, 76%) and **26f** (13.2 mg, 24%) as a colorless and a yellow oil, respectively. **1f**: Spectral data was identical to literature compound [38]. ^{1}H NMR (300 MHz, $CDCl_3$) δ 6.99 (s, 2H), 6.78 (s, 1H), 2.30 (s, 6H), 2.22–2.14 (m, 1H), 1.08–1.02 (m, 2H), 0.71–0.66 (m, 2H). **26f**: Spectral data was identical to literature compound [58]. ^{1}H NMR (300 MHz, $CDCl_3$) δ 7.12 (s, 4H), 6.85 (s, 2H), 2.28 (s, 12H).

Cyclopropyl(2,4-dimethylphenyl)sulfane (1g) and 1,2-bis(2,4-dimethylphenyl)disulfane (26g). The general procedure was followed on 0.371 mmol scale starting from 2,4-dimethylbenzenethiol (**14g**). The residue was purified on silica gel (100% Hex) to afford **1g** (20.5 mg, 31%) and **26g** (17.3 mg, 33%) as colorless oils. **1g**: Spectral data was identical to literature compound [38]. ^{1}H NMR (300 MHz, $CDCl_3$) δ 7.41 (d, *J* = 3.9 Hz, 1H), 7.00 (d, *J* = 3.9 Hz, 1H), 6.96 (s, 1H), 2.29 (s, 3H), 2.25 (s, 3H), 2.14–2.10 (m, 1H), 1.07–1.04 (m, 2H), 0.69–0.66 (m, 2H). **26g**: Spectral data was identical to literature compound [38]. ^{1}H NMR (300 MHz, $CDCl_3$) δ 7.37 (d, *J* = 7.8 Hz, 2H), 6.99 (s, 2H), 6.93 (d, *J* = 8.4 Hz, 2H), 2.37 (s, 6H), 2.29 (s, 6H).

(4-Fluorophenyl)(cyclopropyl)sulfane (1h). The general procedure was followed on 0.470 mmol scale starting from 4-fluorobenzenethiol (**14h**). The residue was purified on silica gel (100% Hex) to afford **1h** (65.4 mg, 83%) as a colorless oil: Spectral data was identical to literature compound [38]. ^{1}H NMR (300 MHz, $CDCl_3$) δ 7.37–7.31 (m, 2H), 7.04–6.96 (m, 2H), 2.22–2.14 (m, 1H), 1.07–1.01 (m, 2H), 0.71–0.66 (m, 2H).

(4-Bromophenyl)(cyclopropyl)sulfane (1i) and 1,2-bis(4-bromophenyl)disulfane (26i). The general procedure was followed on 0.400 mmol scale starting from 4-bromobenzenethiol (**14i**). The residue was purified on silica gel (100% Hex) to afford **1i** (86.9 mg, 95%) and **26i** (1.5 mg, 2%) as colorless oils. **1i**: Spectral data was identical to literature compound [38]. ^{1}H NMR (300 MHz, $CDCl_3$) δ 7.39 (d, *J* = 8.4 Hz, 2H), 7.22 (d, *J* = 8.4 Hz, 2H), 2.20–2.12 (m, 1H), 1.11–1.04 (m, 2H), 0.71–0.66 (m, 2H). **26i**: Spectral data was identical to literature compound [59]. ^{1}H NMR (300 MHz, $CDCl_3$) δ 7.43 (d, *J* = 8.4, 4H), 7.34 (d, *J* = 8.4 Hz, 4H).

(4-Chlorophenyl)(cyclopropyl)sulfane (1j) and 1,2-bis(4-chlorophenyl)disulfane (26j). The general procedure was followed on 0.400 mmol scale starting from 4-chlorobenzenethiol (**14j**). The residue was purified on silica gel (100% Hex) to afford **1j** (52.9 mg, 72%) and **26j** (12.6 mg, 22%) as a colorless oil and a white solid, respectively. **1j**: Spectral data was identical to literature compound [38]. ^{1}H NMR (300 MHz, $CDCl_3$) δ 7.30–7.22 (m, 4H), 2.20–2.12 (m, 1H), 1.10–1.03 (m, 2H), 0.70–0.65 (m, 2H). **26j**: mp 71.0–73.0 °C. Spectral data was identical to literature compound [60]. ^{1}H NMR (300 MHz, $CDCl_3$) δ 7.39 (d, *J* = 8.4 Hz, 4H), 7.27 (d, *J* = 8.7, 4H).

Cyclopropyl(4-(trifluoromethyl)phenyl)sulfane (1k). The general procedure was followed on 0.400 mmol scale starting from 4-(trifluoromethyl)benzenethiol (**14k**). The residue was purified on silica gel (100% Hex) to afford **1k** (63.2 mg, 72%) as a light yellow oil: Spectral data was identical to literature compound [38]. ^{1}H NMR (300 MHz, $CDCl_3$) δ 7.52 (d, *J* = 8.4 Hz, 2H), 7.43 (d, *J* = 8.4 Hz, 2H), 2.24–2.15 (m, 1H), 1.18–1.07 (m, 2H), 0.74–0.65 (m, 2H).

Cyclopropyl(4-nitrophenyl)sulfane (1l). The general procedure was followed on 0.400 mmol scale starting from 4-nitrobenzenethiol (**14l**). The residue was purified on silica gel (from 100% Hex to 15% EtOAc/Hex) to afford **1l** (60.7 mg, 78%) as a yellow oil: Spectral data was identical to literature compound [38]. ^{1}H NMR (300 MHz, $CDCl_3$) δ 8.13 (d, *J* = 8.7 Hz, 2H), 7.44 (d, *J* = 9.0 Hz, 2H), 2.25–2.17 (m, 1H), 1.23–1.16 (m, 2H), 0.77–0.72 (m, 2H).

Cyclopropyl(4-methoxyphenyl)sulfane (1m) and 1,2-bis(4-methoxyphenyl)disulfane (26m). The general procedure was followed on 0.400 mmol scale starting from 4-methoxyben-

zenethiol (**14m**). The residue was purified on silica gel (from 100% Hex to 20% EtOAc/Hex) to afford **1m** (57.4 mg, 80%) and **26m** (1.1 mg, 2%) as yellow oils. **1m**: Spectral data was identical to literature compound [38]. ^{1}H NMR (300 MHz, $CDCl_3$) δ 7.34 (d, *J* = 9.0 Hz, 2H), 6.86 (d, *J* = 8.7 Hz, 2H), 3.80 (s, 3H), 2.22–2.14 (m, 1H), 1.01–0.95 (m, 2H), 0.70–0.65 (m, 2H). **26m**: Spectral data was identical to literature compound [61]. ^{1}H NMR (300 MHz, $CDCl_3$) δ 7.40 (d, *J* = 9.0 Hz, 4H), 6.83 (d, *J* = 8.7 Hz, 4H), 3.80 (s, 6H).

(3-Bromophenyl)(cyclopropyl)sulfane (1n) and 1,2-bis(3-bromophenyl)disulfane (26n). The general procedure was followed on 0.484 mmol scale starting from 3-bromobenzenethiol (**14n**). The residue was purified on silica gel (100% Hex) to afford **1n** (49.9 mg, 45%) and **26n** (5.5 mg, 6%) as a colorless and a yellow oil, respectively. **1n**: Spectral data was identical to literature compound [38]. ^{1}H NMR (300 MHz, $CDCl_3$) δ 7.51–7.50 (t, *J* = 0.9 Hz, 1H), 7.27–7.24 (m, 2H), 7.13 (t, *J* = 3.9 Hz, 1H), 2.19–2.15 (m, 1H), 1.12–1.09 (m, 2H), 0.72–0.69 (m, 2H). **26n**: Spectral data was identical to literature compound [38]. ^{1}H NMR (300 MHz, $CDCl_3$) δ 7.64–7.62 (m, 2H), 7.42–7.35 (m, 4H), 7.18 (t, *J* = 7.8 Hz, 2H).

Methyl 2-(cyclopropylthio)benzoate (1o) and dimethyl 2,2'-disulfanediyldibenzoate (26o). The general procedure was followed on 0.400 mmol scale starting from methyl 2-mercaptobenzoate (**14o**). The residue was purified on silica gel (from 100% Hex to 20% EtOAC/Hex) to afford **1o** (36.7 mg, 44%) and **26o** (24.1 mg, 36%) as a yellow oil and a white solid, respectively. **1o**: Spectral data was identical to literature compound [38]. ^{1}H NMR (300 MHz, $CDCl_3$) δ 7.99 (dd, *J* = 8.0, 1.7 Hz, 1H), 7.79 (dd, *J* = 8.1, 1.2 Hz, 1H), 7.47 (ddd, *J* = 8.7, 7.2, 1.5 Hz, 1H), 7.15 (ddd, *J* = 9.0, 7.2, 1.2 Hz, 1H), 3.89 (s, 3H), 2.12–2.04 (m, 1H), 1.17–1.10 (m, 2H), 0.74–0.69 (m, 2H). **26o**: mp 133.0–135.5 °C. Spectral data was identical to literature compound [62]. ^{1}H NMR (300 MHz, $CDCl_3$) δ 8.06 (dd, *J* = 7.8, 1.5 Hz, 2H), 7.76 (dd, *J* = 8.3, 1.1 Hz, 2H), 7.41 (ddd, *J* = 8.3, 7.3, 1.3 Hz, 2H), 7.23 (dd, *J* = 7.5, 1.2, 2H), 3.99 (s, 6H).

Supporting Information

Supporting Information File 1

Copies of NMR spectra of synthesized compounds.
[https://www.beilstein-journals.org/bjoc/content/supplementary/1860-5397-15-113-S1.pdf]

Acknowledgements

This work was supported by Boehringer Ingelheim Pharmaceuticals, Inc. through a Scientific Advancement Grant, by a provincial Fonds de Recherche du Québec, Nature et Technologies (FRQNT) team grant and by the Centre in Green Chemistry and Catalysis (CGCC).

ORCID® iDs

Emeline Benoit - https://orcid.org/0000-0002-1692-676X

References

1. Fyfe, M. C. T.; White, J. R.; Taylor, A.; Chatfield, R.; Wargent, E.; Printz, R. L.; Sulpice, T.; McCormack, J. G.; Procter, M. J.; Reynet, C.; Widdowson, P. S.; Wong-Kai-In, P. *Diabetologia* **2007,** *50,* 1277–1287. doi:10.1007/s00125-007-0646-8
2. Mao, W.; Ning, M.; Liu, Z.; Zhu, Q.; Leng, Y.; Zhang, A. *Bioorg. Med. Chem.* **2012,** *20,* 2982–2991. doi:10.1016/j.bmc.2012.03.008
3. ClinicalTrialsgov identifier: NCT01247363: A Study of LY2608204 in Patients with Type 2 Diabetes.
4. Deshpande, A. M.; Bhuniya, D.; De, S.; Dave, B.; Vyavahare, V. P.; Kurhade, S. H.; Kandalkar, S. R.; Naik, K. P.; Kobal, B. S.; Kaduskar, R. D.; Basu, S.; Jain, V.; Patil, P.; Chaturvedi Joshi, S.; Bhat, G.; Raje, A. A.; Reddy, S.; Gundu, J.; Madgula, V.; Tambe, S.; Shitole, P.; Umrani, D.; Chugh, A.; Palle, V. P.; Mookhtiar, K. A. *Eur. J. Med. Chem.* **2017,** *133,* 268–286. doi:10.1016/j.ejmech.2017.03.042
5. ClinicalTrials.gov identifier: NCT01247363: Phase 1 study of LY2608204 in patients with Type 2 Diabetes Melitus.
6. Lücking, U.; Jautelat, R.; Krüger, M.; Brumby, T.; Lienau, P.; Schäfer, M.; Briem, H.; Schulze, J.; Hillisch, A.; Reichel, A.; Wengner, A. M.; Siemeister, G. *ChemMedChem* **2013,** *8,* 1067–1085. doi:10.1002/cmdc.201300096
7. Nishimura, N.; Norman, M. H.; Liu, L.; Yang, K. C.; Ashton, K. S.; Bartberger, M. D.; Chmait, S.; Chen, J.; Cupples, R.; Fotsch, C.; Helmering, J.; Jordan, S. R.; Kunz, R. K.; Pennington, L. D.; Poon, S. F.; Siegmund, A.; Sivits, G.; Lloyd, D. J.; Hale, C.; Jean, D. J. St. *J. Med. Chem.* **2014,** *57,* 3094–3116. doi:10.1021/jm5000497
8. Lohier, J.-F.; Glachet, T.; Marzag, H.; Gaumont, A.-C.; Reboul, V. *Chem. Commun.* **2017,** *53,* 2064–2067. doi:10.1039/c6cc09940h
9. Reck, M.; Horn, L.; Novello, S.; Barlesi, F.; Albert, I.; Juhász, E.; Kowalski, D.; Robinet, G.; Cadranel, J.; Bidoli, P.; Chung, J.; Fritsch, A.; Drews, U.; Wagner, A.; Govindan, R. *J. Thorac. Oncol.* **2019,** *14,* 701–711. doi:10.1016/j.jtho.2019.01.010
10. Bumgardner, C. L.; Lever, J. R.; Purrington, S. T. *Tetrahedron Lett.* **1982,** *23,* 2379–2382. doi:10.1016/s0040-4039(00)87347-5
11. Trost, B. M.; Vladuchick, W. C. *Synthesis* **1978,** 821. doi:10.1055/s-1978-24897
12. Kwon, T. W.; Smith, M. B. *Synth. Commun.* **1992,** *22,* 2273–2285. doi:10.1080/00397919208019081
13. Trost, B. M.; Keeley, D. E.; Arndt, H. C.; Bogdanowicz, M. J. *J. Am. Chem. Soc.* **1977,** *99,* 3088–3100. doi:10.1021/ja00451a040
14. Horiguchi, Y.; Suehiro, I.; Sasaki, A.; Kuwajima, I. *Tetrahedron Lett.* **1993,** *34,* 6077–6080. doi:10.1016/s0040-4039(00)61732-x
15. Grover, H. K.; Emmett, M. R.; Kerr, M. A. *Org. Biomol. Chem.* **2015,** *13,* 655–671. doi:10.1039/c4ob02117g
16. Bernard, A. M.; Frongia, A.; Secci, F.; Delogu, G.; Ollivier, J.; Piras, P. P.; Salaün, J. *Tetrahedron* **2003,** *59,* 9433–9440. doi:10.1016/j.tet.2003.09.074

17. Bernard, A. M.; Frongia, A.; Secci, F.; Piras, P. P. *Chem. Commun.* **2005,** 3853–3855. doi:10.1039/b505707h
18. Masson, E.; Leroux, F. *Helv. Chim. Acta* **2005,** *88,* 1375–1386. doi:10.1002/hlca.200590110
19. Banning, J. E.; Prosser, A. R.; Alnasleh, B. K.; Smarker, J.; Rubina, M.; Rubin, M. *J. Org. Chem.* **2011,** *76,* 3968–3986. doi:10.1021/jo200368a
20. Lin, H.-C.; Tsai, R.-T.; Wu, H.-P.; Lee, H.-Y.; Lee, G.-A. *Tetrahedron* **2016,** *72,* 184–191. doi:10.1016/j.tet.2015.11.024
21. Kozhushkov, S. I.; Brandl, M.; de Meijere, A. *Eur. J. Org. Chem.* **1998,** 1535–1542. doi:10.1002/(sici)1099-0690(199808)1998:8<1535::aid-ejoc1535>3.3.co;2-g
22. Volta, L.; Stirling, C. J. M. *Phosphorus, Sulfur Silicon Relat. Elem.* **2009,** *184,* 1508–1522. doi:10.1080/10426500902947856
23. Tanaka, K.; Uneme, H.; Matsui, S.; Kaji, A. *Bull. Chem. Soc. Jpn.* **1982,** *55,* 2965–2972. doi:10.1246/bcsj.55.2965
24. Gagnon, A.; Dansereau, J.; Le Roch, A. *Synthesis* **2017,** *49,* 1707–1745. doi:10.1055/s-0036-1589482
25. Gagnon, A.; Benoit, E.; Le Roch, A. *Sci. Synth., Knowl. Updates* **2018,** *4,* 1.
26. Gagnon, A.; Albert, V.; Duplessis, M. *Synlett* **2010,** 2936–2940. doi:10.1055/s-0030-1259023
27. Petiot, P.; Gagnon, A. *Eur. J. Org. Chem.* **2013,** 5282–5289. doi:10.1002/ejoc.201300850
28. Petiot, P.; Gagnon, A. *Heterocycles* **2014,** *88,* 1615–1624. doi:10.3987/com-13-s(s)114
29. Dansereau, J.; Gautreau, S.; Gagnon, A. *ChemistrySelect* **2017,** *2,* 2593–2599. doi:10.1002/slct.201700438
30. Petiot, P.; Dansereau, J.; Gagnon, A. *RSC Adv.* **2014,** *4,* 22255–22259. doi:10.1039/c4ra02467b
31. Crifar, C.; Petiot, P.; Ahmad, T.; Gagnon, A. *Chem. – Eur. J.* **2014,** *20,* 2755–2760. doi:10.1002/chem.201303684
32. Petiot, P.; Dansereau, J.; Hébert, M.; Khene, I.; Ahmad, T.; Samaali, S.; Leroy, M.; Pinsonneault, F.; Legault, C. Y.; Gagnon, A. *Org. Biomol. Chem.* **2015,** *13,* 1322–1327. doi:10.1039/c4ob02497d
33. Ahmad, T.; Dansereau, J.; Hébert, M.; Grand-Maître, C.; Larivée, A.; Siddiqui, A.; Gagnon, A. *Tetrahedron Lett.* **2016,** *57,* 4284–4287. doi:10.1016/j.tetlet.2016.08.021
34. Hébert, M.; Petiot, P.; Benoit, E.; Dansereau, J.; Ahmad, T.; Le Roch, A.; Ottenwaelder, X.; Gagnon, A. *J. Org. Chem.* **2016,** *81,* 5401–5416. doi:10.1021/acs.joc.6b00767
35. Gagnon, A.; St-Onge, M.; Little, K.; Duplessis, M.; Barabé, F. *J. Am. Chem. Soc.* **2007,** *129,* 44–45. doi:10.1021/ja0676758
36. Gagnon, A.; Duplessis, M.; Alsabeh, P.; Barabé, F. *J. Org. Chem.* **2008,** *73,* 3604–3607. doi:10.1021/jo702377h
37. Benoit, E.; Dansereau, J.; Gagnon, A. *Synlett* **2017,** *28,* 2833–2838. doi:10.1055/s-0036-1590832
38. Benoit, E.; Bueno, B.; Choinière, C.; Gagnon, A. *J. Organomet. Chem.* **2019,** *893,* 72–77. doi:10.1016/j.jorganchem.2019.04.032
39. Bénard, S.; Neuville, L.; Zhu, J. *J. Org. Chem.* **2008,** *73,* 6441–6444. doi:10.1021/jo801033y
40. Bénard, S.; Neuville, L.; Zhu, J. *Chem. Commun.* **2010,** *46,* 3393–3395. doi:10.1039/b925499d
41. Tsuritani, T.; Strotman, N. A.; Yamamoto, Y.; Kawasaki, M.; Yasuda, N.; Mase, T. *Org. Lett.* **2008,** *10,* 1653–1655. doi:10.1021/ol800376f
42. Racine, E.; Monnier, F.; Vors, J.-P.; Taillefer, M. *Chem. Commun.* **2013,** *49,* 7412–7414. doi:10.1039/c3cc42575d
43. Haneda, S.; Sudo, K.; Hayashi, M. *Heterocycles* **2012,** *84,* 569–575. doi:10.3987/com-11-s(p)20
44. Tambe, Y. B.; Sharma, S.; Pathak, A.; Reddy, L. K. *Synth. Commun.* **2012,** *42,* 1341–1348. doi:10.1080/00397911.2010.539758
45. Chan, D. M. T.; Monaco, K. L.; Wang, R.-P.; Winters, M. P. *Tetrahedron Lett.* **1998,** *39,* 2933–2936. doi:10.1016/s0040-4039(98)00503-6
46. Evans, D. A.; Katz, J. L.; West, T. R. *Tetrahedron Lett.* **1998,** *39,* 2937–2940. doi:10.1016/s0040-4039(98)00502-4
47. Lam, P. Y. S.; Clark, C. G.; Saubern, S.; Adams, J.; Winters, M. P.; Chan, D. M. T.; Combs, A. *Tetrahedron Lett.* **1998,** *39,* 2941–2944. doi:10.1016/s0040-4039(98)00504-8
48. Evano, G.; Blanchard, N., Eds. *Copper-Mediated Cross-Coupling Reactions;* John Wiley and Sons Ltd.: Hoboken, NJ, U.S.A., 2013. doi:10.1002/9781118690659
49. Evano, G.; Blanchard, N.; Toumi, M. *Chem. Rev.* **2008,** *108,* 3054–3131. doi:10.1021/cr8002505
50. Monnier, F.; Taillefer, M. *Angew. Chem., Int. Ed.* **2009,** *48,* 6954–6971. doi:10.1002/anie.200804497
51. Sambiagio, C.; Marsden, S. P.; Blacker, A. J.; McGowan, P. C. *Chem. Soc. Rev.* **2014,** *43,* 3525–3550. doi:10.1039/c3cs60289c
52. Derosa, J.; O'Duill, M. L.; Holcomb, M.; Boulous, M. N.; Patman, R. L.; Wang, F.; Tran-Dubé, M.; McAlpine, I.; Engle, K. M. *J. Org. Chem.* **2018,** *83,* 3417–3425. doi:10.1021/acs.joc.7b03100
53. Xu, H.-J.; Zhao, Y.-Q.; Feng, T.; Feng, Y.-S. *J. Org. Chem.* **2012,** *77,* 2878–2884. doi:10.1021/jo300100x
54. Herradura, P. S.; Pendola, K. A.; Guy, R. K. *Org. Lett.* **2000,** *2,* 2019–2022. doi:10.1021/ol005832g
55. Hayashi, M.; Okunaga, K.-i.; Nishida, S.; Kawamura, K.; Eda, K. *Tetrahedron Lett.* **2010,** *51,* 6734–6736. doi:10.1016/j.tetlet.2010.10.070
56. Figuly, G. D.; Martin, J. C. *J. Org. Chem.* **1980,** *45,* 3728–3729. doi:10.1021/jo01306a041
57. Taniguchi, N. *Synlett* **2005,** 1687–1690. doi:10.1055/s-2005-871545
58. Spurg, A.; Schnakenburg, G.; Waldvogel, S. R. *Chem. – Eur. J.* **2009,** *15,* 13313–13317. doi:10.1002/chem.200902466
59. Loghmani-Khouzani, H.; Poorheravi, M. R.; Sadeghi, M. M. M.; Caggiano, L.; Jackson, R. F. W. *Tetrahedron* **2008,** *64,* 7419–7425. doi:10.1016/j.tet.2008.05.034
60. Shojaei, A.; Rezvani, M.; Heravi, M. *J. Serb. Chem. Soc.* **2011,** *76,* 955–963.
61. Oba, M.; Tanaka, K.; Nishiyama, K.; Ando, W. *J. Org. Chem.* **2011,** *76,* 4173–4177. doi:10.1021/jo200496r
62. Misra, A. K.; Agnihotri, G. *Synth. Commun.* **2004,** *34,* 1079–1085. doi:10.1081/scc-120028640

BEILSTEIN JOURNAL OF ORGANIC CHEMISTRY

Allylic cross-coupling using aromatic aldehydes as α-alkoxyalkyl anions

Akihiro Yuasa, Kazunori Nagao and Hirohisa Ohmiya*

Letter

Open Access

Address:
Division of Pharmaceutical Sciences, Graduate School of Medical Sciences, Kanazawa University, Kakuma-machi, Kanazawa 920-1192, Japan

Email:
Hirohisa Ohmiya* - ohmiya@p.kanazawa-u.ac.jp

* Corresponding author

Keywords:
aldehyde; copper; copper catalysis; cross-coupling; palladium; synthetic method

Beilstein J. Org. Chem. **2020,** *16,* 185–189.
doi:10.3762/bjoc.16.21

Received: 15 October 2019
Accepted: 03 February 2020
Published: 07 February 2020

This article is part of the thematic issue "Copper-catalyzed reactions for organic synthesis".

Guest Editor: O. Riant

Abstract

The allylic cross-coupling using aromatic aldehydes as α-alkoxyalkyl anions is described. The synergistic palladium/copper-catalyzed reaction of aromatic aldehydes, allylic carbonates, and a silylboronate produces the corresponding homoallylic alcohol derivatives. This process involves the catalytic formation of a nucleophilic α-silyloxybenzylcopper(I) species and the subsequent palladium-catalyzed allylic substitution.

Introduction

α-Alkoxy-substituted carbanions (α-alkoxyalkyl anions) are useful C(sp^3) nucleophiles for the construction of alcohol units found in a majority of pharmaceuticals, agrochemicals and bioactive natural products. Generally, α-alkoxyalkyl anions are presynthesized as stoichiometric organometallic reagents such as organolithium, organozinc, organocuprate, organostannane, organosilane and organoboron compounds [1-6]. Alternatively, we showed that easily available aromatic aldehydes can be used as α-alkoxyalkyl anions for catalytic carbon–carbon bond formations [7-9]. For example, a nucleophilic α-silyloxybenzylcopper(I) species can be generated catalytically from aromatic aldehydes through the 1,2-addition of a silylcopper(I) species followed by [1,2]-Brook rearrangement and then successfully trapped with aryl bromides under palladium catalysis (Scheme 1). This system was extended to an asymmetric version using the chiral α-silyloxybenzylcopper(I) species having a chiral NHC ligand. In the asymmetric system, one example of allylic carbonate was used as the carbon electrophile [8,10,11]. This paper describes in full detail the racemic system using allylic carbonates. The allylic cross-coupling of aromatic aldehydes and allylic carbonates with a silylboronate by the merging of a copper–*N*-heterocyclic carbene catalyst and a palladium–bisphosphine catalyst produced homoallylic alcohol derivatives [12-14].

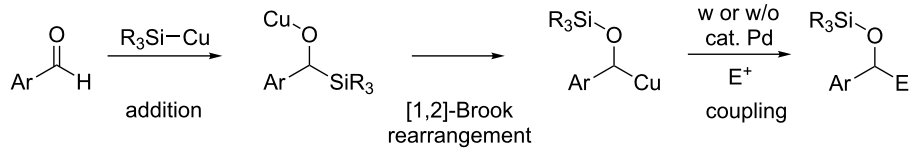

Scheme 1: Our strategy.

Results and Discussion

Specifically, the three-component allylic cross-coupling reaction of benzaldehyde (**1a**, 0.4 mmol), *tert*-butyl cinnamyl carbonate (**2a**, 0.2 mmol) and (dimethylphenylsilyl)boronic acid pinacol ester [$PhMe_2SiB(pin)$] (0.4 mmol) occurred in the presence of catalytic amounts of $Pd(OCOCF_3)_2$ (3 mol %), DPPF (3 mol %), (SIPr)CuCl (15 mol %) and KO*t*-Bu (25 mol %) in toluene at 80 °C to afford homoallylic alcohol derivative **3aa** in 64% yield (based on **2a**) (Scheme 2). The reaction yielded small amounts of side products such as cinnamylsilane and benzyl silyl ether, which are derived from the Pd-catalyzed allylic silylation of **2a** and the Cu-catalyzed silylation of **1a** and the subsequent [1,2]-Brook rearrangement, respectively. In this coupling reaction, (SIPr)CuCl was a slightly better copper complex than (IPr)CuCl (62%), (SIMes)CuCl (60%) and (IMes)CuCl (53%) in terms of the chemical yield. Notably, the allylic cross-coupling reaction did not occur at all without $Pd(OCOCF_3)_2$–DPPF or (SIPr)CuCl, and thus the palladium and copper catalysts cooperatively acted in the allylic cross-coupling.

Scheme 3 shows the substrate range of aromatic aldehydes **1** and allylic carbonates **2**. Methyl, *tert*-butyl and fluoro substituents were tolerated at the *ortho*- or *para*-positions of the aromatic aldehyde (**3ba**–**da**). 2,6-Dimethylphenyl- or 1-naphthyl moieties as the γ-substituent of the primary allylic carbonate were tolerated in the reaction (**3ab** and **3ac**). Cinnamyl carbonates having a fluoro or acetal substituent were also suitable coupling partners (**3ad** and **3ae**).

The synergistic palladium/copper catalysis was used for the reaction of a secondary allylic carbonate. For example, the allylic cross-coupling of **2a'**, a constitutional isomer of **2a**, with benzaldehyde (**1a**) afforded the linear allylation product **3aa** with complete regioselectivity. The symmetric secondary allylic carbonate was converted to the corresponding homoallylic alcohol derivative in 50% yield (**3af**).

To gain understanding into the mechanism of this synergistic palladium/copper-catalyzed allylic cross-coupling, a stoichiometric experiment was conducted (Scheme 4). The reaction of the SIPr-ligated α-silyloxybenzylcopper **4** with the cinnamyl–palladium complex **5**, which was prepared in situ from $[(cinnamyl)PdCl]_2$ and DPPF, gave the corresponding homoallylic alcohol derivative **3aa**.

Based on previous reports and the outcome obtained by the stoichiometric experiment in Scheme 4, a possible reaction pathway involving a cooperative action of palladium and copper catalysis can be proposed as illustrated in Scheme 5. The reaction of SIPr-ligated CuCl (**A**), KO*t*-Bu and a silylboronate produces a silylcopper(I) species **B**. The 1,2-addition of silylcopper(I) **B** to the aromatic aldehyde **1** [15-19] and the subsequent [1,2]-Brook rearrangement from the obtained α-silyl-substituted copper(I) alkoxide **C** forms the key intermediate, an α-silyloxybenzylcopper(I) species **D**. The transmetallation between **D** and an allylpalladium(II) species **F** that is generated through the oxidative addition of an allylic carbonate **2** across a palladium(0)–DPPF complex **E**, followed by

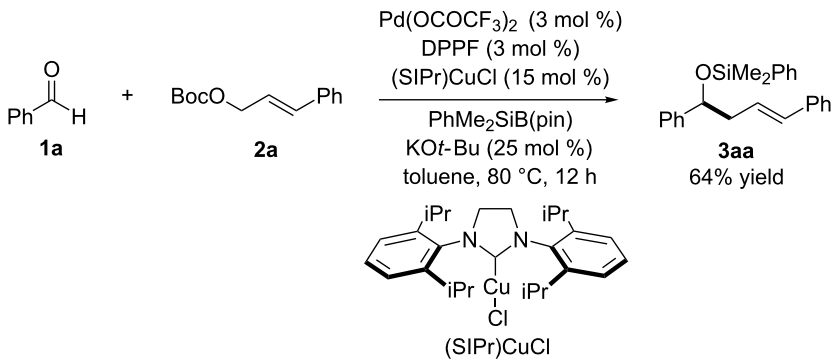

Scheme 2: Allylic cross-coupling using aldehydes as α-alkoxyalkyl anions.

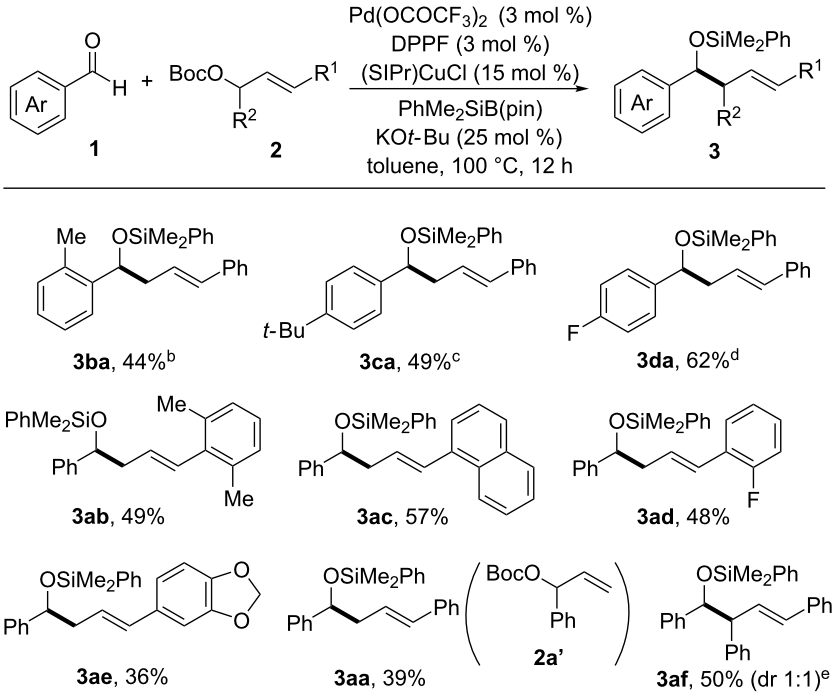

Scheme 3: Substrate scope and reaction conditions. a) reactions were carried out with **1** (0.4 mmol), **2** (0.2 mmol), $PhMe_2SiBpin$ (0.4 mmol), $Pd(OCOCF_3)_2$ (3 mol %), DPPF (3 mol %), (SIPr)CuCl (15 mol %), KO*t*-Bu (25 mol %) in toluene (2 mL) at 100 °C for 12 h. b) $Pd(OCOCF_3)_2$/DPPF (3 mol %), (SIPr)CuCl (25 mol %) and KO*t*-Bu (35 mol %) were used and the reaction temperature was decreased to 80 °C. c) $Pd(OCOCF_3)_2$/DPPF (3 mol %), (SIPr)CuCl (25 mol %) and KO*t*-Bu (35 mol %) were used. d) The reaction temperature was decreased to 80 °C. e) $Pd(OCOCF_3)_2$/DPPF (5 mol %), (SIPr)CuCl (25 mol %) and KO*t*-Bu (35 mol %) were used.

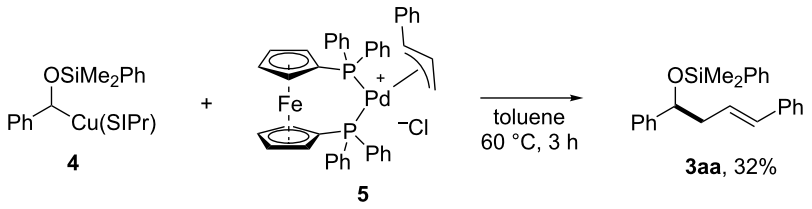

Scheme 4: Stoichiometric reaction.

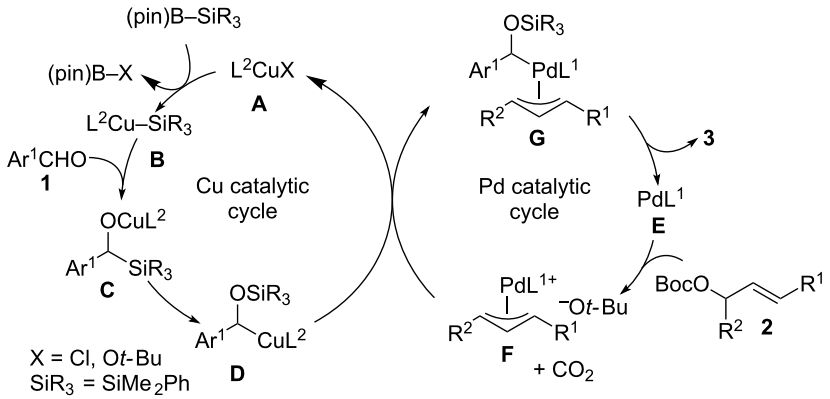

Scheme 5: Possible pathway.

reductive elimination from **G** produces the homoallylic alcohol **3** and then regenerate **A** and **E** for the next catalytic cycle [20-23].

Conclusion

In summary, we developed an umpolung strategy for catalytically formed α-alkoxyalkyl anions from aromatic aldehydes for the use in allylic cross-coupling reactions. The synergistic palladium/copper-catalyzed reaction of aromatic aldehydes, allylic carbonates, and a silylboronate delivered the homoallylic alcohol derivatives. This process involves the catalytic formation of a nucleophilic α-silyloxybenzylcopper(I) species and the subsequent palladium-catalyzed allylic substitution.

Experimental

SIPrCuCl (14.7 mg, 0.03 mmol), and KO*t*-Bu (4.5 mg, 0.04 mmol) were placed in a vial containing a magnetic stirring bar. The vial was sealed with a Teflon®-coated silicon rubber septum, and then the vial was evacuated and filled with nitrogen. Toluene (0.6 mL) was added to the vial, and then the mixture was stirred at 25 °C for 10 min. Next, $PhMe_2SiB(pin)$ (104.9 mg, 0.4 mmol) and benzaldehyde (**1a**, 42.4 mg, 0.4 mmol) were added, and the mixture (mixture A) was stirred at 25 °C for 10 min. Meanwhile, $Pd(OCOCF_3)_2$ (2.0 mg, 0.006 mmol) and DPPF (3.3 mg, 0.006 mmol) were placed in another vial. This vial was sealed with a Teflon®-coated silicon rubber septum and then evacuated and filled with nitrogen. After toluene (0.8 mL) was added to the vial, the mixture was stirred at 25 °C for 10 min. Next, KO*t*-Bu (1.1 mg, 0.01 mmol) and allylic carbonate **2a** (46.9 mg, 0.2 mmol) were added to the vial, and the mixture (mixture B) was stirred at 25 °C for 10 min. Finally, the palladium solution (mixture B) was transferred to the vial (mixture A) containing the copper complex with toluene (0.6 mL). After 12 h stirring at 80 °C, the reaction mixture was diluted with diethyl ether (1 mL). The reaction mixture was filtered through a short plug of aluminum oxide (1 g) with diethyl ether as an eluent. After volatiles were removed under reduced pressure, GPC (EtOAc) followed by flash chromatography on silica gel (0–1% EtOAc/hexane) gave product **3aa** in 64% isolated yield (45.7 mg, 0.13 mmol).

Supporting Information

Supporting Information File 1

Experimental procedures, spectroscopic and analytical data, and copies of NMR spectra for newly synthesized compounds.
[https://www.beilstein-journals.org/bjoc/content/supplementary/1860-5397-16-21-S1.pdf]

Funding

This work was supported by JSPS KAKENHI Grant Number JP18H01971 to Scientific Research (B), JSPS KAKENHI Grant Number JP17H06449 (Hybrid Catalysis), and Kanazawa University SAKIGAKE project 2018 (to H.O.).

ORCID® iDs

Hirohisa Ohmiya - https://orcid.org/0000-0002-1374-1137

References

1. Hoppe, D.; Hense, T. *Angew. Chem., Int. Ed. Engl.* **1997,** *36,* 2282–2316. doi:10.1002/anie.199722821
2. Still, W. C. *J. Am. Chem. Soc.* **1978,** *100,* 1481–1487. doi:10.1021/ja00473a025
3. Papillon, J. P. N.; Taylor, R. J. K. *Org. Lett.* **2002,** *4,* 119–122. doi:10.1021/ol016986e
4. Linderman, R. J.; Godfrey, A.; Horne, K. *Tetrahedron Lett.* **1987,** *28,* 3911–3914. doi:10.1016/s0040-4039(00)96418-9
5. Arai, N.; Suzuki, K.; Sugizaki, S.; Sorimachi, H.; Ohkuma, T. *Angew. Chem., Int. Ed.* **2008,** *47,* 1770–1773. doi:10.1002/anie.200704696
6. Laitar, D. S.; Tsui, E. Y.; Sadighi, J. P. *J. Am. Chem. Soc.* **2006,** *128,* 11036–11037. doi:10.1021/ja064019z
7. Takeda, M.; Yabushita, K.; Yasuda, S.; Ohmiya, H. *Chem. Commun.* **2018,** *54,* 6776–6779. doi:10.1039/c8cc01055b
8. Yabushita, K.; Yuasa, A.; Nagao, K.; Ohmiya, H. *J. Am. Chem. Soc.* **2019,** *141,* 113–117. doi:10.1021/jacs.8b11495
9. Takeda, M.; Mitsui, A.; Nagao, K.; Ohmiya, H. *J. Am. Chem. Soc.* **2019,** *141,* 3664–3669. doi:10.1021/jacs.8b13309
10. Nahra, F.; Macé, Y.; Lambin, D.; Riant, O. *Angew. Chem., Int. Ed.* **2013,** *52,* 3208–3212. doi:10.1002/anie.201208612
11. Jia, T.; Cao, P.; Wang, B.; Lou, Y.; Yin, X.; Wang, M.; Liao, J. *J. Am. Chem. Soc.* **2015,** *137,* 13760–13763. doi:10.1021/jacs.5b09146
12. Kim, I. S.; Ngai, M.-Y.; Krische, M. J. *J. Am. Chem. Soc.* **2008,** *130,* 6340–6341. doi:10.1021/ja802001b
13. Ketcham, J. M.; Shin, I.; Montgomery, T. P.; Krische, M. J. *Angew. Chem., Int. Ed.* **2014,** *53,* 9142–9150. doi:10.1002/anie.201403873
14. Denmark, S. E.; Matesich, Z. D. *J. Org. Chem.* **2014,** *79,* 5970–5986. doi:10.1021/jo501004j
15. Kleeberg, C.; Feldmann, E.; Hartmann, E.; Vyas, D. J.; Oestreich, M. *Chem. – Eur. J.* **2011,** *17,* 13538–13543. doi:10.1002/chem.201102367
16. Cirriez, V.; Rasson, C.; Hermant, T.; Petrignet, J.; Díaz Álvarez, J.; Robeyns, K.; Riant, O. *Angew. Chem., Int. Ed.* **2013,** *52,* 1785–1788. doi:10.1002/anie.201209020
17. Delvos, L. B.; Hensel, A.; Oestreich, M. *Synthesis* **2014,** *46,* 2957–2964. doi:10.1055/s-0034-1378542
18. Oestreich, M.; Hartmann, E.; Mewald, M. *Chem. Rev.* **2013,** *113,* 402–441. doi:10.1021/cr3003517
19. Hensel, A.; Oestreich, M. Asymmetric Addition of Boron and Silicon Nucleophiles. In *Progress in Enantioselective Cu(I)-catalyzed Formation of Stereogenic Centers;* Harutyunyan, S., Ed.; Top. Organomet. Chem., Vol. 58; Springer: Cham, Switzerland, 2016; pp 135–167. doi:10.1007/3418_2015_156
20. Pye, D. R.; Mankad, N. P. *Chem. Sci.* **2017,** *8,* 1705–1718. doi:10.1039/c6sc05556g

21. Semba, K.; Nakao, Y. *J. Am. Chem. Soc.* **2014,** *136,* 7567–7570. doi:10.1021/ja5029556
22. Smith, K. B.; Logan, K. M.; You, W.; Brown, M. K. *Chem. – Eur. J.* **2014,** *20,* 12032–12036. doi:10.1002/chem.201404310
23. Friis, S. D.; Pirnot, M. T.; Buchwald, S. L. *J. Am. Chem. Soc.* **2016,** *138,* 8372–8375. doi:10.1021/jacs.6b04566

License and Terms

BEILSTEIN JOURNAL OF ORGANIC CHEMISTRY

Combination of multicomponent KA^2 and Pauson–Khand reactions: short synthesis of spirocyclic pyrrolocyclopentenones

Riccardo Innocenti[1], Elena Lenci[1], Gloria Menchi[1] and Andrea Trabocchi[*1,2]

Full Research Paper

Open Access

Address:
[1]Department of Chemistry “Ugo Schiff”, University of Florence, Via della Lastruccia 13, 50019 Sesto Fiorentino, Florence, Italy, and [2]Interdepartmental Center for Preclinical Development of Molecular Imaging (CISPIM), University of Florence, Viale Morgagni 85, 50134 Florence, Italy

Email:
Andrea Trabocchi[*] - andrea.trabocchi@unifi.it

* Corresponding author

Keywords:
chemical libraries; chemoinformatics; Cu-catalysis; cycloadditions; molecular scaffolds; multicomponent reactions

Beilstein J. Org. Chem. **2020,** *16,* 200–211.
doi:10.3762/bjoc.16.23

Received: 18 November 2019
Accepted: 23 January 2020
Published: 12 February 2020

This article is part of the thematic issue "Copper-catalyzed reactions for organic synthesis".

Guest Editor: G. Evano

Abstract

The Cu-catalyzed multicomponent ketone–amine–alkyne (KA^2) reaction was combined with a Pauson–Khand cycloaddition to give access of unprecedented constrained spirocyclic pyrrolocyclopentenone derivatives following a DOS couple-pair approach. The polyfunctional molecular scaffolds were tested on the cyclopentenone reactivity to further expand the skeletal diversity, demonstrating the utility of this combined approach in generating novel spiro compounds as starting material for the generation of chemical libraries. The chemoinformatics characterization of the newly-synthesized molecules gave evidence about structural and physicochemical properties with respect to a set of blockbuster drugs, and showed that such scaffolds are drug-like but more spherical and three-dimensional in character than the drugs.

Introduction

The screening of small molecule libraries is a well-established approach in early-stage drug discovery to identify hit candidates for the development of drug leads. The application of unconventional molecular scaffolds to develop chemical libraries can increase the chance of finding compounds able to address the so-called “undruggable” targets, such as protein–protein interactions [1]. In this context, molecules containing one or more rings are of primary interest, as they will suffer a reduced conformational entropy penalty upon binding to a protein target, and the approach of constraining the ligand conformation with a ring is widely used in drug design [2]. Accordingly, with increasing interest for sp^3-rich molecules, spirocyclic compounds are being considered valuable as molecular platforms for the generation of high-quality small molecule

collections, taking advantage of the stereochemical diversity, and of their three-dimensional shape and structural bias to develop lead compounds, specifically in the field of protein–protein interactions [3-6]. Spiranic rings such as spiroketals are present in numerous natural products [7-9], a wide array of spirocyclic compounds are being studied in drug discovery and their chemical space have been systematically charted and characterized recently by Bajorath and co-workers (Figure 1) [10]. This study revealed that spirocycles are found only in few approved drugs [11] and that there is a significant potential to explore the chemical space of spirocyclic scaffolds, especially in the case of the condensed ones. Thus, new synthetic routes towards the synthesis of building blocks containing spiranic rings have increasingly appeared in the recent literature [12].

Among the synthetic approaches to improve the quality and quantity of small molecules members of chemical libraries, diversity-oriented synthesis (DOS) [13-16], has been proposed as a paradigm for developing large collections of structurally diverse small molecules in a way to generate the maximum diversity and complexity from simple starting materials applying divergent synthetic strategies, such as the use of complexity-generating reactions and the build/couple/pair approach [17,18]. The application of multicomponent approaches has proven to be very useful as starting points in DOS [19-22], such as the exploitation of the Petasis three-component [23-29] and the Ugi four-component reactions [30-33], showing interesting properties for the generation of compounds characterized by high stereochemical and skeletal diversity. Although not fully exploited so far, some contributions on the diversity-oriented synthesis of spirocyclic compounds have appeared in the literature recently, also employing multicomponent approaches to give the spirocyclic adduct after a cyclization step [34-36]. We recently focused our interest to the cyclopentenone ring [37], as this heterocycle is a powerful synthon for the synthesis of a variety of bioactive target molecules, due to the broad diversity of chemical modifications available for the enone structural motif [38]. The most common approach to access such chemotype is the Pauson–Khand (PK) reaction [39,40], consisting of a [2 + 2 + 1] cycloaddition between an olefin, alkyne, and carbon monoxide. This reaction has been also applied in cascade approaches [41], and in combination with RCM [42], Diels–Alder [43] and Staudinger [44] reactions to produce novel structurally complex chemical entities. Following our interest to DOS as a synthetic strategy for the generation of molecular scaffolds according to a couple/pair approach [45-47], we reasoned to combine the copper-catalyzed ketone–amine–alkyne (KA^2) multicomponent coupling reaction [48] with the Pauson–Khand cycloaddition as the pairing reaction to achieve spirocyclic pyrrolocyclopentenone derivatives. Specifically, the KA^2 reaction was envisaged taking into account cyclic ketones, to install a quaternary carbon atom carrying the required 1,6-enyne moiety for the subsequent Pauson–Khand reaction, thus achieving the corresponding tricylic structure in three single steps (Scheme 1b). This unprecedent molecular scaffold repre-

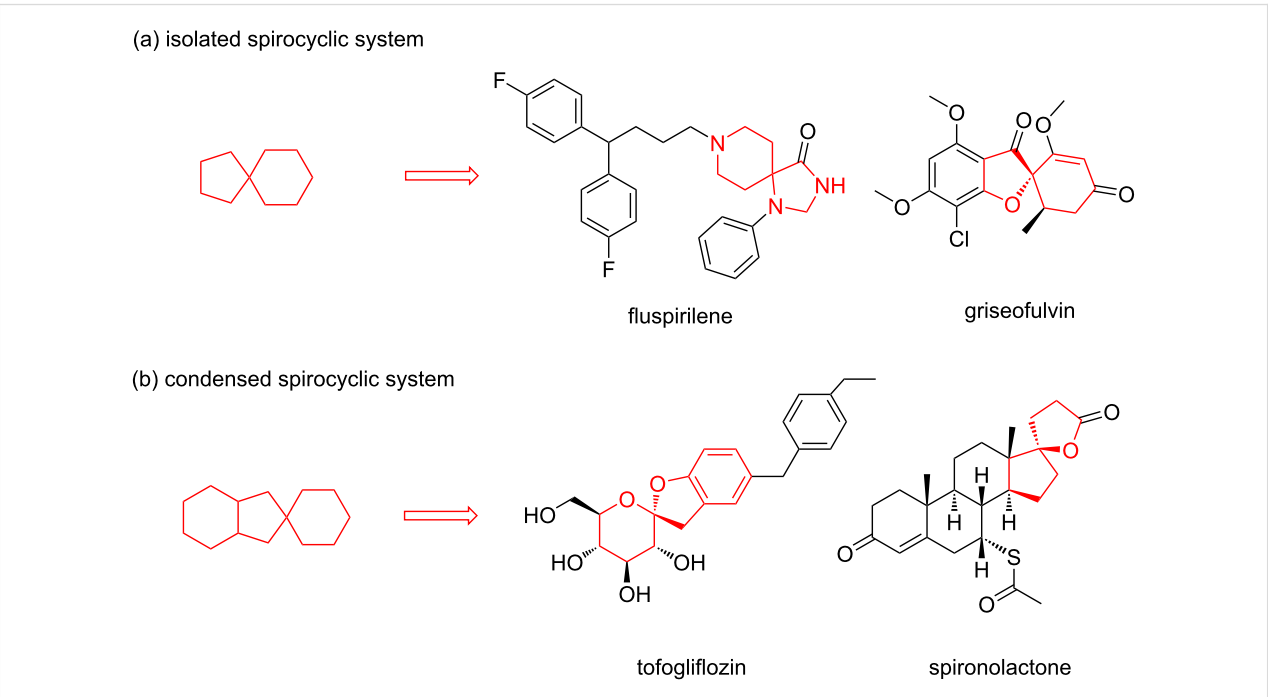

Figure 1: Chemical structure of representative approved drugs containing a spirocyclic moiety.

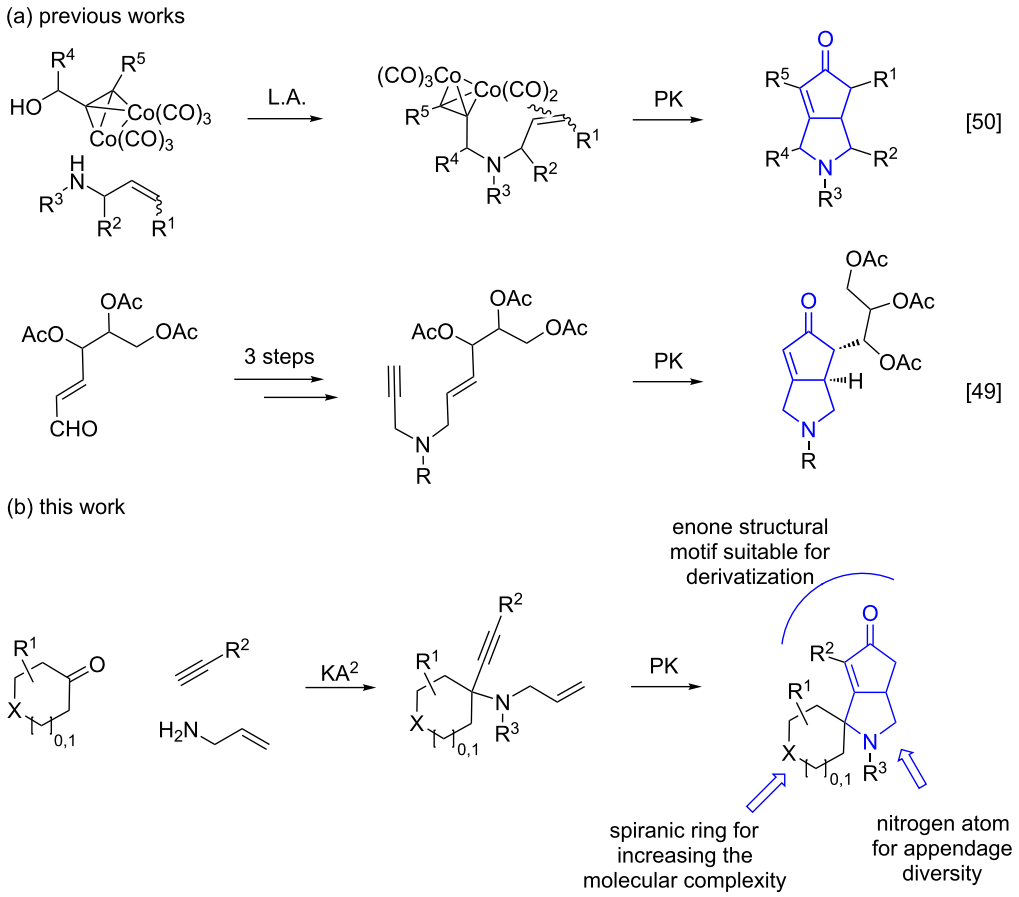

Scheme 1: Synthetic strategies for accessing pyrrolocyclopentenone derivatives, including the novel couple/pair approach that combines the KA^2 and PK multicomponent reactions. L.A. = Lewis acid; PK = Pauson–Khand.

sents a valuable template for medicinal chemistry purpose, as the pyrrolocyclopentenone core is contained in a variety of bioactive molecules [49,50], and can serve as an advanced intermediate for the synthesis of different compounds, such as (−)-kainic acid [51,52]. Previous similar approaches reported only planar pyrrolocyclopentenones starting from propargyl alcohol–cobalt complexes and allyl amides [50], or carbohydrate-derived allylpropargylamine [49] (Scheme 1a).

Results and Discussion

Cyclohexanone (**1**) and phenylacetylene (**2**) were taken into account for the optimization of the KA^2 reaction conditions with allylamine, in order to attain a quaternary carbon atom containing suitable alkenyl and alkynyl appendages for subsequent Pauson–Khand intramolecular cycloaddition (Scheme 2).

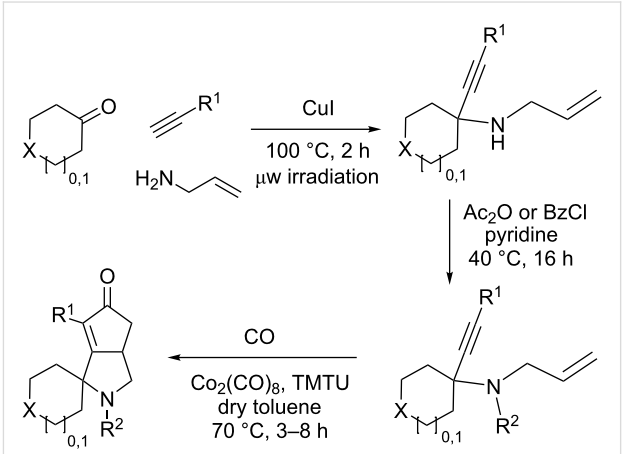

Scheme 2: Couple/pair approach using combined KA^2 and Pauson–Khand multicomponent reactions.

The KA^2 reaction was assayed following the reported method [48] employing copper catalysis, and tested on our starting material upon variation of copper salts, solvents and temperature, resulting in the neat reaction under CuI catalysis being optimal when carried out for 2 h at 100 °C under microwave irradiation (see Supporting Information File 1), as it can promote metal-catalyzed reactions [53]. The scope of the combined approach employing KA^2 and Pauson–Khand reactions was studied by varying the alkyne and ketone components, along with the

acylating moiety being installed before the Pauson–Khand reaction (Scheme 2 and Table 1). The acylation of the amino group was found necessary to allow for the cobalt-catalyzed reaction to proceed under a CO atmosphere. This step was also carried out in one pot after the KA^2 reaction by diluting with pyridine and adding the acylating reagent, to achieve the corresponding product in slightly lower yield. Attempts to carry out the Pauson–Khand reaction directly on the amino group before the acylation step did not work, nor using a modified approach using ammonium chloride and 1.5 equivalents of $Co_2(CO)_8$

Table 1: Scope of the combined KA^2 and Pauson–Khand multicomponent processes.[a]

entry	ketone	alkyne	yield, %	
			KA^2 product	PK product
1	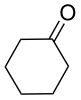 **1**	 **2**	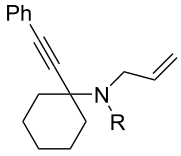 **3**: R = H, 82% **4**: R = Ac, 61%	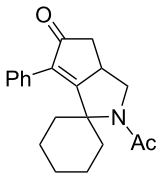 **5**, 73%
2	**1**	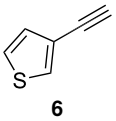 **6**	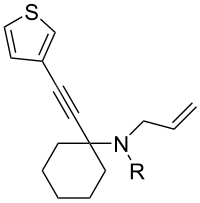 **7**: R = H, 74% **8**: R = Ac, 78%	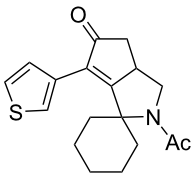 **9**, 68%
3	**1**	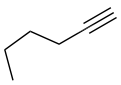 **10**	–	–
4	**1**	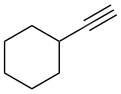 **11**	–	–
5	 **12**	**2**	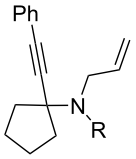 **13**: R = H, 61% **14**: R = Ac, 56%	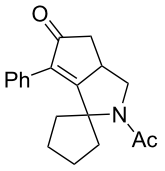 **15**, 72%
6	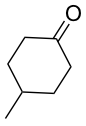 **16**	**2**	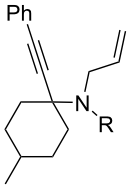 **17**: R = H, 82% **18**: R = Ac, 68%	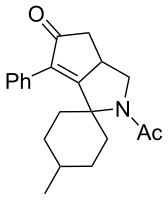 **19**, 72%
7	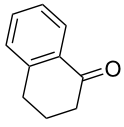 **20**	**2**	–	–

Table 1: Scope of the combined KA^2 and Pauson–Khand multicomponent processes.[a] (continued)

8	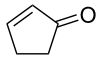 **21**	**2**		
9	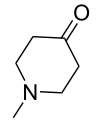 **22**	**2**	–	–
10	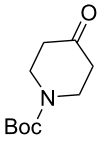 **23**	**2**	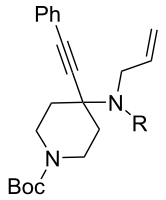 **24**: R = H, 83% **25**: R = Ac, 63%	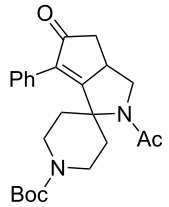 **26**, 79%
11	**23**	**6**	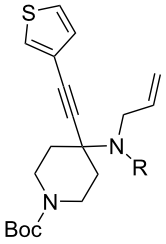 **27**: R = H, 62% **28**: R = Ac, 63%	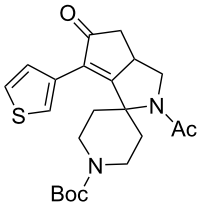 **29**, 68%
12	**23**	**2**	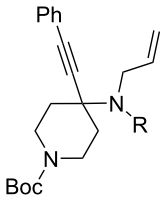 **24**: R = H, 83% **30**: R = Bz, 68%	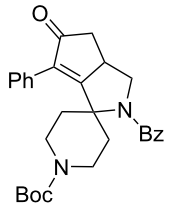 **31**, 78%
13	**23**	**2**	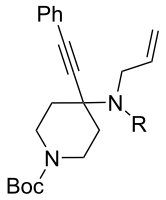 **24**: R = H, 83% **32**: R = Ts, 63%	–
14	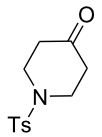 **33**	**2**	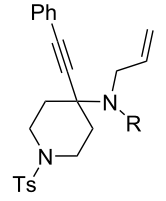 **34**: R = H, 71% **35**: R = Ac, 52%	–

[a]Reaction conditions. KA^2 reaction: ketone (1 equiv), alkyne (1.2 equiv) and amine (1.2 equiv), CuI (0.2 equiv), 100 °C, 2 h, microwave irradiation. Amine protection: pyridine (2 mL/mmol), acetic anhydride (4 mL/mmol), 40 °C, 16 h. Pauson–Khand reaction: enyne (1 equiv), $Co_2(CO)_8$ (0.1 equiv), *N,N,N′,N′*-tetramethylthiourea (0.6 equiv), toluene (20 mL/mmol), CO atmosphere, 70 °C, 3–8 h.

under an inert atmosphere, as reported for similar reactions in the presence of basic nitrogen atoms [28].

The variation of the alkyne component proved to give the KA^2 coupling adduct when aromatic terminal alkynes were used, as shown in Table 1, entries 1 and 2 for those containing phenyl and thienyl moieties, resulting in 82% and 74% yield for the KA^2 step. Subsequent acylation and pairing steps proved to proceed in good yield, thus furnishing the corresponding spirocyclopentenone derivatives **5** and **9** with an aromatic appendage at the carbonyl alpha carbon. On the contrary, when aliphatic alkynes were applied in the KA^2 process, no reaction with allylamine and cyclohexanone was achieved, suggesting a role of the aromatic ring in activating the alkyne towards the copper-catalyzed process (Table 1, entries 3 and 4), as previously reported in other works [54]. Use of cyclopentanone, thus varying the ring size of the cyclic ketone, resulted in the conversion to the title spirocyclopentenone derivative, although in slightly lower yield as compared for the homologous ketone (Table 1, entry 5). No conversion to the KA^2 adduct was achieved by using unsaturated or aromatic ketones (Table 1, entries 7 and 8, respectively), confirming an important role of the electronic content of the components in the outcome of the multicomponent coupling reaction. Similarly, the use of piperidone as the ketone component proved to work only when the amino group was protected as Boc, whereas the *N*-methyl derivative did not proceed to the coupling product (Table 1, entries 10 and 9, respectively). Indeed, the Boc-piperidone furnished the corresponding spirocyclopentenone derivatives upon changing both the aromatic alkyne or the acylating agent (Table 1, entries 10–12). When the Boc group was replaced with the tosyl one as the *N*-substituent, such chemical moiety proved to impair the subsequent Pauson–Khand reaction (Table 1, entry 13), possibly due to a coordinating effect towards the cobalt catalyst. Such an effect was confirmed when the *N*-tosylpiperidone was used as the ketone component, as also in this case the presence of the tosyl group impaired the acetylated KA^2 adduct from reacting under Pauson–Khand conditions (Table 1,entry 14).

The synthetic utility of the spiro derivatives resulting from the combined KA^2/Pauson–Khand process to generate second-generation molecular scaffolds was tested on compound **5** by applying representative reactions on the enone structural motif (Scheme 3).

The chemoselective carbonyl reduction to obtain the corresponding allylic alcohol derivative **36** was achieved in 92% under Luche reduction conditions employing $NaBH_4/CeCl_3$ in MeOH/DCM, resulting in the selective synthesis of the *syn*-alcohol, as a consequence of the formation of the equatorial alcohol favored by reduced gauche interactions [55]. Subsequent epoxidation at the double bond directed by the hydroxy group and using *m*-chloroperbenzoic acid allowed to install two additional stereocenters with complete control of the relative stereochemistry in 68% yield. Such two-step synthesis proved to proceed also in one-pot, resulting in the generation of the stereochemically dense epoxyalcohol **37** in 68% overall yield. The treatment of compound **5** with EtMgBr as a Grignard

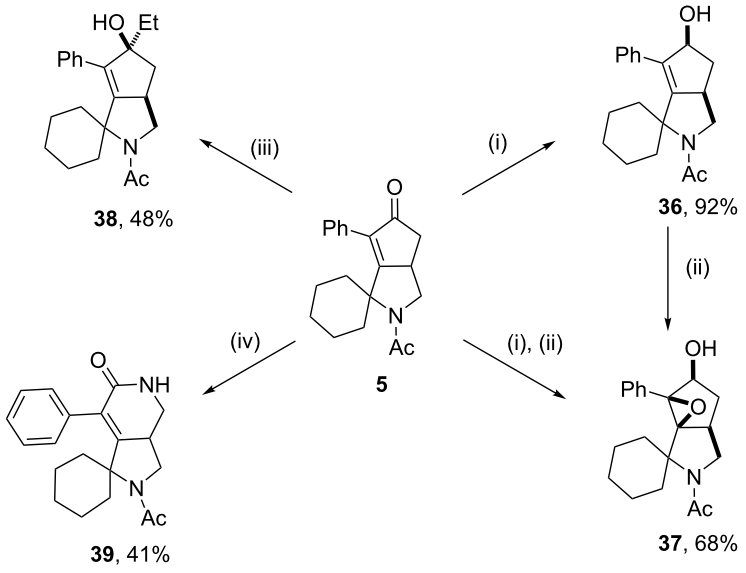

Scheme 3: Follow-up chemistry on compound **5** taking advantage of the enone chemistry. Reaction conditions. (i) $NaBH_4$ (2 equiv), $CeCl_3{\cdot}7H_2O$ (2 equiv), DMC/MeOH 1:1 (20 mL/mmol), 25 °C, 1 h; (ii) *m*-CPBA (1 equiv), DCM (6.5 mL/mmol), 0 °C, 4 h; (iii) EtMgBr 3 M in Et_2O (5 equiv), $CeCl_3$ (1 equiv), THF (6 mL/mmol), 0 °C, 30 min; (iv) NaN_3 (1.8 equiv), TFA (5 mL/mmol), reflux, 16 h.

reagent in the presence of $CeCl_3$ gave the corresponding tertiary alcohol **38** with similar stereochemical features as of **36** in the formation of the equatorial alcohol, although in lower yield. The use of $CeCl_3$ together with EtMgBr was found particularly effective to suppress conjugate additions, with similar yield as reported for analogous substrates [56]. Subsequent acid-catalyzed displacement of the hydroxy moiety with aniline in the presence of camphorsulfonic acid did not give the desired amine, supporting the hypothesis of steric hindrance at such position [57]. Similarly, Simmons–Smith cyclopropanation reaction [58] did not work, and so as for the cycloaddition reaction with Danishefsky's diene, possibly due to steric hindrance imposed by the adjacent phenyl and cyclohexyl rings [59]. The treatment of compound **5** under Schmidt reaction conditions with sodium azide in TFA [60] resulted in the conversion to the corresponding six-membered ring lactam **39** in 41% yield, demonstrating the reactivity of the enone **5** at the carbonyl group and showing stability towards harsh acidic conditions.

The structural assignment of compound **36** was assessed by detailed 1D and 2D NMR studies, and corroborated with molecular modeling calculations. NOESY-1D experiments carried out with a mixing time of 500 ms allowed to identify the unique rotamer possessing a Z geometry, as evinced by a NOE interaction between H_d and the methyl group. The *cis* relationship between the OH group and the pyrrolidine ring, resulting from the chemo- and stereoselective *syn* reduction of the carbonyl group, was evinced by NOESY-1D experiments showing intense NOE effects between H_c and H_a protons, as also shown in NOESY 2D spectrum (see Figure 2 and Supporting Information File 1). A similar analysis allowed the structural assignment for **38**.

Chemoinformatic analysis

The structural features of the compounds so obtained and representative functionalized molecular scaffolds were analyzed in terms of chemical properties and shape analysis in the context of the chemical space [61] using principal component analysis (PCA) and principal moments of inertia (PMI) analysis. PCA is a statistical tool to condense multidimensional chemical properties (i.e., molecular weight, logP, ring complexity) into single dimensional numerical values (principal components), to simplify the comparison with different sets of compounds. ChemGPS-NP [62-64] was chosen for the PCA analysis, providing a comprehensive exploration of the chemical space in terms of global mapping onto a consistent 8-dimensional map of structural characteristics [65]. In particular, the first and the second dimensions (PC1 and PC2) are the most interesting ones, being associated respectively with size, shape, and polarizability and with aromatic and conjugation related properties. The analysis of PC1 vs PC2 of compounds **3–39**, in comparison with a reference set of 40 brand-name blockbuster drugs

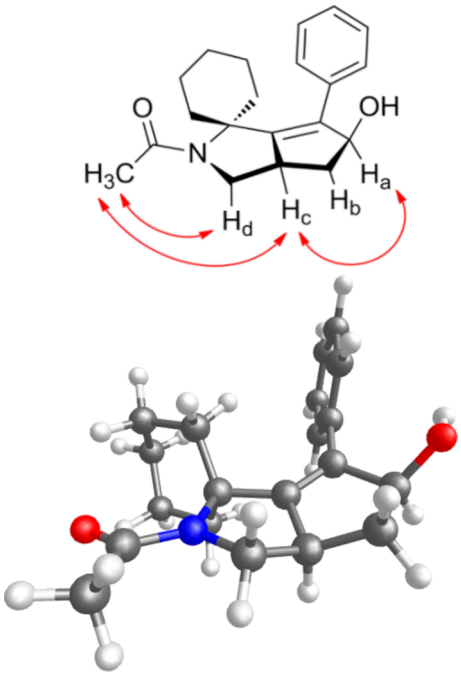

Figure 2: Top: Selected NOE contacts from NOESY 1D spectra of compound **36**; bottom: low energy conformer of **36**, Z rotamer, using ab initio calculation at the HF/3-21G* level.

[66,67] (Figure 3), showed the different distribution of compounds **3–39** in two different clusters. Most of the compounds reside in the first cluster, positioned in the negative direction of x axis, in a region that shows good overlap with drugs like levaquin, which is characterized by a complex tricyclic skeleton. The addition of a second aromatic ring, as the benzoyl or tosyl group of compounds **30–32**, **34** and **35**, increased the aromatic- and conjugation-related character of the structure, thus resulting in shifting those compounds to a second cluster being positioned in the positive direction for both axes, together with drugs possessing large aromatic content, as benazepril and seroquel.

The principal moments of inertia (PMI) analysis was also taken into account for the three-dimensional shape analysis of compounds **3–39** in the context of chemical space, again with reference to a set of BB drugs. The three principal moments of inertia (I_{xx}, I_{yy}, I_{zz}) and the corresponding normalized principal moments of inertia were determined according to Sauer and Schwarz [68] for the lowest energy conformation of all the compounds and the reference drugs. Then, the normalized PMI ratios were plotted on a triangular graph where the vertices (0,1), (0.5,0.5), and (1,1) represent a perfect rod (i.e., 2-butyne), disc (i.e., benzene), and sphere (i.e., adamantane), respectively (Figure 4). This analysis showed that all compounds **3–39** pos-

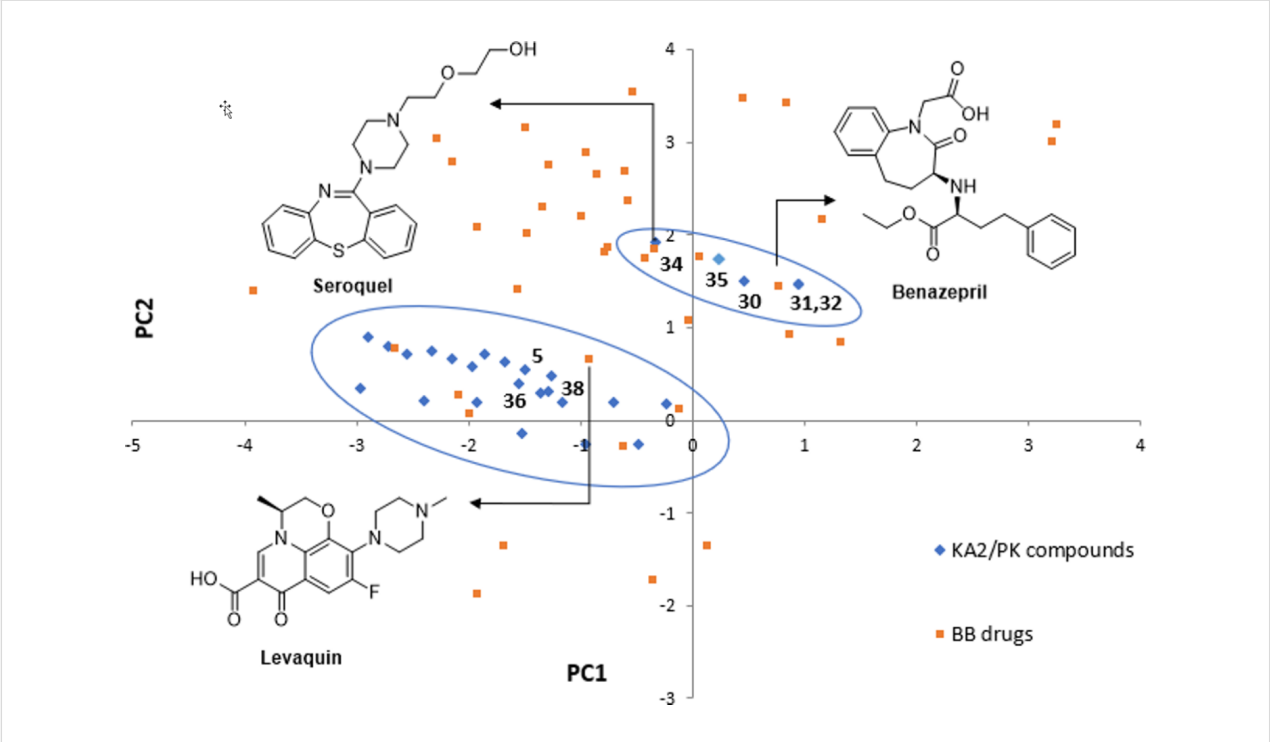

Figure 3: PCA plot resulting from the correlation between PC1 vs PC2, showing the positioning in the chemical space of compounds **3**–**39** (blue diamonds) with respect to the reference set of brand-name blockbuster drugs (orange squares).

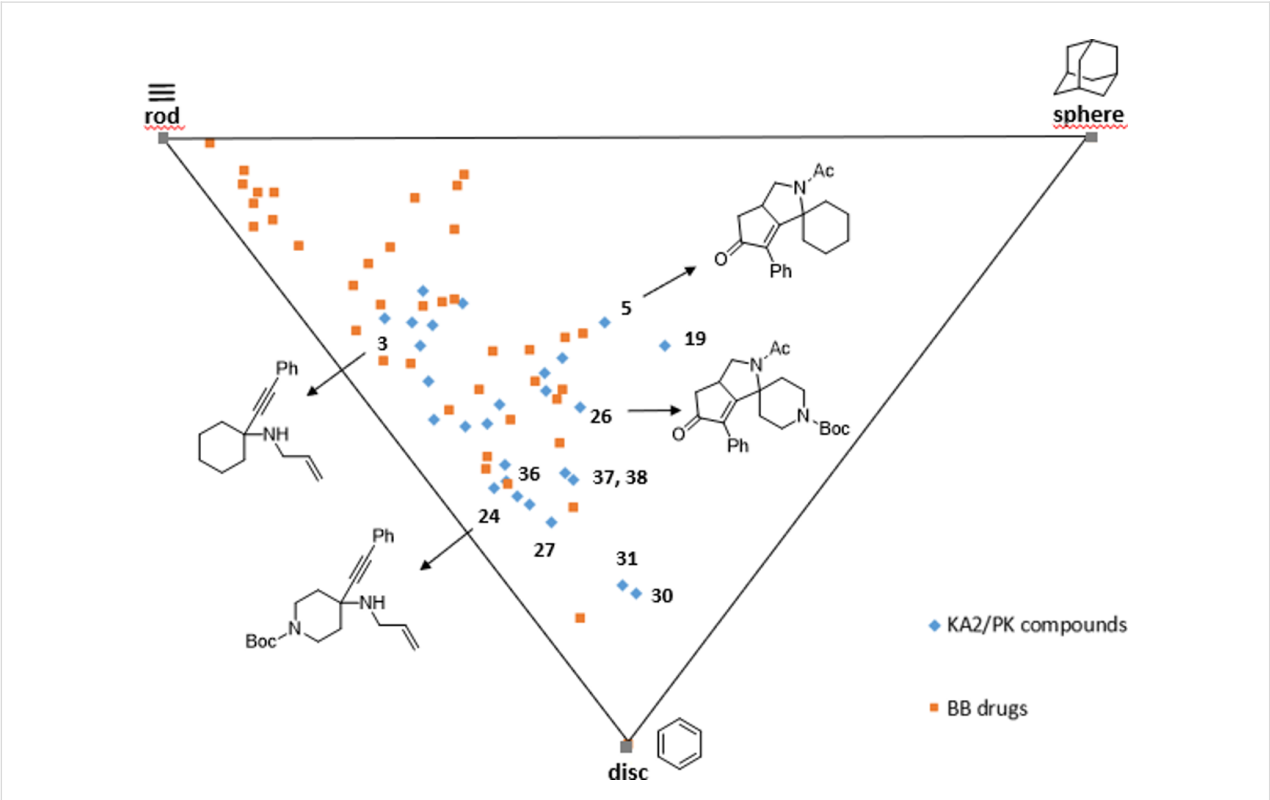

Figure 4: PMI plot showing the skeletal diversity of compounds **3**–**39** (blue diamonds) with respect to the reference set of brand-name blockbuster drugs (orange squares).

sess lower tendency to stay in the rod side of the triangle, as compared to BB drugs, suggesting for these compounds a higher shape complexity, as due to the presence of quaternary carbon atoms introduced by the KA^2 coupling reaction. The intramolecular Pauson–Khand cyclization proved to be even more efficient in increasing the three-dimensional character of these compounds, as spiro tricyclic products were found to be more shifted towards the sphere-disc region of this chemical space, especially if compared to their corresponding starting materials (see Figure 4, compounds **5** and **26** with respect to **3** and **24**, respectively). This feature is promising in view of expanding the array of molecular scaffolds of this nature for drug discovery purpose, as a higher scaffold complexity is generally associated with a more successful outcome in drug discovery and development [69-71]. On the other hand, the reduction of the carbonyl group into an alcohol was not significant in increasing the three-dimensional character of the structure, as compounds **36**–**38** were found to be more shifted towards the rod-sphere axes as compared to the parent compound **5**.

Conclusion

Spirocyclic compounds are valuable molecular platforms for the generation of high-quality small molecule collections, taking advantage of their three-dimensional shape and structural bias to develop lead compounds. The combination of multicomponent KA^2 and Pauson–Khand reactions using representative cyclic ketones, allylamine and phenylacetylene gave access to highly constrained spirocyclopentenone derivatives following a DOS couple-pair approach. A representative spirocyclopentenone derivative was applied to follow-up chemistry employing the enone reactivity to further expand the skeletal diversity, resulting in additional chemotypes useful as starting compounds for appendage diversity in the generation of chemical libraries. The chemoinformatics characterization of the newly-synthesized molecules gave evidence about structural and physicochemical properties with respect to a set of blockbuster drugs, and showed that such scaffolds are drug-like but more spherical and three-dimensional in character than the drugs. These combined approaches are being applied in chemistry as more efficient synthetic approaches to expand the array of polyfunctional sp^3-rich molecular scaffolds in the effort of increasing the synthetically-accessible chemical space.

Experimental

General procedure (A) for the KA^2 coupling reaction. CuI (0.2 equiv) was added in a dry sealed vial for microwave synthesis under a nitrogen flow. Then, ketone (1 equiv), alkyne (1.2 equiv) and amine (1.2 equiv) were successively added under a nitrogen flow, and the mixture was heated under microwave irradiation to 100 °C for 2 h. Then, EtOAc was added and the organic phase was washed with 5% NH_4OH (3 × 20 mL) and brine. The organic phase was dried with Na_2SO_4 and concentrated under reduced pressure. The crude product was purified by flash chromatography using the indicated solvent mixture as eluent.

General procedure (B) for the amine protection. The KA^2 product was dissolved in pyridine (2 mL/mmol) and acetic anhydride (4 mL/mmol) was added dropwise to the reaction mixture at 0 °C. Then, the reaction mixture was heated to 40 °C for 16 h, followed by EtOAc addition. The organic phase was washed with 1 M HCl (3 × 20 mL), satd. Na_2CO_3 (3 × 20 mL) and brine. The organic phase was dried over Na_2SO_4 and concentrated under reduced pressure. The crude product was purified by flash chromatography using the indicated solvent mixture as eluent.

General procedure for the Pauson–Khand (C) reaction. In a dry round bottom flask under a nitrogen flow $Co_2(CO)_8$ (0.1 equiv), *N*,*N*,*N*',*N*'-tetramethylthiourea (0.6 equiv) and a solution of the enyne compound (1 equiv) were successively added in dry toluene (20 mL/mmol). Then, the reaction mixture was kept under a CO atmosphere and stirred at 70 °C until disappearance of the starting material as monitored by TLC. Then, the mixture was filtered on Celite and concentrated under reduced pressure. The crude product was purified by flash chromatography using the indicated solvent mixture as eluent.

Molecular modelling. Calculations were performed using SPARTAN Version 5.11. Conformational searches of **36** were carried out using Monte Carlo method within MMFF94 force field, and the AM1 semiempirical method [72] was used to optimize the global minimum conformer. The geometry of the most abundant minimum energy conformer was successively subjected to ab initio single point energy calculation at the 3-21G*/ HF level of quantum chemical theory.

PCA analysis. The web-based public tool ChemGPS-NP was used for PCA analysis of compounds **3**–**39**, to compare their chemical properties with those of blockbuster drugs. ChemGPS-NP can be applied for comprehensive chemical space navigation and exploration in terms of global mapping on to a consistent 8-dimensional map of structural characteristics. The first four dimensions of the ChemGPS-NP map capture 77% of data variance. Chemical compounds were positioned onto this map using interpolation in terms of PCA score prediction. SMILES codes for all compounds were retrieved using ChemBioDraw Ultra 12.0 and submitted to ChemGPS-NP for achieving the corresponding PC scores (see Supporting Informations). The PCA data were then used for the construction of PC1 vs PC2.

PMI analysis. Principal moments of inertia analysis was carried out by calculation of the lowest energy conformation of compounds **3**–**39** and block buster drugs. The conformation calculation was performed using the built-in AMMP molecular mechanics algorithm with default parameters of the VEGA ZZ molecular modelling software package v.3.0.1. Once the lowest energy conformer was calculated, the three principal moments of inertia (I_{xx}, I_{yy}, I_{zz}) and normalized principal moments of inertia, npr1 (I_{xx}/I_{zz}) and npr2 (I_{yy}/I_{zz}) were determined and plotted on a triangular graph with the vertices (0,1), (0.5,0.5) and (1,1) representing a perfect rod, disc and sphere, respectively.

Supporting Information

Supporting Information File 1

Table of reaction conditions for KA^2; experimental procedures, characterization data and copies of ^{1}H and ^{13}C NMR spectra for all new compounds; copies of NOESY-1D, gCOSY, NOESY and cartesian coordinates of compound **36**; Smiles codes, PCA and PMI data for compounds **3**–**39**.
[https://www.beilstein-journals.org/bjoc/content/supplementary/1860-5397-16-23-S1.pdf]

Funding

Financial support from MIUR (PRIN2015, cod. 20157WW5EH), Fondazione CR Firenze (cod. 2017.0721), CNR roadmap europea ESFRI:CISPIM and University of Florence are acknowledged.

ORCID® iDs

Elena Lenci - https://orcid.org/0000-0001-7408-2828
Andrea Trabocchi - https://orcid.org/0000-0003-1774-9301

References

1. Wells, J. A.; McClendon, C. L. *Nature* **2007,** *450,* 1001–1009. doi:10.1038/nature06526
2. Zheng, Y.; Tice, C. M.; Singh, S. B. *Bioorg. Med. Chem. Lett.* **2014,** *24,* 3673–3682. doi:10.1016/j.bmcl.2014.06.081
3. Griggs, S. D.; Tape, D. T.; Clarke, P. A. *Org. Biomol. Chem.* **2018,** *16,* 6620–6633. doi:10.1039/c8ob01271g
4. Aldeghi, M.; Malhotra, S.; Selwood, D. L.; Chan, A. W. E. *Chem. Biol. Drug Des.* **2014,** *83,* 450–461. doi:10.1111/cbdd.12260
5. Lovering, F.; Bikker, J.; Humblet, C. *J. Med. Chem.* **2009,** *52,* 6752–6756. doi:10.1021/jm901241e
6. Lovering, F. *Med. Chem. Commun.* **2013,** *4,* 515–519. doi:10.1039/c2md20347b
7. Zhang, F.-M.; Zhang, S.-Y.; Tu, Y.-Q. *Nat. Prod. Rep.* **2018,** *35,* 75–104. doi:10.1039/c7np00043j
8. Lenci, E.; Menchi, G.; Saldívar-Gonzalez, F. I.; Medina-Franco, J. L.; Trabocchi, A. *Org. Biomol. Chem.* **2019,** *17,* 1037–1052. doi:10.1039/c8ob02808g
9. Favre, S.; Vogel, P.; Gerber-Lemaire, S. *Molecules* **2008,** *13,* 2570–2600. doi:10.3390/molecules13102570
10. Müller, G.; Berkenbosch, T.; Benningshof, J. C. J.; Stumpfe, D.; Bajorath, J. *Chem. – Eur. J.* **2017,** *23,* 703–710. doi:10.1002/chem.201604714
11. Knox, C.; Law, V.; Jewison, T.; Liu, P.; Ly, S.; Frolkis, A.; Pon, A.; Banco, K.; Mak, C.; Neveu, V.; Djoumbou, Y.; Eisner, R.; Guo, A. C.; Wishart, D. S. *Nucleic Acids Res.* **2011,** *39,* D1035–D1041. doi:10.1093/nar/gkq1126
12. Marson, C. M. *Chem. Soc. Rev.* **2011,** *40,* 5514–5533. doi:10.1039/c1cs15119c
13. Schreiber, S. L. *Science* **2000,** *287,* 1964–1969. doi:10.1126/science.287.5460.1964
14. Trabocchi, A., Ed. *Diversity-Oriented Synthesis: Basics and Applications in Organic Synthesis, Drug Discovery, and Chemical Biology;* John Wiley and Sons: Hoboken, NJ, U.S.A., 2013. doi:10.1002/9781118618110
15. Spring, D. R. *Org. Biomol. Chem.* **2003,** *1,* 3867–3870. doi:10.1039/b310752n
16. Pavlinov, I.; Gerlach, E. M.; Aldrich, L. N. *Org. Biomol. Chem.* **2019,** *17,* 1608–1623. doi:10.1039/c8ob02327a
17. Burke, M. D.; Schreiber, S. L. *Angew. Chem., Int. Ed.* **2004,** *43,* 46–58. doi:10.1002/anie.200300626
18. Yi, S.; Varun, B. V.; Choi, Y.; Park, S. B. *Front. Chem. (Lausanne, Switz.)* **2018,** *6,* 507. doi:10.3389/fchem.2018.00507
19. De Moliner, F.; Banfi, L.; Riva, R.; Basso, A. *Comb. Chem. High Throughput Screening* **2011,** *14,* 782–810. doi:10.2174/138620711796957099
20. Eckert, H. *Molecules* **2012,** *17,* 1074–1102. doi:10.3390/molecules17011074
21. Biggs-Houck, J. E.; Younai, A.; Shaw, J. T. *Curr. Opin. Chem. Biol.* **2010,** *14,* 371–382. doi:10.1016/j.cbpa.2010.03.003
22. Sunderhaus, J. D.; Martin, S. F. *Chem. – Eur. J.* **2009,** *15,* 1300–1308. doi:10.1002/chem.200802140
23. Flagstad, T.; Hansen, M. R.; Le Quement, S. T.; Givskov, M.; Nielsen, T. E. *ACS Comb. Sci.* **2015,** *17,* 19–23. doi:10.1021/co500091f
24. Muncipinto, G.; Kaya, T.; Wilson, J. A.; Kumagai, N.; Clemons, P. A.; Schreiber, S. L. *Org. Lett.* **2010,** *12,* 5230–5233. doi:10.1021/ol102266j
25. Schreiber, S. L. *Nature* **2009,** *457,* 153–154. doi:10.1038/457153a
26. García-Cuadrado, D.; Barluenga, S.; Winssinger, N. *Chem. Commun.* **2008,** 4619–4621. doi:10.1039/b807869f
27. Nielsen, T. E.; Schreiber, S. L. *Angew. Chem., Int. Ed.* **2008,** *47,* 48–56. doi:10.1002/anie.200703073
28. Kumagai, N.; Muncipinto, G.; Schreiber, S. L. *Angew. Chem., Int. Ed.* **2006,** *45,* 3635–3638. doi:10.1002/anie.200600497
29. Lenci, E.; Rossi, A.; Menchi, G.; Trabocchi, A. *Org. Biomol. Chem.* **2017,** *15,* 9710–9717. doi:10.1039/c7ob02454a
30. Moni, L.; De Moliner, F.; Garbarino, S.; Saupe, J.; Mang, C.; Basso, A. *Front. Chem. (Lausanne, Switz.)* **2018,** *6,* 369. doi:10.3389/fchem.2018.00369
31. Vázquez-Vera, Ó.; Sánchez-Badillo, J. S.; Islas-Jácome, A.; Rentería-Gómez, M. A.; Pharande, S. G.; Cortes-García, C. J.; Rincón-Guevara, M. A.; Ibarra, I. A.; Gámez-Montaño, R.; González-Zamora, E. *Org. Biomol. Chem.* **2017,** *15,* 2363–2369. doi:10.1039/c6ob02572b

32. García-González, M. C.; Hernández-Vázquez, E.; Gordillo-Cruz, R. E.; Miranda, L. D. *Chem. Commun.* **2015,** *51,* 11669–11672. doi:10.1039/c5cc02927a
33. Moni, L.; Banfi, L.; Basso, A.; Brambilla, A.; Riva, R. *Beilstein J. Org. Chem.* **2014,** *10,* 209–212. doi:10.3762/bjoc.10.16
34. Tan, W.; Zhu, X.-T.; Zhang, S.; Xing, G.-J.; Zhu, R.-Y.; Shi, F. *RSC Adv.* **2013,** *3,* 10875–10886. doi:10.1039/c3ra40874d
35. Zhuang, Q.-Y.; Wang, X.; Gao, Y.; Shi, F.; Jiang, B.; Tu, S.-J. *ACS Comb. Sci.* **2011,** *13,* 84–88. doi:10.1021/co100034v
36. Pereshivko, O. P.; Peshkov, V. A.; Ermolat'ev, D. S.; Van Hove, S.; Van Hecke, K.; Van Meervelt, L.; Van der Eycken, E. V. *Synthesis* **2011,** 1587–1594. doi:10.1055/s-0030-1260012
37. Innocenti, R.; Menchi, G.; Trabocchi, A. *Synlett* **2018,** 820–824. doi:10.1055/s-0036-1591521
38. Simeonov, S. P.; Nunes, J. P. M.; Guerra, K.; Kurteva, V. B.; Afonso, C. A. M. *Chem. Rev.* **2016,** *116,* 5744–5893. doi:10.1021/cr500504w
39. Ricker, J. D.; Geary, L. M. *Top. Catal.* **2017,** *60,* 609–619. doi:10.1007/s11244-017-0741-0
40. Shibata, T.; Toshida, N.; Yamasaki, M.; Maekawa, S.; Takagi, K. *Tetrahedron* **2005,** *61,* 9974–9979. doi:10.1016/j.tet.2005.08.016
41. Pérez-Castells, J. *Top. Organomet. Chem.* **2006,** *19,* 207–257. doi:10.1007/3418_008
42. Rosillo, M.; Arnáiz, E.; Abdi, D.; Blanco-Urgoiti, J.; Domínguez, G.; Pérez-Castells, J. *Eur. J. Org. Chem.* **2008,** 3917–3927. doi:10.1002/ejoc.200800332
43. Choi, S. Y.; Lee, S. I.; Park, K. H.; Chung, Y. K. *Synlett* **2007,** 1857–1862. doi:10.1055/s-2007-984511
44. Olier, C.; Azzi, N.; Gil, G.; Gastaldi, S.; Bertrand, M. P. *J. Org. Chem.* **2008,** *73,* 8469–8473. doi:10.1021/jo801668b
45. Lenci, E.; Innocenti, R.; Menchi, G.; Trabocchi, A. *Front. Chem. (Lausanne, Switz.)* **2018,** *6,* 522. doi:10.3389/fchem.2018.00522
46. Lenci, E.; Menchi, G.; Guarna, A.; Trabocchi, A. *J. Org. Chem.* **2015,** *80,* 2182–2191. doi:10.1021/jo502701c
47. Ciofi, L.; Morvillo, M.; Sladojevich, F.; Guarna, A.; Trabocchi, A. *Tetrahedron Lett.* **2010,** *51,* 6282–6285. doi:10.1016/j.tetlet.2010.09.103
48. Pereshivko, O. P.; Peshkov, V. A.; Van der Eycken, E. V. *Org. Lett.* **2010,** *12,* 2638–2641. doi:10.1021/ol1008312
49. Areces, P.; Durán, M. Á.; Plumet, J.; Hursthouse, M. B.; Light, M. E. *J. Org. Chem.* **2002,** *67,* 3506–3509. doi:10.1021/jo011129+
50. Jeong, N.; Yoo, S.-e.; Lee, S. J.; Lee, S. H.; Chung, Y. K. *Tetrahedron Lett.* **1991,** *32,* 2137–2140. doi:10.1016/s0040-4039(00)71257-3
51. Oe, K.; Ohfune, Y.; Shinada, T. *Org. Lett.* **2014,** *16,* 2550–2553. doi:10.1021/ol5009526
52. Mollica, A.; Costante, R.; Stefanucci, A.; Novellino, E. *Protein Pept. Lett.* **2015,** *22,* 696–711. doi:10.2174/0929866522666150206170716
53. Larhed, M.; Hallberg, A. *Drug Discovery Today* **2001,** *6,* 406–416. doi:10.1016/s1359-6446(01)01735-4
54. Cheng, M.; Zhang, Q.; Hu, X.-Y.; Li, B.-G.; Ji, J.-X.; Chan, A. S. C. *Adv. Synth. Catal.* **2011,** *353,* 1274–1278. doi:10.1002/adsc.201000914
55. Thede, K.; Diedrichs, N.; Ragot, J. P. *Org. Lett.* **2004,** *6,* 4595–4597. doi:10.1021/ol0479904
56. Imamoto, T.; Takiyama, N.; Nakamura, K.; Hatajima, T.; Kamiya, Y. *J. Am. Chem. Soc.* **1989,** *111,* 4392–4398. doi:10.1021/ja00194a037
57. Whitby, R. J.; Dixon, S.; Maloney, P. R.; Delerive, P.; Goodwin, B. J.; Parks, D. J.; Willson, T. M. *J. Med. Chem.* **2006,** *49,* 6652–6655. doi:10.1021/jm060990k
58. Jung, M. E.; Dwight, T. A.; Vigant, F.; Østergaard, M. E.; Swayze, E. E.; Seth, P. P. *Angew. Chem., Int. Ed.* **2014,** *53,* 9893–9897. doi:10.1002/anie.201405283
59. Inokuchi, T.; Okano, M.; Miyamoto, T.; Madon, H. B.; Takagi, M. *Synlett* **2000,** 1549–1552. doi:10.1055/s-2000-7940
60. Kawanaka, Y.; Kobayashi, K.; Kusuda, S.; Tatsumi, T.; Murota, M.; Nishiyama, T.; Hisaichi, K.; Fujii, A.; Hirai, K.; Nishizaki, M.; Naka, M.; Komeno, M.; Nakai, H.; Toda, M. *Bioorg. Med. Chem.* **2003,** *11,* 689–702. doi:10.1016/s0968-0896(02)00540-0
61. Dobson, C. M. *Nature* **2004,** *432,* 824–828. doi:10.1038/nature03192
62. Larsson, J.; Gottfries, J.; Muresan, S.; Backlund, A. *J. Nat. Prod.* **2007,** *70,* 789–794. doi:10.1021/np070002y
63. Rosén, J.; Lövgren, A.; Kogej, T.; Muresan, S.; Gottfries, J.; Backlund, A. *J. Comput.-Aided Mol. Des.* **2009,** *23,* 253–259. doi:10.1007/s10822-008-9255-y
64. ChemGPS-NP website. http://chemgps.bmc.uu.se/ (accessed Jan 10, 2020).
65. Oprea, T. I.; Gottfries, J. *J. Comb. Chem.* **2001,** *3,* 157–166. doi:10.1021/cc0000388
66. Kopp, F.; Stratton, C. F.; Akella, L. B.; Tan, D. S. *Nat. Chem. Biol.* **2012,** *8,* 358–365. doi:10.1038/nchembio.911
67. Bauer, R. A.; Wurst, J. M.; Tan, D. S. *Curr. Opin. Chem. Biol.* **2010,** *14,* 308–314. doi:10.1016/j.cbpa.2010.02.001
68. Sauer, W. H. B.; Schwarz, M. K. *J. Chem. Inf. Comput. Sci.* **2003,** *43,* 987–1003. doi:10.1021/ci025599w
69. Flagstad, T.; Min, G.; Bonnet, K.; Morgentin, R.; Roche, D.; Clausen, M. H.; Nielsen, T. E. *Org. Biomol. Chem.* **2016,** *14,* 4943–4946. doi:10.1039/c6ob00961a
70. Stotani, S.; Lorenz, C.; Winkler, M.; Medda, F.; Picazo, E.; Ortega Martinez, R.; Karawajczyk, A.; Sanchez-Quesada, J.; Giordanetto, F. *ACS Comb. Sci.* **2016,** *18,* 330–336. doi:10.1021/acscombsci.6b00005
71. Clemons, P. A.; Bodycombe, N. E.; Carrinski, H. A.; Wilson, J. A.; Shamji, A. F.; Wagner, B. K.; Koehler, A. N.; Schreiber, S. L. *Proc. Natl. Acad. Sci. U. S. A.* **2010,** *107,* 18787–18792. doi:10.1073/pnas.1012741107
72. Govender, K.; Gao, J.; Naidoo, K. J. *J. Chem. Theory Comput.* **2014,** *10,* 4694–4707. doi:10.1021/ct500372s

License and Terms

BEILSTEIN JOURNAL OF ORGANIC CHEMISTRY

Copper-catalyzed enantioselective conjugate addition of organometallic reagents to challenging Michael acceptors

Delphine Pichon, Jennifer Morvan, Christophe Crévisy and Marc Mauduit*

Review

Open Access

Address:
Université de Rennes, Ecole Nationale Supérieure de Chimie de Rennes, CNRS, ISCR – UMR 6226, F-35000 Rennes, France

Email:
Marc Mauduit* - marc.mauduit@ensc-rennes.fr

* Corresponding author

Keywords:
acylimidazole; *N*-acyloxazolidinone; *N*-acylpyrrole; *N*-acylpyrrolidinone; aldehyde; amide; copper catalysis; electron-deficient alkenes; enantioselective conjugate addition; Michael acceptor; thioester

Beilstein J. Org. Chem. **2020,** *16,* 212–232.
doi:10.3762/bjoc.16.24

Received: 22 November 2019
Accepted: 04 February 2020
Published: 17 February 2020

This article is part of the thematic issue "Copper-catalyzed reactions for organic synthesis".

Guest Editor: G. Evano

Abstract

The copper-catalyzed enantioselective conjugate addition (ECA) of organometallic nucleophiles to electron-deficient alkenes (Michael acceptors) represents an efficient and attractive methodology for providing a wide range of relevant chiral molecules. In order to increase the attractiveness of this useful catalytic transformation, some Michael acceptors bearing challenging electron-deficient functions (i.e., aldehydes, thioesters, acylimidazoles, *N*-acyloxazolidinones, *N*-acylpyrrolidinones, amides, *N*-acylpyrroles) were recently investigated. Remarkably, only a few chiral copper-based catalytic systems have successfully achieved the conjugate addition of different organometallic reagents to these challenging Michael acceptors, with excellent regio- and enantioselectivity. Furthermore, thanks to their easy derivatization, the resulting chiral conjugated products could be converted into various natural products. The aim of this tutorial review is to summarize recent advances accomplished in this stimulating field.

Introduction

Generating high molecular complexity and controlling multiple stereogenic centers in a minimum number of steps is nowadays one of the most important challenges in organic chemistry for the synthesis of complex chiral molecules. The transition metal (TM)-catalyzed enantioselective conjugate addition (ECA) of nucleophiles to electron-deficient alkenes (Michael acceptors) is one of the most relevant and versatile methods to achieve this goal [1-4]. Among the plethora of metals studied, copper-based catalytic systems proved to be highly efficient for the conjugate addition of various organometallic reagents, such as diorganozinc, triorganoaluminium, and Grignard reagents to Michael acceptors. In that respect, since the pioneering example reported by Alexakis and co-workers in 1993 [5], a wide range of cyclic and acyclic electron-deficient alkenes, such as α,β-unsaturated ketones, esters, nitriles, sulfones, or nitroolefines, was intensively studied, leading to the expected 1,4-products in excellent yields and remarkable enantioselectivities. More recently, tremendous breakthroughs were achieved in this

field, notably by the formation of all-carbon quaternary chiral centers [6] and the challenging 1,6-, 1,8-, or 1,10-selective addition to cyclic or aliphatic polyenic substrates [7-9]. Furthermore, Cu ECA transformations were also successfully applied to the synthesis of natural products [10]. Nevertheless, it is worth to underline that the choice of the electron-withdrawing group (EWG) on the Michael substrates appears not so simple. First, the hardness of the involved organometallic reagents has to be considered in order to overcome or limit undesirable side reactions. Although the main role of copper is to form a transient organocuprate reactive species with the hard nucleophiles to avoid the formation of the nondesired 1,2-product, some Grignard or aluminium reagents remain too reactive and incompatible with some electron-withdrawing functions. In contrast, some organometallic reagents, such as dimethylzinc, are poorly reactive and require a higher electrophilicity of the Michael acceptors to provide the desired conjugated products. Second, in order to be attractive for the total synthesis of relevant molecules, the involved EWG should preferably allow readily applicable and practicable postfunctionalizations [10].

Among the plethora of studied Michael acceptors, α,β-unsaturated aldehydes, thioesters, acylimidazoles, *N*-acyloxazolidinones, *N*-acylpyrrolidinones, amides, and *N*-acylpyrroles have been scarcely investigated in Cu ECA despite their usefulness for postfunctionalizations. This tutorial review aims to describe the early examples and recent advances in copper-catalyzed asymmetric conjugate additions of dialkylzinc, Grignard, or trialkylaluminium reagents toward those challenging substrates and their fruitful application in the total synthesis of natural products.

Review

Enantioselective conjugate addition to challenging Michael acceptors

Copper-catalyzed ECA to α,β-unsaturated aldehydes

Nowadays, β-substituted enals represent probably the most challenging Michael acceptors in the copper-catalyzed ECA of organometallic reagents [11-13]. This challenge is reinforced by the fact that the resulting chiral β-functionalized aldehydes are considered as an important motif that is ubiquitous in numerous natural molecules. However, as depicted in Scheme 1, due to their stronger reactivity than that of usual esters or ketones, a competitive 1,2-addition to the carbonyl function of enals could occur, leading to the corresponding alcohol as a byproduct. Moreover, even if the 1,4-addition is favored, thanks to the copper/ligand catalytic species, the resulting metallic enolate intermediate can also react with the starting material to form the aldol byproduct, significantly altering the yield of the expected 1,4-product (Scheme 1).

The first successful copper-catalyzed ECA to α,β-unsaturated aldehydes with organozinc and Grignard reagents was reported by Alexakis and co-workers in 2010 [14]. After screening various chiral phosphine-based ligands, the combinations of either phosphoramidite **L1** with $Cu(OTf)_2$, or (*R*)-BINAP (**L2**) with copper thiophenecarboxylate (CuTC) appeared to be the most efficient for the addition of Et_2Zn to a variety of cyclic and acyclic aldehydes **1**. High 1,4-regioselectivities and promising stereoselectivities ranging from 27 to 90% ee were achieved (Scheme 2a). It is noteworthy that the addition of dimethylzinc was also successfully achieved, as the desired 1,4-methylated

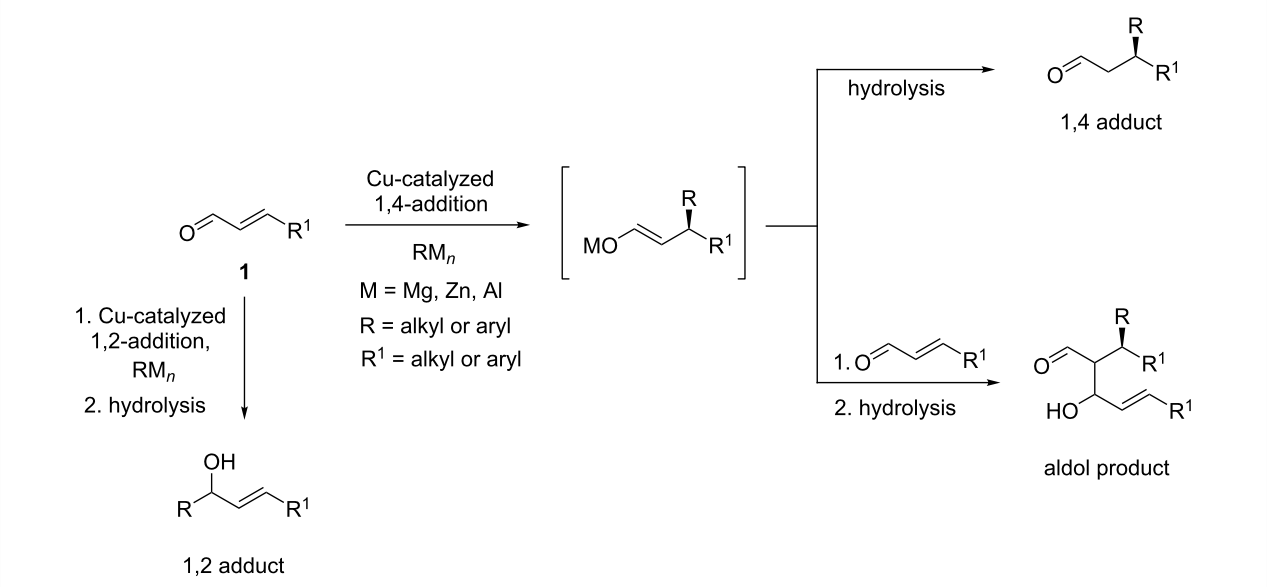

Scheme 1: Competitive side reactions in the Cu ECA of organometallic reagents to α,β-unsaturated aldehydes.

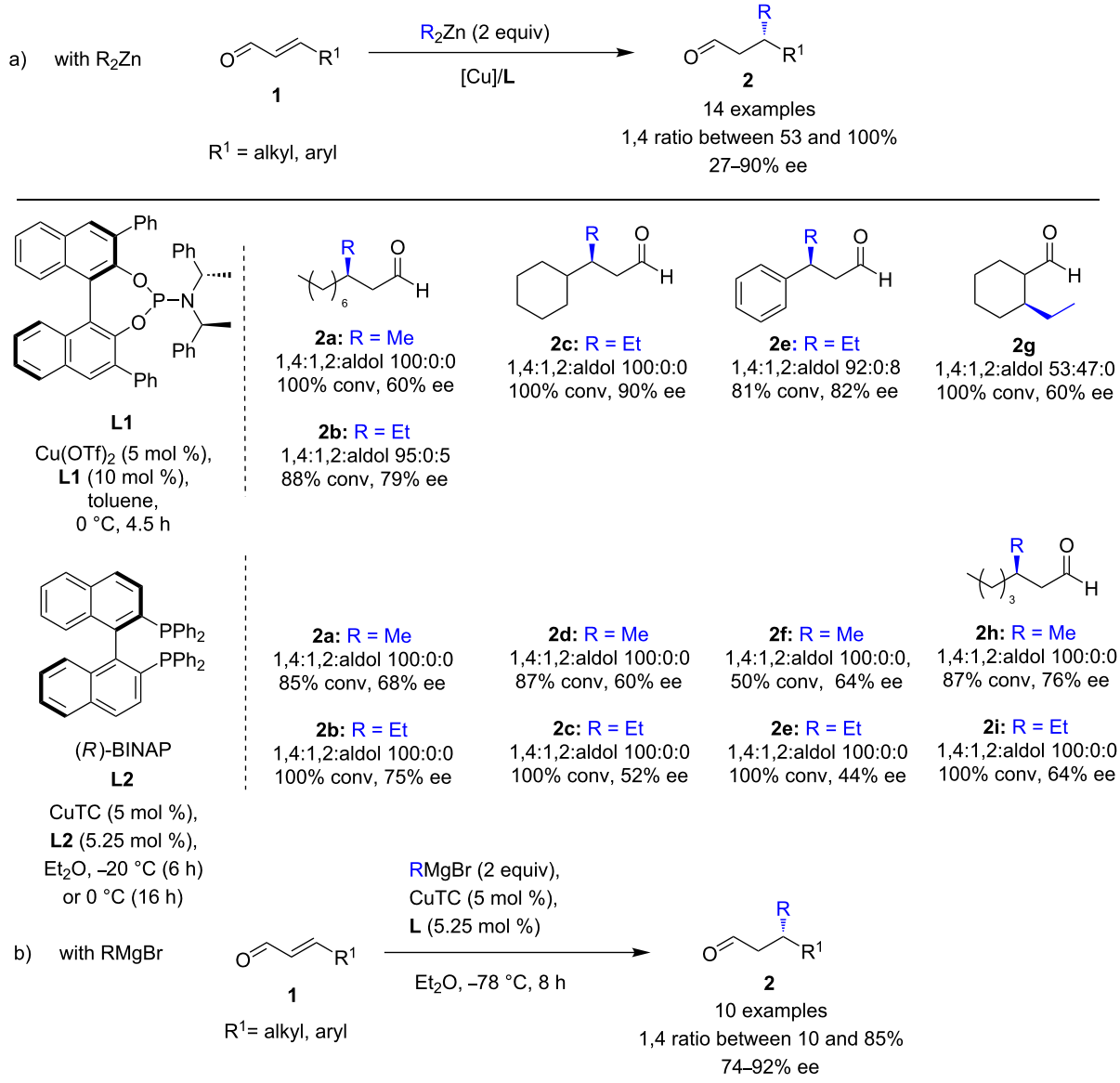

Scheme 2: Cu-catalyzed ECA of α,β-unsaturated aldehydes with phosphoramidite- (a) and phosphine-based ligands (b).

products were exclusively formed in moderate to good yields, with ee values of up to 76%. When the conjugate addition was performed with Grignard reagents, significant amounts of 1,2-products and enols were formed, despite the use of cryogenic conditions. (*R*)-BINAP (**L2**) gave the best regio- and enantioselectivity, with 62% of the 1,4-product and 89% ee with EtMgBr (Scheme 2b). To overcome the low regioselectivity, the authors took into account previous works showing that the 1,4-regioselectivity in the addition of cuprates to enals could be improved in the presence of a slight excess of TMSCl [15-19]. Indeed, using TMSCl in combination with (*R*)-TolBINAP (**L3**), a promising 85% regioselectivity was observed, without altering the enantioselectivity (90% ee), whereas only 32% of the desired 1,4- product was obtained without TMSCl [20]. With those optimized conditions, various enals and Grignard reagents were screened. Nevertheless, despite the presence of TMSCl, the 1,4:1,2 ratio varied significantly (from 85:15 to 10:90), while the level of enantioselectivity remained relatively good, reaching up to 90%.

Following this, Alexakis and Quintard invented an efficient stepwise one-pot copper-catalyzed asymmetric ECA/organocatalyzed α-substitution of enals [21]. By using (*R*)-BINAP (**L2**)/CuTC in combination with chiral prolinol derivatives **L4–6** as organocatalysts, various α,β-functionalized aldehydes were synthesized in good isolated yields (57–74%) and remarkable enantioselectivity (99%) from diethylzinc or dimethylzinc as nucleophiles and vinyl sulfones as electrophiles (Scheme 3). Of note,

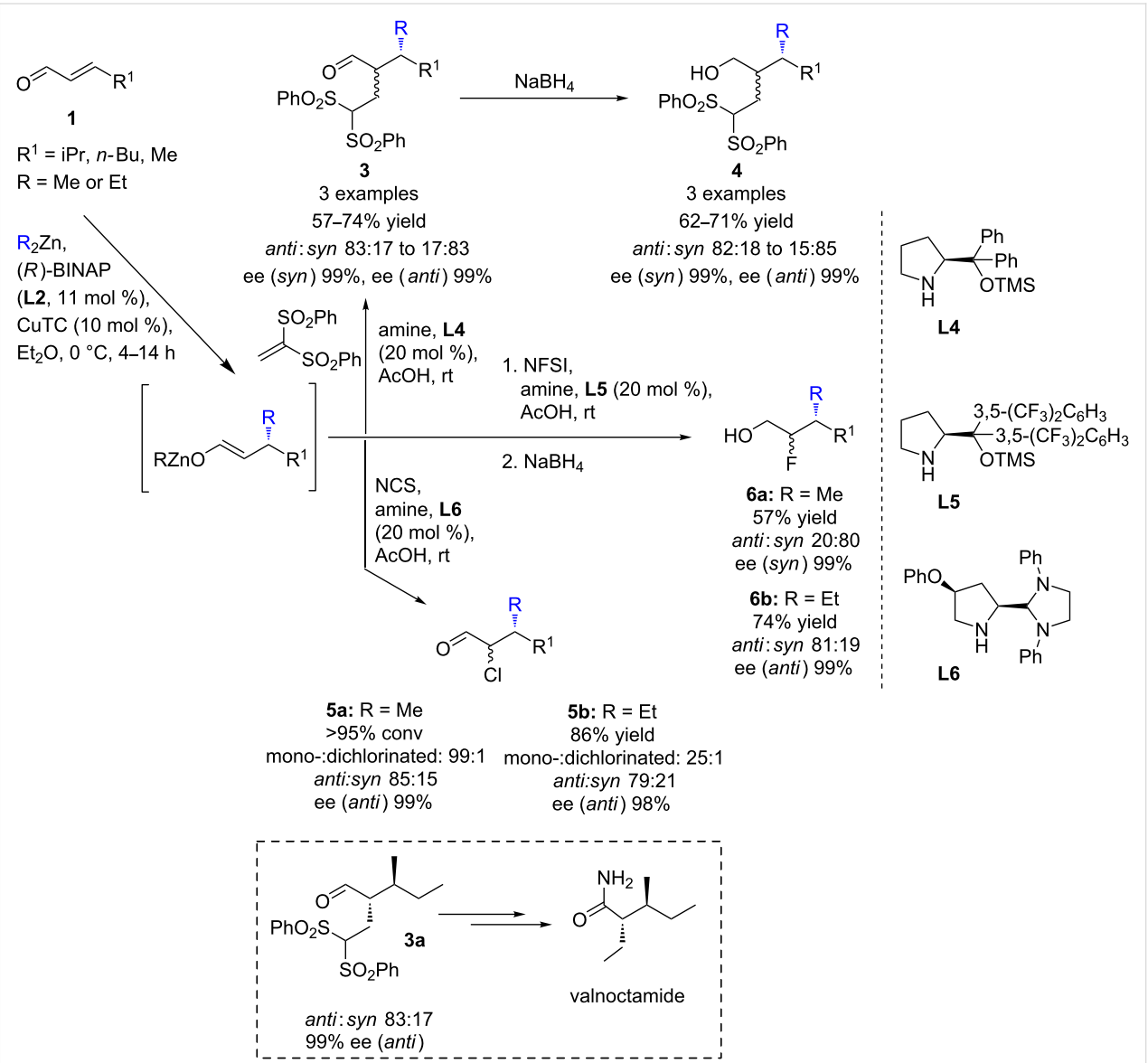

Scheme 3: One-pot Cu-catalyzed ECA/organocatalyzed α-substitution of enals.

both the *anti*- and the *syn*-product could be predominantly formed (with a *anti*:*syn* ratio from 83:17 to 15:85), and no diastereocontrol occurred in the absence of the organocatalyst. Interestingly, this simple protocol was successfully applied to the enantioselective synthesis of valnoctamide, a commercialized mild tranquilizer. Finally, this methodology was extended to the sequential Michael/halogenation reaction using NFSI or NCS as electrophiles, with similar efficiency.

Similarly, a cocatalyzed enantioselective β-functionalization of enals was developed by Córdova, Ibrahem, and co-workers in 2011 (Scheme 4) [22]. By mixing high catalytic loadings of $Cu(OTf)_2$, PPh_3, and TMS-protected diarylprolinol **L4**, the conjugate addition of Et_2Zn or Me_2Zn to various β-substituted enals proved to be highly enantioselective (ee up to 96%), but moderate to good 1,4:1,2 ratios were obtained (51:49 to 97:3). Of note, chiral phosphines were also screened, but without any improvement of selectivity. Furthermore, this methodology was then efficiently applied to the total synthesis of several bisabolane sesquiterpenes, which exhibited anticancer and antimicrobial activities or are employed as ingredients in perfumes and cosmetics (Scheme 4).

The last report on ECAs of enals [23] was disclosed in 2016 by Alexakis and co-workers [24]. They achieved to develop three sets of optimized conditions for the CuTC-catalyzed conjugate addition of diorganozinc compounds, Grignard, and triorganoaluminium reagents to α,β-unsaturated aldehydes (Scheme 5). With diethyl- and dimethylzinc, and in the presence of the most efficient chiral ligand (*R*)-H_8-BINAP (**L7**), moderate to excellent regioselectivities (1,4:1,2 ratios up to 100:0) were observed, and the desired 1,4-products were formed with remarkable enantioselectivities (58 to 96% ee). With Grignard reagents, the best ee values (45 to 90%) were obtained with (*R*)-TolBINAP (**L3**), but despite the presence of TMSCl, the regioselectivities remained modest, with a highest 1,4:1,2 ratio of 85:15. At last, (*R*)-SEGPHOS (**L8**) promoted the conjugate addition of Me_3Al to cinnamaldehyde, with a remarkable 96% ee and a moderate 1,4:1,2 ratio. However, albeit no trace of aldol byproduct was detected, the reaction was incomplete (66% conversion). The use of TMSCl improved the conversion to 88%, but this was detrimental to the enantiocontrol (8% ee). These methodologies were applied to the straightforward synthesis of valuable (*R*)-citronellal and (*S*)-Florhydral®, which were obtained with excellent enantioselectivities (87 and 96%,

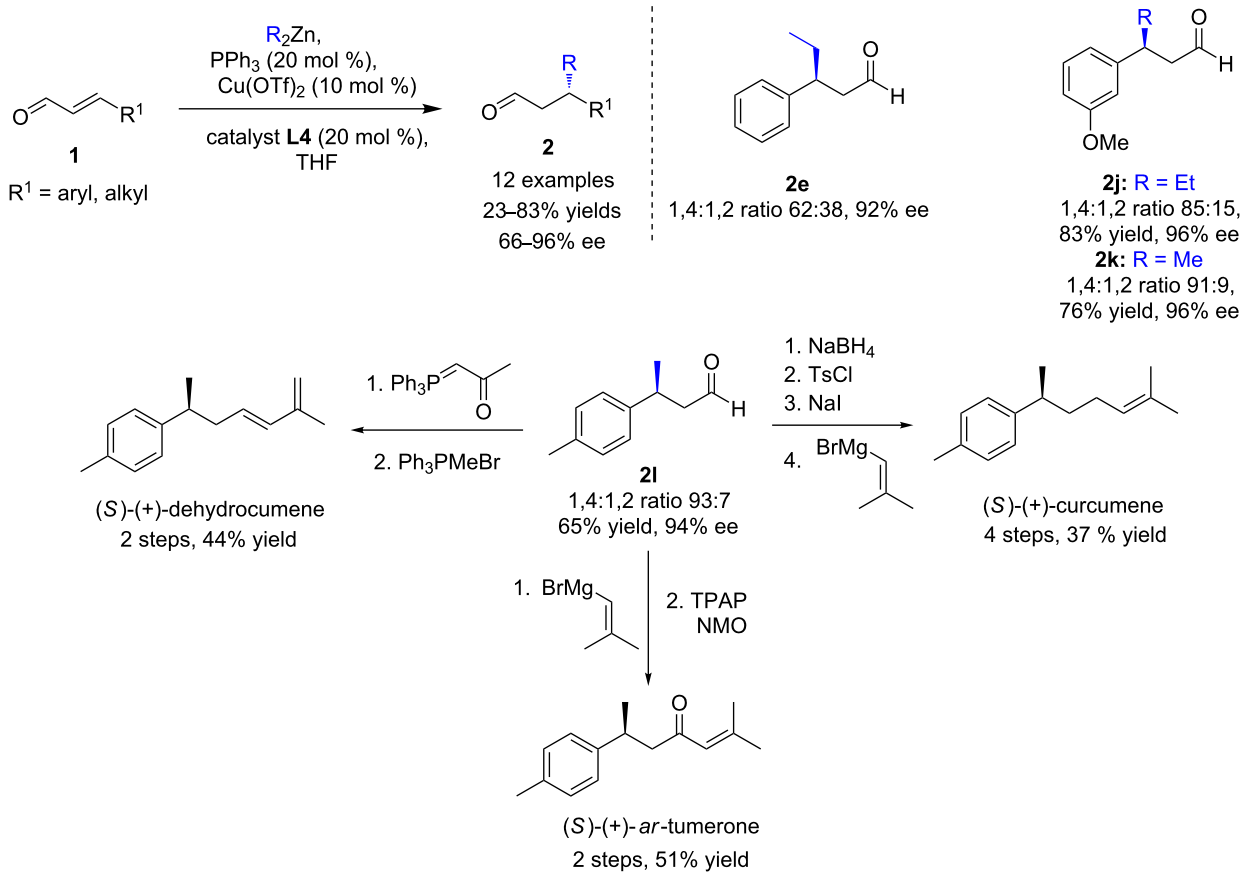

Scheme 4: Combination of copper and amino catalysis for enantioselective β-functionalizations of enals.

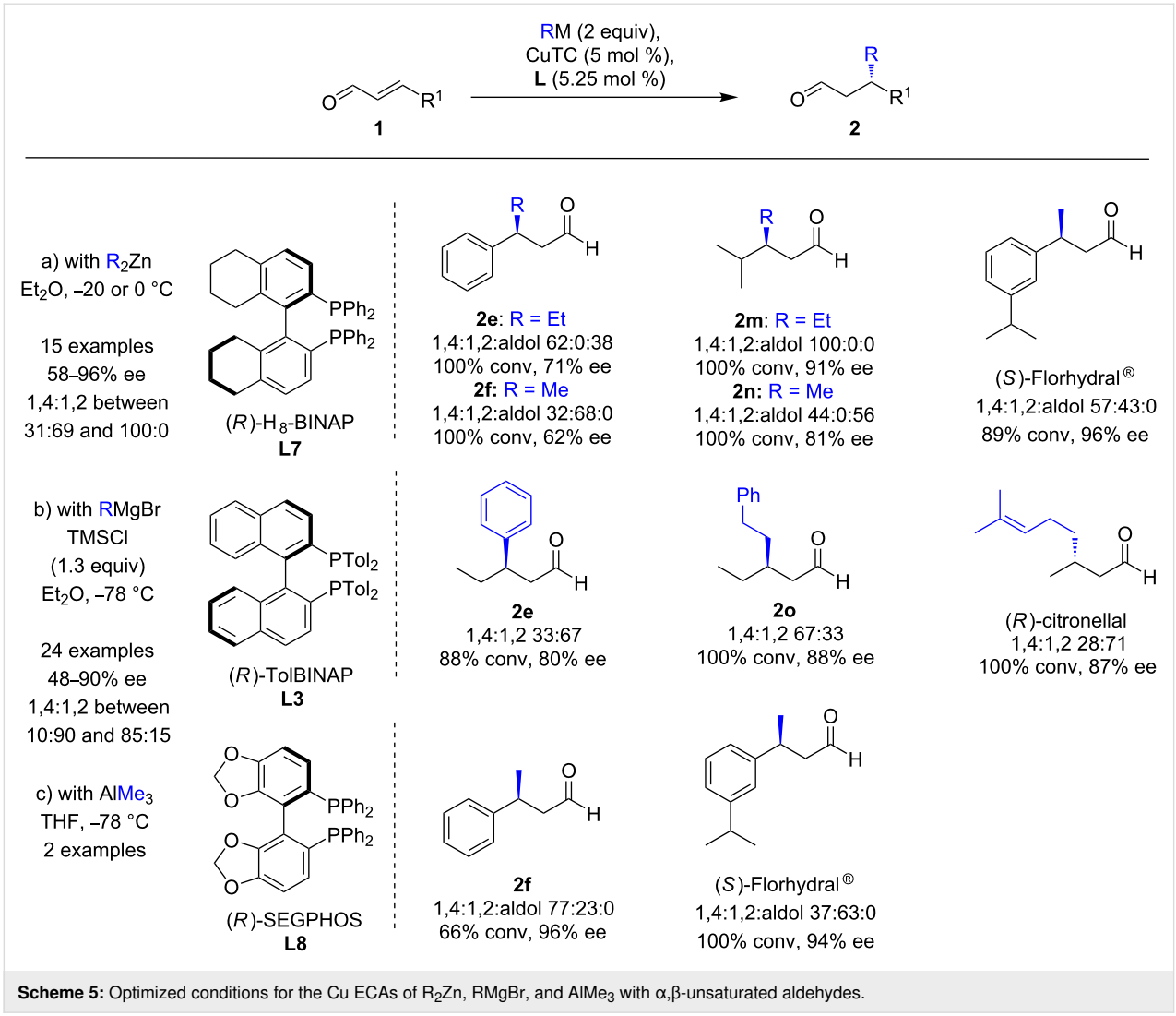

Scheme 5: Optimized conditions for the Cu ECAs of R_2Zn, RMgBr, and $AlMe_3$ with α,β-unsaturated aldehydes.

respectively). However, moderate to significant amounts of the 1,2-products were also formed.

As highlighted by these pioneering works, the direct copper-catalyzed conjugate addition of organometallic reagents to α,β-unsaturated aldehydes still remains an important challenge. Albeit some promising excellent regioselectivities and high enantioselectivities were achieved, this was often limited to a few organometallic reagents/enal substrates, as mentioned above. In that respect, indirect pathways were developed as alternative strategies, involving electron-deficient functions that can subsequently easily be converted to aldehydes.

α,β-Unsaturated thioesters

In 2005, Feringa, Minnaard, and co-workers were the first to report the ECA of Grignard reagents to α,β-unsaturated thioesters [25]. Advantageously, the latter were also readily accessible but significantly more reactive than α,β-unsaturated esters. Indeed, the thioester fragments featured a reduced electron delocalization compared to oxoesters, which resulted in a higher reactivity in conjugate additions, even with the less reactive MeMgBr. As depicted in Scheme 6, excellent yields and remarkable enantioselectivities (up to 96%) were obtained in ECAs of linear aliphatic Grignard reagents (in particular MeMgBr) to a wide range of substrates, catalyzed by CuBr·SMe_2/(*R*,*S*)-Josiphos (**L9**).

However, the catalytic system was poorly selective toward sterically hindered organomagnesium nucleophiles (15–25% ee). The synthetic versatility of the thioester function was illustrated in the synthesis of (−)-lardolure (26% overall yield over 12 steps) via a relevant diastereoselective and enantioselective iterative route, affording the highly desirable deoxypropionate moiety in high 97% de. The Josiphos (**L9**)/CuBr·SMe_2 catalytic system was also efficient to promote the ECAs of MeMgBr to the less reactive aromatic α,β-unsaturated thioesters (ee

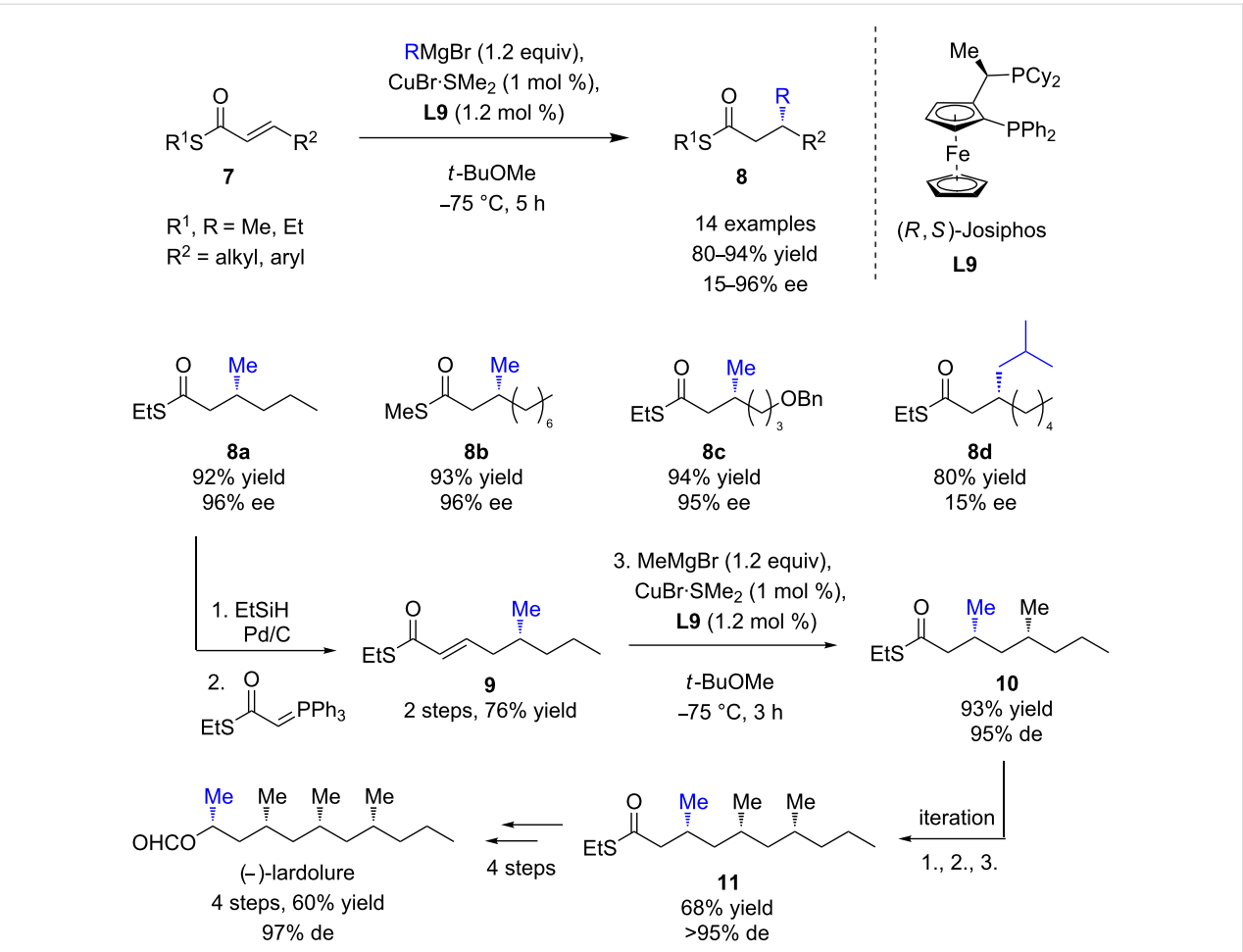

Scheme 6: CuECA of Grignard reagents to α,β-unsaturated thioesters and their application in the asymmetric total synthesis of (–)-lardolure.

values up to >99%) [26]. In order to extend their methodology to less reactive bulky Grignard reagents and/or substrates, a catalytic system of wider application, involving (*S*)-TolBINAP (*ent*-**L3**)/CuI was developed by the same authors [26]. The expected 1,4-products were isolated in good yields and moderate to excellent enantioselectivities (up to 99% ee, Scheme 7), depending on the steric hindrance of the reagent. Unfortunately, the addition of PhMgBr remained unsuccessful. This powerful catalytic protocol was illustrated by Bates and Sridhar in the enantioselective total synthesis of (−)-mintlactone [27]. The key step, furnishing the β-methylated thioester **8j**, was accomplished in a good yield of 84% and a high ee of 94% (Scheme 7).

In 2008, Feringa and Minnaard evaluated the ECA of Grignard reagents to γ-substituted α,β-unsaturated thioesters that could lead to vicinal (i.e., 1,2-relation) dialkyl arrays, a highly desirable moiety that is ubiquitous in a wide range of natural products [28]. As depicted in Scheme 8, TolBINAP (**L3**)/CuI, which appeared to be a better catalytic system than Josiphos (**L9**)/CuBr·SMe$_2$, afforded either the *syn* or *anti* 1,4 product **13** in good isolated yields and excellent diastereoselectivities and enantioselectivities (dr up to 99:1 and ee up to >99.5). The value of the protocol was successfully illustrated through the enantioselective total syntheses of (−)-lasiol and (+)-faranal, two useful natural pheromones.

Shortly after, Feringa, Minnaard, and co-workers demonstrated the efficiency of (*S*,*R*)-reversed Josiphos (**L10**) in the copper-catalyzed 1,6-ECA of MeMgBr to α,β,γ,δ-bisunsaturated thioesters [29,30]. The expected 1,6-products were selectively formed (the 1,6:1,4 ratio ranged from 85:15 to 99:1) in high yields (78–88%) and good enantioselectivities (82–89%, Scheme 9). It is worth to note that this protocol failed in the case of linear dienoates [29]. Interestingly, after a subsequent reconjugation step in the presence of DBU, the resulting enantioenriched γ-methylated α,β-unsaturated thioester **18a** was subsequently reacted in a 1,4-ECA reaction catalyzed by Josiphos (**L9**)/CuBr·SMe$_2$. Using both enantiomers of the chiral ligand, either *anti*- or *syn*-1,3-deoxypropionate units were pro-

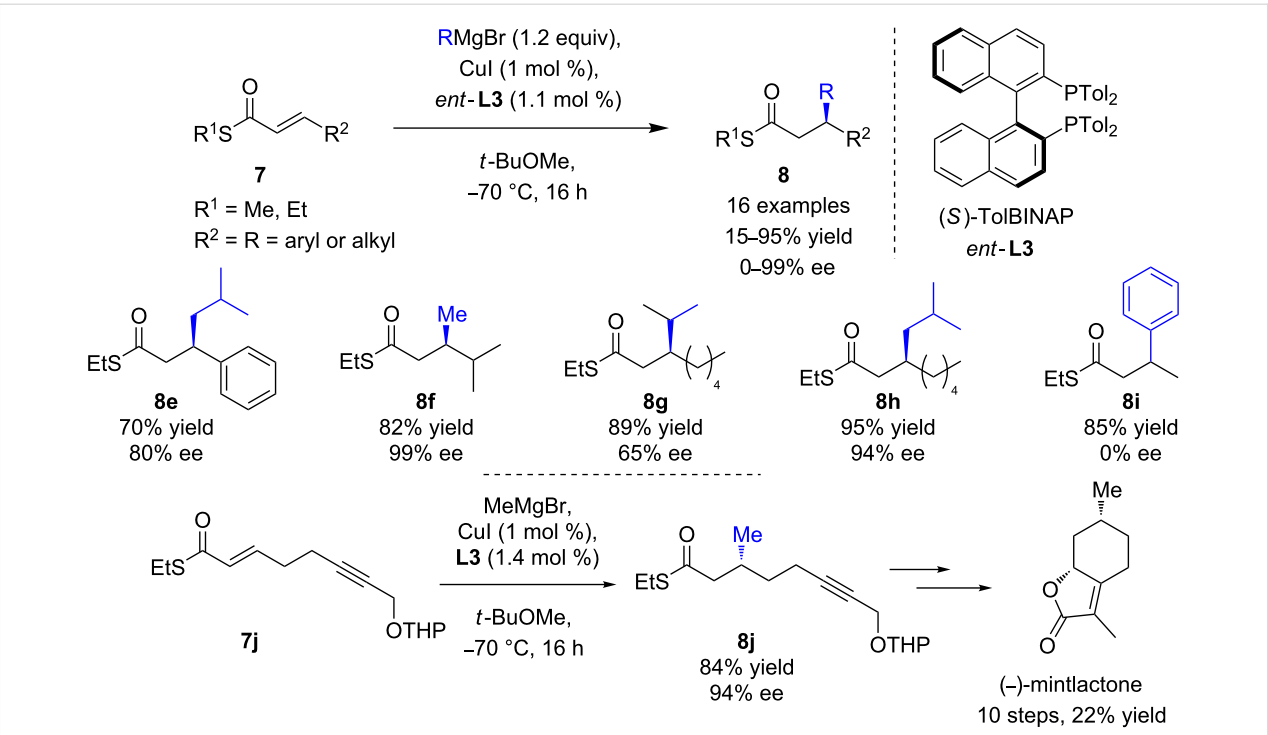

Scheme 7: Improved Cu ECA of Grignard reagents to α,β-unsaturated thioesters, and their application in the asymmetric total synthesis of (−)-mintlactone.

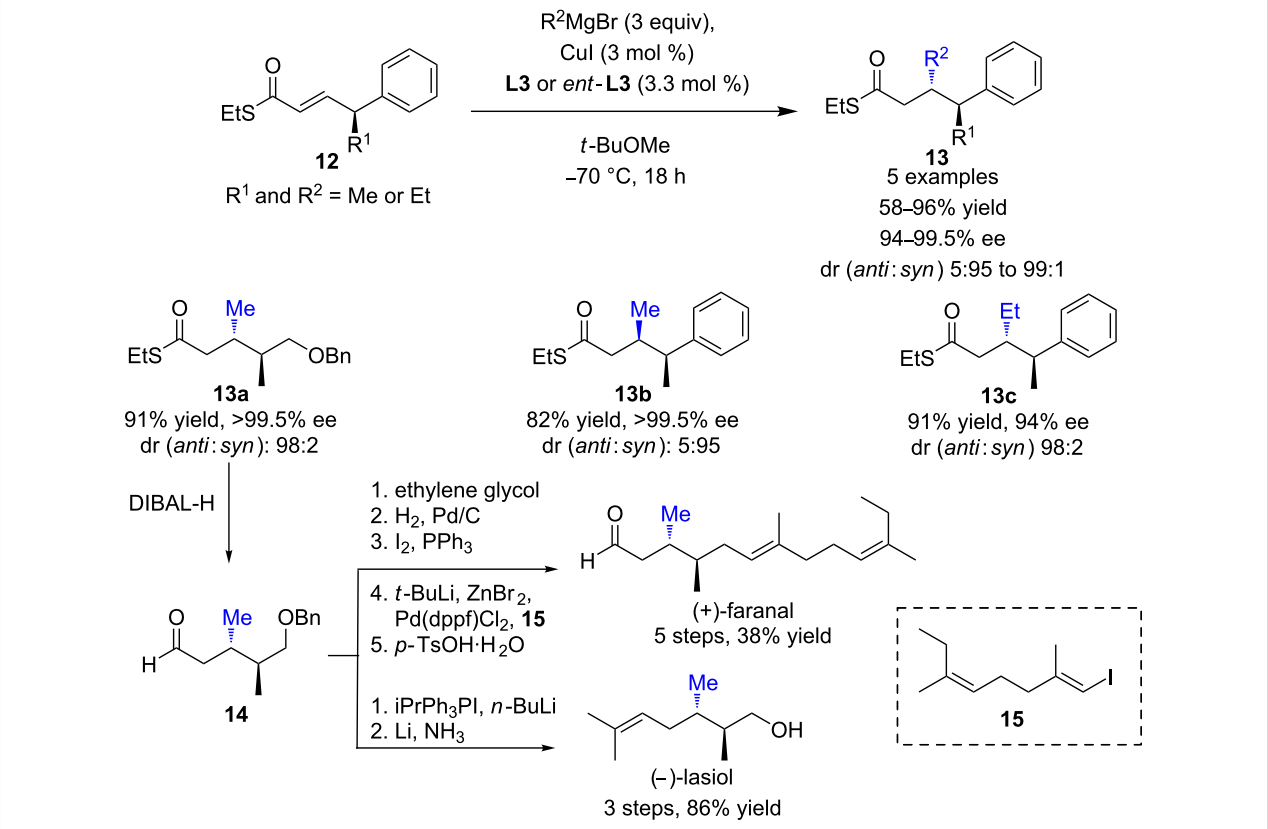

Scheme 8: Catalytic enantioselective synthesis of vicinal dialkyl arrays via Cu ECA of Grignard reagents to γ-substituted α,β-unsaturated thioesters.

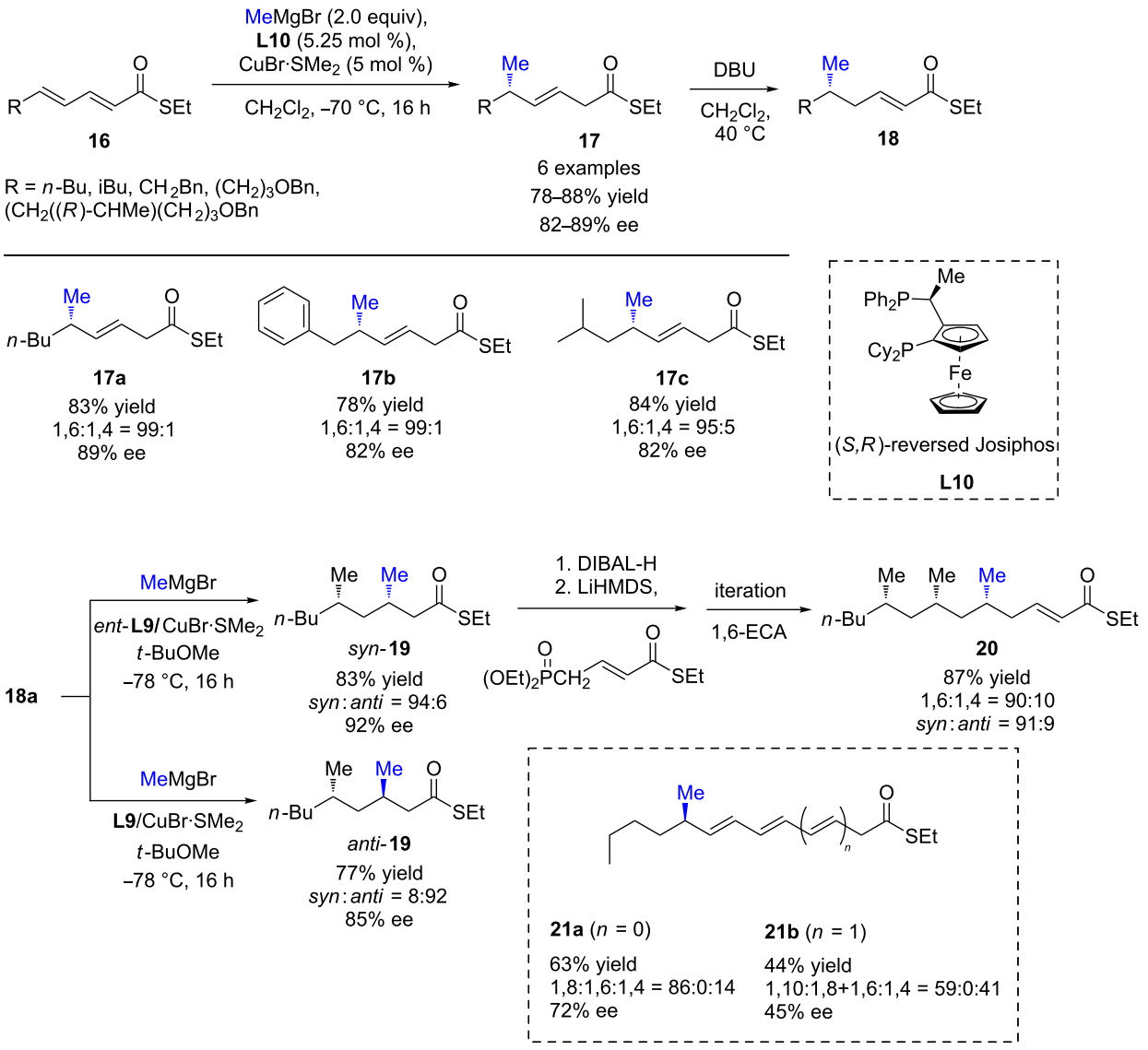

Scheme 9: 1,6-Cu ECA of MeMgBr to α,β,γ,δ-bisunsaturated thioesters: an iterative approach to deoxypropionate units.

duced in good yields and excellent enantioselectivities (85–92% ee). Furthermore, an iterative procedure was also performed leading to all-*syn* or *anti*/*syn*-5,7,9-stereotriads, with high yields and stereoselectivity. This methodology was also tested on linear polyenic thioesters [9]. The challenging 1,8- and 1,10-products **21a**/**b** were obtained, but the stereoselectivity dropped when the distance between the reacting olefin and the ester function was increased (1,8-ECA 72% ee; 1,10-ECA 45% ee). However, the regioselectivity (59–86%) and yield (44–63%) remained decent.

The efficiency of TolBINAP (**L3**)/CuI was also demonstrated in the ECA of Grignard reagents to the 4-chloro-α,β-unsaturated thioester **22** [31]. Interestingly, the presence of the internal chloro leaving group allowed a powerful tandem conjugate addition–enolate trapping that led to valuable *trans*-1-alkyl-2-substituted cyclopropanes (Scheme 10). Various Grignard reagents were used, affording the corresponding cyclopropanes in moderate to high yields (50–92%) and good to excellent ee values (70–96%), except for PhMgBr (26% ee).

In 2010, Hall and Lee described a successful synthesis of enantioenriched boronate derivatives through catalytic ECA of Grignard reagents to 3-boronyl α,β-unsaturated thioesters (Scheme 11) [32]. By applying an **L3**/CuI catalytic protocol previously developed by Feringa and Minnaard, MeMgBr and a range of aromatic Grignard reagents were selectively introduced, leading to the expected 1,4-products in high yields

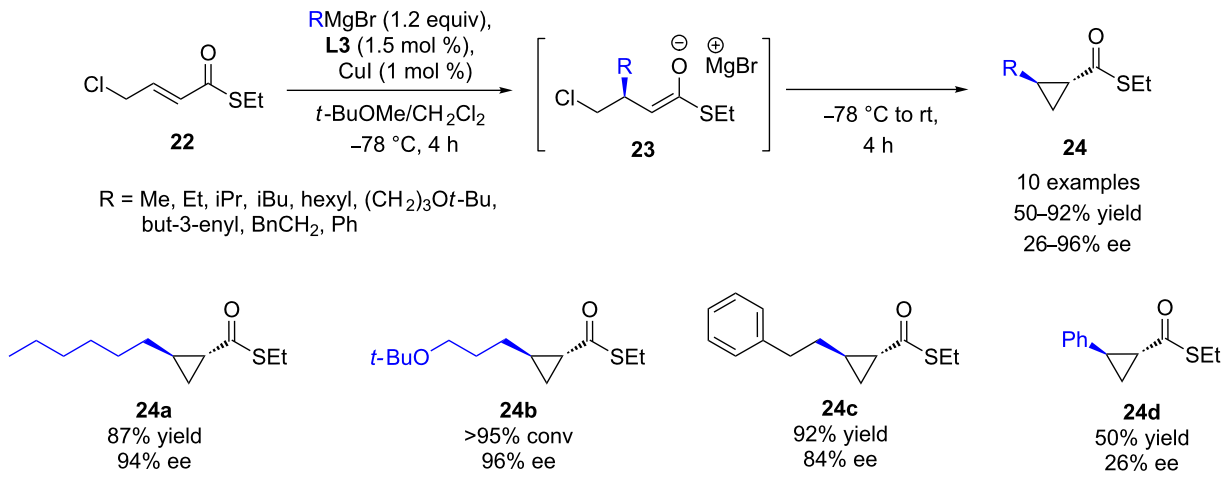

Scheme 10: Tandem Cu ECA/intramolecular enolate trapping involving 4-chloro-α,β-unsaturated thioester **22**.

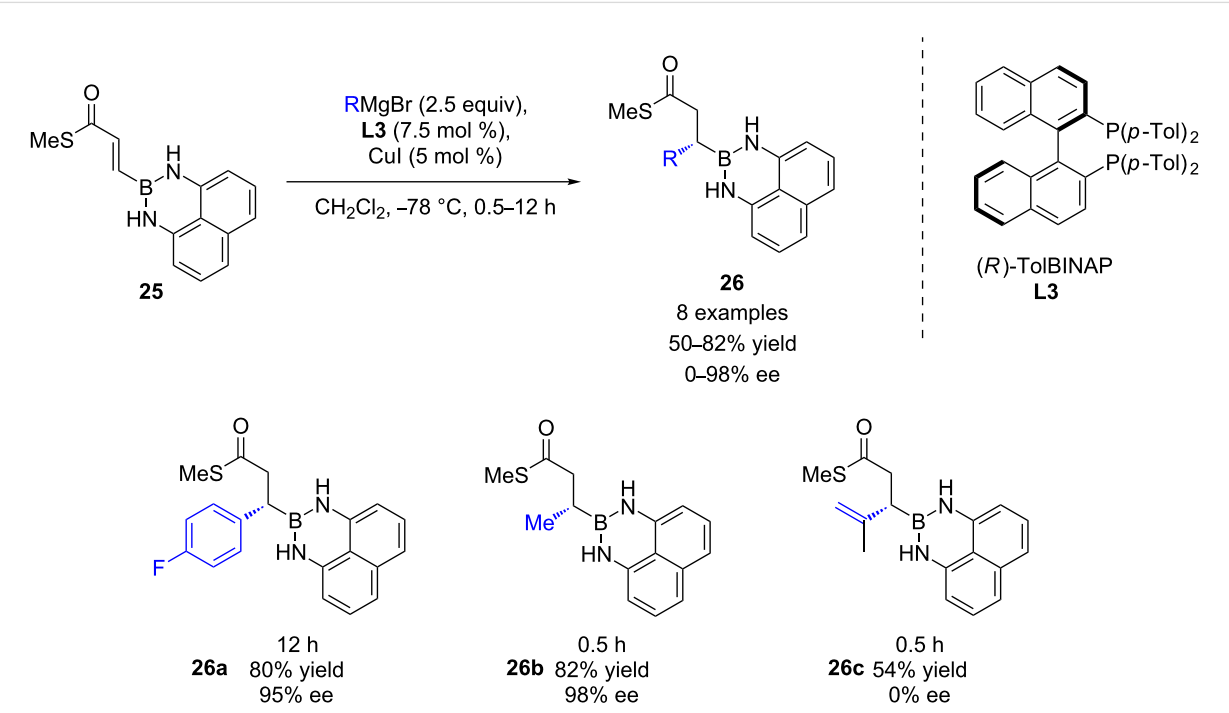

Scheme 11: Cu ECA of Grignard reagents to 3-boronyl α,β-unsaturated thioesters.

(50–82%) and ee values (82–98%). Unfortunately, *ortho*-substituted aromatic or hindered alkenyl reagents led to the corresponding products without showing any enantioselectivity.

Very recently, Fletcher and Gao reported the first copper-catalyzed ECA of alkylzirconium reagents to α,β-unsaturated thioesters [33]. Starting from diversely functionalized alkenes, the resulting hydrozirconated adducts were reacted with various β-substituted Michael acceptors in the presence of CuCl and the chiral phosphoramidite **L11** (Scheme 12). Remarkably, the corresponding 1,4-products were isolated in moderate to good yields (around 70%) and up to 99% ee. The high versatility of the protocol was illustrated by the synthesis of commercially relevant fragrances (phenoxanol and hydroxycitronellal). Additionally, an efficient iterative route was also described, allowing to produce the highly functionalized deoxypropionate fragment **30** in good overall yields and excellent stereocontrol for all stereogenic centers (up to 98:2 dr).

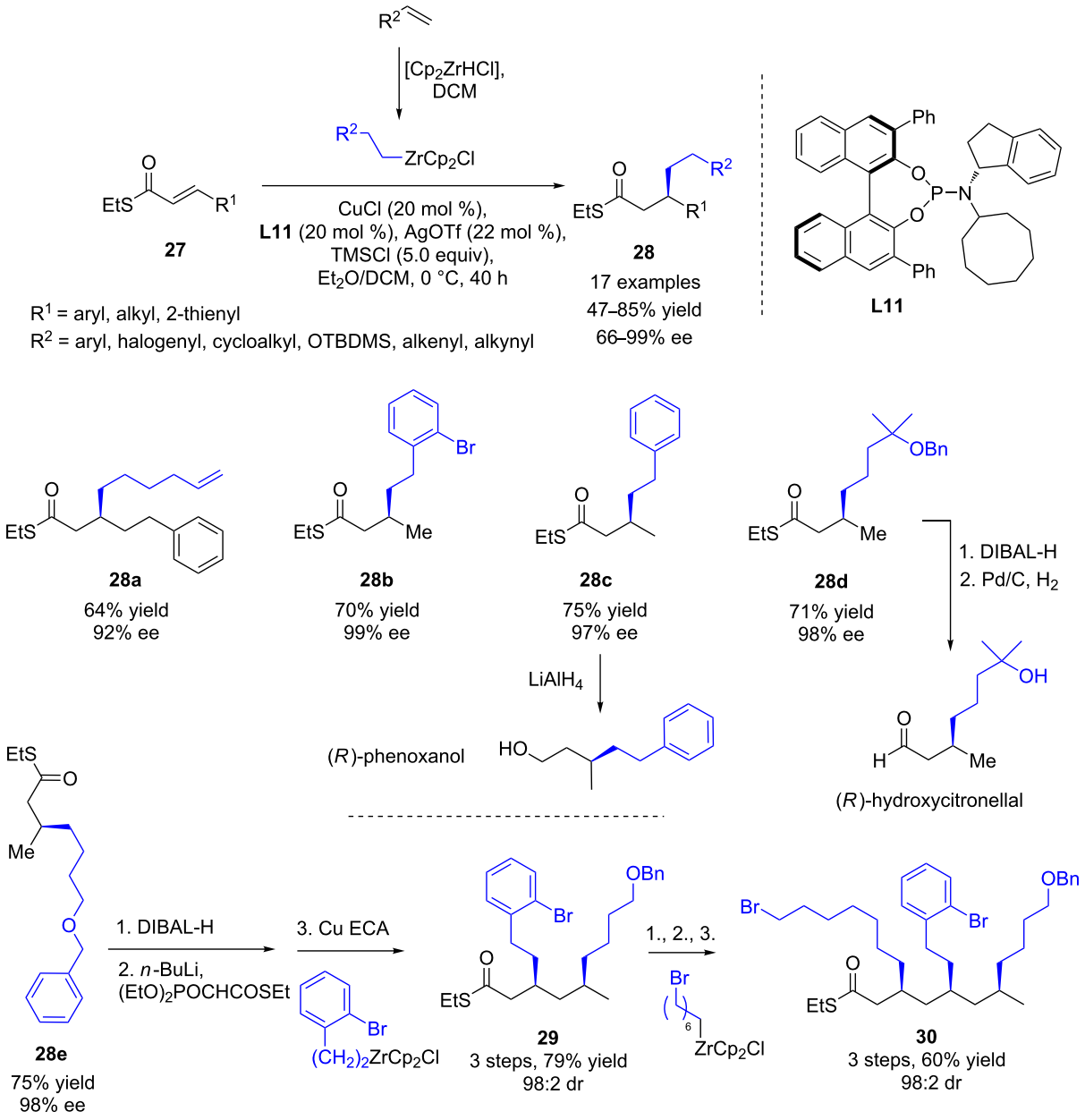

Scheme 12: Cu ECA of alkylzirconium reagents to α,β-unsaturated thioesters.

α,β-Unsaturated acylimidazoles

The pioneering and successful use of α,β-unsaturated acylimidazoles as Michael acceptors in enantioselective catalysis was reported by Evans and co-workers in 2005 [34]. The selected asymmetric transformation was the Friedel–Crafts 1,4-addition involving indole derivatives as nucleophiles, catalyzed by a scandium(III) triflate complex with chiral bis(oxazolinyl)pyridine ligands. As highlighted by Evans, the acylimidazole moiety constituted a privileged surrogate of esters, amides, ketones, and aldehydes. Indeed, this peculiar function, which was readily accessible from the corresponding aldehydes or Weinreb amides, could be efficiently converted into a wide range of carbonyl derivatives, as depicted in Scheme 13.

The successful use of α,β-unsaturated acylimidazole in Cu ECAs using organometallic reagents has been introduced very recently. Pioneering works in this field were published in 2011 by Roelfes, Liskamp, and co-workers, with the 1,4-addition of dimethyl malonate to cinnamyl 2-acyl-1-methylimidazole (**31**). Unfortunately, in the presence of $Cu(NO_3)_2$ and the triazacyclo-

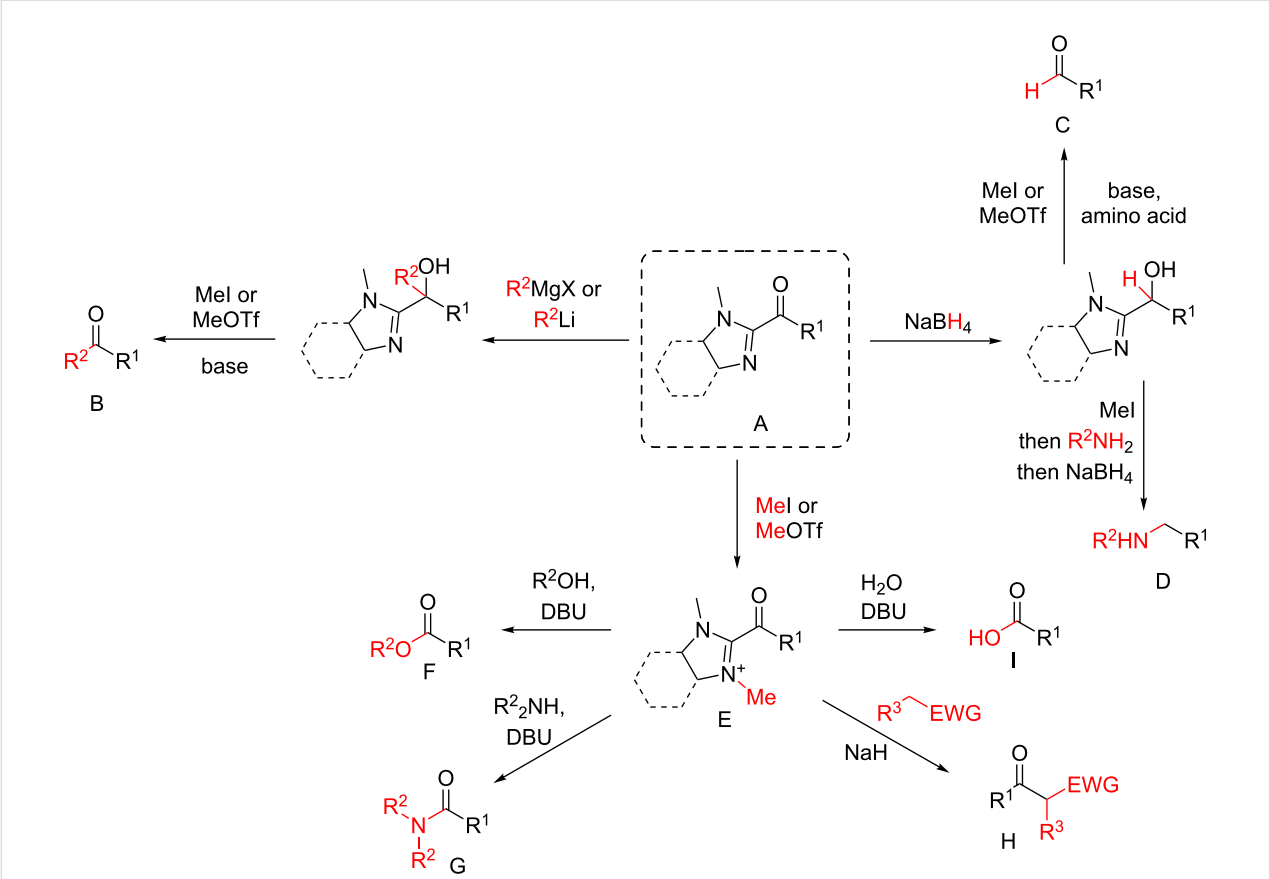

Scheme 13: Conversion of acylimidazoles into aldehydes, ketones, acids, esters, amides, and amines.

phane-based ligand **L12**, the product was obtained in a good yield of 90%, but a poor enantioselectivity (24% ee) was observed (Scheme 14) [35].

In 2012, Sawamura and co-workers described the first highly enantioselective copper-catalyzed conjugate addition of alkyl boranes to α,β-unsaturated 2-acyl-1-methylbenzimidazoles **33** [36]. Based on a previous study dealing with the CuCl/IMes-catalyzed addition of various alkylated 9BBN derivatives [37], the authors screened a set of various chiral NHC precursors. The imidazolium compound **L13** appeared to be the most efficient one, affording the desired 1,4 products in high yields (57 to 93%) and excellent ee values (up to 93%, Scheme 15). Advantageously, this methodology was highly tolerant towards a wide range of functional groups, whether on alkylboranes or on substrates.

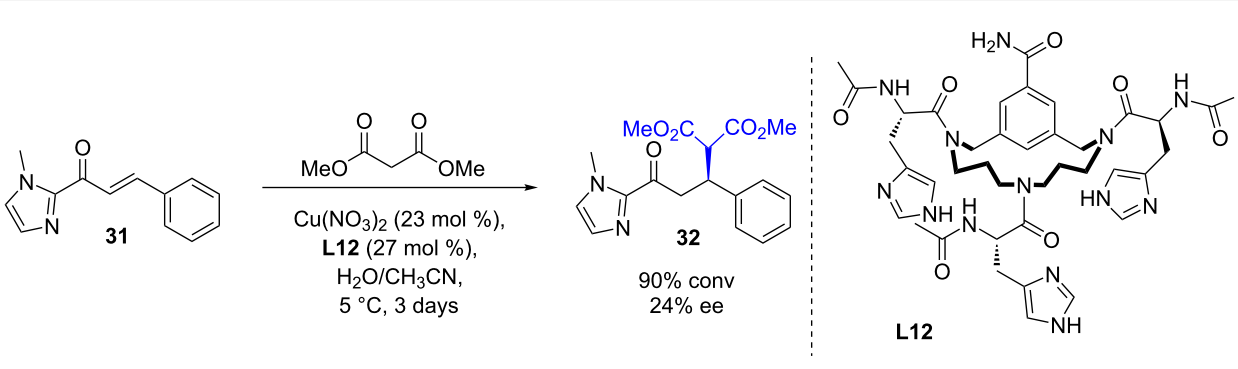

Scheme 14: Cu ECA of dimethyl malonate to α,β-unsaturated acylimidazole **31** with triazacyclophane-based ligand **L12**.

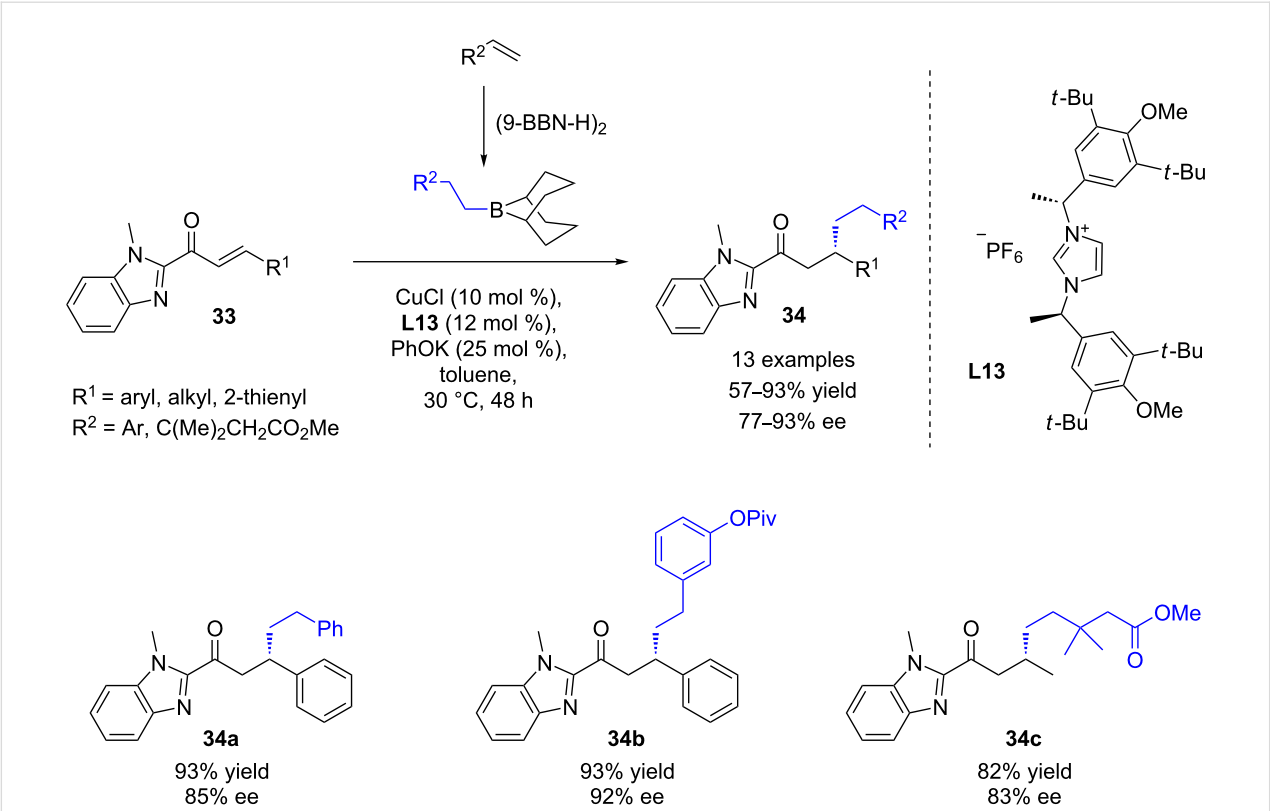

Scheme 15: Cu/**L13**-catalyzed ECA of alkylboranes to α,β-unsaturated acylimidazoles.

In 2015, Mauduit, Campagne, and co-workers set up a highly enantioselective 1,4-addition of dimethylzinc to a wide scope of α,β-unsaturated acylimidazoles **35** [38]. Among the various ligands screened in combination with copper(II) triflate, the hydroxyalkyl-chelating NHC precursor **L14** proved to be the most efficient one, giving the 1,4 product with moderate to good yields (34–86%) and excellent enantioinduction (86 to 95% ee, Scheme 16). The methodology was successfully applied to various extended Michael acceptor systems (dienic or trienic acylimidazoles), leading preferably to the corresponding 1,4 products in moderate to good yields (28–85%) with remarkable regio- (>95%) and enantioselectivities (91–95% ee) [39]. Interestingly, DFT calculations supported the crucial role of the imidazole moiety towards the 1,4-addition (vs 1,6 or 1,8) [39].

Thanks to the efficient post-transformation of the acylimidazole function, the synthetic potential of this methodology was illustrated in the synthesis of relevant molecules, such as a ionone derivative, (+)-*ar*-turmerone, and (+)-Florhydral®, which were formed in good yields, without alteration of their optical purity [38,39].

Moreover, an iterative Cu ECA process allowing the selective introduction of a second methyl stereogenic center was then explored to develop a straightforward access to 1,3-deoxypropionate units, a scaffold ubiquitous in numerous natural products (Scheme 17) [40]. Starting from enantioenriched β-methylated aldehyde **37**, the regeneration of the α,β-unsaturated 2-acyl-1-methylimidazole moiety was performed in high yield and *E*/*Z* selectivity via a two-step protocol. The resulting Michael acceptor was then engaged in an ECA to afford the expected 1,3-dimethyl product in 69% yield and a good diastereomeric excess of 94% (Scheme 17). Following this iterative methodology, the synthesis of 3,5,7-all-*syn*- and *anti*,*anti*-stereotriads **40a**/**b** were successfully achieved in high diastereomeric ratios (up to >95:5) and good overall yields from (*R*)- or (*S*)-citronellal.

More recently, Mauduit, Campagne, and co-workers reported an efficient Cu/Taniaphos-catalyzed β-borylation of an α,β-unsaturated acylimidazole, leading to various enantioenriched β-hydroxy products after oxidation (up to >98% ee) [41]. Interestingly, following the aforementioned iterative ECA strategy, the postfunctionalized chiral acylimidazole **41** derived from (*S*)-citronellal was efficiently converted to highly desirable *anti*,*syn*- and *anti*,*anti*-3,5,7-(Me,OR,Me)-substituted products **42a**/**b**, which were isolated in good yields and excellent diastereomeric ratios (up to >95:5, Scheme 18).

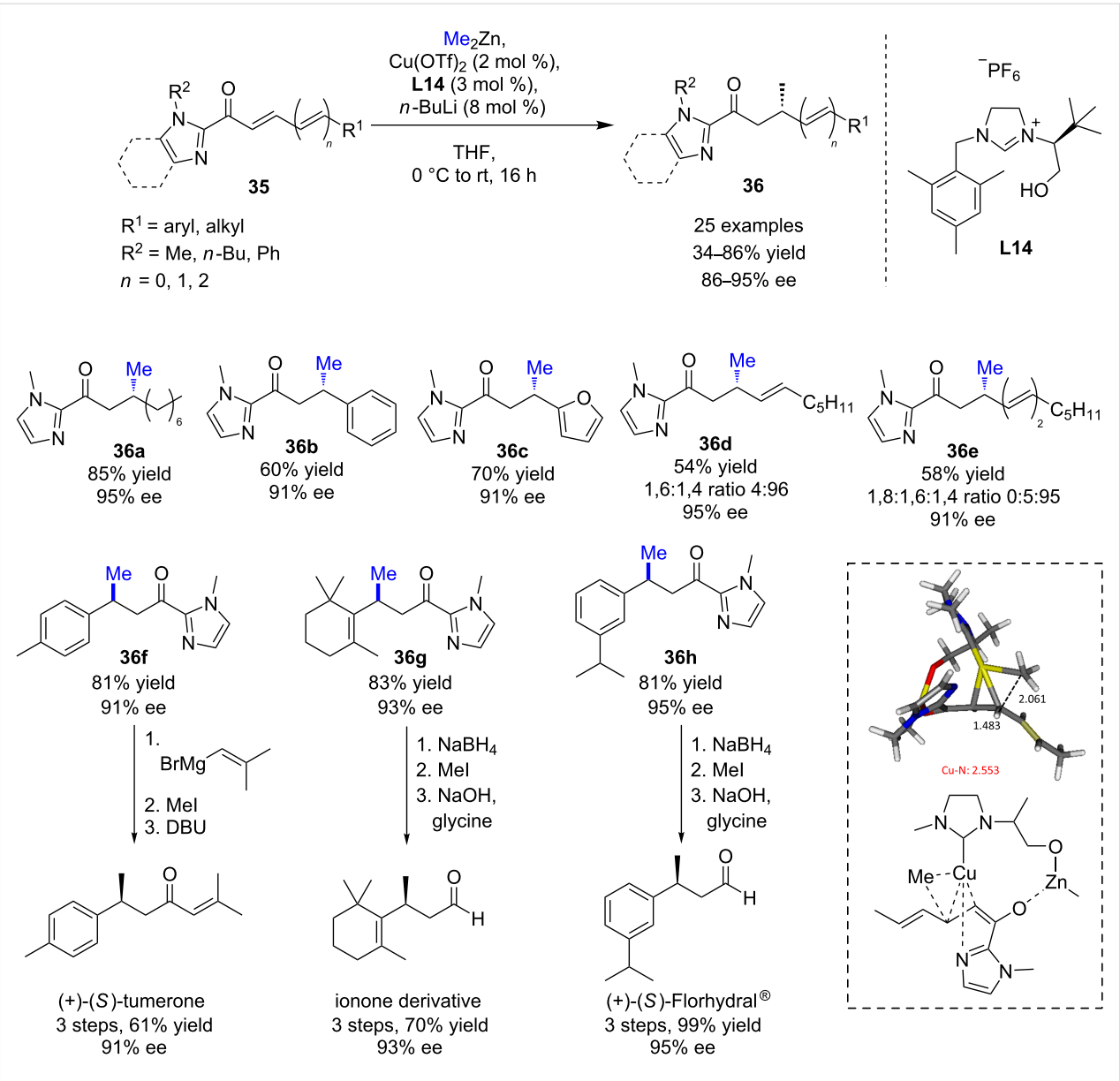

Scheme 16: Cu/hydroxyalkyl-NHC-catalyzed ECA of dimethylzinc to α,β-unsaturated acylimidazoles.

α,β-Unsaturated *N*-acyloxazolidinone, *N*-acylpyrrolidinone, and amide derivatives

Similar to acylimidazole Michael acceptors, the first use of α,β-unsaturated *N*-acyloxazolidinones was also described in asymmetric Friedel–Crafts 1,4-additions catalyzed by chiral copper/bisoxazolidine Lewis acids [42-46]. Thanks to the easy post-transformation of the oxazolidine moiety, the resulting enantio-enriched products (up to 99% ee) were successfully converted to relevant molecules, such as *trans*-whisky lactone [43].

In 2003, Hoveyda and Hird reported the first 1,4-addition of alkylmetal nucleophiles to α,β-unsaturated *N*-acyloxazolidinones (Scheme 19) [47]. The chiral triamidophosphane ligand **L15a** as a copper(I) triflate complex efficiently promoted the catalytic conjugate addition of dialkylzinc species to various *N*-acyloxazolidinone Michael acceptors, in most of the cases with high isolated yields (61 to 95%) and excellent enantioselectivities (up to >98%). Furthermore, the resulting enantio-enriched β-alkylated *N*-acyloxazolidinones could be converted to various derivatives (aldehydes, ketones, Weinreb amides, or carboxylic acids) in good yields and without alteration of the ee values. In 2006, aminohydroxyphosphine **L15b** was used as a new designer ligand by Nakamura and co-workers for the addition of diethylzinc to crotonyl *N*-acyloxazolidinone [48]. The 1,4-product was also formed in high enantioselectivity (>98% ee) and high yield (91%).

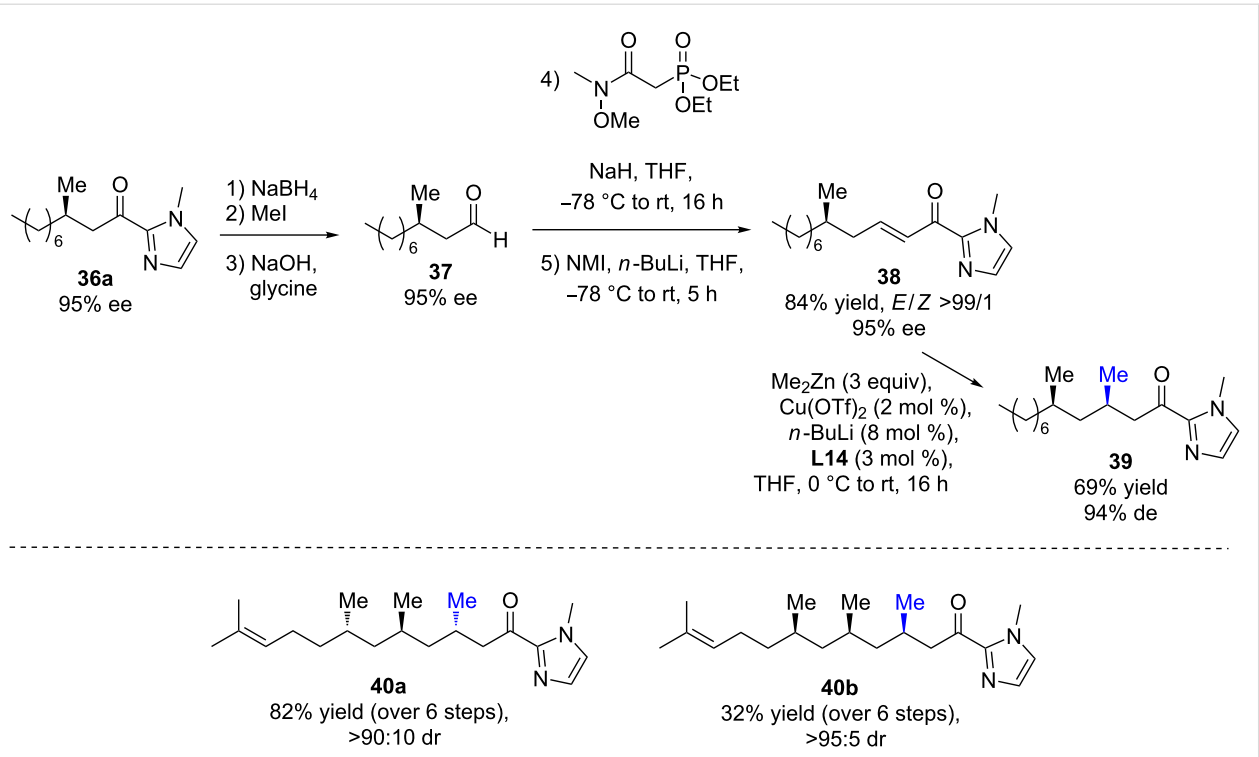

Scheme 17: Stereocontrolled synthesis of 3,5,7-all-*syn* and *anti*,*anti*-stereotriads via iterative Cu ECAs.

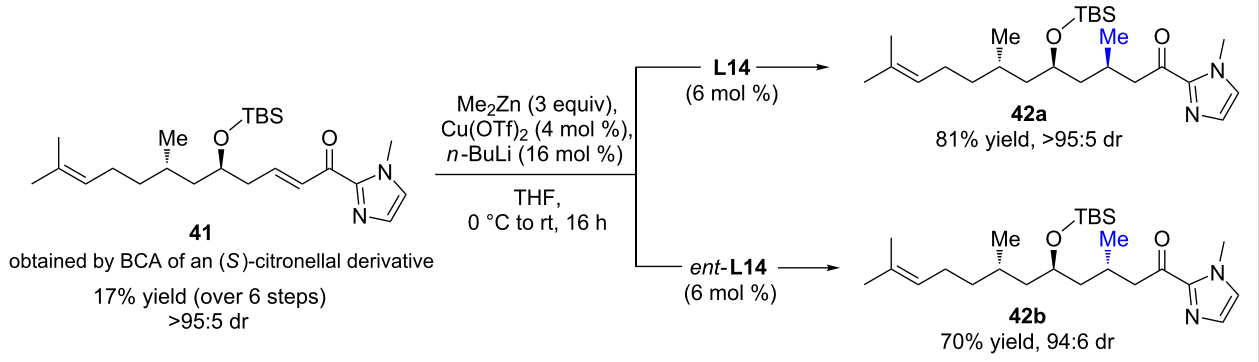

Scheme 18: Stereocontrolled synthesis of *anti*,*syn*- and *anti*,*anti*-3,5,7-(Me,OR,Me) units via iterative Cu ECA/BCA.

The same year, Pineschi et al. evaluated various α,β-unsaturated acyl derivatives for the copper/(*R*,*S*,*S*)-phosphoramidite **L16**-catalyzed addition of diethylzinc (Scheme 20) [49]. Although the Michael acceptor bearing the *N*-acyloxazolidinone moiety that was successfully used by Hoveyda (95% ee) gave a lower enantioselectivity (64%), a more satisfactory enantiocontrol was obtained with the substrate having a 2-pyrrolidinone fragment (87% ee). The scope was then extended to various α,β-unsaturated *N*-acyl-2-pyrrolidinones and dialkylzinc reagents, leading to the corresponding 1,4-products in low to good yields (7–88%), with good to excellent enantioinduction (60 to >99% ee). Trimethylaluminium reagents were also investigated, but unfortunately, only low ee values were observed (20–36% ee), whereas no reactivity was observed with α,β-unsaturated amides.

Although Pineschi's conditions were ineffective for amides [49], Harutyunyan and co-workers achieved an important breakthrough by reporting the first enantioselective alkylation of α,β-unsaturated amides [50]. Indeed, due to their poor reactivity compared to other Michael acceptors, catalytic asymmetric conjugate additions of organometallic reagents to *N*,*N*-

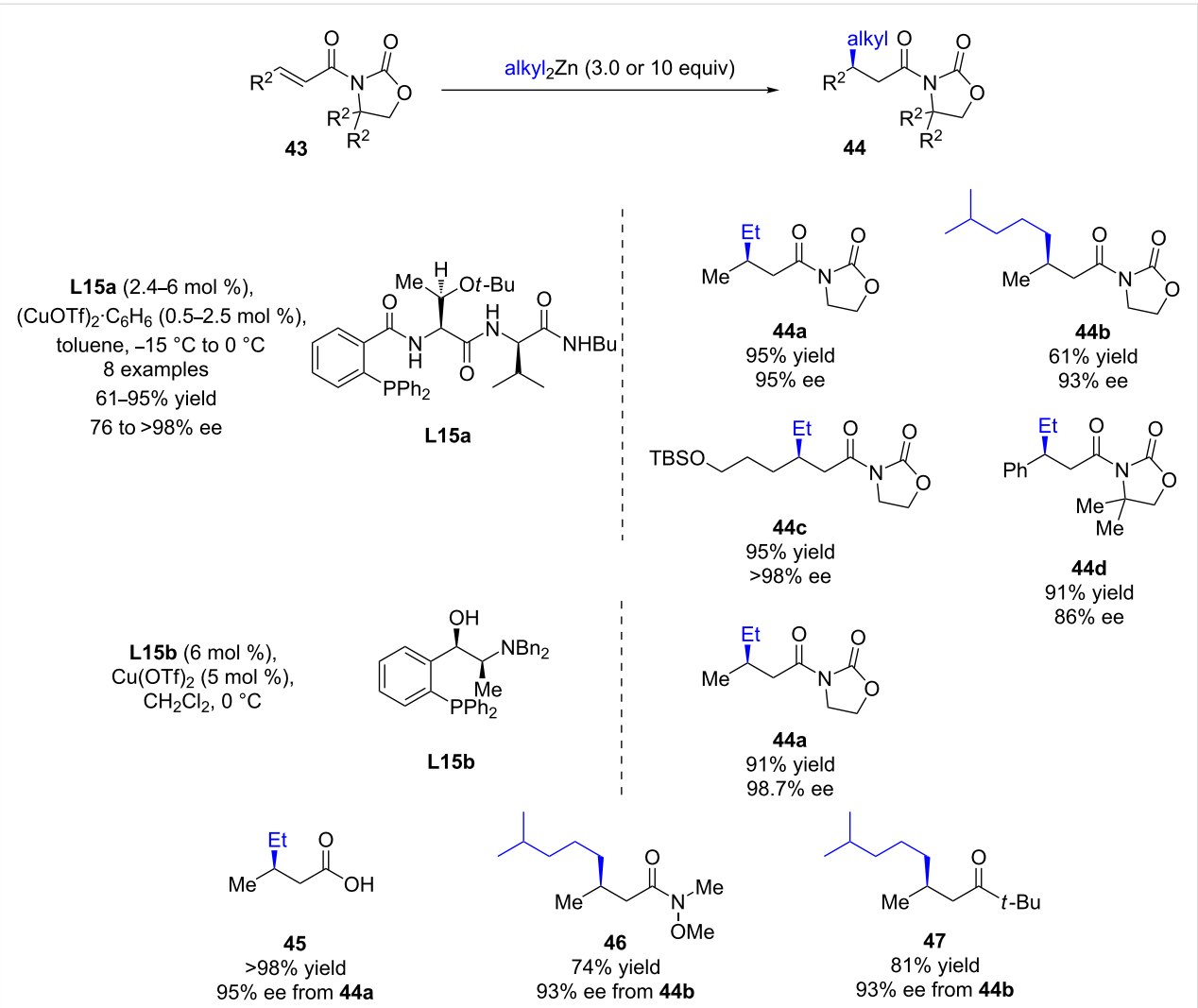

Scheme 19: Cu-catalyzed ECA of dialkylzinc reagents to α,β-unsaturated *N*-acyloxazolidinones.

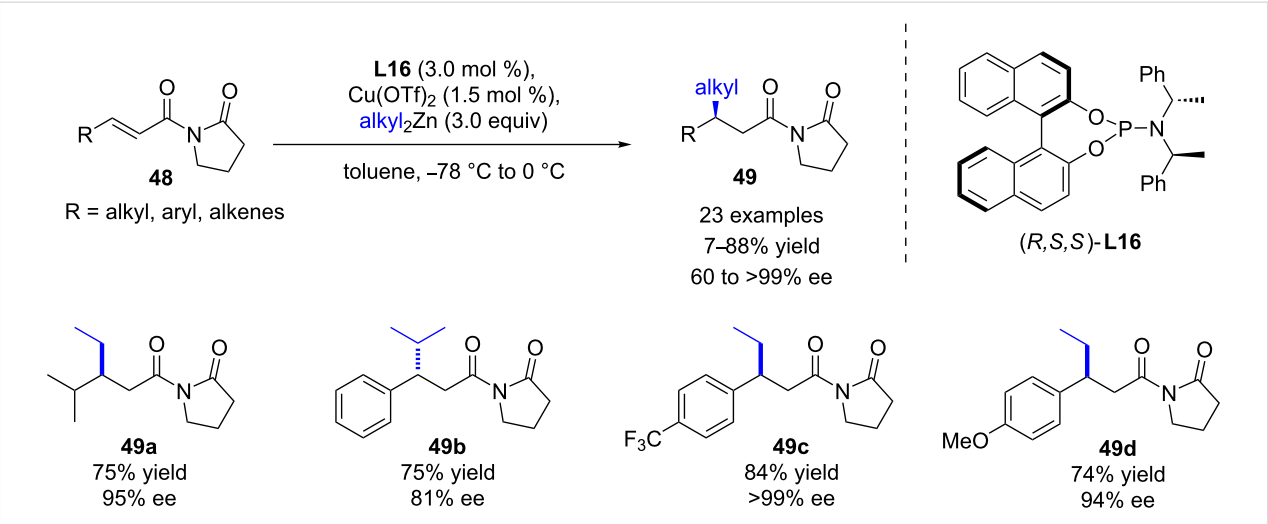

Scheme 20: Cu/phosphoramidite **L16**-catalyzed ECA of dialkylzincs to α,β-unsaturated *N*-acyl-2-pyrrolidinones.

dialkylenamides remained a real challenge. However, thanks to the synergistic action of the boron-based Lewis acid $BF_3{\cdot}Et_2O$, $CuBr{\cdot}SMe_2$, and the chiral (*R,S*)-Josiphos ligand (**L9**), an efficient (yields up to 86%) and highly regio- and enantioselective (ee values up to 99%) protocol was developed for 1,4-additions of various Grignard reagents to a wide scope of substrates (Scheme 21). Notably, the introduction of methyl and functionalized alkyl groups was performed with remarkable stereoselectivity (97–99%). Furthermore, this catalytic system was easily upscalable (up to 10 g), and the chiral catalyst could be recycled without any loss of efficiency. Unfortunately, although a wide range of Grignard reagents led to excellent results, PhMgBr provided low conversion and the racemic 1,4-product. Additionally, amide substrates featuring a bis(*para*-methoxybenzyl) moiety could be converted into relevant β-alkyl-substituted chiral amines, ubiquitous in numerous pharmaceutical ingredients, such as **52**, a direct precursor of a drug candidate. Moreover, tandem ECA/enolate trapping was also studied, providing the *trans*-cyclopentane product **56** as a single diastereoisomer (92% ee).

In 2018, the same authors reported the 1,6- and 1,4-additions of various Grignard reagents to a wide scope of conjugated dienyl amides (Scheme 22) [51]. Interestingly, the authors observed

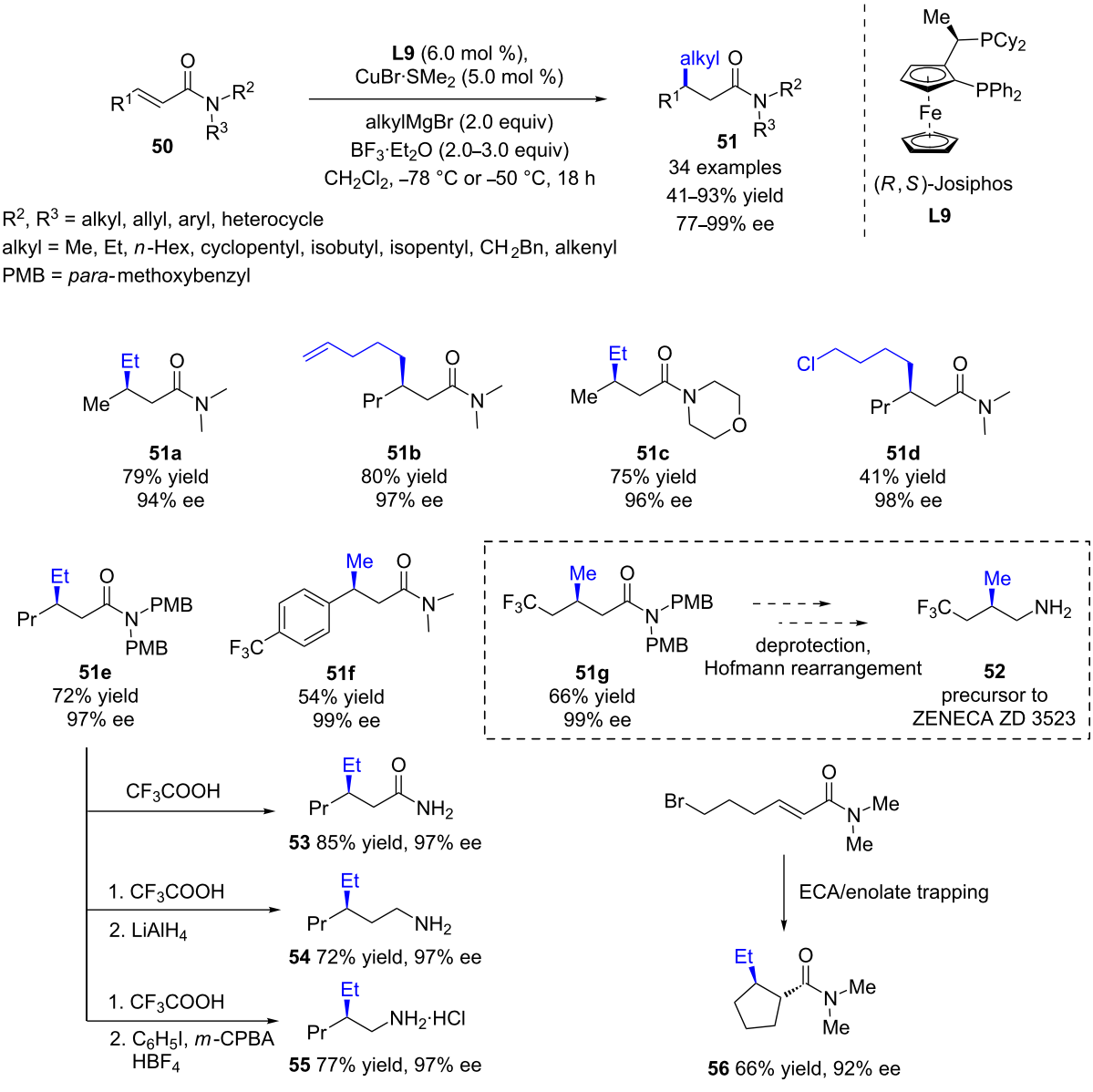

Scheme 21: Cu/(*R*,*S*)-Josiphos (**L9**)-catalyzed ECA of Grignard reagents to α,β-unsaturated amides.

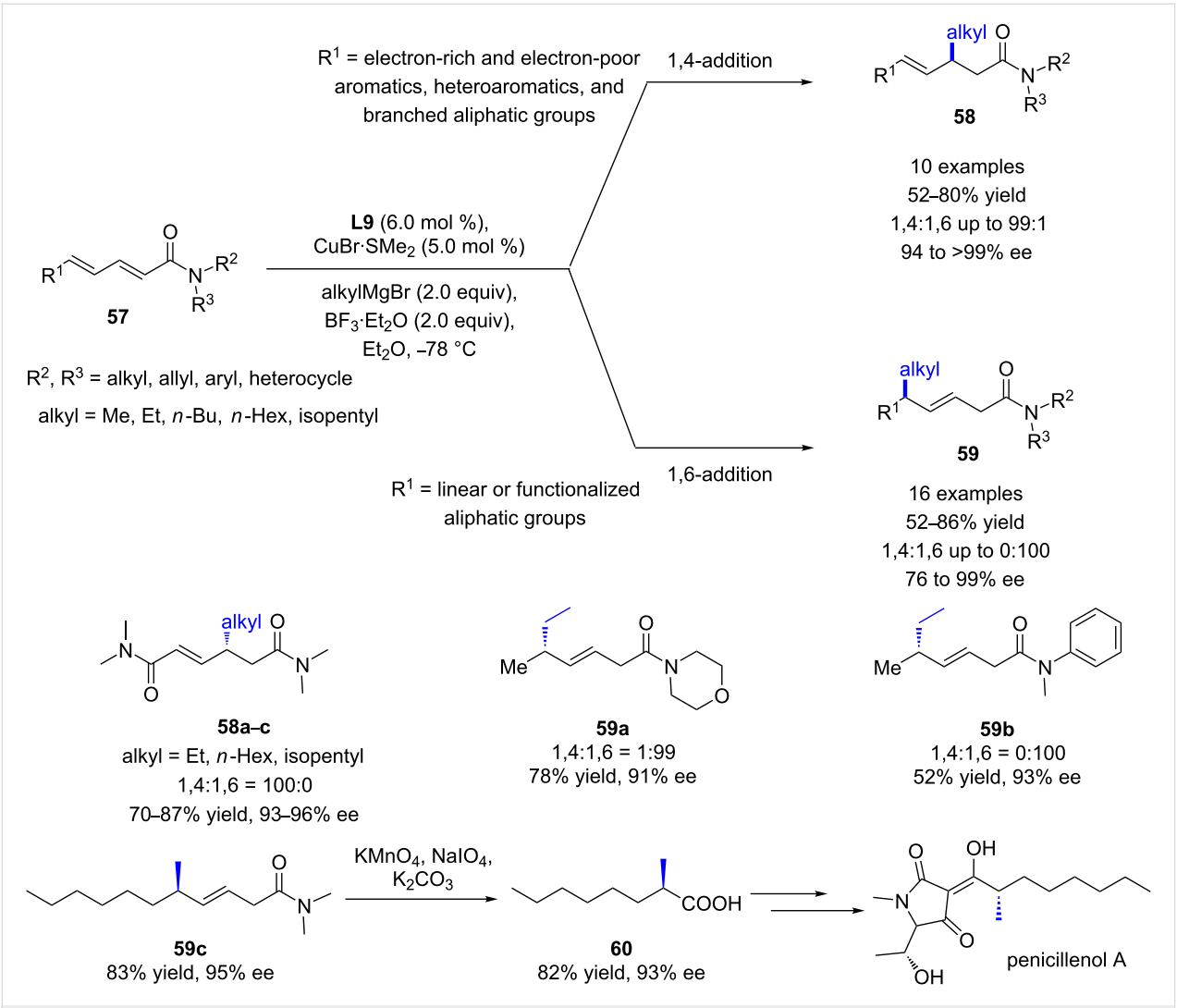

Scheme 22: Cu/Josiphos (**L9**)-catalyzed ECA of Grignard reagents to polyunsaturated amides.

that the regioselectivity was directed by the substituent in the δ-position of the substrate: dienic amides featuring linear or functionalized aliphatic substituents in the δ-position led predominantly to 1,6-products, whereas those featuring electron-rich and electron-poor aromatic, heteroaromatic, and branched aliphatic substituents in the δ-position afforded preferably the 1,4-products. Importantly, when the morpholine moiety was used as N-substituent, the addition of diethylzinc to the enamide afforded the 1,6-addition product with 78% isolated yield and 91% ee. It is worth to underline that the morpholine group could easily allow further postfunctionalizations. Furthermore, thanks to the highly 1,6-enantioselective additions of methylmagnesium bromide (95% ee), this methodology was applied to the synthesis of the natural product penicillenol A by oxidative cleavage of the resulting 1,6 product **59c**, affording the key synthon **60** with a slight erosion of the optical purity (Scheme 22).

α,β-Unsaturated *N*-acylpyrroles

α,β-Unsaturated *N*-acylpyrroles were also investigated as Michael acceptors in enantioselective conjugate additions using organometallic reagents. In 2013, Endo and Shibata described a catalytic system based on multinuclear copper/aluminium complexes and phenolphosphine-based ligands **L17a**/**b** and **L18**, allowing the selective 1,4-addition of trimethylaluminium to three α,β-unsaturated *N*-acylpyrroles with moderate to good yields (54 to 87%) and excellent enantioselectivities (94 to 97% ee, Scheme 23) [52]. This methodology was successfully applied to the synthesis of various natural molecules, such as (*S*)-Florhydral® and (*S*)-(+)-*ar*-turmerone or key intermediates in the synthesis of 8-deoxyanisatin and frondosin.

Conclusion

The enantioselective Cu-catalyzed conjugate addition of organometallic reagents to Michael acceptors has been exten-

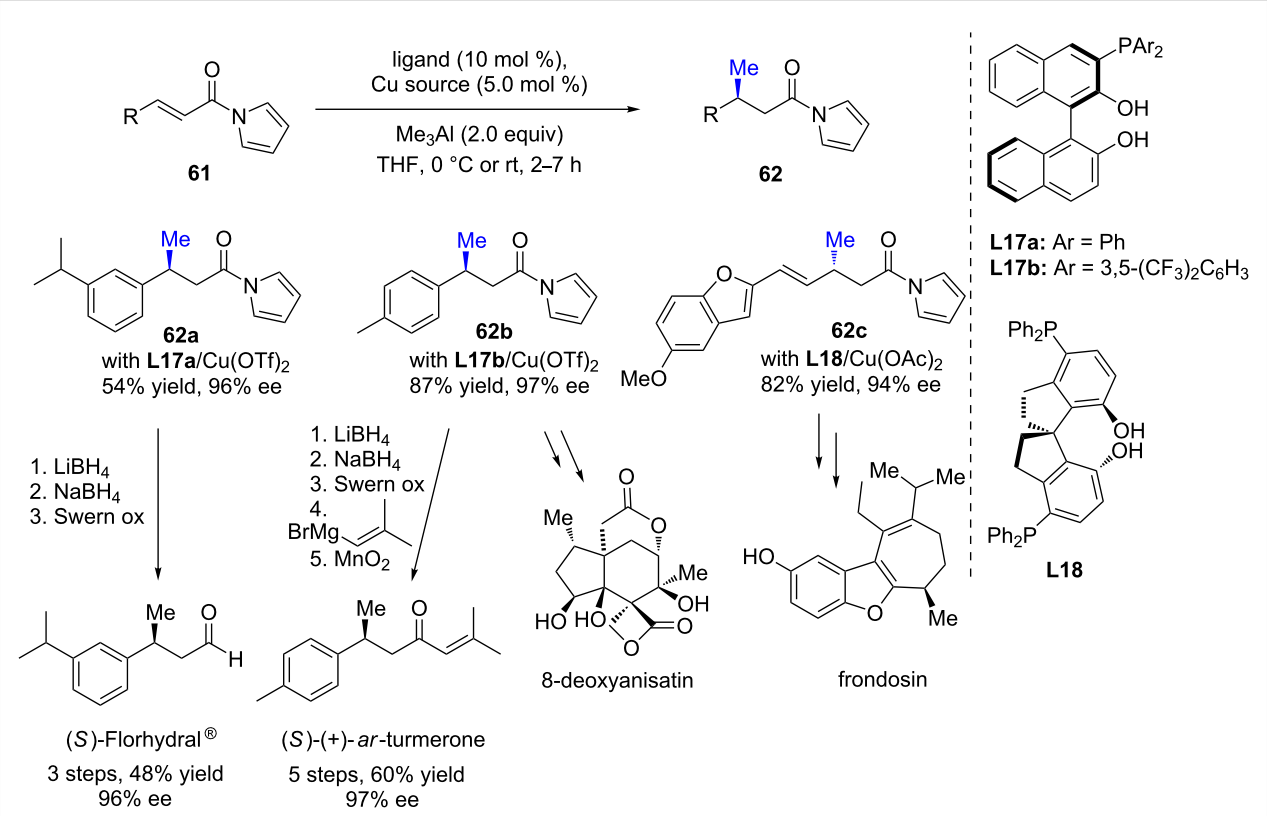

Scheme 23: Cu-catalyzed ECA of trimethylaluminium to *N*-acylpyrrole derivatives.

sively studied for many decades and led to remarkable results. However, for a long time, some classes of Michael acceptors (α,β-unsaturated aldehydes, thioesters, acylimidazoles, *N*-acyloxazolidinone, *N*-acylpyrrolidinone, amides, *N*-acylpyrroles) have been neglected to varying degrees, probably owing to their particular reactivity, which led to less impressive results. Nevertheless, these substrates present a high potential in total synthesis, since the chiral products can be easily transformed into various natural compounds. For example, the aldehyde function, which is directly obtained from α,β-unsaturated aldehydes or is accessible through postderivatization of either acylimidazole or thioester functions, is present in many natural compounds and is also a key functional group for many synthetic strategies. Furthermore, some of the functional groups listed above can be converted into various other synthetically useful groups, such as ketones, esters, carboxylic acids, and (Weinreb) amide groups.

More recently, some works were reported, which showed that through a judicious selection of chiral ligands and a fine-tuning of the reactivities of both partners, interesting selectivities could be reached with these more challenging electron-deficient alkenes, including, in some cases, di- or trienic acceptors, which accordingly extends the scope and the synthetic applicability of the method. The potential of the methodology has been illustrated through the efficient conversion of some 1,4-products into various chiral natural products. In addition, iterative procedures leading to chiral 1,3,5-(Me,Me,Me) and 1,3,5-(Me,OH,Me) motifs in a stereocontrolled way were successfully applied from α,β-unsaturated acylimidazoles and α,β-unsaturated thioesters, and thus opening a new field for the total synthesis of natural products. We hope that the results collected in this review will encourage chemists on one hand to continue the search for improved procedures combining simple, easily accessible chiral ligands, lower catalytic loadings, high ee values and productivity, and a wide scope, and on the other hand, to include this highly promising methodology in many synthetic strategies.

Acknowledgements

We are grateful to the Ecole Nationale Supérieure de Chimie de Rennes (ENSCR) and the Centre National de la Recherche Scientifique (CNRS).

Funding

M.M., C.C. and J.M. thank the Région Bretagne (ARED 2018 “Biometa” N° 601). M.M and D.P. thank the Agence Nationale

de la Recherche (ANR-16-CE07-0019 Hel-NHC) for their financial support.

ORCID® iDs

Delphine Pichon - https://orcid.org/0000-0002-2307-6388
Jennifer Morvan - https://orcid.org/0000-0003-1210-7975
Christophe Crévisy - https://orcid.org/0000-0001-5145-1600
Marc Mauduit - https://orcid.org/0000-0002-7080-9708

References

1. Mauduit, M.; Baslé, O.; Clavier, H.; Crévisy, C.; Denicourt-Nowicki, A. Metal-Catalyzed Asymmetric Nucleophilic Addition to Electron-Deficient Alkenes. In *Comprehensive Organic Synthesis,* 2nd ed.; Molander, G. A.; Knochel, P., Eds.; Elsevier: Amsterdam, Netherlands, 2014; Vol. 4, pp 189–341. doi:10.1016/b978-0-08-097742-3.00406-7
2. Alexakis, A.; Bäckvall, J. E.; Krause, N.; Pàmies, O.; Diéguez, M. *Chem. Rev.* **2008,** *108,* 2796–2823. doi:10.1021/cr0683515
3. Harutyunyan, S. R.; den Hartog, T.; Geurts, K.; Minnaard, A. J.; Feringa, B. L. *Chem. Rev.* **2008,** *108,* 2824–2852. doi:10.1021/cr068424k
4. Jerphagnon, T.; Pizzuti, M. G.; Minnaard, A. J.; Feringa, B. L. *Chem. Soc. Rev.* **2009,** *38,* 1039–1075. doi:10.1039/b816853a
5. Alexakis, A.; Frutos, J.; Mangeney, P. *Tetrahedron: Asymmetry* **1993,** *4,* 2427–2430. doi:10.1016/s0957-4166(00)82216-8
6. Martin, D.; Kehrli, S.; d'Augustin, M.; Clavier, H.; Mauduit, M.; Alexakis, A. *J. Am. Chem. Soc.* **2006,** *128,* 8416–8417. doi:10.1021/ja0629920
7. Tissot, M.; Li, H.; Alexakis, A. Copper-catalyzed asymmetric conjugate addition and allylic substitution of organometallic reagents to extended multiple bond systems. In *Copper catalyzed asymmetric synthesis;* Alexakis, A.; Krause, N.; Woodward, S., Eds.; Wiley-VCH: Weinheim, Germany, 2014; pp 69–84. doi:10.1002/9783527664573.ch3
8. Schmid, T. E.; Drissi-Amraoui, S.; Crévisy, C.; Baslé, O.; Mauduit, M. *Beilstein J. Org. Chem.* **2015,** *11,* 2418–2434. doi:10.3762/bjoc.11.263
9. den Hartog, T.; Huang, Y.; Fañanás-Mastral, M.; Meuwese, A.; Rudolph, A.; Pérez, M.; Minnaard, A. J.; Feringa, B. L. *ACS Catal.* **2015,** *5,* 560–574. doi:10.1021/cs501297s
   See for mechanistic considerations.
10. Calvo, B. C.; Buter, J.; Minnaard, A. J. Applications to the synthesis of natural products. In *Copper-Catalyzed Asymmetric Synthesis;* Alexakis, A.; Krause, N.; Woodward, S., Eds.; Wiley-VCH: Weinheim, Germany, 2014; pp 373–448. doi:10.1002/9783527664573.ch14
11. Jones, P.; Reddy, C. K.; Knochel, P. *Tetrahedron* **1998,** *54,* 1471–1490. doi:10.1016/s0040-4020(97)10382-9
    See for previous results in copper-free conjugate addition of organometallic reagents to α,β-unsaturated aldehydes.
12. Bräse, S.; Höfener, S. *Angew. Chem., Int. Ed.* **2005,** *44,* 7879–7881. doi:10.1002/anie.200501732
    See for the first enantioselective copper-free conjugate addition of organometallic reagents to α,β-unsaturated aldehydes.
13. Marshall, J. A.; Herold, M.; Eidam, H. S.; Eidam, P. *Org. Lett.* **2006,** *8,* 5505–5508. doi:10.1021/ol062154a
    See for the first copper-catalyzed diastereoselective conjugate addition of organometallic reagents to α,β-unsaturated aldehydes.
14. Palais, L.; Babel, L.; Quintard, A.; Belot, S.; Alexakis, A. *Org. Lett.* **2010,** *12,* 1988–1991. doi:10.1021/ol100441r
15. Corey, E. J.; Boaz, N. W. *Tetrahedron Lett.* **1985,** *26,* 6015–6018. doi:10.1016/s0040-4039(00)95113-x
16. Corey, E. J.; Boaz, N. W. *Tetrahedron Lett.* **1985,** *26,* 6019–6022. doi:10.1016/s0040-4039(00)95114-1
17. Alexakis, A.; Berlan, J.; Besace, Y. *Tetrahedron Lett.* **1986,** *27,* 1047–1050. doi:10.1016/s0040-4039(86)80044-2
18. Nakamura, E.; Matsuzawa, S.; Horiguchi, Y.; Kuwajima, I. *Tetrahedron Lett.* **1986,** *27,* 4029–4032. doi:10.1016/s0040-4039(00)84902-3
19. Chuit, C.; Foulon, J. P.; Normant, J. F. *Tetrahedron* **1980,** *36,* 2305–2310. doi:10.1016/0040-4020(80)80126-8
20. Gremaud, L.; Palais, L.; Alexakis, A. *Chimia* **2012,** *66,* 196–200. doi:10.2533/chimia.2012.196
21. Quintard, A.; Alexakis, A. *Adv. Synth. Catal.* **2010,** *352,* 1856–1860. doi:10.1002/adsc.201000309
22. Afewerki, S.; Breistein, P.; Pirttilä, K.; Deiana, L.; Dziedzic, P.; Ibrahem, I.; Córdova, A. *Chem. – Eur. J.* **2011,** *17,* 8784–8788. doi:10.1002/chem.201100756
23. Fañanas-Mastral, M.; Feringa, B. L. *J. Am. Chem. Soc.* **2010,** *132,* 13152–13153. doi:10.1021/ja105585y
    See for a relevant alternative copper catalytic process based on the in situ enantioselective allylic alkylation of α,β-unstaurated aldehydes leading to β-substituted aldehydes with high ee values (up to 94%).
24. Goncalves-Contal, S.; Gremaud, L.; Palais, L.; Babel, L.; Alexakis, A. *Synthesis* **2016,** *48,* 3301–3308. doi:10.1055/s-0035-1562487
25. Des Mazery, R.; Pullez, M.; López, F.; Harutyunyan, S. R.; Minnaard, A. J.; Feringa, B. L. *J. Am. Chem. Soc.* **2005,** *127,* 9966–9967. doi:10.1021/ja053020f
26. Maciá Ruiz, B.; Geurts, K.; Fernández-Ibáñez, M. Á.; ter Horst, B.; Minnaard, A. J.; Feringa, B. L. *Org. Lett.* **2007,** *9,* 5123–5126. doi:10.1021/ol702425a
27. Bates, R. W.; Sridhar, S. *J. Org. Chem.* **2008,** *73,* 8104–8105. doi:10.1021/jo801433f
28. van Zijl, A. W.; Szymanski, W.; Lopez, F.; Minnaard, A. J.; Feringa, B. L. *J. Org. Chem.* **2008,** *73,* 6994–7002. doi:10.1021/jo8010649
29. den Hartog, T.; Harutyunyan, S. R.; Font, D.; Minnaard, A. J.; Feringa, B. L. *Angew. Chem., Int. Ed.* **2008,** *47,* 398–401. doi:10.1002/anie.200703702
30. den Hartog, T.; Jan van Dijken, D.; Minnaard, A. J.; Feringa, B. L. *Tetrahedron: Asymmetry* **2010,** *21,* 1574–1584. doi:10.1016/j.tetasy.2010.04.057
31. den Hartog, T.; Rudolph, A.; Macia, B.; Minnaard, A. J.; Feringa, B. L. *J. Am. Chem. Soc.* **2010,** *132,* 14349–14351. doi:10.1021/ja105704m
32. Lee, J. C. H.; Hall, D. G. *J. Am. Chem. Soc.* **2010,** *132,* 5544–5545. doi:10.1021/ja9104057
33. Gao, Z.; Fletcher, S. P. *Chem. Commun.* **2017,** *53,* 10216–10219. doi:10.1039/c7cc05433e
34. Evans, D. A.; Fandrick, K. R.; Song, H.-J. *J. Am. Chem. Soc.* **2005,** *127,* 8942–8943. doi:10.1021/ja052433d
35. Bauke Albada, H.; Rosati, F.; Coquière, D.; Roelfes, G.; Liskamp, R. M. J. *Eur. J. Org. Chem.* **2011,** 1714–1720. doi:10.1002/ejoc.201001522
36. Yoshida, M.; Ohmiya, H.; Sawamura, M. *J. Am. Chem. Soc.* **2012,** *134,* 11896–11899. doi:10.1021/ja304481a
37. Ohmiya, H.; Yoshida, M.; Sawamura, M. *Org. Lett.* **2011,** *13,* 482–485. doi:10.1021/ol102819k
38. Drissi-Amraoui, S.; Morin, M. S. T.; Crévisy, C.; Baslé, O.; Marcia de Figueiredo, R.; Mauduit, M.; Campagne, J.-M. *Angew. Chem., Int. Ed.* **2015,** *54,* 11830–11834. doi:10.1002/anie.201506189

39. Drissi-Amraoui, S.; Schmid, T. E.; Lauberteaux, J.; Crévisy, C.; Baslé, O.; de Figueiredo, R. M.; Halbert, S.; Gérard, H.; Mauduit, M.; Campagne, J.-M. *Adv. Synth. Catal.* **2016,** *358,* 2519–2540. doi:10.1002/adsc.201600458
40. ter Horst, B.; Feringa, B. L.; Minnaard, A. J. *Chem. Commun.* **2010,** *46,* 2535–2547. doi:10.1039/b926265b
See for a review on iterative ECA processes.
41. Lauberteaux, J.; Crévisy, C.; Baslé, O.; de Figueiredo, R. M.; Mauduit, M.; Campagne, J.-M. *Org. Lett.* **2019,** *21,* 1872–1876. doi:10.1021/acs.orglett.9b00479
42. Kitajima, H.; Katsuki, T. *Synlett* **1997,** 568–570. doi:10.1055/s-1997-3235
43. Nishikori, H.; Ito, K.; Katsuki, T. *Tetrahedron: Asymmetry* **1998,** *9,* 1165–1170. doi:10.1016/s0957-4166(98)00080-9
44. Evans, D. A.; Willis, M. C.; Johnston, J. N. *Org. Lett.* **1999,** *1,* 865–868. doi:10.1021/ol9901570
45. Evans, D. A.; Rovis, T.; Johnson, J. S. *Pure Appl. Chem.* **1999,** *71,* 1407–1415. doi:10.1351/pac199971081407
46. Evans, D. A.; Scheidt, K. A.; Johnston, J. N.; Willis, M. C. *J. Am. Chem. Soc.* **2001,** *123,* 4480–4491. doi:10.1021/ja010302g
47. Hird, A. W.; Hoveyda, A. H. *Angew. Chem., Int. Ed.* **2003,** *42,* 1276–1279. doi:10.1002/anie.200390328
48. Hajra, A.; Yoshikai, N.; Nakamura, E. *Org. Lett.* **2006,** *8,* 4153–4155. doi:10.1021/ol0618306
49. Pineschi, M.; Del Moro, F.; Di Bussolo, V.; Macchia, F. *Adv. Synth. Catal.* **2006,** *348,* 301–304. doi:10.1002/adsc.200505309
50. Rodríguez-Fernández, M.; Yan, X.; Collados, J. F.; White, P. B.; Harutyunyan, S. R. *J. Am. Chem. Soc.* **2017,** *139,* 14224–14231. doi:10.1021/jacs.7b07344
51. Guo, Y.; Kootstra, J.; Harutyunyan, S. R. *Angew. Chem., Int. Ed.* **2018,** *57,* 13547–13550. doi:10.1002/anie.201808392
52. Endo, K.; Hamada, D.; Yakeishi, S.; Shibata, T. *Angew. Chem., Int. Ed.* **2013,** *52,* 606–610. doi:10.1002/anie.201206297

License and Terms

BEILSTEIN JOURNAL OF ORGANIC CHEMISTRY

Copper-promoted/copper-catalyzed trifluoromethylselenolation reactions

Clément Ghiazza and Anis Tlili*

Review

Open Access

Address:
Institute of Chemistry and Biochemistry, Univ Lyon, Université Lyon 1, CNRS, 43 Bd du 11 Novembre 1918, F-69622 Villeurbanne, France

Email:
Anis Tlili* - anis.tlili@univ-lyon1.fr

* Corresponding author

Keywords:
copper catalysis; fluorine; homogenous catalysis; trifluoromethylselenolation

Beilstein J. Org. Chem. **2020,** *16,* 305–316.
doi:10.3762/bjoc.16.30

Received: 02 November 2019
Accepted: 07 February 2020
Published: 03 March 2020

This article is part of the thematic issue "Copper-catalyzed reactions for organic synthesis".

Guest Editor: G. Evano

Abstract

Copper catalysis and, more generally, copper chemistry are pivotal for modern organofluorine chemistry. Major advances have been made in the field of trifluoromethylselenolations of organic compounds where copper catalysis played a crucial role. Recent developments in this field are highlighted in this minireview.

Introduction

In recent years, the incorporation of fluorine or fluorinated motifs into organic molecules has gained widespread interest. This is mainly due to the new properties associated with the introduction of these modifications. In particular, chalcogen trifluoromethyl motifs are of prime interest since they confer very high lipophilicity [1,2]. In this context, transition-metal catalysis plays a key role in the formation of carbon–chalcogen trifluoromethyl bonds. Major advances have been made in the last ten years especially for C–OCF_3 [3-5] and C–SCF_3 [6-8] bond-forming processes. Today, the incorporation of OCF_3 as well as SCF_3 is routinely used to design new active compounds [8]. The development of new methodologies based on copper catalysis/chemistry is playing a pivotal role due to the low cost and toxicity of the corresponding copper reagents [9]. Due to their stability, these usually contain copper–chalcogen trifluoromethyl σ-bonds. Likewise, the research on new methods enabling the incorporation of $SeCF_3$ has continuously been growing and today, a plethora of strategies have been reported [10,11]. Therein, the design of new catalysts and reagents is a key factor to foster the development of new methods for C–$SeCF_3$ bond-forming processes. Although many methods are available for the introduction of the trifluoromethylselenyl group, only little information is available related to the physicochemical properties of the products. However, it has been noted that the $SeCF_3$ motif is by far one of the most lipophilic fluorinated groups, and thus potentially increases the bioavailability

of the targeted drugs [10]. The focus of this minireview is to highlight the efforts made to use copper reagents for the promotion of trifluoromethylselenolation reactions.

Review

Overview on copper-promoted and copper-catalyzed processes for the introduction of $SeCF_3$ groups

Copper(I) trifluoromethylselenolate complexes

Copper(I) trifluoromethylselenolate was first prepared in 1985 by the group of Yagupolskii [12]. Then, $CuSeCF_3$·DMF was tested in the trifluoromethylselenolation of (hetero)aryl iodides and showed promising results. However, the reactions were performed mainly with activated aryl iodides, and a high temperature was required to achieve acceptable yields. Three decades later, the group of Weng reported the synthesis of discrete $SeCF_3$-containing copper/bipyridine (bpy) complexes [13]. Noteworthy, depending on the nature of the bidentate ligand used, the corresponding copper complex could be isolated as monomer or dimer, and both were air-stable. Among the new complexes, the reactivity of $[(bpy)CuSeCF_3]_2$ in trifluoromethylselenolations was thoroughly investigated using a large panel of starting materials.

The group of Weng first explored the trifluoromethylselenolation of alkyl halides [13] and then propargylic chlorides and allylic bromides (Scheme 1) [14]. Overall, the reactions were performed at temperatures between 70–100 °C with an excess of the trifluoromethylselenyl source, and the desired corresponding products were generally obtained in very good yields.

The application scope of the $[(bpy)CuSeCF_3]_2$ complex was then extended to aromatic halides for the formation of $C(sp^2)$–$SeCF_3$ bonds. The authors demonstrated that a very broad range of (hetero)aryl halides and vinyl halides could be trifluoromethylselenolated that way (Scheme 2) [13,15-17]. Mechanistically, the authors postulated the involvement of copper(I)/(III) oxidation states.

Oxidative cross-coupling reactions between terminal alkynes using the $[(bpy)CuSeCF_3]_2$ complex were also undertaken by the same group to form C(sp)–$SeCF_3$ bonds (Scheme 3) [18]. Therein, Dess–Martin periodinane (DMP) was used as the oxidant and potassium fluoride as the base, and the reactions were performed at room temperature in DMF as the solvent. The desired compounds were obtained in moderate to very good yields. Both electron-withdrawing and -donating groups were tolerated on the arylacetylene derivatives. Heteroaromatic as well as aliphatic alkyne derivatives could also be smoothly converted in these transformation. Noteworthy, the authors demonstrated that the reaction could easily be scaled up when almost two grams of a trifluoromethylselenolated alkyne product could be isolated.

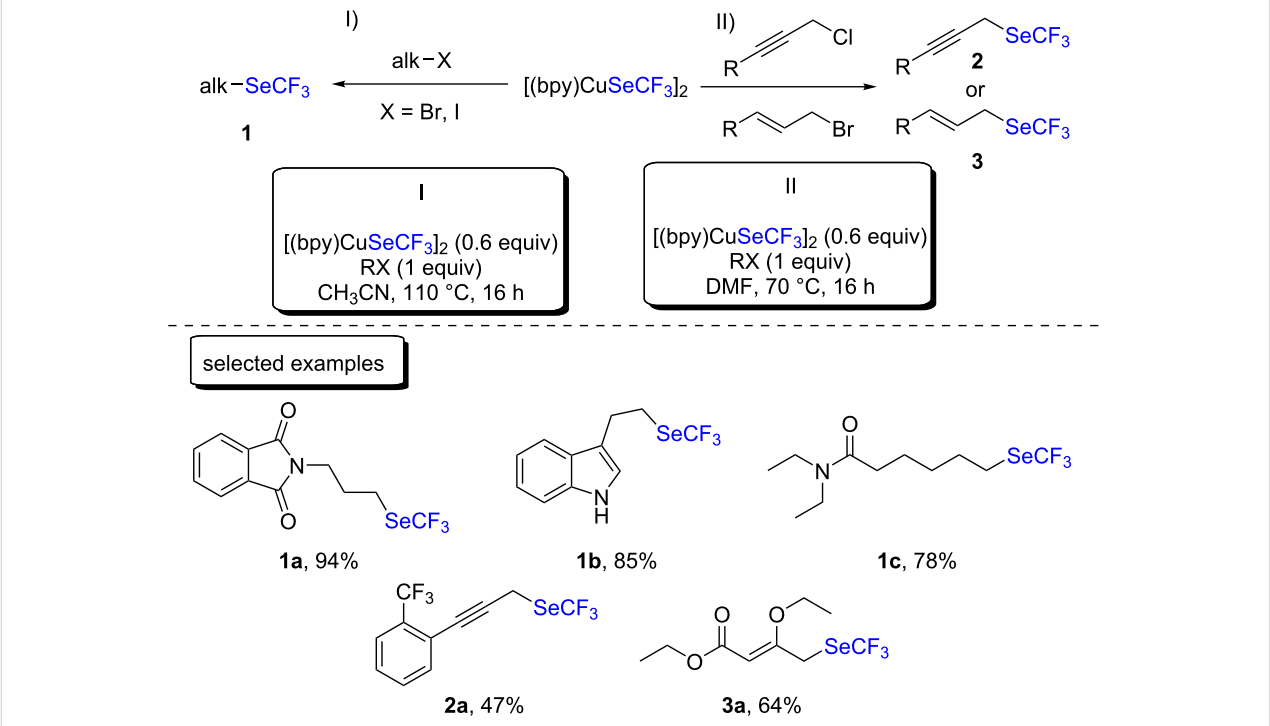

Scheme 1: Process for the formation of $C(sp^3)$–$SeCF_3$ bonds with $[(bpy)CuSeCF_3]_2$ developed by the group of Weng.

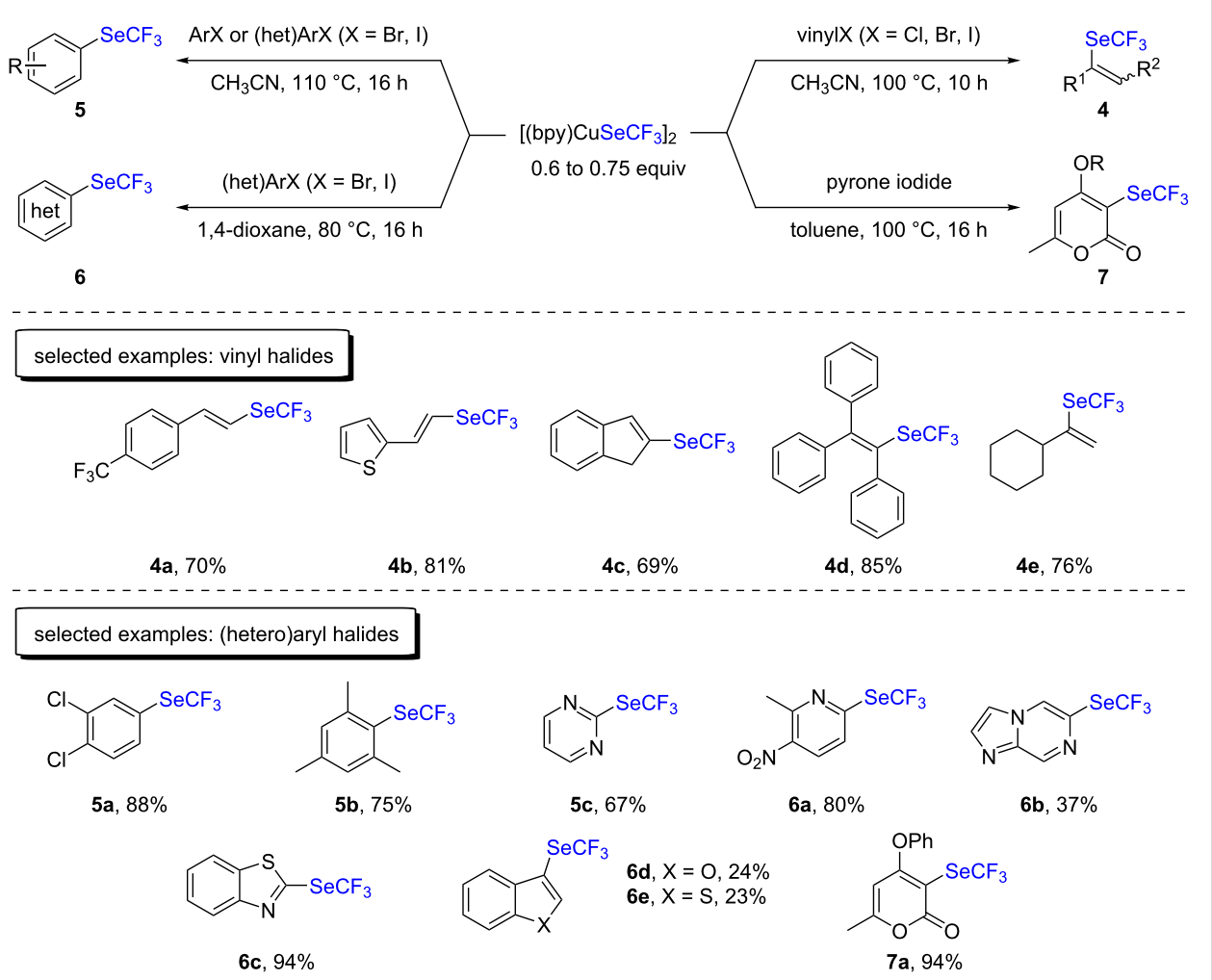

Scheme 2: Trifluoromethylselenolation of vinyl and (hetero)aryl halides with $[(bpy)CuSeCF_3]_2$ by the group of Weng.

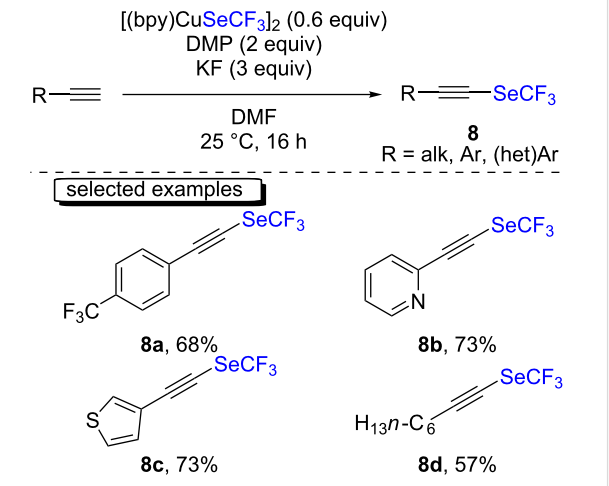

Scheme 3: Trifluoromethylselenolation of terminal alkynes using $[(bpy)CuSeCF_3]_2$ by the group of You and Weng.

After that, the same group studied the α-trifluoromethylselenolation of ketones and esters starting from the corresponding halides or diazoacetates (Scheme 4) [19,20]. Both methods led to the desired products with moderate to very good yields, and the reactions were performed at temperatures between 40–45 °C. Interestingly, a tertiary α-bromoketone furnished the product in 66% yield, excluding an S_N2 mechanism. However, it is worth mentioning that diazoacetates bearing pyridine motifs were not suitable to be used under these conditions.

Following this, the same group studied the direct trifluoromethylselenolation of α-brominated unsaturated carbonyl compounds with $[(bpy)CuSeCF_3]_2$ and CsF as the base (Scheme 5, top) [21]. The products were obtained with good yields as a mixture of *E*/*Z* isomers. The authors postulated the formation of a copper(III) complex in the reaction, resulting from an oxidative addition of the trifluoromethylselenolated copper(I) complex to the α-brominated unsaturated carbonyl

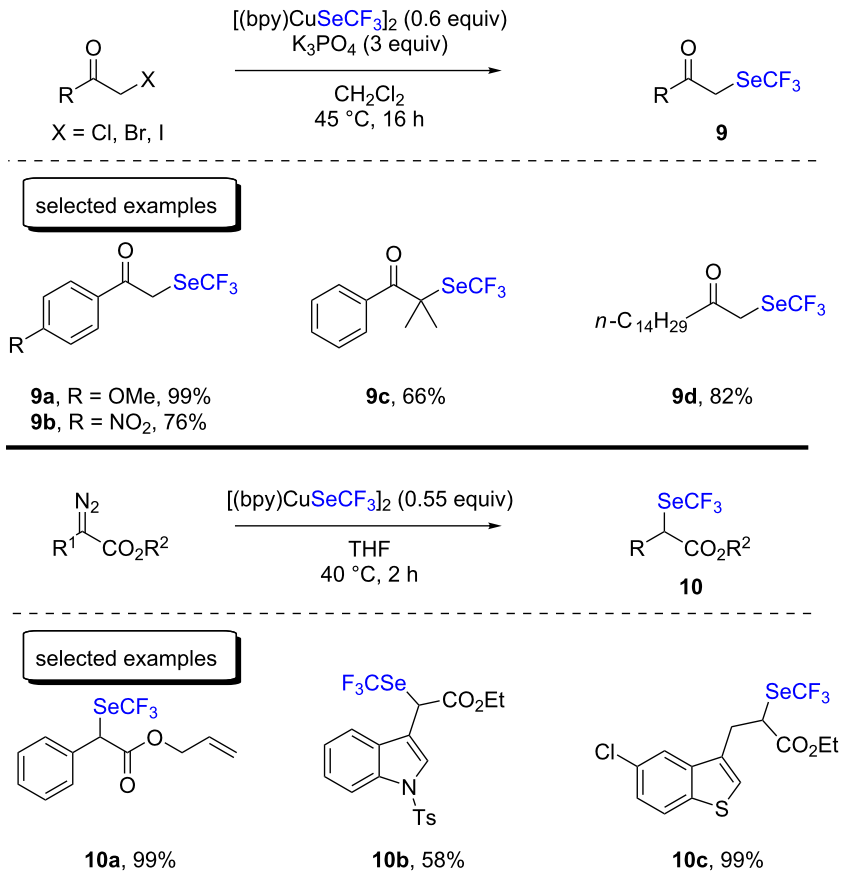

Scheme 4: Trifluoromethylselenolation of carbonyl compounds with $[(bpy)CuSeCF_3]_2$ by the group of Weng.

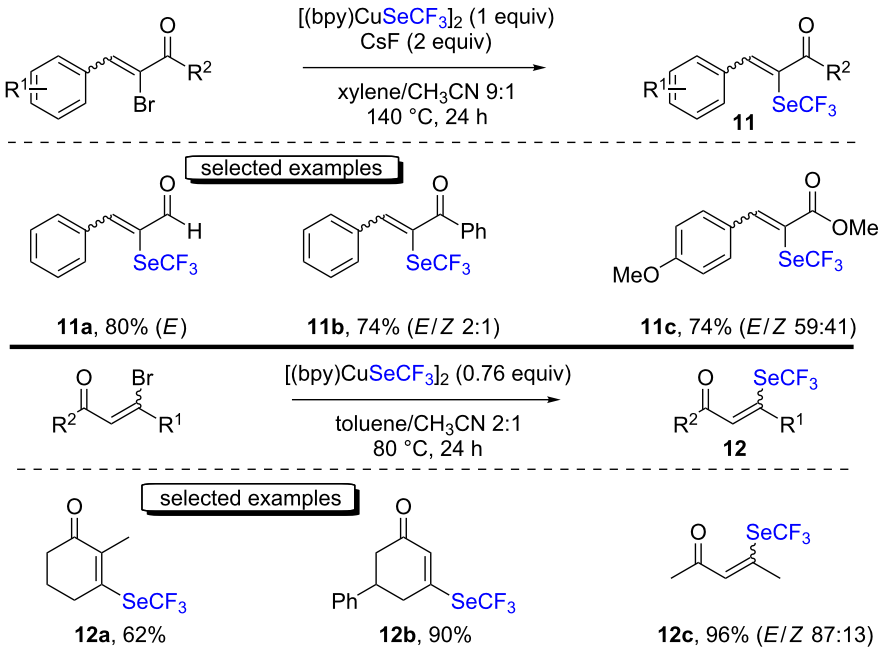

Scheme 5: Trifluoromethylselenolation of α,β-unsaturated ketones with $[(bpy)CuSeCF_3]_2$ by the group of Weng.

compound. Afterwards, a reductive elimination would take place to afford the α-trifluoromethylselenylated α,β-unsaturated carbonyl compound and copper(I) bromide.

The same group also reported the trifluoromethylselenolation of β-brominated unsaturated carbonyl compounds under base-free conditions (Scheme 5, bottom) [22]. Good to excellent yields were obtained for the products. The authors demonstrated that no major alterations were observed in the presence of TEMPO, and thus a radical pathway was considered as less likely. Contrarily to the precedent mechanism, the authors proposed a 1,4-addition of $^{-}SeCF_3$, and a bromide elimination to occur.

The synthesis of trifluoromethylseleno esters was also explored by the group of Weng from readily available acid chlorides (Scheme 6) [23]. Therein, the key was the addition of a catalytic amount of iron powder as the Lewis acid to foster C–Cl bond cleavage and to access the desired products with high yields. The reaction encompassed a broad range of functional groups, including acetate, halides, and heteroaromatic species.

More recently, the same group reported the synthesis of 2-trifluoromethylselenylated benzofused heterocycles (Scheme 7) [24]. This tandem process consisted in a first Pd-catalyzed cyclization of 2-(2,2-dibromovinyl)phenols/-thio-

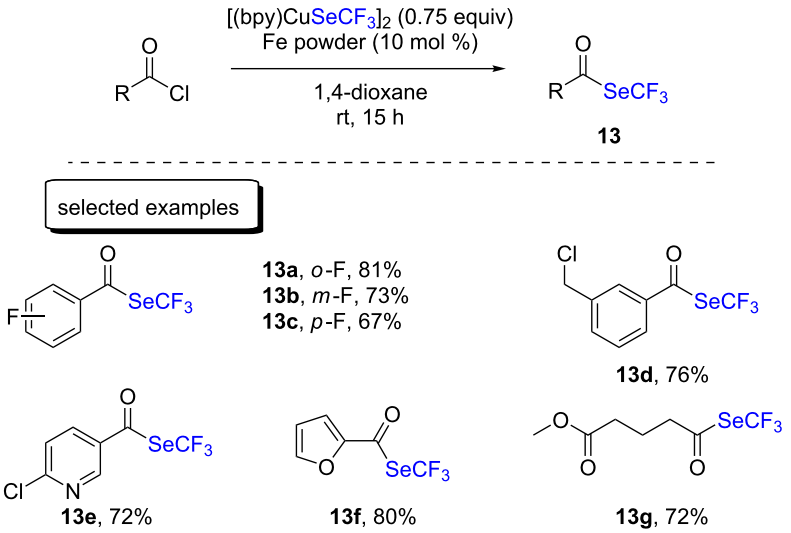

Scheme 6: Trifluoromethylselenolation of acid chlorides with $[(bpy)CuSeCF_3]_2$ by the group of Weng.

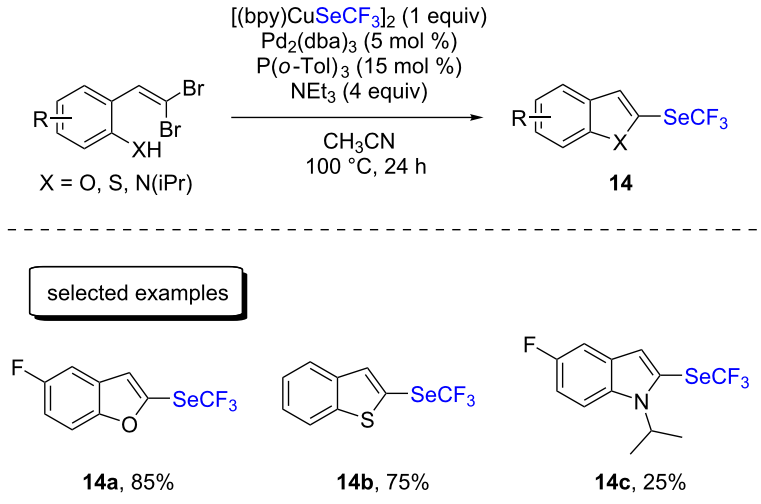

Scheme 7: Synthesis of 2-trifluoromethylselenylated benzofused heterocycles with $[(bpy)CuSeCF_3]_2$ by the group of Weng.

phenols/-anilines, leading to the corresponding 2-brominated heterocycle. This intermediate was then trifluoromethylselenylated by $[(bpy)CuSeCF_3]_2$. While benzofurans and benzothiophenes were prepared in moderate to good yields, only marginal yields were obtained with indole derivatives (up to 25%). Finally, the reactions could easily be scaled up to a gram scale.

The group of Liang reported the difunctionalization of terminal styrenes and arylacetylene derivatives by introducing $SeCF_3$ with the $[(bpy)CuSeCF_3]_2$ copper complex developed by the group of Weng and difluoroalkyl groups with ICF_2CO_2Et (Scheme 8) [25]. Only six examples were reported, with good yields. Mechanistically, the authors proposed that an electron transfer took place between the copper(I) complex and ICF_2CO_2Et, forming, after iodine transfer, a new carbon-centered radical and a copper(II) complex. The center of the radical then shifted to the terminal carbon atom of the unsaturated compound. The latter reacted with the copper(II) complex, forming a new copper(III) intermediate. After reductive elimination, the desired difunctionalized compounds were formed.

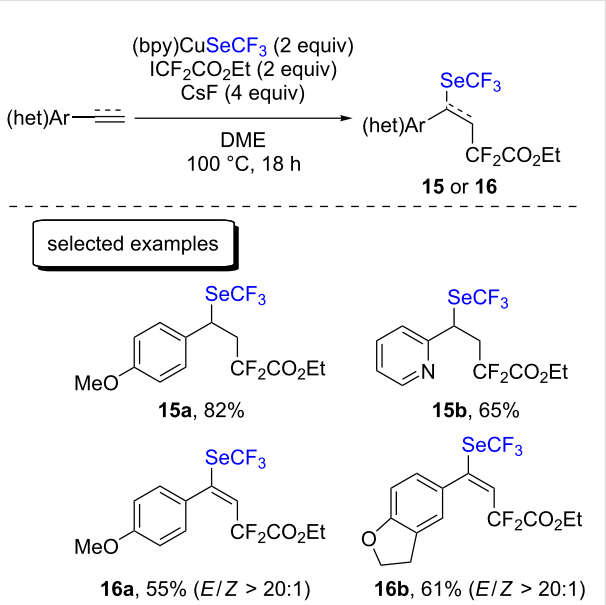

Scheme 8: Difunctionalization of terminal alkenes and alkynes with $[(bpy)CuSeCF_3]_2$ by the group of Liang.

Tetramethylammonium trifluoromethylselenolate salt (Me_4NSeCF_3)

Tetramethylammonium trifluoromethylselenolate was reported by the group of Tyrra in 2003. Therein, the association of the Ruppert–Prakash reagent with ammonium fluoride in the presence of a slight excess of Se allowed the facile synthesis of Me_4NSeCF_3 (Scheme 9) [26]. Today, Me_4NSeCF_3 is routinely used by several research groups. In the past five years, this stable and easy-to-handle reagent was involved in several cross-coupling processes, including copper chemistry.

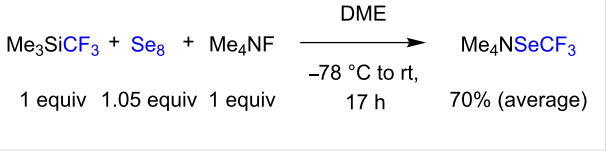

Scheme 9: Synthesis of Me_4NSeCF_3.

In this context, in 2015, the group of Rueping reported an oxidative trifluoromethylselenolation process of terminal alkynes and boronic acid derivatives (Scheme 10) [27]. Using a stoichiometric amount of copper/ligand and molecular oxygen as the oxidant, the substrates were successfully converted to the trifluoromethylselenylated analogs in good to very good yields. The substrate scope highlighted a broad functional group tolerance, including electron-withdrawing and -donating groups, heterocycles, and ferrocene moieties.

One year later, the group of Goossen demonstrated the direct conversion of diazo compounds into trifluoromethylselenolated products using a catalytic amount of copper(I) thiocyanate (Scheme 11) [28,29]. The reaction proceeded under mild conditions, and the desired products were usually obtained with very good to excellent yields. The authors postulated the in situ formation of $CuSeCF_3$ as the catalytically activated species that was able to reduce the diazonium salt and transfer $SeCF_3$.

Trifluoromethylselenyl chloride ($ClSeCF_3$) and trifluoromethyltolueneselenosulfonate ($TsSeCF_3$)

Known since the 1950s, trifluoromethylselenyl chloride ($ClSeCF_3$) was scarcely studied until recently. In fact, this reagent is very volatile [30,31] and potentially toxic by analogy with $ClSCF_3$ [32]. However, to avoid the direct synthesis of $ClSeCF_3$, the group of Billard proposed a one-pot two-step procedure where $ClSeCF_3$ is generated in situ [33].

This strategy was then applied to the trifluoromethylselenolation of alkynes by using copper(I) acetylides [34]. With bipyridine as the ligand, the trifluoromethylselenolation of alkynes was reported to occur with moderate to very good yields. The conditions were compatible with aromatic as well as aliphatic substrates and tolerated sensitive functional groups, such as hydroxy functions or esters (Scheme 12).

Boronic acids were also engaged in combination with $ClSeCF_3$ in the presence of stoichiometric amounts of copper(II) acetate, resulting in marginal to moderate yields, as can be seen in Scheme 12 [35].

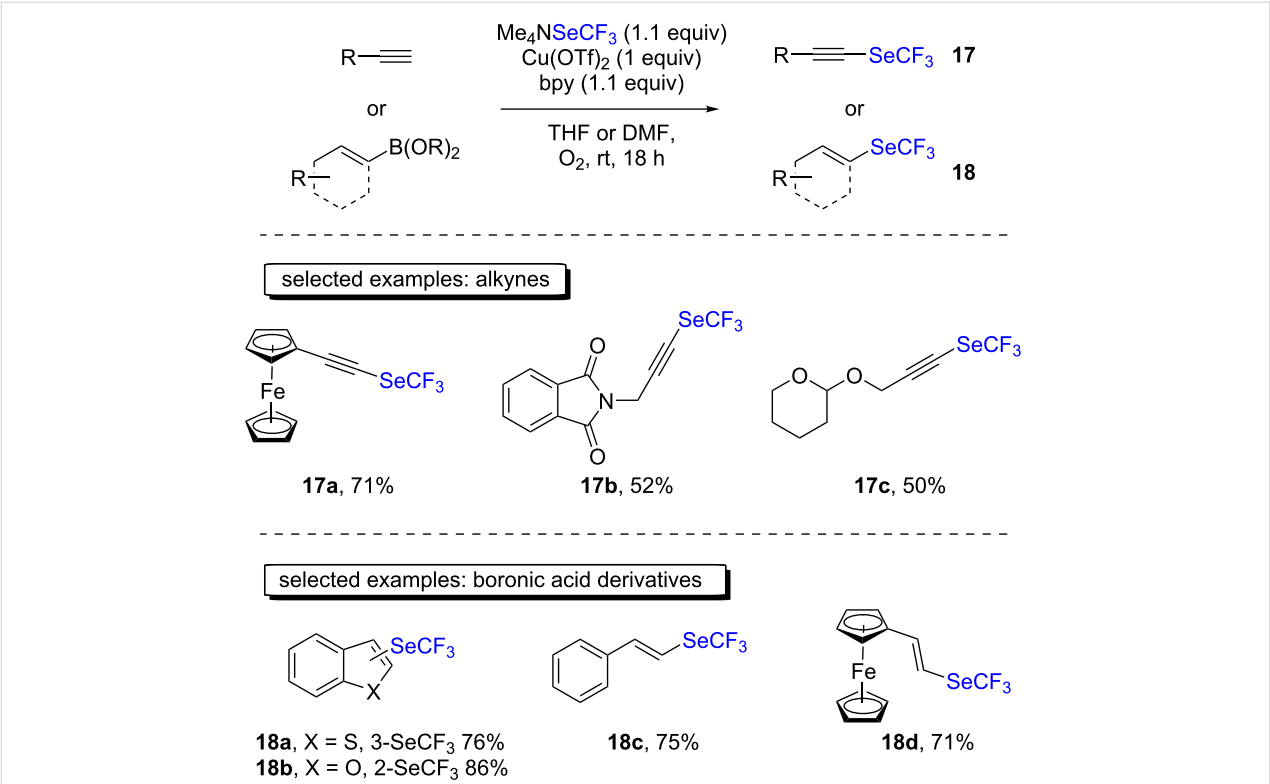

Scheme 10: Oxidative trifluoromethylselenolation of terminal alkynes and boronic acid derivatives with Me_4NSeCF_3 by the group of Rueping.

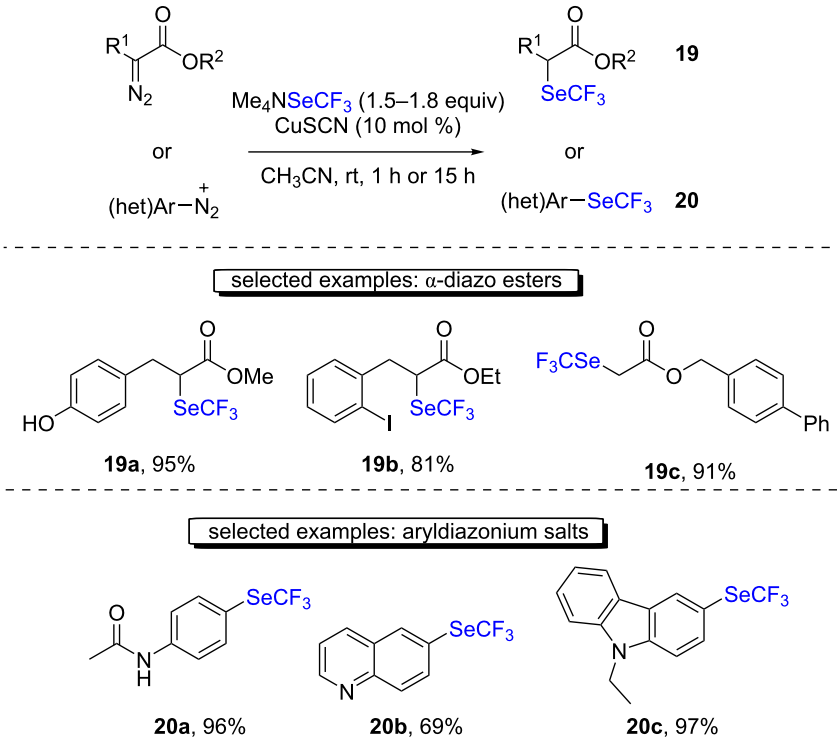

Scheme 11: Trifluoromethylselenolation of diazoacetates and diazonium salts with Me_4NSeCF_3 by the group of Goossen.

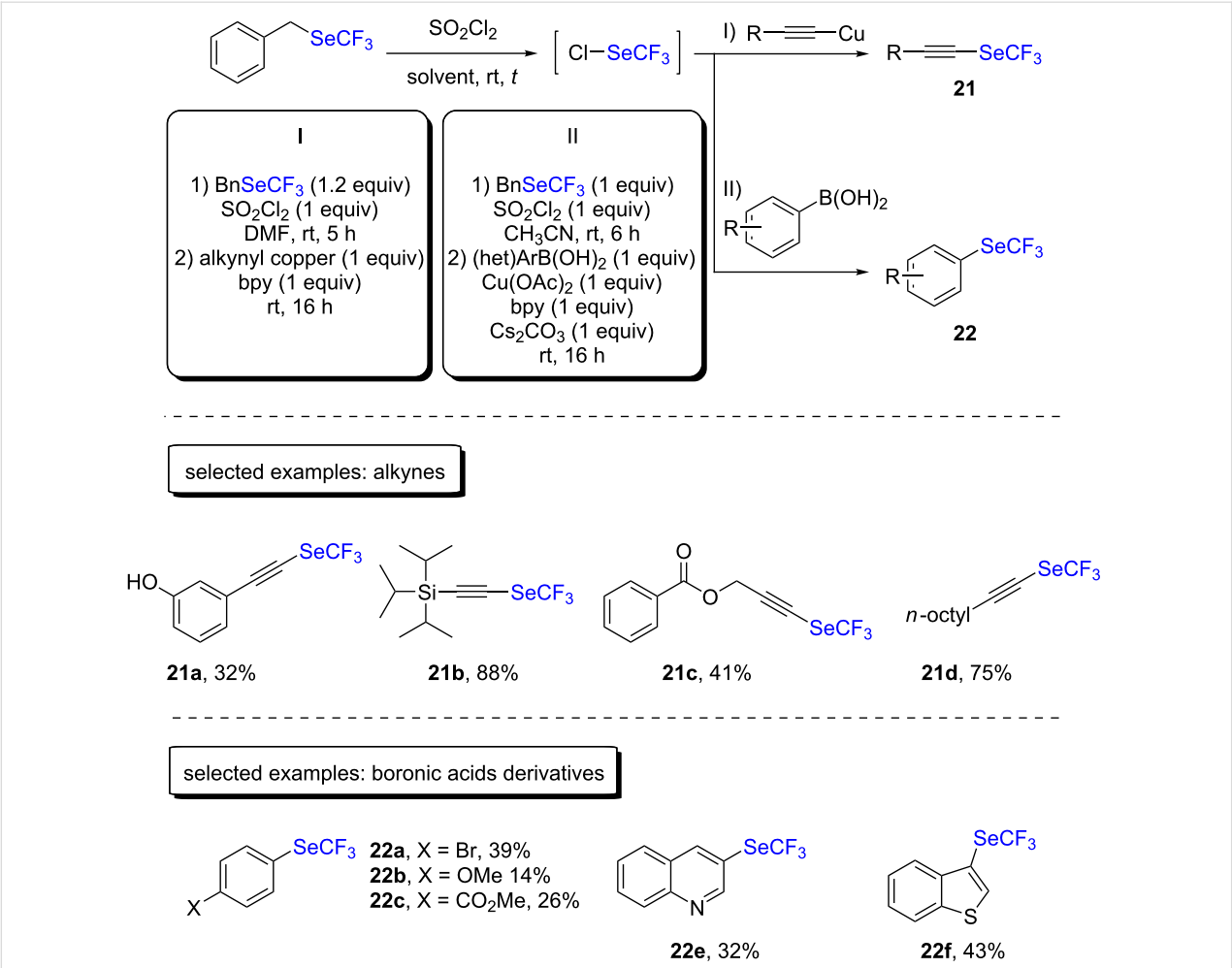

Scheme 12: Trifluoromethylselenolation with $ClSeCF_3$ by the group of Tlili and Billard.

Due to the limitations of $ClSeCF_3$ as an electrophilic reagent for trifluoromethylselenolations in cross-coupling reactions, our group developed a new bench-stable reagent, namely trifluoromethyltolueneselenosulfonate ($TsSeCF_3$) [36]. Trifluoromethyltolueneselenosulfonate can be prepared from in situ-generated $ClSeCF_3$ and sodium sulfinate on a gram scale. This new reagent is ready-to-use and can easily be handled. With this new reagent in hand, our group firstly studied the reactivity with boronic acids (Scheme 13). Therein, a catalytic amount of copper(II) acetate and bipyridine (10 mol % each) was used. Moderate to very good yields were obtained for both electron-deficient and electron-rich substrates. The scope also encompassed heteroaromatic as well as vinylic compounds. Mechanistic experiments allowed us to propose a plausible mechanism in which an arylcopper(I) species was the key intermediate.

Terminal alkynes were also investigated under similar reaction conditions (Scheme 13) [37]. Aromatic and π-activated aliphatic substrates led to the desired products in moderate to very good yields. Moreover, vinyl sulfone derivatives were formed when the starting alkyne derivatives contained an oxygen atom. This way, α-trifluoromethylselenylated vinylsulfones were obtained in moderate to excellent yields (Scheme 13). Mechanistic experiments revealed that copper(I) acetylides were the active species for the synthesis of the trifluoromethylselenylated alkynes. The latter was also a key intermediate for the formation of α-trifluoromethylselenylated vinylsulfone.

It is worth noting that the strategy for the trifluoromethylselenolation of boronic acid developed in our laboratory was applied in 2019 for the synthesis of the selenylated analog **30** of Pretomanid, an antituberculosis drug (Scheme 14) [38]. The key step was the trifluoromethylselenolation of boronic acid **26** under standard conditions (Scheme 13), followed by a mesylation and a reaction with the commercially available alcohol **29** to yield the desired compound **30**. Preliminary results indicated that the physicochemical properties remained widely unchanged. However, further studies must be undertaken in order

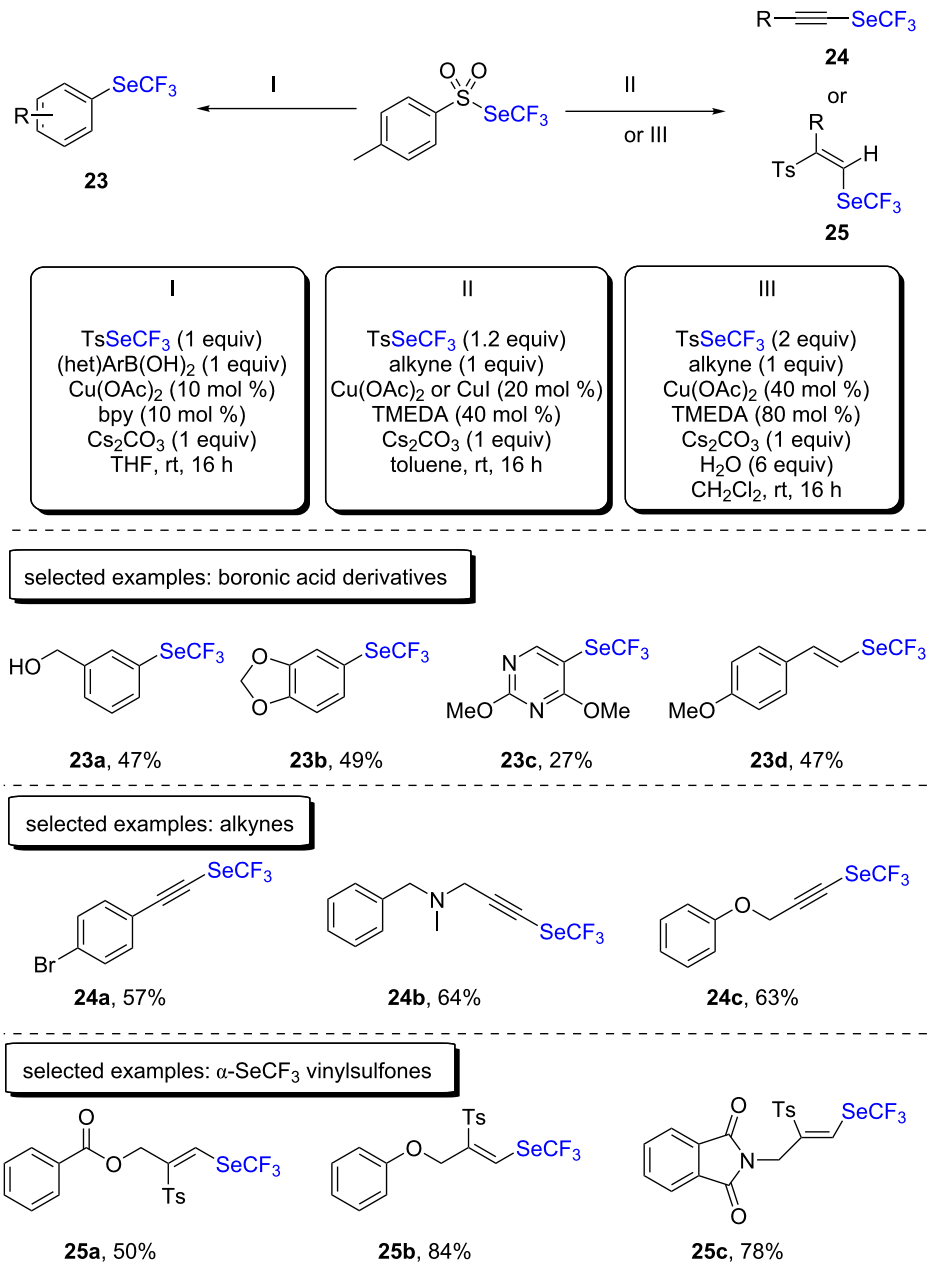

Scheme 13: Trifluoromethylselenolation with $TsSeCF_3$ by the group of Tlili and Billard.

to gain knowledge on the bioactivity of this $SeCF_3$-containing analog.

In situ synthesis of trifluoromethylselenolated compounds using copper complexes

One-pot procedures that rely on the tandem formation of C–Se and Se–fluoroalkyl bonds have emerged in the last five years.

In 2014, Hor and Weng reported the trifluoromethylselenolation of (hetero)aryl iodides and alkyl bromides with the Ruppert–Prakash reagent, $TMSCF_3$, elemental selenium, potassium fluoride, and silver carbonate under copper catalysis (Scheme 15, conditions I) [39]. Mechanistically, the authors proposed the formation of a silver(I)–$SeCF_3$ adduct, followed by a transmetallation step, yielding the active $CuSeCF_3$ species. Good to very good yields were obtained on a broad scope, including amide-, ester-, and heterocycle-containing substrates.

In 2019, Deng and Xiao proposed an alternative strategy based on the use of a three-component system consisting of

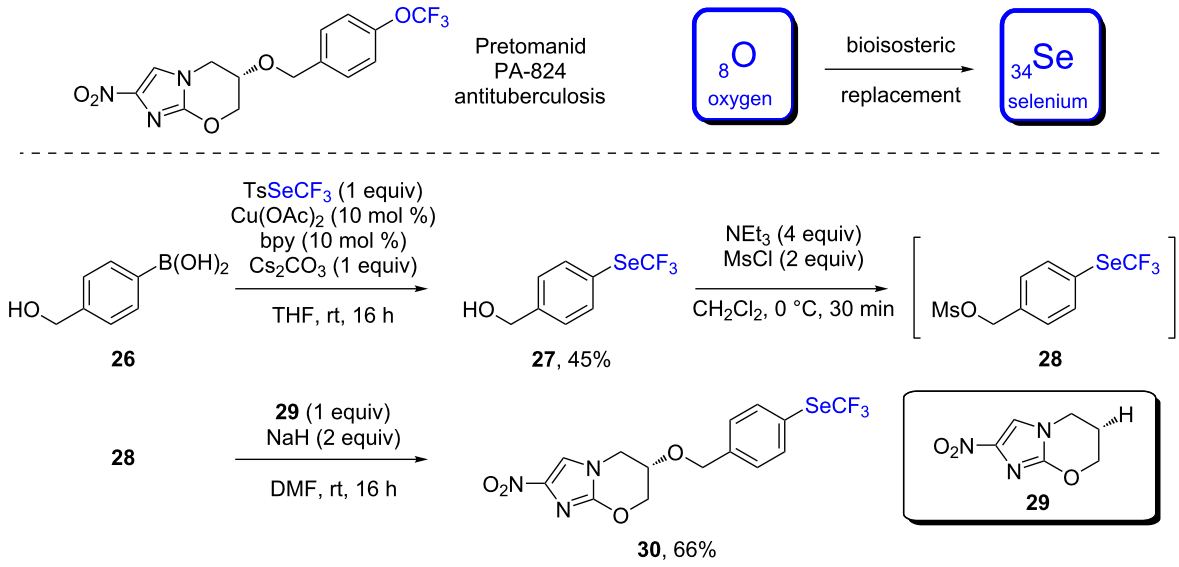

Scheme 14: Copper-catalyzed synthesis of a selenylated analog **30** of Pretomanid developed by the group of Tlili and researchers from Novartis.

$Ph_3P^+CF_2CO_2^-/Se_8/CsF$ (Scheme 15, conditions II) [40]. It should be noted that three equivalents of both the copper source and the ligand were needed in order to obtain high yields. Benzylic bromides and chlorides furnished the desired products in moderate to good yields. However, less activated substrates led to marginal amounts of the trifluoromethylselenylated compounds. Also, when secondary benzylic halides were used in the reaction, low yields were observed, which is in line with an S_N2 mechanism. The authors proposed a mechanism where difluorocarbene is first generated upon thermal decomposition of the starting difluorophosphobetaine. The carbene then reacts with elemental selenium to yield difluoroselenophosgene, and in the presence of fluoride anions, this species is in an equilibrium with the $^-SeCF_3$ anion. As proposed by Hor and Weng, Deng and Xiao also suggested that $CuSeCF_3$ was the active species in the mechanism.

In 2016, the group of Rueping described a sequential copper-catalyzed selenocyanation of aryldiazonium salts, followed by trifluoromethylation in a one-pot procedure with the Ruppert–Prakash reagent (Scheme 15, conditions III) [41]. The corresponding trifluoromethylselenylated (hetero)aryl products were obtained in moderate to good yields using both electron-deficient and -rich starting materials, respectively. Interestingly, the authors demonstrated the feasibility of the reaction by starting directly with *p*-nitroaniline. Moreover, the authors demonstrated that the reaction could easily be scaled up to a 7 mmol scale, and the desired product was obtained in a comparable yield of 70%, and 73% starting from the corresponding aryldiazonium salt.

Conclusion

In conclusion, as highlighted in this minireview, several elegant procedures based on the use of copper reagents allow to directly access trifluoromethylselenolated compounds. Today, the straightforward construction of C–$SeCF_3$ bonds is accessible through several different pathways. On the one hand, the use discrete copper–$SeCF_3$ complexes allows the trifluoromethylselenolation of a large panel of starting materials. Therein, the main drawback is the generation of a stoichiometric amount of a copper salt as a byproduct of the reaction. On the other hand, Me_4NSeCF_3 is a very attractive reagent that already demonstrated its versatility in numerous processes. Nevertheless, its use in oxidative cross-coupling reactions requires stoichiometric amounts of the oxidant, which limits the attractiveness of the method in some cases. Finally, the newly developed electrophilic reagent $TsSeCF_3$ also demonstrated its compatibility in copper-based process and allowed the use of catalytic amounts of copper. The compound is synthesized starting with volatile $ClSeCF_3$, which is the major drawback. Altogether, the presented methodologies cover a wide range of starting materials. Interestingly, the application of these methodologies was already demonstrated for the synthesis of bioactive analogs. To the best of our knowledge, to date there are no $SeCF_3$-containing drug candidates or bioactive molecules in clinical trials. This could be explained by the lack of physicochemical data on the $SeCF_3$ moiety. More efforts must be devoted to exploring the altered properties of the trifluoromethylselenylated compounds. The encouraging results obtained will definitely pave the way for further applications, and put this emerging fluorinated group at the forefront of drug design.

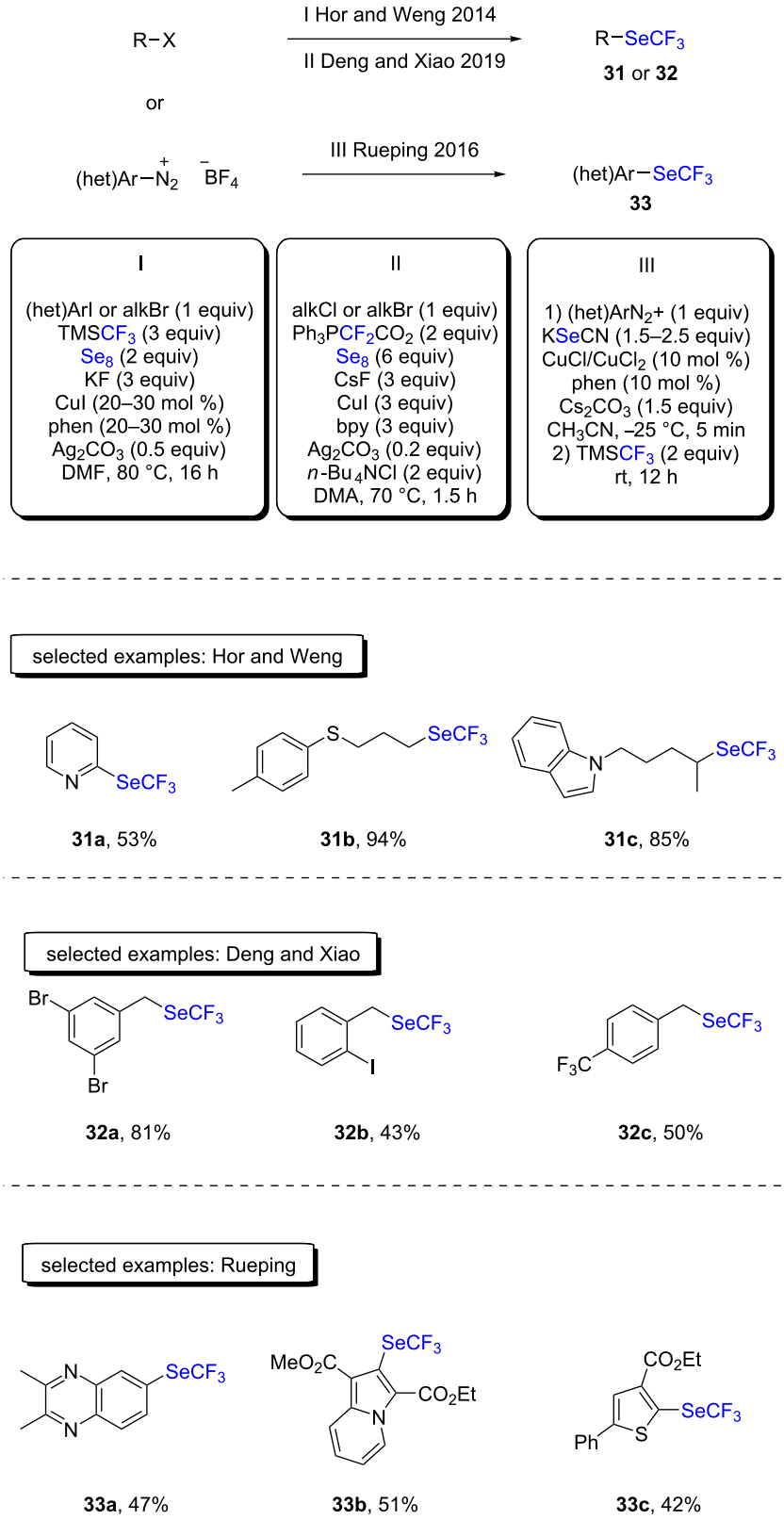

Scheme 15: One-pot procedures for C–$SeCF_3$ bond formations developed by Hor and Weng, Deng and Xiao, and Rueping.

Funding

C.G. held a doctoral fellowship from la region Rhône-Alpes. The authors are grateful to the CNRS, ICBMS (UMR 5246), ICL (Institut de Chimie de Lyon) for financial support.

ORCID® iDs

Anis Tlili - https://orcid.org/0000-0002-3058-2043

References

1. Hansch, C.; Leo, A.; Taft, R. W. *Chem. Rev.* **1991,** *91,* 165–195. doi:10.1021/cr00002a004
2. Kirsch, P. *Modern Fluoroorganic Chemistry;* Wiley-VCH: Weinheim, Germany, 2013. doi:10.1002/9783527651351
3. Leroux, F. R.; Manteau, B.; Vors, J.-P.; Pazenok, S. *Beilstein J. Org. Chem.* **2008,** *4,* No. 13. doi:10.3762/bjoc.4.13
4. Besset, T.; Jubault, P.; Pannecoucke, X.; Poisson, T. *Org. Chem. Front.* **2016,** *3,* 1004–1010. doi:10.1039/c6qo00164e
5. Tlili, A.; Toulgoat, F.; Billard, T. *Angew. Chem., Int. Ed.* **2016,** *55,* 11726–11735. doi:10.1002/anie.201603697
6. Xu, X.-H.; Matsuzaki, K.; Shibata, N. *Chem. Rev.* **2015,** *115,* 731–764. doi:10.1021/cr500193b
7. Barata-Vallejo, S.; Bonesi, S.; Postigo, A. *Org. Biomol. Chem.* **2016,** *14,* 7150–7182. doi:10.1039/c6ob00763e
8. Toulgoat, F.; Billard, T. Toward CF_3S Group: From Trifluoromethylation of Sulfides to Direct Trifluoromethylthiolation. In *Modern Synthesis Processes and Reactivity of Fluorinated Compounds;* Groult, H.; Leroux, F. R.; Tressaud, A., Eds.; Progress in Fluorine Science; Elsevier: Amsterdam, Netherlands, 2017; pp 141–179. doi:10.1016/b978-0-12-803740-9.00006-8
9. Evano, G.; Blanchard, N., Eds. *Copper-Mediated Cross-Coupling Reactions;* John Wiley & Sons, Inc.: Hoboken, NJ, 2013.
10. Tlili, A.; Ismalaj, E.; Glenadel, Q.; Ghiazza, C.; Billard, T. *Chem. – Eur. J.* **2018,** *24,* 3659–3670. doi:10.1002/chem.201704637
11. Ghiazza, C.; Billard, T.; Tlili, A. *Chem. – Eur. J.* **2019,** *25,* 6482–6495. doi:10.1002/chem.201806234
12. Kondratenko, N. V.; Kolomeytsev, A. A.; Popov, V. I.; Yagupolskii, L. M. *Synthesis* **1985,** 667–669. doi:10.1055/s-1985-31301
13. Chen, C.; Ouyang, L.; Lin, Q.; Liu, Y.; Hou, C.; Yuan, Y.; Weng, Z. *Chem. – Eur. J.* **2014,** *20,* 657–661. doi:10.1002/chem.201303934
14. Rong, M.; Huang, R.; You, Y.; Weng, Z. *Tetrahedron* **2014,** *70,* 8872–8878. doi:10.1016/j.tet.2014.09.091
15. Wu, C.; Huang, Y.; Chen, Z.; Weng, Z. *Tetrahedron Lett.* **2015,** *56,* 3838–3841. doi:10.1016/j.tetlet.2015.04.088
16. Tian, Q.; Weng, Z. *Chin. J. Chem.* **2016,** *34,* 505–510. doi:10.1002/cjoc.201600052
17. Zhang, Y.; Yang, D.-Y.; Weng, Z. *Tetrahedron* **2017,** *73,* 3853–3859. doi:10.1016/j.tet.2017.05.051
18. Wang, Y.; You, Y.; Weng, Z. *Org. Chem. Front.* **2015,** *2,* 574–577. doi:10.1039/c5qo00045a
19. Yang, Y.; Lin, X.; Zheng, Z.; Lin, G.; Zhang, Y.; You, Y.; Weng, Z. *J. Fluorine Chem.* **2017,** *204,* 1–5. doi:10.1016/j.jfluchem.2017.10.001
20. Chen, T.; You, Y.; Weng, Z. *J. Fluorine Chem.* **2018,** *216,* 43–46. doi:10.1016/j.jfluchem.2018.10.002
21. Zhu, P.; He, X.; Chen, X.; You, Y.; Yuan, Y.; Weng, Z. *Tetrahedron* **2014,** *70,* 672–677. doi:10.1016/j.tet.2013.11.093
22. Hou, C.; Lin, X.; Huang, Y.; Chen, Z.; Weng, Z. *Synthesis* **2015,** *47,* 969–975. doi:10.1055/s-0034-1379972
23. Wang, J.; Zhang, M.; Weng, Z. *J. Fluorine Chem.* **2017,** *193,* 24–32. doi:10.1016/j.jfluchem.2016.11.006
24. Zhang, M.; Weng, Z. *Org. Lett.* **2019,** *21,* 5838–5842. doi:10.1021/acs.orglett.9b01922
25. Zhang, B.-S.; Gao, L.-Y.; Zhang, Z.; Wen, Y.-H.; Liang, Y.-M. *Chem. Commun.* **2018,** *54,* 1185–1188. doi:10.1039/c7cc09083h
26. Tyrra, W.; Naumann, D.; Yagupolskii, Y. L. *J. Fluorine Chem.* **2003,** *123,* 183–187. doi:10.1016/s0022-1139(03)00118-0
27. Lefebvre, Q.; Pluta, R.; Rueping, M. *Chem. Commun.* **2015,** *51,* 4394–4397. doi:10.1039/c4cc10212f
28. Matheis, C.; Krause, T.; Bragoni, V.; Goossen, L. J. *Chem. – Eur. J.* **2016,** *22,* 12270–12273. doi:10.1002/chem.201602730
29. Matheis, C.; Wagner, V.; Goossen, L. J. *Chem. – Eur. J.* **2016,** *22,* 79–82. doi:10.1002/chem.201503524
30. Magnier, E.; Wakselman, C. *Collect. Czech. Chem. Commun.* **2002,** *67,* 1262–1266. doi:10.1135/cccc20021262
31. Dale, J. W.; Emeléus, H. J.; Haszeldine, R. N. *J. Chem. Soc.* **1958,** 2939–2945. doi:10.1039/jr9580002939
32. Stump, E. C. *Chem. Eng. News* **1967,** *45,* 44.
33. Glenadel, Q.; Ismalaj, E.; Billard, T. *J. Org. Chem.* **2016,** *81,* 8268–8275. doi:10.1021/acs.joc.6b01344
34. Ghiazza, C.; Billard, T.; Tlili, A. *Chem. – Eur. J.* **2017,** *23,* 10013–10016. doi:10.1002/chem.201702028
35. Ghiazza, C.; Tlili, A.; Billard, T. *Molecules* **2017,** *22,* 833. doi:10.3390/molecules22050833
36. Glenadel, Q.; Ghiazza, C.; Tlili, A.; Billard, T. *Adv. Synth. Catal.* **2017,** *359,* 3414–3420. doi:10.1002/adsc.201700904
37. Ghiazza, C.; Debrauwer, V.; Billard, T.; Tlili, A. *Chem. – Eur. J.* **2018,** *24,* 97–100. doi:10.1002/chem.201705231
38. Ghiazza, C.; Billard, T.; Dickson, C.; Tlili, A.; Gampe, C. M. *ChemMedChem* **2019,** *14,* 1586–1589. doi:10.1002/cmdc.201900452
39. Chen, C.; Hou, C.; Wang, Y.; Hor, T. S. A.; Weng, Z. *Org. Lett.* **2014,** *16,* 524–527. doi:10.1021/ol403406y
40. Chen, X.-L.; Zhou, S.-H.; Lin, J.-H.; Deng, Q.-H.; Xiao, J.-C. *Chem. Commun.* **2019,** *55,* 1410–1413. doi:10.1039/c8cc09719d
41. Nikolaienko, P.; Rueping, M. *Chem. – Eur. J.* **2016,** *22,* 2620–2623. doi:10.1002/chem.201504601

License and Terms

BEILSTEIN JOURNAL OF ORGANIC CHEMISTRY

Recent advances in photocatalyzed reactions using well-defined copper(I) complexes

Mingbing Zhong[1], Xavier Pannecoucke[1], Philippe Jubault[1] and Thomas Poisson[*1,2]

Review

Open Access

Address:
[1]Normandie Université, INSA Rouen, UNIROUEN, CNRS, COBRA (UMR 6014), 76000 Rouen, France and [2]Institut Universitaire de France, 1 rue Descartes, 75231 Paris, France

Email:
Thomas Poisson[*] - thomas.poisson@insa-rouen.fr

* Corresponding author

Keywords:
ATRA reactions; copper catalysis; energy transfer; oxidation; PCET reactions; photocatalysis; reduction

Beilstein J. Org. Chem. **2020,** *16,* 451–481.
doi:10.3762/bjoc.16.42

Received: 17 December 2019
Accepted: 12 March 2020
Published: 23 March 2020

This article is part of the thematic issue "Copper-catalyzed reactions for organic synthesis".

Guest Editor: G. Evano

Abstract

This review summarizes the recent advances in photocatalysis using copper complexes. Their applications in various reactions, such as ATRA, reduction, oxidation, proton-coupled electron transfer, and energy transfer reactions are discussed.

Introduction

For a decade, the realm of catalysis has known a significant renewal with the rise of photocatalysis [1]. The fact that a reaction can be carried out, and, more specifically, catalyzed in the presence of visible light and a photosensitive catalyst (organic or organometallic) provided a drastic change of paradigm to the community. Indeed, photocatalysis allows carrying out photochemical reactions in the visible region (redox transformation and energy transfer process). This tremendous progress provided a huge gain of selectivity in photochemical transformations. Indeed, as most organic molecules absorb light in the UV region (UV-A, UV-B, or UV-C), selectivity was a key point to address in photochemistry and photocatalysis using visible light tackled this issue. Moreover, the use of inexpensive and energy-efficient visible light-emitting diodes (LEDs) was an impressive development. Furthermore, photocatalysis allowed to realize elusive transformations as this approach provided better control over the formation of radicals or the reduction or oxidation of reagents, for instance. For all these reasons, photocatalysis is nowadays at the forefront of cutting-edge research in organic chemistry.

Despite the impressive advances reported since the renewal of the field in 2008 [2-4], several issues still have to be addressed. Indeed, most of the developed reactions relied on the use of organometallic complexes of expensive noble metals, such as iridium and ruthenium [5]. Even though their efficiency is outstanding, their use for industrial purposes might be hampered. Indeed, the limited availability of these metals and their prices often prohibit the development of economically efficient chemical processes [6]. In addition, the depletion of natural resources raises questions about the future availability of these metals at a reasonable cost. With regards to organic dyes, impressive de-

velopments have been achieved, but these catalysts might suffer from a low photochemical stability, and thus hampering their use and recyclability [7]. Therefore, alternative solutions have to be developed. Among them, the use of first-row transition metals [8,9], particularly copper, is an interesting approach [10-13]. The high abundance, low price, low toxicity, and intrinsic properties (redox potential, four oxidation states, etc.) of copper are excellent and promising features to be used in the development of new photocatalysts. However, the study, development, and use of these complexes have been underexplored since the pioneering work of McMillin [14] and Sauvage [15], compared to the tremendous expansion of photocatalyzed reactions using Ru and Ir complexes. Indeed, copper-based photocatalysts are often considered less efficient due to a lower luminescence lifetime compared to Ir and Ru complexes [6].

Review

In this review, we summarized the recent significant advances that were made in the use of copper-based photocatalysts for synthetically useful transformations. The use of either homoleptic or heteroleptic complexes in atom transfer radical addition (ATRA) reactions, reductions, oxidations, proton-coupled electron transfer (PCET) reactions, and reactions based on energy transfer will be discussed.

1 Homoleptic Cu(I) complexes

Homoleptic complexes based on bisnitrogen ligands, and particularly phenanthroline derivatives, were used in the pioneering reports from McMillin [14] and Sauvage [15]. For decades, their use in organic synthesis, and particularly catalysis, has been ignored. However, since 2012, a renewed interest toward their use in catalysis has been witnessed.

1.1 ATRA reactions

Atom transfer radical addition reactions are linchpin transformations in organic synthesis as they allow an easy difunctionalization of alkenes. Usually, these reactions require the use of a radical initiator or thermal activation to initiate the radical chain. Recently, photocatalysis appeared as an interesting alternative to catalyze such transformations, and copper-based catalysts provided interesting reactivities.

In 2012, the Reiser group reported a visible light-driven coupling reaction of olefin derivatives with bromo- and iodoalkanes using the Sauvage catalyst as a Cu(I) photocatalyst (Scheme 1) [16]. The $[Cu(I)(dap)_2]Cl$ complex had a strong absorption under irradiation at 530 nm using a green LED. Different organic halides and alkenes were reacted, leading to the product by an ATRA reaction pathway with moderate to good

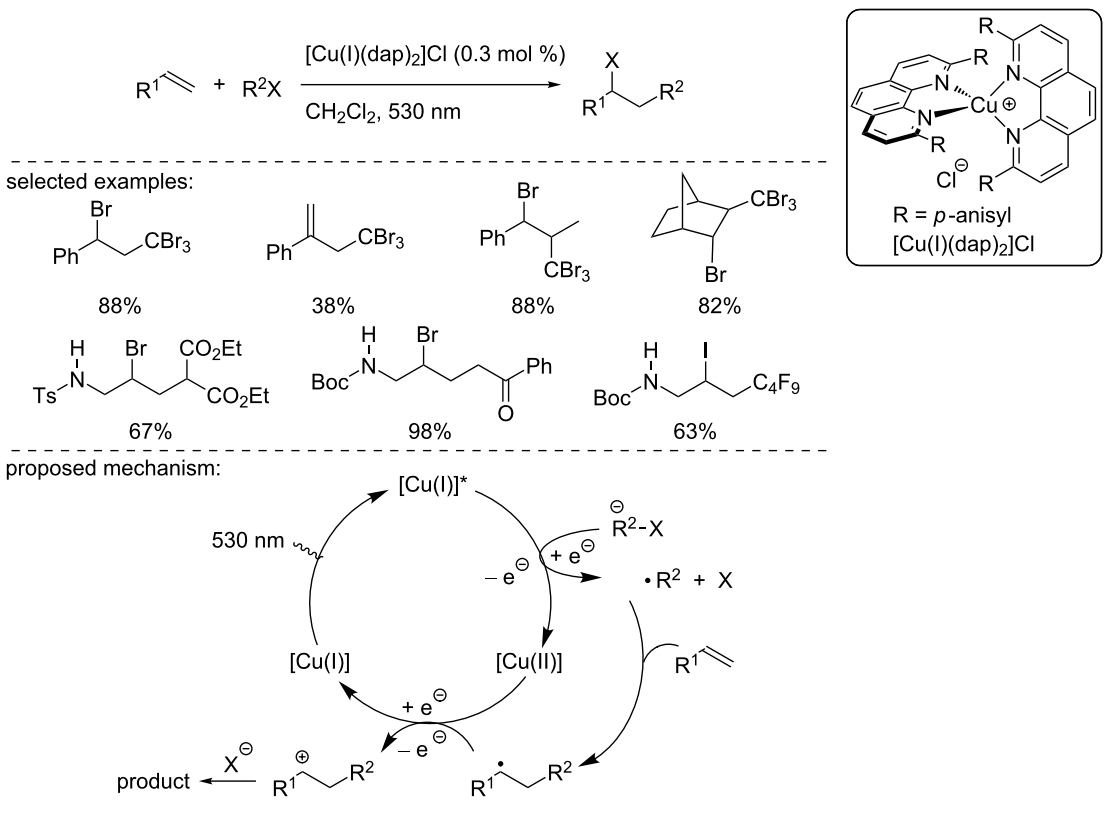

Scheme 1: $[Cu(I)(dap)_2]Cl$-catalyzed ATRA reaction under green light irradiation.

yield at room temperature (Scheme 1). The authors suggested a possible mechanism based on the measured and reported redox potential (Scheme 1).

Upon irradiation at 530 nm using green light, the Cu(I) catalyst transitions to an excited state. Then, the excited copper complex transfers an electron to the alkyl halide, which can generate an alkyl radical that subsequently adds to the alkene. The resulting C-centered radical is oxidized by the Cu(II) complex, regenerating the Cu(I) catalyst, and the formed carbocation is trapped by the halide. Worth to mention is that very recently, Reiser and Engl demonstrated the possible use of $[Cu(dmp)_2Cl]Cl$ as an efficient catalysts in a similar transformation [17].

In another study, Reiser and co-workers described a related allylation process of organic halides with allyltributyltin in the presence of $[Cu(I)(dap)_2]Cl$ as the catalyst [16]. This reaction was applied to a broad range of substrates, including a *para*-nitrophenyl ketones and furanyl ketones, for instance, with good yield. To explain the reaction outcome, the authors suggested that the $[Cu(I)(dap)_2]Cl$ catalyst acted as an electron shuttle between the halide derivative and the allylmetal reagent, precluding a direct electron transfer between the allylstannane and the haloketone. Hence, after being excited by light, the excited [Cu(I)]* complex gave an electron to the α-haloketone. Then, the ketone radical combined with allyltributyltin to generate a Bu_3Sn radical. A final electron transfer from the Bu_3Sn radical to [Cu(II)] regenerated the Cu(I) catalyst (Scheme 2).

Based on this work, in 2015, Reiser and co-workers reported another ATRA reaction to carry out the trifluoromethylchloro-

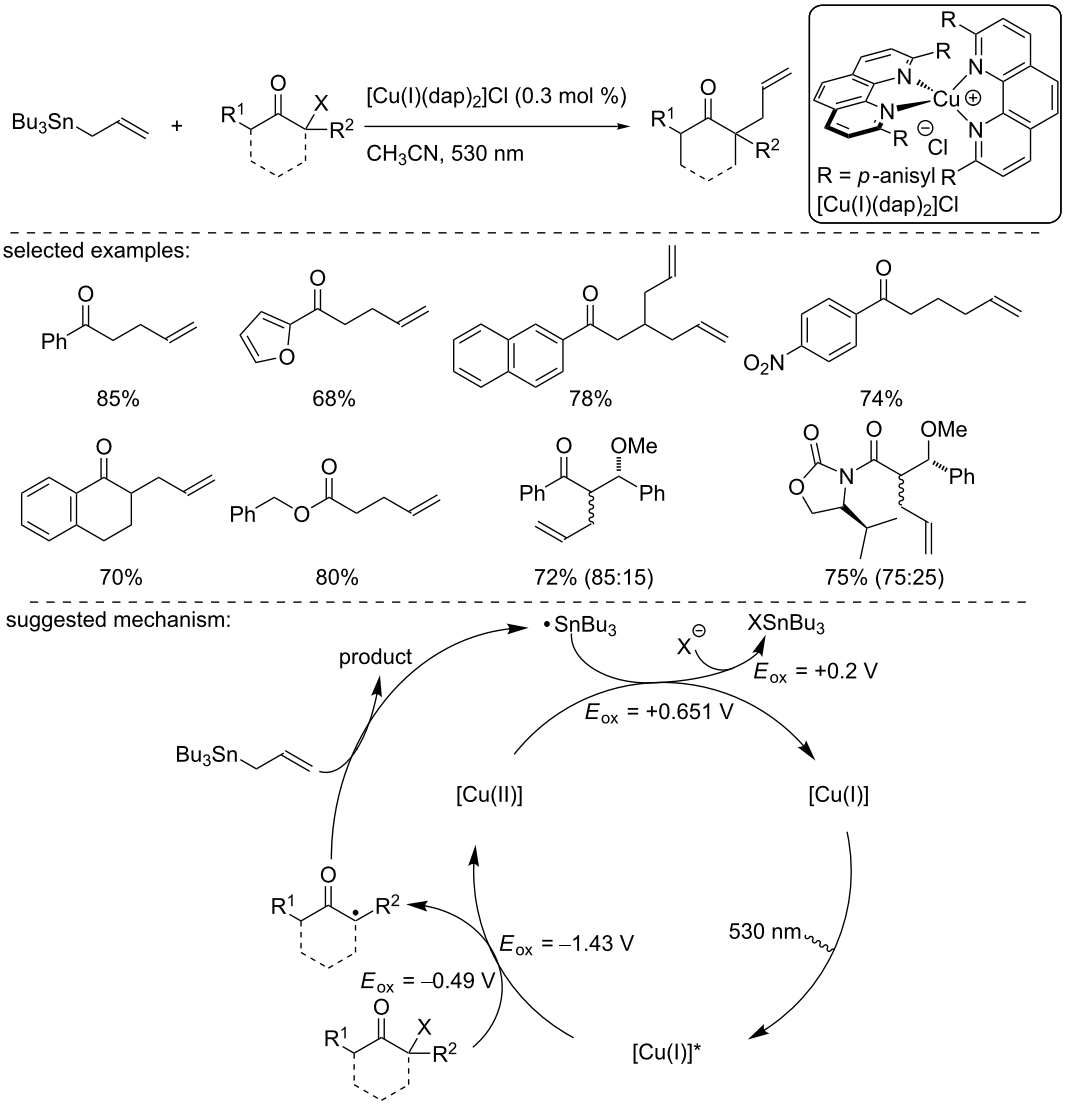

Scheme 2: Photocatalytic allylation of α-haloketones.

sulfonylation of alkenes (Scheme 3) [18]. They used the same catalyst as above, $[Cu(I)(dap)_2]Cl$, to introduce the CF_3 group to different alkenes under green LED irradiation (530 nm), with CF_3SO_2Cl as the CF_3 source. Depending on the substrates, both chlorosulfonylated and chlorotrifluoromethylated products could be obtained. For allylbenzene as well as terminal and cyclic alkenes, the trifluoromethylchlorosulfonylated adducts were isolated in good yield and selectivity. When an electron-donating group (e.g., NH, NHCO, and NMe_2) was in close proximity to the alkene, the pathway of the addition changed and the chlorotrifluoromethylated adduct was formed. To explain the reaction mechanism, the authors suggested the following pathway: Upon irradiation at 530 nm using green light, the Cu(I) catalyst transitions to the excited state. Then, the excited copper complex undergoes an electron transfer to CF_3SO_2Cl, allowing the formation of the CF_3 radical, and the resulting Cu(II) species binds to the SO_2Cl anion, known to be unstable when free. Then, the CF_3 radical adds to the alkene, followed by the addition of SO_2Cl to produce the desired product. However, when the reaction rate is slower, the SO_2Cl anion decomposes to neutral SO_2 and a chloride anion due to the weak nature of the Cu–SO_2Cl bond. The SO_2 extrusion explains the formation of the chlorotrifluoromethylated product (Scheme 3).

In 2019, Bissember and co-workers reported the synthesis of new homoleptic copper complexes by modifying the structure of the phenanthroline ligand at the 1- and 10-positions with various aromatic substituents [19]. These complexes were fully characterized and evaluated in a similar reaction. They observed that the variation of the electronic and steric parameters of the ligand could modulate the selectivity toward the chlorotrifluoromethylated and chlorosulfonylated products.

Earlier, in 2015, the group of Dolbier had reported a similar reaction with fluoroalkylsulfonyl chlorides [20]. This ATRA

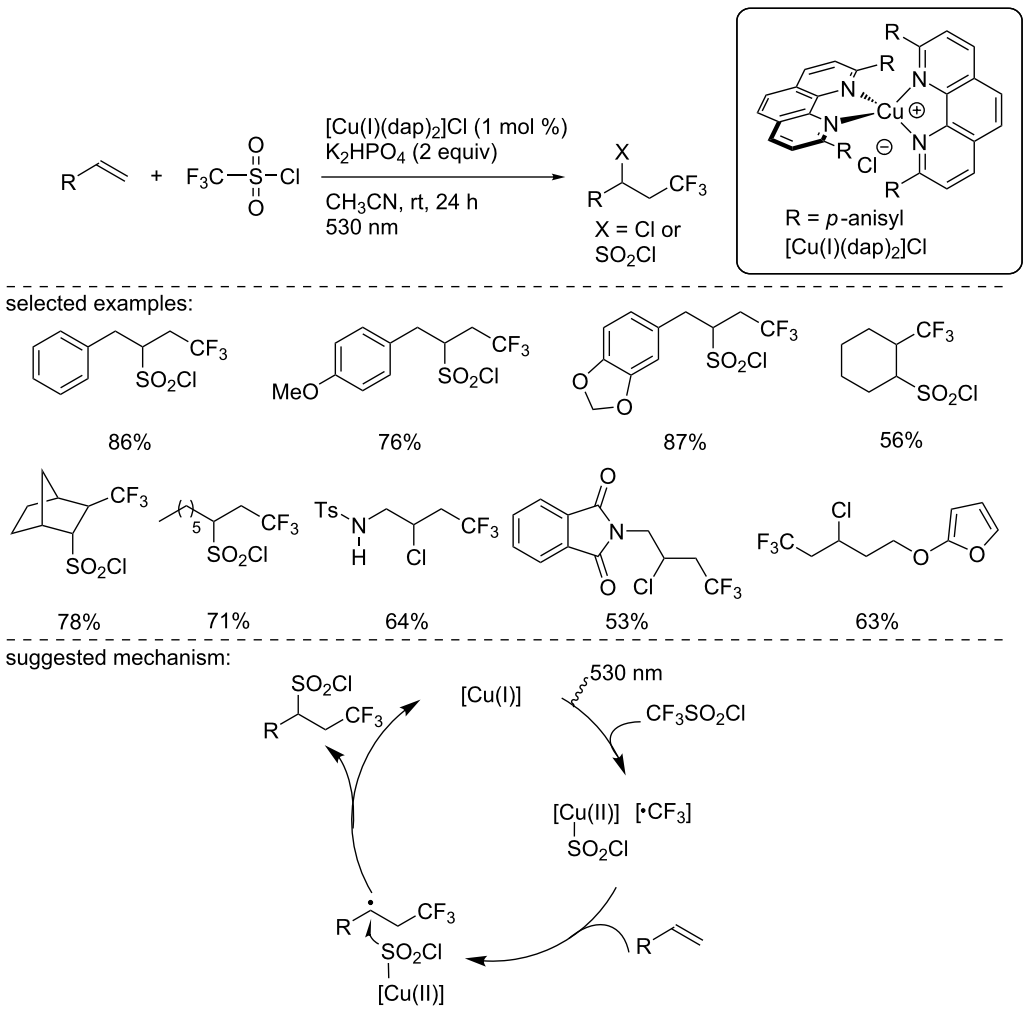

Scheme 3: $[Cu(I)(dap)_2]Cl$-photocatalyzed chlorosulfonylation and chlorotrifluoromethylation of alkenes.

reaction was carried out with various fluoroalkylsulfonyl chlorides, such as CFH_2SO_2Cl, CF_2HSO_2Cl, CF_3SO_2Cl, $CF_3CH_2SO_2Cl$, and $C_4F_9SO_2Cl$, electron-deficient alkenes, including α,β-unsaturated ketones, amides, esters, carboxylic acids, sulfones, and phosphonates (Scheme 4). In contrast to Reiser's protocol, solely chlorofluoroalkylated products were isolated in good yields, and no traces of the chlorosulfonylated alkenes were detected.

In 2016, Reiser's group used a similar protocol to synthesize trifluoromethylated sultones from alkenol and sulfonyl chlorides with the catalyst $[Cu(I)(dap)_2]Cl$ under green light irradiation (Scheme 5) [21]. Fluorinated sultones are important scaffolds for pharmaceutical syntheses. To illustrate the synthetic utility of the method, a novel benzoxathiin analog was synthesized using this reaction as the key step. The authors suggested a similar radical pathway as the one described previously (Scheme 3). This mechanism involved the formation of a CF_3 radical through a single-electron transfer between the excited complex $[Cu(I)(dap)_2]^{+}$* and triflyl chloride. This radical added to the alkene, and the SO_2Cl anion coordinated to the [Cu(II)] species. Upon electron back transfer to regenerate the [Cu(I)] catalyst, SO_2Cl was also incorporated into the product. Finally, an intramolecular cyclization process gave the desired product (Scheme 5).

Two years later, Reiser's group reported another ATRA reaction of perfluoroalkyl iodides with alkenes and alkynes. $[Cu(I)(dap)_2]Cl$ was found to be the best catalyst for this transformation proceeding upon irradiation at 530 nm (green LED, Scheme 6) [22]. Indeed, the comparison of this Cu catalyst with $[Ru(bpy)_3]Cl_2$ and $Ir(ppy)_3$ clearly demonstrated the higher efficiency, good yield, selectivity, and excellent functional group tolerance of the method. Further, the authors carried out an interesting mechanistic study: From their observations, they ruled out a possible radical chain process (path I) because the reaction with styrene cannot be initiated by heating or through a radical initiator. In addition, the authors precluded a possible photocatalytic process (path II). And indeed, even though from a comparison of the redox potential of $[Cu(I)(dap)_2]Cl$ and $[Ru(bpy)_3]Cl_2$, the latter should have been capable to promote the photocatalytic reaction, the ruthenium complex was unsuc-

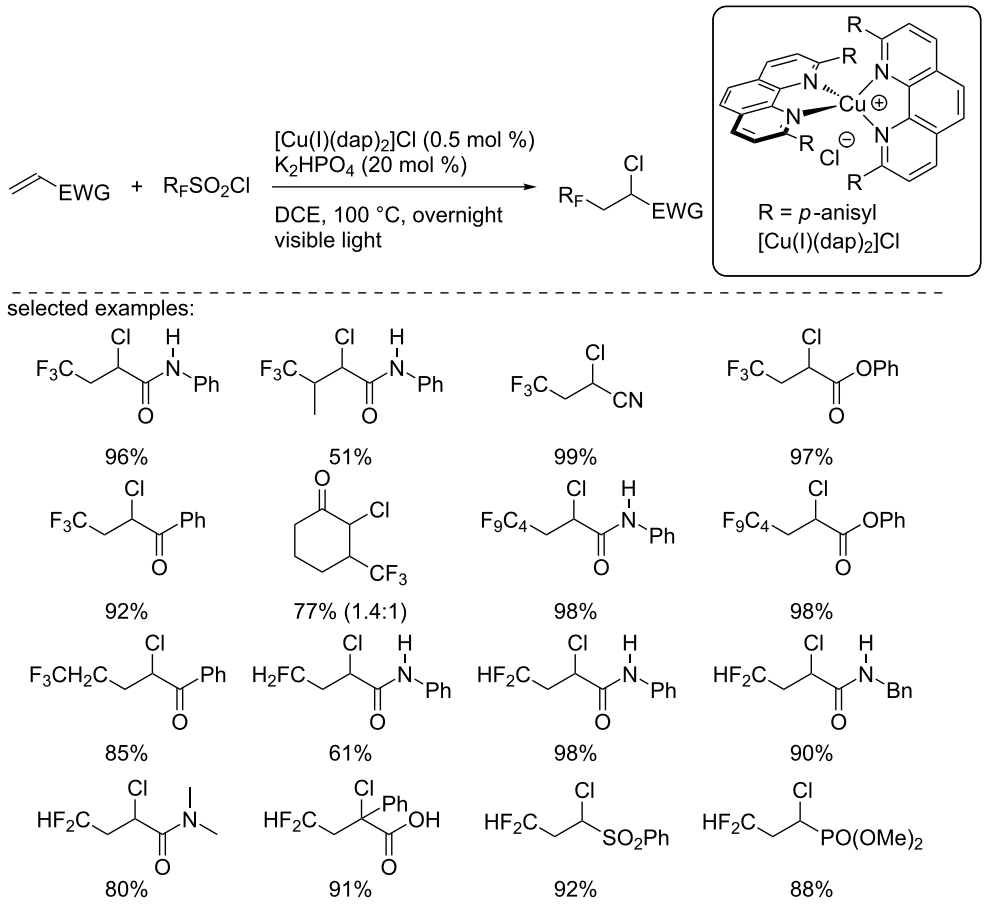

Scheme 4: Photocatalytic perfluoroalkylchlorination of electron-deficient alkenes using the Sauvage catalyst.

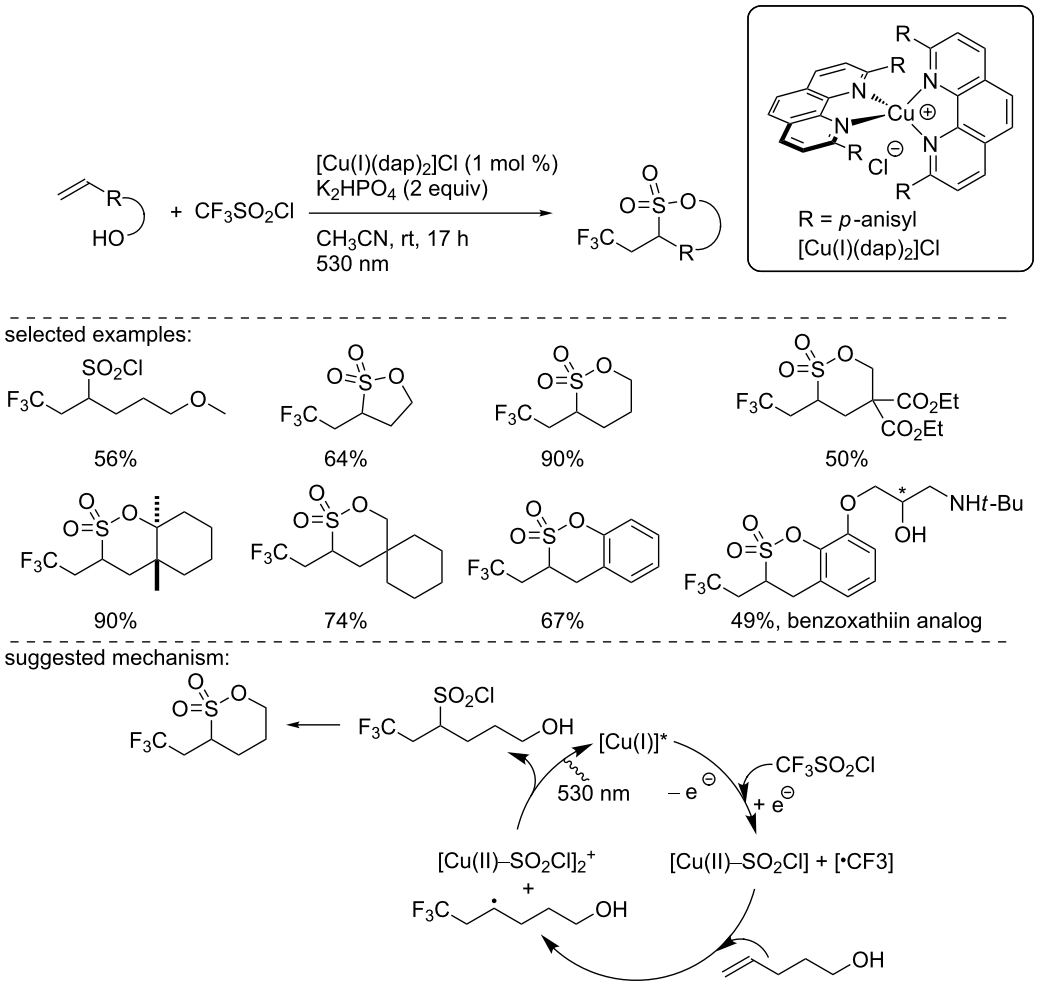

Scheme 5: Photocatalytic synthesis of fluorinated sultones.

cessful. Hence, to explain the reaction outcome, the authors suggested two possible pathways: First, a common reductive SET between the [Cu(I)] species and the perfluorinated iodoalkane, affording the perfluorinated C-centered radical and the [Cu(II)] complex [Cu(II)(dap)I]Cl. The perfluorinated radical then adds to the alkene to form a new C-centered radical. The first possible pathway relied on a rebound cycle where this radical recombined with the [Cu(II)] complex to generate a [Cu(III)] species. Then, a reductive elimination closes the catalytic cycle, delivering the product and regenerating the catalyst, along with an exchange of the ligand iodide for DAP (path III). Another possibility was the trapping of the radical with the iodine ligand of the [Cu(II)] catalyst (path IV).

In 2019, Reiser's group described a chlorosulfonylation reaction of alkenes and alkynes with $[Cu(I)(dap)_2]Cl$ or $[Cu(II)(dap)_2]Cl_2$ under visible light irradiation (Scheme 7) [23]. The scope of this transformation was excellent, demonstrating good functional group tolerance and the products were obtained in good to excellent yields. Note that the reaction yields were similar or even sometimes higher when the $[Cu(II)(dap)_2]Cl_2$ complex was used as a catalyst. To explain the reaction outcome, the authors suggested the involvement of a [Cu(I)] complex as the catalytically active species, even when $[Cu(II)(dap)_2]Cl_2$ was used. Indeed, they suggested the formation of the [Cu(I)] species from a homolytic cleavage of the Cu(II)–Cl bond under light irradiation [24]. First, the excited [Cu(I)]* complex is involved in an SET with the sulfonyl chloride, forming the sulfonyl radical and a [Cu(II)] species binding a chloride anion. The sulfonyl radical stemming from this reduction can add to the alkene, forming a C-centered radical. Then, two plausible pathways were suggested. First, a chlorine ligand transfer to the C-centered radical can proceed, delivering the product and producing the [Cu(I)] species in the ground state. Another possible pathway focused on a rebound between the [Cu(II)] species and the C-centered radical to form

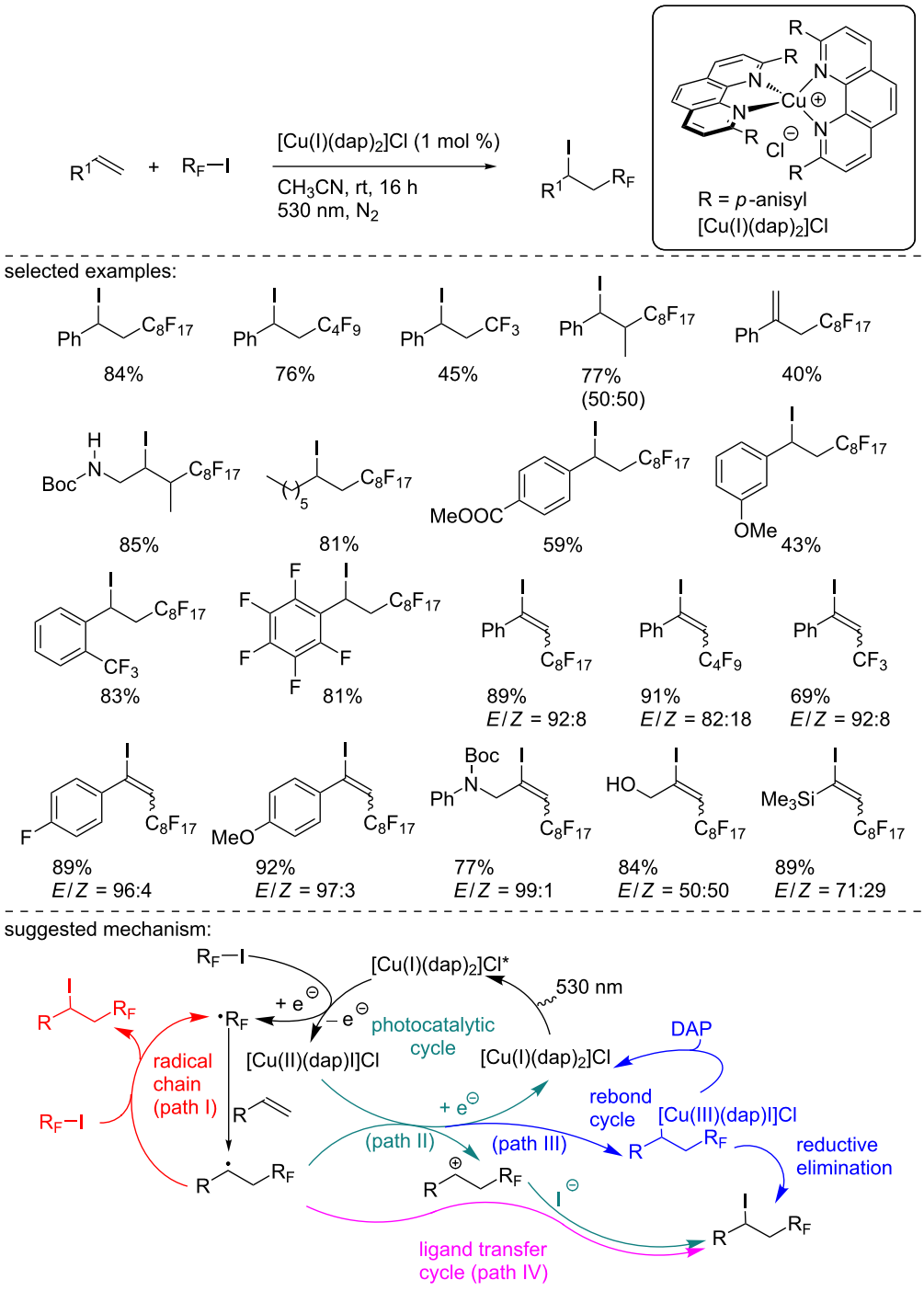

Scheme 6: Photocatalyzed haloperfluoroalkylation of alkenes and alkynes.

a [Cu(III)] species that can deliver the product through a reductive elimination, along with the [Cu(I)] species in the ground state.

1.2 Reduction reactions

In 2013, Fensterbank, Goddard, and Ollivier reported the use of the homoleptic complex $[Cu(I)(dpp)_2]PF_6$ for the reduction of symmetrical diaryliodonium salts (Scheme 8) [25]. This copper-catalyzed photocatalytic reduction generated an aryl radical that was trapped with various allylating reagents. First, the phenyl radical generated from the corresponding diphenyliodonium salt was added to various allyl sulfones substituted in the 2-position. The products were isolated in moderate to good yields. Using the more reactive allyl sulfone, a panel of symmetrical

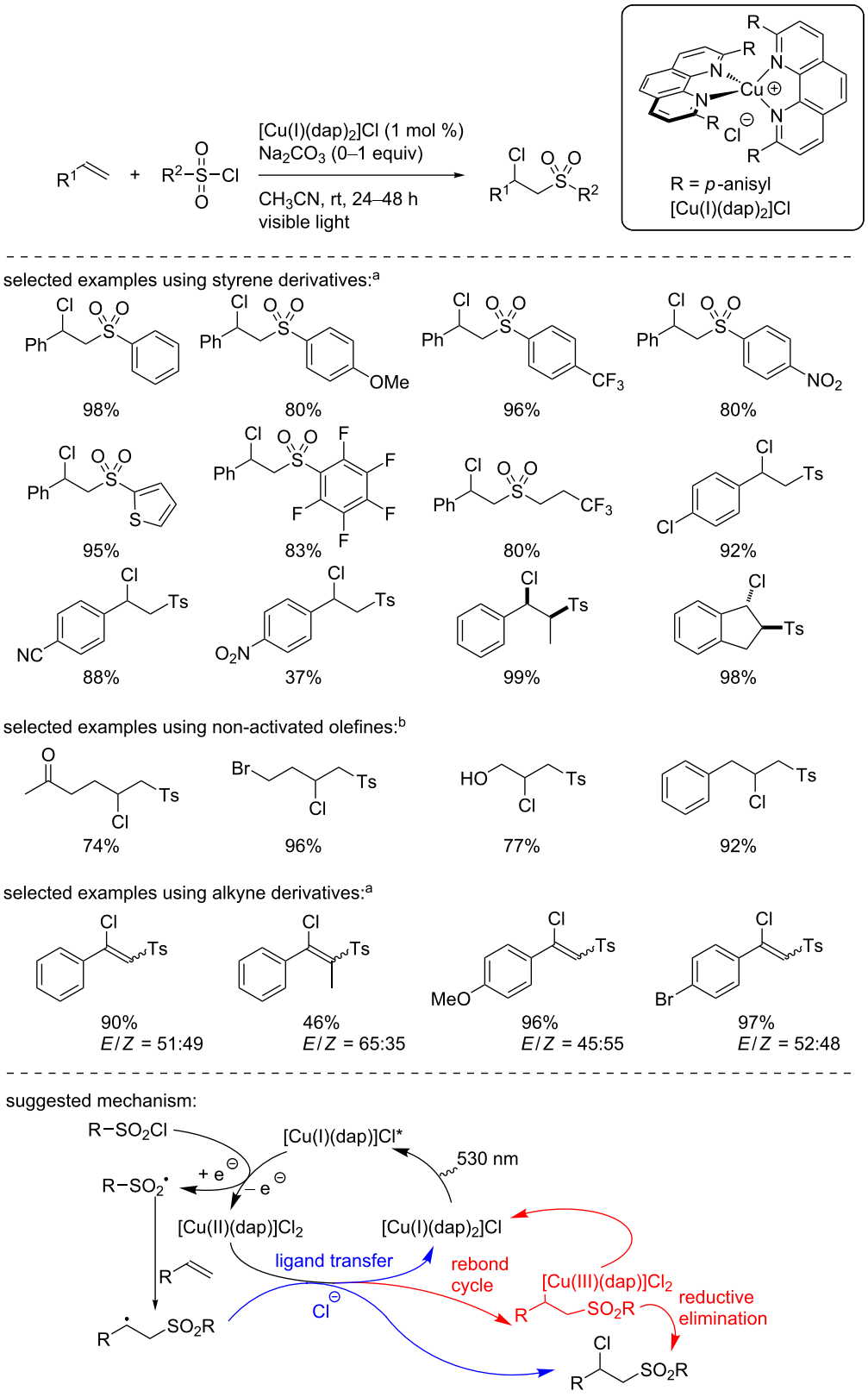

Scheme 7: Chlorosulfonylation of alkenes catalyzed by [Cu(I)(dap)$_2$]Cl. [a]No Na_2CO_3 was added. [b]1 equiv of Na_2CO_3 was used.

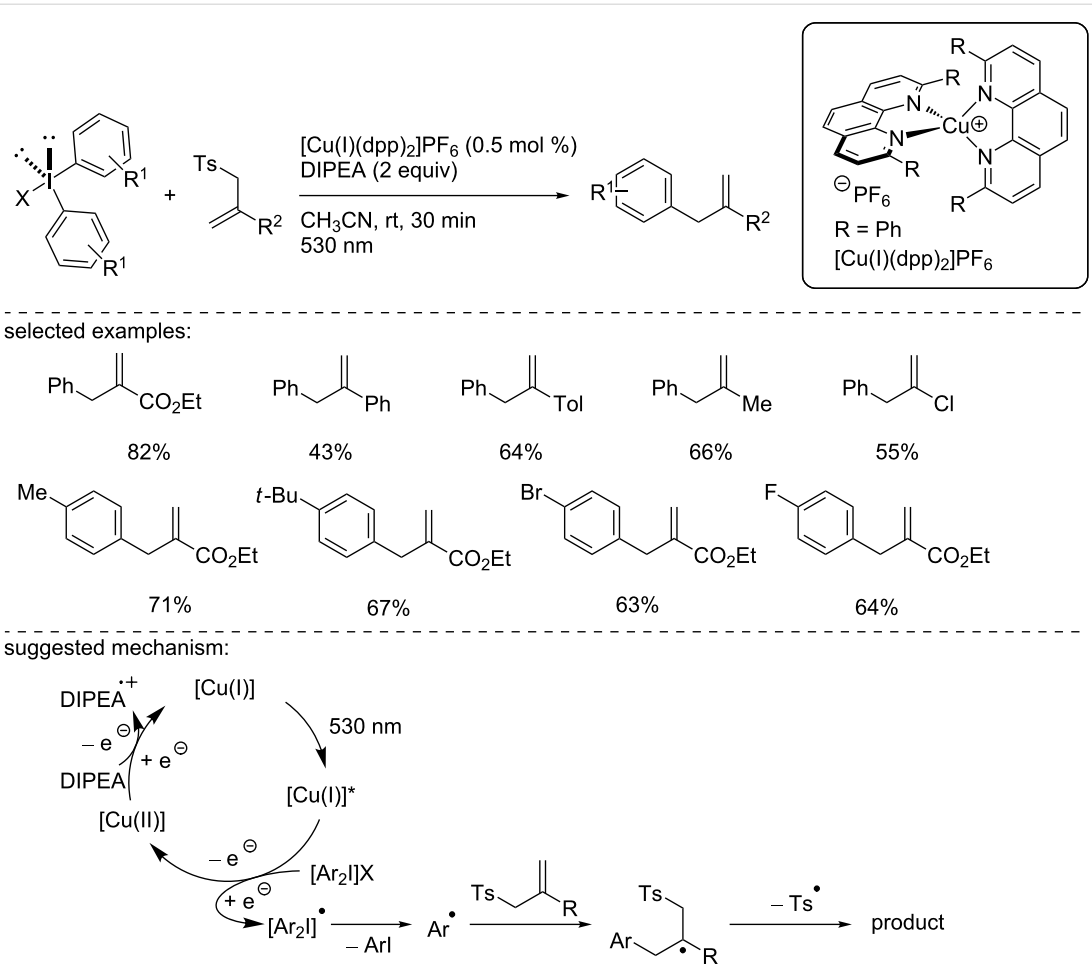

Scheme 8: Copper-photocatalyzed reductive allylation of diaryliodonium salts.

diaryliodonium salts was reacted, giving the products in good yields. The authors conducted some mechanistic studies and suggested a plausible catalytic cycle involving [Cu(I)]/[Cu(I)]*/[Cu(II)] species. The $[Cu(I)(dpp)_2]PF_6$ complex can be excited under visible light irradiation (530 nm), and the resulting excited [Cu(I)]* complex undergoes an SET to reduce the diaryliodonium species, providing the oxidized [Cu(II)] complex. The reduced diaryliodonium species collapses into an aryl radical and the corresponding aryl iodide. The aryl radical can then add to the allylating reagent, which, after tosyl radical elimination, provides the desired product. Finally, the active catalyst is regenerated thanks to the use of DIPEA as a sacrificial reductant. Note that this reaction was inefficient with aryl iodides, and no significant selectivity was observed when nonsymmetrical iodonium salts were reacted under the optimized reaction conditions.

Later in 2015, Greaney and co-workers described the copper-photocatalyzed azidation of styrene olefins and the concomitant introduction of a nucleophile (Scheme 9) [26]. Using the Zhdankin reagent as the azidyl radical precursor and the Sauvage catalyst $[Cu(I)(dap)_2]Cl$ in methanol, various styrenes were readily converted into the azidomethoxylated products in good to excellent yields. The reaction was also extended to α- and β-substituted styrenes, cyclic alkenes, and heteroaromatic derivatives. Noteworthy, when the reaction was carried out in acetonitrile, azido bromination and diazidation reactions were possible using 10 equivalents of NaBr and NaN_3, respectively. Notably, when the reaction was carried out in the dark, the diazidation reaction of the olefins occurred, while the use of Ir or Ru complexes in this transformation led to the degradation of the reagents. As this process did not involve a photocatalytic pathway, it will not be discussed here. To explain the reaction outcome, based on literature data, the authors hypothesized a catalytic cycle involving [Cu(I)]/[Cu(I)]*/[Cu(II)] species and the reduction of the Zhdankin reagent by the copper catalyst to form an azidyl radical, which then reacted with the olefin. The resulting benzyl radical could then be oxidized, probably by the catalyst in the +II oxidation state, to generate a benzylic carbocation and the active [Cu(I)] catalyst. Finally, the solvent or the

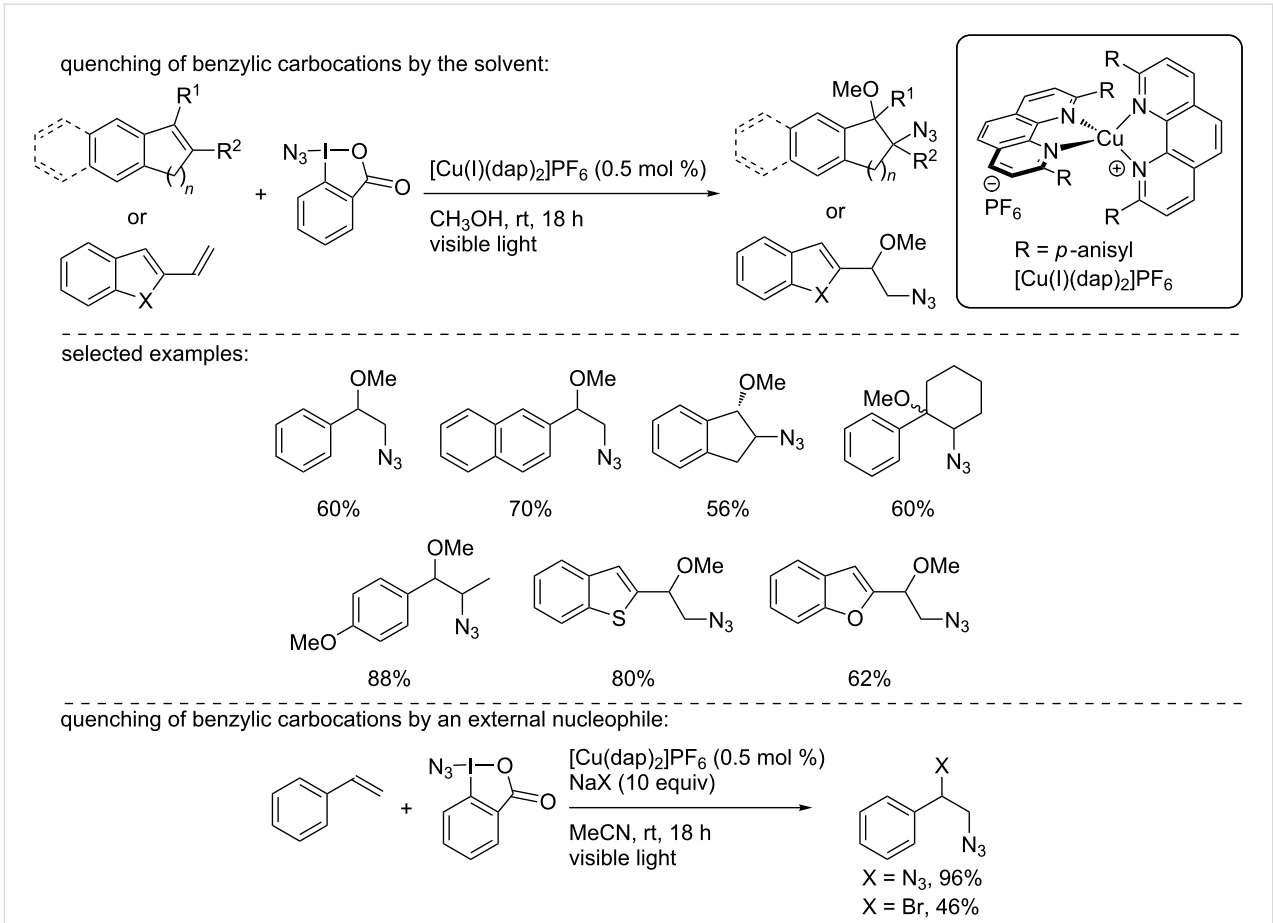

Scheme 9: Copper-photocatalyzed azidomethoxylation of olefins.

nucleophile introduced to the reaction medium reacted with the latter.

Later, Greaney and co-workers reported the photocatalytic azidation of benzylic C–H bonds (Scheme 10) [27]. Using the Sauvage catalyst $[Cu(I)(dap)_2]PF_6$ and the Zhdankin reagent, a large panel of substrates was functionalized under visible light irradiation. The functional group tolerance of the process was excellent and the products were obtained in moderate to excellent isolated yields. The authors suggested a chain radical process to explain the formation of the product. The copper photocatalyst initiated the formation of the azidyl radical, which abstracted the benzylic hydrogen atom from the substrate. Then, the benzylic radical reacted with the Zhdankin reagent, producing the azidated product and propagating the radical chain through the reaction of the iodane radical with the benzylic substrate.

In 2018, Dilman and co-workers reported the catalytic formation of the trifluoromethyl radical through the photocatalytic reduction of a borate complex (Scheme 11) [28]. To carry out this reduction, the authors used the PF_6 salt of the Sauvage catalyst under blue LED irradiation in MeOH to perform the trifluoromethyl methoxylation of styrene derivatives. The methodology was applied to a broad range of styrene derivatives, showing a good functional group tolerance. Noteworthy, α-, β-, and α,β-substituted styrenes were readily functionalized in good to excellent yields. To explain the reaction outcome, the authors suggested a reduction of the trifluoromethyl borate complex according to an SET with the excited copper(I) complex. The resulting substituted pyridyl radical eliminated a trifluoromethyl radical, which then reacted with the alkene. Then, the formed benzylic radical was oxidized to the corresponding carbocation, regenerating the photocatalyst in the ground state. The benzylic carbocation was finally trapped with MeOH, which was used as the solvent to form the trifluoromethyl methoxylated product.

In the same publication, Dilman and co-workers reported the addition of a trifluoromethyl radical to silyl enol ethers derived from ketones using the same reaction conditions (Scheme 12) [28].

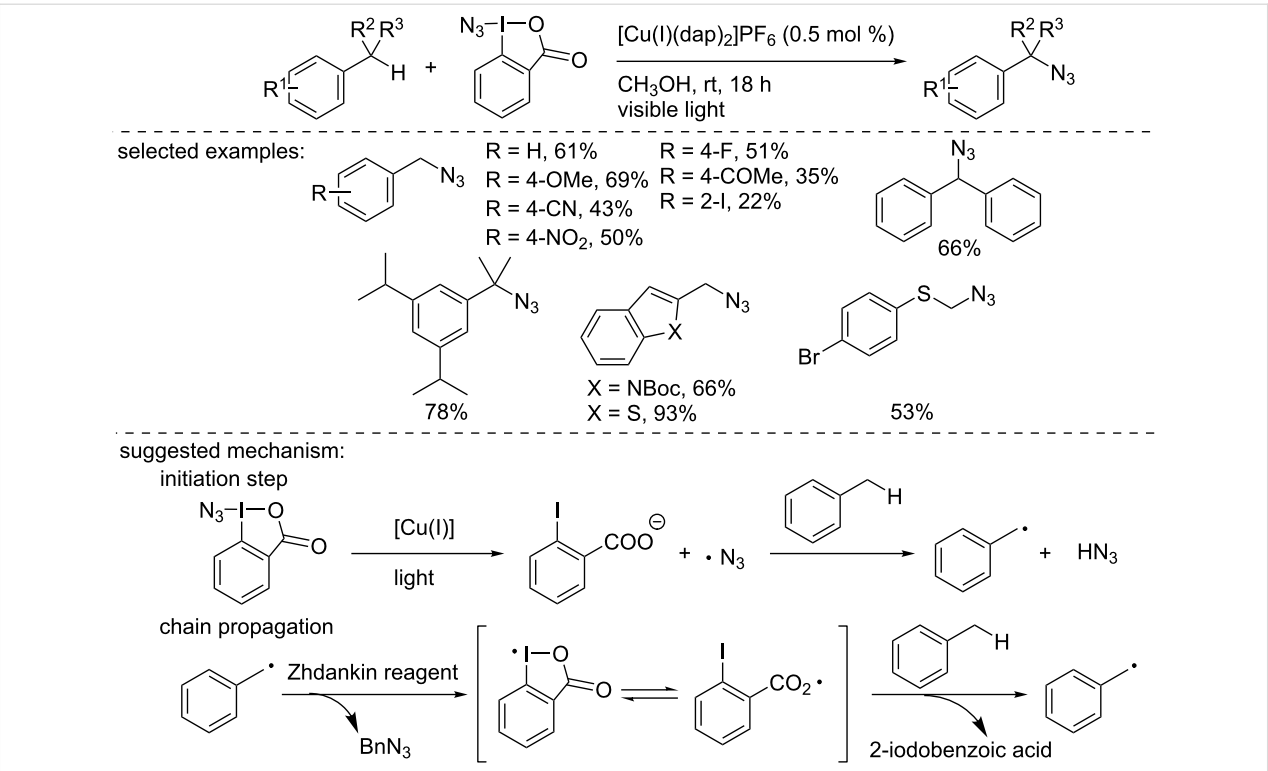

Scheme 10: Benzylic azidation initiated by $[Cu(I)(dap)_2]Cl$.

1.3 Oxidation reactions

In 2015, Bissember and co-workers used the Sauvage catalyst to generate an α-amino radical, which was used to perform the synthesis of annulated tetrahydroquinolines and octahydroisoquinolo[2,1-*a*]pyrrolo[3,4-*c*]quinolines (Scheme 13) [29]. Importantly, the formation of the key α-amino radical resulted from an oxidation reaction catalyzed by the copper catalyst in the oxidation state +II. Using the $[Cu(I)(dap)_2]Cl$ complex as the catalyst and 2 equivalents of TFA under air, *N*,*N*-dialkylated aniline derivatives were reacted with various *N*-substituted maleimides and benzylidenemalonitrile to provide polysubstituted tetrahydroquinolines in moderate to good yields. When *N*-aryltetrahydroisoquinoline was used instead of *N*,*N*-dialkylated anilines, octahydroisoquinolo[2,1-*a*]pyrrolo[3,4-*c*]quinoline derivatives were obtained for the first time.

This transformation starts with the oxidation of the excited photocatalyst with O_2. The aniline is then oxidized into an N-centered radical cation, which further gives the α-amino radical. The latter reacts with the maleimide to provide a transient radical, which undergoes an intramolecular cyclization to give the aryl radical anion. A final oxidation/deprotonation sequence delivers the product.

In 2018, Reiser and co-workers reported the use of the $[Cu(dap)_2]Cl$ catalyst in the oxoazidation of styrene derivatives (Scheme 14) [30]. Under green light irradiation, a large panel of styrene derivatives was converted into the corresponding α-azidoketones in good to excellent yields. Interestingly, the reaction was extended to the heteroaromatic derivatives, such as thiophene or benzofuran and to β-substituted styrenes. The authors conducted mechanistic studies and demonstrated the role of $[Cu(dap)_2]Cl$ as a precatalyst since the catalytically active species was a [Cu(II)] complex. To explain the formation of the product, the authors suggested that after excitation, the [Cu(I)] catalyst is oxidized to a [Cu(II)] species along with the loss of a DAP ligand. Then, the [Cu(II)] complex reacts with $TMSN_3$ to form a [Cu(II)]–N_3 species that gives an azide radical through a homolytic dissociation induced by light irradiation. The formed azide radical reacts with the styrene to form a benzylic radical that is then oxidized by O_2. The resulting peroxyl radical reacts with the Cu complex, forming a new [Cu(II)] species that collapses to deliver the product and regenerates the active [Cu(II)] catalyst.

2 Heteroleptic Cu(I) complexes

Heteroleptic copper complexes appeared as an interesting and promising alternative to the homoleptic examples. Indeed, they usually possess an increased lifetime of the triplet excited state due to a particular geometry that prevents the reorganization from a tetrahedral geometry in the ground state to a square planar geometry [31]. Moreover, the synthesis of these com-

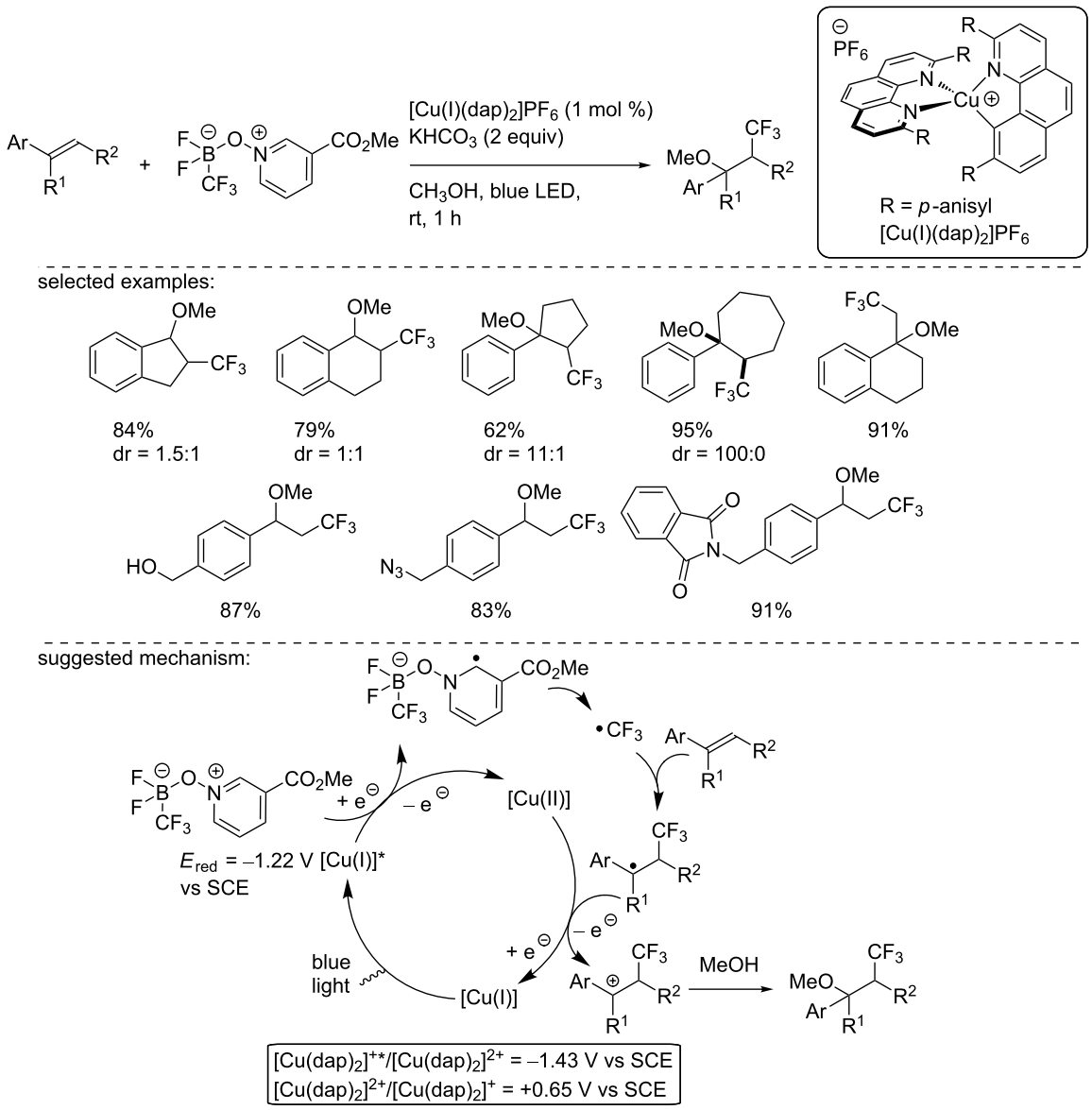

Scheme 11: Trifluoromethyl methoxylation of styryl derivatives using $[Cu(I)(dap)_2]PF_6$. All redox potentials are reported vs SCE.

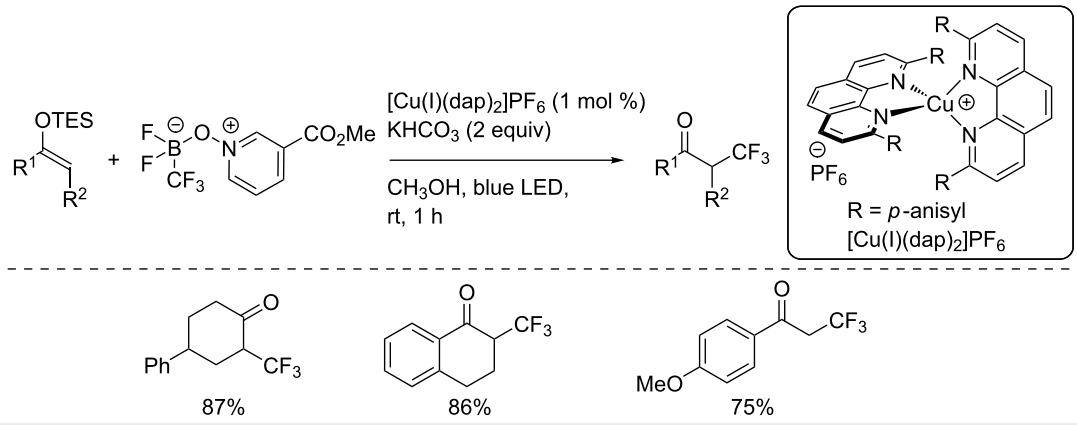

Scheme 12: Trifluoromethylation of silyl enol ethers.

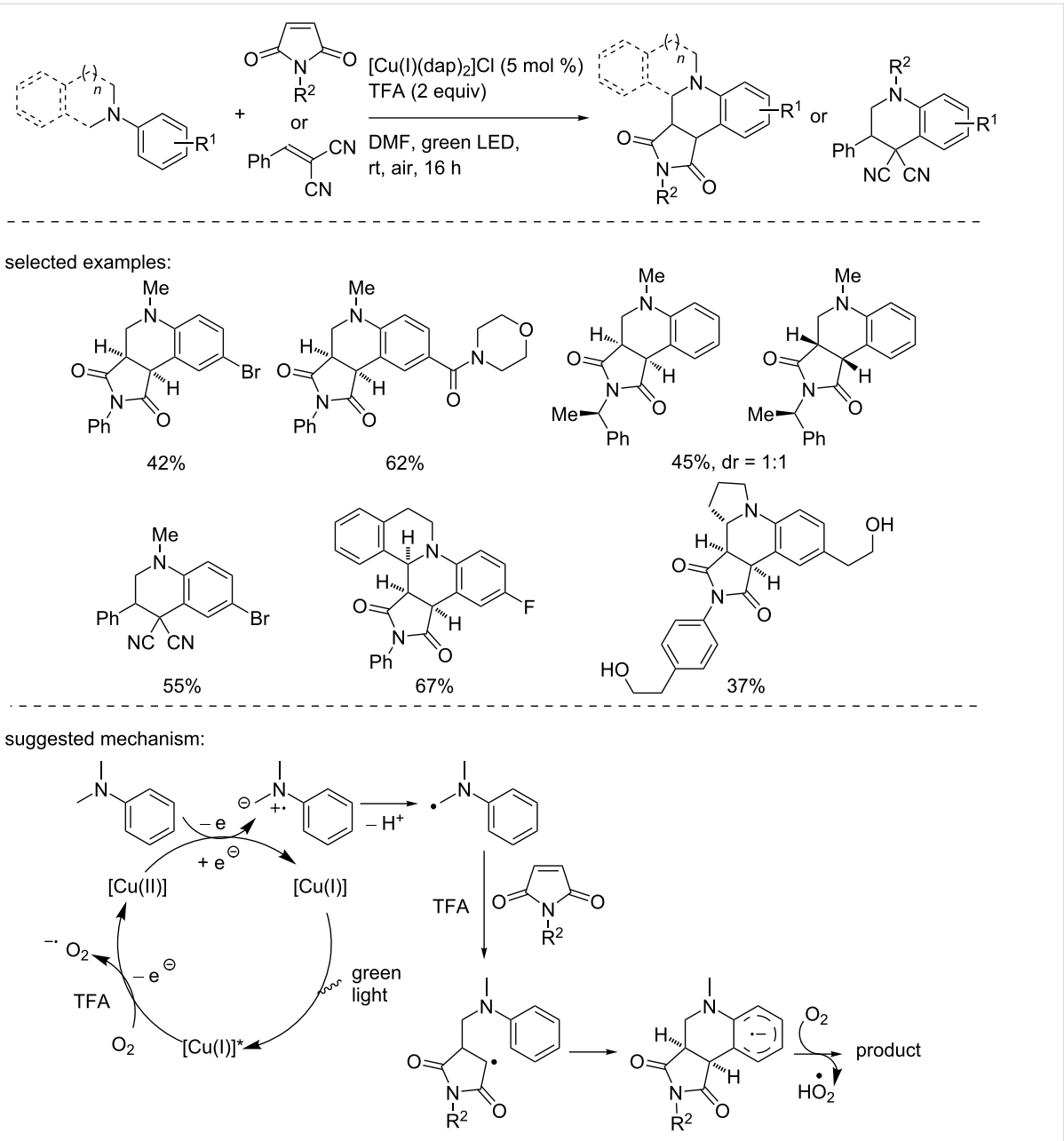

Scheme 13: Synthesis of annulated heterocycles upon oxidation with the Sauvage catalyst.

pounds is usually facile, and they can be readily obtained in a crystalline form. Herein, we will report their use in ATRA reactions, reductions, oxidations, as well as in PCET and energy transfer reactions.

2.1 ATRA reactions

In 2015, Reiser and co-workers reported the synthesis of a novel copper-based heteroleptic complex bearing a phenanthroline derivative and a bisisonitrile ligand, [Cu(I)(dpp)(binc)]BF_4, which was fully characterized (Scheme 15) [32]. This complex proved to have a similar or higher excited state lifetime (17 μs) compared to the previously reported complexes and a redox potential of −1.88 V vs SCE in the excited state ([Cu(I)]*/[Cu(II)]). Upon irradiation at 455 nm, the authors used this complex in ATRA reactions, with various ATRA reagents, including α-bromomalonates and benzyl bromides, in combination with a broad range of alkenes (allylamine, homoallyl alcohol, styrene derivatives, and silyl enol ethers). The corresponding products were isolated in moderate to excellent yields. The authors suggested a classical mechanism for this ATRA. First, the excited copper complex reduced the organohalide to form a C-centered radical. The latter reacted

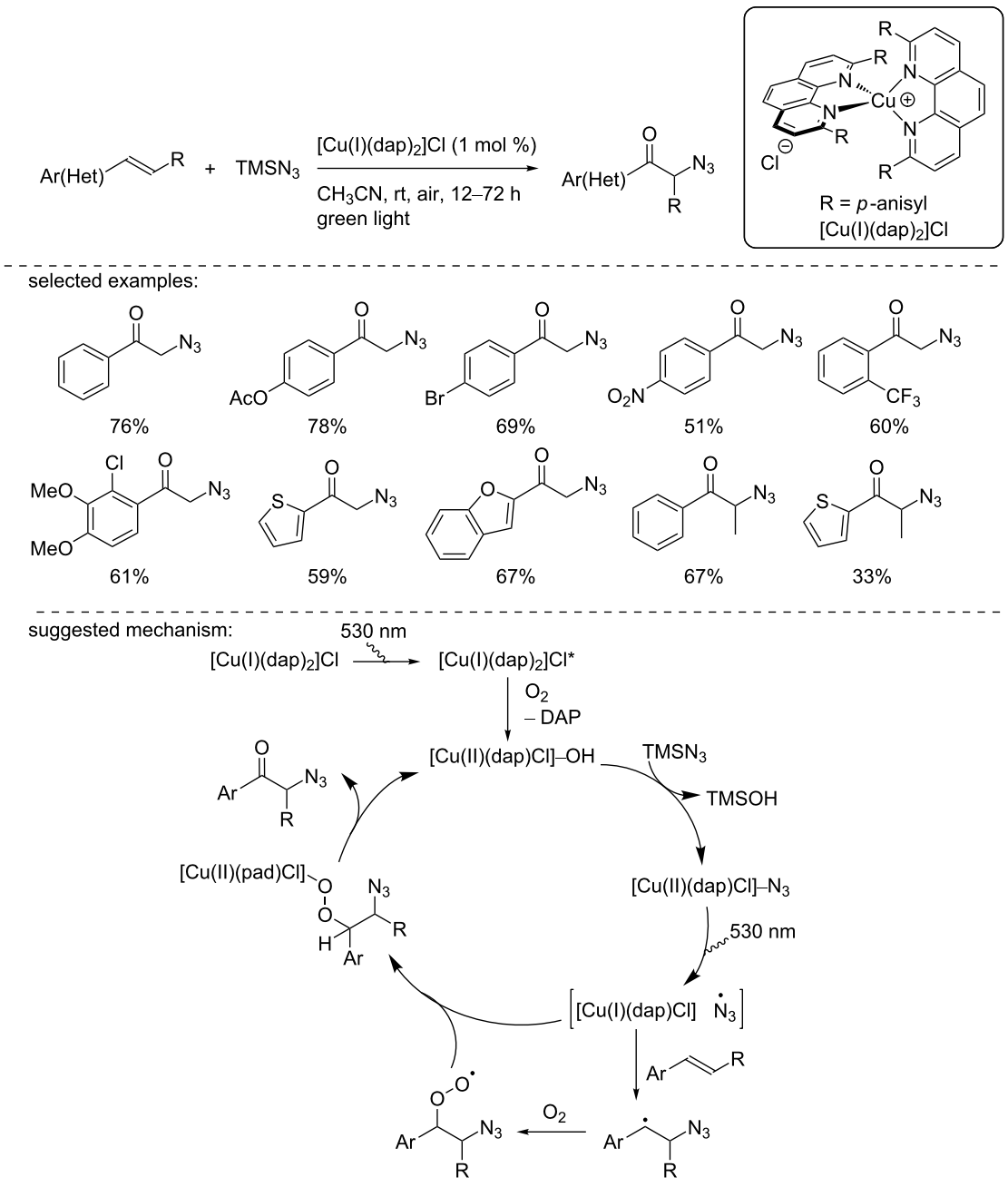

Scheme 14: Oxoazidation of styrene derivatives using $[Cu(dap)_2]Cl$ as a precatalyst.

with the olefin to form a new carbon-centered radical. Then, the catalyst in the oxidation state +II oxidized the newly formed radical to the corresponding carbocation along with the regeneration of the catalyst in the ground state. Finally, the carbocation was trapped by the anion generated in the first reduction step.

In the same report, Reiser and co-workers reported an allylation reaction using the $[Cu(I)(dpp)(binc)]BF_4$ complex (Scheme 16) [32]. The reaction of α-bromomalonates with allyl- and crotylsilanes afforded the allylated products in good yields. To explain the reaction outcome, the authors suggested a reduction of the α-bromomalonate by the excited Cu(I) complex. Then, the generated radical adds to the allylsilane, releasing a silyl radical. Then, the latter oxidizes the Cu(II) complex and regenerates the catalyst in the ground state.

In 2018, Yamaguchi and Itoh reported the ATRA of CBr_4 to various alkenes, including styrene derivatives and aliphatic-substituted olefins (Scheme 17) [33]. The reaction was carried

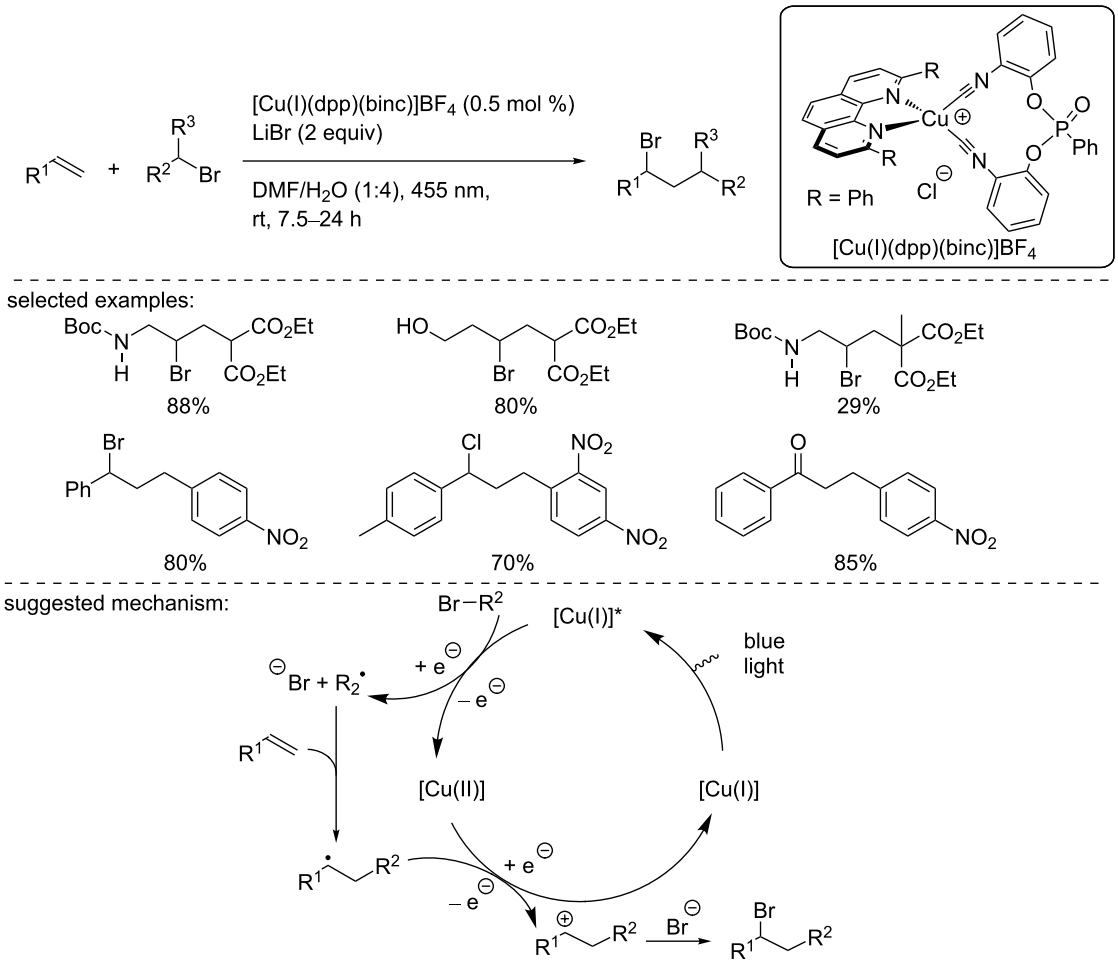

Scheme 15: [Cu(I)(dpp)(binc)]PF_6-catalyzed ATRA reaction.

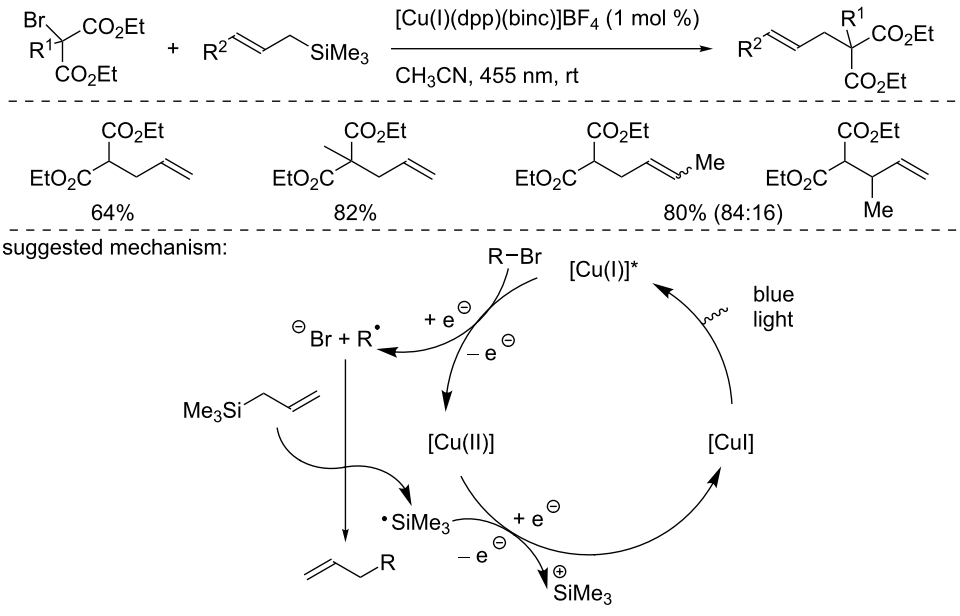

Scheme 16: Allylation reaction of α-bromomalonate catalyzed by [Cu(I)(dpp)(binc)]PF_6 following an ATRA mechanism.

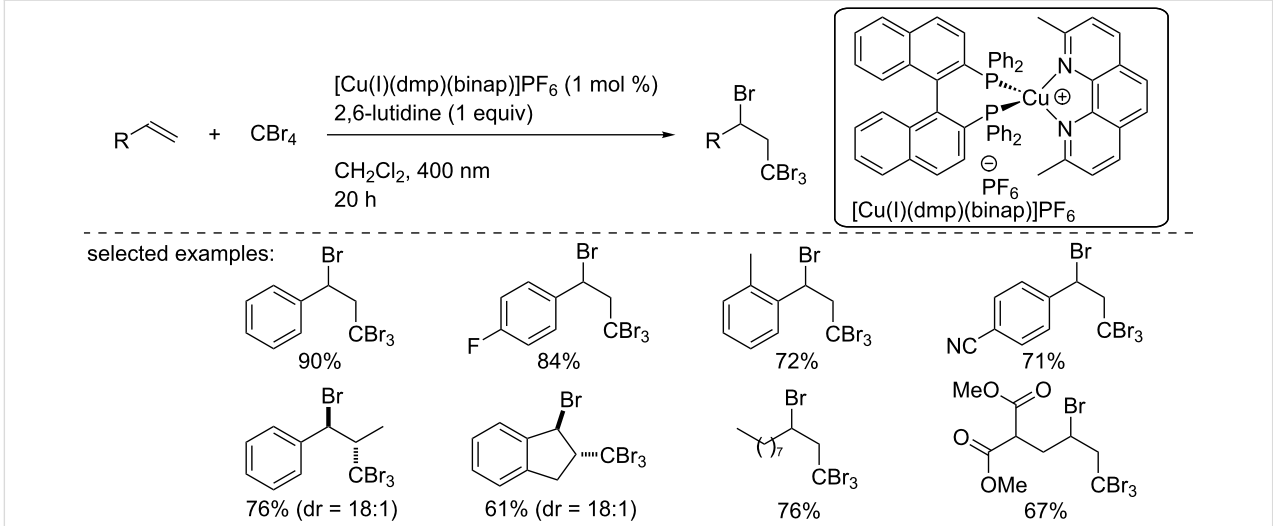

Scheme 17: Bromo/tribromomethylation reaction using [Cu(I)(dmp)(BINAP)]PF_6.

out using the complex [Cu(I)(dmp)(binap)]PF_6, and the desired tribromomethylated products were isolated in good to excellent yields. The authors suggested a similar mechanism to the one described by Reiser and co-workers in Scheme 14.

In 2018, Hu and co-worker described the synthesis of a new heteroleptic copper complex bearing a substituted bipyridine ligand (Scheme 18) [34]. The novel copper catalyst was fully characterized by X-ray crystallographic analysis, UV–visible

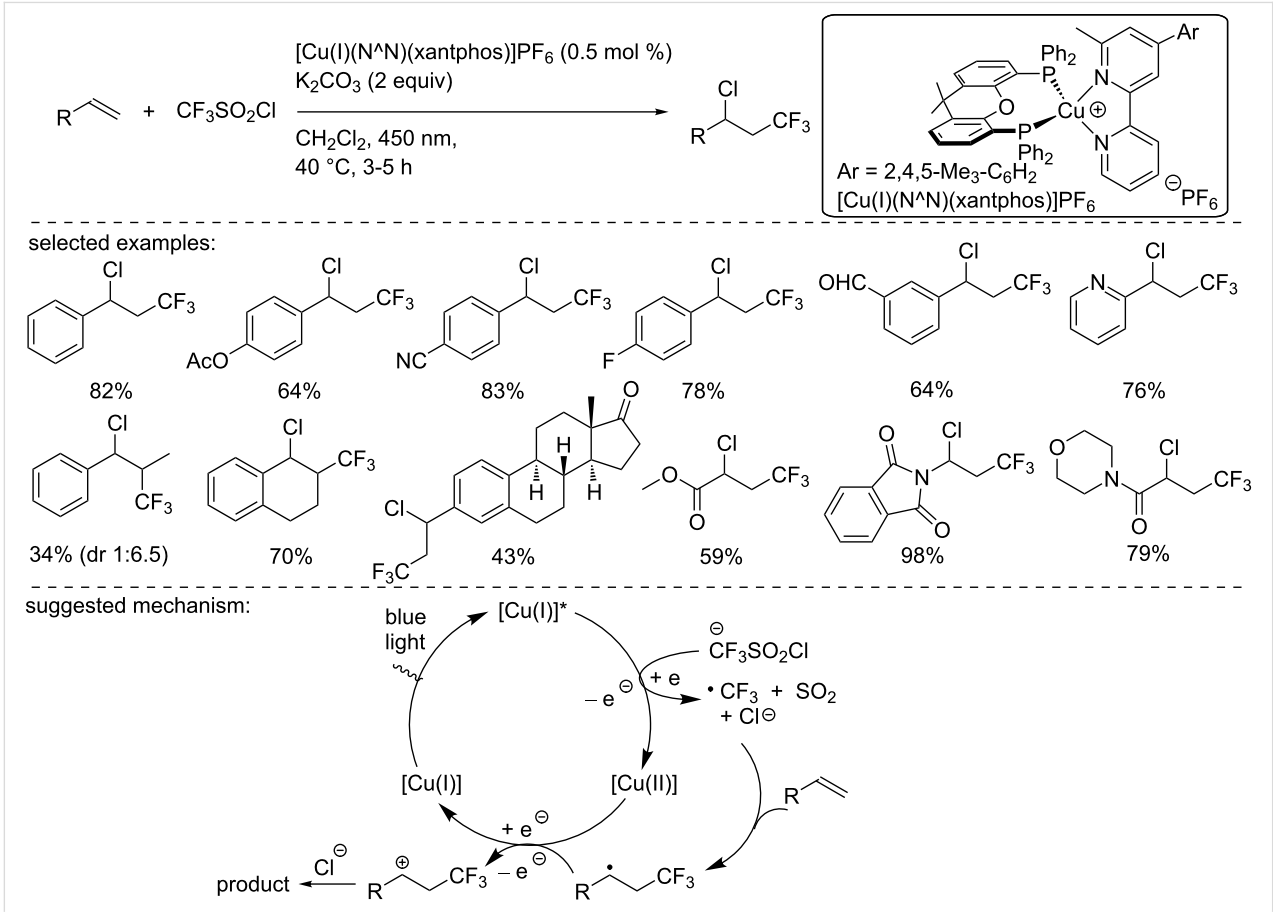

Scheme 18: Chlorotrifluoromethylation of alkenes catalyzed by [Cu(I)(N^N)(xantphos)]PF_6.

absorption and emission as well as cyclic voltammetry. The catalyst [Cu(I)(N^N)(DPEPhos)]PF_6 was used in the chlorotrifluoromethylation of alkenes using CF_3SO_2Cl as the ATRA reagent. The reaction was carried out under blue light irradiation (450 nm). The methodology was applied to a broad range of substrates, including (α-)styryl derivatives, cyclic derivatives, acrylates, enol acetates, and enamines. The functional group tolerance of the transformation was fairly decent and demonstrated the synthetic utility of this reaction manifold. To explain the reaction outcome, the authors suggested the following mechanism: The excited copper catalyst reduces the CF_3SO_2Cl reagent, resulting in the formation of a sulfonyl radical, which, after elimination of SO_2, generates the trifluoromethyl radical. This radical then reacts with the olefin to form a carbon-centered radical. Then, two plausible pathways were suggested: The first one involved an oxidation of this carbon-centered radical by the Cu(II) complex, followed by trapping of the carbocation with the chloride anion initially generated in the first reduction step. Alternatively, the authors suggested a possible mechanism involving a radical propagation.

In another report, Hu and co-worker developed a chlorosulfonylation of terminal alkenes and alkynes using the previously developed copper-based photocatalyst (Scheme 19) [35]. The reaction was tolerant to a broad range of arylchlorosulfonyl derivatives when the reaction was carried out with styrene, including sterically hindered and heteroaromatic substrates. Aliphatic sulfonyl chlorides were also tolerated, although the yields were slightly lower. With respect to the alkenes, the reactions proceeded nicely with styrene derivatives as well as with α- and β-substituted styrenes and methyl methacrylate. However, aliphatic substituted alkenes were not suitable substrates or provided the desired products in very low yields (<10%). Finally, the reaction was extended to phenylacetylene derivatives, and the chlorosulfonylated alkenes were isolated in moderate yields.

2.2 Reduction reactions

In 2017, Evano and co-workers reported the photocatalytic reduction of aryl and alkyl iodides and bromides catalyzed by a heteroleptic copper complex, [Cu(I)(bcp)(DPEPhos)]PF_6, under blue light irradiation (Scheme 20) [36]. The reduction of aryl iodides proceeded well, regardless of the electron density of the aromatic ring, and the products were isolated in good to excellent yield, with an excellent functional group tolerance. Moreover, a complex steroid derivative was efficiently reduced under the standard conditions. Activated aryl bromides were also

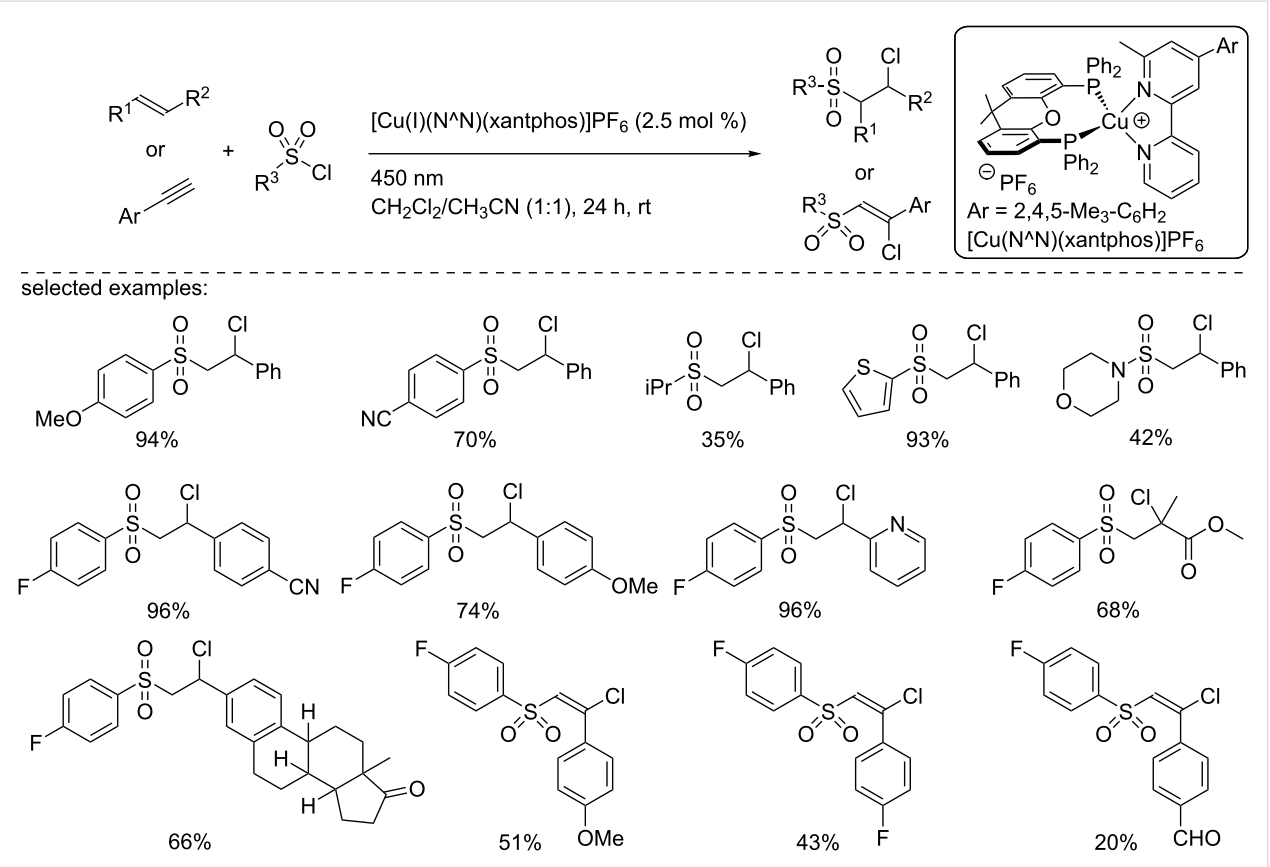

Scheme 19: Chlorosulfonylation of styrene and alkyne derivatives by ATRA reactions.

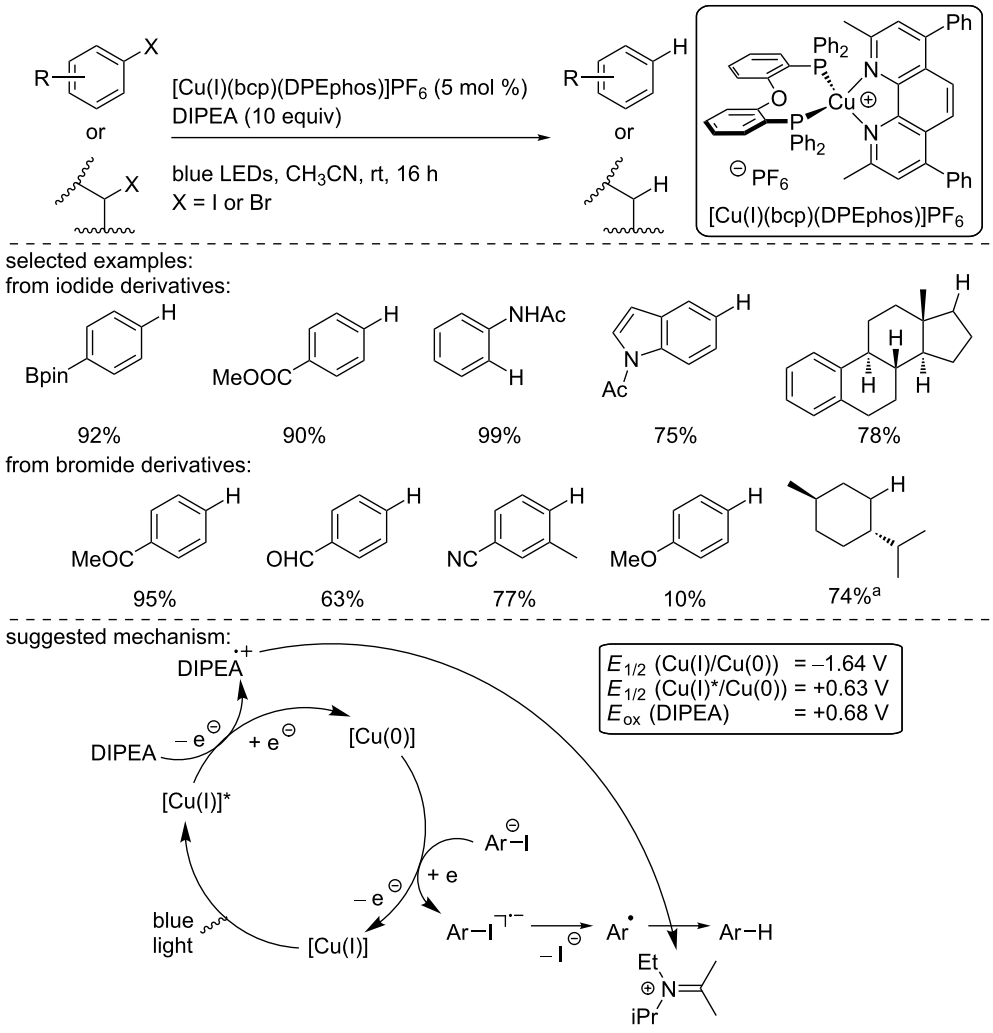

Scheme 20: Reduction of aryl and alkyl halides with the complex [Cu(I)(bcp)(DPEPhos)]PF_6. [a]Irradiation was carried out at 420 nm. All redox potential are reported vs SCE.

readily reduced under similar conditions, even if they were tedious electron-rich aryl bromide substrates, giving low yield, probably due to their intrinsic reduction potential. Interestingly, the bromide substrate derived from menthol was readily reduced in an excellent 74% isolated yield. The authors conducted some mechanistic studies (including cyclic voltammetry and Stern–Volmer quenching experiments, for instance), and, based on their findings, suggested the following mechanism: After irradiation under blue light, the excited [Cu(I)]* complex is reduced by the organic base DIPEA to produce a [Cu(0)] complex. The latter undergoes an SET with the aryl iodide to generate the radical anion from aryl iodide, which collapses into the aryl radical while the photocatalyst in the ground state is regenerated. Finally, the aryl radical abstracts a hydrogen atom from the oxidized DIPEA to produce the reduced aryl derivative.

Within the same study, Evano and co-workers took advantage of the developed photocatalytic reduction of aryl iodides and bromides into the corresponding aryl radical to use the latter in further transformations (Scheme 21). First, a 5-*exo-trig* cyclization was carried out to access indolines, dihydrobenzofurans, indanes, cyclopentane, and pyrrolidines. The cyclized products were isolated in good to excellent yields. Finally, a Meerwein arylation reaction was developed through the copper photocatalyzed formation of an aryl radical according to a reductive process. A large panel of aryl iodides was added to various pyrroles and electron-rich aromatic derivatives. The arylated products were obtained in moderate to good yields, and the functional group tolerance was excellent.

Later in 2018, Evano and co-workers used their methodology to reduce aryl iodide for the synthesis of the alkaloids rosettacin,

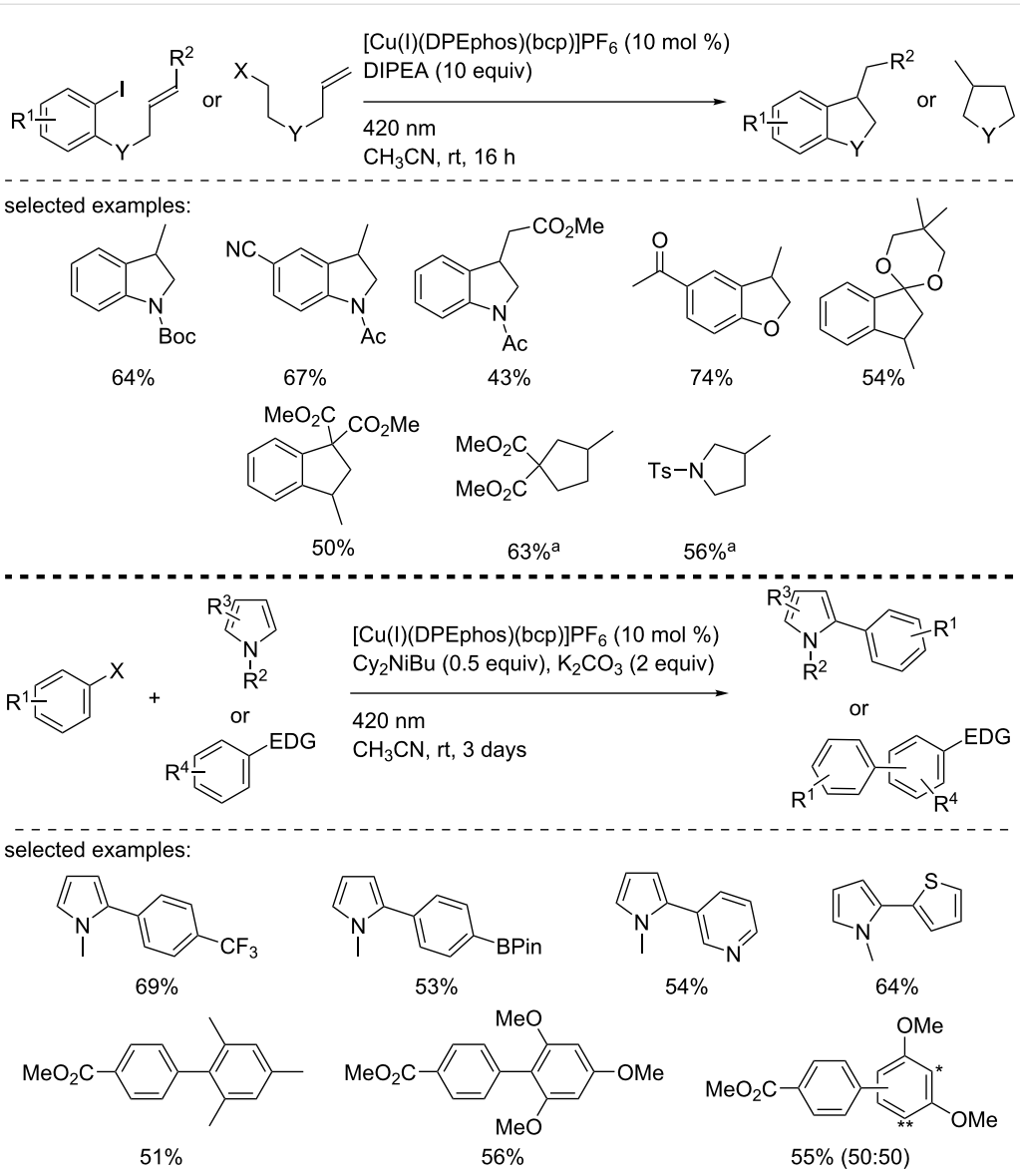

Scheme 21: Meerwein arylation of electron-rich aromatic derivatives and 5-*exo-trig* cyclization catalyzed by the photocatalyst [Cu(I)(bcp)(DPEPhos)]PF_6. [a]5 mol % of catalyst and 5 equiv of DIPEA were used.

luotonin A, and deoxyvasicinone (Scheme 22) [37]. The developed strategy relied on the addition of an aryl radical on ynamides or cyanamides, followed by a final cyclization. Using similar reaction conditions as those used for the Meerwein arylation, the three alkaloids were synthesized in good to excellent yield in a straightforward manner.

In 2017, Fu, Peters, and co-workers reported the copper-photocatalyzed intramolecular decarboxylative C–N coupling of NHP esters using an in situ-formed heteroleptic copper complex (Scheme 23) [38]. This protocol, a versatile alternative to the Curtius rearrangement, was applied to a large variety of substrates, including primary/secondary alkyl, cycloalkyl, and benzyl NHP esters. The products were obtained in good yields. The functional group tolerance of the process was excellent and was further demonstrated in the course of a robustness screen. Supported by mechanistic experiments, including UV–vis analysis, crossover studies, trapping with TEMPO, and the use of a radical clock, the authors suggested the following mechanism, although the nature of the heteroleptic copper complex has not been clearly determined. However, the involvement of [Cu(I)(dmp)(xantphos]BF_4 was precluded, since the preformed complex proved to be inefficient under the standard reaction conditions. The authors suggested first the photoexcitation of a [Cu(I)] species. Then, the excited [Cu(I)]* species reduces the NHP ester to form a carboxyl radical and the phthalimide anion,

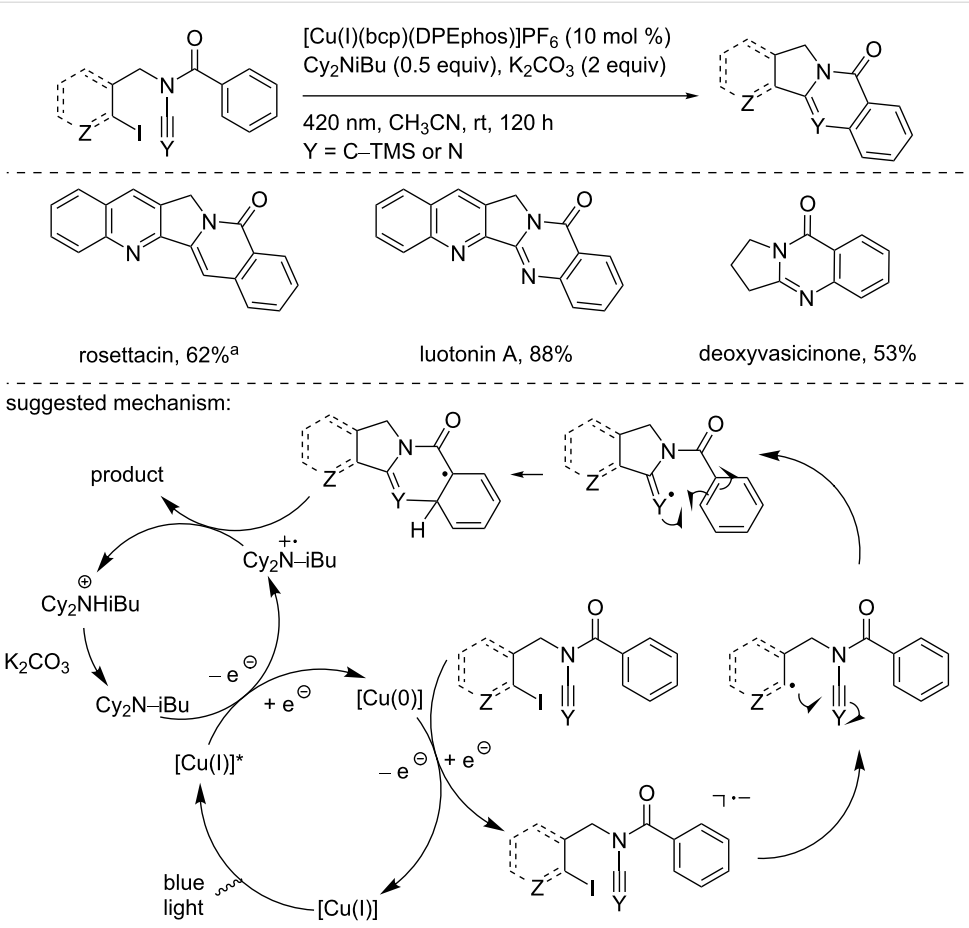

Scheme 22: [Cu(I)(bcp)(DPEPhos)]PF_6-photocatalyzed synthesis of alkaloids. [a]Yield over two steps (cyclization and TMS deprotection).

which binds to the [Cu(II)] species. After the elimination of CO_2, the recombination of the alkyl radical with the [Cu(II)] species bearing the phthalimide forms the product and regenerates the active [Cu(I)] catalyst.

Collins and co-workers described the use of [Cu(I)(dq)(binap)]BF_4 as an efficient catalyst for the reductive decarboxylative coupling of a NHP ester derived from cyclohexanecarboxylic acid with a bromoalkyne (Scheme 24) [39]. The catalyst was selected using a combinatorial approach for the selection of the optimal catalyst structure. The product was isolated in an excellent 87% yield.

In 2018, Wang, Xu, and co-workers described the reductive decarboxylative alkylation of glycine and glycine-containing peptides using an in situ-formed heteroleptic copper complex, [Cu(I)(dmp)(xantphos)]PF_6 (Scheme 25) [40]. Under blue light irradiation, glycine esters were readily alkylated using NHP esters in the presence of DABCO as a base. A large panel of NHP esters was introduced to ethyl *N*-phenylglycine ester, and the alkylated products were obtained in good to excellent yields. In addition, various glycine derivatives were also alkylated in good yields. Finally, the authors demonstrated the synthetic interest of their methodology through the alkylation of di- and tripeptides. The authors studied the reaction mechanism and suggested the following one: First, the excited in situ-formed copper complex reduced the NHP ester, as demonstrated by the Stern–Volmer quenching experiment. The formed radical anion collapsed into the corresponding alkyl radical and the phthalimide anion. Then, the oxidized copper complex oxidized the glycine ester, regenerating the catalyst, furnishing the N-centered radical cation. Then, the latter underwent a 1,2-hydride shift in the presence of the base (or the phthalimide anion) to form the α-amino radical that recombined with the alkyl radical formed in the initial step.

In early 2019, our research group reported the copper-photocatalyzed borylation of organic halides using [Cu(I)(DMEGqu)(DPEPhos)]PF_6 as the photocatalyst (Scheme 26) [41]. The photocatalytic Miyaura borylation reaction was carried out using aryl iodides bearing either electron-donating or electron-withdrawing groups in good to excellent

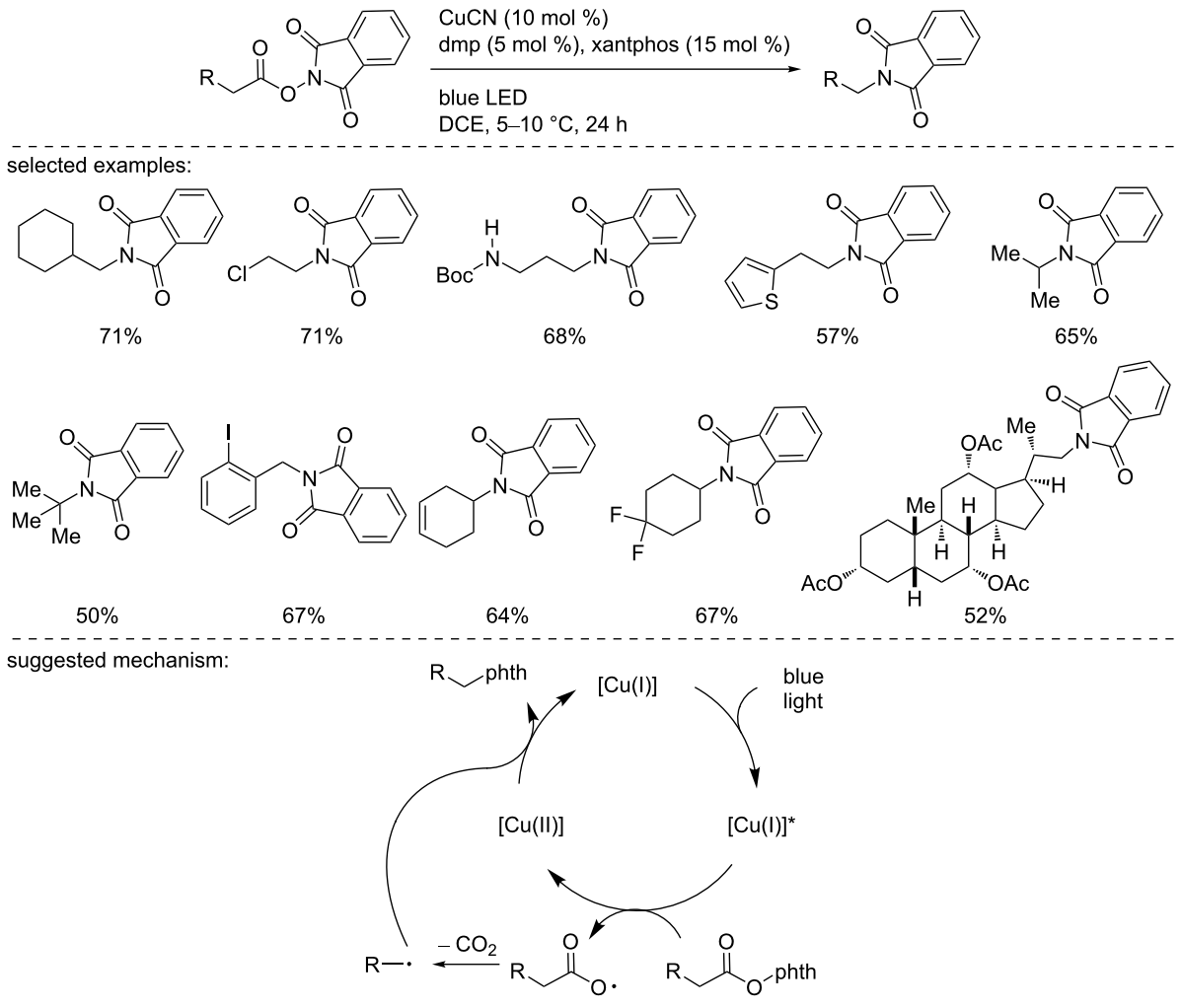

Scheme 23: Copper-photocatalyzed decarboxylative amination of NHP esters.

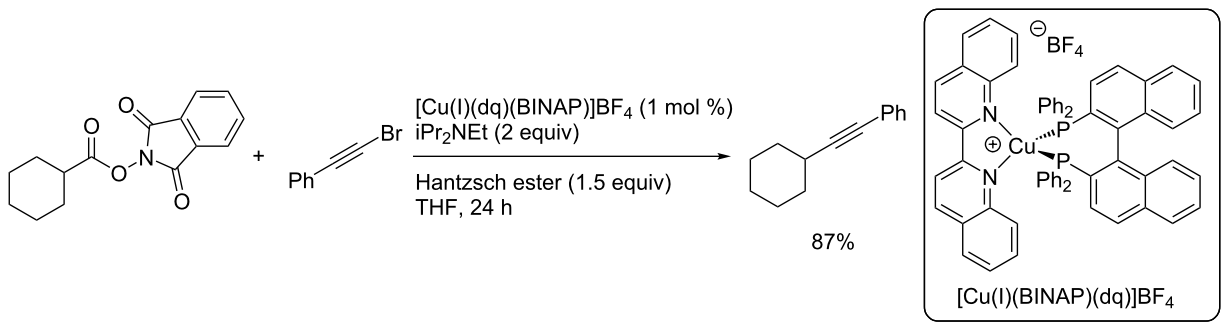

Scheme 24: Photocatalytic decarboxylative alkynylation using [Cu(I)(dq)(binap)]BF_4.

yields. Activated aryl bromides and heteroaryl bromides were also successfully converted to the corresponding arylboronic esters in good to excellent yields. The methodology was also extended to a set of vinyl iodides, providing the vinylboronic esters in moderate to good yields. Notably, alkyl iodides were also suitable substrates. The methodology proved to be compatible with a broad range of functional groups. To demonstrate the synthetic utility of the process, the reaction was developed

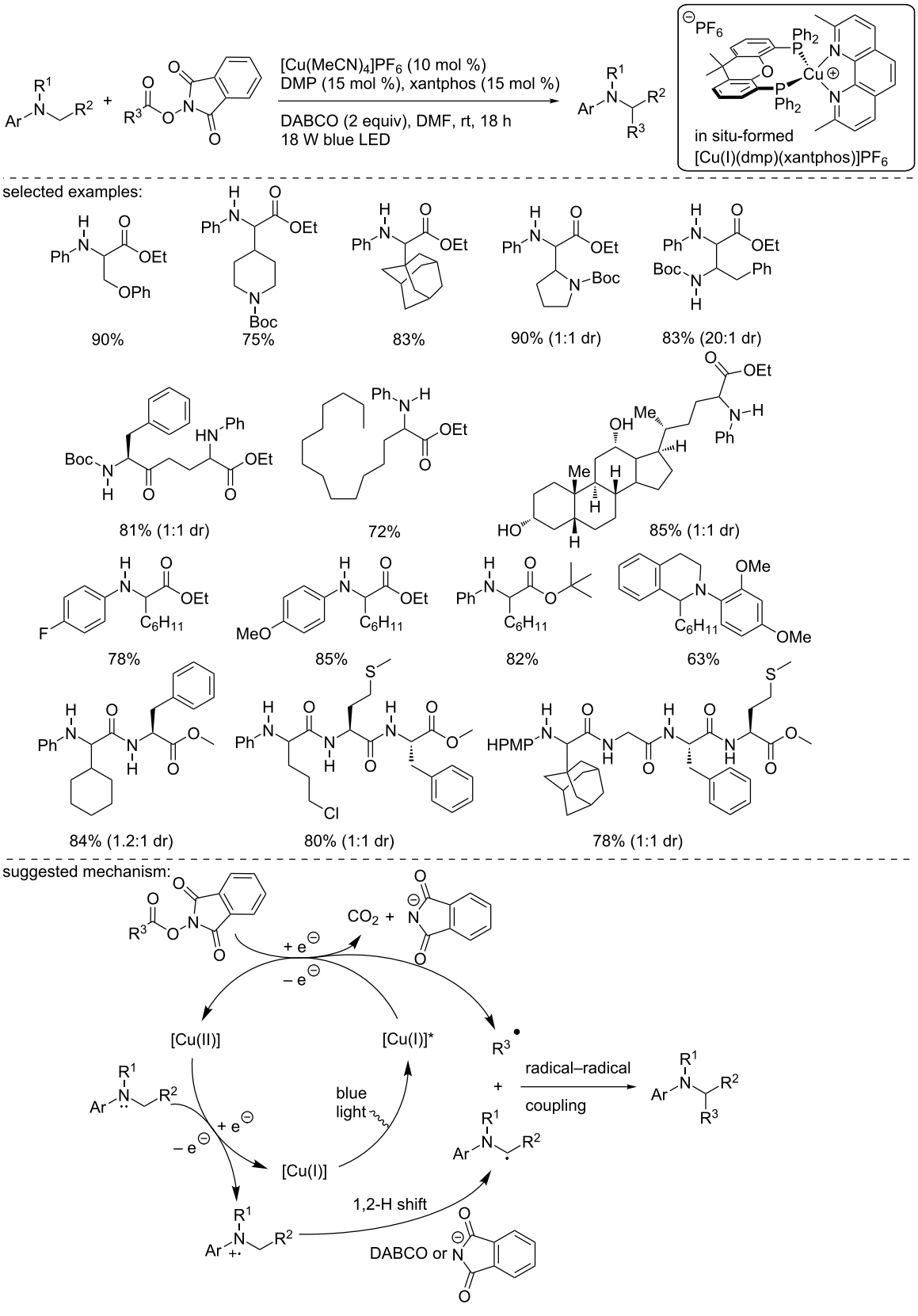

Scheme 25: Copper-photocatalyzed alkylation of glycine esters.

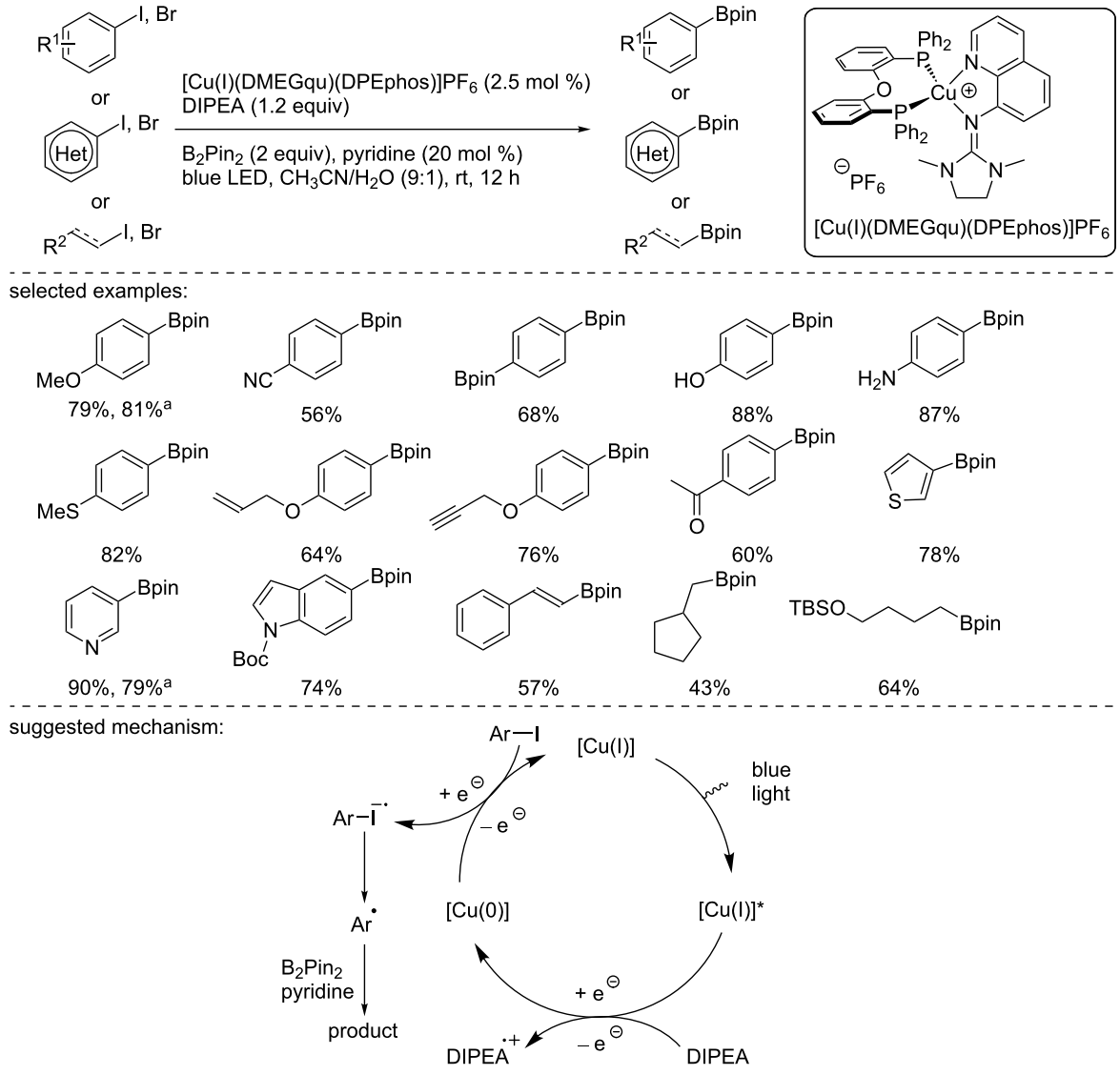

Scheme 26: Copper-photocatalyzed borylation of organic halides. [a]Under continuous flow conditions.

under continuous flow conditions to afford an easy and straightforward scale-up of the method (up to 5 g). Mechanistic studies were carried out, suggesting a possible [Cu(I)]/[Cu(I)]*/[Cu(0)] reaction manifold. The copper photocatalyst in the excited state is reduced to the [Cu(0)] complex by the sacrificial organic reductant DIPEA. The in situ-formed [Cu(0)] species reduces the organic halide to generate the corresponding radical anion, which loses the halide anion and gives rise to the corresponding C-centered radical. A subsequent trapping with B_2Pin_2 affords the borylated product.

In 2019, Wang, Duan, and co-workers reported the reductive α- and δ-functionalization of alcohol using *N*-alkoxyphthalimide derivatives and glycine esters under basic or acidic conditions, respectively [42]. With regards to the α-functionalization, various *N*-arylated glycine esters were used as reaction partners with a broad range of *N*-alkoxyphthalimide derivatives, using [Cu(I)(dmp)(xantphos)]BF_4 as the catalyst and DABCO as the base (Scheme 27). The products were obtained in moderate to good yields and moderate diastereoselectivities. The reaction was applied to *N*-alkoxyphthalimides derived from aliphatic and benzyl alcohols and heteroaromatic ones. To explain the reaction outcome, the authors suggested the reduction of the *N*-alkoxyphthalimide by the excited copper catalyst, [Cu(I)]*. Then, this radical collapses into an α-oxy carbon-centered radical thanks to an intramolecular proton transfer. This carbon-centered radical then recombines with the α-amino radical that arises from the oxidation of the amine with the formed [Cu(II)]

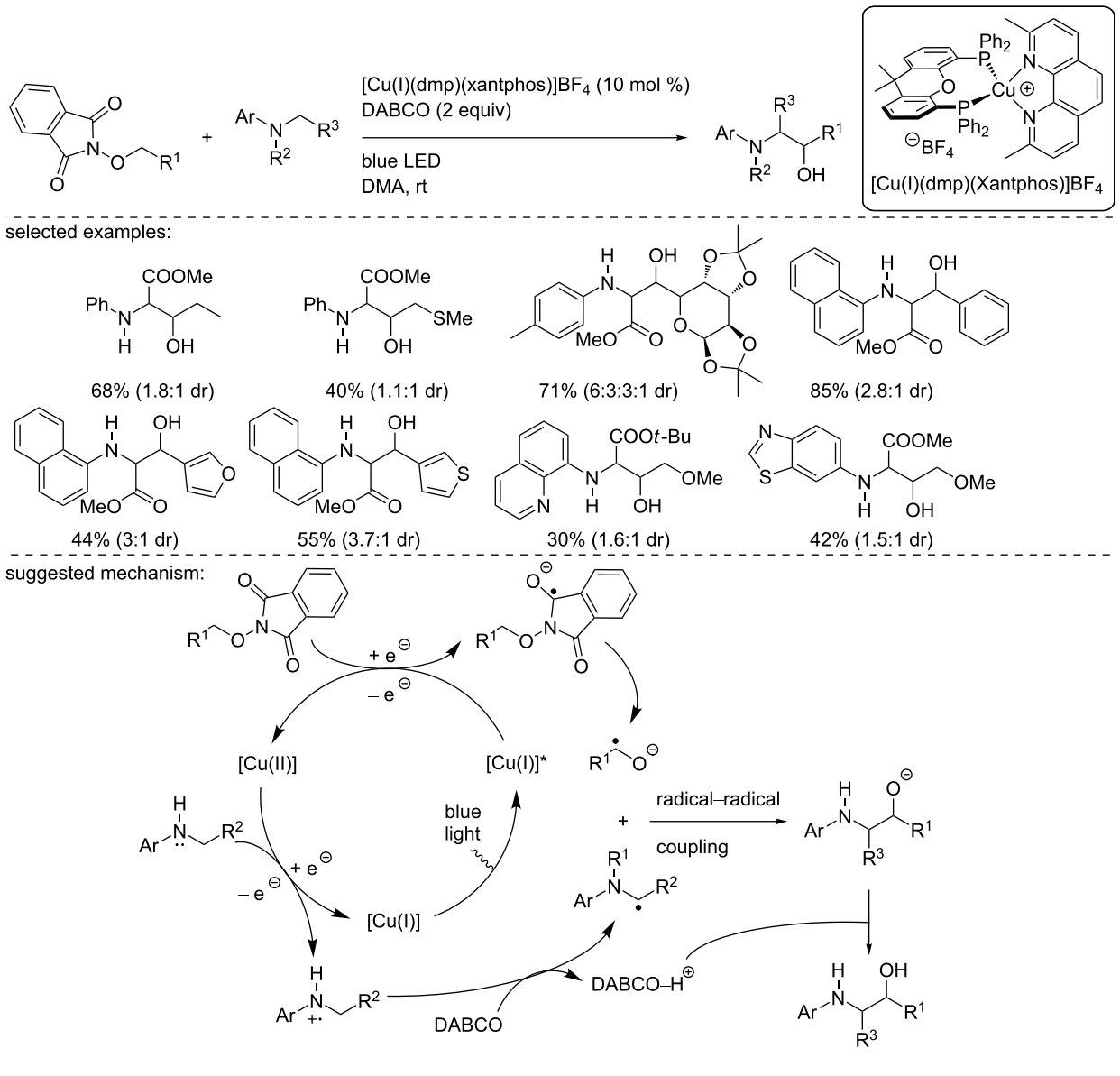

Scheme 27: Copper-photocatalyzed α-functionalization of alcohols with glycine ester derivatives.

complex, followed by a deprotonation by DABCO. The resulting alkoxide is finally converted into the alcohol by the protonated DABCO.

During this study, the authors found that replacement of the base by the Brønsted acid (*R*)-1,1-binaphtyl-2,2-diyl hydrogen phosphate ((*R*)-BNDHP) under similar reaction conditions and using the same copper catalyst provided the δ-functionalization of the alcohol (Scheme 28). This reaction manifold was applied to a large variety of *N*-alkoxyphthalimide derivatives using glycine ester derivatives and was also extended to more complex structures, including di- and tripeptides. These examples demonstrated the synthetic utility of the methodology. The reaction pathway was explained as follows by the authors: Similarly to the α-functionalization, the excited copper photocatalyst reduces the *N*-alkoxyphthalimide. Then, in the presence of the acid, it is protonated and collapses into the corresponding alkoxy radical. This radical carries out a 1,5-HAT to generate a carbon-centered radical. Finally, this radical recombines with the α-amino radical generated from the above-mentioned pathway.

2.3 Oxidation reactions

In 2012, Collins and co-workers described a copper-catalyzed photocyclization to synthesize [5]helicene (Scheme 29) [43]. Using the in situ-formed [Cu(I)(dmp)(xantphos)]BF_4

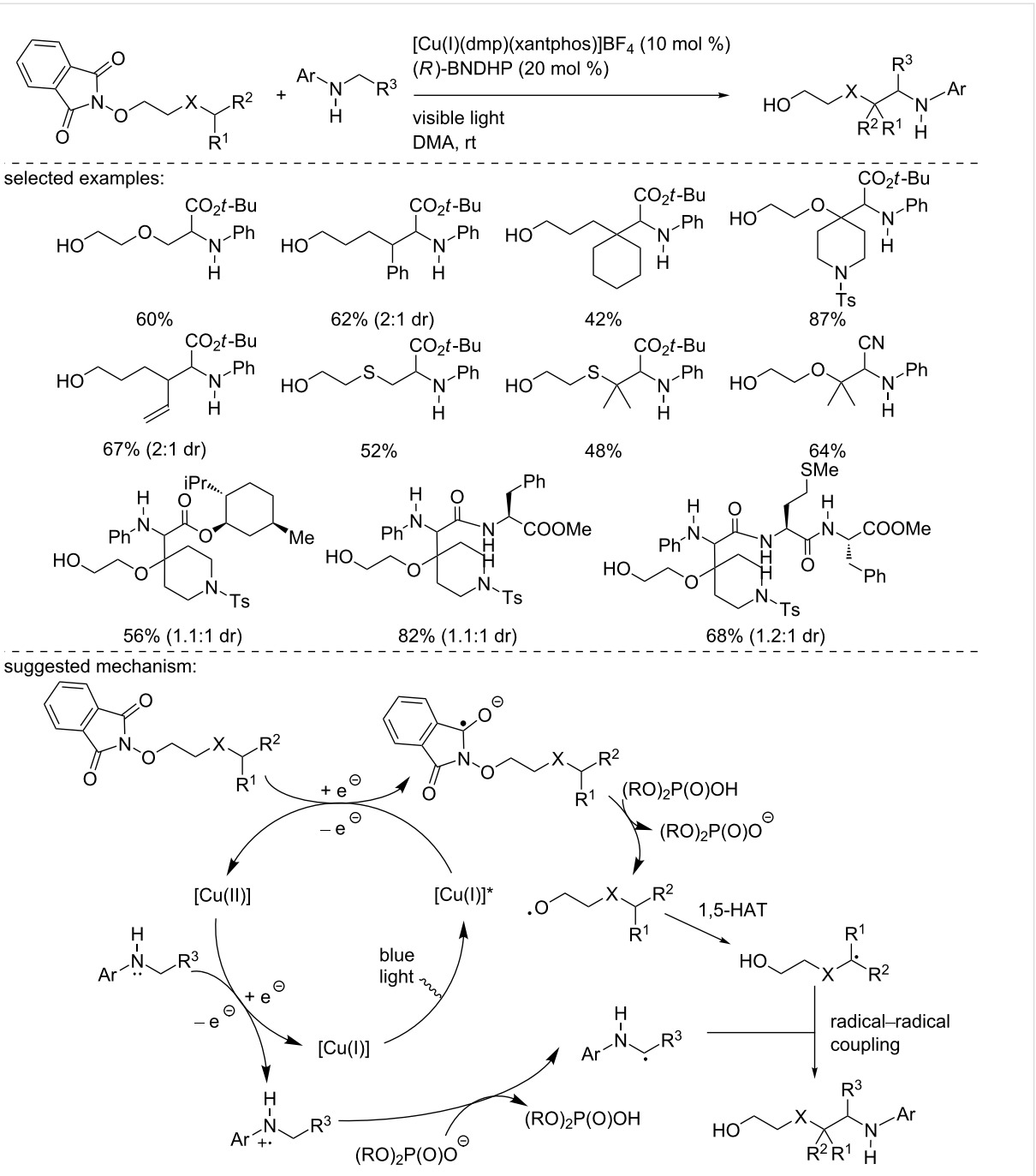

Scheme 28: δ-Functionalization of alcohols using [Cu(I)(dmp)(xantphos)]BF_4.

(25 mol %) in the presence of iodine and propylene oxide as the oxidant system under visible light irradiation, [5]helicene was synthesized in 57% yield. Importantly, the reaction scale was increased to 1 g under continuous flow conditions. Then, the reaction was extended to the cyclization of a stilbene derivative into phenanthrene in a moderate 23% isolated yield. To explain the reaction pathway, the authors suggested an oxidative mechanism.

One year later, 2013, Collins and co-workers extended this concept to the synthesis of carbazole derivatives under continuous flow conditions (Scheme 30) [44]. Using, the [Cu(I)(dmp)(xantphos)]BF_4 catalyst, the oxidative cyclization of various triarylamines was carried out in the presence of I_2 and propylene oxide as a proton scavenger under flow conditions (0.05 mL/min; residence time = 20 h). The use of flow conditions drastically enhanced the kinetics of the

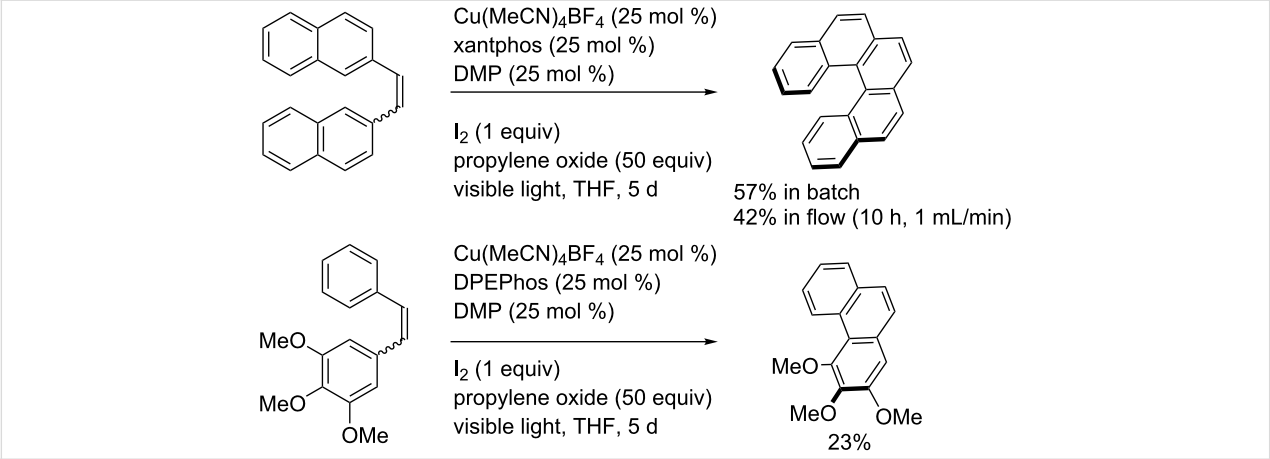

Scheme 29: Photocatalytic synthesis of [5]helicene and phenanthrene.

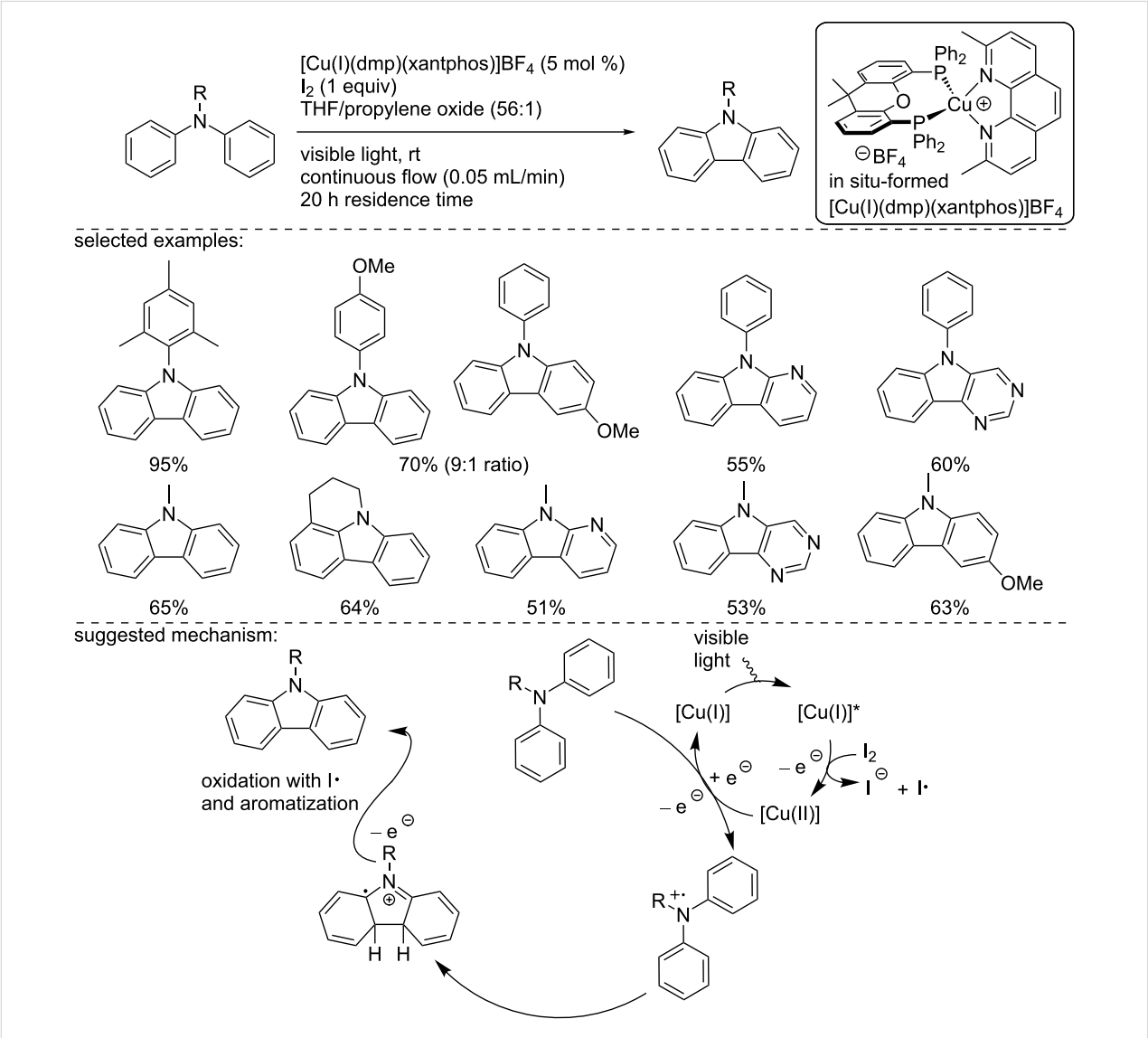

Scheme 30: Oxidative carbazole synthesis using in situ-formed [Cu(I)(dmp)(xantphos)]BF_4.

reaction, moving from 120 h reaction time in batch to 20 h using a continuous flow reactor. The reaction allowed the synthesis of a large panel of carbazoles. The selectivity of the reaction using an unsymmetrical triarylamine depended on the electronic density of the aromatic ring, furnishing, in some cases constitutional isomers. Importantly, in the case of heteroaryl-substituted triarylamines, the heterocycle was incorporated in the carbazole structure, and a single isomer was formed. Then, the methodology was extended to *N*-alkyldiarylamines, the products were isolated in good yields, and no dealkylation was observed for *N*-methyldiarylamines. To explain the reaction outcome, the authors suggested a mechanism involving oxidative quenching. First, the excited [Cu(I)]* species was oxidized in the presence of iodine, furnishing a [Cu(II)] complex. Then, an oxidation of the diarylamine occurred, generating the N-centered radical cation, which undergoes an intramolecular cyclization. A final oxidation of the aryl radical intermediate with an iodine radical, followed by aromatization, generated the desired carbazole.

Later in 2015, the group of Che described the synthesis of a zwitterionic copper(I) complex having a phenanthroline ligand (bcp) and a *nido*-carborane-diphosphine ligand. This complex was used in a benchmark reaction in photocatalysis, the oxidation of *N*-aryl tetrahydroisoquinoline (Scheme 31) [45]. Upon oxidation, the in situ-formed iminium ion was reacted with nitroalkanes, enamines, and indoles. In all cases, the 1-substituted tetrahydroisoquinolines were isolated in good to excellent yields. The reaction mechanism suggested by the authors was in agreement with the literature [46]: The excited copper catalyst oxidizes the tetrahydroisoquinoline and forms an N-centered radical cation. The copper catalyst is regenerated upon oxidation with O_2. The resulting superoxide radical anion allowed the formation of the α-amino radical that is then oxidized to the dihydroisoquinolinium species. Then, the latter reacted with the nucleophile (nitroalkanes, catalytically in situ-formed enamines and indoles) to furnish the product.

2.4 Proton-coupled electron transfer (PCET)

The PCET reaction is an interesting and unusual sequence to functionalize molecules. Indeed, it relies on a redox transformation with a concerted proton and electron exchange. Note that this process can occur either through an oxidative or a reductive pathway [47-49].

In 2018, during the development of a combinatorial approach to select the best copper-based photocatalyst, Collins and co-workers reported the synthesis of a bicyclic lactone by a PCET reaction manifold (Scheme 32) [39]. Using their methodology, the authors discovered the [Cu(I)(quinitri)(xantphos)]BF_4 catalyst as the best one, which afford the *cis*-lactone in 79% isolated yield.

In 2019, Collins and co-workers reported the synthesis of a new bifunctional copper photocatalyst for the reductive pinacol coupling of ketones and aldehydes (Scheme 33) [50]. This new catalyst was designed to activate the ketones or aldehydes due to an acidic proton present on the structure and to carry out an SET when excited by light. This approach represents the first report describing the design of a Cu-based photocatalyst able to carry out an SET and an activation of the substrate, in this case through H-bonding. This close proximity increased the yield of the transformation and avoided the presence of a Brønsted acid in the reaction media. As such, Collins and co-workers developed the catalyst [Cu(I)(pypzs)(BINAP)]BF_4 where the ligand (5-(4-fluorosulfonyl)amino-3-(2pyridyl)pyrazole)) (pypzs) had an acidic proton prone to activate the carbonyl group during the pinacol coupling reaction. In the presence of 2 mol % of the catalyst, the Hantzsch ester (HEH), as a hydrogen atom donor, under blue light irradiation, a large panel of ketones and aldehydes was readily converted into the corresponding 1,2-diols in moderate to excellent yields. The functional group tolerance of the reaction was excellent as bromides, phenols, thioethers, esters, boronic esters, and heterocycles, including pyridine and quinolines, were well tolerated. The authors carried out mechanistic studies and demonstrated the H-bonding ability of their catalyst by NMR studies. The following mechanism was suggested to explain the reaction pathway: After irradiation, the copper catalyst, in an excited state, is quenched by the HEH, as demonstrated by a quenching experiment. Then, the reduced catalyst is involved in a hydrogen bond interaction with the carbonyl derivative, attributed to the acidic proton present on the pypzs ligand, and activates the carbonyl group. The PCET occurs, furnishing a ketyl radical that can react with another molecule (ketone or aldehyde), delivering the pinacol product. A final HAT with another equivalent of HEH or HEH^+ delivers the product, and the resulting radical cation of the Hantzsch ester allows the regeneration of the catalyst in the ground state.

2.5 Reaction based on an energy transfer (EnT)

Reactions based on energy transfer represent an interesting class of photocatalyzed transformations. Indeed, this reaction sequence relies on the deactivation of an excited molecule through a transfer of energy to a second one. Then, this second molecule is raised to the excited state and can then react [51,52].

During the course of the design of a library of copper photocatalysts through a combinatorial approach, Collins and co-workers reported the copper-photocatalyzed vinyl azide

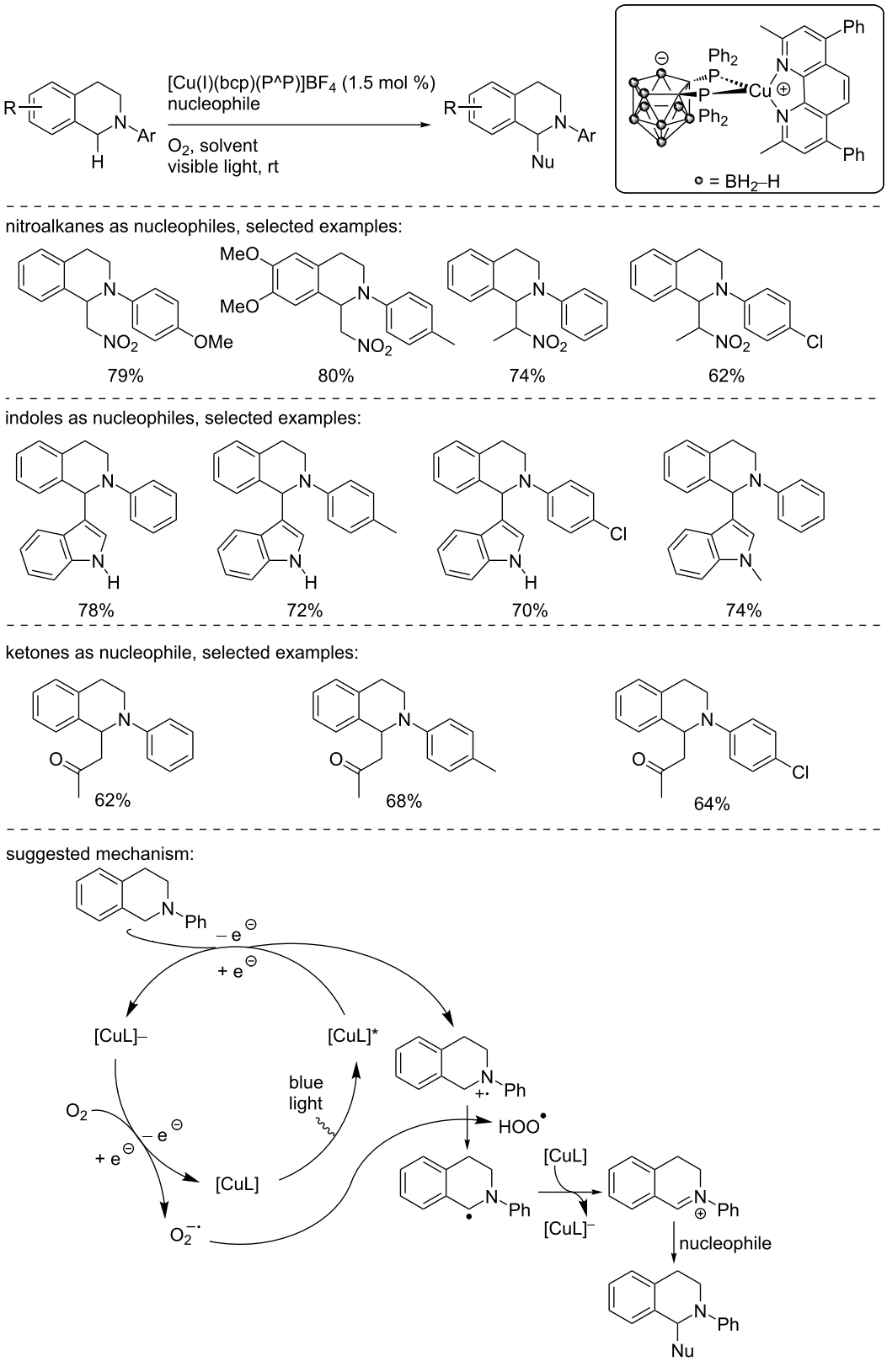

Scheme 31: Copper-photocatalyzed functionalization of *N*-aryl tetrahydroisoquinolines.

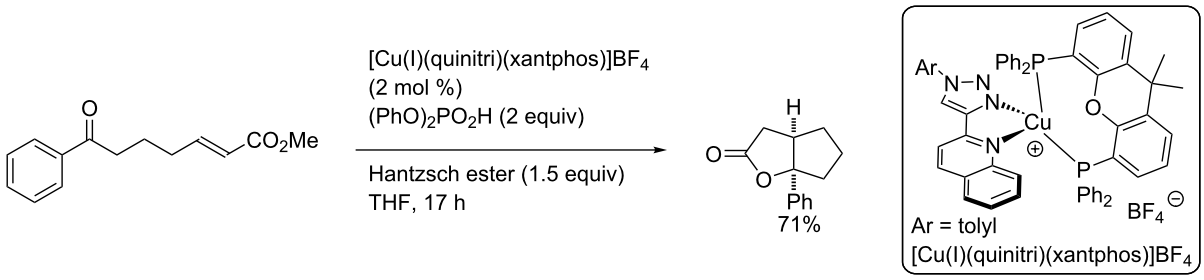

Scheme 32: Bicyclic lactone synthesis using a copper-photocatalyzed PCET reaction.

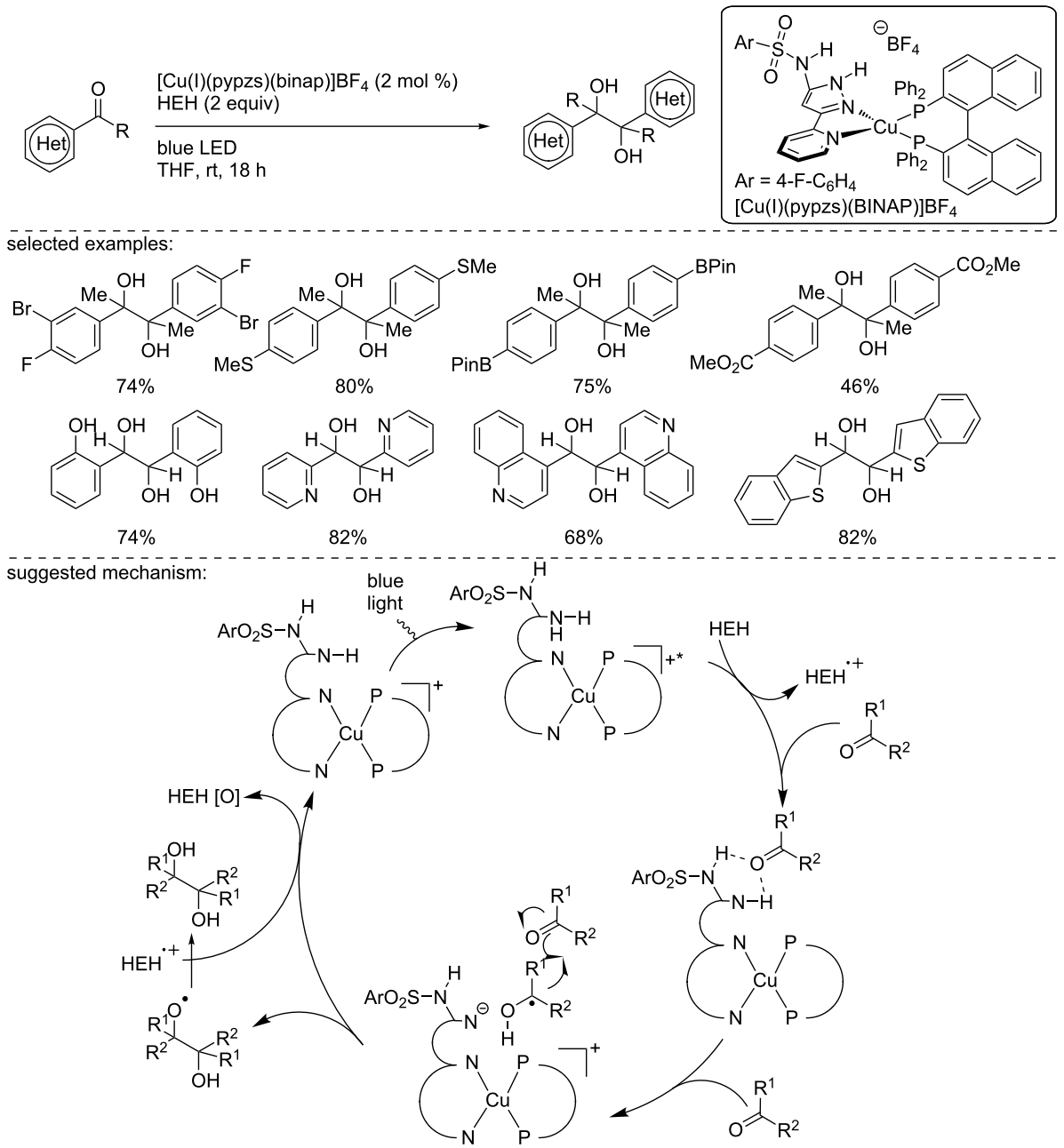

Scheme 33: Photocatalytic Pinacol coupling reaction catalyzed by [Cu(I)(pypzs)(BINAP)]BF_4. The ligands of the copper complex are omitted for clarity.

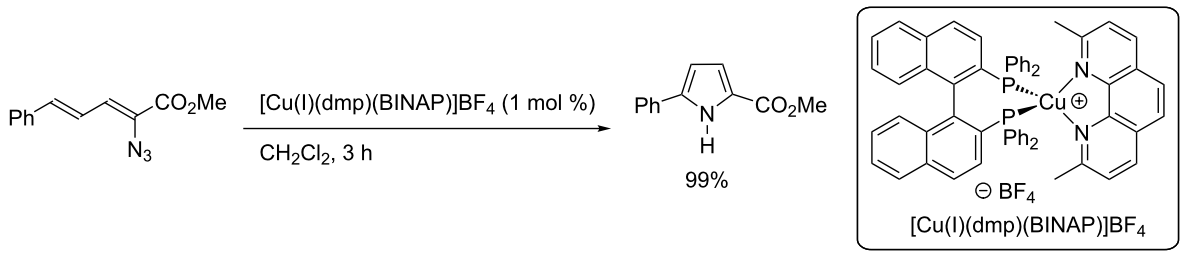

Scheme 34: Azide photosensitization using a Cu-based photocatalyst.

sensitization to allow the formation of the corresponding 2,5-disubstituted pyrrole (Scheme 34) [39]. The reaction was promoted by a visible-light irradiation (450 nm) using the complex [Cu(I)(dmp)(BINAP)]BF_4, and the desired pyrrole was obtained in quantitative yield.

Conclusion

Over the last decade, photocatalysis using homoleptic or heteroleptic copper complexes experienced a significant growth. The use of these inexpensive and readily available complexes in a broad range of applications, as discussed in this review, clearly demonstrate the growing importance of these catalysts. We do believe that the field of copper photocatalysis using well-defined complexes is still in its infancy, and for sure, new and unexpected reactivities will be discovered in a near future by using these catalysts.

Funding

This work was partially supported by Normandie Université (NU), the Région Normandie, the Centre National de la Recherche Scientifique (CNRS), Université de Rouen Normandie (URN), INSA Rouen Normandie, Labex SynOrg (ANR-11-LABX-0029), and Innovation Chimie Carnot (I2C). M. Z. thanks the China Scholarship Council (CSC) for a doctoral fellowship. T. P. thanks the Institut Universitaire de France, the CNRS Emergence program, and the Agence Nationale pour la Recherche (ANR-18-CE07-0004-01) for funding.

ORCID® iDs

Thomas Poisson - https://orcid.org/0000-0002-0503-9620

References

1. Stephenson, C.; Yoon, T.; MacMillan, D. W. C. *Visible Light Photocatalysis in Organic Chemistry;* Wiley-VCH: Weinheim, Germany, 2018. doi:10.1002/9783527674145
2. Nicewicz, D. A.; MacMillan, D. W. C. *Science* **2008,** *322,* 77–80. doi:10.1126/science.1161976
3. Yoon, T. P.; Ischay, M. A.; Du, J. *Nat. Chem.* **2010,** *2,* 527–532. doi:10.1038/nchem.687
4. Narayanam, J. M. R.; Stephenson, C. R. J. *Chem. Soc. Rev.* **2011,** *40,* 102–113. doi:10.1039/b913880n
5. Prier, C. K.; Rankic, D. A.; MacMillan, D. W. C. *Chem. Rev.* **2013,** *113,* 5322–5363. doi:10.1021/cr300503r
6. For instance: Cu = 5.6 €/kg; Ru = 6854 €/kg; Ir = 40579 €/kg; Pd = 43163 €/kg; Rh = 143949 €/kg; Metal trade market, London 10/11/2019.
7. Romero, N. A.; Nicewicz, D. A. *Chem. Rev.* **2016,** *116,* 10075–10166. doi:10.1021/acs.chemrev.6b00057
8. Wenger, O. S. *J. Am. Chem. Soc.* **2018,** *140,* 13522–13533. doi:10.1021/jacs.8b08822
9. Larsen, C. B.; Wenger, O. S. *Chem. – Eur. J.* **2018,** *24,* 2039–2058. doi:10.1002/chem.201703602
10. Reiser, O. *Acc. Chem. Res.* **2016,** *49,* 1990–1996. doi:10.1021/acs.accounts.6b00296
11. Paria, S.; Reiser, O. *ChemCatChem* **2014,** *6,* 2477–2483. doi:10.1002/cctc.201402237
12. Hernandez-Perez, A. C.; Collins, S. K. *Acc. Chem. Res.* **2016,** *49,* 1557–1565. doi:10.1021/acs.accounts.6b00250
13. Hossain, A.; Bhattacharyya, A.; Reiser, O. *Science* **2019,** *364,* eaav9713. doi:10.1126/science.aav9713
14. McMillin, D. R.; Buckner, M. T.; Ahn, B. T. *Inorg. Chem.* **1977,** *16,* 943–945. doi:10.1021/ic50170a046
15. Kern, J.-M.; Sauvage, J.-P. *J. Chem. Soc., Chem. Commun.* **1987,** 546–548. doi:10.1039/c39870000546
16. Pirtsch, M.; Paria, S.; Matsuno, T.; Isobe, H.; Reiser, O. *Chem. – Eur. J.* **2012,** *18,* 7336–7340. doi:10.1002/chem.201200967
17. Engl, S.; Reiser, O. *Eur. J. Org. Chem.* **2020,** 1523–1533. doi:10.1002/ejoc.201900839
18. Bagal, D. B.; Kachkovskyi, G.; Knorn, M.; Rawner, T.; Bhanage, B. M.; Reiser, O. *Angew. Chem., Int. Ed.* **2015,** *54,* 6999–7002. doi:10.1002/anie.201501880
19. Nicholls, T. P.; Caporale, C.; Massi, M.; Gardiner, M. G.; Bissember, A. C. *Dalton Trans.* **2019,** *48,* 7290–7301. doi:10.1039/c8dt04116d
20. Tang, X.-J.; Dolbier, W. R., Jr. *Angew. Chem., Int. Ed.* **2015,** *54,* 4246–4249. doi:10.1002/anie.201412199
21. Rawner, T.; Knorn, M.; Lutsker, E.; Hossain, A.; Reiser, O. *J. Org. Chem.* **2016,** *81,* 7139–7147. doi:10.1021/acs.joc.6b01001
22. Rawner, T.; Lutsker, E.; Kaiser, C. A.; Reiser, O. *ACS Catal.* **2018,** *8,* 3950–3956. doi:10.1021/acscatal.8b00847
23. Hossain, A.; Engl, S.; Lutsker, E.; Reiser, O. *ACS Catal.* **2019,** *9,* 1103–1109. doi:10.1021/acscatal.8b04188
24. Kochi, J. K. *J. Am. Chem. Soc.* **1962,** *84,* 2121–2127. doi:10.1021/ja00870a025
25. Baralle, A.; Fensterbank, L.; Goddard, J.-P.; Ollivier, C. *Chem. – Eur. J.* **2013,** *19,* 10809–10813. doi:10.1002/chem.201301449

26. Fumagalli, G.; Rabet, P. T. G.; Boyd, S.; Greaney, M. F. *Angew. Chem., Int. Ed.* **2015,** *54,* 11481–11484. doi:10.1002/anie.201502980
27. Rabet, P. T. G.; Fumagalli, G.; Boyd, S.; Greaney, M. F. *Org. Lett.* **2016,** *18,* 1646–1649. doi:10.1021/acs.orglett.6b00512
28. Smirnov, V. O.; Maslov, A. S.; Kokorekin, V. A.; Korlyukov, A. A.; Dilman, A. D. *Chem. Commun.* **2018,** *54,* 2236–2239. doi:10.1039/c8cc00245b
29. Nicholls, T. P.; Constable, G. E.; Robertson, J. C.; Gardiner, M. G.; Bissember, A. C. *ACS Catal.* **2016,** *6,* 451–457. doi:10.1021/acscatal.5b02014
30. Hossain, A.; Vidyasagar, A.; Eichinger, C.; Lankes, C.; Phan, J.; Rehbein, J.; Reiser, O. *Angew. Chem., Int. Ed.* **2018,** *57,* 8288–8292. doi:10.1002/anie.201801678
31. Cuttell, D. G.; Kuang, S.-M.; Fanwick, P. E.; McMillin, D. R.; Walton, R. A. *J. Am. Chem. Soc.* **2002,** *124,* 6–7. doi:10.1021/ja012247h
32. Knorn, M.; Rawner, T.; Czerwieniec, R.; Reiser, O. *ACS Catal.* **2015,** *5,* 5186–5193. doi:10.1021/acscatal.5b01071
33. Matsuo, K.; Yamaguchi, E.; Itoh, A. *Asian J. Org. Chem.* **2018,** *7,* 2435–2438. doi:10.1002/ajoc.201800533
34. Alkan-Zambada, M.; Hu, X. *Organometallics* **2018,** *37,* 3928–3935. doi:10.1021/acs.organomet.8b00585
35. Alkan-Zambada, M.; Hu, X. *J. Org. Chem.* **2019,** *84,* 4525–4533. doi:10.1021/acs.joc.9b00238
36. Michelet, B.; Deldaele, C.; Kajouj, S.; Moucheron, C.; Evano, G. *Org. Lett.* **2017,** *19,* 3576–3579. doi:10.1021/acs.orglett.7b01518
37. Baguia, H.; Deldaele, C.; Romero, E.; Michelet, B.; Evano, G. *Synthesis* **2018,** *50,* 3022–3030. doi:10.1055/s-0037-1610134
38. Zhao, W.; Wurz, R. P.; Peters, J. C.; Fu, G. C. *J. Am. Chem. Soc.* **2017,** *139,* 12153–12156. doi:10.1021/jacs.7b07546
39. Minozzi, C.; Caron, A.; Grenier-Petel, J.-C.; Santandrea, J.; Collins, S. K. *Angew. Chem., Int. Ed.* **2018,** *57,* 5477–5481. doi:10.1002/anie.201800144
40. Wang, C.; Guo, M.; Qi, R.; Shang, Q.; Liu, Q.; Wang, S.; Zhao, L.; Wang, R.; Xu, Z. *Angew. Chem., Int. Ed.* **2018,** *57,* 15841–15846. doi:10.1002/anie.201809400
41. Nitelet, A.; Thevenet, D.; Schiavi, B.; Hardouin, C.; Fournier, J.; Tamion, R.; Pannecoucke, X.; Jubault, P.; Poisson, T. *Chem. – Eur. J.* **2019,** *25,* 3262–3266. doi:10.1002/chem.201806345
42. Wang, C.; Yu, Y.; Liu, W.-L.; Duan, W.-L. *Org. Lett.* **2019,** *21,* 9147–9152. doi:10.1021/acs.orglett.9b03524
43. Hernandez-Perez, A. C.; Vlassova, A.; Collins, S. K. *Org. Lett.* **2012,** *14,* 2988–2991. doi:10.1021/ol300983b
44. Hernandez-Perez, A. C.; Collins, S. K. *Angew. Chem., Int. Ed.* **2013,** *52,* 12696–12700. doi:10.1002/anie.201306920
45. Wang, B.; Shelar, D. P.; Han, X.-Z.; Li, T.-T.; Guan, X.; Lu, W.; Liu, K.; Chen, Y.; Fu, W.-F.; Che, C.-M. *Chem. – Eur. J.* **2015,** *21,* 1184–1190. doi:10.1002/chem.201405356
46. Rueping, M.; Vila, C.; Koenigs, R. M.; Poscharny, K.; Fabry, D. C. *Chem. Commun.* **2011,** *47,* 2360–2362. doi:10.1039/c0cc04539j
47. Warren, J. J.; Tronic, T. A.; Mayer, J. M. *Chem. Rev.* **2010,** *110,* 6961–7001. doi:10.1021/cr100085k
48. Weinberg, D. R.; Gagliardi, C. J.; Hull, J. F.; Murphy, C. F.; Kent, C. A.; Westlake, B. C.; Paul, A.; Ess, D. H.; McCafferty, D. G.; Meyer, T. J. *Chem. Rev.* **2012,** *112,* 4016–4093. doi:10.1021/cr200177j
49. Miller, D. C.; Tarantino, K. T.; Knowles, R. R. *Top. Curr. Chem.* **2016,** *374,* No. 30. doi:10.1007/s41061-016-0030-6
50. Caron, A.; Morin, É.; Collins, S. K. *ACS Catal.* **2019,** *9,* 9458–9464. doi:10.1021/acscatal.9b01718
51. Strieth-Kalthoff, F.; James, M. J.; Teders, M.; Pitzer, L.; Glorius, F. *Chem. Soc. Rev.* **2018,** *47,* 7190–7202. doi:10.1039/c8cs00054a and references cited therein.
52. Zhou, Q.-Q.; Zou, Y.-Q.; Lu, L.-Q.; Xiao, W.-J. *Angew. Chem., Int. Ed.* **2019,** *58,* 1586–1604. doi:10.1002/anie.201803102

License and Terms

BEILSTEIN JOURNAL OF ORGANIC CHEMISTRY

Aerobic synthesis of *N*-sulfonylamidines mediated by N-heterocyclic carbene copper(I) catalysts

Faïma Lazreg[1], Marie Vasseur[1], Alexandra M. Z. Slawin[1] and Catherine S. J. Cazin[*2]

Full Research Paper

Open Access

Address:
[1]School of Chemistry, University of St Andrews, St Andrews, KY16 9ST, UK and [2]Centre for Sustainable Chemistry and Department of Chemistry, Ghent University, Krijgslaan 281-S3, 9000 Ghent, Belgium

Email:
Catherine S. J. Cazin[*] - catherine.cazin@ugent.be

* Corresponding author

Keywords:
catalysis; copper; copper catalysis; N-heterocyclic carbene; solvent-free; sulfonylamidines

Beilstein J. Org. Chem. **2020,** *16,* 482–491.
doi:10.3762/bjoc.16.43

Received: 13 December 2019
Accepted: 04 March 2020
Published: 24 March 2020

This article is part of the thematic issue "Copper-catalyzed reactions for organic synthesis".

Guest Editor: G. Evano

Abstract

A new catalytic strategy for the one-pot synthesis of *N*-sulfonylamidines is described. The cationic copper(I) complexes were found to be highly active and efficient under mild conditions in air and in the absence of solvent. A copper acetylide is proposed as key intermediate in this transformation.

Introduction

Amide derivatives represent a ubiquitous molecular construct in chemistry [1-3]. This structural motif favours rearrangements that lead to high reactivity and associated bioactivity [4,5]. Indeed, the presence of an *N*-atom in the amidine structure leads to opportunities as ligands and organocatalysts [6-8]. *N*-Sulfonylamidines and *N*-sulfonylimidates are members of a specific class of these amidines. One initial methodology developed for the formation of sulfonylamidines was based on the cleavage of the bond between the N-4 and C-benzene in thiadiazine ring-type molecules [9]. To date, only few examples of copper-based catalysts have been reported to enable access to such compounds [10-13]. Chang and co-workers were pioneers in this area [10-12]. A three-component reaction between alkyne, sulfonyl azide and amine/alcohol was described as a synthetic route to generate sulfonyltriazole intermediates. However, the presence of additives and high catalyst loading (CuI 10 mol %) were required for the synthesis of *N*-sulfonylimidates (Scheme 1, left).

Over the last two decades, NHCs (NHC = N-heterocyclic carbene) have become ligands of choice to permit the stabilisation and formation of highly reactive transition metal species [14]. Thus, significant advances have been achieved using this supporting ligand family [15-19]. Recently, our group contributed to this area, reporting on the synthesis of the first heteroleptic bis-NHC and mixed NHC/phosphine copper(I) complexes [20-22]. Interestingly, these new copper-based complexes have shown excellent activity in the [3 + 2] cycloaddition reaction of azides/sulfonyl azides and alkynes (Scheme 1, right) [22]. Based on these earlier results, the reactivity of these

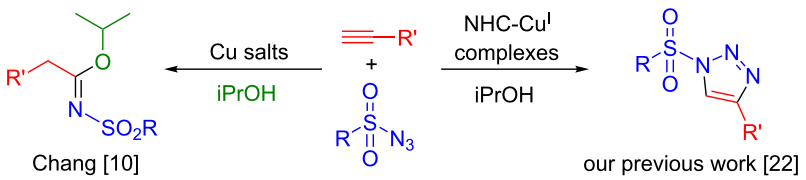

Scheme 1: Formation of sulfonyltriazoles and sulfonamidines.

catalysts was investigated in the context of achieving formation of the challenging sulfonamide derivatives.

Herein, we report the high efficiency of cationic copper(I) complexes for the formation of *N*-sulfonylamidines via a three-component reaction performed in air, using solvent-free conditions and in the absence of any additive.

Results and Discussion

$[Cu(ICy)_2]BF_4$ (**1**), [Cu(IPr)(ICy)]BF_4 (**2**) and [Cu(IPr)(P*t*-Bu_3)]BF_4 (**3**) were initially selected as optimum candidates [22]. This class of catalysts was expanded through the synthesis of the pyridine derivative **4**, of the heteroleptic normal/mesoionic carbene complex **5**, and of the homoleptic mesoionic triazole derivative **6** (Figure 1). This special class of ligands presents unique electronic and steric properties and lead to unusual reactivity [23-28].

[Cu(IPr)(Pyr)]OTf (**4**) was obtained by the reaction of the isolated hydroxide derivative [Cu(IPr)(OH)] [29] with pyridinium trifluoromethanesulfonate, while the biscarbene complexes **5** and **6** were obtained from the corresponding [Cu(NHC)Cl] through the in situ formation of the corresponding hydroxide complex [Cu(NHC)(OH)] [20] which deprotonates the triazolium salt (Scheme 2).

The reactivity of a series of cationic copper(I) complexes (**1**–**6**) was evaluated at 0.5 mol % loading using tosyl azide, phenylacetylene and diisopropylamine as benchmark substrates [31,32]. Various solvents were evaluated at room temperature under aerobic conditions (see Supporting Information File 1 for details). Tetrahydrofuran (THF), 1,2-DCE, 1,4-dioxane and acetonitrile proved to be the most suitable solvents for this transformation (Table 1). Interestingly, similar results were obtained for complexes **1**–**5**, while **6** displayed superior activity.

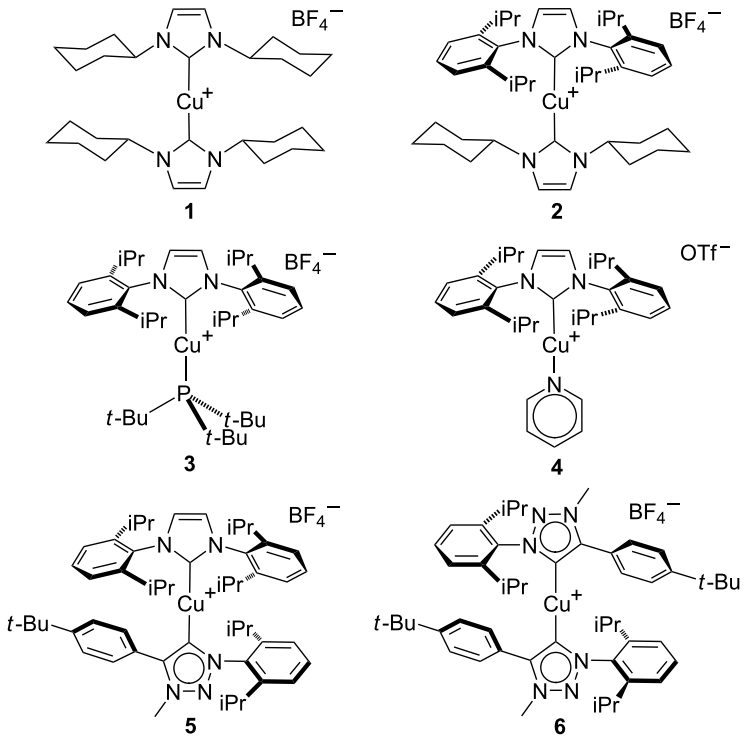

Figure 1: Catalytic systems used in this study.

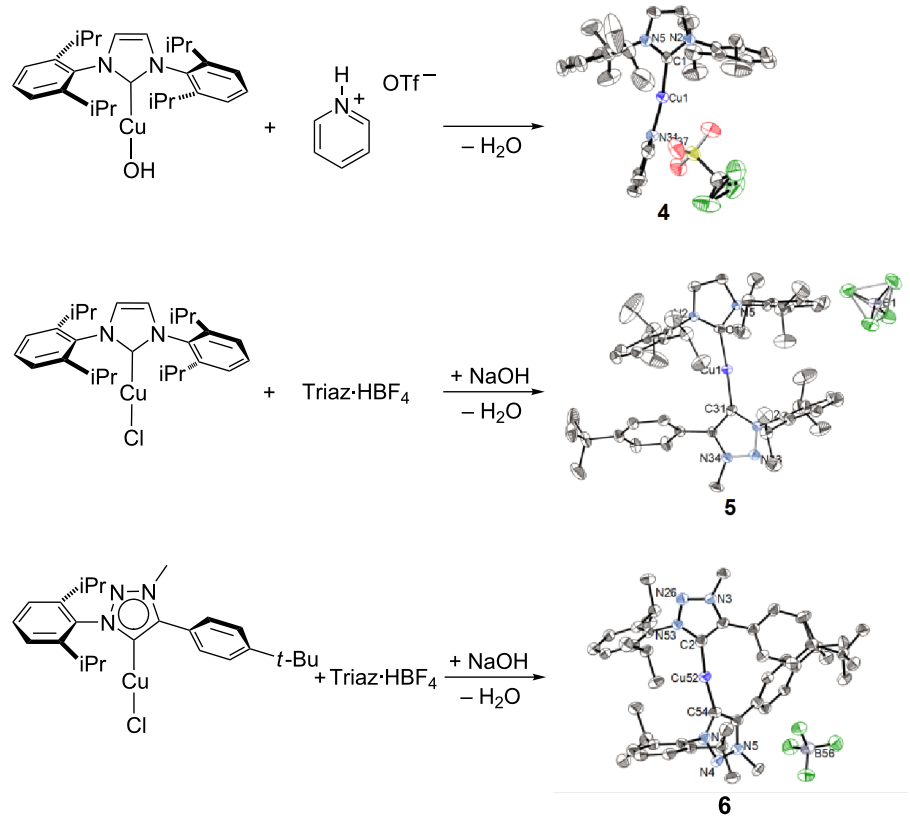

Scheme 2: Synthetic access to complexes **4**–**6** [30].

Table 1: Catalyst and solvent optimisation.[a,b]

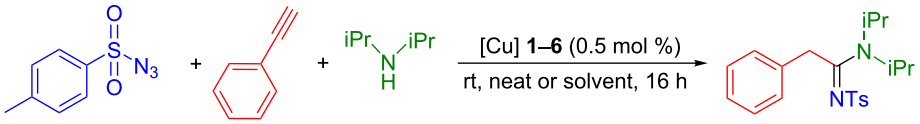

Entry	Complex	Solvent	Conv.[c] (%)
1	**1**	THF	49
2	**2**	THF	47
3	**3**	THF	42
4	**4**	THF	42
5	**5**	THF	46
6	**6**	THF	71
7	**6**	neat	65
8	**6**	1,2-DCE	63
9	**6**	water	41
10	**6**	1,4-dioxane	58
11	**1**	neat	30
12	**2**	neat	58
13	**5**	neat	55

[a]Reaction conditions: phenylacetylene (0.5 mmol), tosyl azide (0.6 mmol), diisopropylamine (0.6 mmol), [Cu] (0.5 mol %), solvent (1 mL), 16 hours. [b]See Supporting Information File 1 for full optimisation. [c]Conversion was determined by GC analysis based on phenylacetylene using mesitylene (42 µL) as internal standard.

Indeed, 71% conversion to the desired product was observed using the homoleptic cationic MIC (mesoionic carbene) complex **6** (Table 1, entry 6). For complexes **1**–**5**, the conversion proved modest and ranged between 42 and 49% (Table 1, entries 1–5).

Subsequently, solvent-free conditions were investigated (Table 1, entries 7 and 11–13). Interestingly, the absence of solvent proved to be highly effective, except for $[Cu(ICy)_2]BF_4$ **1** (Table 1 entry 11). An encouraging 65% conversion was obtained using $[Cu(Triaz)_2]BF_4$ **6** (Table 1, entry 7), while complexes **2** and **5** showed comparable results (Table 1, entries 12 and 13). Complex **6** was also shown to be active in water and in 1,4-dioxane. Based on these results, a reaction scope was conducted under solvent-free conditions, in air, using 1 mol % of $[Cu(Triaz)_2]BF_4$ **6** (Scheme 3).

Functionalised azides were reacted with phenylacetylene and diisopropylamine resulting in good to high yields (Scheme 3, **10a**–**g**). The presence of an activating/deactivating group in *para*-position of the aryl ring was evaluated in order to assess the substrate tolerance. Electron-donating groups, such as methyl, methoxy or naphthyl enhanced considerably the reactivity leading to quantitative conversion with respectively 96% (**10a**), 95% (**10c**) and 93% (**10g**) isolated yields, in reaction times of 3 to 4.5 hours. Regarding the 2,4,6-triisopropylsulfonyl azide, a slight decrease in the reactivity was observed (66%, **10f**), presumably due to the steric hindrance of the substrate. Electron-withdrawing groups such as bromo (**10d**) or cyano (**10e**) appeared to disfavour the reaction resulting in lower yields. Indeed for the cyanosulfonyl azide, under solvent-free conditions, only 38% of the desired product was obtained after 24 hours. This lower yield could also be due to the starting material being a solid which leads to poorer mixing and mass transport issues. Interestingly, when conducted in THF, an increase to 68% isolated yield was observed after 4 hours, supporting our inhomogeneity/transport hypothesis. In the case of the bromosulfonyl azide, a 73% conversion was obtained after 4 hours at 40 °C.

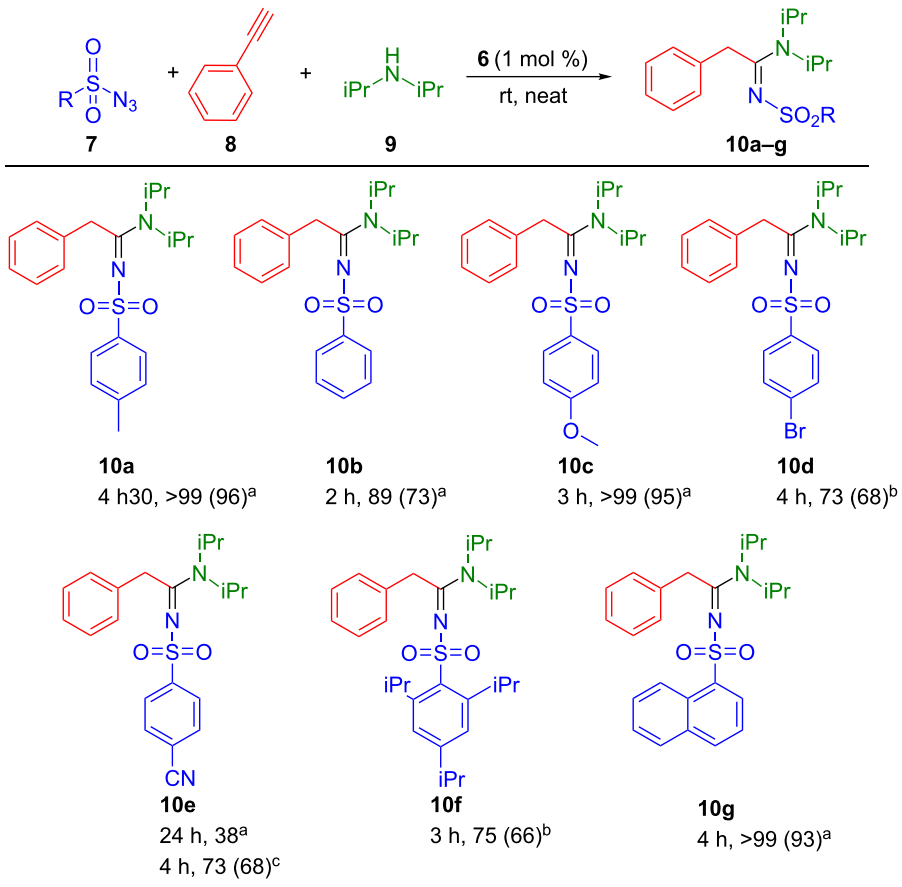

Scheme 3: Variation of sulfonylazides. Reaction conditions: phenylacetylene (0.5 mmol), sulfonyl azide (0.6 mmol), diisopropylamine (0.6 mmol), **6** (1 mol %). Conversion determined by ^{1}H NMR based on alkyne using mesitylene (42 µL) as internal standard. Isolated yield in parentheses. [a]Solvent-free conditions, rt. [b]Solvent-free conditions, 40 °C. [c]THF (1 mL), rt.

Various terminal aryl/alkyl-substituted alkynes were investigated in the presence of tosyl azide and diisopropylamine (Scheme 4). Under standard conditions, good to excellent yields were obtained. The presence of functional groups in *para*-position of the aryl ring leads to a decrease of the conversion to approximately 50% (**11a**, **11b**, **11c** and **11d**). The reactivity was considerably enhanced by increasing the temperature to 40 °C and/or the use of THF as reaction solvent. Interestingly, *ortho*- and *meta*-substitution of the aryl rings are well tolerated (**11e–i**). In the case of 9-ethynylphenanthrene, which is a solid substrate, solvent-free conditions lead to 78% isolated yield at 40 °C. Diynes were also investigated and excellent isolated yields were achieved (92% and 85% for **11j** and **11k**, respectively). Regarding the alkyl-alkynes, longer reactions times as

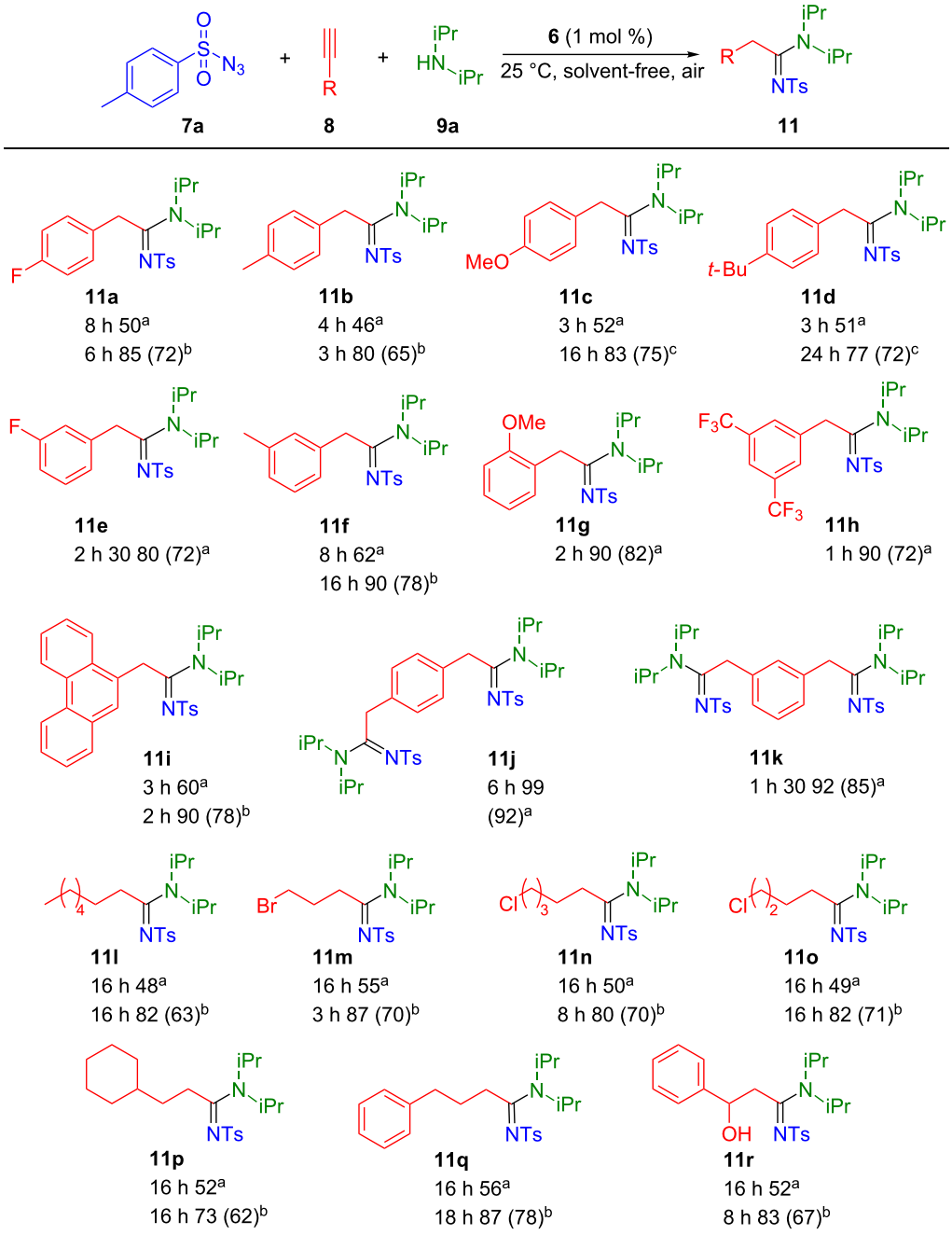

Scheme 4: Variation of alkynes. Reaction conditions: alkyne (0.5 mmol), tosyl azide (0.6 mmol), diisopropylamine (0.6 mmol), **6** (1 mol %). Conversion determined by ^{1}H NMR based on alkyne using mesitylene (42 µL) as internal standard. Isolated yield in parenthesis. [a]Solvent-free conditions, rt. [b]Solvent-free conditions, 40 °C. [c]THF (1 mL), rt.

well as higher temperature were required to reach high conversion. Interestingly, in the case of **11r**, the desired product was obtained in 67% isolated yield.

The effect of the amines was also investigated. Amongst the amines evaluated, dicyclohexylamine (for **12a**) and isopropylamine (for **12b**) lead to good isolated yields (64% and 72%, Scheme 5). In contrast, with diphenylamine, only 20% of the desired product was observed (**12c**).

Interestingly, with benzyl azide, a substrate not containing a sulfonyl moiety, the product obtained is the 1,2,3-triazole derivative [33], resulting from a [3 + 2] cycloaddition of azide and alkyne (Scheme 6).

The catalytic system was also shown applicable to phosphoryl azides; and reaction of phenylacetylene with diisopropylamine and diphenylphosphoryl azide leads to the formation of the corresponding phosphorylamidine product [34] in good yield (Scheme 7), using 2 mol % of catalyst under mild conditions (solvent-free, room temperature).

A proposed reaction mechanism occurring via formation of a copper-acetylide species is proposed and illustrated in

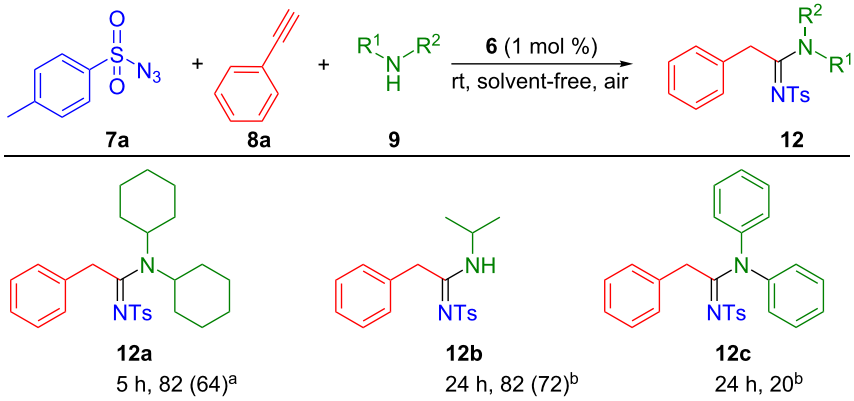

Scheme 5: Variation of the amine substrate. Reaction conditions: phenylacetylene (0.5 mmol), tosyl azide (0.6 mmol), amine (0.6 mmol), **6** (1 mol %). Conversion determined by ^{1}H NMR based on alkyne using mesitylene (42 µL) as internal standard. Isolated yield in parenthesis. [a]Solvent-free conditions, 40 °C. [b]THF (1 mL), rt.

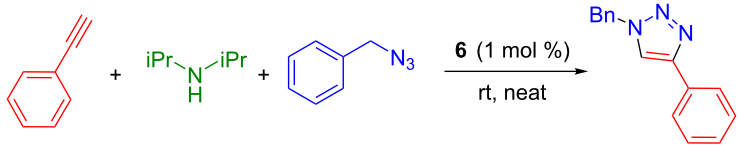

Scheme 6: Reactivity of "non-sulfonyl" azide [33]. Reaction conditions: phenylacetylene (0.5 mmol), benzyl azide (0.6 mmol), diisopropylamine (0.6 mmol), 24 h.

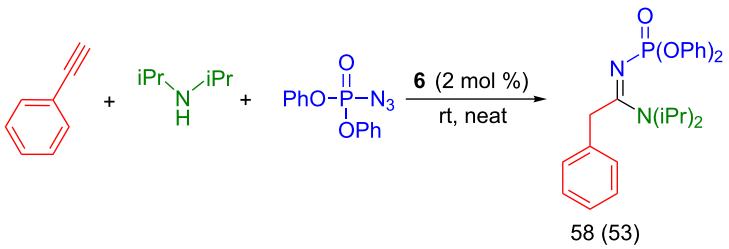

Scheme 7: Reactivity of diphenylphosphoryl azide. Reaction conditions: phenylacetylene (0.5 mmol), diphenylphosphoryl azide (0.6 mmol), diisopropylamine (0.6 mmol), [Cu] (2 mol %), 24 h. Conversion determined by GC based on phenylacetylene using mesitylene (42 µL) as internal standard. Isolated yield in parentheses.

Scheme 8. The bis-NHC copper(I) complex **6** reacts with the alkyne leading to the formation of an acetylide derivative **A** (left hand side, Scheme 8), with concomitant loss of a NHC ligand through the formation of the corresponding triazolium salt **B**. The intermediate **A** can then react with the azide substrate to form a triazolyl–copper complex **C**. The latter can liberate the amidine product and regenerate either catalyst **6** (triazolium salt **B** is source of proton) or directly the acetylide complex **A** (phenylacetylene is source of proton).

In order to support this mechanism, a number of stoichiometric reactions were conducted (see Supporting Information File 1). In a first instance, **6** was reacted with phenylacetylene at room temperature. This led to the rapid formation of the copper acetylide complex **A** with concomitant loss of the triazolium salt Triaz·HBF$_4$ (**B**, Scheme 9). To further confirm the formation of **A**, [Cu(Triaz)Cl] was reacted with phenylacetylene and sodium hydroxide (4 equiv), in toluene for 24 hours under an inert atmosphere. The independent synthesis of **A** was successfully achieved in this manner (Scheme 10). The latter was then reacted with tosyl azide. An immediate colour change resulted and based on ^{1}H NMR data, two new species were formed. They were identified as the sulfonyltriazole and an unstable organometallic compound, presumably the triazolylcopper(I) complex **C**. These results corroborated the proposed hypothesis regarding the formation of a triazole intermediate during the catalytic cycle.

To support the relevance of the Cu-acetylide species in catalysis, the benchmark reaction was conducted at 1 mol % catalyst of the isolated acetylide complex (Scheme 11). After 45 minutes, 80% conversion into the sulfonamidine product was

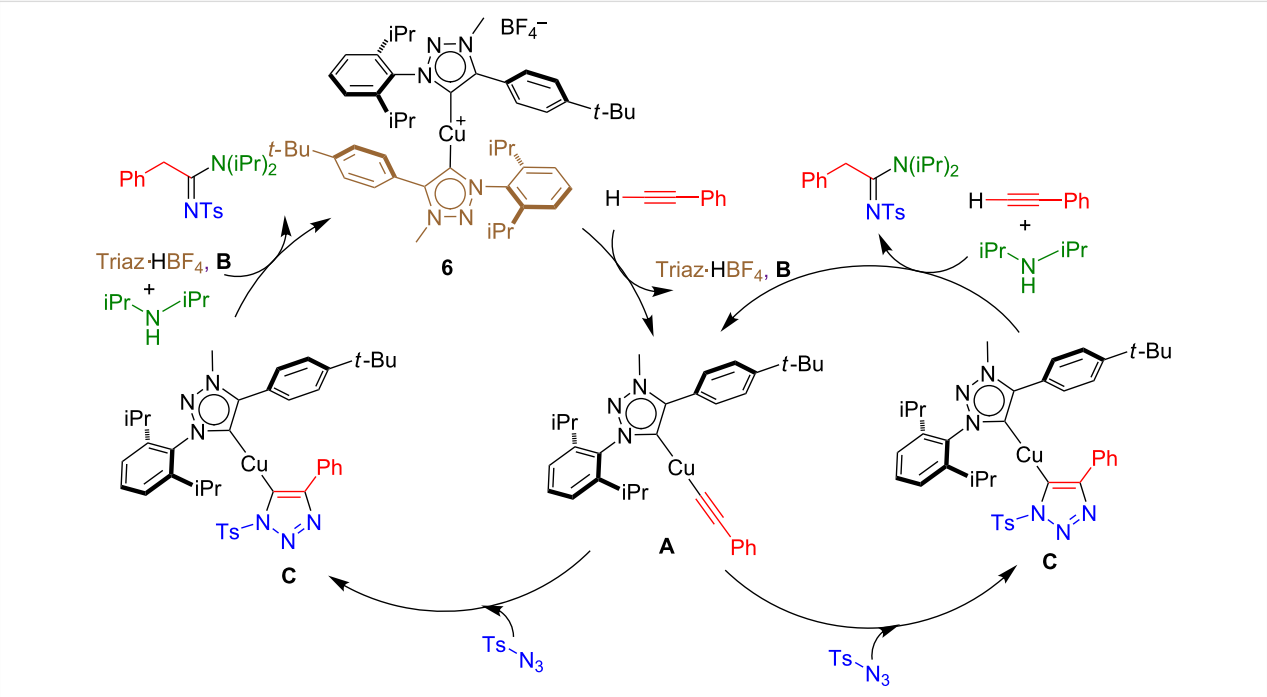

Scheme 8: Proposed mechanism for the formation of sulfonamidine.

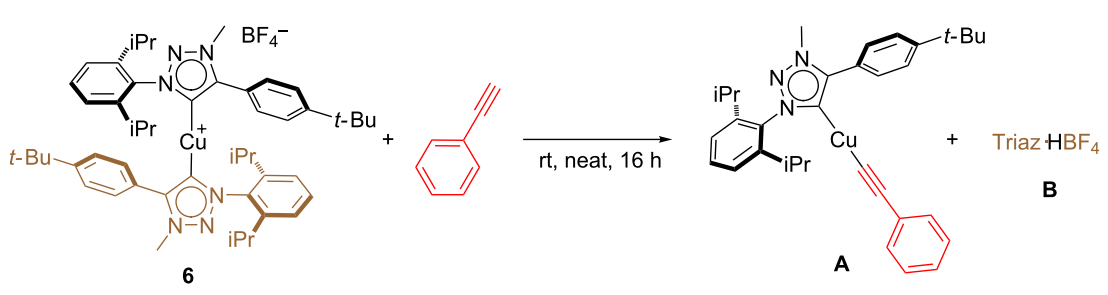

Scheme 9: Stoichiometric reaction between **6** and **8**.

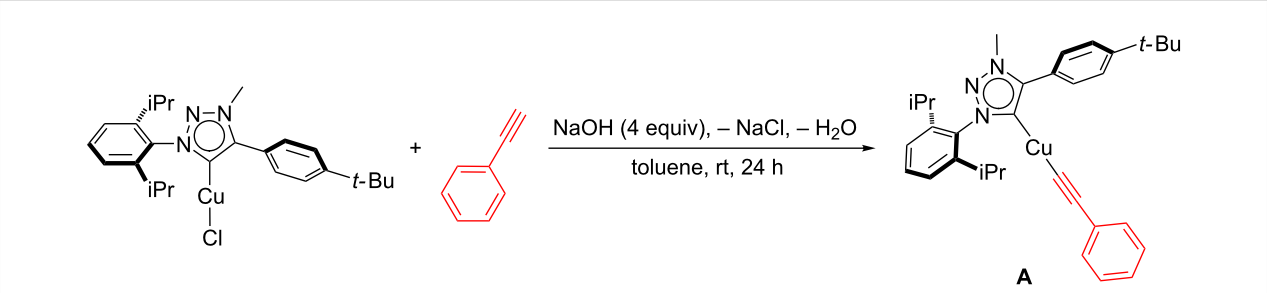

Scheme 10: Synthesis of copper-acetylide intermediate **A** via [Cu(Cl)(Triaz)].

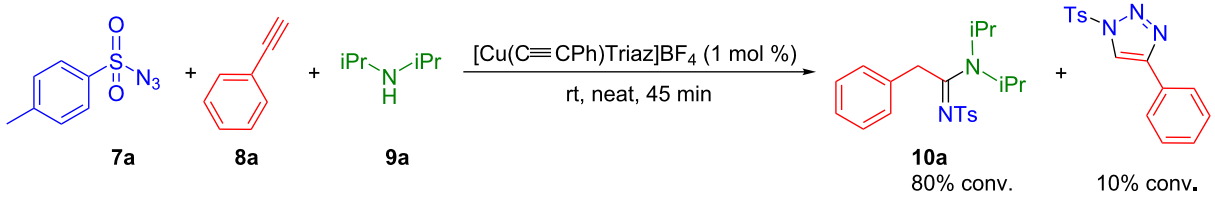

Scheme 11: Catalytic reaction involving copper-acetylide complex **A**.

observed. Of note, the presence of sulfonyltriazole was also observed (10%).

Conclusion

Cationic bis-carbene copper(I) complexes were shown to promote the formation of *N*-sulfonamidines in a Click reaction [35,36]. The new developed mesoionic NHC copper(I) complexes were found highly efficient under solvent-free and aerobic conditions. Stoichiometric reactions support the release of one NHC and the formation of a copper(I) acetylide as key elements in the catalytic cycle.

Experimental

***N,N'*-Bis{2,6-(diisopropyl)phenyl}imidazol-2-ylidene(pyridine)copper(I) triflate, [Cu(IPr)(Pyr)]OTf (4).** In a glovebox, a vial was charged with [Cu(OH)(IPr)] (200 mg, 0.41 mmol), pyridinium trifluoromethanesulfonate (94.0 mg, 1 equiv, 0.41 mmol) and THF (2 mL). The reaction mixture was stirred at room temperature for 15 hours. The solution was concentrated and diethyl ether (10 mL) was added. The precipitate was collected by filtration and washed with diethyl ether (3 × 5 mL). The desired compound was obtained as a colourless solid (201 mg, 92%). ^{1}H NMR (400 MHz, CD_2Cl_2, 298 K) δ (ppm) 0.82 (d, $^3J_{HH}$ = 6.9 Hz, 12H, CHCH_3 (IPr)), 1.01 (d, $^3J_{HH}$ = 6.9 Hz, 12H, CHCH_3 (IPr)), 1.44 (s, 9H, C(CH_3)$_3$), 2.36 (septet, $^3J_{HH}$ = 6.9 Hz, 4H, C*H*CH$_3$ (IPr)), 3.98 (s, 3H, CH_3), 7.06 (s, 2H, H^4 and H^5), 7.19 (d, $^3J_{HH}$ = 7.8 Hz, 4H, C$_{Ar}$*H* (IPr)), 7.50 (t, $^3J_{HH}$ = 7.8 Hz, 2H, C$_{Ar}$*H* (IPr)); ^{13}C{^{1}H} NMR (100 MHz, CD_2Cl_2, 298 K, TMS) δ (ppm) 23.5 (s, CH*C*H$_3$ (Triaz)), 24.8 (s, CH*C*H$_3$ (Triaz)), 28.8 (s, 2 *C*HCH$_3$ (Triaz)), 124.4 (s, *C*$_{Ar}$H), 124.5 (s, *C*$_{Ar}$H), 131.0 (s, *C*$_{Ar}$H), 134.2 (s, *C*$_{Ar}$H), 140.8 (s, *C*^{IV}), 145.8 (s, *C*H (IPr)), 148.9 (s, *C*^{IV}), 177.5 (s, *C*$_{carbene}$); ^{19}F{^{1}H} NMR (282 MHz, $CDCl_3$, 298 K) δ (ppm) −78.6 (s); anal. calcd for $C_{33}H_{41}CuF_3N_3O_3S$: C, 58.26; H, 6.07; N, 6.18; found: C, 58.39; H, 6.16; N, 6.08.

1-{2,6-(Diisopropyl)phenyl}-3-methyl-4-(4-*tert*-butylphenyl)-1,2,3-triazol-5-ylidene-(*N,N'*-bis{2,6-(diisopropyl)-phenyl}imidazol-2-ylidene)copper(I) tetrafluoroborate, [Cu(IPr)(Triaz)]BF$_4$ (5). In a glovebox, a microwave vial was charged with [Cu(Cl)(IPr)] (200.0 mg, 0.41 mmol), NaOH (66.0 mg, 4 equiv, 1.64 mmol), Triaz·HBF$_4$ (190.0 mg, 1 equiv, 0.41 mmol) and acetonitrile (2 mL). The reaction mixture was stirred during 2 h at 80 °C in a microwave. The solution was concentrated and diethyl ether (10 mL) was added. The precipitate was collected by filtration and washed with diethyl ether (3 × 5 mL). The desired compound was obtained as a colourless solid (346 mg, 92%). ^{1}H NMR (400 MHz, CD_2Cl_2, 298 K) δ (ppm) 0.77 (d, $^3J_{HH}$ = 6.9 Hz, 6H, CHCH_3 (Triaz)), 0.82 (d, $^3J_{HH}$ = 6.9 Hz, 12H, CHCH_3 (IPr)), 0.96 (d, $^3J_{HH}$ = 6.9 Hz, 6H, CHCH_3 (Triaz)), 1.01 (d, $^3J_{HH}$ = 6.9 Hz, 12H, CHCH_3 (IPr)), 1.44 (s, 9H, C(CH_3)$_3$) 1.99 (septet, $^3J_{HH}$ = 6.9 Hz, 2H, C*H*CH$_3$ (Triaz)), 2.36 (septet, $^3J_{HH}$ = 6.9 Hz, 4H, C*H*CH$_3$ (IPr)), 3.98 (s, 3H, CH_3), 6.98 (d, $^3J_{HH}$ = 8.3 Hz, 2H, C$_{Ar}$*H* (Triaz)), 7.06 (s, 2H, H^4 and H^5), 7.10 (d, $^3J_{HH}$ = 7.9 Hz, 2H, C$_{Ar}$*H* (Triaz)), 7.19 (d, $^3J_{HH}$ = 7.8 Hz, 4H, C$_{Ar}$*H* (IPr)), 7.36 (d, $^3J_{HH}$ =

8.4 Hz, 2H, $C_{Ar}H$ (Triaz)), 7.43 (t, $^3J_{HH}$ = 7.9 Hz, 1H, $C_{Ar}H$ (Triaz)), 7.50 (t, $^3J_{HH}$ = 7.8 Hz, 2H, $C_{Ar}H$ (IPr)); $^{13}C\{^1H\}$ NMR (75 MHz, CD_2Cl_2, 298 K) δ (ppm) 23.4 (s, $CHCH_3$ (Triaz)), 24.8 (s, $CHCH_3$ (IPr)), 24.4 (s, $CHCH_3$ (IPr)), 24.7 (s, $CHCH_3$ (Triaz)), 28.4 (s, $CHCH_3$ (Triaz)), 28.6 (s, $CHCH_3$ (IPr)), 31.3 (s, CCH_3), 35.0 (s, C^{IV}), 37.6 (s, CH_3), 123.4 (s, C^{IV}), 123.9 (s, $C_{Ar}H$), 124.2 (s, C^4 and C^5), 124.4 (s, $C_{Ar}H$), 126.6 (s, $C_{Ar}H$), 129.4 (s, $C_{Ar}H$), 130.5 (s, $C_{Ar}H$), 130.9 (s, $C_{Ar}H$), 134.3 (s, C^{IV}), 144.8 (s, C^{IV}), 145.2 (s, C^{IV}), 152.0 (s, C^{IV}), 152.8 (s, C^{IV}), 179.4 (s, $C_{carbene}$); $^{19}F\{^1H\}$ NMR (282 MHz, $CDCl_3$, 298 K) δ (ppm) −155.0 (s, BF_4), −155.1 (s, BF_4); anal. calcd for $C_{52}H_{69}BCuF_4N_5$: C, 68.30; H, 7.61; N, 7.66; found: C, 68.15; H, 7.72; N, 7.68.

Bis{1-{2,6-(diisopropyl)phenyl}-3-methyl-4-(4-*tert*-butylphenyl)-1,2,3-triazol-5-ylidene}copper(I) tetrafluoroborate, [Cu(Triaz)$_2$]BF$_4$ (6). In a glovebox, a vial was charged with [Cu(Cl)(Triaz)] (150.0 mg, 0.32 mmol), NaOH (50 mg, 4 equiv, 1.28 mmol), Triaz.HBF$_4$ (148 mg, 1 equiv, 0.32 mmol) and acetonitrile (2 mL). The reaction mixture was stirred during 2 h at 80 °C in a microwave. The solution was concentrated (0.5 mL) and diethyl ether (10 mL) was added. The precipitate was collected by filtration and washed with diethyl ether (3 × 5 mL). The desired compound was obtained as a colourless solid (281 mg, 97%). ^1H NMR (400 MHz, $CDCl_3$, 298 K, TMS) δ (ppm) 0.79 (d, $^3J_{HH}$ = 6.8 Hz, 12H, $CHCH_3$ (IPr)), 1.08 (d, $^3J_{HH}$ = 6.8 Hz, 12H, $CHCH_3$ (IPr)), 1.38 (s, 18H, $C(CH_3)_3$), 2.10 (septet, $^3J_{HH}$ = 6.8 Hz, 4H, $CHCH_3$ (IPr)), 4.20 (s, 6H, CH_3), 7.19 (d, $^3J_{HH}$ = 7.8 Hz, 4H, $C_{Ar}H$ (IPr)), 7.34 (m, 8H, $C_{Ar}H$), 7.49 (t, $^3J_{HH}$ = 7.7 Hz, 2H, $C_{Ar}H$ (IPr)); $^{13}C\{^1H\}$ NMR (75 MHz, $CDCl_3$, 298 K, TMS) δ (ppm) 23.8 (s, $CHCH_3$ (Triaz)), 24.2 (s, $CHCH_3$ (Triaz)), 28.4 (s, $CHCH_3$ (Triaz)), 31.3 (s, CCH_3), 35.0 (s, C^{IV}), 37.8 (s, CH_3), 123.6 (s, C^{IV}), 124 (s, $C_{Ar}H$), 126.2 (s, $C_{Ar}H$), 129.0 (s, $C_{Ar}H$), 131.1 (s, $C_{Ar}H$), 134.3 (s, C^{IV}), 145.0 (s, C^{IV}), 149.2 (s, C^{IV}), 153.4 (s, C^{IV}); $^{19}F\{^1H\}$ NMR (282 MHz, $CDCl_3$, 298 K) δ (ppm) −154.9 (s, BF_4), −155.0 (s, BF_4); anal. calcd for $C_{50}H_{66}BCuF_4N_6$: C, 66.62; H, 7.38; N, 9.32; found: C, 66.55; H, 7.46; N, 9.47.

General catalytic procedure. A vial was charged with [Cu(Triaz)$_2$]BF$_4$ (4.5 mg, 1 mol %), the alkyne (0.5 mmol), the azide (0.6 mmol) and the amine (0.6 mmol). The reaction was stirred neat for the appropriate amount of time. Dichloromethane (2 mL) and a saturated aqueous solution of ammonium chloride (3 mL) were added and the reaction mixture stirred during 30 minutes. The aqueous layer was extracted with dichloromethane (3 × 10 mL). The combined organic layers were dried over $MgSO_4$, filtered and the solvent was removed under vacuum. The crude product was purified by flash column chromatography or by recrystallization. The reported yields are the average of two reactions.

Supporting Information

Supporting Information File 1
Experimental and characterisation data.
[https://www.beilstein-journals.org/bjoc/content/supplementary/1860-5397-16-43-S1.pdf]

Supporting Information File 2
Crystal data for **4**.
[https://www.beilstein-journals.org/bjoc/content/supplementary/1860-5397-16-43-S2.cif]

Supporting Information File 3
Crystal data for **5**.
[https://www.beilstein-journals.org/bjoc/content/supplementary/1860-5397-16-43-S3.cif]

Supporting Information File 4
Crystal data for **6**.
[https://www.beilstein-journals.org/bjoc/content/supplementary/1860-5397-16-43-S4.cif]

Acknowledgements
The authors gratefully acknowledge the ESPRC National Mass Spectroscopy Facilities for the HMRS analysis at the University of Swansea.

ORCID® iDs
Alexandra M. Z. Slawin - https://orcid.org/0000-0002-9527-6418
Catherine S. J. Cazin - https://orcid.org/0000-0002-9094-8131

References
1. Zabicky, J. *The Chemistry of Amides;* Interscience: London, New York, 1970. doi:10.1002/9780470771235
2. Gautier, J.-A.; Miocque, M.; Farnoux, C. C. Preparation and synthetic uses of amidines. *Amidines and Imidates Vol. 1 (1975);* John Wiley & Sons, Ltd: Chichester, United Kingdom; pp 283–348. doi:10.1002/9780470771495.ch7
3. Bielawski, K.; Bielawska, A.; Sosnowska, K.; Miltyk, W.; Winnicka, K.; Pałka, J. *Biochem. Pharmacol.* **2006,** *72,* 320–331. doi:10.1016/j.bcp.2006.04.028
4. Sondhi, S. M.; Singh, J.; Kumar, A.; Jamal, H.; Gupta, P. P. *Eur. J. Med. Chem.* **2009,** *44,* 1010–1015. doi:10.1016/j.ejmech.2008.06.029
5. Özden, S.; Atabey, D.; Yıldız, S.; Göker, H. *Bioorg. Med. Chem.* **2005,** *13,* 1587–1597. doi:10.1016/j.bmc.2004.12.025
6. Barker, J.; Kilner, M. *Coord. Chem. Rev.* **1994,** *133,* 219–300. doi:10.1016/0010-8545(94)80059-6
7. Oakley, S. H.; Soria, D. B.; Coles, M. P.; Hitchcock, P. B. *Dalton Trans.* **2004,** 537–546. doi:10.1039/b314707j
8. Ahmad, S. M.; Braddock, D. C.; Cansell, G.; Hermitage, S. A.; Redmond, J. M.; White, A. J. P. *Tetrahedron Lett.* **2007,** *48,* 5948–5952. doi:10.1016/j.tetlet.2007.06.112

9. Iwakawa, T.; Tamura, H.; Masuko, M.; Murabayashi, A.; Hayase, Y. *J. Pestic. Sci. (Jpn. Ed., 1976-2002)* **1992,** *17,* 131–135. doi:10.1584/jpestics.17.2_131
10. Bae, I.; Han, H.; Chang, S. *J. Am. Chem. Soc.* **2005,** *127,* 2038–2039. doi:10.1021/ja0432968
11. Yoo, E. J.; Ahlquist, M.; Bae, I.; Sharpless, K. B.; Fokin, V. V.; Chang, S. *J. Org. Chem.* **2008,** *73,* 5520–5528. doi:10.1021/jo800733p
12. Yavari, I.; Ahmadian, S.; Ghazanfarpur-Darjani, M.; Solgi, Y. *Tetrahedron Lett.* **2011,** *52,* 668–670. doi:10.1016/j.tetlet.2010.11.135
13. Yang, T.; Cui, H.; Zhang, C.; Zhang, L.; Su, C.-Y. *Inorg. Chem.* **2013,** *52,* 9053–9059. doi:10.1021/ic4012229
14. Shi, S.; Nolan, S. P.; Szostak, M. *Acc. Chem. Res.* **2018,** *51,* 2589–2599. doi:10.1021/acs.accounts.8b00410
15. Cazin, C. S. J., Ed. *N-Heterocyclic Carbenes in Transition Metal Catalysis and Organocatalysis;* Springer: Dordrecht, Netherlands, 2011; Vol. 32. doi:10.1007/978-90-481-2866-2
16. Nolan, S. P. *N-Heterocyclic Carbenes in Synthesis;* Wiley-VCH: Weinheim, Germany, 2006. doi:10.1002/9783527609451
17. Díez-González, S.; Marion, N.; Nolan, S. P. *Chem. Rev.* **2009,** *109,* 3612–3676. doi:10.1021/cr900074m
18. Raubenheimer, H. G.; Cronje, S.; Olivier, P. J. *J. Chem. Soc., Dalton Trans.* **1995,** 313–316. doi:10.1039/dt9950000313
19. Egbert, J. D.; Cazin, C. S. J.; Nolan, S. P. *Catal. Sci. Technol.* **2013,** *3,* 912–926. doi:10.1039/c2cy20816d
20. Lazreg, F.; Cordes, D. B.; Slawin, A. M. Z.; Cazin, C. S. J. *Organometallics* **2015,** *34,* 419–425. doi:10.1021/om500882t
21. Lazreg, F.; Cazin, C. J. S. NHC–Copper Complexes and their Applications. *N-Heterocyclic Carbenes;* Wiley-VCH: Weinheim, Germany, 2014; pp 199–242. doi:10.1002/9783527671229.ch08
22. Lazreg, F.; Cazin, C. S. J. *Organometallics* **2018,** *37,* 679–683. doi:10.1021/acs.organomet.7b00506
23. Yoo, E. J.; Bae, I.; Cho, S. H.; Han, H.; Chang, S. *Org. Lett.* **2006,** *8,* 1347–1350. doi:10.1021/ol060056j
24. Martin, D.; Melaimi, M.; Soleilhavoup, M.; Bertrand, G. *Organometallics* **2011,** *30,* 5304–5313. doi:10.1021/om200650x
25. Mathew, P.; Neels, A.; Albrecht, M. *J. Am. Chem. Soc.* **2008,** *130,* 13534–13535. doi:10.1021/ja805781s
26. Schuster, O.; Yang, L.; Raubenheimer, H. G.; Albrecht, M. *Chem. Rev.* **2009,** *109,* 3445–3478. doi:10.1021/cr8005087
27. Guisado-Barrios, G.; Soleilhavoup, M.; Bertrand, G. *Acc. Chem. Res.* **2018,** *51,* 3236–3244. doi:10.1021/acs.accounts.8b00480
28. Bidal, Y. D.; Lesieur, M.; Melaimi, M.; Nahra, F.; Cordes, D. B.; Athukorala Arachchige, K. S.; Slawin, A. M. Z.; Bertrand, G.; Cazin, C. S. J. *Adv. Synth. Catal.* **2015,** *357,* 3155–3161. doi:10.1002/adsc.201500453
29. Fortman, G. C.; Slawin, A. M. Z.; Nolan, S. P. *Organometallics* **2010,** *29,* 3966–3972. doi:10.1021/om100733n
30. CCDC 1443106 (**4**), CCDC 1443107 (**5**), CCDC 1443108 (**6**) contain the supplementary crystallographic data for this contribution. These data can be obtained free of charge from the Cambridge Crystallographic Data Centre via http://www.ccdc.cam.ac.uk/data_request/cif.
31. Shojaei, S.; Ghasemi, Z.; Shahrisa, A. *Appl. Organomet. Chem.* **2017,** *31,* e3788. doi:10.1002/aoc.3788
32. Mandal, S.; Gauniyal, H. M.; Pramanik, K.; Mukhopadhyay, B. *J. Org. Chem.* **2007,** *72,* 9753–9756. doi:10.1021/jo701565m
33. Lazreg, F.; Slawin, A. M. Z.; Cazin, C. S. J. *Organometallics* **2012,** *31,* 7969–7975. doi:10.1021/om3006195
34. Kim, S. H.; Jung, D. Y.; Chang, S. *J. Org. Chem.* **2007,** *72,* 9769–9771. doi:10.1021/jo7016247
35. Worrell, B. T.; Malik, J. A.; Fokin, V. V. *Science* **2013,** *340,* 457–460. doi:10.1126/science.1229506
36. Jin, L.; Tolentino, D. R.; Melaimi, M.; Bertrand, G. *Sci. Adv.* **2015,** *1,* e1500304. doi:10.1126/sciadv.1500304

License and Terms

BEILSTEIN JOURNAL OF ORGANIC CHEMISTRY

Controlling alkyne reactivity by means of a copper-catalyzed radical reaction system for the synthesis of functionalized quaternary carbons

Goki Hirata, Yu Yamane, Naoya Tsubaki, Reina Hara and Takashi Nishikata*

Letter

Open Access

Address:
Graduate School of Science and Engineering, Yamaguchi University
2-16-1 Tokiwadai, Ube, Yamaguchi, 755-8611, Japan

Email:
Takashi Nishikata* - nisikata@yamaguchi-u.ac.jp

* Corresponding author

Keywords:
copper catalyst; 1,3-enyne; functionalized quaternary carbon; indolinone; tandem alkyl radical addition

Beilstein J. Org. Chem. **2020,** *16,* 502–508.
doi:10.3762/bjoc.16.45

Received: 17 December 2019
Accepted: 13 March 2020
Published: 26 March 2020

This article is part of the thematic issue "Copper-catalyzed reactions for organic synthesis".

Guest Editor: G. Evano

Abstract

A terminal alkyne is one of the most useful reactants for the synthesis of alkyne and alkene derivatives. Because an alkyne undergoes addition reaction at a C–C triple bond or cross-coupling at a terminal C–H bond. Combining those reaction patterns could realize a new reaction methodology to synthesize complex molecules including C–C multiple bonds. In this report, we found that the reaction of 3 equivalents of terminal alkyne **1** (aryl substituted alkyne) and an α-bromocarbonyl compound **2** (tertiary alkyl radical precursor) undergoes tandem alkyl radical addition/Sonogashira coupling to produce 1,3-enyne compound **3** possessing a quaternary carbon in the presence of a copper catalyst. Moreover, the reaction of α-bromocarbonyl compound **2** and an alkyne **4** possessing a carboxamide moiety undergoes tandem alkyl radical addition/C–H coupling to produce indolinone derivative **5**.

Introduction

Terminal alkynes are undoubtedly useful functional groups for organic synthesis, and they can undergo a variety of reactions [1]. The C–C triple bond of an alkyne is suitable for addition reactions, whereas the terminal hydrogen atom is a good target for cross-coupling by using Sonogashira and related coupling reactions [2-4]. Although there are many reports on alkyne transformations, one recent development in this area has been the reaction of alkynes with tertiary alkyl electrophiles to produce functionalized quaternary carbon atoms via addition [5-10] or coupling [11-16].

Recently, we have prepared quaternary carbon centers via radical reactions by using α-bromocarbonyl compounds (a tertiary alkyl source) and olefins or heteroatoms in the presence of a copper catalyst [17-19]. During our studies, we found that combinations of alkynes and tertiary alkyl radicals generated

from the reaction of a copper catalyst and an α-bromocarbonyl compound can undergo i) Sonogashira type couplings via an alkynyl-Cu intermediate [20], ii) *cis*-hydro tertiary alkylations via 1-alkenyl-Cu [21], and iii) *trans*-hydro tertiary alkylations via atom-transfer radical addition (ATRA) [21] (Scheme 1, i–iii). Therefore, we postulated that if we could control the reactivities of the alkynyl–Cu and ATRA adducts, a tandem tertiary alkylation followed by an alkynylation could occur to produce a 1,3-enyne possessing a quaternary carbon center with good regio- and stereoselectivity (Scheme 1, this work). Similarly, Zhu's group has reported that the reaction of an alkyne and an α-bromocarbonyl compound furnishes a highly functionalized 1,3-enyne compound via ATRA followed by an alkynylation reaction [22], but both Pd and Cu are required as catalysts in that case. Our methodology can realize a Pd-free catalyst system to prepare complex quaternary carbon atoms. Herein, we report the Cu-catalyzed control of the reactivity of an alkyne (addition and coupling) undergoing tandem tertiary alkylation and alkynylation to produce a 1,3-enyne containing a quaternary carbon center with good regio- and stereoselectivity.

Results and Discussion

In our preliminary research, we tried various Cu salts, including CuI, CuBr, CuCl, CuOAc, and CuOTf, and ligands, including PPh_3, 1,10-phenanthroline (1,10-Phen), *N*,*N*,*N*',*N*'',*N*''-pentamethyldiethylenetriamine, and tris(2-pyridylmethyl)amine, in the reaction of phenylacetylene (**1a**) and α-bromoester **2a**. From these experiments, CuBr and 1,10-Phen acted as a good catalyst system for obtaining 1,3-enyne **3a** in 62% yield with good regio- and stereoselectivity (Table 1, entry 1). On the basis of this preliminary result, we also tried other conditions. Toluene was very effective in our previous reaction system [17] but was not effective at all in this case (Table 1, entry 2). The reaction without NaI resulted in the formation of **3a**-**Br** in 30% yield, instead of **3a** (Table 1, entry 3). If KI was used instead of NaI, the yield of **3a** decreased (Table 1, entry 4). We will discuss the proposed reaction mechanism later in the text, but the formation of **3a**-**I** via ATRA could be important for the alkynylation reaction. Generally, the Sonogashira coupling requires both a Pd catalyst and a Cu co-catalyst [2-4]. However, couplings with terminal alkynes can be carried out in the absence of the Pd catalyst [23-32]; this is the so-called Castro–Stephens reaction [33]. The effect of the base was very important for producing the main product **3a** (Table 1, entries 5–8). If the reaction was performed in the presence of a base other than Cs_2CO_3, a decreased yield of **3a** was observed. Finally, an increased amount of catalyst was effective for obtaining the highest yield (Table 1, entry 9). The total yield was moderate, but the yields for each step of this two-step tandem reaction system (ATRA followed by Castro–Stephens coupling) should be over 80%.

Under the optimized conditions, the reactivities of alkynes **1** and α-bromocarbonyl compounds **2** were examined (Figure 1). The two-step tandem alkyne transformation produced various 1,3-enynes **3** with concomitant formation of ATRA adducts as side-products. It was very difficult to separate the products by silica-gel column chromatography; therefore, we are reporting the ^{1}H NMR and GPC yields of **3**. (The pure products were obtained by gel permeation chromatography (GPC).) For example, α-bromocarbonyl compounds **2** possessing various degrees of steric bulkiness (ethyl groups) at the carbonyl α-position or a

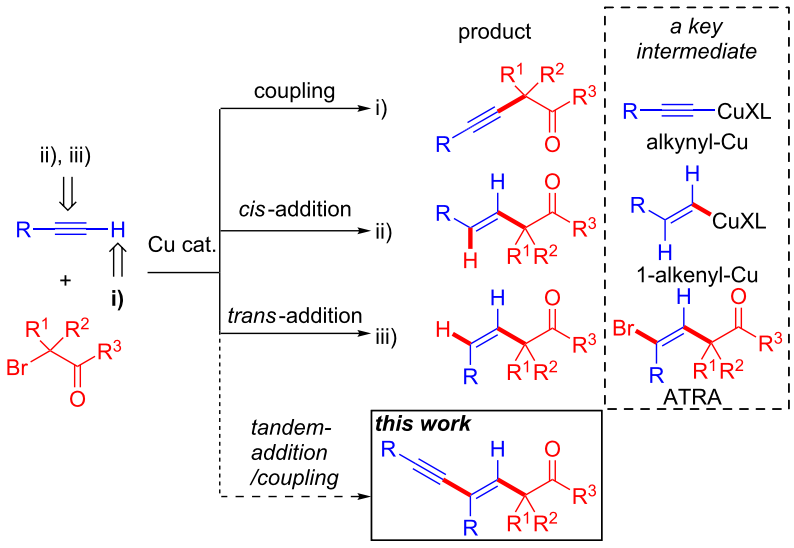

Scheme 1: Reaction modes of alkyne.

Table 1: Optimization.[a]

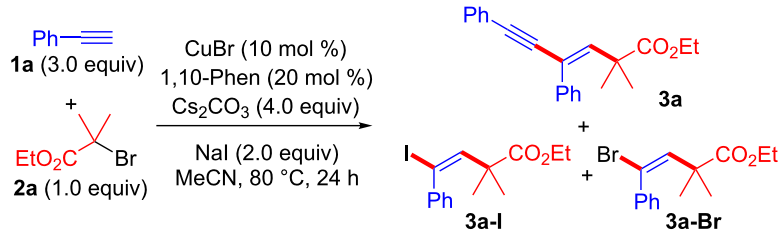

entry	changes from standard conditions	**3a** (%)	**3a-I** (%)	**3a-Br** (%)
1	none	62	10	trace
2	toluene instead of MeCN	trace	–	–
3	without NaI	<5	0	30
4	KI instead of NaI	30	7	7
5	Hunig's base instead of Cs_2CO_3	trace	60	trace
6	iPr_2NH instead of Cs_2CO_3	trace	65	trace
7	K_2CO_3 instead of Cs_2CO_3	6	58	trace
8	K_3PO_4 instead of Cs_2CO_3	26	20	trace
9	15 mol % CuBr and 30 mol % 1,10-Phen	66(52)[b]	7	trace

[a]Conducted at 80 °C for 24 h in MeCN with CuBr (10 mol %), 1,10-Phen (20 mol %), Cs_2CO_3 (4.0 equiv), NaI (2.0 equiv), **1a** (3.0 equiv) and **2a** (1.0 equiv). Yields were determined by ^{1}H NMR analysis. [b]GPC yield.

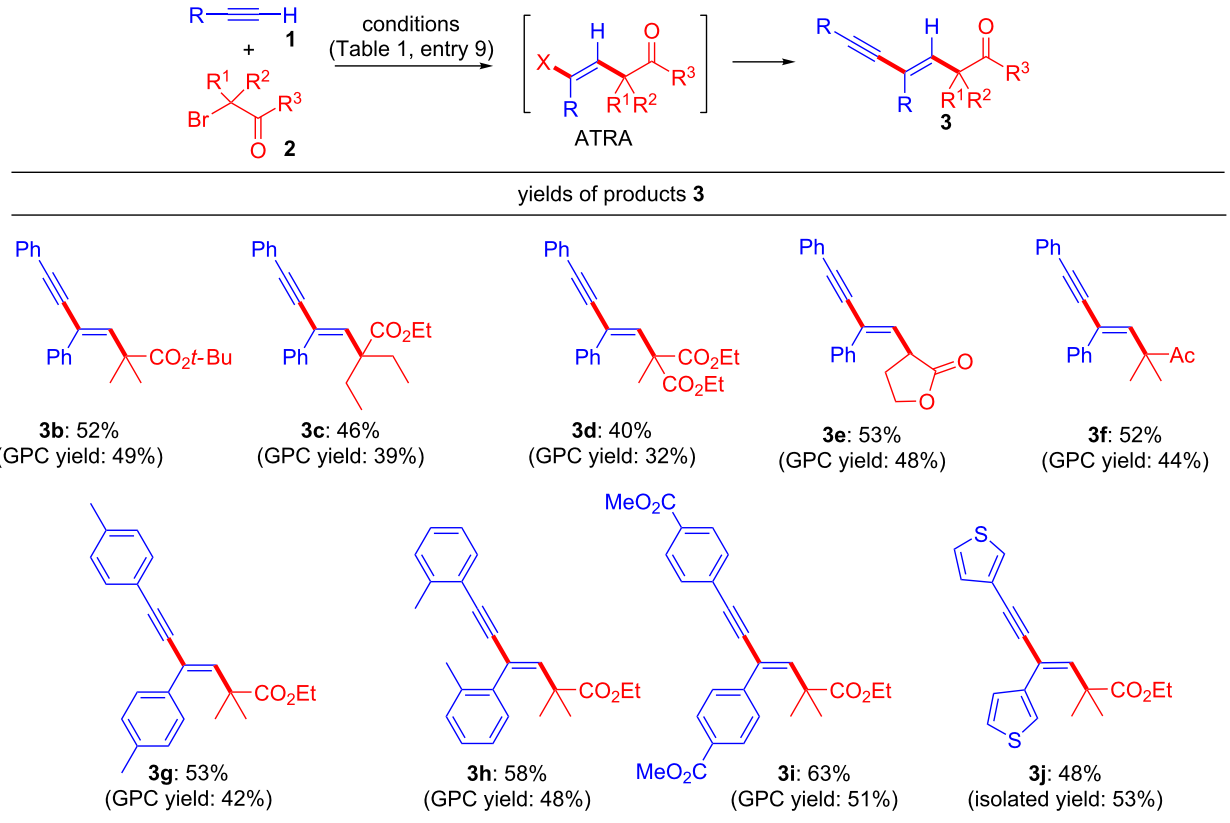

Figure 1: Substrate scope of **1** and **2**. [a]Conducted at 80 °C for 24 h in MeCN with CuBr (10 mol %), 1,10-Phen (20 mol %), Cs_2CO_3 (4.0 equiv), NaI (2.0 equiv), **1** (3.0 equiv) and **2** (1.0 equiv). Yields were determined by ^{1}H NMR analysis.

tert-butyl ester group reacted with **1a** to produce **3b** and **3c** in moderate yields. Bromomalonate, bromolactone, and bromoketone derivatives resulted in the formation of **3d**, **3e**, and **3f** in 40%, 53%, and 52% yield, respectively. *Ortho* and *meta* substituted arylalkynes **1** reacted with **2a** to produce **3g** and **3h**, respectively. An arylalkyne **1** possessing an electron-withdrawing group (ester) yielded **3i** without affecting the reactivity of **2**. Sulfur functional groups tend to decrease the catalytic activity of copper salts, but thienyl-substituted alkyne **1** reacted with **2a** to produce **3j** in 48% yield.

Although the exact reaction mechanism is currently unclear, one possibility involves a radical pathway including cross-coupling with an alkynyl copper species (Scheme 2). After the generation of **A**, addition of **A** to **1** takes place to give the radical intermediate **B**. This then reacts with the Cu(II) species to produce intermediate **C**, with concomitant formation of a Cu(I) species. The brominated intermediate **C** undergoes a cross-coupling reaction with the alkynyl copper species to give the desired product **3**. We have detected brominated intermediate **C** during the reaction. We have also examined the reaction between **3a-Br** (intermediate **C**) and the alkynyl copper species (**1a-Cu**) (Scheme 3). The result showed that **3a-Br** reacted with the alkynyl copper species to produce the desired product **3a** in reasonable yield. This reaction should be a Sonogashira coupling without a Pd catalyst [23,24,30].

Interestingly, if the reaction of **2a** and electron-deficient alkyne **4a** was performed under the conditions shown in Table 1, entry 9, the C–H cyclized product **5a** was obtained instead of **3k**. In this case, an alkyl radical addition followed by C–H cyclization via an alkenyl radical intermediate could be occur (Scheme 4). A Pd-catalyzed cascade reaction (C–C bond formation/C–H cyclization process) of *N*-arylpropynamide **4** for the preparation of indolinone derivatives **5** was previously reported by Li's group [34,35]. In another report on C–H cyclization by Lei's group, Ni-catalyzed aromatic C–H alkylation occurs via a radical reaction [36]. Both cases were helpful in our development of the current Cu-catalyzed cascade C–H cyclization system.

After careful optimization, we found that CuI, 1,10-Phen, Cy_2NMe as a base, and 1,4-dioxane were effective for obtaining the best yields of products **5** (Figure 2). In this examination, product isolation was difficult because of the formation of stereoisomers (*E* and *Z* stereoisomers of **5**). The yields shown in

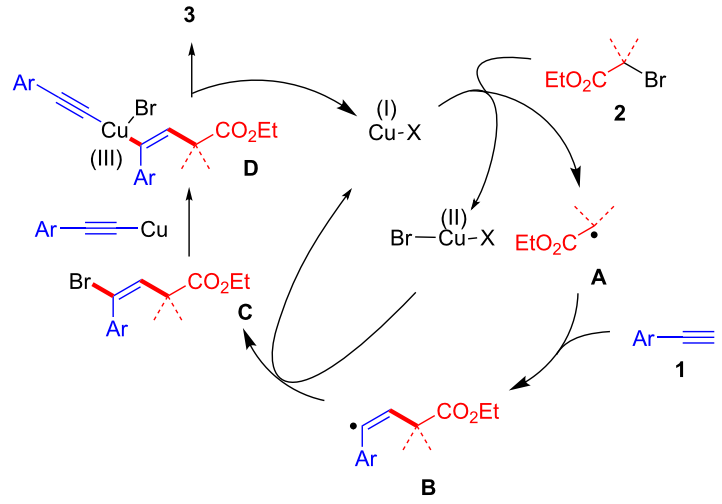

Scheme 2: Proposed mechanism.

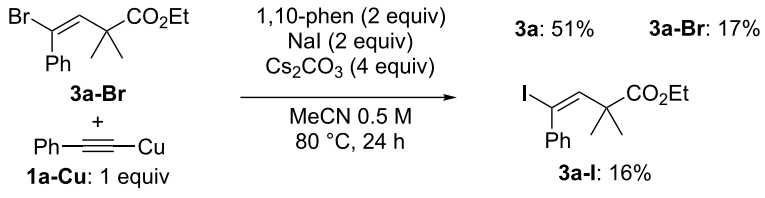

Scheme 3: Control experiment.

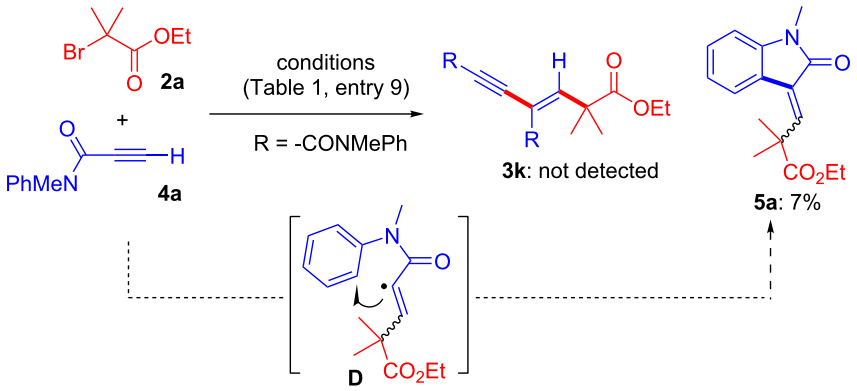

Scheme 4: Reaction of **2a** and **4a**.

Figure 2 were including isomers (We also put yield of pure *E*-**5** as an NMR yield.). Although the chemical yields of **5** were moderate, the stereoselectivities in this reaction were good (the major stereoisomers of **5** produced were *E*). We tested compounds **2** possessing acyclic and cyclic structures and compounds **4** possessing MeO, F, and *N*-Et moieties as substrates for the reaction; however, no big differences were observed. The C–H cyclized products were not obtained from the reaction of compound **4** if it did not possess an alkyl substituent on the nitrogen atom of the amide bond.

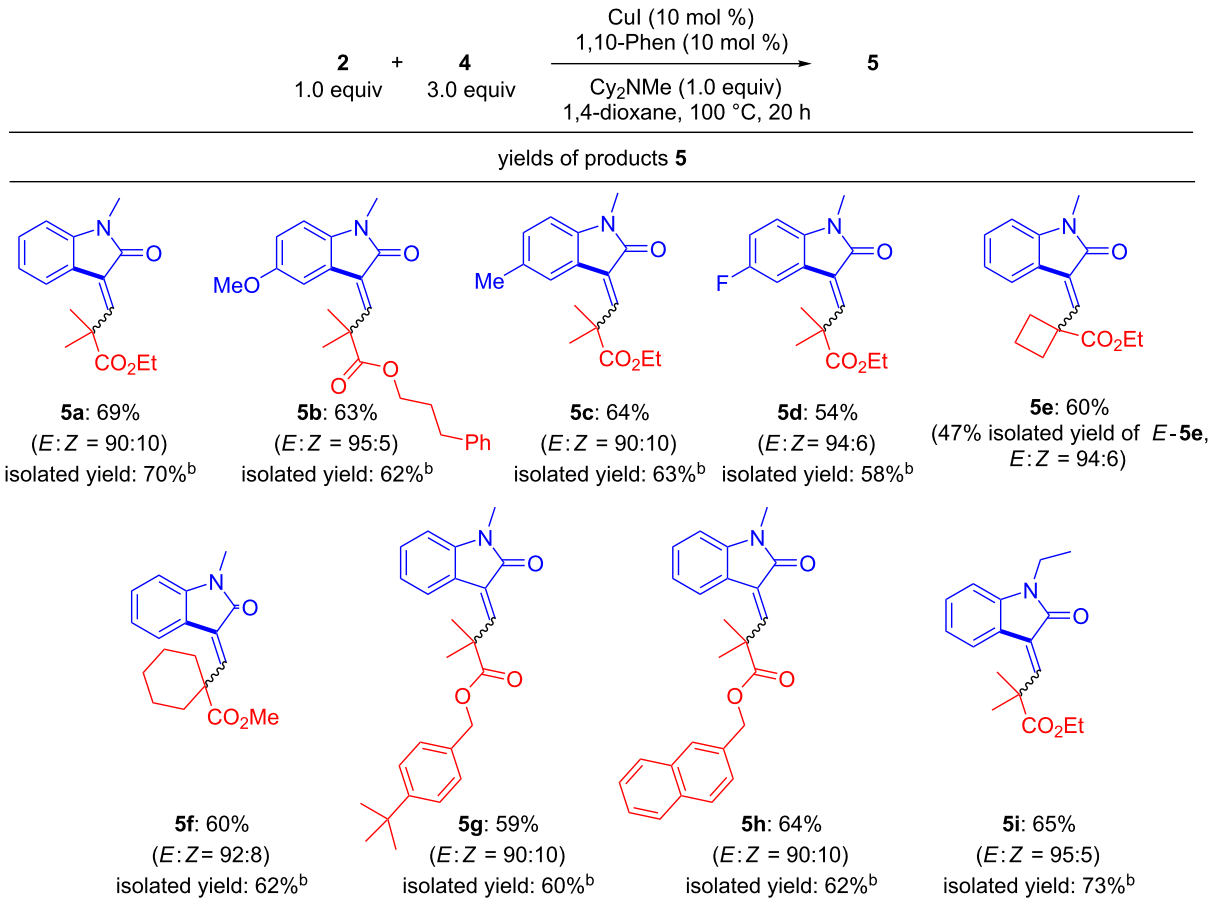

Figure 2: Substrate scope of **2** and **4**. [a]Conducted at 100 °C for 20 h in 1,4-dioxane with CuI (10 mol %), 1,10-Phen (10 mol %), Cy_2NMe (1.0 equiv), **2** (1.0 equiv) and **4** (3.0 equiv). Yields were determined by ^1H NMR analysis. [b]Including *E* and *Z* isomers.

Conclusion

In summary, we have developed two types of tandem reactions catalyzed by a copper salt. The reaction of 2-bromocarbonyl compounds and aryl-substituted alkynes underwent alkyl radical addition at a C–C triple bond followed by Sonogashira coupling to produce 1,3-enyne compounds. On the other hand, the reaction with alkyne possessing a carboxamide moiety underwent tandem alkyl radical addition at the C–C triple bond followed by C–H coupling to produce indolinone derivatives. These results could suggest new aspects of alkyne transformations in a copper catalyzed alkyl radical reaction system.

Supporting Information

Supporting Information File 1

Experimental procedures, compound characterization data, and NMR spectra.
[https://www.beilstein-journals.org/bjoc/content/supplementary/1860-5397-16-45-S1.pdf]

Funding

We warmly thank Yamaguchi university (TN), the Naito foundation, and JSPS KAKENHI Grant Number JP 18H04262(TN) in Precisely Designed Catalysts with Customized Scaffolding.

ORCID® iDs

Goki Hirata - https://orcid.org/0000-0002-2532-9959
Takashi Nishikata - https://orcid.org/0000-0002-2659-4826

References

1. Trost, B. M.; Li, C.-J. *Modern Alkyne Chemistry: Catalytic and Atom-Economic Transformations;* Wiley-VCH: Weinheim, Germany, 2015.
2. Chinchilla, R.; Nájera, C. *Chem. Rev.* **2007,** *107,* 874–922. doi:10.1021/cr050992x
3. Sonogashira, K.; Tohda, Y.; Hagihara, N. *Tetrahedron Lett.* **1975,** *16,* 4467–4470. doi:10.1016/s0040-4039(00)91094-3
4. Liu, W.; Li, L.; Li, C.-J. *Nat. Commun.* **2015,** *6,* 6526. doi:10.1038/ncomms7526
5. Liu, W.; Chen, Z.; Li, L.; Wang, H.; Li, C.-J. *Chem. – Eur. J.* **2016,** *22,* 5888–5893. doi:10.1002/chem.201600219
6. Beringer, F. M.; Galton, S. A. *J. Org. Chem.* **1965,** *30,* 1930–1934. doi:10.1021/jo01017a053
7. Ochiai, M.; Kunishima, M.; Nagao, Y.; Fuji, K.; Shiro, M.; Fujita, E. *J. Am. Chem. Soc.* **1986,** *108,* 8281–8283. doi:10.1021/ja00286a037
8. Bachi, M. D.; Bar-Ner, N.; Crittell, C. M.; Stang, P. J.; Williamson, B. L. *J. Org. Chem.* **1991,** *56,* 3912–3915. doi:10.1021/jo00012a025
9. Fernández González, D.; Brand, J. P.; Waser, J. *Chem. – Eur. J.* **2010,** *16,* 9457–9461. doi:10.1002/chem.201001539
10. Brand, J. P.; Waser, J. *Chem. Soc. Rev.* **2012,** *41,* 4165–4179. doi:10.1039/c2cs35034c
11. Dong, W.; Yuan, Y.; Gao, X.; Keranmu, M.; Li, W.; Xie, X.; Zhang, Z. *Org. Lett.* **2018,** *20,* 5762–5765. doi:10.1021/acs.orglett.8b02463
12. Gao, Y.; Zhang, P.; Li, G.; Zhao, Y. *J. Org. Chem.* **2018,** *83,* 13726–13733. doi:10.1021/acs.joc.8b02001
13. Liu, B.; Yu, J.-X.; Li, Y.; Li, J.-H.; He, D.-L. *Org. Lett.* **2018,** *20,* 2129–2132. doi:10.1021/acs.orglett.8b00236
14. Gao, Y.; Zhang, P.; Ji, Z.; Tang, G.; Zhao, Y. *ACS Catal.* **2017,** *7,* 186–190. doi:10.1021/acscatal.6b03033
15. Che, C.; Huang, Q.; Zheng, H.; Zhu, G. *Chem. Sci.* **2016,** *7,* 4134–4139. doi:10.1039/c5sc04980f
16. Cheung, C. W.; Zhurkin, F. E.; Hu, X. *J. Am. Chem. Soc.* **2015,** *137,* 4932–4935. doi:10.1021/jacs.5b01784
17. Nishikata, T.; Noda, Y.; Fujimoto, R.; Sakashita, T. *J. Am. Chem. Soc.* **2013,** *135,* 16372–16375. doi:10.1021/ja409661n
18. Nishikata, T.; Ishida, S.; Fujimoto, R. *Angew. Chem., Int. Ed.* **2016,** *55,* 10008–10012. doi:10.1002/anie.201603426
19. Ishida, S.; Takeuchi, K.; Taniyama, N.; Sunada, Y.; Nishikata, T. *Angew. Chem., Int. Ed.* **2017,** *56,* 11610–11614. doi:10.1002/anie.201706293
20. Yamane, Y.; Miwa, N.; Nishikata, T. *ACS Catal.* **2017,** *7,* 6872–6876. doi:10.1021/acscatal.7b02615
21. Nakamura, K.; Nishikata, T. *ACS Catal.* **2017,** *7,* 1049–1052. doi:10.1021/acscatal.6b03343
22. Che, C.; Zheng, H.; Zhu, G. *Org. Lett.* **2015,** *17,* 1617–1620. doi:10.1021/acs.orglett.5b00546
23. Okuro, K.; Furuune, M.; Enna, M.; Miura, M.; Nomura, M. *J. Org. Chem.* **1993,** *58,* 4716–4721. doi:10.1021/jo00069a040
24. Gujadhur, R. K.; Bates, C. G.; Venkataraman, D. *Org. Lett.* **2001,** *3,* 4315–4317. doi:10.1021/ol0170105
25. Thathagar, M. B.; Beckers, J.; Rothenberg, G. *Green Chem.* **2004,** *6,* 215–218. doi:10.1039/b401586j
26. Ma, D.; Liu, F. *Chem. Commun.* **2004,** 1934–1935. doi:10.1039/b407090a
27. Wang, Y. F.; Deng, W.; Liu, L.; Guo, Q. X. *Chin. Chem. Lett.* **2005,** *16,* 1197–1200.
28. Saejueng, P.; Bates, C. G.; Venkataraman, D. *Synthesis* **2005,** 1706–1712. doi:10.1055/s-2005-869893
29. Xie, Y.-X.; Deng, C.-L.; Pi, S.-F.; Li, J.-H.; Yin, D.-L. *Chin. J. Chem.* **2006,** *24,* 1290–1294. doi:10.1002/cjoc.200690240
30. Li, J.-H.; Li, J.-L.; Wang, D.-P.; Pi, S.-F.; Xie, Y.-X.; Zhang, M.-B.; Hu, X.-C. *J. Org. Chem.* **2007,** *72,* 2053–2057. doi:10.1021/jo0623742
31. Tang, B.-X.; Wang, F.; Li, J.-H.; Xie, Y.-X.; Zhang, M.-B. *J. Org. Chem.* **2007,** *72,* 6294–6297. doi:10.1021/jo070538o
32. Guan, J. T.; Yu, G.-A.; Chen, L.; Weng, T. Q.; Yuan, J. J.; Liu, S. H. *Appl. Organomet. Chem.* **2009,** *23,* 75–77. doi:10.1002/aoc.1474
33. Stephens, R. D.; Castro, C. E. *J. Org. Chem.* **1963,** *28,* 3313–3315. doi:10.1021/jo01047a008
34. Tang, S.; Peng, P.; Zhong, P.; Li, J.-H. *J. Org. Chem.* **2008,** *73,* 5476–5480. doi:10.1021/jo8008808
35. Jiang, T.-S.; Tang, R.-Y.; Zhang, X.-G.; Li, X.-H.; Li, J.-H. *J. Org. Chem.* **2009,** *74,* 8834–8837. doi:10.1021/jo901963g
36. Liu, C.; Liu, D.; Zhang, W.; Zhou, L.; Lei, A. *Org. Lett.* **2013,** *15,* 6166–6169. doi:10.1021/ol403021p

BEILSTEIN JOURNAL OF ORGANIC CHEMISTRY

Copper-catalyzed enantioselective conjugate reduction of α,β-unsaturated esters with chiral phenol–carbene ligands

Shohei Mimura[1], Sho Mizushima[1], Yohei Shimizu[1,2] and Masaya Sawamura[*1,2]

Full Research Paper

Open Access

Address:
[1]Department of Chemistry, Faculty of Science, Hokkaido University, Kita 10 Nishi 8, Kita-ku, Sapporo, Hokkaido 060-0810, Japan and [2]Institute for Chemical Reaction Design and Discovery (WPI-ICReDD), Hokkaido University, Kita 21 Nishi 10, Kita-ku, Sapporo, Hokkaido 001-0021, Japan

Email:
Masaya Sawamura[*] - sawamura@sci.hokudai.ac.jp

* Corresponding author

Keywords:
catalyst; chiral NHC; conjugate reduction; copper catalysis; enantioselective reaction

Beilstein J. Org. Chem. **2020,** *16,* 537–543.
doi:10.3762/bjoc.16.50

Received: 19 November 2019
Accepted: 05 February 2020
Published: 31 March 2020

This article is part of the thematic issue "Copper-catalyzed reactions for organic synthesis".

Guest Editor: O. Riant

Abstract

A chiral phenol–NHC ligand enabled the copper-catalyzed enantioselective conjugate reduction of α,β-unsaturated esters. The phenol moiety of the chiral NHC ligand played a critical role in producing the enantiomerically enriched products. The catalyst worked well for various (*Z*)-isomer substrates. Opposite enantiomers were obtained from (*Z*)- and (*E*)-isomers, with a higher enantiomeric excess from the (*Z*)-isomer.

Introduction

Since the leading work of Stryker and co-workers on triphenylphosphine-stabilized copper hydride complexes [1,2], copper hydrides have been widely used for conjugate reductions of α,β-unsaturated carbonyl compounds [3]. Especially a chiral copper catalyst combined with a stoichiometric amount of a silane reagent, which generated copper hydride in situ, has successfully been utilized for enantioselective reactions with β,β-disubstituted α,β-unsaturated carbonyl compounds [4-11]. The pioneering work of Buchwald and co-workers on the enantioselective conjugate reduction of α,β-unsaturated esters using a chiral *p*-tol-BINAP/copper catalyst established the excellent utility of chiral bisphosphine ligands for this type of reaction [4]. Surprisingly, however, chiral ligands based on *N*-heterocyclic carbenes (NHCs) [12] have not been applied to the conjugate reduction of α,β-unsaturated carbonyl compounds, while an achiral NHC/copper catalyst has successfully been utilized in this reaction [13].

Meanwhile, we devoted our effort to develop novel enantioselective C–C bond formation reactions utilizing chiral phenol–NHC/copper catalyst systems [14-18], in which the phenol group of the NHC ligand plays crucial roles in both the catalytic activity and stereoselectivity [19-21]. Notably, these catalyst systems were also applicable for three-component

coupling reactions using hydrosilanes as hydride reagents [17]. Based on this knowledge, we decided to investigate the effects of the phenol–NHC ligand on the copper-catalyzed enantioselective conjugate reduction of α,β-unsaturated esters with hydrosilanes, placing a focus on (*Z*)-isomer substrates, which generally gave slightly lower enantiomeric excess with the chiral bisphosphines compared to the (*E*)-isomer substrates.

Results and Discussion

Optimization

The initial investigation of the reaction conditions was carried out with ethyl (*Z*)-3-phenylbut-2-enoate (**1a**) as a substrate (Table 1). When chiral NHC precursor **L1**·HBF_4 (10 mol %) was used in combination with CuCl (10 mol %) and Li*O*t-Bu (20 mol %) for the conjugate reduction of **1a** with diethoxymethylsilane (4 equiv) as a reductant and *t*-AmOH (1 equiv) as a protonation reagent in DMA as the solvent at 25 °C for 15 h, the product **2a** was produced in 98% yield (^{1}H NMR analysis) with a promising enantioselectivity of 69% ee (Table 1, entry 1). When the phenolic hydroxy group of **L1** was changed to a methoxy group (in **L2**), the enantioselectivity drastically dropped to −10% ee, while the yield remained 99% (Table 1, entry 2). Similarly, *N*,*N*′-dimesityl-NHC **L3**, which lacked an oxygen functionality in the *N*-aryl group, showed poor enantioselectivity (9% ee) with high yield (99%

Table 1: Optimization of the copper-catalyzed enantioselective conjugate reduction of **1a**.[a]

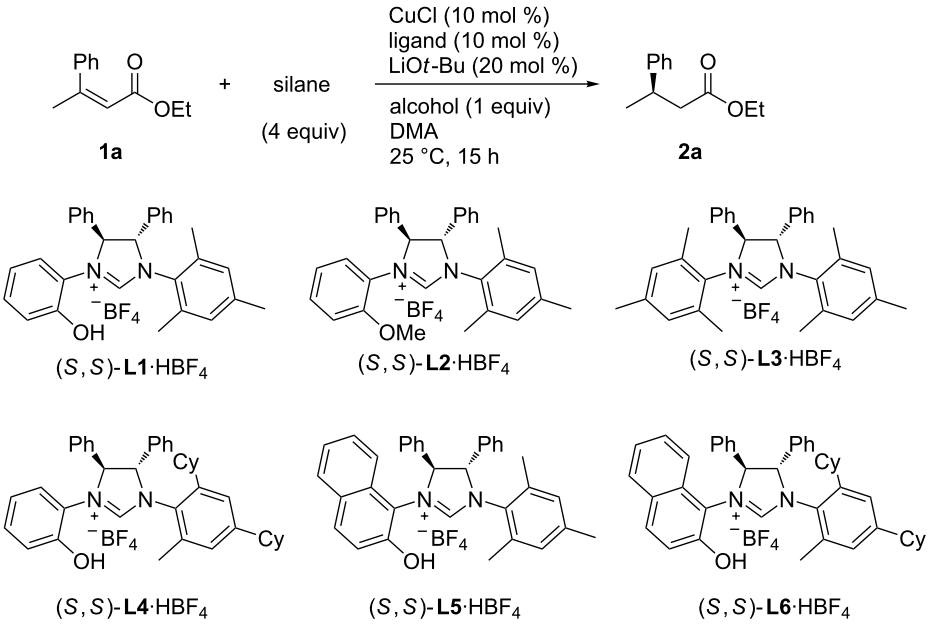

entry	ligand	silane	alcohol	yield (%)	ee (%)
1	(*S*,*S*)-**L1**·HBF_4	$(EtO)_2MeSiH$	*t*-AmOH	98	69
2	(*S*,*S*)-**L2**·HBF_4	$(EtO)_2MeSiH$	*t*-AmOH	99	−10
3	(*S*,*S*)-**L3**·HBF_4	$(EtO)_2MeSiH$	*t*-AmOH	99	9
4	(*S*,*S*)-**L4**·HBF_4	$(EtO)_2MeSiH$	*t*-AmOH	97	90
5	(*S*,*S*)-**L5**·HBF_4	$(EtO)_2MeSiH$	*t*-AmOH	99	26
6	(*S*,*S*)-**L6**·HBF_4	$(EtO)_2MeSiH$	*t*-AmOH	97	58
7	(*S*,*S*)-**L4**·HBF_4	$(MeO)_2MeSiH$	*t*-AmOH	98	84
8	(*S*,*S*)-**L4**·HBF_4	$(TMSO)_2MeSiH$	*t*-AmOH	94	71
9	(*S*,*S*)-**L4**·HBF_4	$(EtO)_3SiH$	*t*-AmOH	0	–
10	(*S*,*S*)-**L4**·HBF_4	PMHS	*t*-AmOH	5	–
11	(*S*,*S*)-**L4**·HBF_4	$(EtO)_2MeSiH$	*t*-BuOH	99	82
12	(*S*,*S*)-**L4**·HBF_4	$(EtO)_2MeSiH$	iPrOH	7	–
13	(*S*,*S*)-**L4**·HBF_4	$(EtO)_2MeSiH$	MeOH	4	–

[a]The yield was determined by ^{1}H NMR analysis using 1,1,2,2-tetrachloroethane as an internal standard. The enantiomeric excess (ee) was determined by HPLC analysis with a chiral stationary phase column CHIRALCEL® OD-H.

yield, Table 1, entry 3). Thus, the hydroxy group of **L1** was essential for the enantioselectivity by the catalyst. When the mesityl group of **L1** was changed to a bulkier 2-Me-4,6-Cy_2-C_6H_2 group in **L4**, the enantioselectivity was markedly improved to 90% ee, with a high yield (97%, Table 1, entry 4). A naphthol substituent on the nitrogen atom of the NHC (in **L5** and **L6**) instead of the phenol substituent was not suitable, giving significantly lower enantioselectivities (Table 1, entry 5, 99% yield, 26% ee; entry 6, 97% yield, 58% ee).

Further optimization of the conditions was conducted with **L4**. Changing the silane group affected both the reactivity and selectivity (Table 1, entries 7–10), while the replacement of the ethoxy groups of $(EtO)_2MeSiH$ with methoxy or trimethylsilyloxy groups resulted in only moderate reductions in the enantioselectivity and high yields. At the same time, trialkoxysilane $(EtO)_3SiH$ and polymeric silane PMHS gave only trace amounts of the product.

The nature of the alcoholic protonation reagent also had a strong impact. The presence of a tertiary alcohol, *t*-AmOH or *t*-BuOH, was essential for the reaction to occur with a reasonable yield, while iPrOH and MeOH markedly suppressed the reaction (Table 1, entries 12 and 13). However, the bulkier *t*-AmOH was superior to *t*-BuOH in terms of enantioselectivity (Table 1, entries 4 and 11).

Substrate scope

Having established optimized conditions for the reaction of **1a** (**2a**, 97% yield, 90% ee (*R*), Table 2, entry 1), the scope of α,β-unsaturated carbonyl compounds was examined. Because the separation of the product from silicon-based byproducts was troublesome, the isolated yields were lower than the yields determined by NMR spectroscopy (**2a**, 52%, Table 2, entry 1).

When (*E*)-**1a** was used as the substrate, the opposite enantiomer (*S*)-**2a** was obtained in >99% yield, with slightly lower en-

Table 2: Substrate scope of the copper-catalyzed enantioselective conjugate reduction.[a]

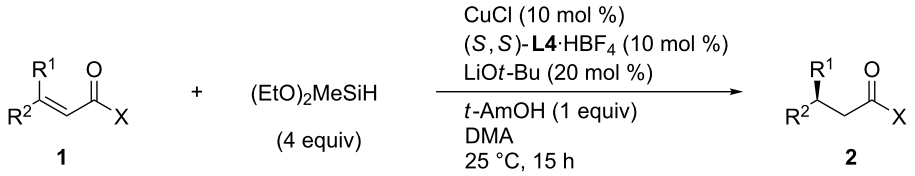

entry	substrate	product	yield (%)	ee (%)
1	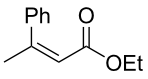 **1a**	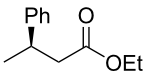 **2a**	97 (52)	90
2	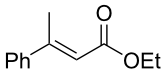 (*E*)-**1a**	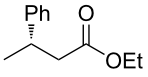 (*S*)-**2a**	>99 (75)	82
3[b]	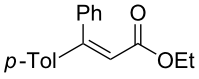 **1b**	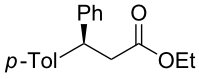 **2b**	>99 (60)	75
4	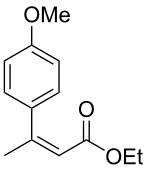 **1c**	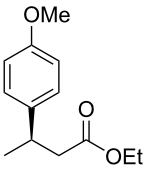 **2c**	>99 (44)	84
5	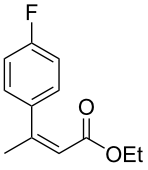 **1d**	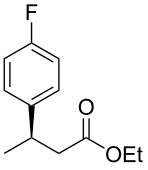 **2d**	96 (74)	76

Table 2: Substrate scope of the copper-catalyzed enantioselective conjugate reduction.[a] (continued)

6[b,c]	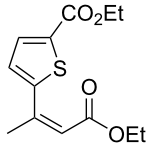 **1e**	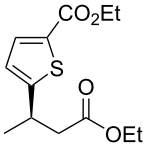 **2e**	>99 (75)	84
7	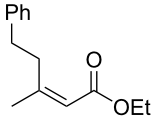 **1f**	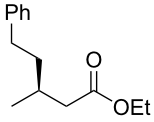 **2f**	>99 (45)	85
8[b,c]	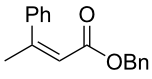 **1g**	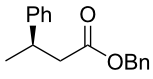 **2g**	>99 (55)	70
9	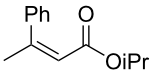 **1h**	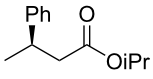 **2h**	>99 (79)	83
10	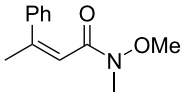 **1i**	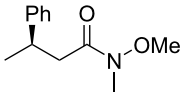 **2i**	81 (59)	79

[a]The yields were determined by ^{1}H NMR analysis using 1,1,2,2-tetrachloroethane as an internal standard. Isolated yields are shown in parentheses. [b]*t*-BuOH was used instead of *t*-AmOH. [c]$(EtO)_2MeSiH$ (1 equiv) was used.

antioselectivity (Table 2, entry 2, 82% ee (*S*) vs 90% ee (*R*) in entry 1). The inversion of the absolute configuration of the product depended on the *E*/*Z* geometry of the substrates, and this was analogous to the reported results obtained with the chiral bisphosphine ligand systems, while the observation of a higher enantioselectivity for the (*Z*)-isomer substrate **1a** was characteristic for the phenol–NHC chiral ligand [4,6,8]. The result suggested that the chiral catalyst may mainly discriminate the hydrogen atom and the ethoxycarbonyl group at the α-position rather than the two substituents at the β-position. In good agreement with this assumption is the reaction of substrate **1b**, carrying a phenyl group and a *p*-tolyl group as β-substituents, which seemed to be difficult for the catalyst to differentiate, both sterically and electronically, affording the product **2b** in good enantioselectivity (Table 2, entry 3, >99% yield, 75% ee).

Next, the effects of the β-substituent (R^1) were examined. Both electron-donating and -withdrawing substituents on the *para*-position of the β-aryl substituent gave excellent reactivities and good enantioselectivities (Table 2, entry 4, **2c**: >99% yield, 84% ee; entry 5, **2d**: 96% yield, 76% ee). Further, a heteroaryl substituent, 2-ethoxycarbonylthiophene, was tolerated (Table 2, entry 6, **2e**: >99% yield, 84% ee), and a β-alkyl-substituted substrate **1f** was also competent (entry 7, **2f**: >99% yield, 85% ee).

The structure of the ester moiety affected the stereoselectivities: Lower enantioselectivities were observed with benzyl ester **2g** (Table 2, entry 8, >99% yield, 70% ee) and isopropyl ester **2h** (Table 2, entry 9, >99% yield, 83% ee). In addition to the α,β-unsaturated esters, an α,β-unsaturated Weinreb amide **1i** afforded the corresponding product **2i** with comparable results (Table 2, entry 10, 81% yield, 79% ee).

Proposed catalytic cycle

Based on the experimental observations and previous knowledge of the catalysis of phenol–NHC chiral ligands [14-18], we propose a catalytic cycle as shown in Scheme 1. LiO*t*-Bu abstracts the two protons of the acidic imidazolium C–H and phenol O–H groups of the **L4**·HBF_4 adduct in the presence of CuCl to generate a phenoxy copper(I) species **A**. As a result, all LiO*t*-Bu (20 mol %) is consumed in this step. Thus, the system is neutral. Transmetalation between **A** and $(EtO)_2MeSiH$ produces the copper hydride species **B**. This transmetalation adds the silyl group to the phenoxy oxygen atom of the NHC ligand. The coordination of an α,β-unsaturated carbonyl compound **1** to the copper atom occurs in such a way that the bulky *O*-silyl group of the copper catalyst can avoid steric repulsions with the alkoxycarbonyl group of the substrate **1**, forming π-complex **C**, and thus explaining the marked influence of the hydrosilane structure on the enantioselectivity. During this stereodetermining step, coordination of the phenoxy oxygen

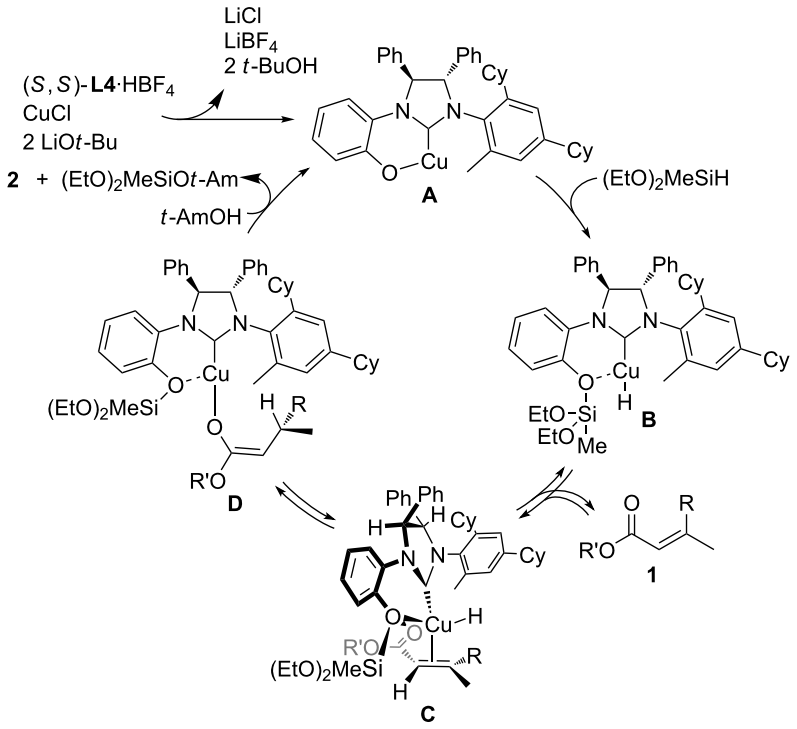

Scheme 1: Proposed catalytic cycle.

atom to the copper atom may render the chiral environment better defined. Then, the π-complex **C** undergoes 1,4-hydrocupration to afford copper enolate **D**. During our initial investigations, we observed configurational isomerization from **1a** to (*E*)-**1a** when the reaction was conducted in the absence of alcoholic protonation reagents. This observation implied that the 1,4-hydrocupration step (**C** to **D**) is reversible. Finally, protonation of **D** by *t*-AmOH gives the product **2** and silyl ether $(EtO)_2MeSiOt$-Am, regenerating the phenoxy copper(I) complex **A**. Due to the reversibility of the 1,4-hydrocupration, the choice of the alcoholic protonation reagent affects both the reactivity and enantioselectivity.

Conclusion

A chiral phenol–NHC ligand efficiently promoted the enantioselective conjugate reduction of α,β-unsaturated esters with a hydrosilane. To the best of our knowledge, this is the first demonstration of the applicability of chiral NHC ligands in Cu-catalyzed enantioselective conjugate reductions. The phenolic *N*-substituent of the chiral NHC ligand was essential for the high enantioselectivity. Good enantioselectivities were observed for the various (*Z*)-configured substrates with different β-substituents. Further investigations on the catalyst development based on this knowledge are ongoing in our laboratory.

Experimental

A typical procedure for the copper-catalyzed enantioselective conjugate reduction (Table 1, entry 4; Table 2, entry 1): In a glove box, CuCl (1.5 mg, 0.015 mmol), **L4**·HBF_4 (9.8 mg, 0.015 mmol), and Li*Ot*-Bu (2.4 mg, 0.03 mmol) were placed in a vial containing a magnetic stirring bar. The vial was sealed with a teflon-coated silicon rubber septum. *N*,*N*-Dimethylacetamide (0.90 mL) was added to the vial, and then the mixture was stirred at room temperature for 5 min. Next, *t*-AmOH (16.3 μL, 0.15 mmol) was added, and the vial was taken out of the glove box. To the reaction mixture was added **1a** (28.5 mg, 0.15 mmol). After stirring for 5 min at room temperature, diethoxymethylsilane (101 μL, 0.60 mmol) was added to the mixture. After stirring for 15 h at 25 °C, the reaction mixture was diluted with diethyl ether (1.0 mL) and quenched with H_2O (0.6 mL). The organic layer was separated, and the aqueous layer was extracted three times with diethyl ether. The combined organic layer was filtered through a short plug of silica gel by using diethyl ether as an eluent. After the solvent was removed under reduced pressure, the yield of the product was determined to be 97% by ^1H NMR analysis with 1,1,2,2-tetrachloroethane as an internal standard. After a rough purification of the crude product by silica gel chromatography (eluent: 0 to 1% EtOAc/hexane), the collected residue was further purified by GPC (eluent: $CHCl_3$) to afford the pure product **2a** as color-

less oil (15.1 mg, 52% yield, 90% ee). ^{1}H NMR (400 MHz, $CDCl_3$) δ 1.17 (t, J = 7.2 Hz, 3H), 1.29 (d, J = 7.2 Hz, 3H), 2.50–2.63 (m, 2H), 3.27 (sext, J = 7.2 Hz, 1H), 4.06 (q, J = 7.2 Hz, 2H), 7.16–7.22 (m, 3H), 7.28 (t, J = 7.2 Hz, 2H); ^{13}C NMR (100.5 Hz, $CDCl_3$) δ 14.1, 21.7, 36.4, 42.9, 60.2, 126.3, 126.7, 128.4, 145.6, 172.3; $[\alpha]_D^{27.3}$ −23.2 (*c* 1.25, $CHCl_3$). The spectral data matched those reported in the literature [22].

The ee value was determined by HPLC analysis with a chiral stationary column CHIRALCEL® OD-H (Daicel Chemical Industries, 4.6 mm, 250 mm, hexane/2-propanol, 98:2, v/v, 0.5 mL/min, 40 °C, 220 nm UV detector, retention time = 9.1 min for the (*R*)-isomer and 13.3 min for the (*S*)-isomer). The absolute configuration of **2a** was assigned by the comparison of the optical rotation with the same compound prepared by a reported method [4].

Supporting Information

Supporting Information File 1

Experimental procedures, characterization data, HPLC charts, and NMR spectra (^{1}H, ^{13}C) for the new compounds.
[https://www.beilstein-journals.org/bjoc/content/supplementary/1860-5397-16-50-S1.pdf]

Acknowledgements

The Institute for Chemical Reaction Design and Discovery (ICReDD) was established by the World Premier International Research Initiative (WPI), MEXT, Japan.

Funding

This work was supported by the JSPS KAKENHI grant-in-aid for Scientific Research (A) to M.S. (No. JP18H03906), JSPS KAKENHI grant-in-aid for Early-Career Scientists (No. 18K14207) to Y.S.

ORCID® iDs

Yohei Shimizu - https://orcid.org/0000-0001-8797-9757
Masaya Sawamura - https://orcid.org/0000-0002-8770-2982

References

1. Mahoney, W. S.; Brestensky, D. M.; Stryker, J. M. *J. Am. Chem. Soc.* **1988,** *110,* 291–293. doi:10.1021/ja00209a048
2. Mahoney, W. S.; Stryker, J. M. *J. Am. Chem. Soc.* **1989,** *111,* 8818–8823. doi:10.1021/ja00206a008
3. Deutsch, C.; Krause, N.; Lipshutz, B. H. *Chem. Rev.* **2008,** *108,* 2916–2927. doi:10.1021/cr0684321
4. Appella, D. H.; Moritani, Y.; Shintani, R.; Ferreira, E. M.; Buchwald, S. L. *J. Am. Chem. Soc.* **1999,** *121,* 9473–9474. doi:10.1021/ja992366l
5. Moritani, Y.; Appella, D. H.; Jurkauskas, V.; Buchwald, S. L. *J. Am. Chem. Soc.* **2000,** *122,* 6797–6798. doi:10.1021/ja0009525
6. Lipshutz, B. H.; Servesko, J. M. *Angew. Chem., Int. Ed.* **2003,** *42,* 4789–4792. doi:10.1002/anie.200352313
7. Hughes, G.; Kimura, M.; Buchwald, S. L. *J. Am. Chem. Soc.* **2003,** *125,* 11253–11258. doi:10.1021/ja0351692
8. Lipshutz, B. H.; Servesko, J. M.; Taft, B. R. *J. Am. Chem. Soc.* **2004,** *126,* 8352–8353. doi:10.1021/ja049135l
9. Huang, S.; Voigtritter, K. R.; Unger, J. B.; Lipshutz, B. H. *Synlett* **2010,** 2041–2042. doi:10.1055/s-0030-1258540
10. Wu, Y.; Qi, S.-B.; Wu, F.-F.; Zhang, X.-C.; Li, M.; Wu, J.; Chan, A. S. C. *Org. Lett.* **2011,** *13,* 1754–1757. doi:10.1021/ol200287z
11. Hou, C.-J.; Guo, W.-L.; Hu, X.-P.; Deng, J.; Zheng, Z. *Tetrahedron: Asymmetry* **2011,** *22,* 195–199. doi:10.1016/j.tetasy.2011.01.022
12. Janssen-Müller, D.; Schlepphorst, C.; Glorius, F. *Chem. Soc. Rev.* **2017,** *46,* 4845–4854. doi:10.1039/c7cs00200a
13. Jurkauskas, V.; Sadighi, J. P.; Buchwald, S. L. *Org. Lett.* **2003,** *5,* 2417–2420. doi:10.1021/ol034560p
14. Harada, A.; Makida, Y.; Sato, T.; Ohmiya, H.; Sawamura, M. *J. Am. Chem. Soc.* **2014,** *136,* 13932–13939. doi:10.1021/ja5084333
15. Ohmiya, H.; Zhang, H.; Shibata, S.; Harada, A.; Sawamura, M. *Angew. Chem., Int. Ed.* **2016,** *55,* 4777–4780. doi:10.1002/anie.201600619
16. Yasuda, Y.; Ohmiya, H.; Sawamura, M. *Angew. Chem., Int. Ed.* **2016,** *55,* 10816–10820. doi:10.1002/anie.201605125
17. Hojoh, K.; Ohmiya, H.; Sawamura, M. *J. Am. Chem. Soc.* **2017,** *139,* 2184–2187. doi:10.1021/jacs.6b12881
18. Yasuda, Y.; Ohmiya, H.; Sawamura, M. *Synthesis* **2018,** *50,* 2235–2246. doi:10.1055/s-0036-1591548
19. Clavier, H.; Coutable, L.; Guillemin, J.-C.; Mauduit, M. *Tetrahedron: Asymmetry* **2005,** *16,* 921–924. doi:10.1016/j.tetasy.2005.01.015
20. Martin, D.; Kehrli, S.; d'Augustin, M.; Clavier, H.; Mauduit, M.; Alexakis, A. *J. Am. Chem. Soc.* **2006,** *128,* 8416–8417. doi:10.1021/ja0629920
21. Shintani, R.; Takatsu, K.; Takeda, M.; Hayashi, T. *Angew. Chem., Int. Ed.* **2011,** *50,* 8656–8659. doi:10.1002/anie.201103581
22. Guo, S.; Zhou, J. *Org. Lett.* **2016,** *18,* 5344–5347. doi:10.1021/acs.orglett.6b02662

BEILSTEIN JOURNAL OF ORGANIC CHEMISTRY

Copper-catalyzed *O*-alkenylation of phosphonates

Nuria Vázquez-Galiñanes, Mariña Andón-Rodríguez, Patricia Gómez-Roibás and Martín Fañanás-Mastral*

Letter

Open Access

Address:
Centro Singular de Investigación en Química Biolóxica e Materiais Moleculares (CiQUS), Departamento de Química Orgánica, Universidade de Santiago de Compostela, 15782 Santiago de Compostela, Spain

Email:
Martín Fañanás-Mastral* - martin.fananas@usc.es

* Corresponding author

Keywords:
alkenylation; copper; C(sp^2)–O bond formation; hypervalent iodine; phosphonates

Beilstein J. Org. Chem. **2020,** *16,* 611–615.
doi:10.3762/bjoc.16.56

Received: 30 January 2020
Accepted: 27 March 2020
Published: 03 April 2020

This article is part of the thematic issue "Copper-catalyzed reactions for organic synthesis".

Guest Editor: G. Evano

Abstract

Copper catalysis allows the direct oxygen alkenylation of dialkyl phosphonates with alkenyl(aryl)iodonium salts with selective transfer of the alkenyl group. This novel methodology proceeds with a wide range of phosphonates under mild conditions and gives straightforward access to valuable enol phosphonates in very good yields.

Introduction

Organophosphorus compounds represent an important class of products with a wide range of applications in biology, agriculture and synthetic organic chemistry [1-3]. In particular, *O*-alkenyl phosphonate esters (i.e., enol phosphonates) have been described as potent insecticides and show antifungal activity [4]. While several methods are available for the preparation of cyclic enol phosphonates [5-10], the synthesis of the acyclic counterparts has received less attention. Current methodologies for the synthesis of acyclic mixed enol phosphonates include the Perkow-type reaction between phosphonites and α-halocarbonyl compounds [11], the mercury-catalyzed addition of phosphonic acid monoesters to terminal alkynes [12,13] and multistep procedures involving a Mitsunobu reaction between 2-hydroxyalkyl phenyl selenides and phosphonic acid monoesters followed by an oxidation/elimination step [14] or reaction of an enolate with a phosphonic dichloride and subsequent treatment with an alcohol [15] (Scheme 1a). However, these procedures are subject to selectivity problems, involve toxic and hazardous materials or are limited to the restricted availability of the corresponding phosphorus reagents. Therefore, the development of alternative methods for the synthesis of acyclic enol phosphonates is highly desirable.

Diaryliodonium and aryl(alkenyl)iodonium salts, which are air- and moisture-stable, nontoxic and easy to prepare compounds, have become efficient reagents for mild and selective arylation and alkenylation reactions in organic synthesis [16-18]. In particular, the use of these hypervalent iodine reagents in copper

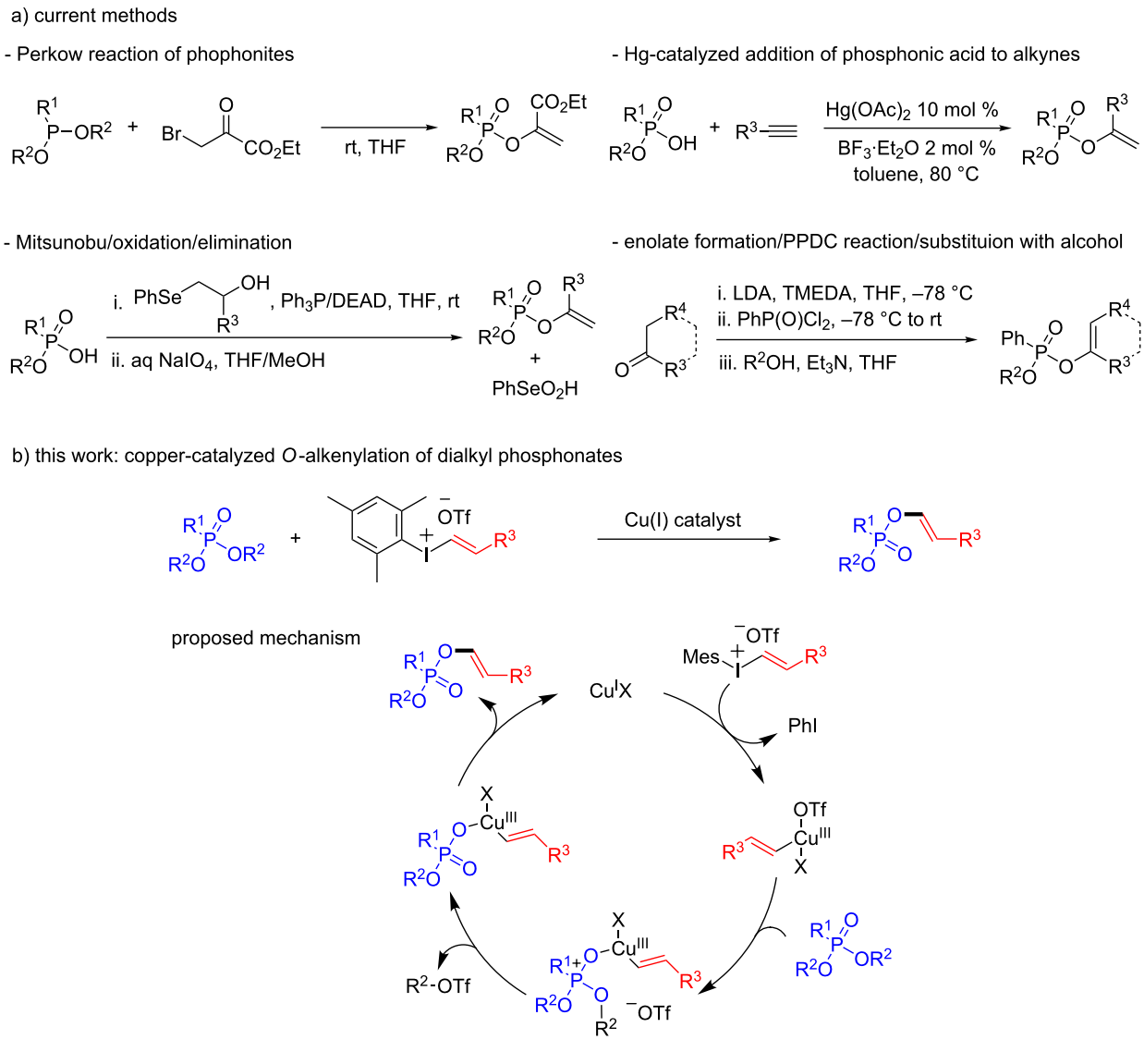

Scheme 1: Synthesis of mixed alkyl alkenyl phosphonates.

catalysis has allowed to perform a wide range of previously unknown synthetic transformations [19-29]. In these reactions, aryl(vinyl)Cu(III) species [30,31] have been proposed as key intermediates to undergo reactions with a variety of nucleophiles. Fañanás-Mastral and Feringa recently reported a catalytic method for the synthesis of mixed alkyl aryl phosphonates based on a copper-catalyzed arylation of phosphonates with diaryliodonium salts [32]. Encouraged by this work, in the context of an electrophilic alkenylation of phosphonates, we reasoned that the action of a copper catalyst on an alkenyl(aryl)iodonium salt [33,34] would generate an alkenyl–copper(III) species which might undergo nucleophilic attack of the Lewis-basic oxygen of a dialkyl phosphonate. The resulting phosphonium-like intermediate would evolve by Arbuzov-type substitution of one of the alkyl groups, and final reductive elimination would form the new C(sp^2)–O bond, providing an acyclic enol phosphonate with concomitant regeneration of the Cu(I) catalyst (Scheme 1b). Herein we report the successful realization of such a copper-catalyzed oxygen-alkenylation strategy and show that a range of readily available, dialkyl phosphonates and alkenyl(aryl)iodonium salts can be combined to form enol phosphonates in high yield and excellent selectivity.

Results and Discussion

We started our studies by investigating the reaction between diethyl phosphonate **1a** and styryl(mesityl)iodonium triflate (**2a**, Table 1). We first run the reaction under the conditions re-

Table 1: Optimization studies[a].

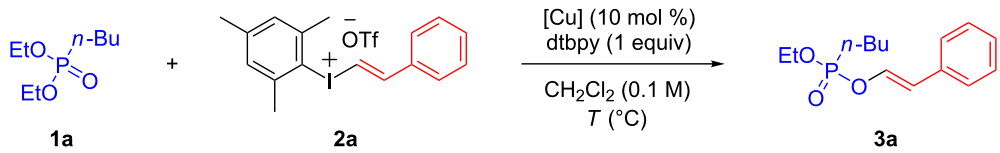

1a **2a** **3a**

entry	**2a** (equiv)	[Cu]	*T* (°C)	conv (%)[b]	**3a** (%)[b]
1	1.5	CuCl	40	42	34
2	1.5	CuCl	50	63	53
3	1.5	CuOTf·$PhCH_3$	50	32	25
4	1.5	$Cu(OTf)_2$	50	65	60
5	1.5	CuI	50	50	50
6	1.5	CuTC	50	75	69
7	2	CuTC	50	full	82 (78)[c]
8	2	–	50	–	–
9[d]	2	CuTC	50	10	5
10[e]	2[e]	CuTC	50	30	15

[a]Reactions run on a 0.2 mmol scale; [b]Determined by ^1H NMR using 1,3,5-trimethoxybenzene as internal standard. [c]Yield of isolated product shown in brackets. [d]Reaction run in the absence of dtbpy. [e]Styryl(phenyl)iodonium triflate used instead of **2a**.

ported for the copper-catalyzed O-arylation of phosphonates (CuCl as catalyst, 2,6-di-*tert*-butylpyridine (dtbpy) as additive in dichloromethane at 40 °C) [32]. Under those conditions, enol phosphonate **3a** was the only product of the reaction, although low conversion and yield were observed (Table 1, entry 1). A screening of copper complexes at a higher temperature (50 °C) revealed that CuTC (TC = thiophene-2-carboxylate) is the most efficient catalyst for this transformation (Table 1, entries 2–6). Finally, by using 2 equiv of **2a** full conversion was achieved and enol phosphonate **3a** was isolated in 78% yield with full selectivity towards the monoalkenylation product (Table 1, entry 7). Importantly, no reaction was observed in the absence of copper catalyst (Table 1, entry 8), while the absence of dtbpy led to a minimal conversion (Table 1, entry 9). The structure of the alkenyliodonium salt also plays an important role in the outcome of the reaction since the use of a phenyl group instead of the mesityl ligand caused a dramatic decrease in conversion and reaction yield likely due to a faster decomposition of the salt (Table 1, entry 10).

Having established optimized conditions for the copper-catalyzed O-alkenylation of phosphonates, we set out to investigate the scope of the reaction (Scheme 2). This catalytic transformation proved to be very efficient for several diethyl phosphonates bearing alkyl, benzyl and aryl groups providing in all cases the corresponding enol phosphonates **3a–d** in good yields. Importantly, no double alkenylation product was observed in any case. Benzyl and alkyl diethyl phosphonates bearing halide groups also worked well and led to enol phosphonates **3e** and **3f** in good yields without any traces of side products. An acetal-protected aldehyde could also be used providing enol phosphonate **3g** in 52% yield. In this case, prolonged reaction times led to partial evolution of **3g** into enol ether **4**. This transformation may be explained by an acid-mediated elimination of ethanol likely caused by trace formation of triflic acid via decomposition of ethyl triflate. As a limitation, substrates bearing a vinyl substituent or an enolizable ester group did not give any conversion. This methodology is also applicable to other dialkyl phosphonates as illustrated by the synthesis of enol phosphonates **3j**, **3k** and **3l**. Interestingly, the copper-catalyzed alkenylation of phosphonates followed the same reactivity trend as the one described for the arylation reaction [32] with the diisopropyl phosphonates being more efficient than the dimethyl phosphonate esters. It is also important to remark that, in sharp contrast to the copper-catalyzed reaction between *H*-phosphonates and vinyliodonium salts described by Eustache and co-workers [35], no formation of the P-alkenylation product was observed in any case.

Different alkenyliodonium salts were also used for this transformation. Styryl(mesityl)iodonium salts bearing both electron-donating and electron-withdrawing substituents worked well and allowed access to the corresponding enol phosphonates **3m–p** in very good yields. Importantly, the bulky mesityl ligand allowed the selective transfer of the alkenyl group in all cases. In sharp contrast, no alkenylation product was ob-

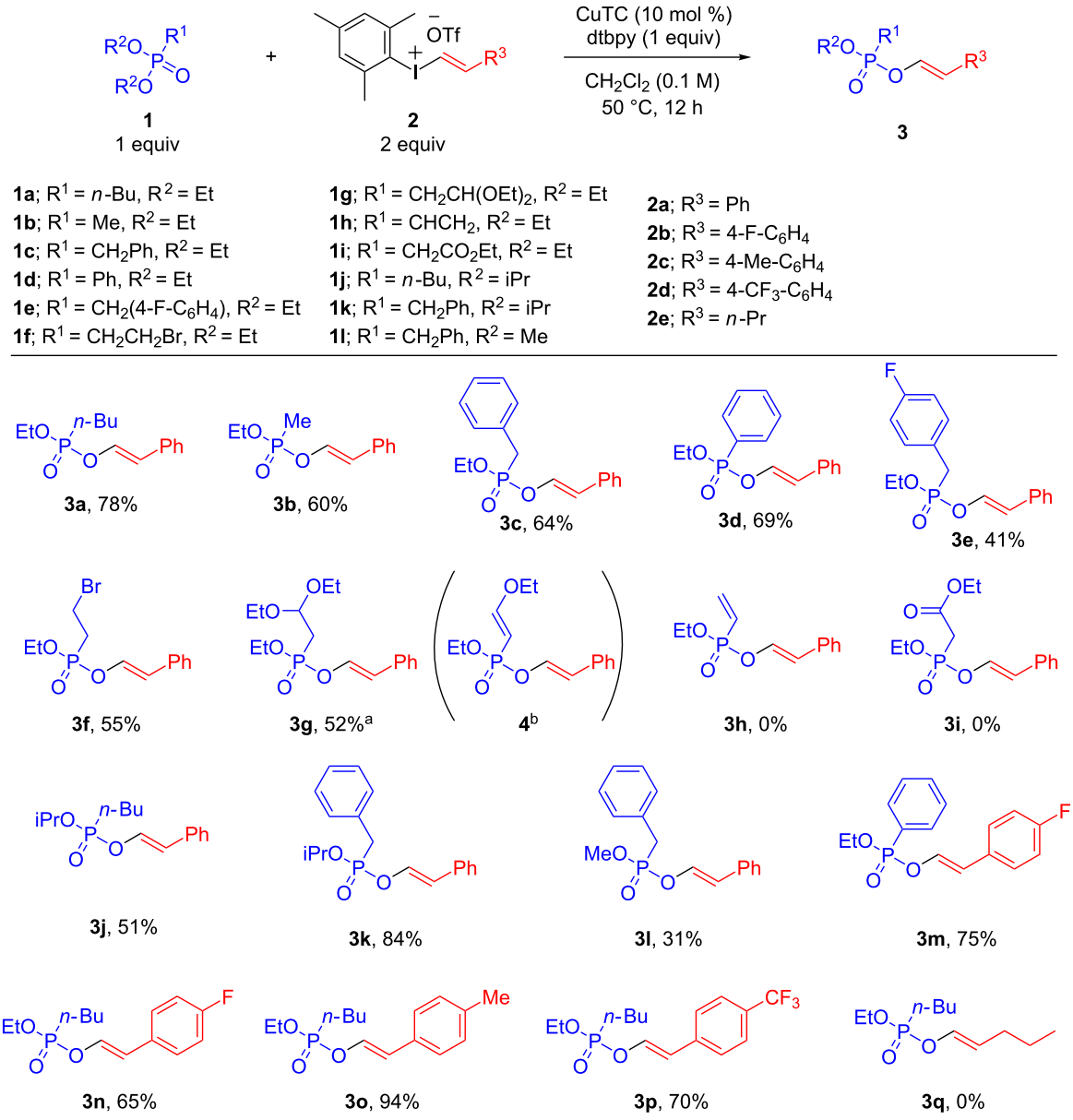

Scheme 2: Scope of the copper-catalyzed alkenylation of dialkyl phosphonates. Reactions run on a 0.2 mmol scale. Yields refer to isolated pure products. [a]Reaction time = 10 h. [b]When reaction was stirred over 18 h a **3g**:**4** mixture was obtained in a 1:1 ratio.

served when alkenyliodonium salts bearing aliphatic substituents were used likely due to a faster decomposition of the salt [36,37].

Conclusion

In summary, we have developed an efficient copper-catalyzed oxygen alkenylation of dialkyl phosphonates with alkenyl(aryl)iodonium salts. The reaction proceeds under mild conditions, with excellent levels of selectivity and affords acyclic enol phosphonates in high yields. We believe that the reaction occurs through the formation of a high valent alkenyl–copper(III) species which gets attacked by the phosphoryl oxygen of the phosphonate.

Supporting Information

Supporting Information File 1

Experimental procedures and characterization data of enol phosphonates **3**.
[https://www.beilstein-journals.org/bjoc/content/supplementary/1860-5397-16-56-S1.pdf]

Funding

Financial support from the AEI (CTQ2017-88451-R), Xunta de Galicia (ED431F 2016/006; ED431C 2018/04; Centro singular de investigación de Galicia accreditation 2016-2019, ED431G/09) and the European Union (ERDF) is gratefully acknowledged. N. V.-G. thanks AEI for a predoctoral FPI fellowship.

ORCID® iDs

Patricia Gómez-Roibás - https://orcid.org/0000-0002-1619-1484
Martín Fañanás-Mastral - https://orcid.org/0000-0003-4903-0502

References

1. McGrath, J. W.; Chin, J. P.; Quinn, J. P. *Nat. Rev. Microbiol.* **2013,** *11,* 412–419. doi:10.1038/nrmicro3011
2. Duke, S. O.; Powles, S. B. *Pest Manage. Sci.* **2008,** *64,* 319–325. doi:10.1002/ps.1518
3. Quin, L. D., Ed. *A Guide to Organophosphorus Chemistry;* Wiley-Interscience: New York, NY, USA, 2000.
4. Engel, R., Ed. *Handbook of Organophosphorus Chemistry;* Marcel Dekker: New York, NY, USA, 1992. doi:10.1201/9781482277241
5. Peng, A.-Y.; Ding, Y.-X. *J. Am. Chem. Soc.* **2003,** *125,* 15006–15007. doi:10.1021/ja038627f
6. Peng, A.-Y.; Ding, Y.-X. *Org. Lett.* **2004,** *6,* 1119–1121. doi:10.1021/ol0499506
7. Unoh, Y.; Hashimoto, Y.; Takeda, D.; Hirano, K.; Satoh, T.; Miura, M. *Org. Lett.* **2013,** *15,* 3258–3261. doi:10.1021/ol4012794
8. Seo, J.; Park, Y.; Jeon, I.; Ryu, T.; Park, S.; Lee, P. H. *Org. Lett.* **2013,** *15,* 3358–3361. doi:10.1021/ol401407v
9. Park, Y.; Seo, J.; Park, S.; Yoo, E. J.; Lee, P. H. *Chem. – Eur. J.* **2013,** *19,* 16461–16468. doi:10.1002/chem.201302652
10. Pérez-Saavedra, B.; Vázquez-Galiñanes, N.; Saá, C.; Fañanás-Mastral, M. *ACS Catal.* **2017,** *7,* 6104–6109. doi:10.1021/acscatal.7b02434
11. Despax, C.; Navech, J. *Tetrahedron Lett.* **1990,** *31,* 4471–4472. doi:10.1016/s0040-4039(00)97651-2
12. Peng, A.; Ding, Y. *Synthesis* **2003,** 205–208. doi:10.1055/s-2003-36818
13. Wasserman, H. H.; Cohen, D. *J. Am. Chem. Soc.* **1960,** *82,* 4435–4436. doi:10.1021/ja01501a084
14. Sheng, S.-R.; Sun, W.-K.; Hu, M.-G.; Liu, X.-L.; Wang, Q.-Y. *J. Chem. Res.* **2007,** 97–99. doi:10.3184/030823407x198221
15. Campbell, I. B.; Guo, J.; Jones, E.; Steel, P. G. *Org. Biomol. Chem.* **2004,** *2,* 2725–2727. doi:10.1039/b411111g
16. Zhdankin, V. V.; Stang, P. J. *Chem. Rev.* **2008,** *108,* 5299–5358. doi:10.1021/cr800332c
17. Merritt, E. A.; Olofsson, B. *Angew. Chem., Int. Ed.* **2009,** *48,* 9052–9070. doi:10.1002/anie.200904689
18. Aradi, K.; Tóth, B. L.; Tolnai, G. L.; Novák, Z. *Synlett* **2016,** *27,* 1456–1485. doi:10.1055/s-0035-1561369
19. Fañanás-Mastral, M. *Synthesis* **2017,** *49,* 1905–1930. doi:10.1055/s-0036-1589483
20. Phipps, R. J.; Grimster, N. P.; Gaunt, M. J. *J. Am. Chem. Soc.* **2008,** *130,* 8172–8174. doi:10.1021/ja801767s
21. Phipps, R. J.; Gaunt, M. J. *Science* **2009,** *323,* 1593–1597. doi:10.1126/science.1169975
22. Zhu, S.; MacMillan, D. W. C. *J. Am. Chem. Soc.* **2012,** *134,* 10815–10818. doi:10.1021/ja305100g
23. Suero, M. G.; Bayle, E. D.; Collins, B. S. L.; Gaunt, M. J. *J. Am. Chem. Soc.* **2013,** *135,* 5332–5335. doi:10.1021/ja401840j
24. Collins, B. S. L.; Suero, M. G.; Gaunt, M. J. *Angew. Chem., Int. Ed.* **2013,** *52,* 5799–5802. doi:10.1002/anie.201301529
25. Xu, Z.-F.; Cai, C.-X.; Liu, J.-T. *Org. Lett.* **2013,** *15,* 2096–2099. doi:10.1021/ol4003543
26. Wang, Y.; Chen, C.; Peng, J.; Li, M. *Angew. Chem., Int. Ed.* **2013,** *52,* 5323–5357. doi:10.1002/anie.201300586
27. Cahard, E.; Male, H. P. J.; Tissot, M.; Gaunt, M. J. *J. Am. Chem. Soc.* **2015,** *137,* 7986–7989. doi:10.1021/jacs.5b03937
28. Beaud, R.; Phipps, R. J.; Gaunt, M. J. *J. Am. Chem. Soc.* **2016,** *138,* 13183–13186. doi:10.1021/jacs.6b09334
29. Teskey, C. J.; Sohel, S. M. A.; Bunting, D. L.; Modha, S. G.; Greaney, M. F. *Angew. Chem., Int. Ed.* **2017,** *56,* 5263–5266. doi:10.1002/anie.201701523
30. Hickman, A. J.; Sanford, M. S. *Nature* **2012,** *484,* 177–185. doi:10.1038/nature11008
31. Casitas, A.; Ribas, X. *Chem. Sci.* **2013,** *4,* 2301–2318. doi:10.1039/c3sc21818j
32. Fañanás-Mastral, M.; Feringa, B. L. *J. Am. Chem. Soc.* **2014,** *136,* 9894–9897. doi:10.1021/ja505281v
33. Ochiai, M.; Sumi, K.; Nagao, Y.; Fujita, E. *Tetrahedron Lett.* **1985,** *26,* 2351–2354. doi:10.1016/s0040-4039(00)95096-2
34. Okuyama, T.; Takino, T.; Sato, K.; Ochiai, M. *J. Am. Chem. Soc.* **1998,** *120,* 2275–2282. doi:10.1021/ja972267c
35. Thielges, S.; Bisseret, P.; Eustache, J. *Org. Lett.* **2005,** *7,* 681–684. doi:10.1021/ol047516y
36. Beringer, F. M.; Bodlaender, P. *J. Org. Chem.* **1969,** *34,* 1981–1985. doi:10.1021/jo01258a107
37. Lockhart, T. P. *J. Am. Chem. Soc.* **1983,** *105,* 1940–1946. doi:10.1021/ja00345a045

BEILSTEIN JOURNAL OF ORGANIC CHEMISTRY

Recent advances in Cu-catalyzed C(sp^3)–Si and C(sp^3)–B bond formation

Balaram S. Takale, Ruchita R. Thakore, Elham Etemadi-Davan and Bruce H. Lipshutz*

Review

Open Access

Address:
Department of Chemistry & Biochemistry, University of California, Santa Barbara, California 93106, USA

Email:
Bruce H. Lipshutz* - lipshutz@chem.ucsb.edu

* Corresponding author

Keywords:
C–B bonds; copper catalysis; C–Si bonds; enantioselective reactions; sp^3 carbon functionalization

Beilstein J. Org. Chem. **2020,** *16,* 691–737.
doi:10.3762/bjoc.16.67

Received: 26 October 2019
Accepted: 10 March 2020
Published: 15 April 2020

This article is part of the thematic issue "Copper-catalyzed reactions for organic synthesis".

Guest Editor: G. Evano

Abstract

Numerous reactions generating C–Si and C–B bonds are in focus owing to the importance of incorporating silicon or boron into new or existing drugs, in addition to their use as building blocks in cross-coupling reactions en route to various targets of both natural and unnatural origins. In this review, recent protocols relying on copper-catalyzed sp^3 carbon–silicon and carbon–boron bond-forming reactions are discussed.

Introduction

Transition-metal-catalyzed silylation and borylation are useful transformations [1], widely studied because organosilicon [2,3] and organoboron compounds [4] are common partners in a variety of important cross-coupling reactions. They are also especially valuable precursors to other functional groups such as organic halides, alcohols [5-7], etc. Moreover, recent drug discovery efforts have shifted towards the incorporation of these non-natural functional groups into existing or new drugs. Examples include the incorporation of silicon bioisosteres that help increase lipophilicity, subsequently altering the existing metabolic pathway of a drug due to differences in its physicochemical properties [8]. On the other hand, the trigonal planar nature of boron can lead to dative bond formation with enzymes, and therefore increase binding affinity. As shown in Scheme 1, several silicon [9-12] and boron-containing [13-16] drugs have already entered the market, or are currently in the drug development pipeline. As the number of drugs containing these functional groups continues to increase, new synthetic pathways for their inclusion will surely attract synthetic organic chemists, as well challenge them to consider both existing approaches and developing new reactions.

Many recent reviews already cover the syntheses and applications of organosilicon [17-20] and organoboron [21-24] com-

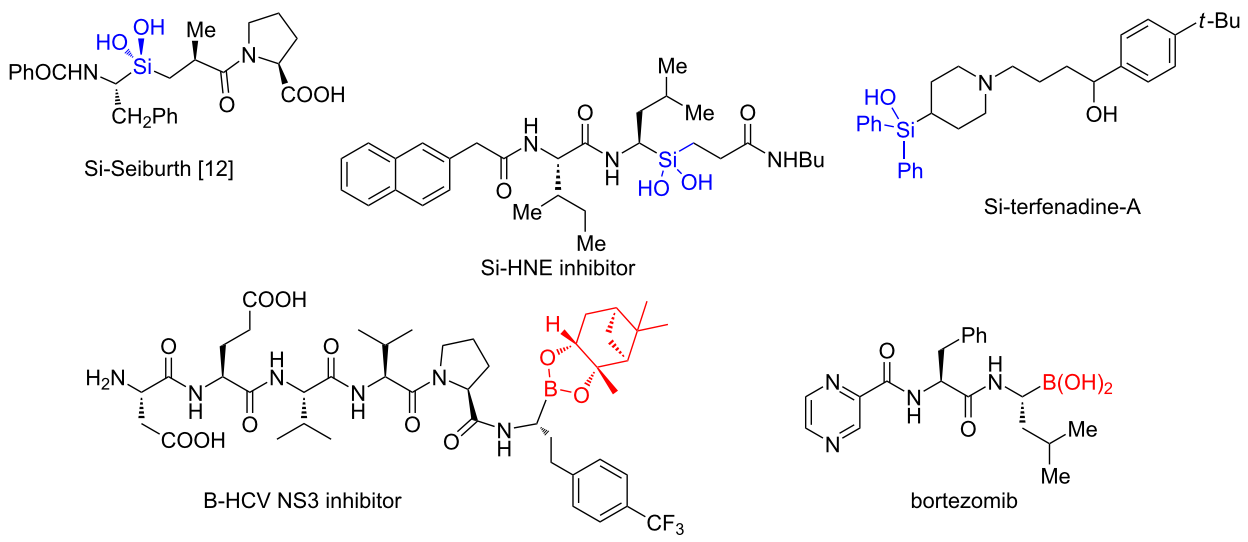

Scheme 1: Pharmaceuticals possessing a silicon or boron atom.

pounds (i.e., C(sp^3)–Si and C(sp^3)–B). Nonetheless, considering the extent of their use and their increasing popularity in the pharmaceutical industry, as well as the significant growth in the development of Cu-catalyzed processes applied to their syntheses, a review on this subject seems quite timely. Therefore, we will focus on highlights of the past 5–6 years in this area, dividing the document into two sections: C–Si and C–B bond formation.

Review

Cu-catalyzed C–Si bond formation

1.1 Substitution reactions

Alkylsilanes are an interesting class of substrates for medicinal and polymer chemistry. Nevertheless, they can be transformed into a variety of building blocks for subsequent use in complex molecule synthesis. The first example of a copper-catalyzed C(sp^3)–Si bond formation was reported by Oshima and co-workers in 1984 [25]. In an attempt to determine the existence of radical behavior of $PhMe_2Si$-MgMe (**2**), they studied the reaction of this Grignard reagent with dodecyl tosylate (**1**, X = OTs), which led to the formation of dodecyl silane **3** (20%) along with tridecane **4** (3%) and dodecane **5** (36%). Similarly, dodecyl bromide (**1**, X = Br) led to the same three products in 22%, 10%, and 24% yields, respectively (Scheme 2).

Later, a far higher yielding C–Si bond formation (66%) was developed by Hayashi [26]. More precisely, they used a catalytic amount of the complex formed from CuCl and NHC ligand **L1**, together with Suginome's reagent (**7**), to successfully convert benzyl phosphate **6** to benzylic silanes **8**. Curiously, the reaction proceeded even in the absence of a ligand, albeit with lower yield (25%; Scheme 3). However, only one example was reported and a more general method for the preparation of alkylsilanes was developed by the Oestreich group in 2016 [27]. The reaction could be performed using CuCN as catalyst in the absence of a ligand. A wide variety of triflates **9**, including some containing a remote tosylate, bromide, alkene, or alkyne functionality, afforded the desired alkylsilanes **10**–**16** in fair to

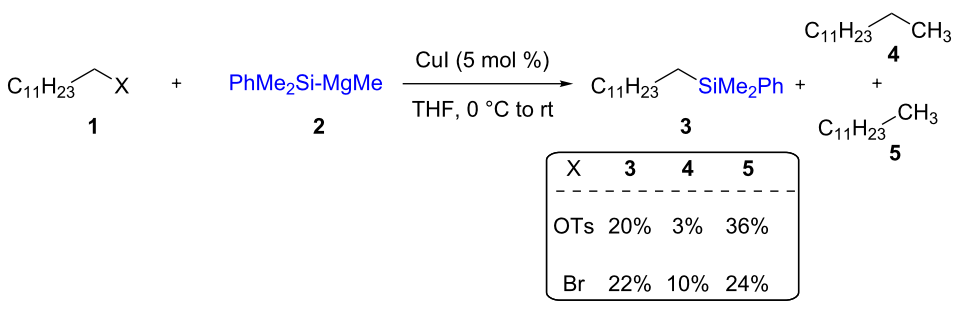

Scheme 2: The first Cu-catalyzed C(sp^3)–Si bond formation.

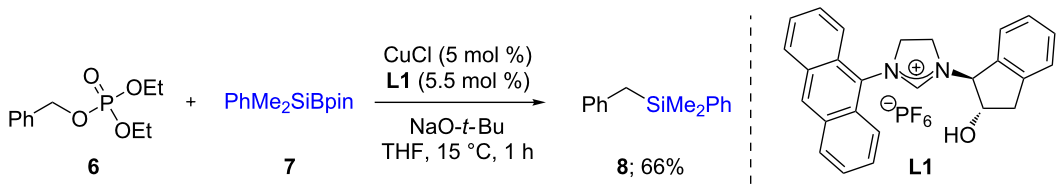

Scheme 3: Conversion of benzylic phosphate **6** to the corresponding silane.

good yields (Scheme 4). It should be mentioned that secondary triflates or halides are not suitable for this transformation, since they lead to products resulting from fast β-elimination.

Considering this limitation, they designed alkyl triflates stabilized by a strong electron-withdrawing group (EWG) directly attached to the triflate bearing carbon. In this way, different classes of substrates bearing either a nitrile (**17**) or ethyl ester (**21**) easily underwent conversion to the corresponding silylated products **18**–**20** in moderate to good yields (Scheme 5). This method was extended to the use of enantiomerically pure substrates, and as expected, inversion of configuration occurred at

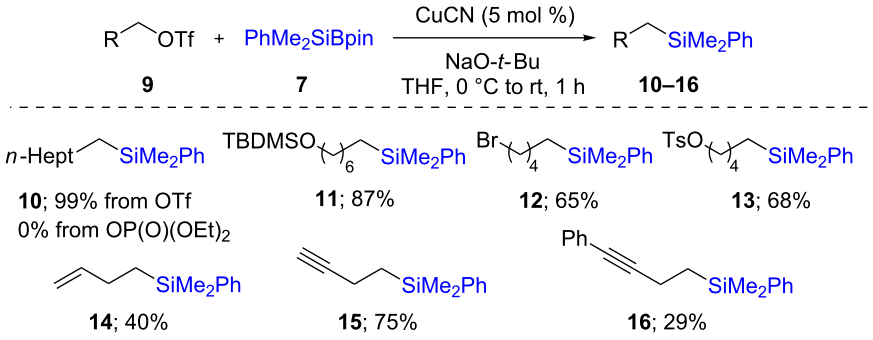

Scheme 4: Conversion of alkyl triflates to alkylsilanes.

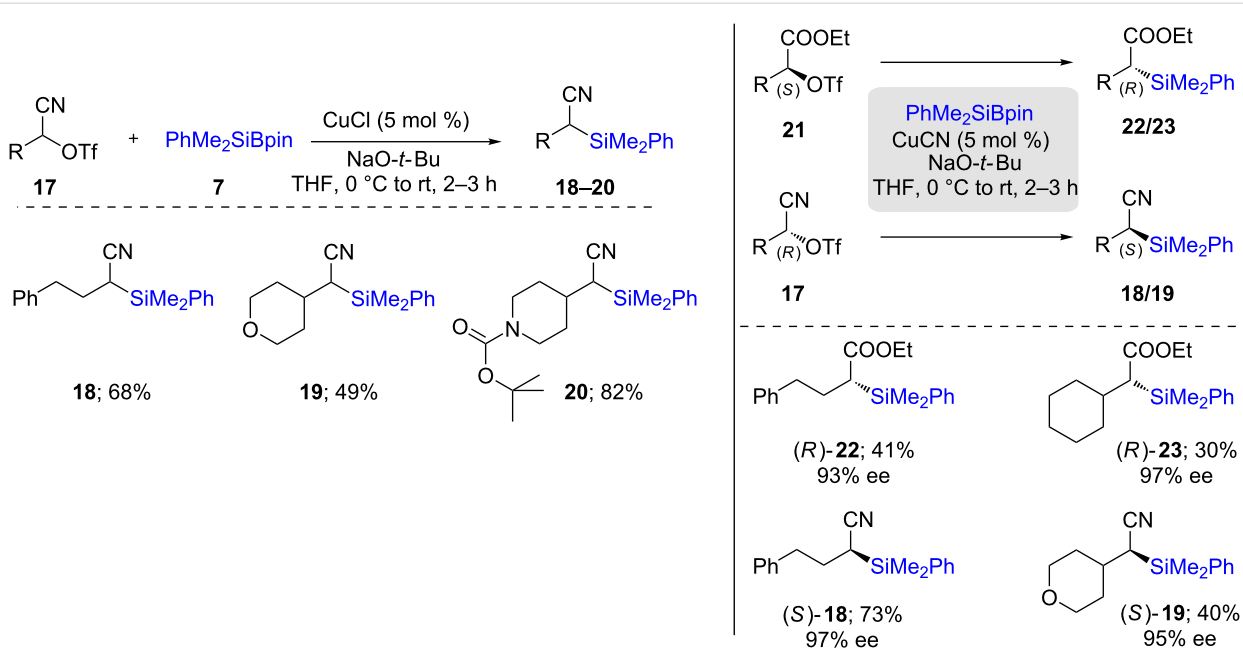

Scheme 5: Conversion of secondary alkyl triflates to alkylsilanes.

the stereogenic carbon centers, where an *S*-configured substrate led to an (*R*)-product (**22/23**), and vice versa (**18/19**) [28].

While the mechanism for the above two protocols are essentially ionic, an alternative method was reported by Oestreich [29] for the synthesis of secondary (**26–28**) and tertiary (**29**) silanes via a radical pathway, in good chemical yields (Scheme 6). It was possible to perform this reaction on a wide array of alkyl iodides using various silylating reagents. One selected application of this reaction, which also supports a radical mechanism, is depicted in Scheme 7. Here, an intermediate radical could easily be intercepted by a tethered alkene in **30** leading to a 5-*exo*-*trig* cyclization and hence, the formation of a 5-membered ring as found in products **31**–**33**. The formation of, e.g., compound **34**, suggested that a specific geometry of the tethered alkene is required, as no 6-membered ring formation was observed. Interestingly, Cárdenas' precursor **35** [30] led, after a cascade of reactions, to the formation of compound **36**. Computational as well as experimental studies suggested that the ligand and thiocyanate anion both play specific roles in the generation of an active Cu species able to trap the Si–Li (previously formed by reaction of LiO-*t*-Bu(THF)$_3$ with PhMe$_2$Si-Bpin; other atoms on Si and Li were omitted for clarity). The resultant Cu–Si species may then form a dative bond with the alkyl iodide leading to an electron transfer to the iodine atom, thereby liberating iodide, an alkyl radical, and a radical cation of the Cu complex. Recombination of the latter radicals leads to the formation of the desired silane along with the regeneration of the active Cu species (Scheme 8).

This strategy was also explored on redox-active alkyl esters derived from *N*-hydroxyphthalimide (NHPI, **37**), in which case the reactions proceeded through a similar radical pathway due to, in part, the alkyl radical surrogate nature of the NHPI esters.

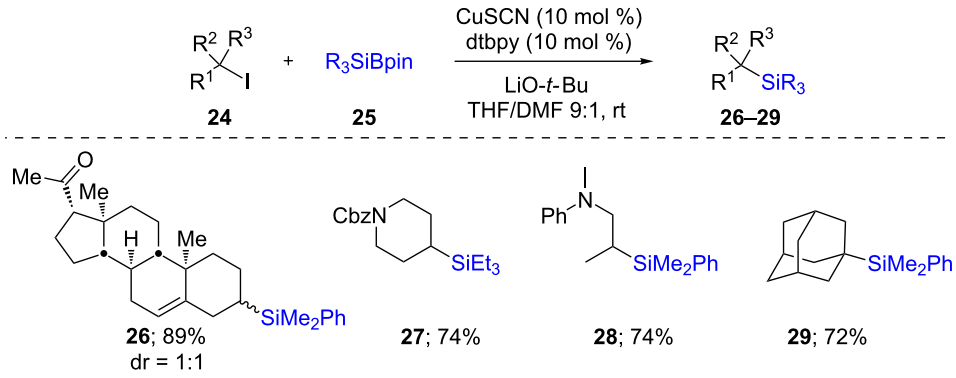

Scheme 6: Conversion of alkyl iodides to alkylsilanes.

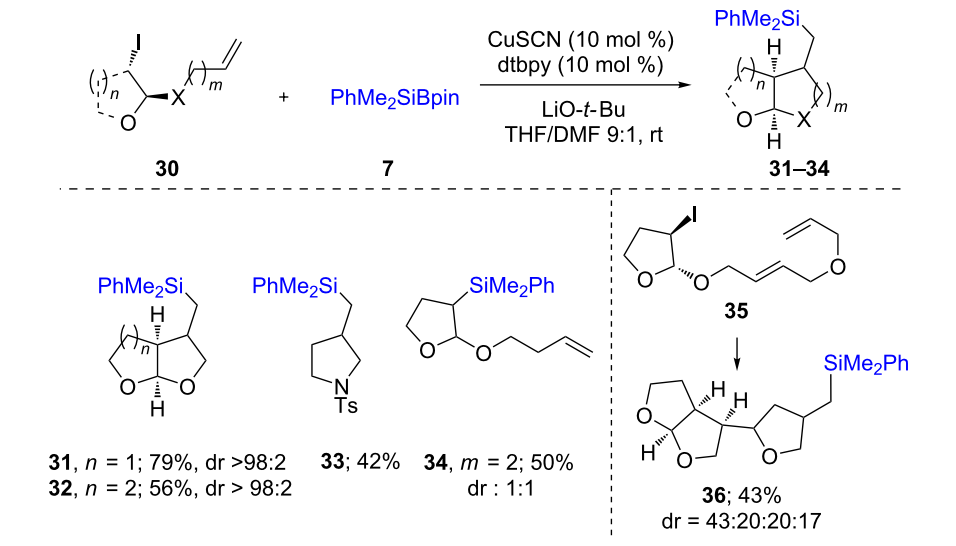

Scheme 7: Trapping of intermediate radical through cascade reaction.

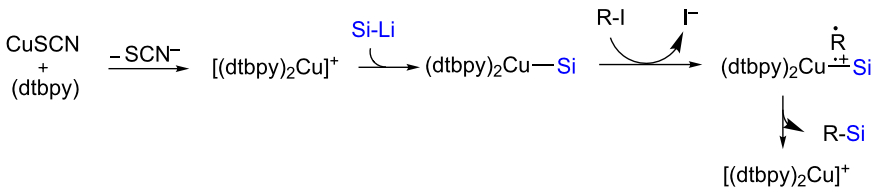

Scheme 8: Radical pathway for conversion of alkyl iodides to alkylsilanes.

The radical generated via decarboxylation of these esters is easily trapped by the in situ-formed Cu–Si species leading ultimately to the formation of the desired C–Si bond. This process could be applied to a variety of substrates leading to the desired products **29** and **38**–**40** (Scheme 9) [31].

This silylation reaction was also performed on geminal dibromides **41**. In such cases, both bromides were replaced by silyl groups. The reaction supposedly occurred partly via ionic silylation (of the first bromide), and partly via a radical pathway (silylation of the second bromide), effected by the presence of catalytic amounts of $CuBr{\cdot}SMe_2$ along with dtbpy as ligand. Whatever the mechanism(s), a variety of substrates were suitable for this transformation, giving the desired products **42**–**44** in good chemical yields (Scheme 10) [32].

1.2 Additions to imines

Among the very first studies on Cu-catalyzed additions to imines one can include the work of Moeller and co-workers published in 2002 in which they performed 1,2-additions of a silyl moiety to iminium ions [33], based on earlier work using silyllithium intermediates [34]. More recently, the Oestreich group described a more general method for the addition of silyl moieties to aldimines or ketimines **45** using 5 mol % CuCN together with Suginome's $PhMe_2Si$-BPin [35] as a silicon pronucleophile (Scheme 11A) [36]. The mechanism followed the

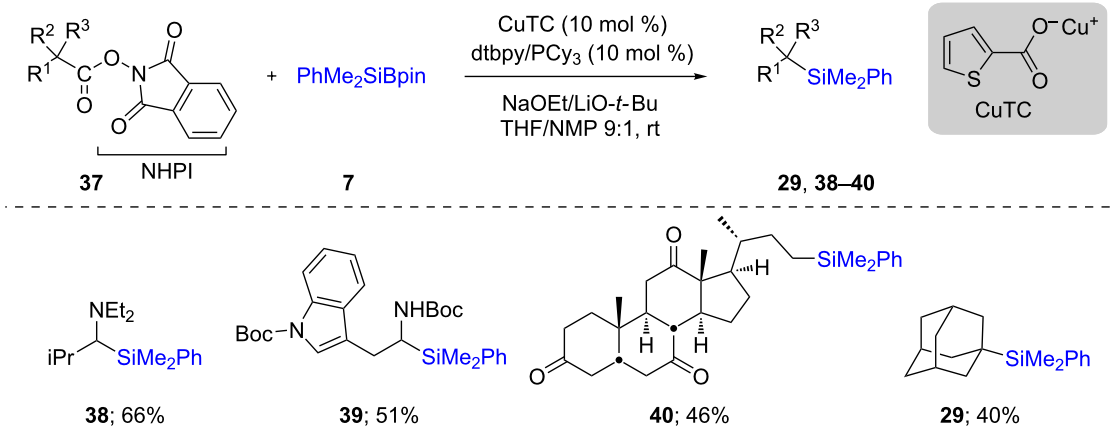

Scheme 9: Conversion of alkyl ester of *N*-hydroxyphthalimide to alkylsilanes.

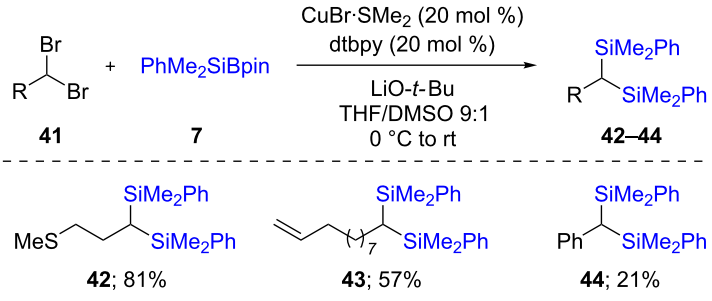

Scheme 10: Conversion of *gem*-dibromides to bis-silylalkanes.

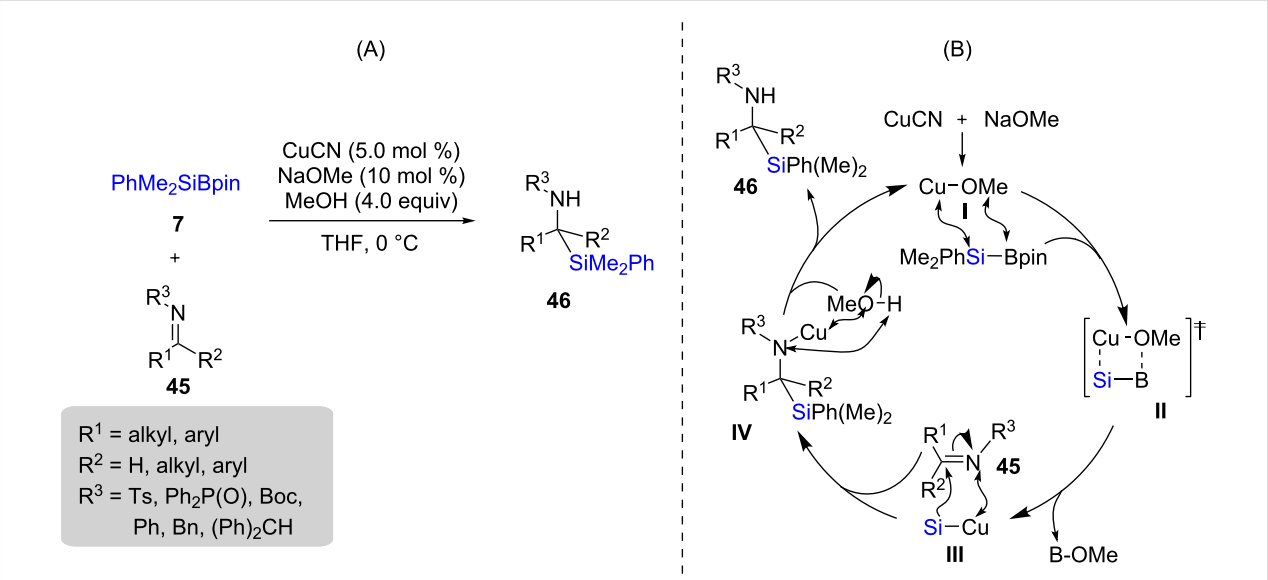

Scheme 11: Conversion of imines to α-silylated amines (A) and the reaction pathway (B).

expected pathway involving transmetallation from boron to copper to form the corresponding Cu–Si species **III**. This intermediate then adds to the imine **45** to give intermediate **IV**, which after undergoing proto-demetallation afforded the final product **46** (Scheme 11B).

Initially, the reaction was limited to the generation of racemic products. Ultimately, optimization using McQuade's six membered *N*-heterocyclic carbene (NHC) **L2** [37] in combination with CuCl led to conditions applicable to different types of aldimines **47** to give both good chemical yields and enantioselectivities associated with products **48**–**51** (Scheme 12). However, these additions were not applicable to neutral imines or ketimines – they are best performed on activated imines (e.g., *N*-sulfonyl imines) [38].

The same year, Sato and co-workers [39] used a comparatively simple ligand to perform asymmetric silylations of imines. Different ethylenediamine-based ligands (**L3**–**L5**) were screened from which **L3** proved to give even better yields and ees (Scheme 13). The use of this ligand was explored with other substrates **56** and found to give excellent chemical yields with good enantioselectivities for products **57**–**59** (Scheme 14). Interestingly, this approach could be extended to the synthesis of amino acids using cesium fluoride in the presence of CO_2 gas to afford **60** and **61**. From the representative examples shown below, it appears that α-amino esters could be obtained in excellent chemical yields with little erosion in enantiopurity.

Similar work was described by Zhao et al. using a C1-symmetric chiral NHC ligand **L6** together with catalytic amounts of

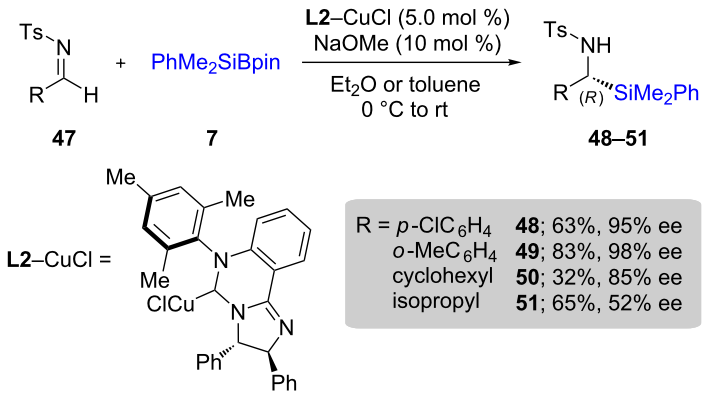

Scheme 12: Conversion of *N*-tosylimines to α-silylated amines.

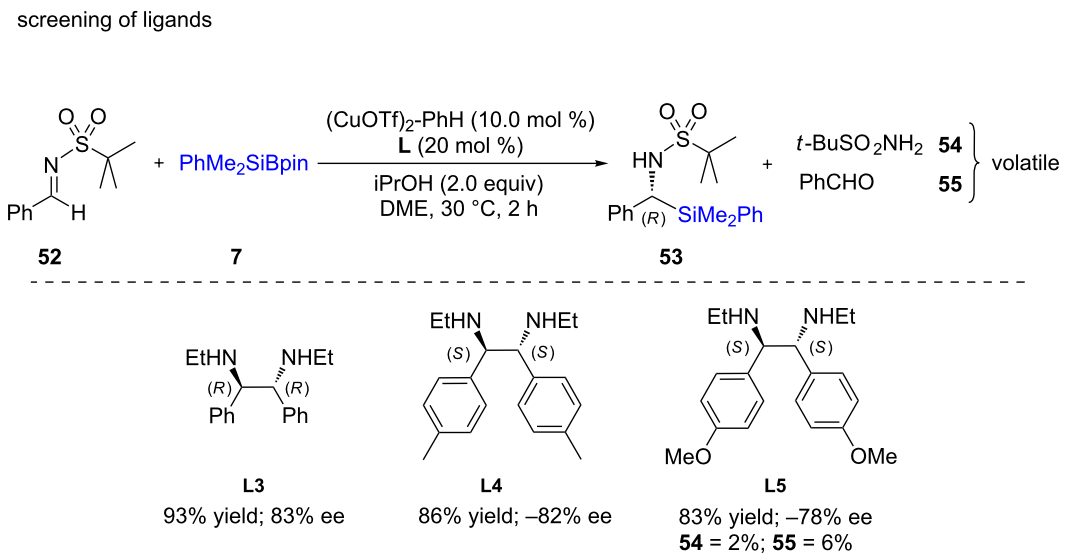

Scheme 13: Screening of diamine ligands.

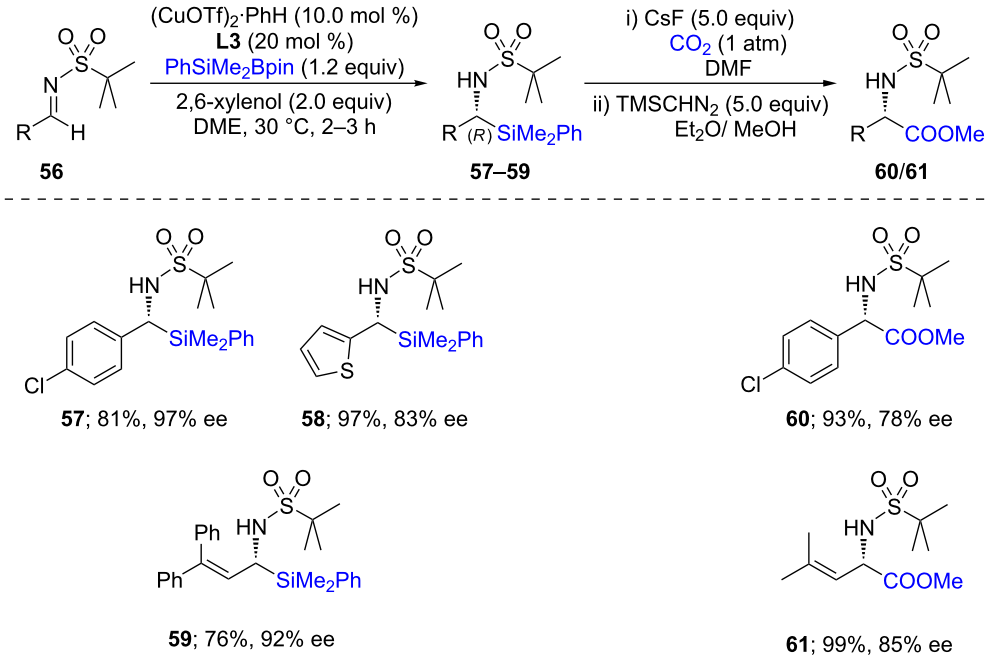

Scheme 14: Conversion of *N*-*tert*-butylsulfonylimines to α-silylated amines.

CuCl. Here again, reactions could be performed on numerous albeit activated aldimines **62**, failing to use unactivated educts [40]. Likewise, the α-silylated sulfonamide **67** was obtained in modest ee, although the chemical yield of the transformation was very low (15%). Changing the protecting group from Ts to methyl (**68**) or Boc (**70**) in the aldimine series did not alter yields or ees significantly. However, with the aniline derivative **69** (R = Ph on nitrogen), the ee dropped precipitously (Scheme 15).

Chen et al. used a paracyclophane-based NHC ligand, along with Cu_2O, to perform similar asymmetric 1,2-silyl additions onto activated imines. For several substrates (**47**) studied, the chemical yields were higher than in previously reported reac-

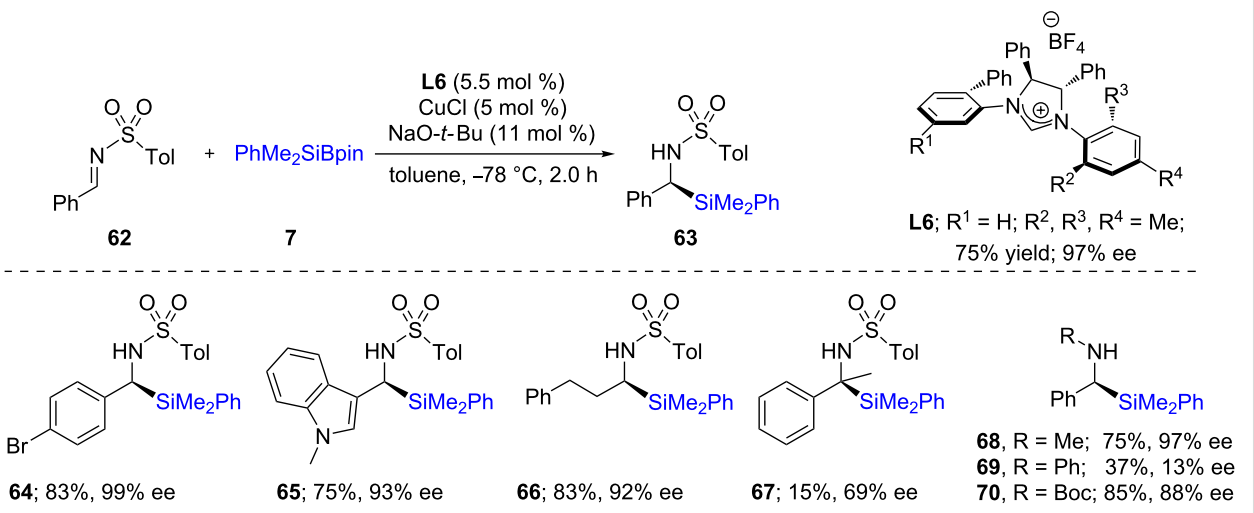

Scheme 15: Conversion of aldimines to nonracemic α-silylated amines.

tions, along with higher ees (Scheme 16, left). Although the synthesis of the ligand was somewhat tedious, the reaction proceeded in shorter reaction times [41]. Another approach, also shown below (Scheme 16, right), involves a metal-free background reaction. This represents the first example done in a water/THF solvent system at room temperature, giving moderate chemical yields and ees. It has been proposed that the ligand itself acts as an organocatalyst, eliminating the need for a copper catalyst.

1.3 Additions to aldehydes

The Oestreich group [42] described NHC–Cu (**74**)/base 1,2-additions at room temperature of silicon pro-nucleophiles onto aldehydes **81** leading to racemic silyl alcohols **82**–**87**

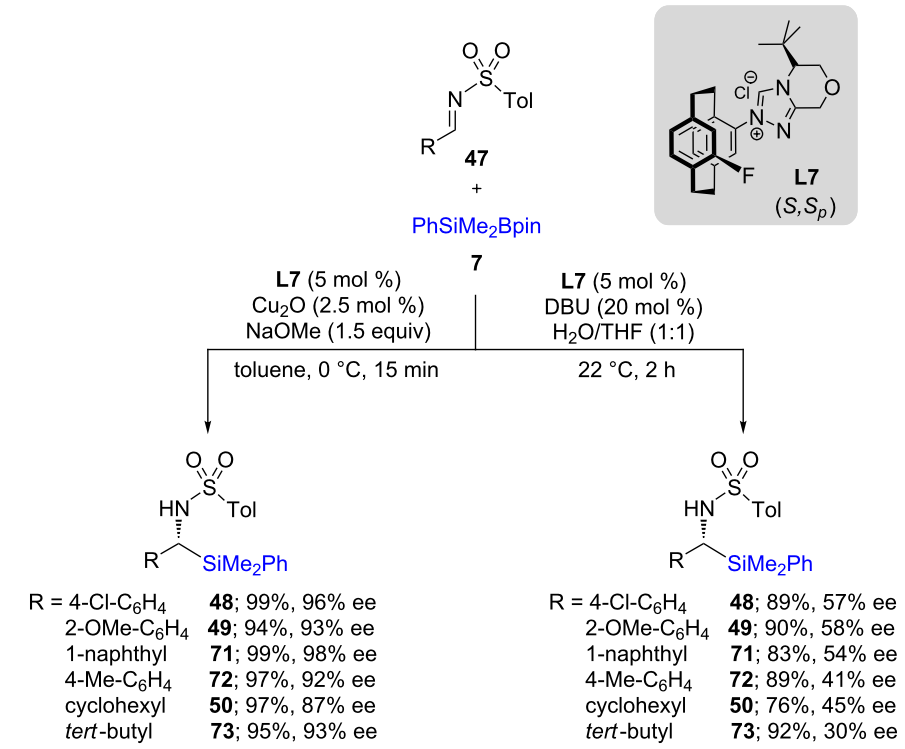

Scheme 16: Conversion of *N*-tosylimines to α-silylated amines.

(Scheme 17B). A detailed mechanistic study revealed that a Cu–Si species is involved, giving intermediate **77**, which subsequently undergoes fast Brook rearrangement to form a C–Cu bond-containing intermediate **78** (Scheme 17A). The O–Cu intermediate **77** can be intercepted either by $PhMe_2SiBpin$ or methanol to give the silylated O-Bpin product **79** or silyl alcohol **80**, respectively. Interestingly, it was eventually realized that the use of the NHC ligand is not required if CuCN is used as the catalyst. Under such conditions, the desired product could be obtained faster than when the NHC was used. However, aldehydes containing reactive functional groups, as in **85**–**87**, gave none of the desired product with either CuCN or the Cu–NHC complex **74**.

On the other hand, Ohmiya and co-workers envisioned inverting the polarity of an aldehyde **81** via conversion into the corresponding α-alkoxyalkyl Cu(I) anion **78**. Utilizing **78**, which undergoes transmetallation to an initially formed Pd(II) intermediate (from oxidative addition) led to cross couplings affording benzhydryl silyl ethers **89**–**92** (Scheme 18), thus showcasing the synergistic relationship between Pd and Cu catalysis [43].

Driven by the success of earlier results, the authors utilized **78** for reductive couplings between ketones **93** and imines **97** as electrophiles to form unsymmetrical 1,2-diols **94**–**96** and 1,2-amino alcohols **98**–**100**, respectively. Palladium was no longer needed for these transformations. The scope of the reaction with ketones was not limited to diaryl species and aryl ketones participated in the reaction, including those with more hindered alkyl groups (Scheme 19) [44].

This discovery was followed by a study from the Riant group [45] that performed asymmetric 1,2-additions on aldehydes using Suginome's reagent in the presence of phosphine-ligated copper (Scheme 20A). After optimization, they found that DTBM-Segphos (**L12**; 10 mol %) together with CuCl (5 mol %) led to moderate yields (46%) and high ee (97%) for this transformation. In an attempt to improve the chemical yield, they prepared a preformed complex of diphosphine copper(I)

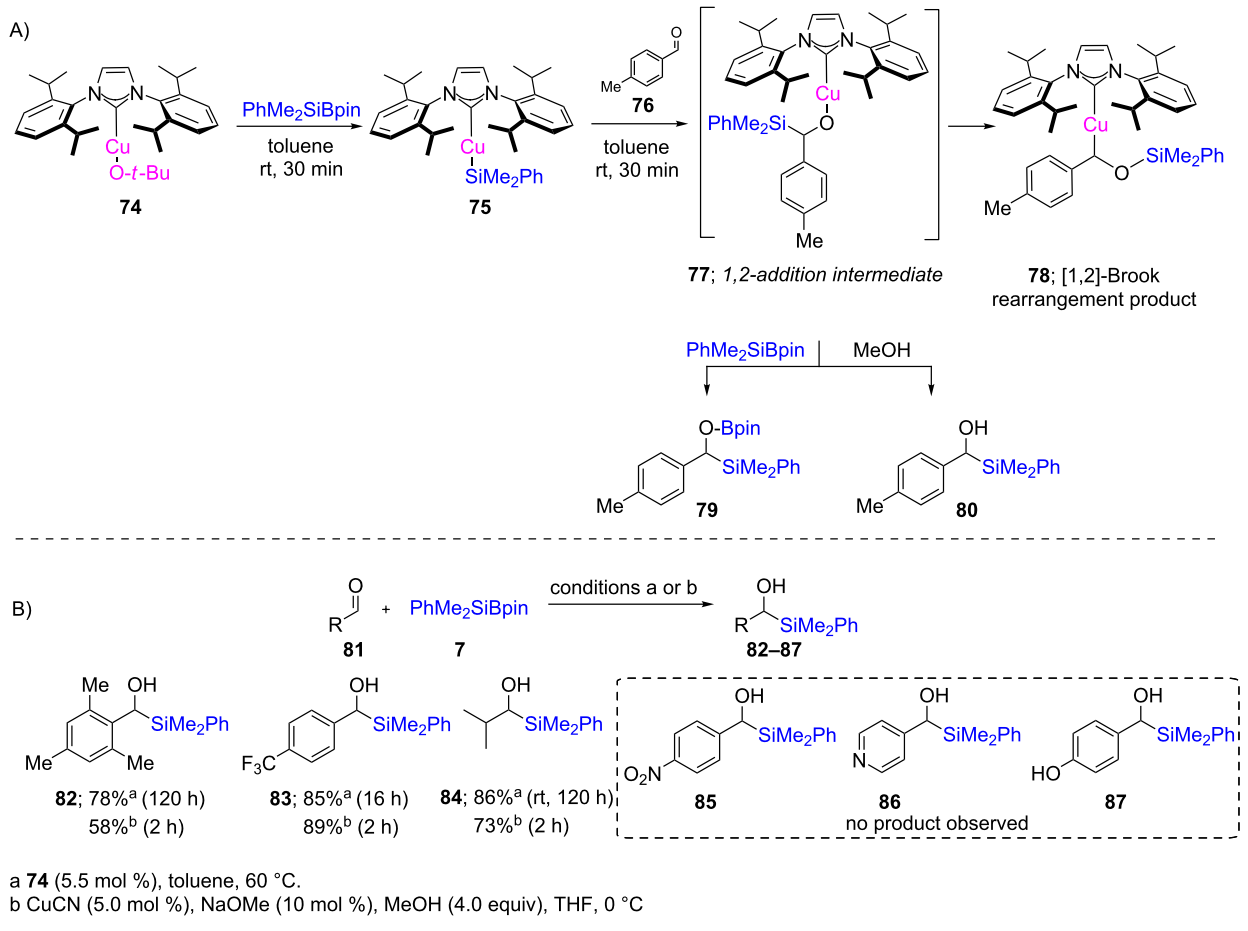

a **74** (5.5 mol %), toluene, 60 °C.
b CuCN (5.0 mol %), NaOMe (10 mol %), MeOH (4.0 equiv), THF, 0 °C

Scheme 17: Reaction pathway [A] and conversion of aldehydes to α-silylated alcohols [B].

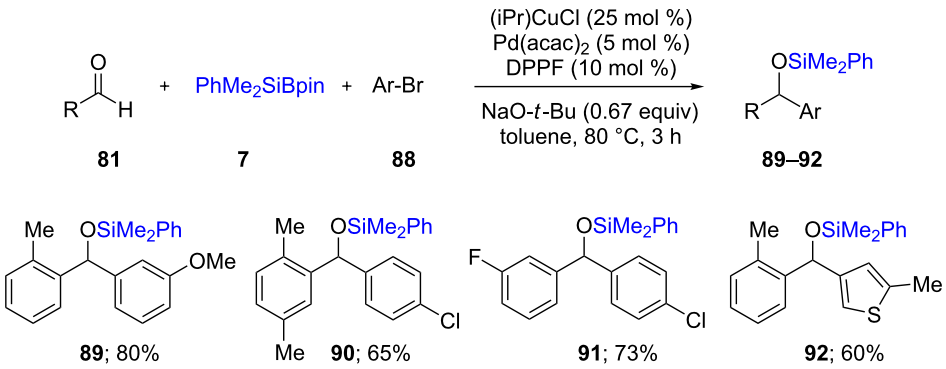

Scheme 18: Conversion of aldehydes to benzhydryl silyl ethers.

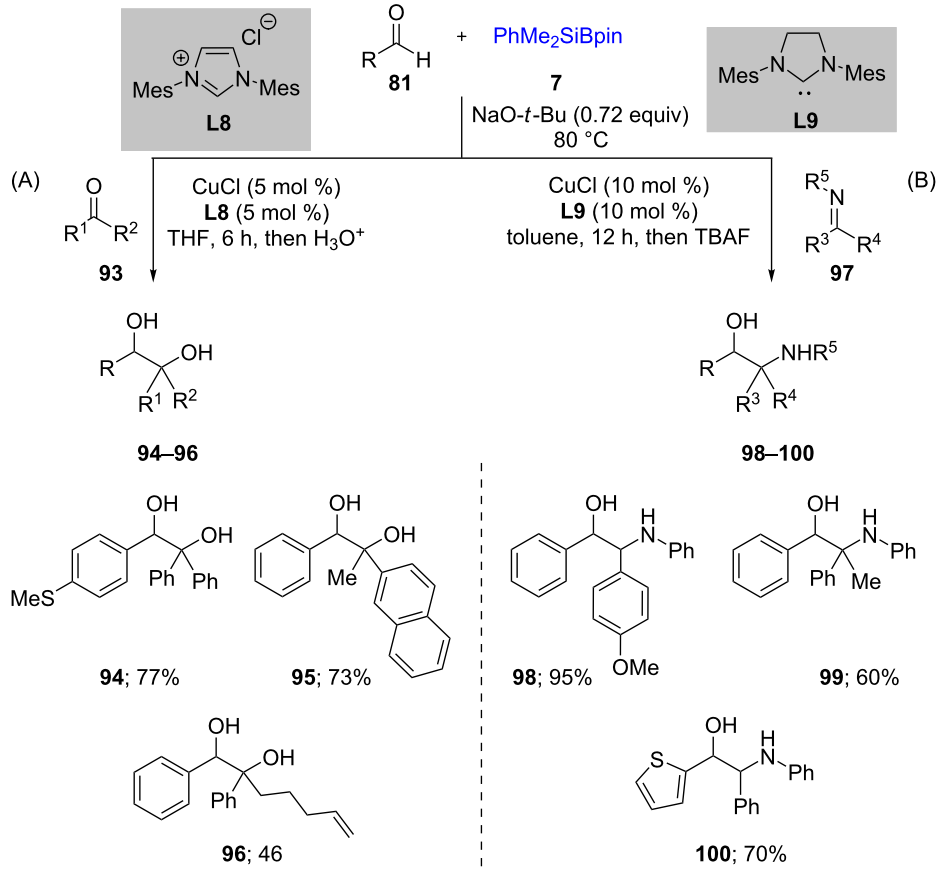

Scheme 19: Conversion of ketones to 1,2-diols (A) and conversion of imines to 1,2-amino alcohols (B).

difluoride, which, indeed, increased the yield to 87% together with raising the ee to 99%. A variety of substrates were then studied using this complex, and in each case, more than 90% ee along with high chemical yields were obtained (Scheme 20B). Simultaneous efforts by Oestreich were also directed towards nonracemic silyl alcohol synthesis using McQuade's NHC **L2** (Scheme 21) [46].

1.4 Additions to unsaturated compounds

Back in 1977, Fleming first described 1,4-additions of cuprates derived from a silyllithium [47] to α,β-unsaturated ketones [48]. There was no effort made at that time to convert these reactions to the corresponding catalytic processes, rather, the accent was more towards using the silyl group introduced as a hydroxy group equivalent [49-51]. Similarly, although the Lipshutz

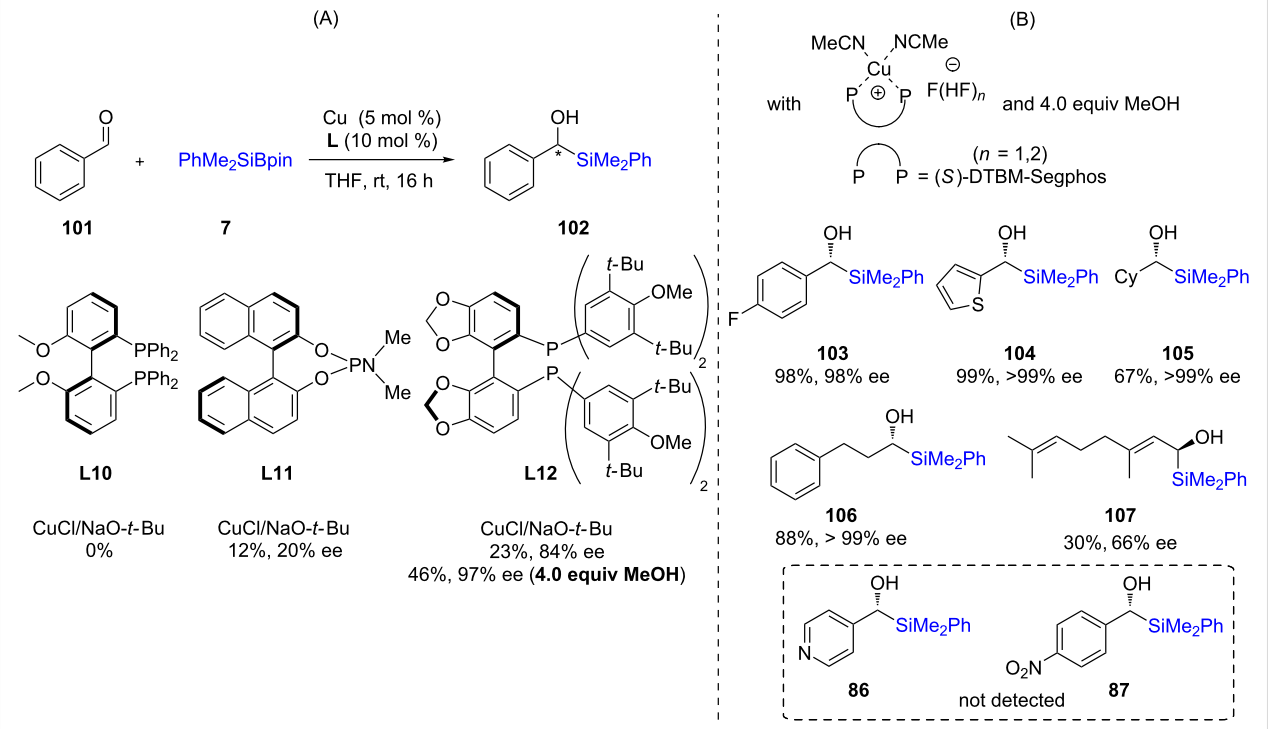

Scheme 20: Ligand screening (A) and conversion of aldehydes to α-silylated alcohols (B).

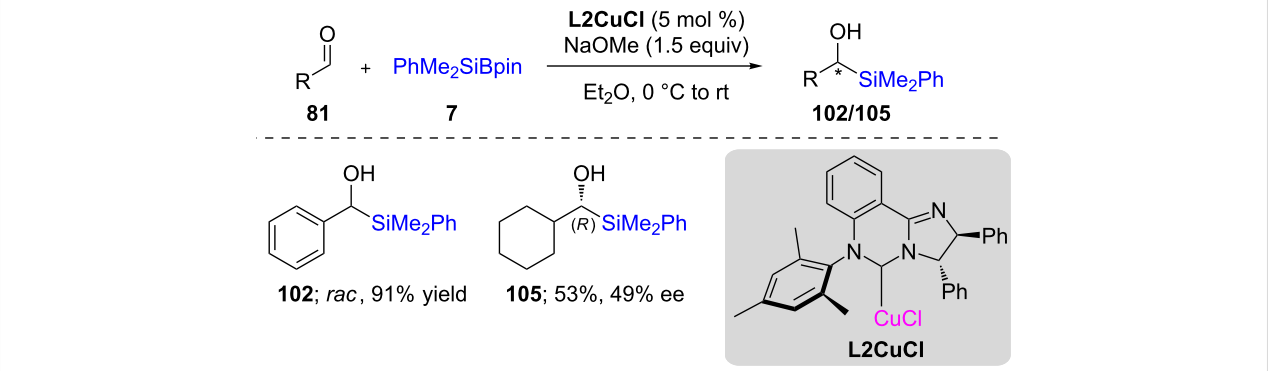

Scheme 21: Conversion of aldehydes to α-silylated alcohols.

group [52] also showed that in situ-formed trialkylsilylcuprates could be used for 1,4-additions with unsaturated ketones **108** in high chemical yields (Scheme 22, left), here, too, a catalytic method had yet to be reported limiting the use of these methods. Almost a decade later, however, Lipshutz et al. revisited this reaction, showing that it could be performed using only 3 mol % of the copper catalyst, while leading to high chemical yields of the desired silylated product **112** (Scheme 22, left) [53]. In the same year, Hosomi and co-workers reported that the alternative silane, 1,1,2,2-tetramethyl-1,2-diphenyldisilane, also commercially available, can be used for nucleophilic additions to α,β-unsaturated ketones. Thus, by cleaving the Si–Si bond in the presence of a Cu(I) salt, an active [Cu–Si] species is generated leading to β-silylated ketones [54]. More than a decade later, Molander et al. made use of the same disilane as a source of the nucleophile for additions to α,β-unsaturated alkenes and alkynes as Michael acceptors bearing sulfones, nitriles, cyano, amido, and carboxyl ester groups to form β-silylated alkanes and alkenes in good to moderate yields [55]. Following this report, Oestreich and co-workers examined asymmetric additions of silicon to unsaturated ketones **113** using P–N-type ligand **L13**. However, the background reaction of the silyl–zinc reagent was predominant leading to poor chirality transfer from the phosphine ligand **L13**, giving essentially the racemic product **114** (Scheme 22, right) [56].

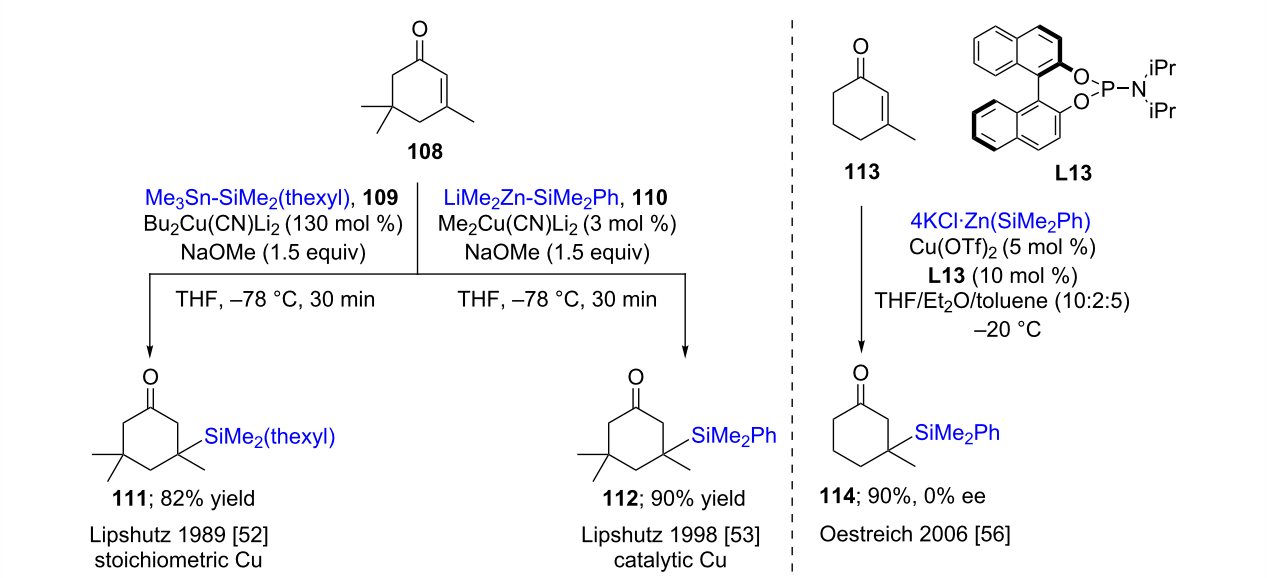

Scheme 22: 1,4-Additions to α,β-unsaturated ketones.

In 2010, Hoveyda [57] used CuCl along with an NHC ligand (**L14**) that enabled 1,4-additions of silicon nucleophiles to unsaturated ketones. The best results were obtained at low temperatures, giving both high chemical yields and products with high enantiomeric ratios. Both cyclic (**117** and **118**) and acyclic (**119**,**120**) ketones could be silylated efficiently (Scheme 23). Interestingly, cyclic enones conjugated to an external double bond, as in **121**, upon exposure to these conditions resulted in

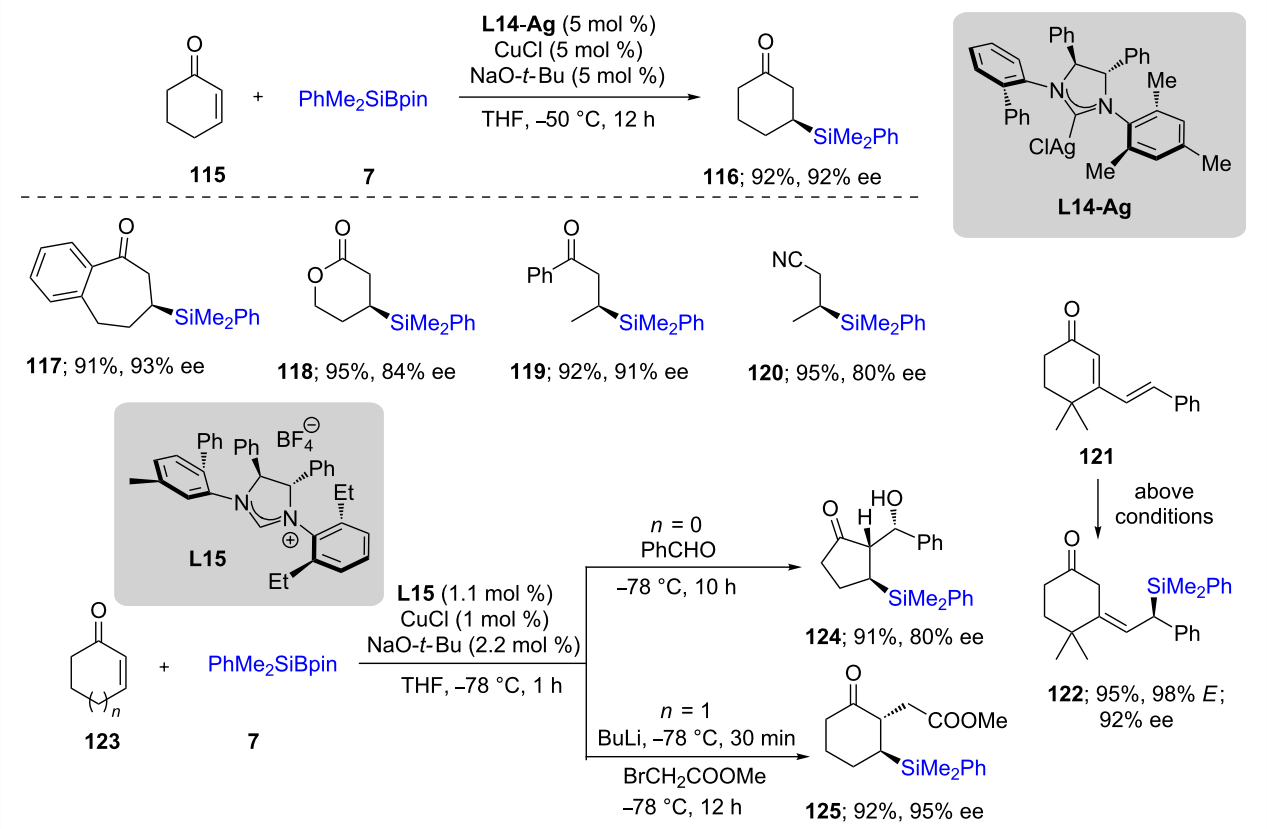

Scheme 23: 1,4-Additions to unsaturated ketones to give β-silylated derivatives.

an excellent selectivity for the 1,6-addition and in high ee for product **122**. Moreover, the intermediates could be trapped in the presence of electrophiles, such as aldehydes or alkyl halides to afford interesting α-substituted products **124** and **125**. This phenomenon was further studied in detail on different dienones [58].

In 2013, Procter and co-workers [59] extended the scope of this silicon addition to unsaturated lactones using copper catalysis together with NHC ligand **L16**. The ligand used previously to great advantage by the Hoveyda and Oestreich groups for conjugate additions did not yield high ees for these substrates. The authors designed a new NHC possessing either an anthryl or naphthyl group, the use of which led to moderate to good enantioselectivities in most cases. An application of this method is shown for the total synthesis of the natural product (+)-blastmycinone (Scheme 24).

As a follow up to this work, the same authors successfully accomplished, for the first time, a silyl transfer to lactams in both high chemical yields and high ees [60]. In this case, a comparatively higher (5 mol %) copper loading was necessary. Not only lactams (Scheme 25) but also acyclic, unsaturated amides could be efficiently silylated under these conditions. Interestingly, this protocol was applied to the total synthesis of (*R*)-oxiracetam (**142**), a drug used for the treatment of Alzheimer's disease [61].

In a similar way, a ligand-free, intramolecular silylarylation of unsaturated amides **143** could be performed, albeit following a radical pathway leading to cyclic products (Scheme 26). From the different radical generators screened, dicumyl peroxide (DCP) was found to be very effective in leading to the corresponding products **144**–**148**. Along with different acrylamides, different hydrosilanes were used as silyl source and the reaction could be applied to a wide variety of substrates, although the methodology required hazardous conditions; i.e., hot benzene [62].

A few years later, similar types of reactions were carried out by Loh and co-workers [63]. In this case, a variety of α,β-unsaturated compounds, that, rather than undergoing intramolecular cyclization, could be intercepted at the intermediate radical stage (**149**) with radical initiator TBHP present in excess, leading to silylated peroxy products **151**–**156**. This approach was applied to different types of conjugated systems, including esters, ketones, amides, alkynes, etc. (Scheme 27).

Kleeberg [64] et al. have contributed to the understanding of the mechanism of silylation reactions of unsaturated compounds. In their studies, it was possible, surprisingly, to isolate and characterize a β-silyl boron enolate complex **158**. On the basis of experimental and NMR studies, they proposed that for α,β-unsaturated ketones, a 1,4-addition product was formed through a transient copper enolate, **157**. With α,β-unsaturated esters, how-

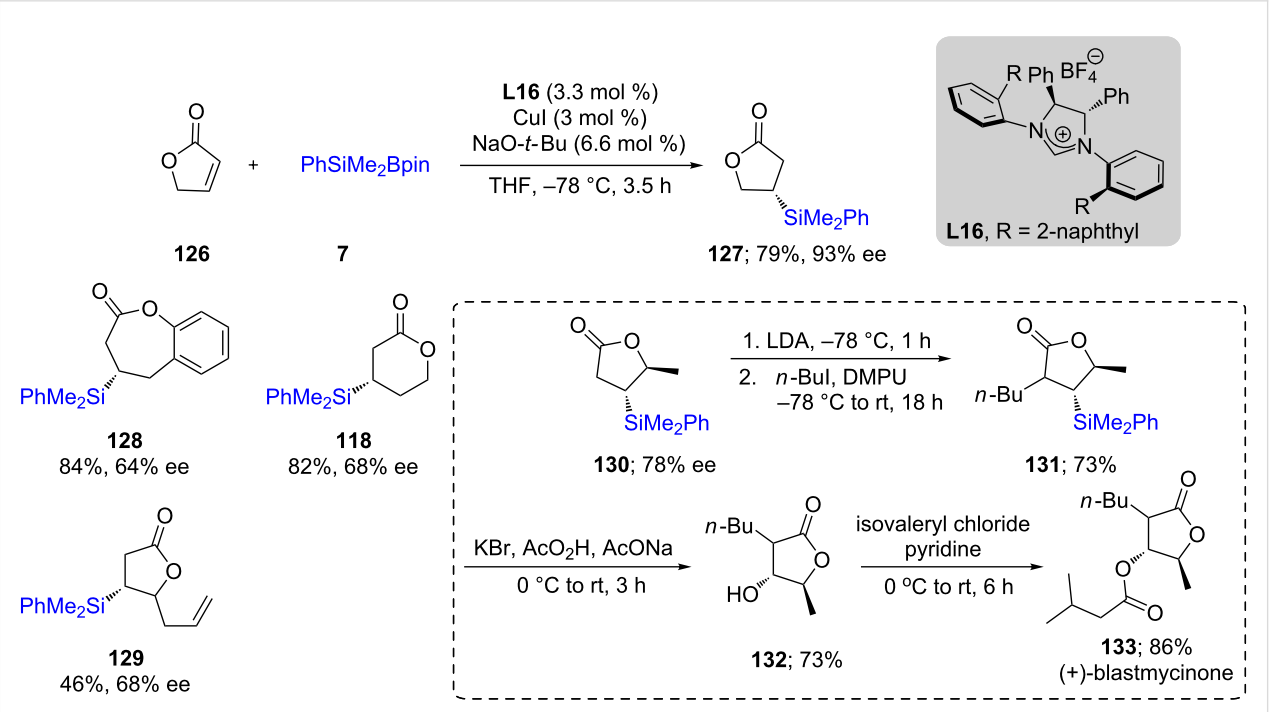

Scheme 24: Additions onto α,β-unsaturated lactones to give β-silylated lactones.

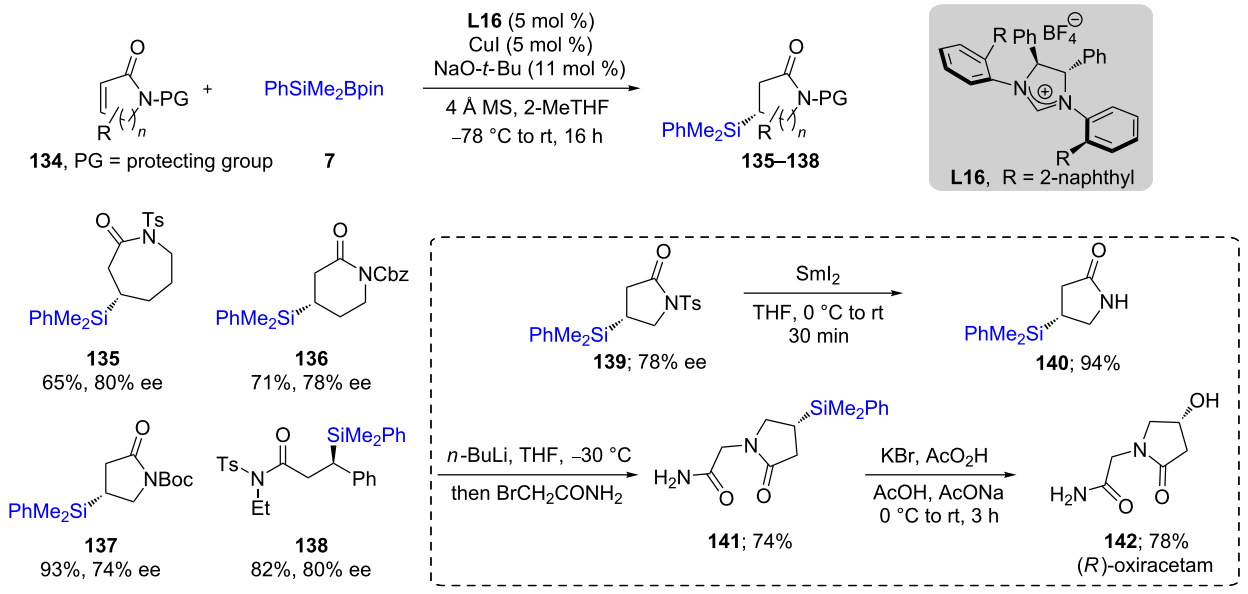

Scheme 25: Conversion of α,β-unsaturated to β-silylated lactams.

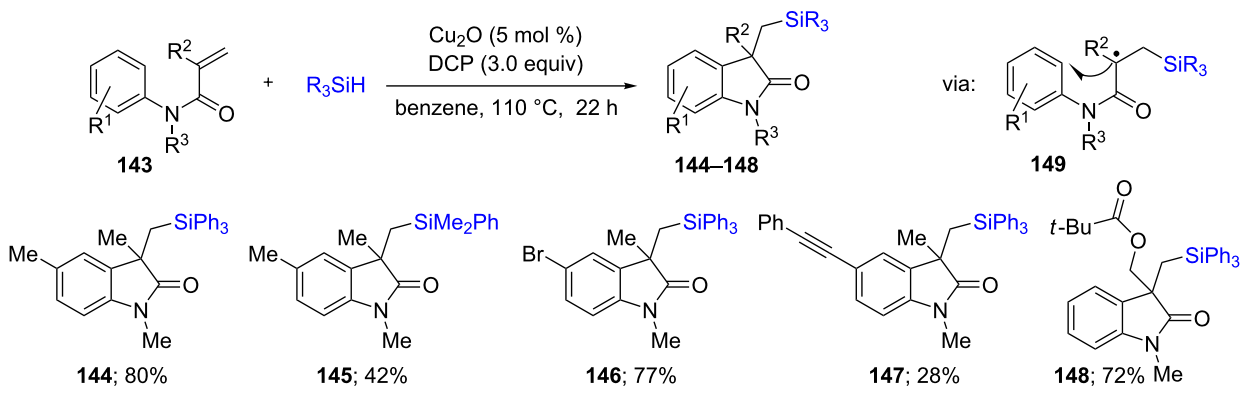

Scheme 26: Conversion of *N*-arylacrylamides to silylated oxindoles.

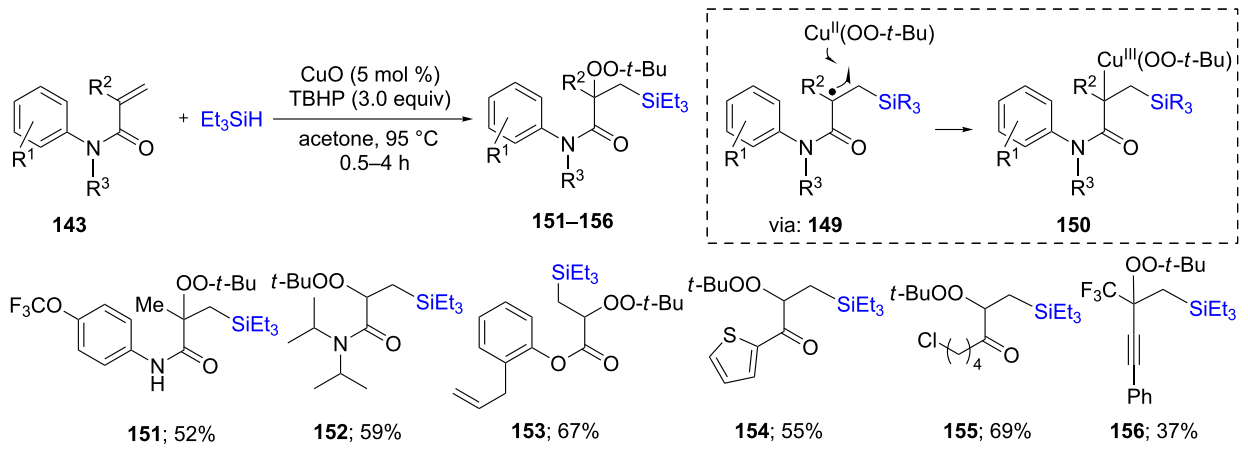

Scheme 27: Conversion of α,β-unsaturated carbonyl compounds to silylated *tert*-butylperoxides.

ever, a carbon enolate, **160**, is the intermediate. In order to maintain a catalytic cycle, iPrOH could be added to regenerate the active Cu species (Scheme 28). This study again proofed that an enol system, as in the case of unsaturated ketones which is not easy to isolate, could be modified in such way that the resultant intermediate is highly stable. For example, Tortosa [65] showed that this type of catalytic system could be applied to the quinone methide system **162**, which is equivalent to dienones (Scheme 29). In this case, however, instead of forming an enol, a highly stable phenol resulted from the addition of silicon at the methide position. The reaction was exclusively done on electron-rich systems **163**–**166**. Nonetheless, further functionalization of one of the silicon-containing products (**166**) was carried out to arrive at the keto phenol derivative **167**.

Loh, Xu, and co-workers [66] explored related reactions involving unsaturated ketimines using copper triflate or copper bis(4-cyclohexylbutyrate) ($Cu(CHB)_2$) to prepare allylic silanes. Interestingly, using one or the other of these two copper sources and a selection of appropriate reaction conditions allowed for the complete reversal in geometrical isomers of the products. For example, the use of $Cu(OTf)_2/Na_3PO_4$ in dioxane/*t*-BuOH resulted in *Z*-isomer formation (93% selectivity; Scheme 30, left; conditions A), while the use of catalytic $Cu(CHB)_2$/diisopropyl ethylamine in *m*-xylenes/*t*-BuOH gave the *E*-isomer (99% selectivity; Scheme 30, right; conditions B). They also screened various bisoxazoline-containing ligands (for example Scheme 31, **L17**) for chiral induction which led to good enantioselectivities, in addition to excellent *E:Z* ratios within the re-

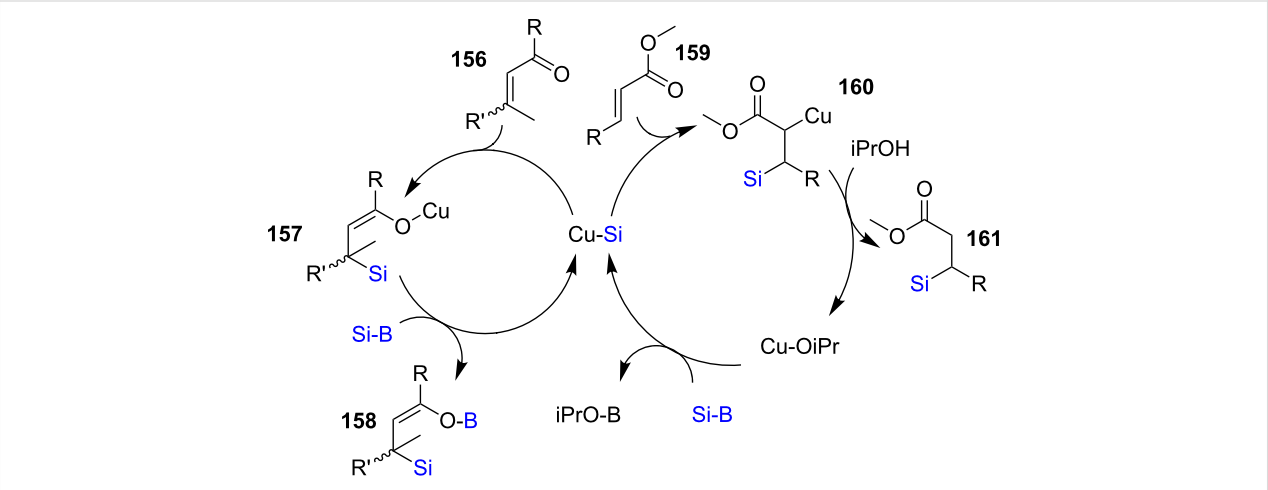

Scheme 28: Catalytic cycle for Cu(I) catalyzed α,β-unsaturated compounds.

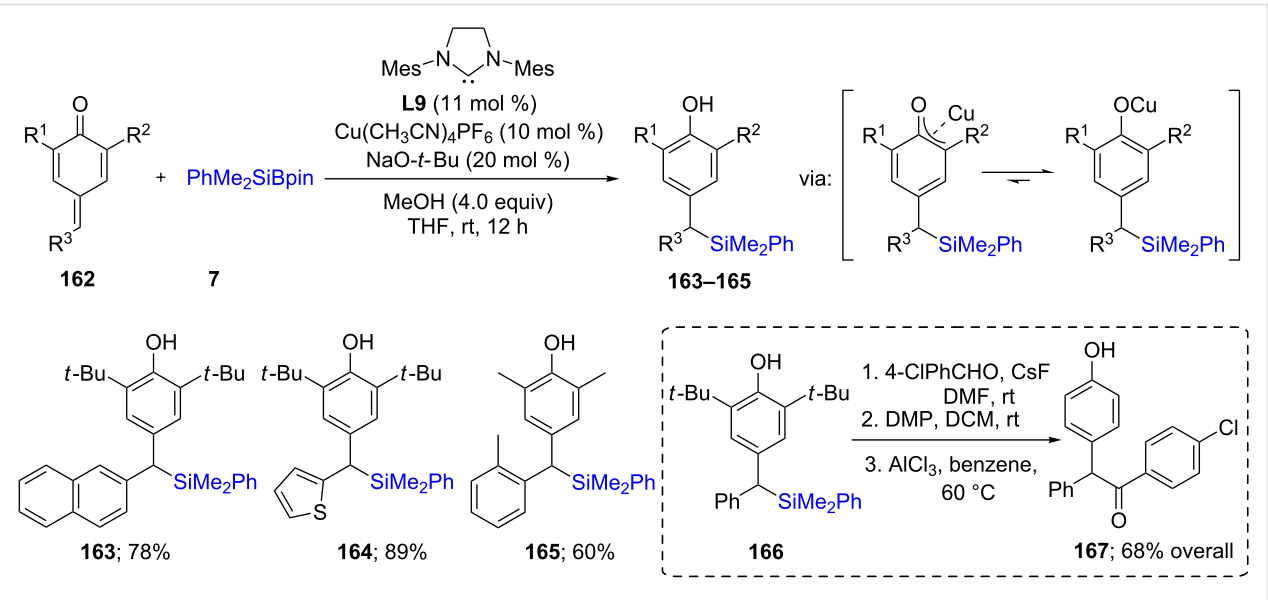

Scheme 29: Conversion of *p*-quinone methides to benzylic silanes.

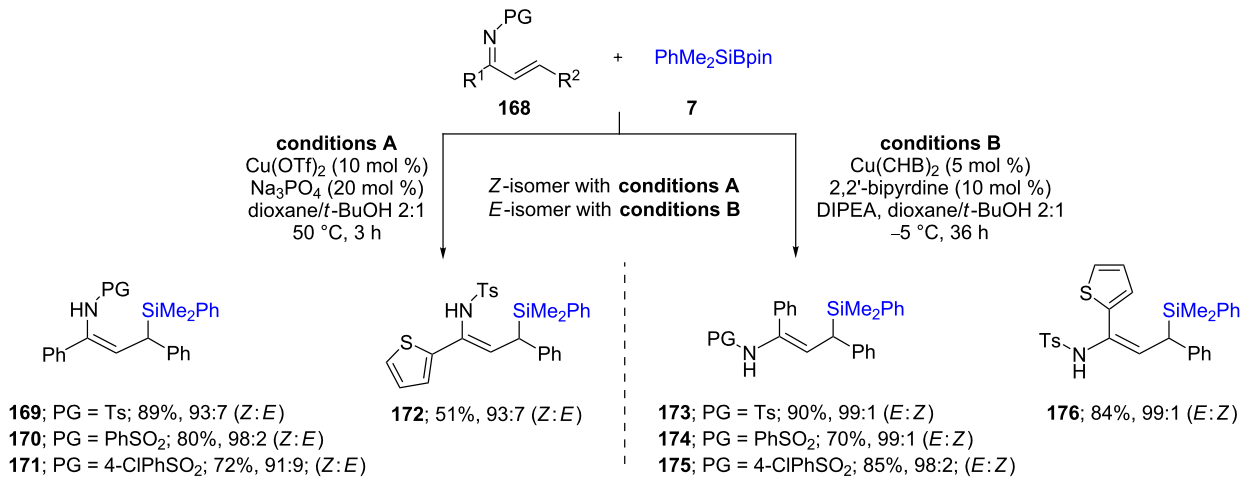

Scheme 30: Conversion of α,β-unsaturated ketimines to regio- and stereocontrolled allylic silanes.

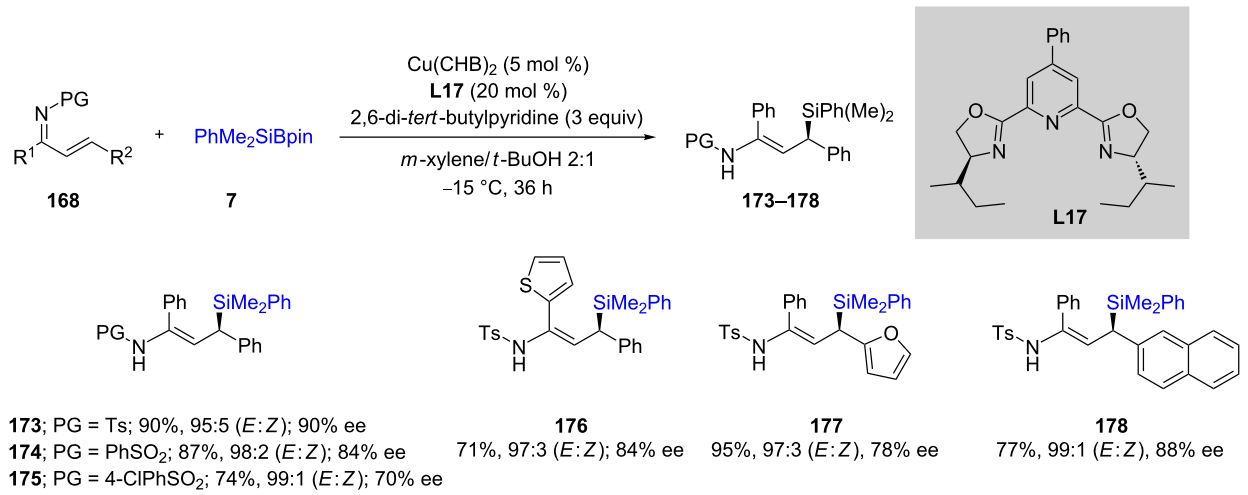

Scheme 31: Conversion of α,β-unsaturated ketimines to enantioenriched allylic silanes.

sulting alkenes. This methodology could be applied to a wide variety of compounds, including those containing heterocycles (**176**–**178**).

In a later study [67], they found that by changing ligands, a dramatic switch in the selectivity could be induced in silyl additions to dienedioates. Interestingly, tricyclohexylphosphonium tetrafluoroborate (**L18**), along with CuCN, resulted in the 1,4-addition as the major pathway (Scheme 32, left). By contrast, the use of the bulkier tris(2,6-dimethoxyphenyl)phosphane (**L19**) led to the formation of 1,6-adducts (Scheme 32, right).

The Oestreich group [68] used silicon-based Grignard reagents **189** to add to conjugated heteroaromatics **188**, e.g., benzoxazole (as an extension to more commonly studies ketones, esters, imines, etc.), leading to products **190**–**194**. The heterocycle played a crucial role, as in its absence, none of the expected product was obtained, e.g., when simple stilbene was used the reaction led to only traces of product **194** (Scheme 33). With benzoxazole-conjugated alkenes, upon treatment with catalytic Cu complexed by a nonracemic Josiphos ligand (**L20**), good chemical yields of the desired enantioenriched products **196**–**199** could be isolated (Scheme 34).

Another class of heterocycles, α-silylated *N*-alkylated indoles **201**–**205** recently reported by Xu and co-workers, were formed using a nonracemic Cu–NHC catalyst through the enantioselective addition of the $PhMe_2Si$ group to α,β-unsaturated carbonyl

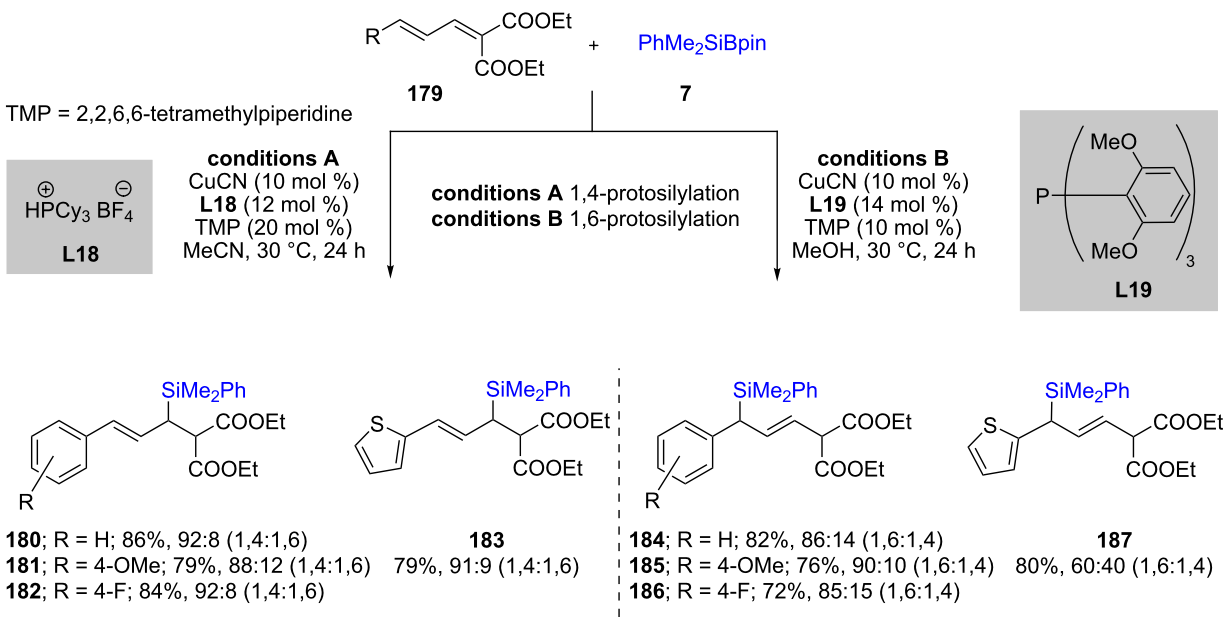

Scheme 32: Regioselective conversion of dienedioates to allylic silanes.

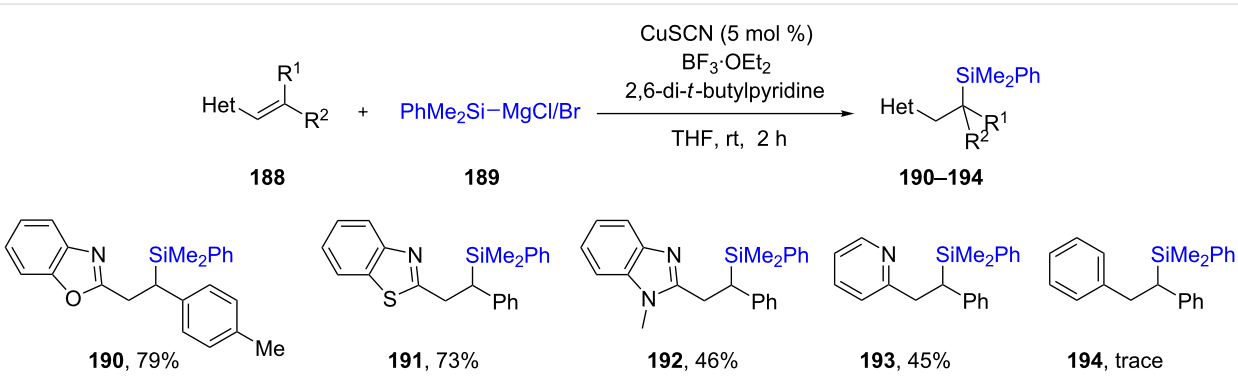

Scheme 33: Conversion of alkenyl-substituted azaarenes to β-silylated adducts.

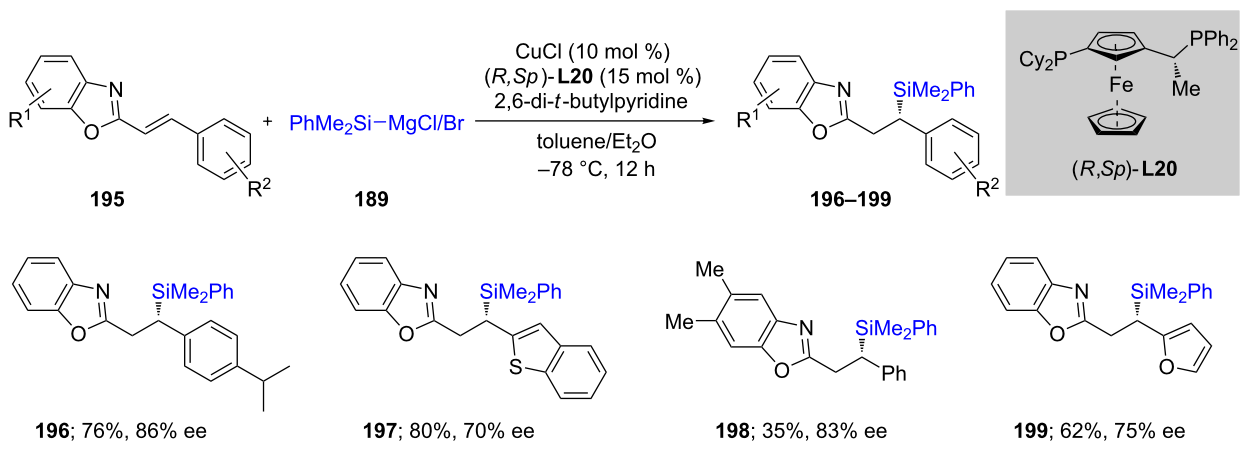

Scheme 34: Conversion of conjugated benzoxazoles to enantioenriched β-silylated adducts.

indoles **200** (Scheme 35). The authors demonstrated a wide substrate scope, including an example of benzimidazole and pyrrole, although with varying chemical yields [69].

Recently Zhang et al. [70] explored various **L22**-containing (NHC)Cu catalysts by means of generating interesting non-racemic aminosilanes. In this case, they performed 1,2-additions on β-amidoacrylates (**200**) using 10 mol % CuCl in THF at room temperature (Scheme 36). In most cases, the chemical yields were very good to excellent, as were the resulting ees of the products **201**–**207**.

The processes described above were run using stoichiometric copper and organic solvents at cryogenic temperatures, hence, they are neither economical nor sustainable [71-73]. Alternatively, the Kobayashi [74] group has shown that such reactions can be done not only more efficiently, but in a far "greener" fashion using water as the solvent, catalytic amounts of copper, and the reaction being done at room temperature. One of the biggest advantages of using water was that this catalytic system behaved as if being run homogeneously in an organic solvent. However, due to a lack of solubility of both the substrate and catalyst in water, it is actually heterogeneous and hence, provided an opportunity for recycling and reuse. This catalyst, therefore, was isolated using simple centrifugation and reused in a second reaction leading to no appreciable loss in catalytic activity en route to product **218**. It was also utilized not only for unsaturated ketones but also to deliver the $PhMe_2Si$ moiety in a

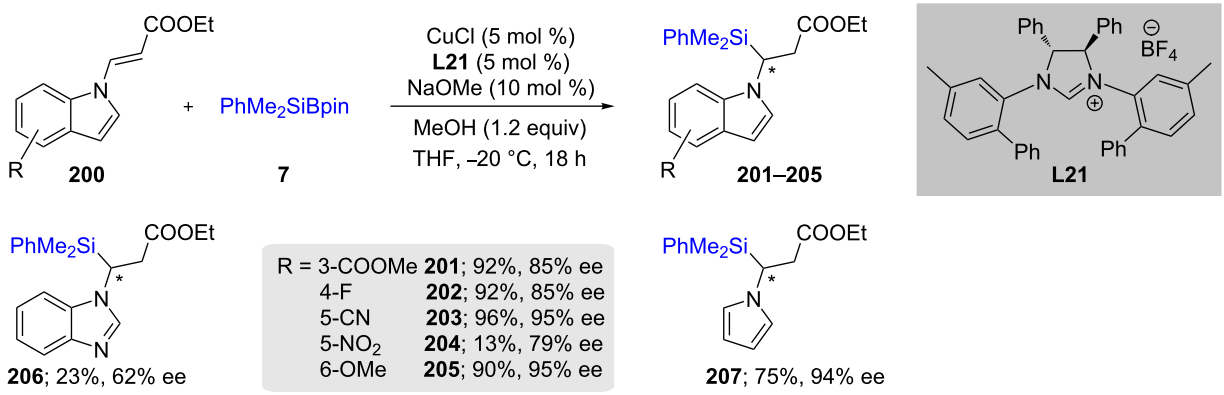

Scheme 35: Conversion of α,β-unsaturated carbonyl indoles to α-silylated *N*-alkylated indoles.

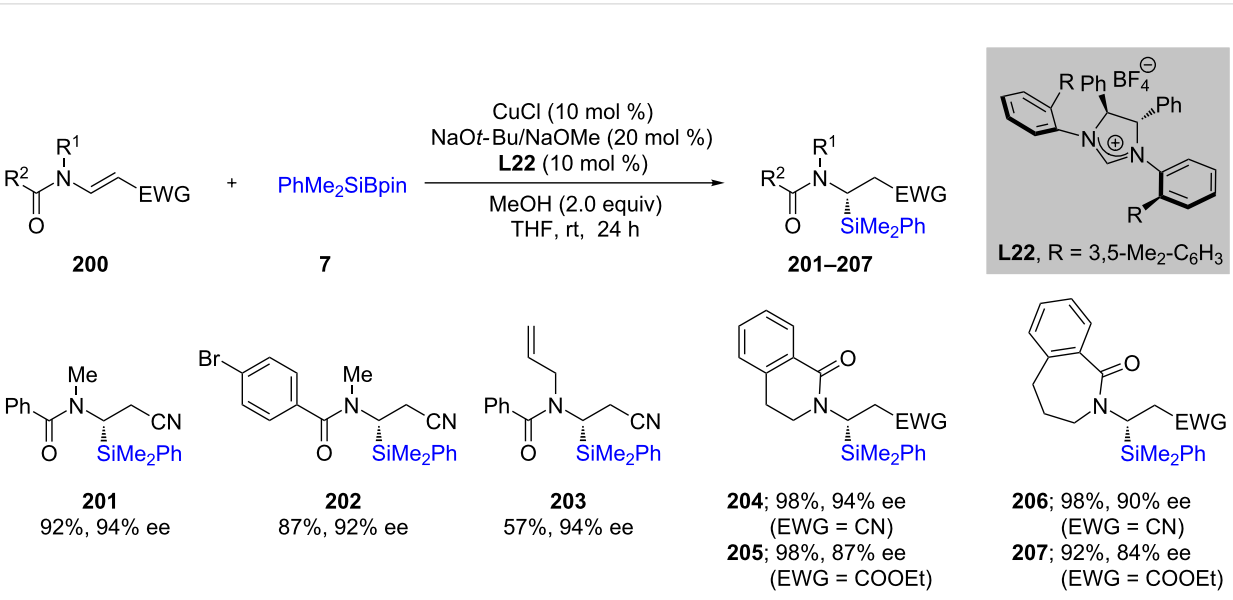

Scheme 36: Conversion of β-amidoacrylates to α-aminosilanes.

1,4-manner to unsaturated nitro and cyano derivatives leading to adducts **209**–**218**, each being obtained in high chemical yield and good enantioselectivity (Scheme 37).

1.5 Miscellaneous reactions

The Tsuji group developed a mild method for the regio-divergent silacarboxylation of allenes **219**. Based on the type of ligands used (e.g., Me-DuPhos; **L24** vs. Cy_3P), either vinyl (**220**–**223**) or allylic (**224**–**228**) silanes could be obtained, respectively, in good yields. Different types of substrates were studied to give maximum selectivity for the desired product (Scheme 38). Also, for cases forming allylic silanes, only *Z*-isomers were obtained [75].

In furthering Zhou's initial report [76], Ollevier and co-workers [77] recently described carbene insertions, starting with **229**, into Si–H bonds, leading to a wide variety of silylated products [18]. The original work by Zhou included asymmetric carbenoid insertions using *spiro*-bisimine ligand **L25** at cryogenic temperatures (Scheme 39A). Ollevier, however, focused on making these reactions more general under ligand-free conditions at ambient temperature, and without the asymmetric component (Scheme 39B). The substrate scope was already broad, including both diazoesters and diazoketones as carbene precursors.

After the impressive report from Dow Corning on the hydrosilylation of alkenes in 2013 [78], recently, the Buchwald group extended this chemistry to the asymmetric hydrosilylation of alkenes [79]. They used nonracemic ligand (*S,S*)-Ph-BPE (**L26**) in combination with catalytic amounts of $Cu(OAc)_2$ and stoichiometric Ph_2SiH_2 at ambient temperature to convert various alkenes to the desired enantiomerically pure silylated products (Scheme 40).

A highly regio- and enantioselective dearomative silyation of indoles using NHC **L27**–ligated CuCl has been disclosed recently [80]. A variety of 3-acylindoles **245** were converted to the desired indolino-silane products **246**–**250** in mostly moderate to good yields with very good enantioselectivities (Scheme 41). A mechanistic investigation revealed the importance of the acyl group at the 3-position. Systematic kinetic studies using NMR experiments suggested that protonation of the intermediate **252** occurs from the sterically favored side,

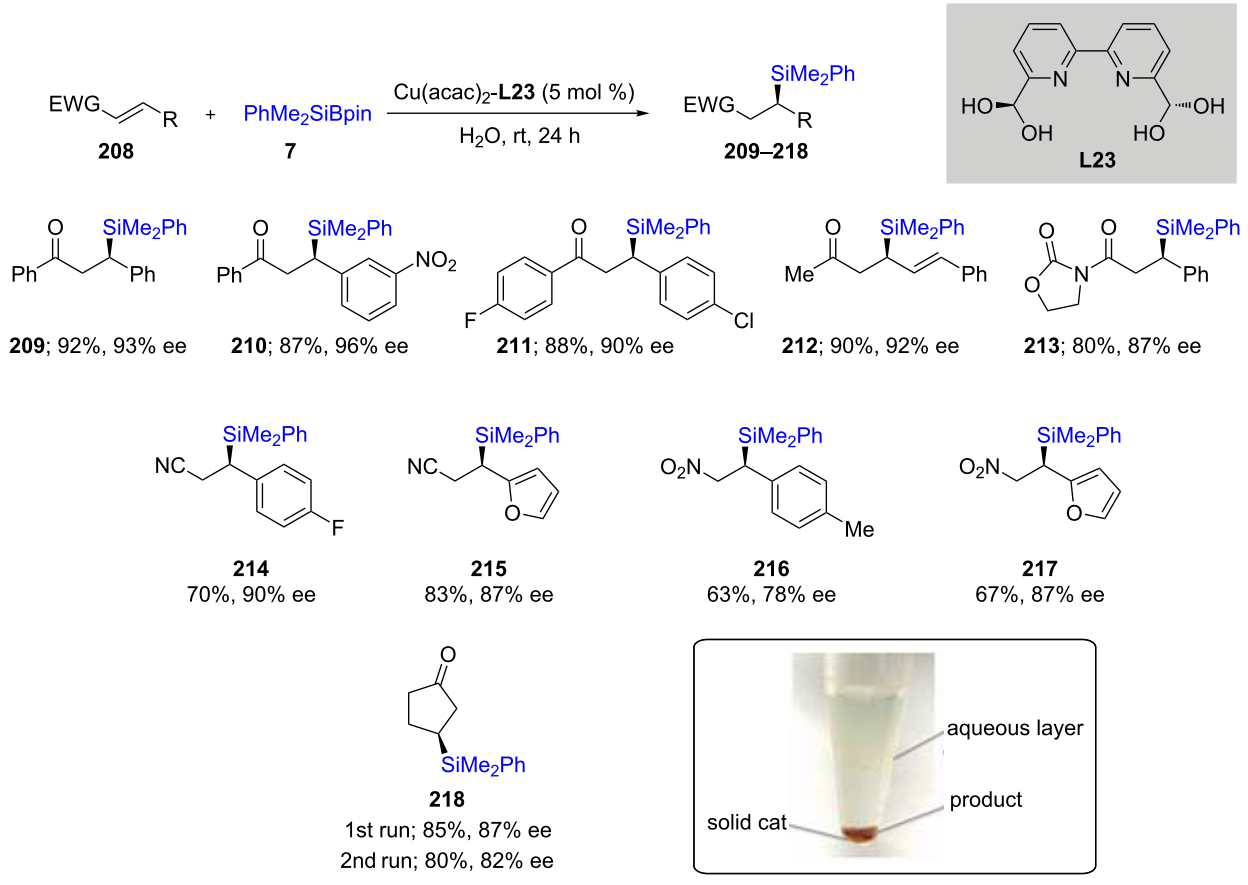

Scheme 37: Conversion of α,β-unsaturated ketones to enantioenriched β-silylated ketones, nitriles, and nitro derivatives in water.

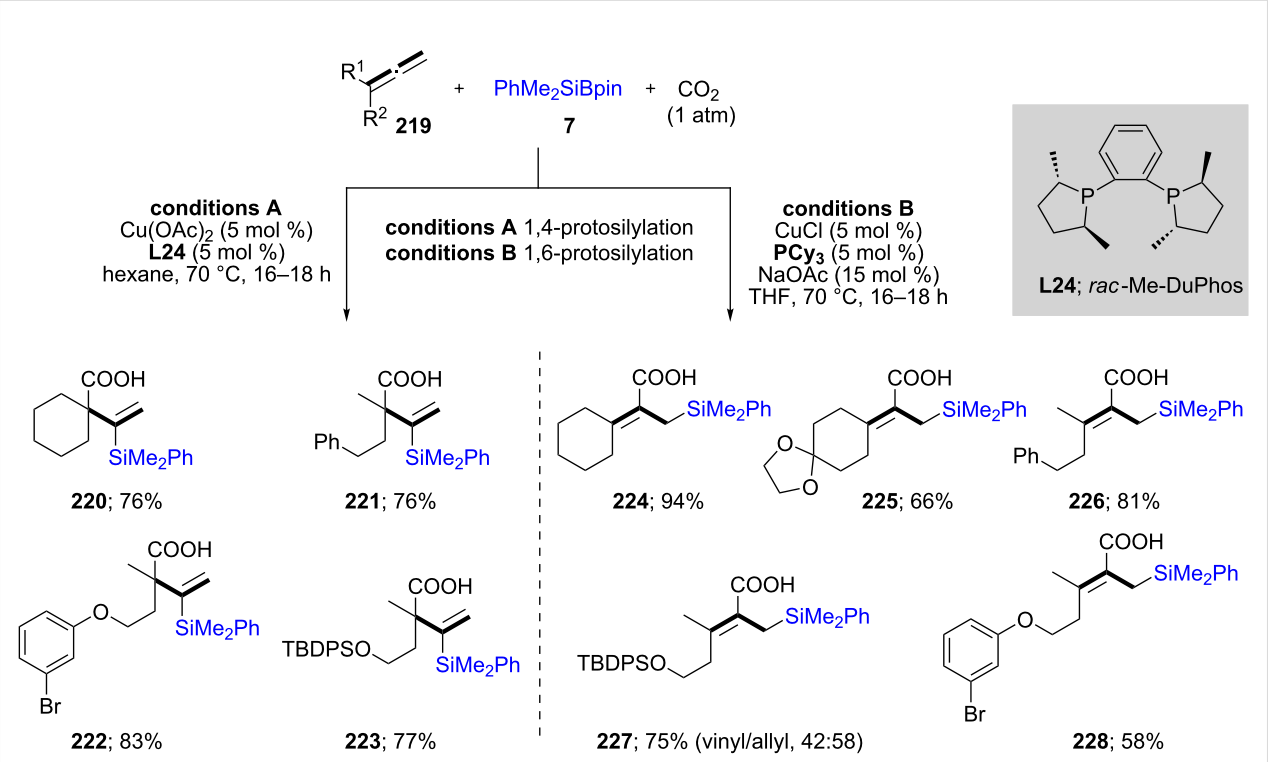

Scheme 38: Regio-divergent silacarboxylation of allenes.

leading to the kinetically stable *cis* product (Scheme 42). Nonetheless, some epimerization under the reaction conditions took place leading to the thermodynamically more stable *trans* product, **246**.

The direct activation of C(sp^3)–H bonds attached to *N*-Cl tosylamines **253** was achieved via a radical pathway affording the products of silylation **254**–**258** in good chemical yields (Scheme 43) [81]. Most benzylic or benzylic-like positions are

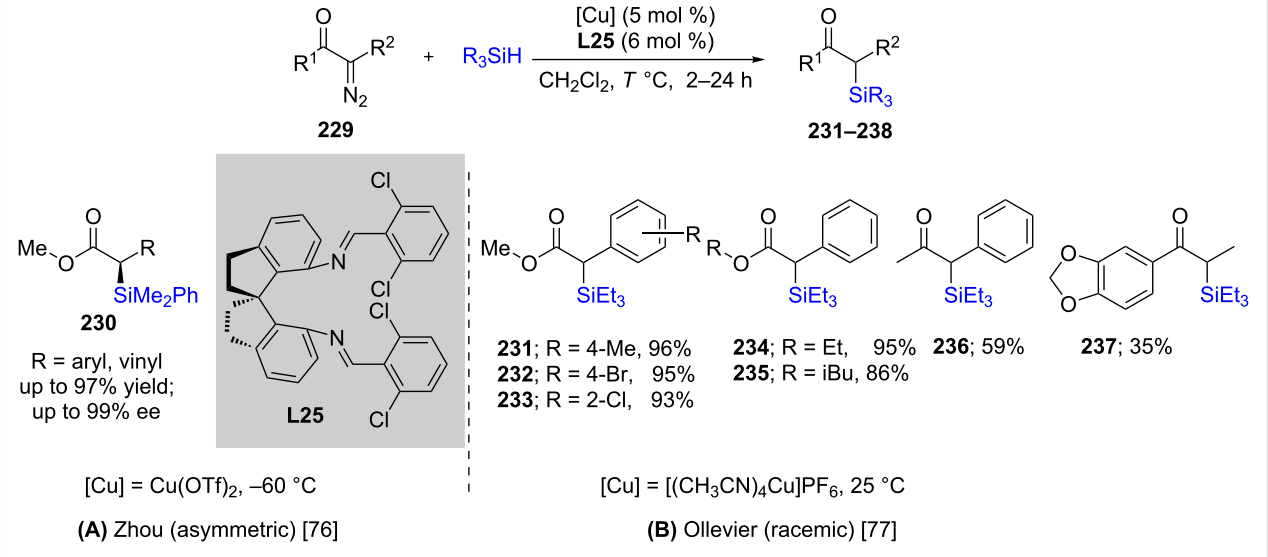

Scheme 39: Silylation of diazocarbonyl compounds, (A) asymmetric and (B) racemic.

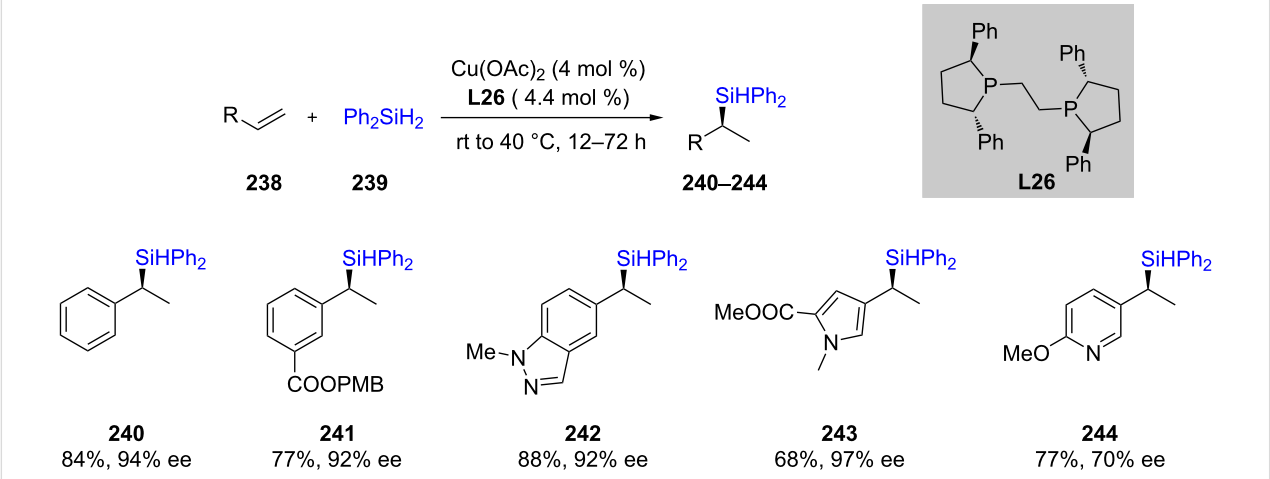

Scheme 40: Enantioselective hydrosilylation of alkenes.

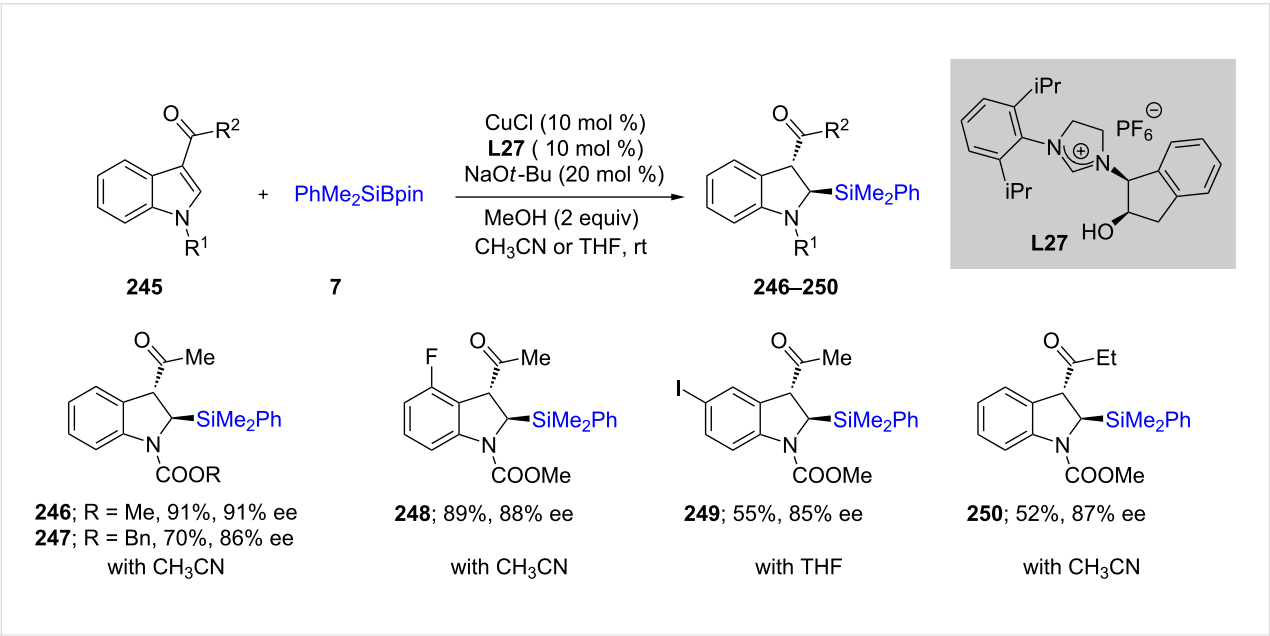

Scheme 41: Conversion of 3-acylindoles to indolino-silanes.

sufficiently activated to give tertiary carbon centers-bearing silicon products, although educts with initial tri-substitution led to lower isolated yields (e.g., **258**).

An unusual type of reaction has been described in which an acyl silane reacts with 1,3-dienes, under Cu catalysis, leading to an interesting class of α-silyl tertiary alcohols (Scheme 44) [82]. In most cases, high chemical yields along with high ees were obtained when phosphoramidite ligand **L28** was used. A wide variety of compounds was prepared, including one with a bisquarternary center (**267**), although the Bpin residue within it could not be oxidized to the desired alcohol due to decomposition. Nonetheless, several products could be transformed into molecules of greater complexity. For example, cyclopropanation could be achieved to give **269**. Additionally, TBS protection of **268** followed by ring closing metathesis (RCM) led to the interesting 6-membered silacycle **270**.

This same research group recently reported on the addition of silyl Grignard reagents to aziridines under copper catalysis [83].

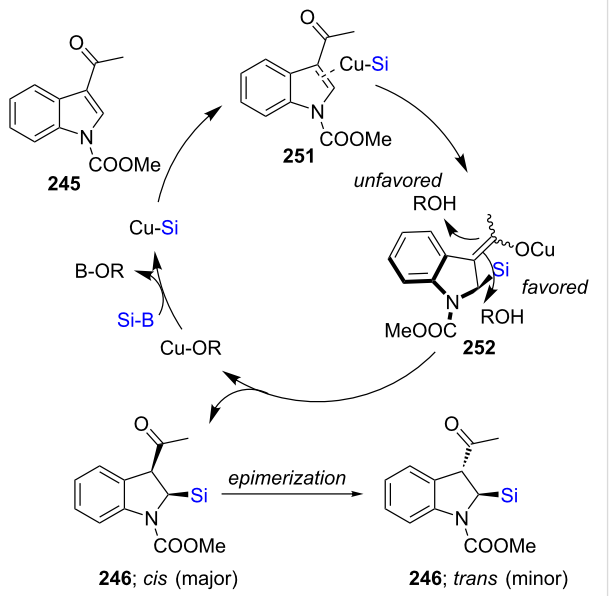

Scheme 42: Proposed mechanism for the silylation of 3-acylindoles.

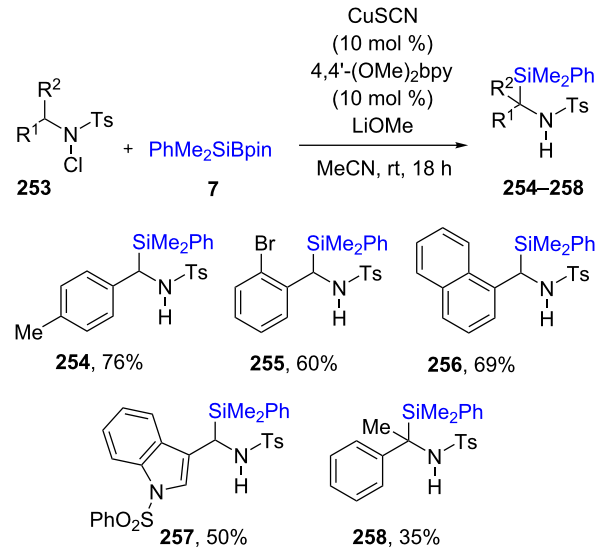

Scheme 43: Silyation of *N*-chlorosulfonamides.

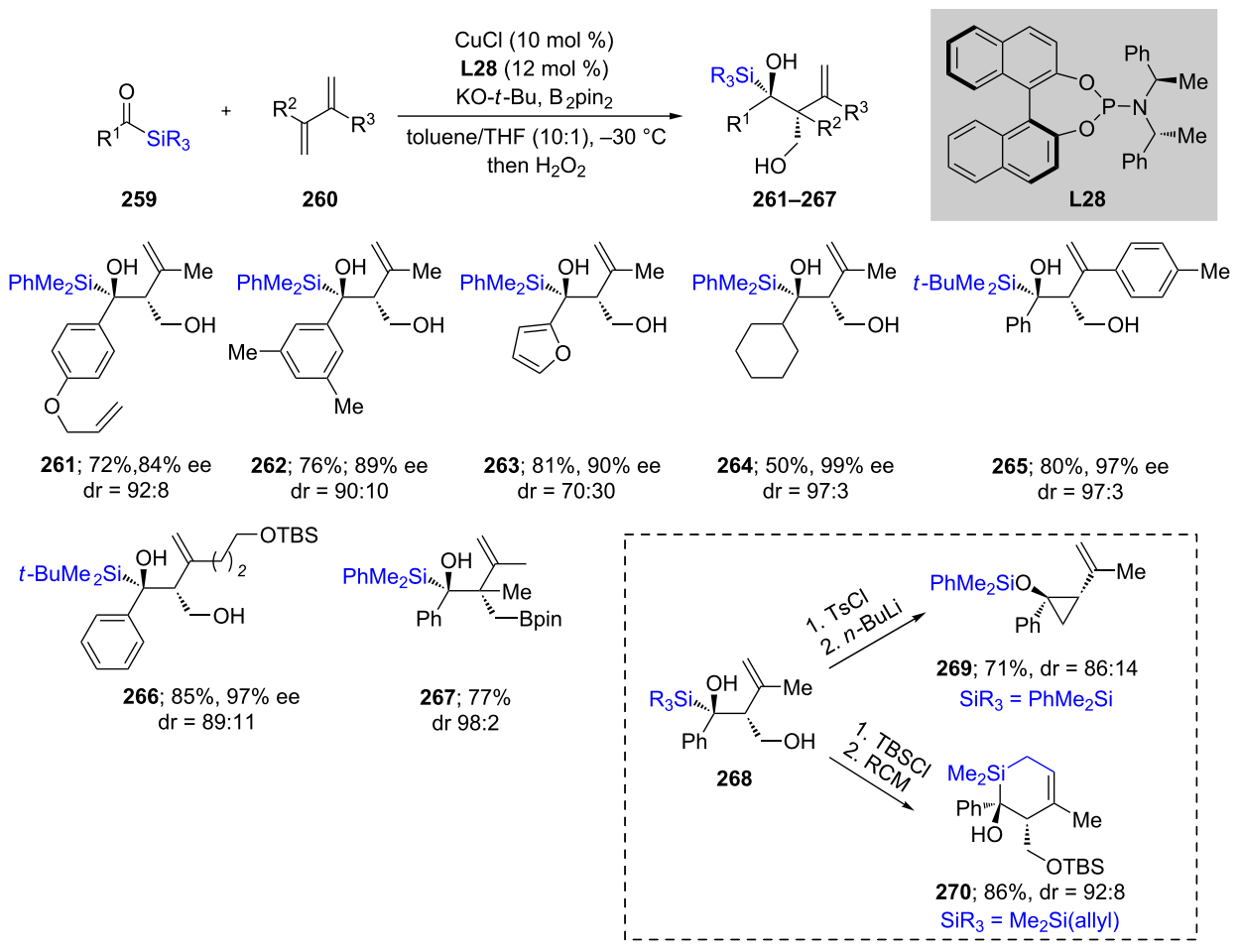

Scheme 44: Conversion of acyl silanes to α-silyl alcohols.

While the use of RMgX led to high chemical yields of the desired products, the corresponding catalytic Cu/zinc reagents gave poor yields (ca. 20%; Scheme 45). A library of aminosilane derivatives was prepared using this strategy to result in branched silyl compounds **272**–**276**. The addition of Grignard-derived copper reagents was stereospecific, where *cis*-aziridines gave *trans* products (e.g., **274**), and vice versa (e.g., **275**). The important aspect shown here is the utility of Suginome's reagent along with LiCl, which completely overrode the need for a Grignard reagent and led to good chemical yields of the desired product (e.g., **272**). In one case examined, a bulky silyl Grignard reagent gave the linear silyl derivative selectively. In addition, a quaternary carbon bearing the $PhMe_2Si$ group could also be prepared in moderate yield (**276**).

The regiocontrolled ring opening reactions of the same aryl-substituted aziridines **277** have also been shown by Minakata and Takeda et al. to be susceptible to dual Pd/Cu catalysis. Depending upon the ligand on each metal, either the 2 or 3-position on the ring could be accessed. A dual catalytic cycle was proposed, where the Cu–Si species formed in situ undergoes transmetallation to the Pd(II) species resulting from the attack of Pd(0) on the aziridine ring, ultimately affording the silylated product with silicon at the benzylic site (Scheme 46). The product featuring the $PhMe_2Si$ residue at the β-location **287**, however, arises by way of a 1,2-addition to an imine, formed from the same Pd(II) intermediate via elimination [84].

Oestrich and co-workers have recently demonstrated non-directed, asymmetric *syn*-addition-silylations of 3,3-disubstituted cyclopropenes **288** using a Cu(I) pre-catalyst and (*R*)-DM-Segphos (**L29**) that take place with high enantio- and diastereoselectivities. They also studied the effect of geminal carbon substituents and found that as the bulk increases, both yields

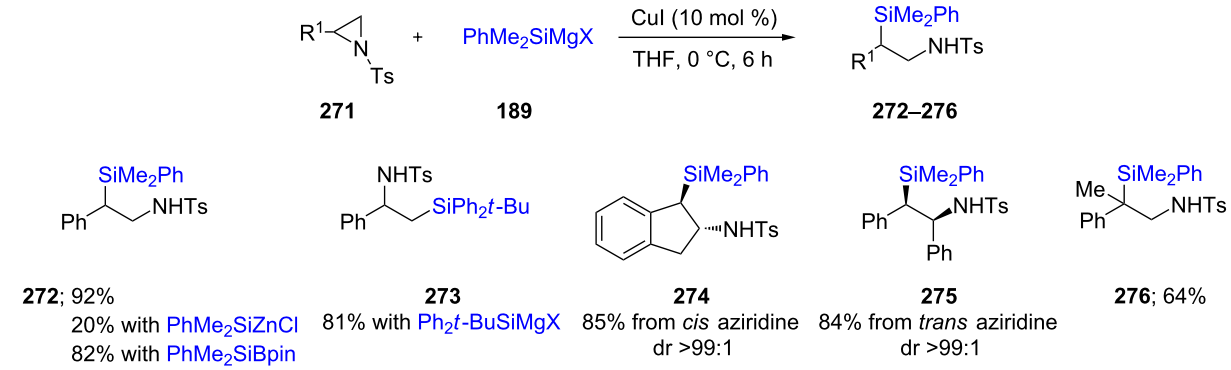

Scheme 45: Conversion of *N*-tosylaziridines to β-silylated *N*-tosylamines.

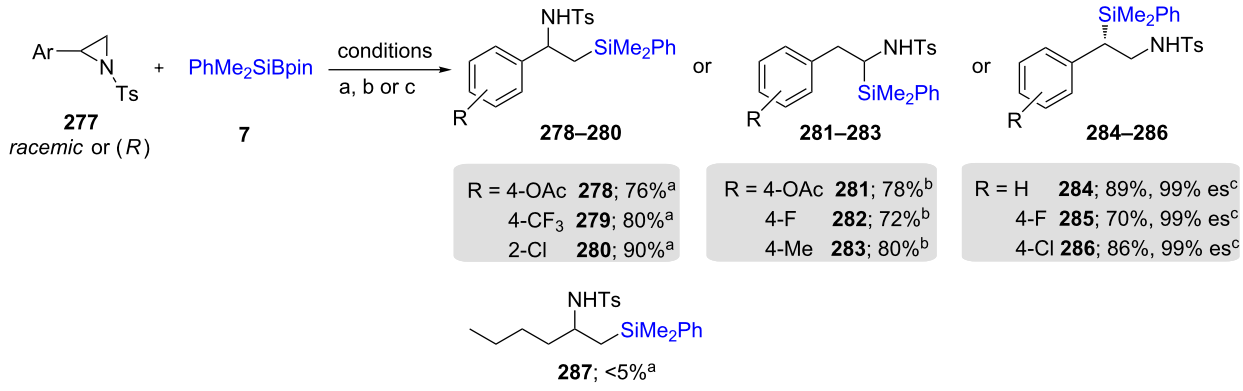

conditions a: $CuSO_4$ (4 mol %), bpy (10 mol %, Cp(allyl)Pd (4 mol %), P-*t*-Bu_2Me, CPME/MeOH (1 mL, *v*/*v* 9:1), 40 °C, 3 h
b: SIPr-Pd-PPh_3 (2 mol %), CuF_2 (4 mol %), bpy (10 mol %), PPh_3 (4 mol %), toluene/MeOH (1 mL, *v*/*v* 9:1), 50 °C, 4 h
c: SIPr-Pd-PPh_3 (2 mol %), CuF_2 (4 mol %), phen (10 mol %), CPME/MeOH (2.5 mL, *v*/*v* 9:1), 50 °C, 12 h
es = enantioselectivity

Scheme 46: Conversion of *N*-tosylaziridines to silylated *N*-tosylamines.

and diastereoselectivities decrease, while enantioselectivities remain unaffected. In addition to the impact of steric effects, variations in the alkyl-substituted silicon reagents also negatively impacted the chemical yields. However, again, there was no effect on enantioselectivity. Interestingly, upon replacement of the alkyl groups on the silicon by three phenyl rings **294** there was no conversion, highlighting the influence of the alkyl groups on silicon (Scheme 47) [85].

Xu and co-workers have described a simultaneous double silylation on conjugated enynes **297**, where either racemic or enantiomerically enriched 1,3-bis(silyl)propenes are formed in good yields (Scheme 48). They proposed a mechanism in which LCu(I)–Si coordinates first with the triple bond, which eventually forms a monosilylated diene. The resulting organocopper species then participates in a second catalytic cycle to furnish the disilylated products [86].

2 Cu-catalyzed carbon–boron bond formation

Organoboron compounds are widely used in C–C and C–X (X = N, O) bond constructions. Straightforward methods for their synthesis involve the copper-catalyzed addition of organoboron compounds to alkynes, alkenes, and unsaturated carbonyl compounds, as well as the nucleophilic borylation of alkyl or aryl halides. While there are reports on the formation of C–B bonds in the presence of NHC complexes [87] with Au [88], Pd [89], Pt [90], and Ir [91] catalysts, the focus here is on Cu-catalyzed reactions. Enantioselective processes have also been studied due to applications of medicinal interest involving optically active organoboron derivatives and their intermediacy as precursors to other functional groups, such as nonracemic alcohols. Achiral substrates in the presence of well-defined chiral copper complexes deliver chiral products, while nonracemic substrates can also react with achiral copper for similar purposes.

In general, the pathway for introducing boron into unsaturated compounds (C–B coupling) mediated by a copper catalyst relies on the reaction of a Cu(I) salt with an alkoxide (M–OR) which then undergoes transmetallation with an organoborane to form, e.g., L-Cu-Bpin (**306**). This species serves as an active catalyst, nucleophilic at boron, via coordination with an alkene (**307**) which undergoes insertion to deliver the B–C bonded species via an intermediate that either undergoes elimination or reacts with an electrophile to form the product (e.g., **308**, **309**, Scheme 49) [92].

2.1 Formation and reactions of allylic C–B bonds

The synthesis of α-stereogenic allylboronates was reported by Ito in 2005 using CuO-*t*-Bu/Xantphos (CuCl and KO-*t*-Bu form CuO-*t*-Bu in situ as the active catalyst precursor), an enantioenriched allyl carbonate, and B_2pin_2 (**310**; Scheme 50) [93].

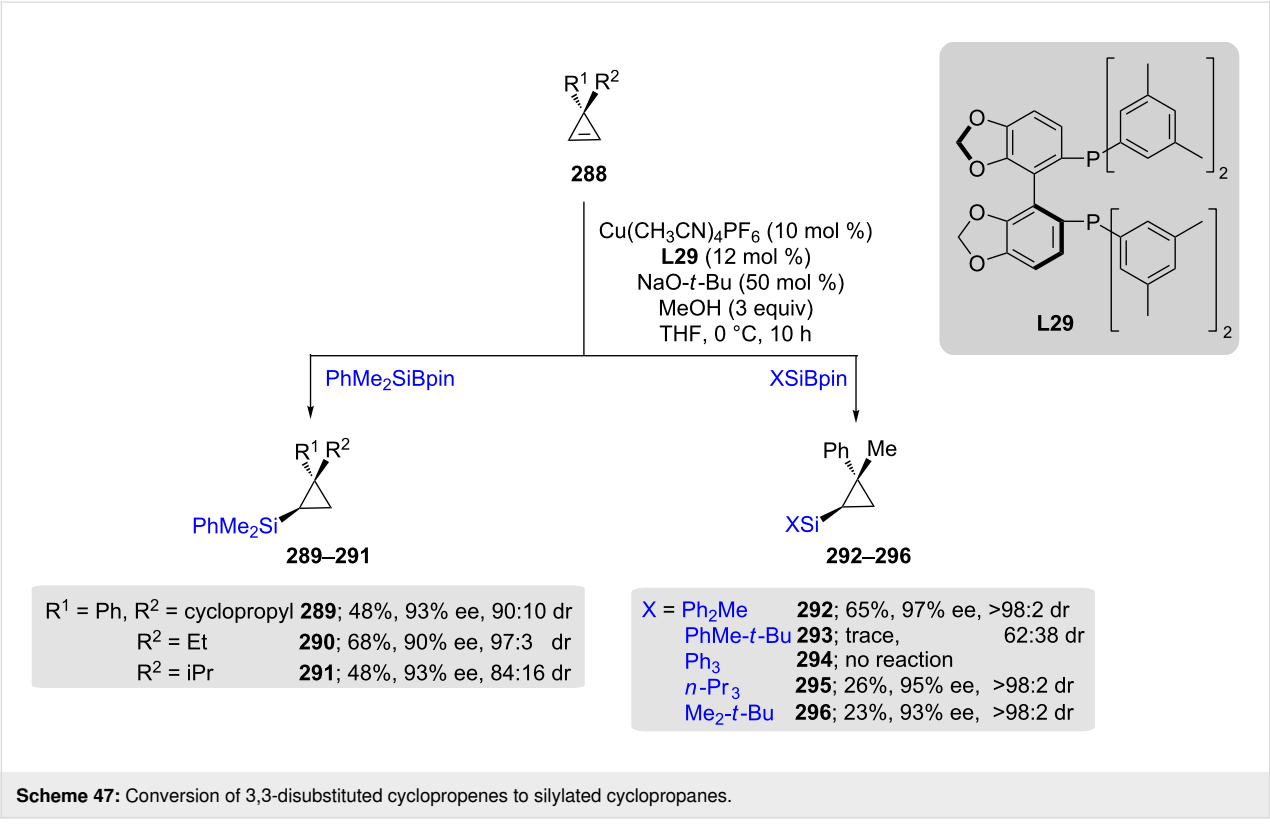

Scheme 47: Conversion of 3,3-disubstituted cyclopropenes to silylated cyclopropanes.

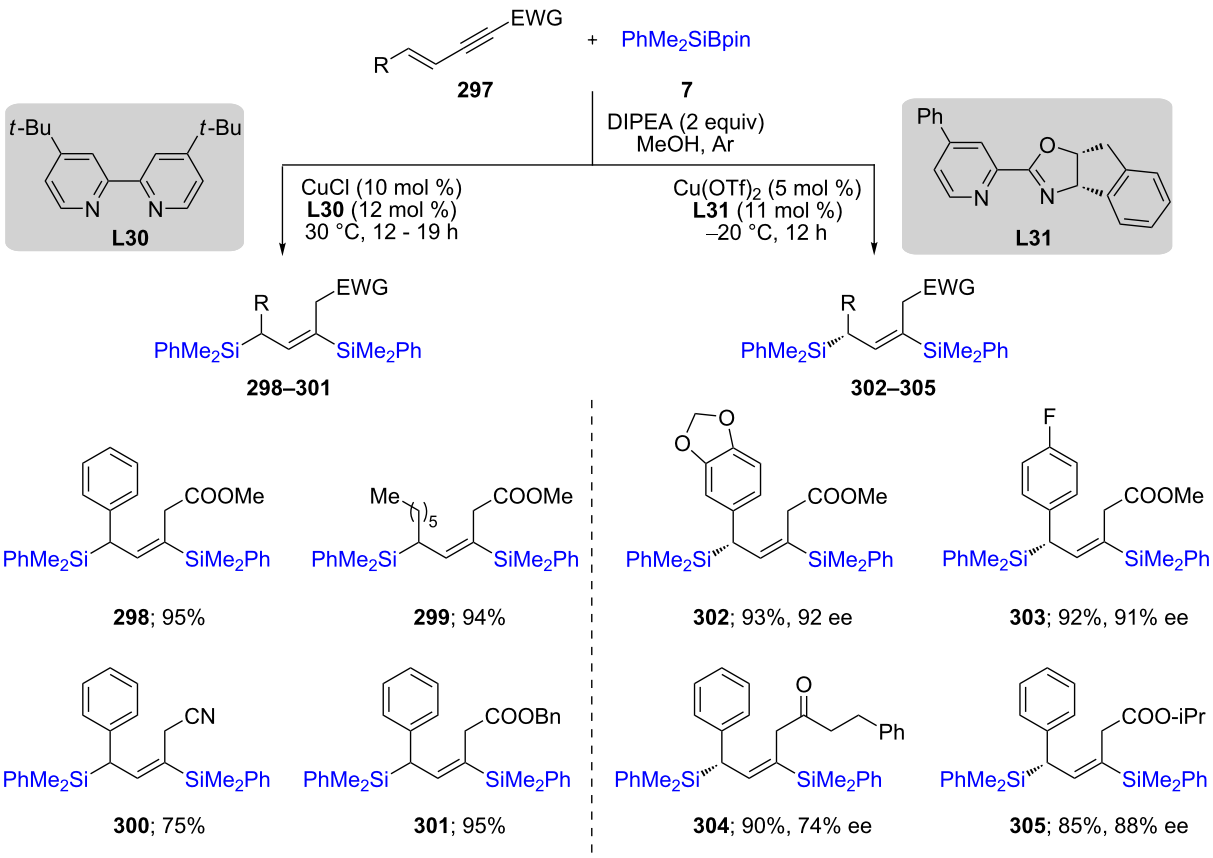

Scheme 48: Conversion of conjugated enynes to 1,3-bis(silyl)propenes.

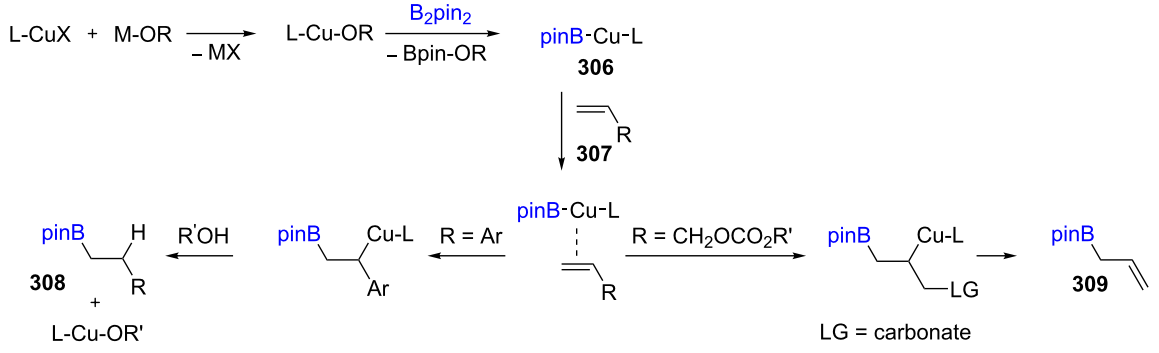

Scheme 49: Proposed sequence for the Cu-catalyzed borylation of substituted alkenes.

Both (*Z*)- and (*E*)-alkenes **311** afforded the (*E*)-alkene **312** as the major product. The targeted γ-borylated compounds (relative to the leaving group) were formed, each with high enantioselectivity, which can be used for further stereoselective C–C and C–X (X = heteroatom) bond formation.

Catalytic Cu(NHC)-mediated formations of enantioenriched α-substituted allylic boronates take place in high yields and site-selectivity (>98% S_N2') starting with either *trans*- or *cis*-disubstituted alkenes **313**, as well as linear or branched alkyl and aryl trisubstituted allylic carbonates **314**. The further oxidation of the boronated products (e.g., **316**) yielded nonracemic secondary (e.g., **317**) and tertiary alcohols (e.g., **319**). The presence of $Cu(OTf)_2$, an imidazolium salt, and NaOMe leads to a chiral NHC–Cu complex, which, in the presence of B_2pin_2, generates the corresponding B–Cu species followed by its addition to

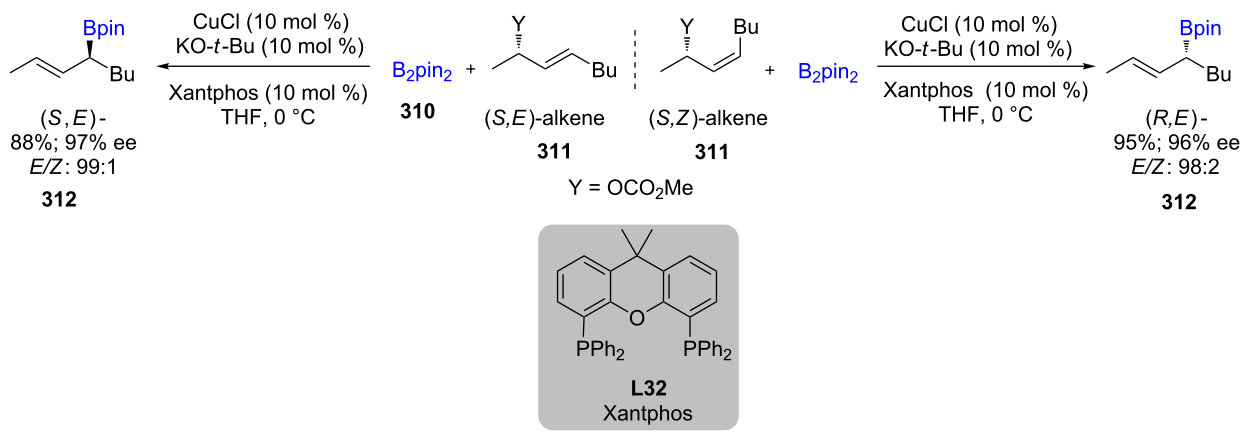

Scheme 50: Cu-catalyzed synthesis of nonracemic allylic boronates.

allylic carbonates to deliver the targeted products (Scheme 51) [94].

In addition to allylic carbonates, allylic acetals (**319**) were also used for C–B bond formation that, in the presence of CuCl/(*R,R*)-BenzP* and stoichiometric amounts of KO-*t*-Bu, provide access to α-chiral linear or carbocyclic (γ-alkoxy-allylic)boronates **320**–**322**. High functional group tolerance and enantioselectivities are characteristics of this reaction. The stereoselective formation of a 3,3-disubstituted cyclopentene scaffold (e.g., **331**), containing three contiguous asymmetric centers, was also developed starting from an achiral cyclic acetal **327**. In addition, the formation of an *anti*-1,2-diol with high enantioselectivity is also another outcome resulting from this protocol (Scheme 52) [95].

Catalytic Cu-mediated conversions of (*Z*)-3-arylallylic phosphates **332** to nonracemic *trans*-2-aryl and -heteroaryl-substituted cyclopropylboronates **333** have been reported to take place in high yields, along with high diastereo- and enantioselectivities. Applications of optimized ligands, such as (*R,R*)-QuinoxP* and (*R,R*)-iPr-DuPhos, for borylation of

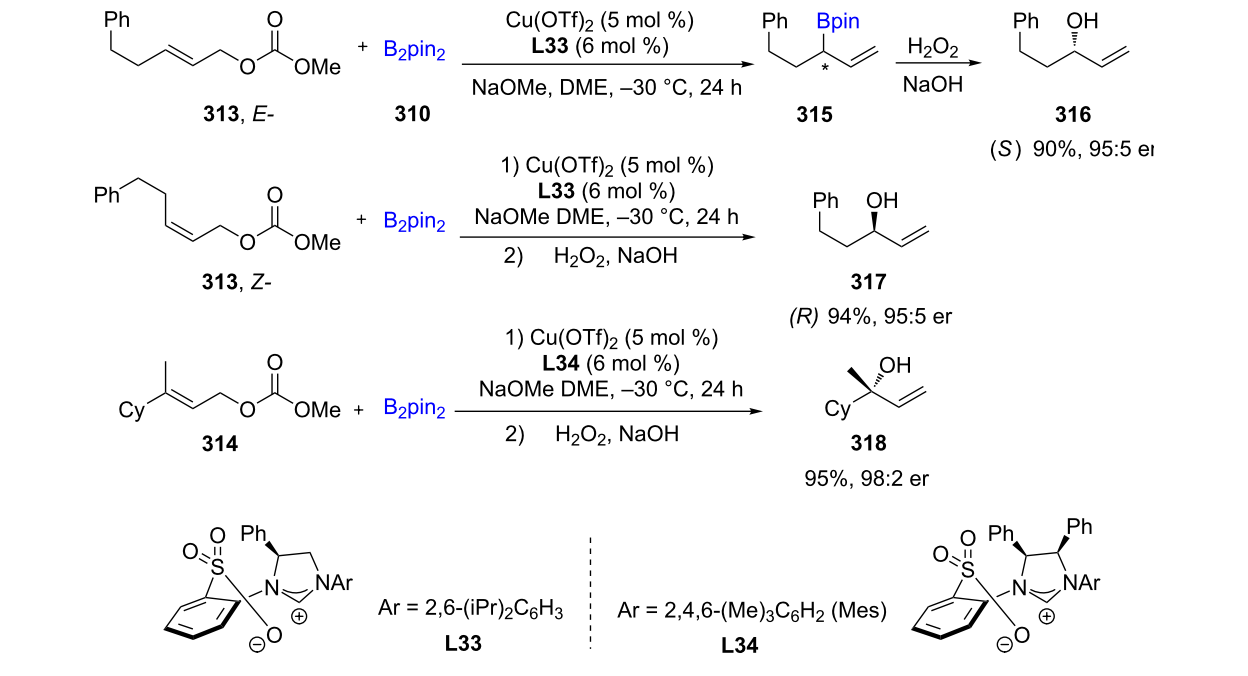

Scheme 51: Cu–NHC catalyzed synthesis of α-substituted allylboronates.

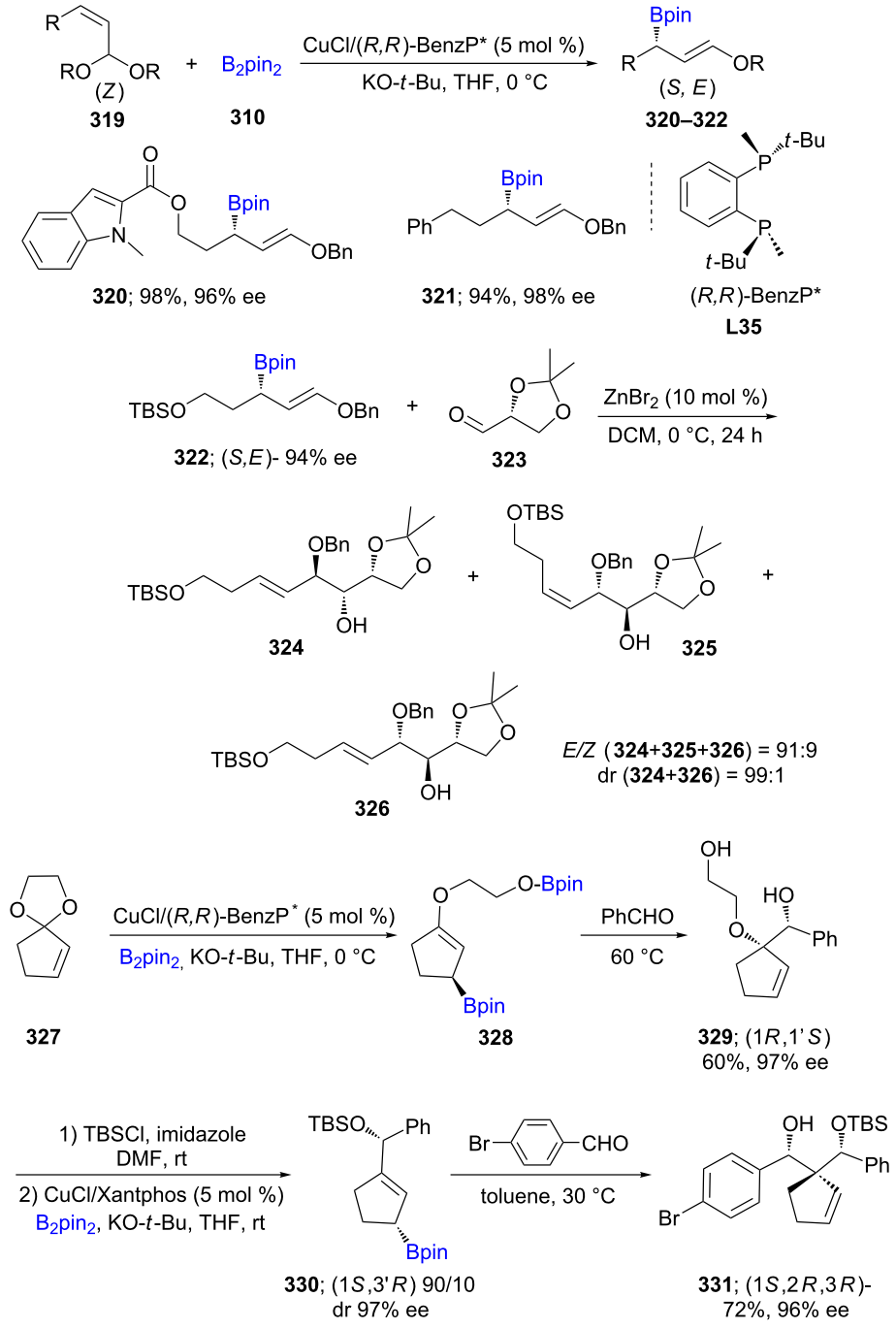

Scheme 52: Synthesis of α-chiral (γ-alkoxyallyl)boronates.

(*E*)-allylic phosphates **334** delivers either the *trans* or *cis*-configuration of these cyclopropyl moieties (**335**; Scheme 53) [96].

The first Cu(I)-catalyzed allylic displacement on alkenes containing a CF_3 group was reported in 2018. Enantioenriched γ,γ-*gem*-difluoroallylic boronates **339**–**341** can be obtained via this process. Once the obtained difluoromethylene scaffolds are formed, they are readily converted to optically active secondary alcohols (e.g., **342**, Scheme 54) [97].

2.2 Regioselective borylation of alkynes, alkenes, and allenes

Cu-catalyzed borylation of C–C multiple bonds involves the formation of nucleophilic Cu–B species that coordinate with a π-system to initially transfer the boryl group. This step is then

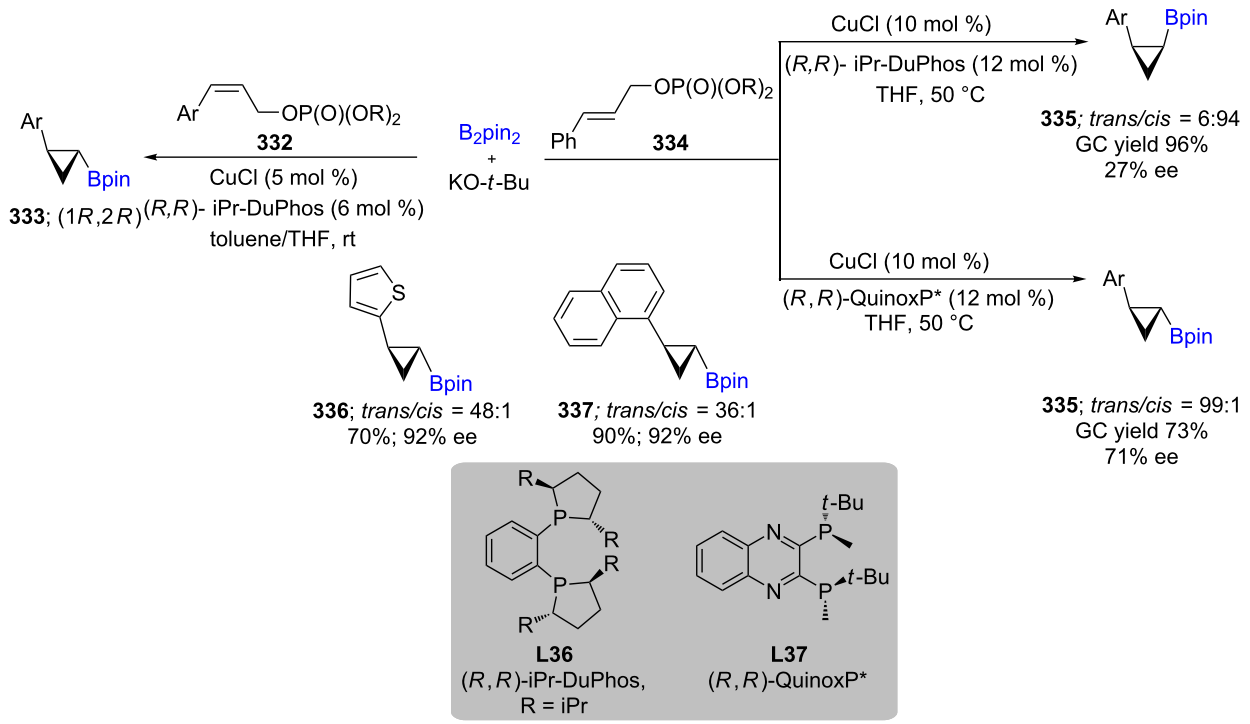

Scheme 53: Cu-mediated formation of nonracemic *cis*- or *trans*- 2-substituted cyclopropylboronates.

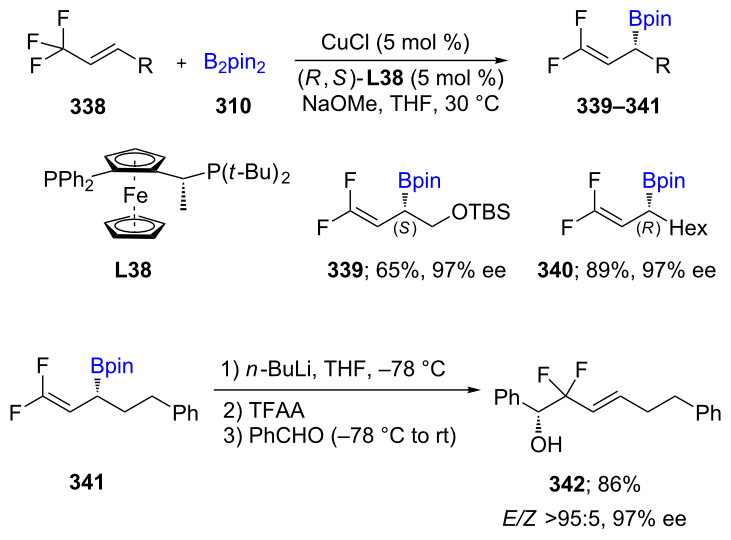

Scheme 54: Cu-catalyzed synthesis of γ,γ-*gem*-difluoroallylboronates.

followed by treatment of the reaction intermediate with an electrophile to deliver the desired borylated compound [98].

An efficient Cu-catalyzed (via in situ formed [(*R*)-DTBM-Segphos]CuH) protocol for an asymmetric net hydroboration of internal alkenes **343** with high regio- and enantioselectivity was reported by Hartwig et al. in 2016 [99]. The newly formed C–B bond reacted with a range of electrophiles to deliver products containing C–C, C–N, and C–X (X = Br, Cl) bonds (e.g., **349**, **350**). Efforts to explore the mechanism revealed a decrease in regioselectivity when the C=C bond is further from the directing group. This was attributed to the importance of both the negative charge at the carbon and the forming C–Cu bond being developed in the transition state, which is stabilized by

the positive charge on the carbon bearing the directing group. Later, in 2017, the same group investigated the details of the mechanism for the hydrofunctionalization of internal alkenes and vinyl arenes (Scheme 55) [100]. Unlike acyclic alkenes, Tortosa et al. utilized cyclobutenes as well as bicyclic cyclobutenes as educts using (*R*)-DM-Segphos for Cu-catalyzed enantioselective borylation, affording cyclobutyl boronates in high yields and with excellent stereocontrol [101]. This work followed on the heels of earlier studies on the borylation of 2,6-disubstituted *p*-quinone methides en route to enantioenriched mono- and dibenzylic boronates [102].

An efficient regio-divergent method starting from a single alkene **307** (e.g., protected allylic alcohols) was explored by varying the ligand on copper. Using catalytic CuCl/Xantphos, direct access to *anti*-Markovnikov alkylborated products (e.g., **353**, **354**) was noted. Alternatively, simply switching from Xantphos to Cy-Xantphos afforded the products of Markovnikov addition (e.g., **351**, **352**). It was shown that the presence of a heteroatom plays a crucial role due to the otherwise non-selective, facile addition of Cu-Bpin to alkenes (Scheme 56) [103]. Based on previous studies on asymmetric 3-component carboboration of styrene derivatives [104] and 1,3-dienes [105] with C(sp^2)-containing electrophiles such as *tert*-butyl allyl carbonate or aldimines using B_2pin_2, Liao et al. reported the same approach, albeit using more challenging C(sp^3) electrophiles (e.g., CH_3I) for the enantioselective methylboration. Both aliphatic alkenes and styrenes could be used with either CuCl/quinoxP* or their in-house-developed chiral sulfoxide phosphine ligand (SOP). Excellent diastereo- and enantioselectivities were obtained. A gram scale synthesis of (*S*)-naproxen was also described as a "real world" application [106].

From previous findings involving trapping of a vinylarene-derived benzylic copper species with an electrophilic source of a cyano residue, Yang and co-workers reported on the Cu-catalyzed borylation of styrenes bearing an allylic group at the

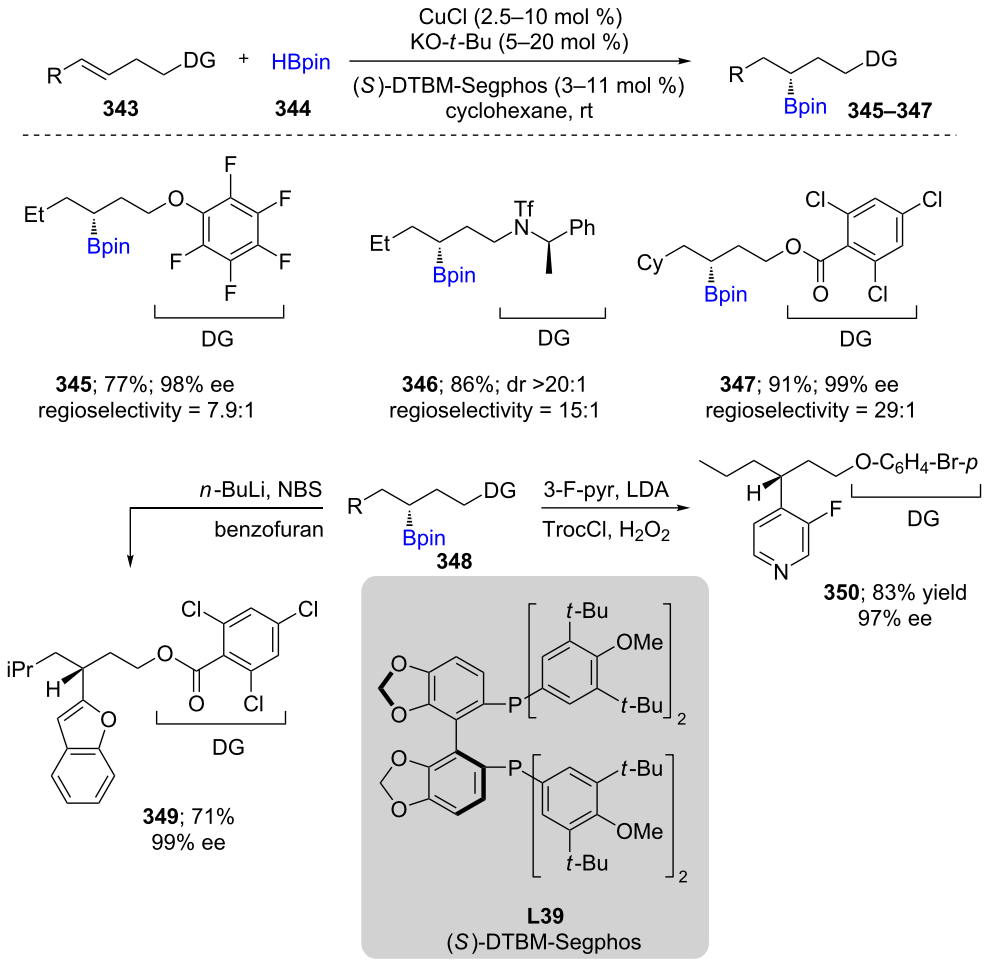

Scheme 55: Cu-catalyzed hydrofunctionalization of internal alkenes and vinylarenes.

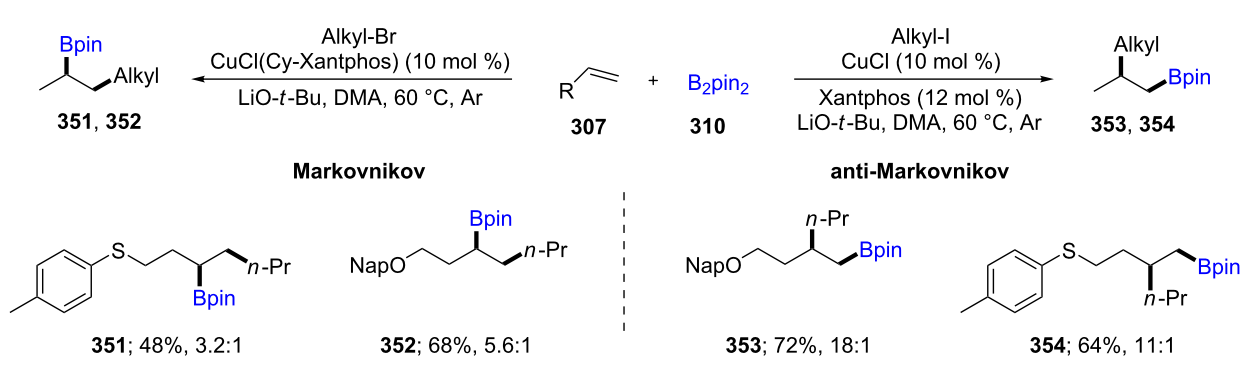

Scheme 56: Cu-catalyzed Markovnikov and *anti*-Markovnikov borylation of alkenes.

1-position. After the initial addition, a cascade of reactions occurred, including cyanation generating a dearomatized intermediate. This species then undergoes [3,3]-sigmatropic rearrangement, positioning the allylic unit in a regio- and stereospecific manner, along with rearomatization to afford the products **357**–**360** (Scheme 57) [107].

The borylfluoromethylation of acrylamides, acrylates, and heteroaromatic-substituted alkenes (**307**) was established using CuBr/JohnPhos/LiO-*t*-Bu and CuCl/IMes/NaO-*t*-Bu, respectively, in the presence of I-CH_2F (**361**) as the methylfluorinating agent, affording products reflecting excellent control of regioselectivity. This transformation is useful for the synthesis, e.g., of monofluorinated ibuprofen, through sequential oxidation of the product with $NaBO_3{\cdot}4H_2O$ and Jones reagent. The catalytic cycle includes formation of (L)Cu-O-*t*-Bu (**366**) which then reacts with B_2R_2 (**310**, B_2mpd_2) to form (L)Cu–BR (**367**). The reaction of this species with the olefin **307** afforded a borylcuprated intermediate **368**, which upon reaction with I-CH_2F leads to the borylfluoromethylated product (e.g., **362**–**365**, Scheme 58) [108].

Yin and co-workers described Cu(I)-catalyzed asymmetric additions to challenging trifluoromethyl and perfluoroalkyl ketones **370**, starting with 1,3-enynes **369** and a slight excess of B_2pin_2 in THF at room temperature. The initial homopropargylic borane adduct, upon oxidation with $NaBO_3{\cdot}H_2O$, yields the desired nonracemic tertiary alcohols **371**–**373** in typically high chemical yields, good diastereoselectivities, and impressive enantioselectivities. The subsequent treatment of these newly formed adducts (e.g., **373** to form products, **374** and **375**; Scheme 59) highlights the utility of this methodology [109].

Following Hoveyda's report on enantioselective Cu-catalyzed conjugate additions of borylated butadiene, generated in situ, to enolates [110], Procter et al. described the regio-divergent conversion of 2-substituted 1,3-dienes **376** into borocyano products using commercially available phosphine ligands

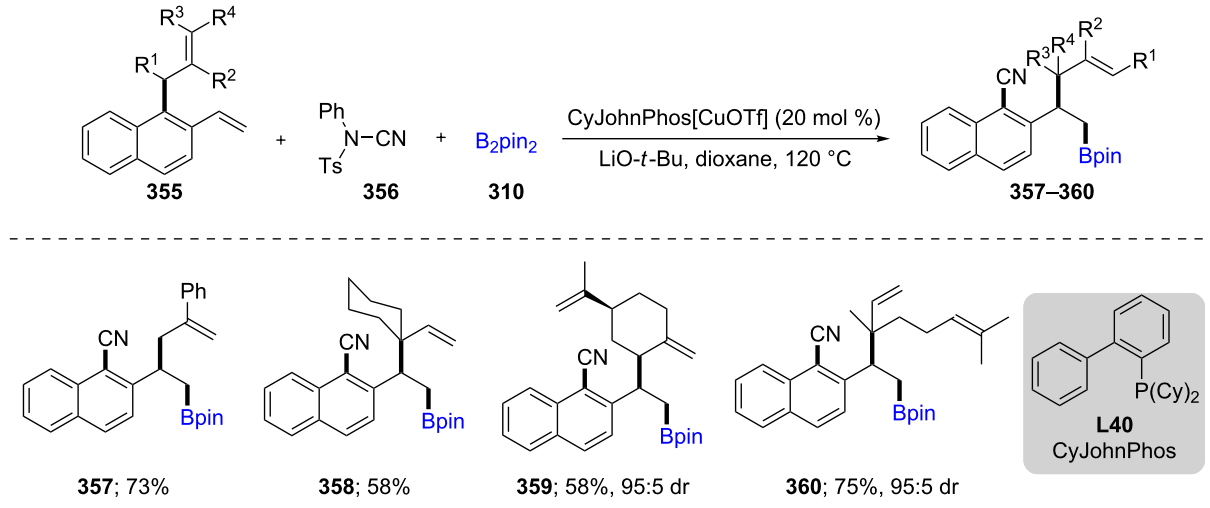

Scheme 57: Cu-catalyzed borylation/ortho-cyanation/Cope rearrangement.

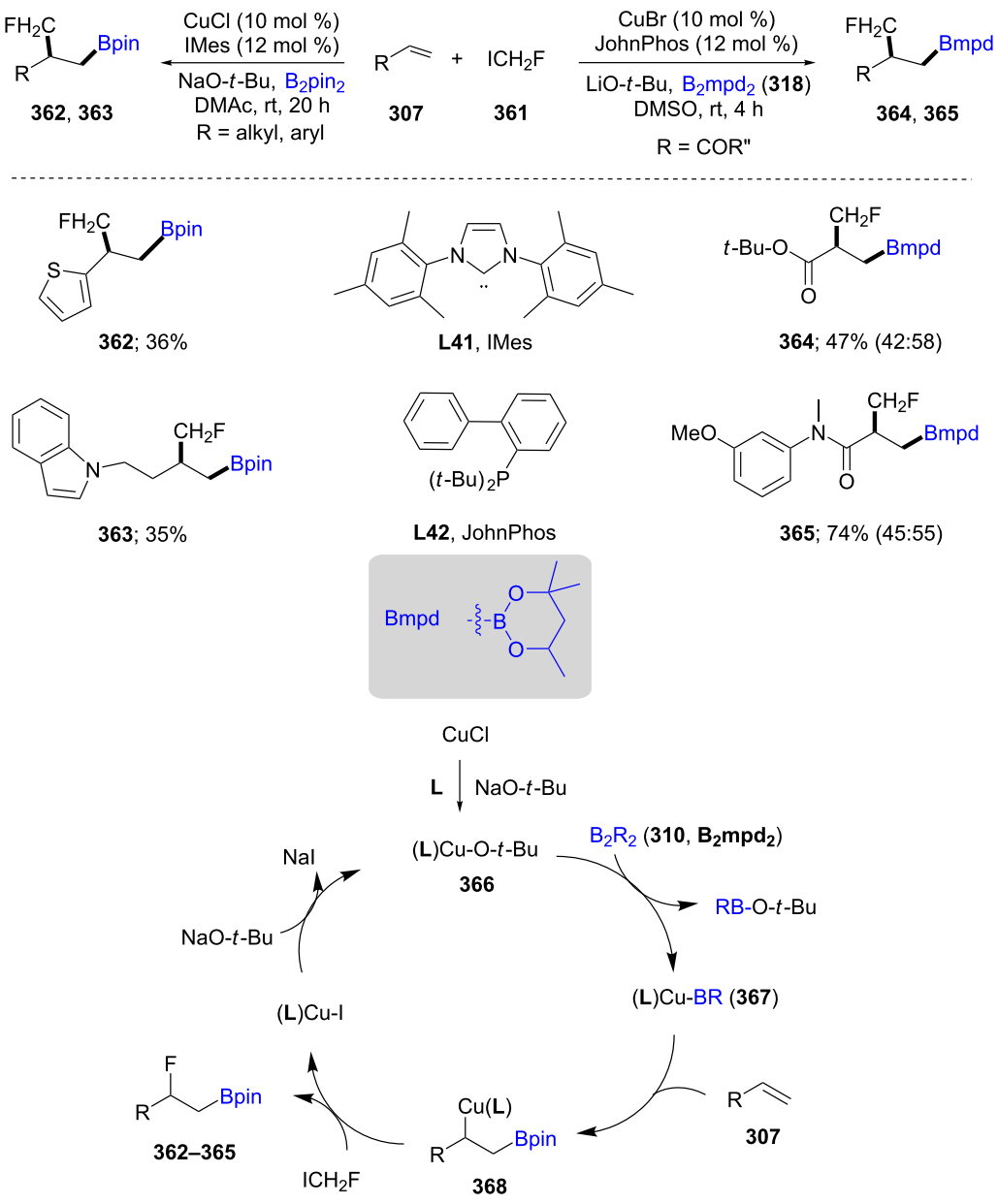

Scheme 58: Borylfluoromethylation of alkenes.

(Scheme 60). Simply switching from a mono to a bidentate ligand resulted in 1,4 to 4,1-borocupration. The formation of allyl–Cu intermediates in the catalytic cycle readily trap available electrophiles, such as *N*-cyanosulfonamides, leading to 1,2 or 4,3-borocyanation in a regiospecific fashion from borocuprative intermediates, respectively [111].

Extending earlier efforts from the Montgomery group for Cu-catalyzed cascade diborylation/ortho-cyanations of terminal allenes [112] and styrene derivatives [113], the cyanoborylation of terminal allenes **382** has also been studied. Using B_2pin_2 in the presence of *N*-cyano-*N*-phenyl-*p*-toluenesulfonamide (NCTs, **377**), under Cu-catalysis led to regio-, chemo-, and diastereoselective trifunctionalized products **383**–**386**. The reaction sequence involves three steps: first, borocupration followed by an electrophilic cyanation, and finally, a second borocupration. It was discovered that steric factors determine the site of the first borocupration, while electronic effects are dominant in the second addition of boron (Scheme 61) [114].

The selective arylborylation of α-alkylstyrenes **387** has been investigated, delivering 1,1-adducts **389**, **390** in the presence of

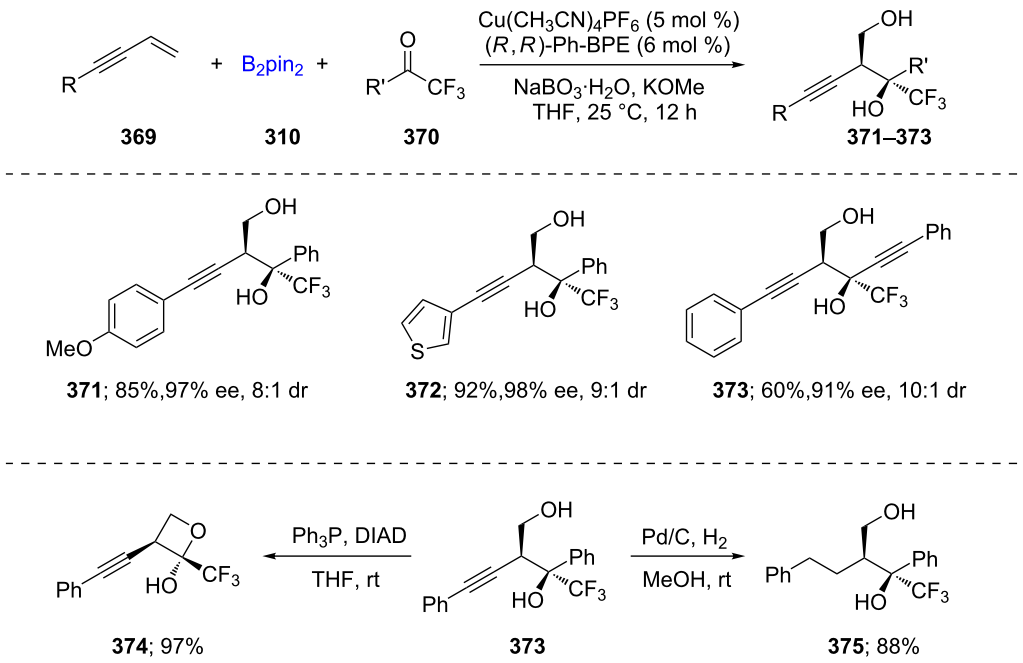

Scheme 59: Cu-catalyzed synthesis of tertiary nonracemic alcohols.

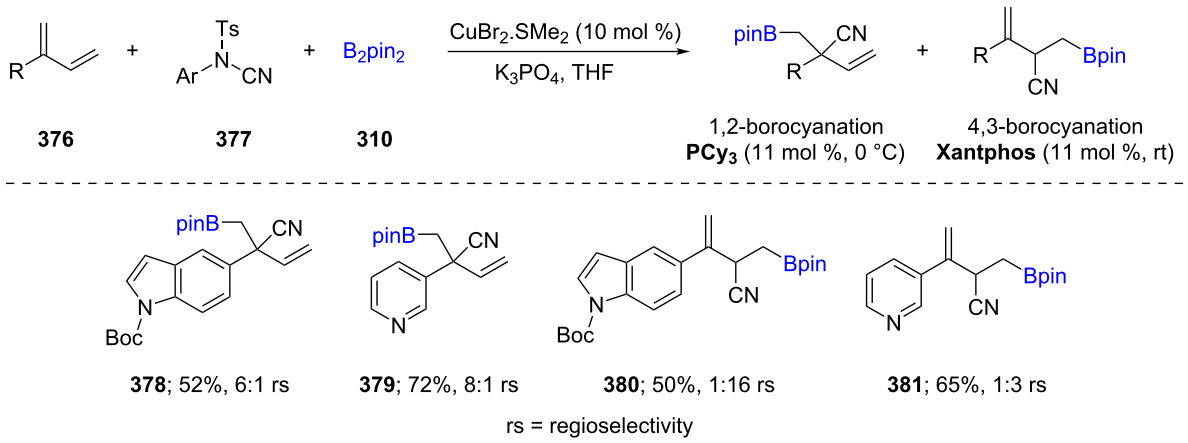

Scheme 60: Synthesis of densely functionalized and synthetically versatile 1,2- or 4,3-borocyanated 1,3-butadienes.

palladacycle PCy_3Pd G3, while 1,2-adducts **391**–**393** result using APhosPd G3. The former reaction proceeds through a second-stage β-hydride elimination/re-insertion pathway, although for the latter set of conditions, a rare cross-coupling takes place (Scheme 62) [115].

The cooperative effect of a catalytic system consisting of Cu/Ni (e.g., $Ni(acac)_2$, CuCl, and PCy_3) was also reported by Nakao et al. leading to regio- and stereoselective arylboration of 1-arylalkenes with aryl chlorides or tosylates. The reactions tolerate a variety of functional groups (including silyl ether, alkoxycarbonyl, and aminocarbonyl) [116]. Following the expected mechanistic sequence, Brown et al. generated a variety of Cu-catalyzed carboborylated products from *trans*-β-substituted styrenes [117] and *cis*-β-substituted styrenes [118] coupled with aryl/heteroaryl halides using SIMesCuCl/Pd-RuPhos G3 to give the *syn*-isomers, while SIMesCuCl/Pd-P-iBu_3 gave the *anti*-isomers. Styrenes could also be coupled with acyl chlorides [119] as electrophiles in the presence of $B_2(pin)_2$. Likewise, these same authors coupled 1,2-disubstituted 1,3-

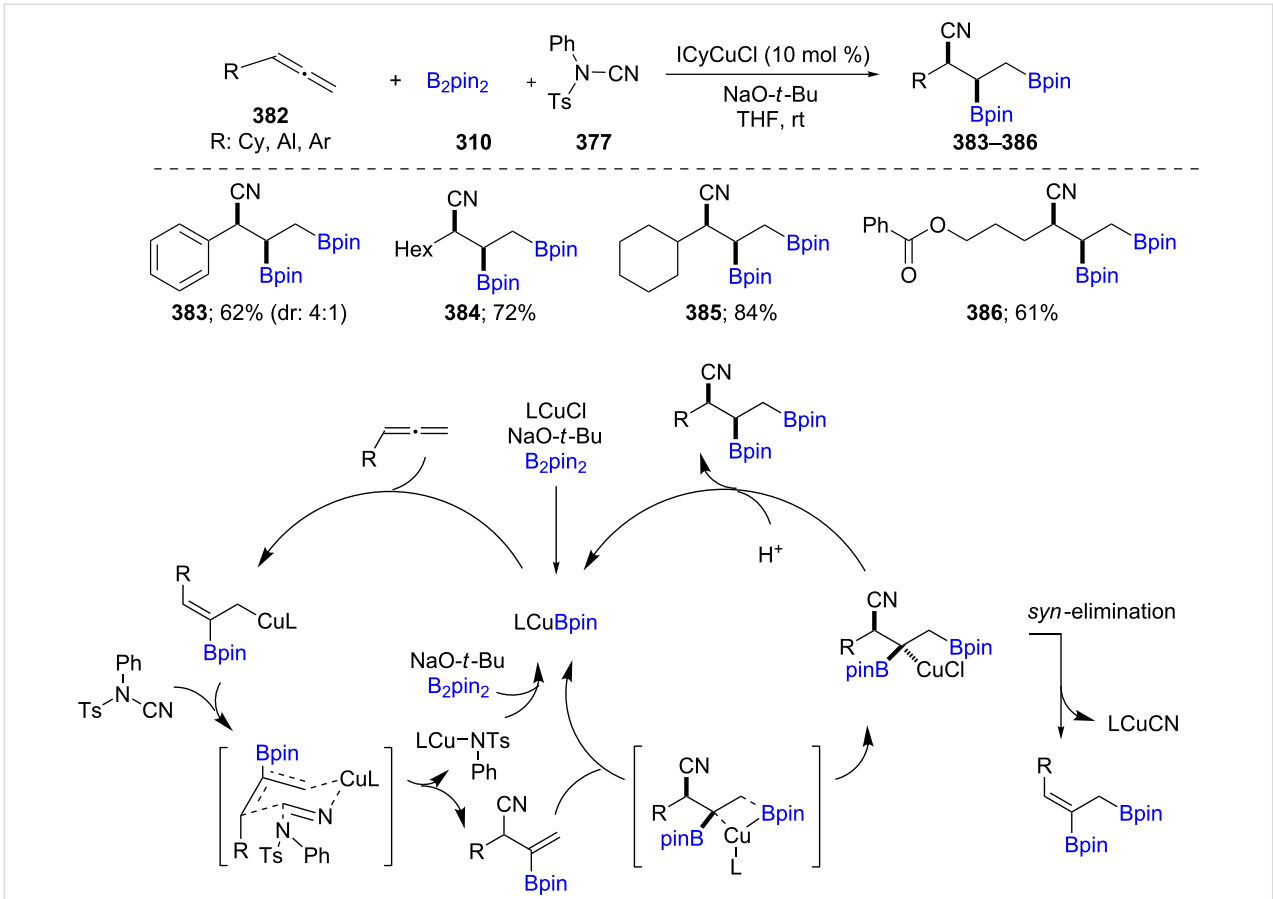

Scheme 61: Cu-catalyzed trifunctionalization of allenes.

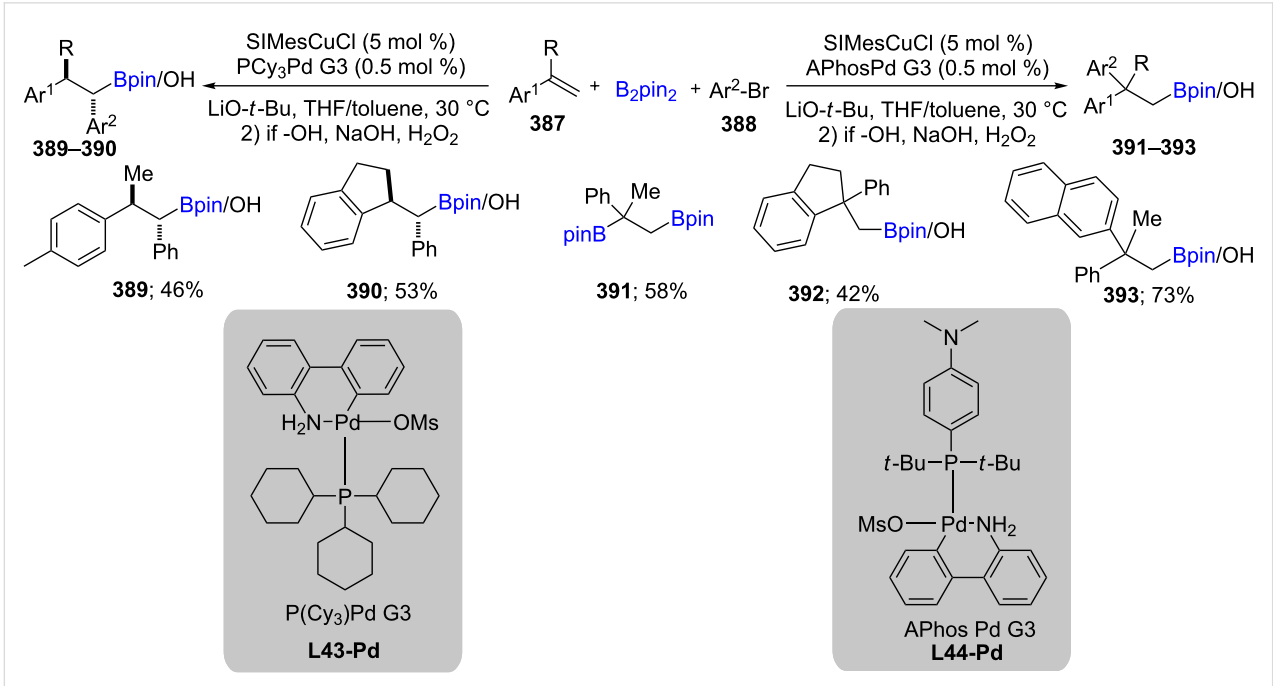

Scheme 62: Cu-catalyzed selective arylborylation of arenes.

dienes with 3-bromopyridine derivatives and $B_2(pin)_2$ under both racemic and non-racemic conditions and short reaction times [120].

Following various reports [121,122] of nonracemic borylative coupling of alkenes with imines, Kanai and coworkers [123] demonstrated a related enantio- and diastereo-divergent borylative coupling of styrenes **395** with *N*-phosphinoyl and *N*-thiophosphinoyl imines **394** to afford α,β-disubstituted γ-borylated nonracemic amines **396**–**399**. A combination of CuMes with either (*R*,*R*)-Ph-BPE or (*R*)-(S_p)-Josiphos afforded the targeted products in high ees (Scheme 63). The asymmetric addition of benzylic–Cu intermediates to imines proceeds through a flexible linear transition state which is sensitive to the steric environment surrounding the copper catalyst. This observation provided the opportunity to achieve either diastereomer depending on the choice of the ligand **L45** or **L46**.

Based on the interest in Cu-catalyzed aminoboration reactions of a variety of alkenes, such as bicyclic alkenes [124], Miura et al. subsequently described the preparation of β-borylalkylamines **401**–**404** from unactivated terminal alkenes **307** (Scheme 64). Using a mixed diborane reagent, such as pinB–Bdan developed by Suginome [125], or B_2pin_2, along with various *N*-hydroxylamine derivatives (**400**) under ligand-influenced Cu catalysis, high regioselectivities were typically obtained [126]. A year later, Popp et al. reported a Cu-catalyzed regiospecific boracarboxylation of vinyl arenes using 1 atm CO_2 and B_2pin_2 in moderate to excellent yields [127].

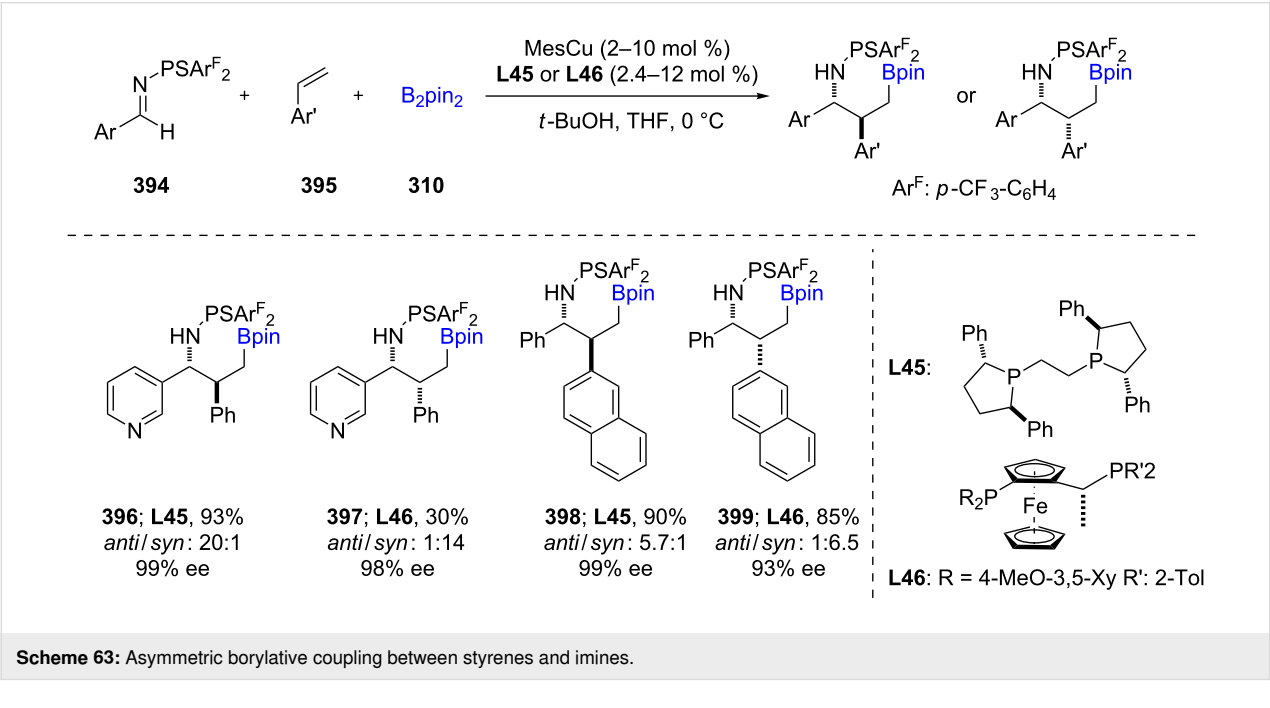

Scheme 63: Asymmetric borylative coupling between styrenes and imines.

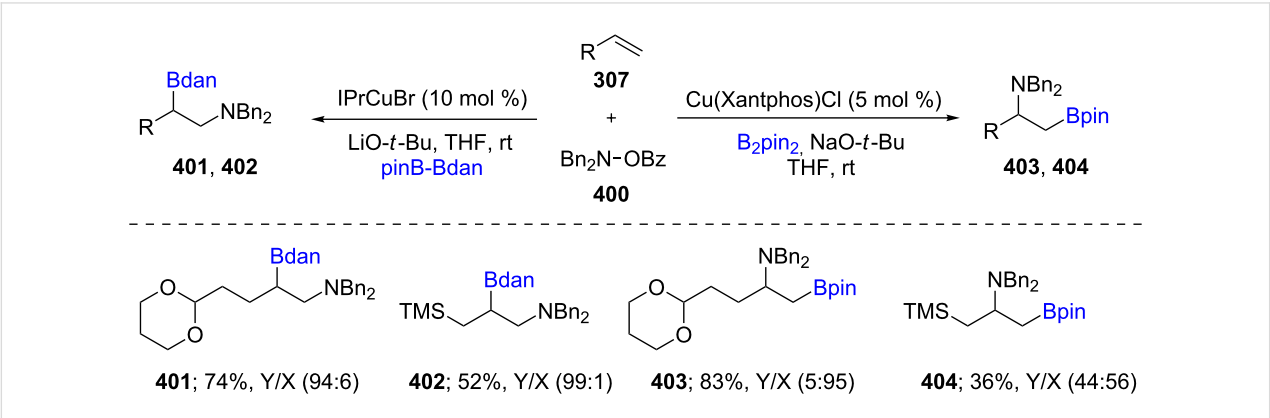

Scheme 64: Regio-divergent aminoboration of unactivated terminal alkenes.

2.3 β-Borylation of α,β-unsaturated compounds

The use of an inexpensive transition metal like copper as catalyst is attractive for β-borylations of α,β-unsaturated carbonyl compounds, that can then be further functionalized. In 2000, an initial report featuring a 1,4-borylation of α,β-unsaturated compounds **405** was reported by Hosomi in the presence of $Cu(OTf)_2{\cdot}C_6H_6/(t\text{-}Bu)_3P$ in DMF. No reaction occurred using $(CuOTf)_2{\cdot}C_6H_6$ in the absence of $(t\text{-}Bu)_3P$. Mechanistic studies showed that the coordination of phosphorus(III) to Cu(I) accelerated the reaction, as was confirmed by ^{31}P NMR. Using equimolar diboron (e.g., B_2pin_2) slightly changed the chemical shift of $(t\text{-}Bu)_3P$ from −30.7 ppm to −31.4 ppm. In addition, a significant downfield shift was observed in the presence of $CuCl/(t\text{-}Bu)_3P$ (−14.2 ppm). Therefore, it can be concluded that the extent of coordination of $(t\text{-}Bu)_3P$ to CuCl is far greater than that with the diboron species, which results in an enhancement of the catalytic activity (Scheme 65) [128].

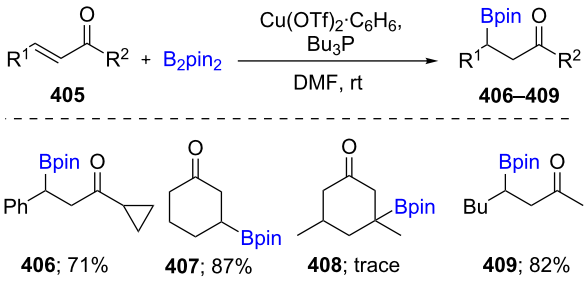

Scheme 65: Cu-catalyzed 1,4-borylation of α,β-unsaturated ketones.

The one-pot borylation/protodeboronation of α,β-unsaturated ketones **405** in the presence of CuBr, B_2pin_2 and H_2O as the hydrogen source was developed under mild reaction conditions to yield saturated ketones **410** and **411** in good to excellent yields. Hydrogen isotope labelling showed that water was likely the source of hydrogen since no reaction was observed under anhydrous conditions. By contrast, the addition of either TEMPO and BHT to the reaction resulted in 99% of the borylated product **414**, which may indicate the presence of a radical intermediate in the second, protodeboronation step. Therefore, the key intermediate is the 1,4-adduct **415**, which in the presence of base and water affords the saturated product (e.g., **410**, **411**; Scheme 66) [129].

The β-borylation of α,β-unsaturated imines **416** was reported using CuCl/L/NaO-*t*-Bu (L = PCy_3, Ph_3P, JosiPhos) which, upon oxidation with $NaBO_3$, delivered the desired β-imino alcohol **418** (Scheme 67). It is postulated that the base is responsible for the displacement of chloride from the catalyst and also cleavage of the B–B bond in B_2pin_2 to form the boryl-copper intermediate. Following this, the metallo-enamine is formed before reacting with an electrophile [130].

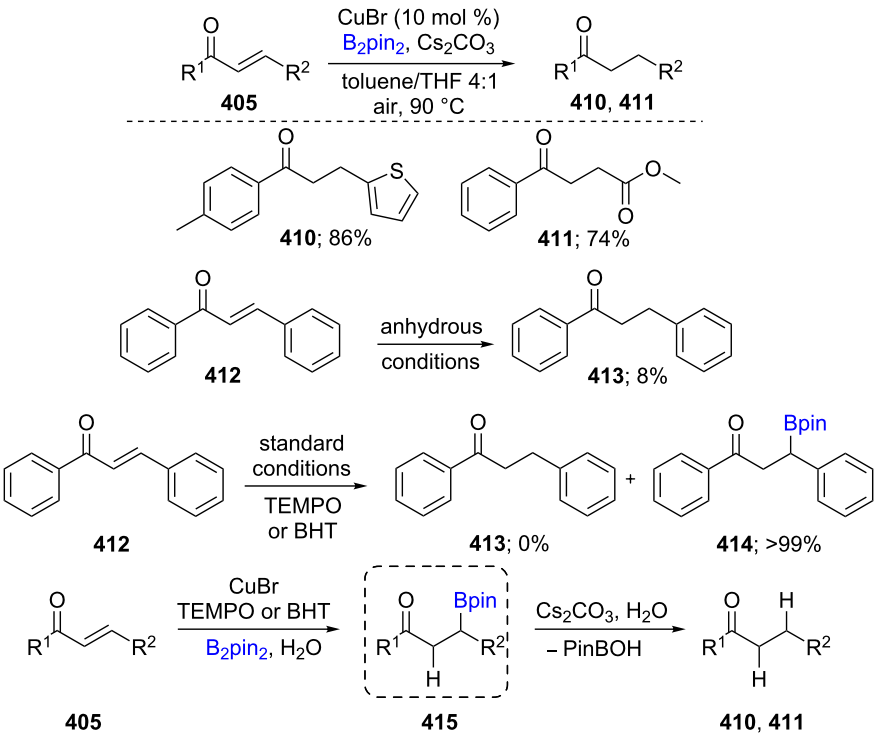

Scheme 66: Cu-catalyzed protodeboronation of α,β-unsaturated ketones.

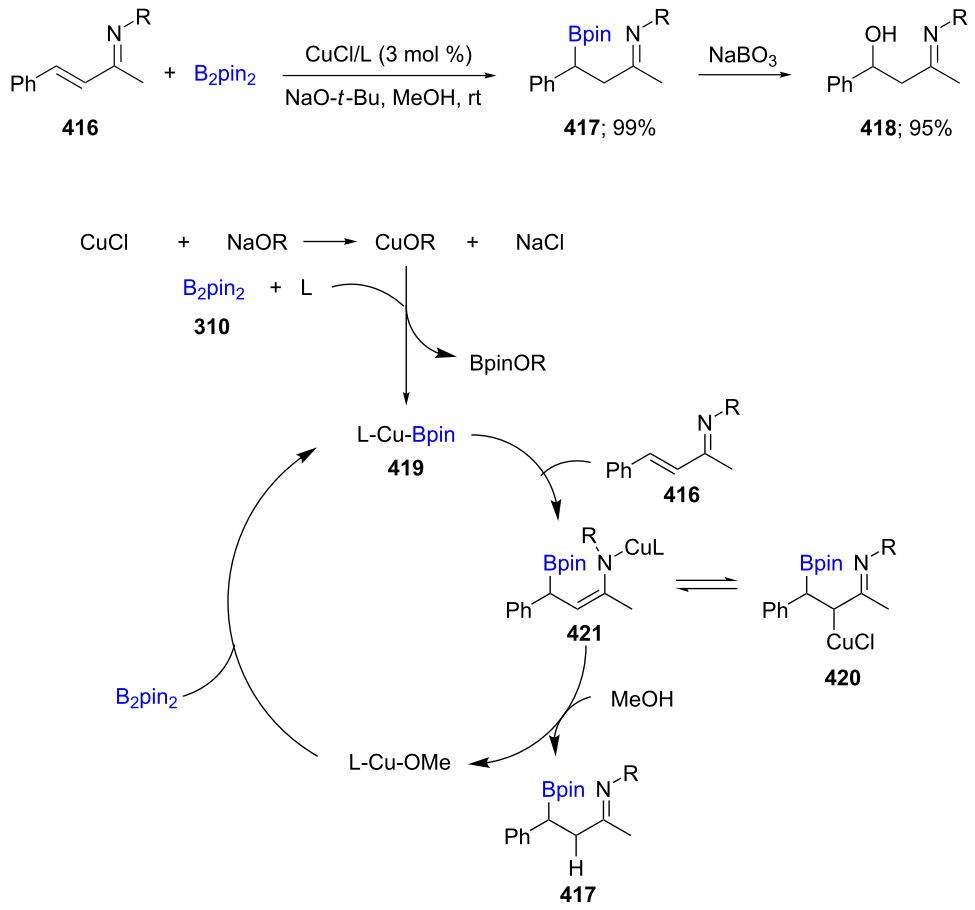

Scheme 67: Cu-catalyzed β-borylation of α,β-unsaturated imines.

A method to prepare β-trifluoroborate salts **423**–**427** each containing a carbonyl group was developed using a combination of CuCl/CyJohnPhos/NaO-*t*-Bu as the catalytic system. The conditions employed $B_2(OH)_4$ as an atom economical source of boron, starting from α,β-unsaturated amides **422**, ketones, and esters in MeOH as the solvent (Scheme 68) [131]. The β-amidotrifluoroborates synthesized through this protocol do not encounter the purification difficulties typically associated with conversions of pinacol esters to trifluoroborates.

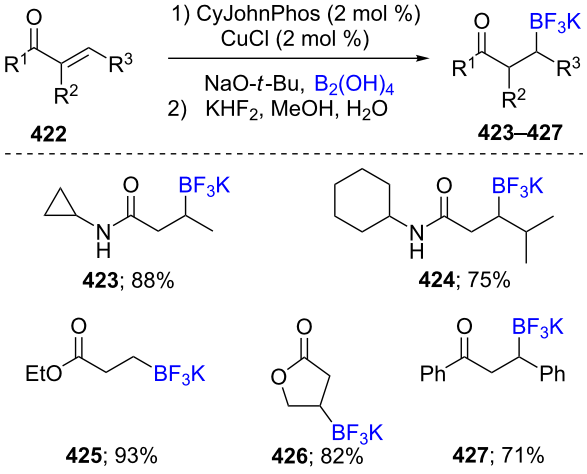

Scheme 68: Cu-catalyzed synthesis of β-trifluoroborato carbonyl compounds.

An asymmetric 1,4-borylation of α,β-unsaturated carbonyl derivatives, e.g., **428** and **429**, was reported using a combination of $Cu(MeCN)_2PF_6$/**L47** with either bisboronic acid (BBA, **430**) or tetrakis(dimethylamino)diboron (**431**) as atom-economical boron sources leading to the desired products **432**–**435** in moderate to good ees (Scheme 69) [132]. In addition, the reaction of potassium *N*-(4-methoxyphenyl)-3-(trifluoroborato)butanamide (**436**) as the nucleophilic coupling partner was investigated with heteroarylchlorides **437** leading to products reflecting a complete inversion of stereochemistry. The screening showed that XPhos-Pd-G2 is the best pre-catalyst for these reactions and it was proposed that the reaction takes place through an S_E2 pathway due to coordination of the carbonyl group of the nucleophile to the boronate intermediate.

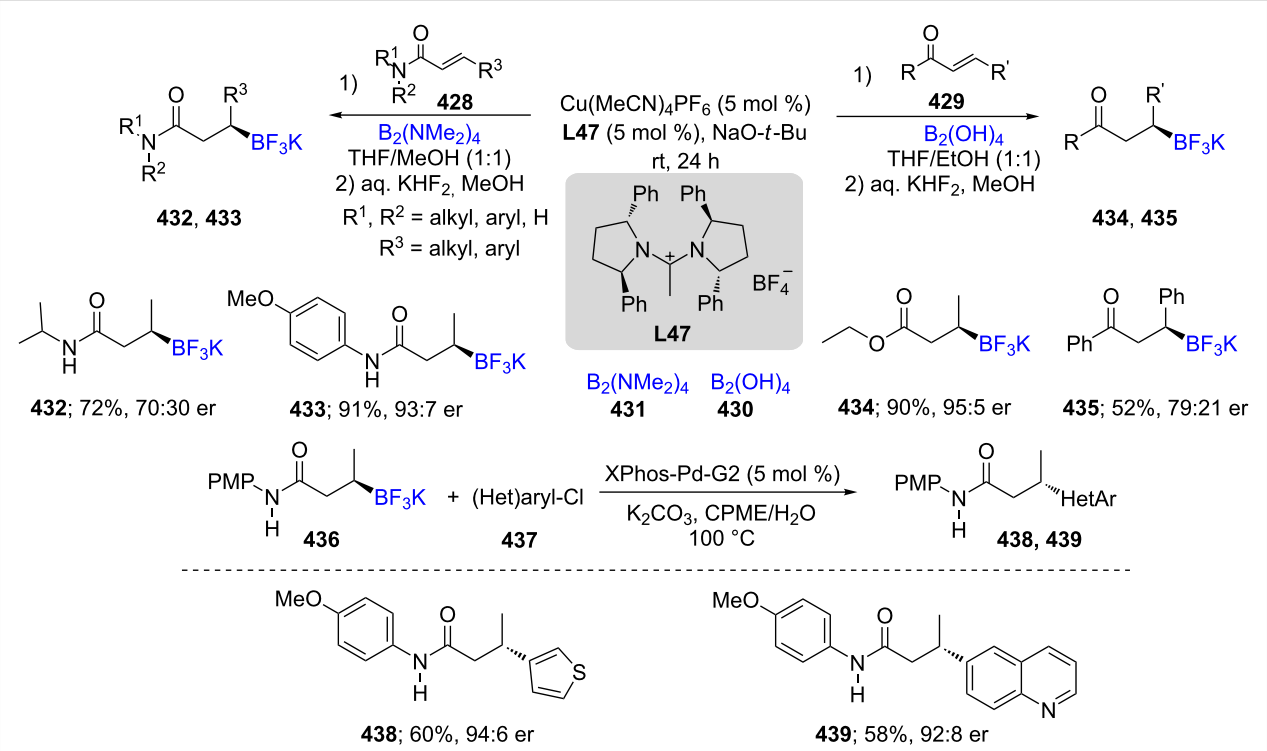

Scheme 69: Asymmetric 1,4-borylation of α,β-unsaturated carbonyl compounds.

Very recently the asymmetric Cu-catalyzed conjugate borylation (ACB) and addition (ACA) reactions onto α,β-unsaturated 2-acyl-*N*-methylimidazoles **440** have been developed using nonracemic Taniaphos (**L48**) as ligand, followed by an oxidation to the secondary alcohols resulting in high enantioselectivities. Aliphatic chains gave a high degree of enantioselectivity (up to 98%), while more moderate ees were noted when the substrates were branched at the γ-site (Scheme 70) [133]. The absolute configuration at each stereogenic center was determined by subsequent conversion of the borylated acylimidazole

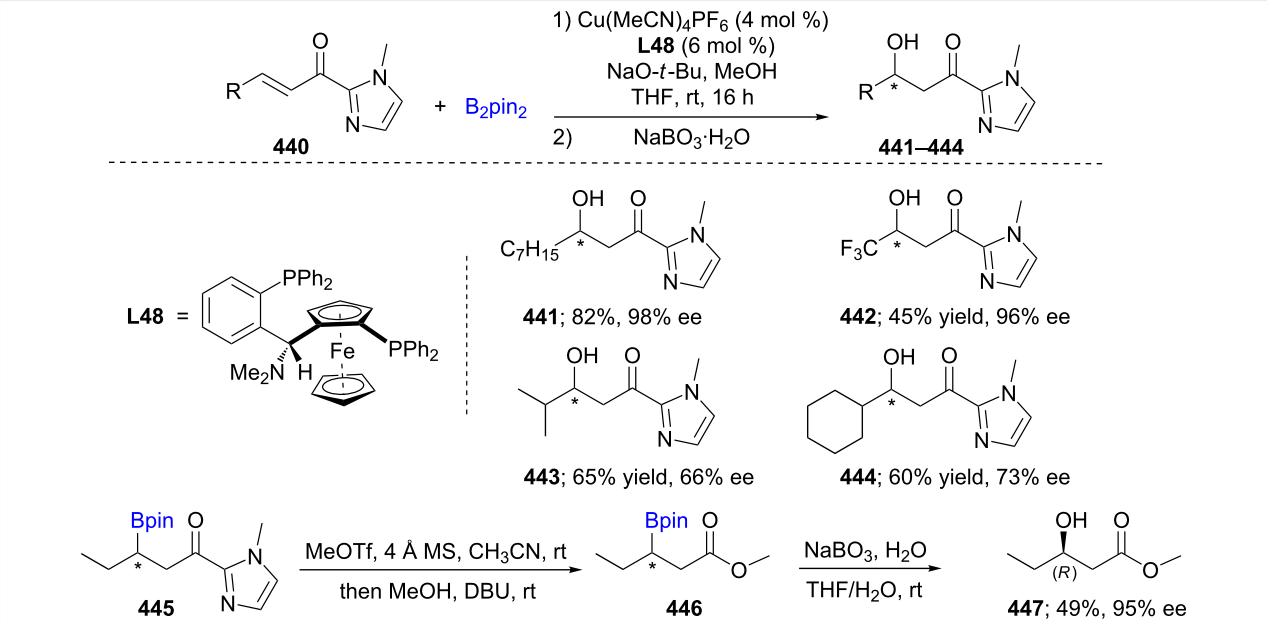

Scheme 70: Cu-catalyzed ACB and ACA reactions of α,β-unsaturated 2-acyl-*N*-methylimidazoles.

445 to the corresponding ester **446**, which then was reacted with $NaBO_3$ to deliver the nonracemic hydroxy derivative **447**.

2.4 Nucleophilic borylation of C=X bonds

The first studies on the borylation of both aliphatic and aromatic aldehydes **448** were carried out using Cu/NHC-ligand complexes generating diborylated products **449**–**451**; Scheme 71, top) [134]. The insertion of an in situ-formed Cu–B species into the aldehyde carbonyl was proposed, leading to the formation of a C–B bond. ^{1}H NMR studies, however, did not confirm the formation of this Cu–O–C–B linkage **452**. Instead, solely the Cu–C–O–B species **453** was observed. Due to the possibility of facile rearrangement of the former to the latter, it could not be concluded that a direct insertion of the aldehyde into the Cu–B bond is taking place.

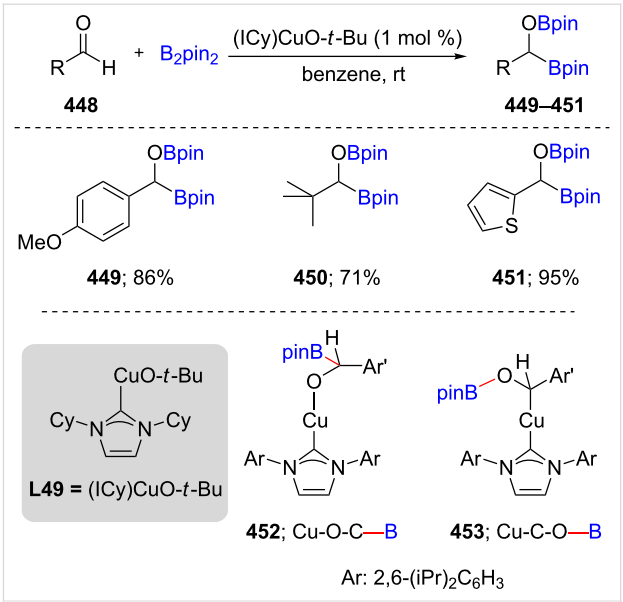

Scheme 71: Cu-catalyzed diborylation of aldehydes.

The enantioselective borylation of aliphatic aldehydes **448** was first reported in 2015 using CuCl/KO-*t*-Bu/(*R*)-(DTBM)-Segphos as the active catalyst in THF for the formation of chiral, nonracemic α-alkoxyorganoboronate esters (up to 99% ee; **454**–**457**). MeOH was used as the proton source. Further functionalization can be considered as an umpolung pathway for the formation of enantioenriched tertiary alcohols through subsequent C–C bond formation (Scheme 72) [135]. The proposed mechanism involves the formation of L–Cu–O–*t*-Bu **458** which reacts with B_2pin_2 to generate L-Cu-Bpin **459**. The

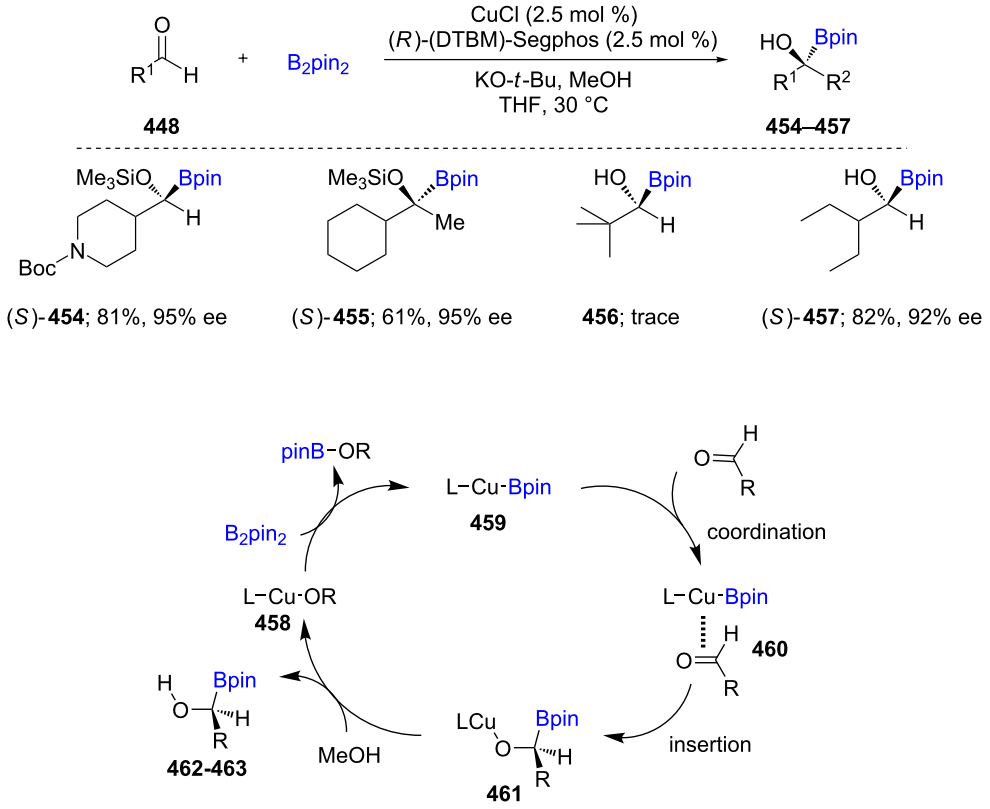

Scheme 72: Umpolung pathway for chiral, nonracemic tertiary alcohol synthesis (top) and proposed mechanism for product formation of **456** and **457** (bottom).

subsequent coordination to the aldehyde results in the intermediate **461**. Upon protonation of **461** the desired enantiomerically enriched borylated products **462** and **463** are obtained.

In 2017, a CuCl/nonracemic NHC combination of reagents was employed as catalyst leading to an efficient enantioselective formation of α-hydroxyboronates **465**–**467** in up to 94% ee from aliphatic ketones **464**. The subsequent treatment with *n*-BuLi followed by an appropriate electrophile led to C–C bond formation, ultimately delivering chiral tertiary alcohols. Mechanistic studies and DFT calculations showed that an in situ-formed borylcopper(I) species is responsible for the 1,2-addition (Scheme 73) [136].

C,O-Diboration of ketones **464** was explored using a catalytic system consisting of (ICy)CuCl/NaO-*t*-Bu (ICy = *N*,*N*-dicyclohexylimidazolyl) in toluene which afforded the products **470** in moderate to high yields. Subsequently, tertiary α-hydroxyboronate esters **471**–**474** were isolated through O–B bond cleavage upon treatment with silica (Scheme 74) [137]. The diastereoselective formation of α-hydroxyboronate esters **477** and **478** starting from cyclic and acyclic ketones **475** and **476**) arises from an extensive steric crowding during the insertion reaction of the coordinated L-Cu-Bpin to the aldehyde **479**. The observed selectivity from Felkin-Anh-controlled addition to the carbonyl is increased here due to steric congestion associated with the Bpin substituent.

2.5 Borylation of C–X bonds

Decades ago, both aryl or vinyl boronates were synthesized via Pd-catalyzed Miyaura borylations using aryl or vinyl halides as substrates, respectively [138]. Unactivated alkyl halides (X = Cl, Br, I, OTs; **481**), however, have been examined far more recently under mild conditions, using a combination of B_2pin_2 together with CuI/Ph_3P and Li-OMe. Those alkyl halides bearing a double or triple bond in an appropriate position deliver cyclized borylated products **486**. Hence, both primary and secondary boronates could be obtained with high functional group tolerance, which is hard to access through previous protocols. Moreover, the desired alkylboronates **487** can be used further for Suzuki–Miyaura coupling reactions with aryl bromides **488** utilizing Ruphos as the ligand on palladium (Scheme 75) [139].

Early in 2019, a highly diastereo- and enantioselective conversion of trisubstituted alkenyl difluorides, where both *Z*- and *E*-olefinic isomers **490** and **492** afforded high levels of *Z*-olefinic boronates **491** and **493** was described. However, the *Z*-configured alkenes together with the catalyst system consisting of CuCl/BenzP* gave the *R*-configured alkylboronates, while a change in the ligand to the BPE ((+)-1,2-*bis*((2*S*,5*S*)-2,5-diphenylphospholano)ethane) series, led to the opposite isomer at the newly formed C(sp^3) center. These fluorine-containing borylated products can be further converted to allylic amines (**495**; Scheme 76) [140].

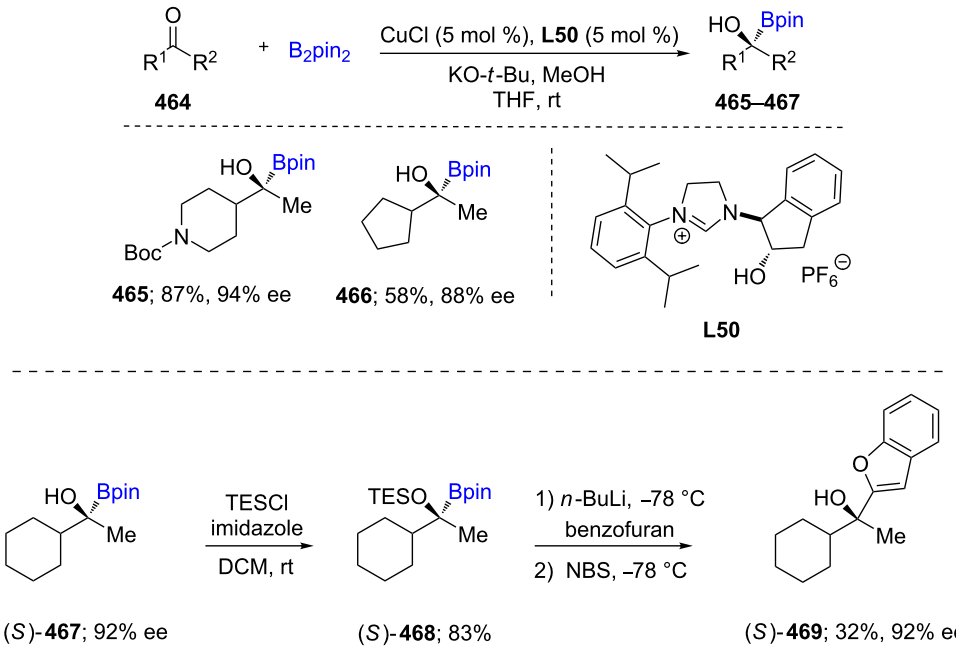

Scheme 73: Cu-catalyzed synthesis of α-hydroxyboronates.

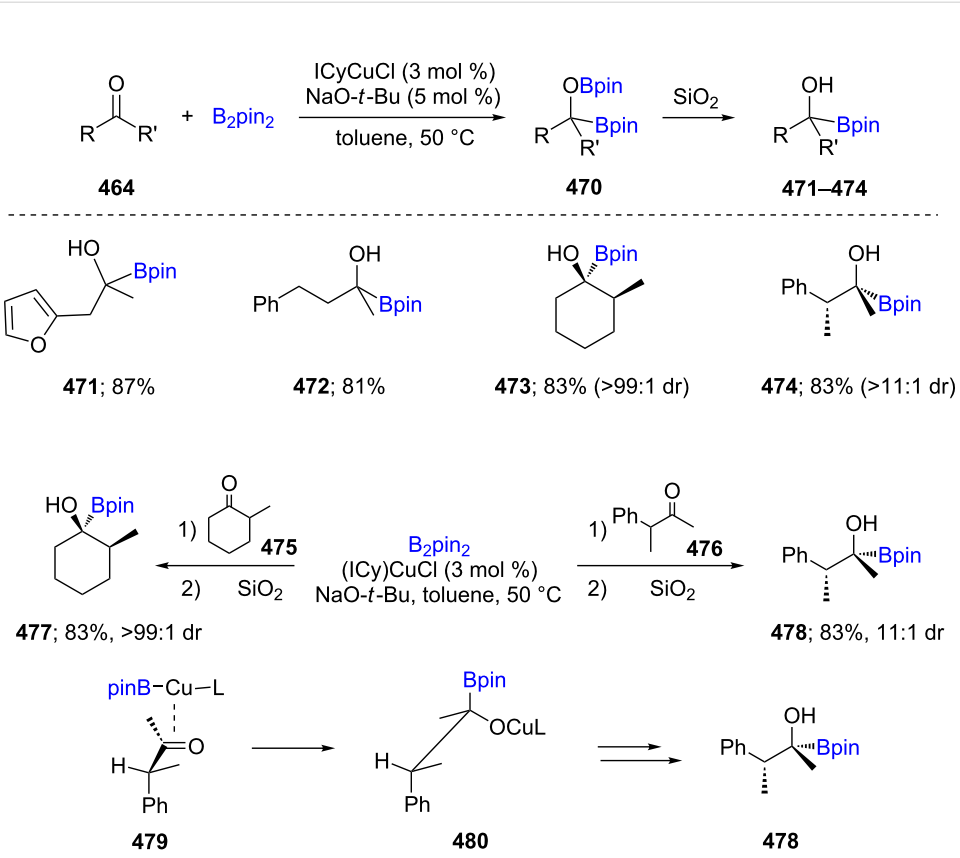

Scheme 74: Cu-catalyzed borylation of ketones.

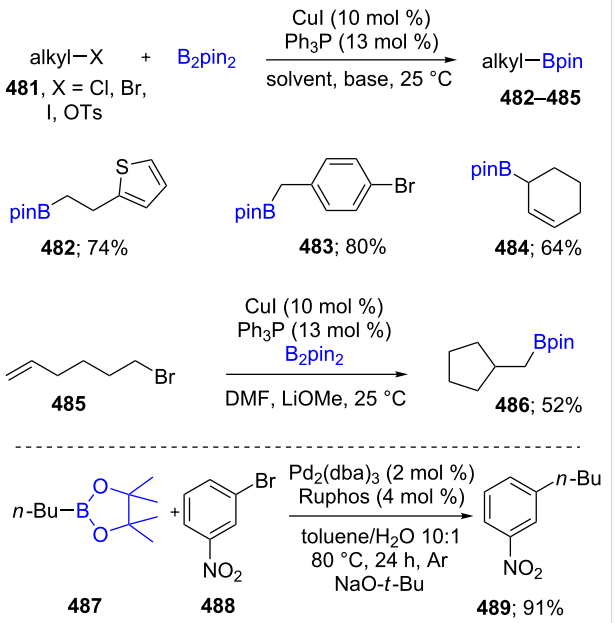

Scheme 75: Cu-catalyzed borylation of unactivated alkyl halides.

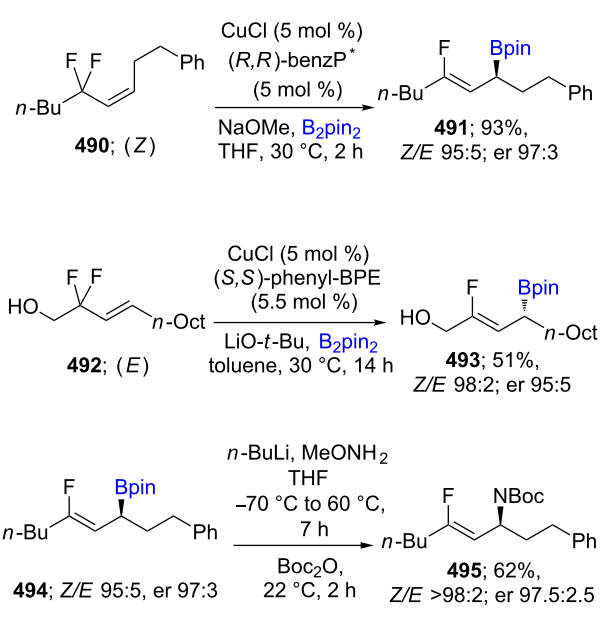

Scheme 76: Cu-catalyzed borylation of allylic difluorides.

Borylation of cyclic and acyclic alkyl halides (X = Cl, Br, I; **496**) was developed using a catalyst derived from CuCl and the ligand Xantphos, with stoichiometric amounts of KO-*t*-Bu in one pot. No reaction was reported, however, using alkyl mesylates. Ring-opened products were observed using cyclopropylmethyl bromide (**500**) which suggests a radical pathway. A variety of functional groups was tolerated, and high diastereoselectivity of the newly formed products was maintained; e.g., in the case of menthyl halides (**499**; Scheme 77) [141].

A novel protocol was developed for the borylation of unactivated alkyl chlorides **496** and bromides using catalytic Cu(II) together with NHC **L51**. Similar to mechanistic studies for catalytic Cu(I) reactions, these Cu(II)–NHC complexes may activate B_2pin_2 forming a copper–boryl species, which further reacts with an alkyl halide as electrophile. The reactions, which could be performed under air, provide the desired borylated products in good yields while tolerating a wide range of functional groups. The reaction of cyclopropylmethyl bromide (**500**) leads to the ring-opened product, while in the case of 6-bromohex-1-ene (**485**), the cyclic alkylboronate (**486**) was formed as the major product. Both results suggest a radical pathway (Scheme 78) [142]. Enantioenriched benzylboronates were also synthesized from racemic benzyl chlorides using $Cu(CH_3CN)_4$/(*S*)-Quinox-*t*-BuAd_2 as the nonracemic catalytic system [143].

Baran et al. reported an inexpensive and ligand-free Cu-catalyzed decarboxylative method for the synthesis of boronic esters **510**–**513** through reaction of an acid with *N*-hydroxyphthalimide, via the in situ-generation of a redox active ester **509** (Scheme 79). The reaction conditions reported are mild, the reactions are fast, and they tolerate a wide variety of functional groups leading to the Bpin-containing products in moderate yields. By contrast, substrates bearing halides were low yielding due to unavoidable protodehalogenation or alternative borylation processes [144].

Direct functionalization of sp^3 C–O bonds present in alcohols is of great interest due to their abundance in nature as well as their commercial availability. As a result, benzylic, allylic, and propargylic alcohols (**514**, **516**, **518**) were employed in the Cu-catalyzed borylation reactions in the presence of B_2pin_2 to afford benzyl-, allyl-, and allenyl boronates, respectively (**515**, **517**, **519**). Structural variations in the alcohols did not appear to inhibit reactivity under the reaction conditions. Mechanistic studies suggested a nucleophilic substitution of Cu(I)–Bpin onto an activated hydroxy-Lewis acid adduct. This reaction proceeds under mild conditions, shows a broad substrate scope, and gives the targeted benzyl-, allyl-, and allenyl boronate products in good chemical yields. $Ti(O\text{-}iPr)_4$ is used in the reaction to activate the alcohol via formation of **521** and iPrOH. The Cu(I) species, formed through reaction of Cu(II) and Xantphos, reacts

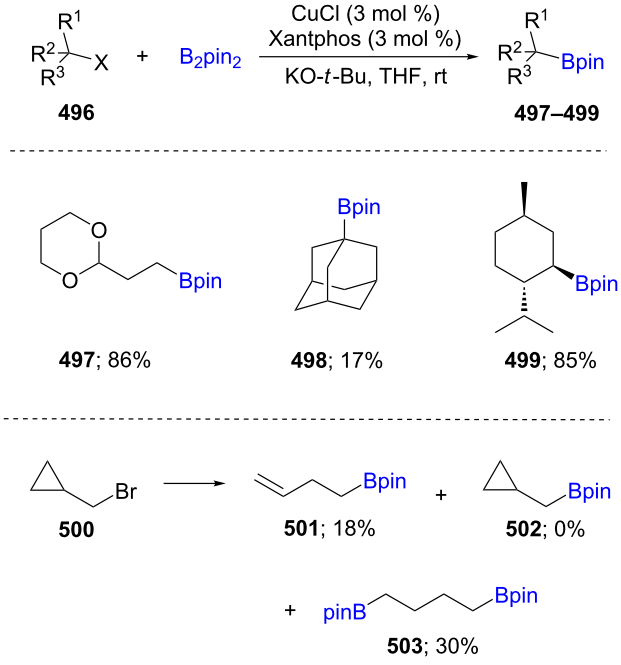

Scheme 77: Cu-catalyzed borylation of cyclic and acyclic alkyl halides.

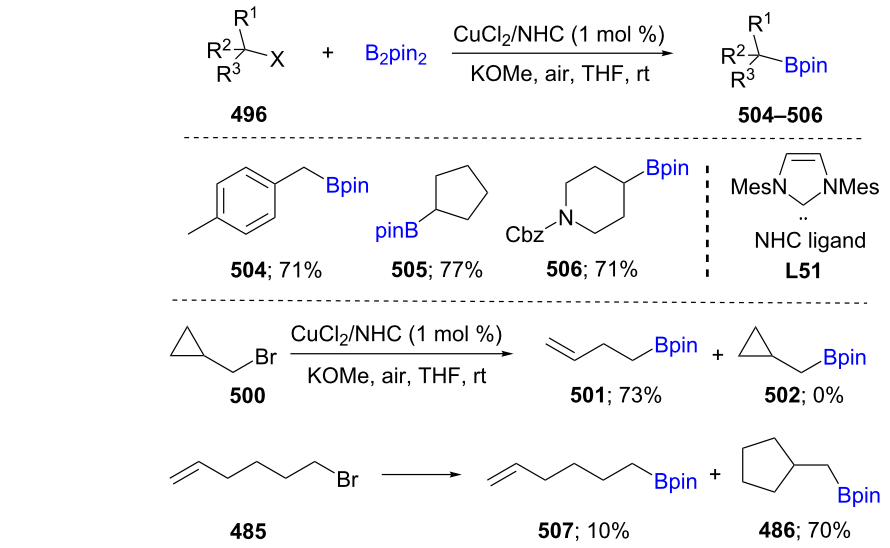

Scheme 78: Cu-catalyzed borylation of unactivated alkyl chlorides and bromides.

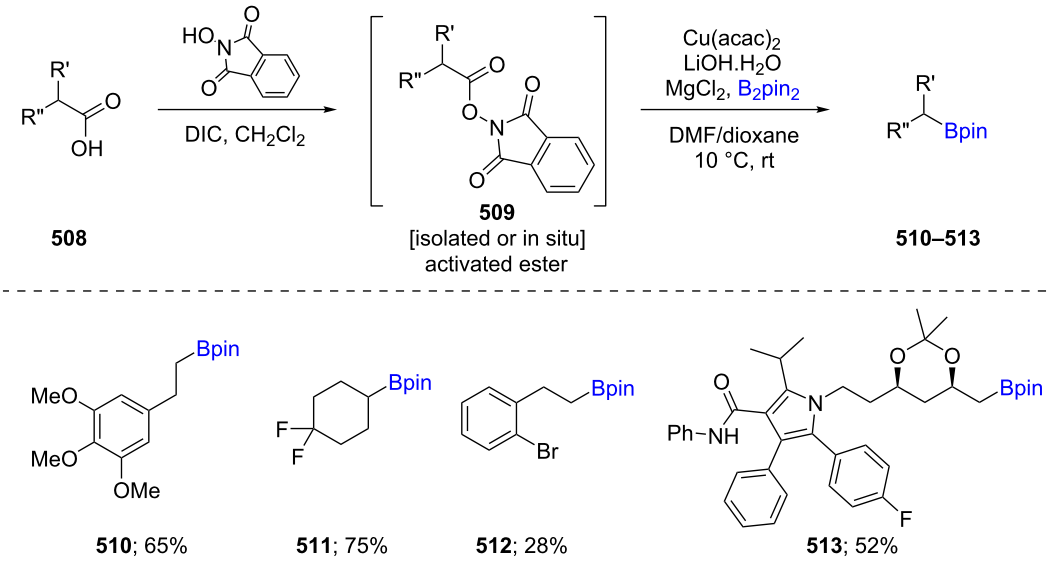

Scheme 79: Cu-catalyzed decarboxylative borylation of carboxylic acids.

with iPrOH, followed by B_2Pin_2 to generate the intermediate L-Cu-Bpin. The *in situ*-formed L-Cu-Bpin then reacts with species **521**, **522**, and **523** to form the desired borylated products **524**, **525**, or **526**, respectively (Scheme 80) [145].

Conclusion

Copper-catalyzed processes as described herein provide an excellent access to both carbon–silicon and carbon–boron intermediates. Given the plethora of known chemical methods utilizing such C–Si and C–B bonds en route to derived, valuable functionalities, it is not surprising that considerable attention has been paid to the developments described herein. Moreover, copper has been, and still is, very attractively priced, being classified as a base metal, and remains an incentive, further encouraging future discoveries. Its participation in achiral and, perhaps more noteworthy, asymmetric catalyses, stems in large measure from both its phosphine and *N*-heterocyclic carbene-derived complexes that impart especially useful

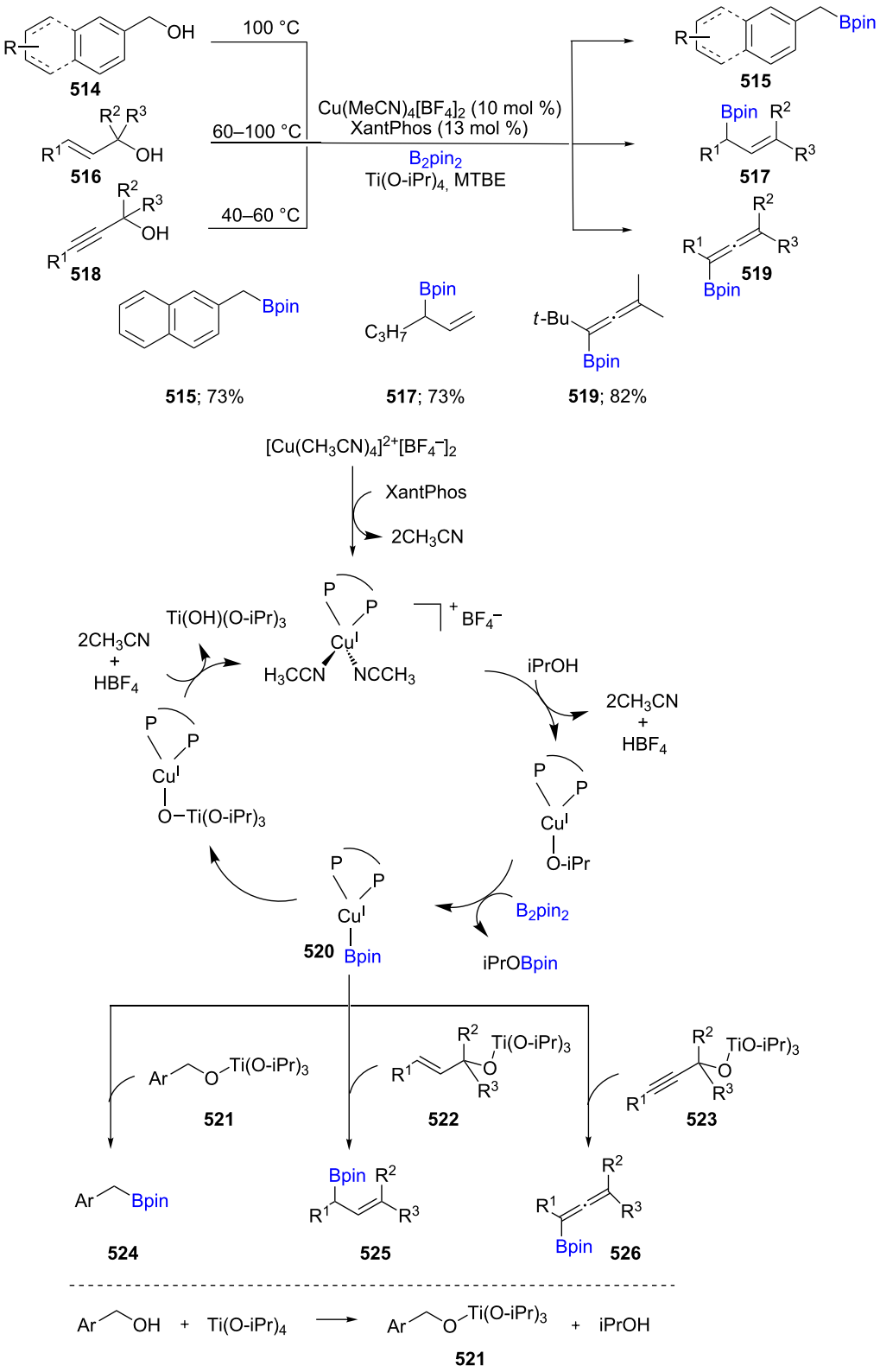

Scheme 80: Cu-catalyzed borylation of benzylic, allylic, and propargylic alcohols.

reactivity and selectivity profiles. And while most of the chemistry discussed to date takes place in organic solvents, its expansion into alternative reaction media (e.g., water) is sure to offer new, exciting, and sustainable opportunities for copper catalysis in the future.

Funding

Financial support provided by the NSF (18-56406) and PHT International (postdoctoral fellowship to B.S.T.) is warmly acknowledged with thanks.

ORCID® iDs

Balaram S. Takale - https://orcid.org/0000-0001-8279-944X

References

1. Cheng, C.; Hartwig, J. F. *Chem. Rev.* **2015,** *115,* 8946–8975. doi:10.1021/cr5006414
2. Hatanaka, Y.; Hiyama, T. *J. Org. Chem.* **1988,** *53,* 918–920. doi:10.1021/jo00239a056
3. Denmark, S. E.; Regens, C. S. *Acc. Chem. Res.* **2008,** *41,* 1486–1499. doi:10.1021/ar800037p
4. Miyaura, N.; Suzuki, A. *Chem. Rev.* **1995,** *95,* 2457–2483. doi:10.1021/cr00039a007
5. Jacob, P., III; Brown, H. C. *J. Org. Chem.* **1977,** *42,* 579–580. doi:10.1021/jo00423a050
6. Essafi, S.; Tomasi, S.; Aggarwal, V. K.; Harvey, J. N. *J. Org. Chem.* **2014,** *79,* 12148–12158. doi:10.1021/jo502020e
7. Brown, H. C.; Rogic, M. M.; Nambu, H.; Rathke, M. W. *J. Am. Chem. Soc.* **1969,** *91,* 2147–2149. doi:10.1021/ja01036a070
8. Franz, A. K.; Wilson, S. O. *J. Med. Chem.* **2013,** *56,* 388–405. doi:10.1021/jm3010114
9. Mortensen, M.; Husmann, R.; Veri, E.; Bolm, C. *Chem. Soc. Rev.* **2009,** *38,* 1002–1010. doi:10.1039/b816769a
10. Fujii, S.; Hashimoto, Y. *Future Med. Chem.* **2017,** *9,* 485–505. doi:10.4155/fmc-2016-0193
11. Geyer, M.; Wellner, E.; Jurva, U.; Saloman, S.; Armstrong, D.; Tacke, R. *ChemMedChem* **2015,** *10,* 911–924. doi:10.1002/cmdc.201500040
12. Singh, S.; Sieburth, S. M. *Org. Lett.* **2012,** *14,* 4422–4425. doi:10.1021/ol301933n
13. Baker, S. J.; Tomsho, J. W.; Benkovic, S. J. *Chem. Soc. Rev.* **2011,** *40,* 4279–4285. doi:10.1039/c0cs00131g
14. Diaz, D. B.; Yudin, A. K. *Nat. Chem.* **2017,** *9,* 731–742. doi:10.1038/nchem.2814
15. Baker, S. J.; Ding, C. Z.; Akama, T.; Zhang, Y.-K.; Hernandez, V.; Xia, Y. *Future Med. Chem.* **2009,** *1,* 1275–1288. doi:10.4155/fmc.09.71
16. Groziak, M. P. *Am. J. Ther.* **2001,** *8,* 321–328. doi:10.1097/00045391-200109000-00005
17. Bähr, S.; Xue, W.; Oestreich, M. *ACS Catal.* **2019,** *9,* 16–24. doi:10.1021/acscatal.8b04230
18. Keipour, H.; Carreras, V.; Ollevier, T. *Org. Biomol. Chem.* **2017,** *15,* 5441–5456. doi:10.1039/c7ob00807d
19. Wilkinson, J. R.; Nuyen, C. E.; Carpenter, T. S.; Harruff, S. R.; Van Hoveln, R. *ACS Catal.* **2019,** *9,* 8961–8979. doi:10.1021/acscatal.9b02762
20. Hensel, A.; Oestreich, M. Asymmetric Addition of Boron and Silicon Nucleophiles. In *Progress in Enantioselective Cu(I)-catalyzed Formation of Stereogenic Centers;* Harutyunyan, S. R., Ed.; Springer: Cham, Switzerland, 2015; pp 135–167. doi:10.1007/3418_2015_156
21. Hemming, D.; Fritzemeier, R.; Westcott, S. A.; Santos, W. L.; Steel, P. G. *Chem. Soc. Rev.* **2018,** *47,* 7477–7494. doi:10.1039/c7cs00816c
22. Neeve, E. C.; Geier, S. J.; Mkhalid, I. A. I.; Westcott, S. A.; Marder, T. B. *Chem. Rev.* **2016,** *116,* 9091–9161. doi:10.1021/acs.chemrev.6b00193
23. Mkhalid, I. A. I.; Barnard, J. H.; Marder, T. B.; Murphy, J. M.; Hartwig, J. F. *Chem. Rev.* **2010,** *110,* 890–931. doi:10.1021/cr900206p
24. Collins, B. S. L.; Wilson, C. M.; Myers, E. L.; Aggarwal, V. K. *Angew. Chem., Int. Ed.* **2017,** *56,* 11700–11733. doi:10.1002/anie.201701963
25. Okuda, Y.; Morizawa, Y.; Oshima, K.; Nozaki, H. *Tetrahedron Lett.* **1984,** *25,* 2483–2486. doi:10.1016/s0040-4039(01)81210-7
26. Takeda, M.; Shintani, R.; Hayashi, T. *J. Org. Chem.* **2013,** *78,* 5007–5017. doi:10.1021/jo400888b
27. Scharfbier, J.; Oestreich, M. *Synlett* **2016,** *27,* 1274–1276. doi:10.1055/s-0035-1561407
28. Scharfbier, J.; Hazrati, H.; Irran, E.; Oestreich, M. *Org. Lett.* **2017,** *19,* 6562–6565. doi:10.1021/acs.orglett.7b03279
29. Xue, W.; Qu, Z.-W.; Grimme, S.; Oestreich, M. *J. Am. Chem. Soc.* **2016,** *138,* 14222–14225. doi:10.1021/jacs.6b09596
30. Guisán-Ceinos, M.; Soler-Yanes, R.; Collado-Sanz, D.; Phapale, V. B.; Buñuel, E.; Cárdenas, D. J. *Chem. – Eur. J.* **2013,** *19,* 8405–8410. doi:10.1002/chem.201300882
31. Xue, W.; Oestreich, M. *Angew. Chem., Int. Ed.* **2017,** *56,* 11649–11652. doi:10.1002/anie.201706611
32. Hazrati, H.; Oestreich, M. *Org. Lett.* **2018,** *20,* 5367–5369. doi:10.1021/acs.orglett.8b02281
33. Sun, H.; Moeller, K. D. *Org. Lett.* **2002,** *4,* 1547–1550. doi:10.1021/ol025776e
34. Min, G. K.; Hernández, D.; Skrydstrup, T. *Acc. Chem. Res.* **2013,** *46,* 457–470. doi:10.1021/ar300200h
35. Suginome, M.; Matsuda, T.; Ito, Y. *Organometallics* **2000,** *19,* 4647–4649. doi:10.1021/om000254t
36. Vyas, D. J.; Fröhlich, R.; Oestreich, M. *Org. Lett.* **2011,** *13,* 2094–2097. doi:10.1021/ol200509c
37. Park, J. K.; Lackey, H. H.; Ondrusek, B. A.; McQuade, D. T. *J. Am. Chem. Soc.* **2011,** *133,* 2410–2413. doi:10.1021/ja1112518
38. Hensel, A.; Nagura, K.; Delvos, L. B.; Oestreich, M. *Angew. Chem., Int. Ed.* **2014,** *53,* 4964–4967. doi:10.1002/anie.201402086
39. Mita, T.; Sugawara, M.; Saito, K.; Sato, Y. *Org. Lett.* **2014,** *16,* 3028–3031. doi:10.1021/ol501143c
40. Zhao, C.; Jiang, C.; Wang, J.; Wu, C.; Zhang, Q.-W.; He, W. *Asian J. Org. Chem.* **2014,** *3,* 851–855. doi:10.1002/ajoc.201402077
41. Chen, Z.; Huo, Y.; An, P.; Wang, X.; Song, C.; Ma, Y. *Org. Chem. Front.* **2016,** *3,* 1725–1737. doi:10.1039/c6qo00386a
42. Kleeberg, C.; Feldmann, E.; Hartmann, E.; Vyas, D. J.; Oestreich, M. *Chem. – Eur. J.* **2011,** *17,* 13538–13543. doi:10.1002/chem.201102367
43. Takeda, M.; Yabushita, K.; Yasuda, S.; Ohmiya, H. *Chem. Commun.* **2018,** *54,* 6776–6779. doi:10.1039/c8cc01055b
44. Takeda, M.; Mitsui, A.; Nagao, K.; Ohmiya, H. *J. Am. Chem. Soc.* **2019,** *141,* 3664–3669. doi:10.1021/jacs.8b13309

45. Cirriez, V.; Rasson, C.; Hermant, T.; Petrignet, J.; Díaz Álvarez, J.; Robeyns, K.; Riant, O. *Angew. Chem., Int. Ed.* **2013,** *52,* 1785–1788. doi:10.1002/anie.201209020
46. Delvos, L. B.; Hensel, A.; Oestreich, M. *Synthesis* **2014,** *46,* 2957–2964. doi:10.1055/s-0034-1378542
47. Lipshutz, B. H. Organocopper Chemistry. In *Organometallics in Synthesis: A Manual,* 2nd ed.; Schlosser, M., Ed.; Wiley-VCH: Weinheim, 2002; pp 665–815. doi:10.1002/9781118750421.ch6
48. Hartmann, E.; Vyas, D. J.; Oestreich, M. *Chem. Commun.* **2011,** *47,* 7917–7932. doi:10.1039/c1cc10528k
49. Ager, D. J.; Fleming, I. *J. Chem. Soc., Chem. Commun.* **1978,** 176–177. doi:10.1039/c39780000177
50. Ager, D. J.; Fleming, I.; Patel, S. K. *J. Chem. Soc., Perkin Trans. 1* **1981,** 2520–2526. doi:10.1039/p19810002520
51. Fleming, I.; Newton, T. W. *J. Chem. Soc., Perkin Trans. 1* **1984,** 1805. doi:10.1039/p19840001805
52. Lipshutz, B. H.; Reuter, D. C.; Ellsworth, E. L. *J. Org. Chem.* **1989,** *54,* 4975–4977. doi:10.1021/jo00282a001
53. Lipshutz, B. H.; Sclafani, J. A.; Takanami, T. *J. Am. Chem. Soc.* **1998,** *120,* 4021–4022. doi:10.1021/ja980152i
54. Ito, H.; Ishizuka, T.; Tateiwa, J.-i.; Sonoda, M.; Hosomi, A. *J. Am. Chem. Soc.* **1998,** *120,* 11196–11197. doi:10.1021/ja9822557
55. Iannazzo, L.; Molander, G. A. *Eur. J. Org. Chem.* **2012,** 4923–4926. doi:10.1002/ejoc.201200767
56. Auer, G.; Weiner, B.; Oestreich, M. *Synthesis* **2006,** 2113–2116. doi:10.1055/s-2006-942405
57. Lee, K.-s.; Hoveyda, A. H. *J. Am. Chem. Soc.* **2010,** *132,* 2898–2900. doi:10.1021/ja910989n
58. Lee, K.-s.; Wu, H.; Haeffner, F.; Hoveyda, A. H. *Organometallics* **2012,** *31,* 7823–7826. doi:10.1021/om300790t
59. Pace, V.; Rae, J. P.; Harb, H. Y.; Procter, D. J. *Chem. Commun.* **2013,** *49,* 5150–5152. doi:10.1039/c3cc42160k
60. Pace, V.; Rae, J. P.; Procter, D. J. *Org. Lett.* **2014,** *16,* 476–479. doi:10.1021/ol4033623
61. Miyamoto, S.; Mori, A. *Neuroscience* **1985,** *11,* 1–8.
62. Zhang, L.; Liu, D.; Liu, Z.-Q. *Org. Lett.* **2015,** *17,* 2534–2537. doi:10.1021/acs.orglett.5b01067
63. Lan, Y.; Chang, X.-H.; Fan, P.; Shan, C.-C.; Liu, Z.-B.; Loh, T.-P.; Xu, Y.-H. *ACS Catal.* **2017,** *7,* 7120–7125. doi:10.1021/acscatal.7b02754
64. Plotzitzka, J.; Kleeberg, C. *Organometallics* **2014,** *33,* 6915–6926. doi:10.1021/om500989w
65. López, A.; Parra, A.; Jarava-Barrera, C.; Tortosa, M. *Chem. Commun.* **2015,** *51,* 17684–17687. doi:10.1039/c5cc06653k
66. Da, B.-C.; Liang, Q.-J.; Luo, Y.-C.; Ahmad, T.; Xu, Y.-H.; Loh, T.-P. *ACS Catal.* **2018,** *8,* 6239–6245. doi:10.1021/acscatal.8b01547
67. Ahmad, T.; Li, Q.; Qiu, S.-Q.; Xu, J.-L.; Xu, Y.-H.; Loh, T.-P. *Org. Biomol. Chem.* **2019,** *17,* 6122–6126. doi:10.1039/c9ob01086f
68. Mao, W.; Xue, W.; Irran, E.; Oestreich, M. *Angew. Chem., Int. Ed.* **2019,** *58,* 10723–10726. doi:10.1002/anie.201905934
69. Shen, J.-J.; Gao, Q.; Wang, G.; Tong, M.; Chen, L.; Xu, S. *ChemistrySelect* **2019,** *4,* 11358–11361. doi:10.1002/slct.201903570
70. Zhang, Y.; Tong, M.; Gao, Q.; Zhang, P.; Xu, S. *Tetrahedron Lett.* **2019,** *60,* 1210–1212. doi:10.1016/j.tetlet.2019.03.072
71. Lipshutz, B. H. *Curr. Opin. Green Sustainable Chem.* **2018,** *11,* 1–8. doi:10.1016/j.cogsc.2017.10.004
72. Lipshutz, B. H.; Gallou, F.; Handa, S. *ACS Sustainable Chem. Eng.* **2016,** *4,* 5838–5849. doi:10.1021/acssuschemeng.6b01810
73. Lipshutz, B. H.; Ghorai, S. *Green Chem.* **2014,** *16,* 3660–3679. doi:10.1039/c4gc00503a
74. Kitanosono, T.; Zhu, L.; Liu, C.; Xu, P.; Kobayashi, S. *J. Am. Chem. Soc.* **2015,** *137,* 15422–15425. doi:10.1021/jacs.5b11418
75. Tani, Y.; Fujihara, T.; Terao, J.; Tsuji, Y. *J. Am. Chem. Soc.* **2014,** *136,* 17706–17709. doi:10.1021/ja512040c
76. Zhang, Y.-Z.; Zhu, S.-F.; Wang, L.-X.; Zhou, Q.-L. *Angew. Chem., Int. Ed.* **2008,** *47,* 8496–8498. doi:10.1002/anie.200803192
77. Keipour, H.; Jalba, A.; Delage-Laurin, L.; Ollevier, T. *J. Org. Chem.* **2017,** *82,* 3000–3010. doi:10.1021/acs.joc.6b02998
78. Brandstadt, K.; Cook, S.; Nguyen, B. T.; Surgenor, A.; Taylor, R.; Tzou, M.-S. Copper Containing Hydrosilylation Catalysts and Compositions Containing the Catalysts. WO Patent 2013043792 A, March 28, 2013.
79. Gribble, M. W., Jr.; Pirnot, M. T.; Bandar, J. S.; Liu, R. Y.; Buchwald, S. L. *J. Am. Chem. Soc.* **2017,** *139,* 2192–2195. doi:10.1021/jacs.6b13029
80. Shi, Y.; Gao, Q.; Xu, S. *J. Org. Chem.* **2018,** *83,* 14758–14767. doi:10.1021/acs.joc.8b02308
81. Feng, J.-J.; Oestreich, M. *Org. Lett.* **2018,** *20,* 4273–4276. doi:10.1021/acs.orglett.8b01698
82. Feng, J.-J.; Oestreich, M. *Angew. Chem., Int. Ed.* **2019,** *58,* 8211–8215. doi:10.1002/anie.201903174
83. Yi, H.; Oestreich, M. *Chem. – Eur. J.* **2019,** *25,* 6505–6507. doi:10.1002/chem.201901128
84. Takeda, Y.; Shibuta, K.; Aoki, S.; Tohnai, N.; Minakata, S. *Chem. Sci.* **2019,** *10,* 8642–8647. doi:10.1039/c9sc02507c
85. Zhang, L.; Oestreich, M. *Chem. – Eur. J.* **2019,** *25,* 14304–14307. doi:10.1002/chem.201904272
86. Meng, F.-F.; Xie, J.-H.; Xu, Y.-H.; Loh, T.-P. *ACS Catal.* **2018,** *8,* 5306–5312. doi:10.1021/acscatal.8b00999
87. Lee, K.-s.; Zhugralin, A. R.; Hoveyda, A. H. *J. Am. Chem. Soc.* **2009,** *131,* 7253–7255. doi:10.1021/ja902889s
88. Ramírez, J.; Sanaú, M.; Fernández, E. *Angew. Chem., Int. Ed.* **2008,** *47,* 5194–5197. doi:10.1002/anie.200800541
89. Guo, W.-H.; Zhao, H.-Y.; Luo, Z.-J.; Zhang, S.; Zhang, X. *ACS Catal.* **2019,** *9,* 38–43. doi:10.1021/acscatal.8b02842
90. Lawson, Y. G.; Gerald Lesley, M. J.; Norman, N. C.; Rice, C. R.; Lawson, Y. G.; Marder, T. B. *Chem. Commun.* **1997,** 2051–2052. doi:10.1039/a705743a
91. Yang, L.; Uemura, N.; Nakao, Y. *J. Am. Chem. Soc.* **2019,** *141,* 7972–7979. doi:10.1021/jacs.9b03138
92. Hemming, D.; Fritzemeier, R.; Westcott, S. A.; Santos, W. L.; Steel, P. G. *Chem. Soc. Rev.* **2018,** *47,* 7477–7494. doi:10.1039/c7cs00816c
93. Ito, H.; Kawakami, C.; Sawamura, M. *J. Am. Chem. Soc.* **2005,** *127,* 16034–16035. doi:10.1021/ja056099x
94. Guzman-Martinez, A.; Hoveyda, A. H. *J. Am. Chem. Soc.* **2010,** *132,* 10634–10637. doi:10.1021/ja104254d
95. Yamamoto, E.; Takenouchi, Y.; Ozaki, T.; Miya, T.; Ito, H. *J. Am. Chem. Soc.* **2014,** *136,* 16515–16521. doi:10.1021/ja506284w
96. Zhong, C.; Kunii, S.; Kosaka, Y.; Sawamura, M.; Ito, H. *J. Am. Chem. Soc.* **2010,** *132,* 11440–11442. doi:10.1021/ja103783p
97. Kojima, R.; Akiyama, S.; Ito, H. *Angew. Chem., Int. Ed.* **2018,** *57,* 7196–7199. doi:10.1002/anie.201803663
98. Dang, L.; Zhao, H.; Lin, Z.; Marder, T. B. *Organometallics* **2007,** *26,* 2824–2832. doi:10.1021/om070103r
99. Xi, Y.; Hartwig, J. F. *J. Am. Chem. Soc.* **2016,** *138,* 6703–6706. doi:10.1021/jacs.6b02478

100. Xi, Y.; Hartwig, J. F. *J. Am. Chem. Soc.* **2017,** *139,* 12758–12772. doi:10.1021/jacs.7b07124
101. Guisán-Ceinos, M.; Parra, A.; Martín-Heras, V.; Tortosa, M. *Angew. Chem., Int. Ed.* **2016,** *55,* 6969–6972. doi:10.1002/anie.201601976
102. Jarava-Barrera, C.; Parra, A.; López, A.; Cruz-Acosta, F.; Collado-Sanz, D.; Cárdenas, D. J.; Tortosa, M. *ACS Catal.* **2016,** *6,* 442–446. doi:10.1021/acscatal.5b02742
103. Su, W.; Gong, T.-J.; Lu, X.; Xu, M.-Y.; Yu, C.-G.; Xu, Z.-Y.; Yu, H.-Z.; Xiao, B.; Fu, Y. *Angew. Chem., Int. Ed.* **2015,** *54,* 12957–12961. doi:10.1002/anie.201506713
104. Jia, T.; Cao, P.; Wang, B.; Lou, Y.; Yin, X.; Wang, M.; Liao, J. *J. Am. Chem. Soc.* **2015,** *137,* 13760–13763. doi:10.1021/jacs.5b09146
105. Jiang, L.; Cao, P.; Wang, M.; Chen, B.; Wang, B.; Liao, J. *Angew. Chem., Int. Ed.* **2016,** *55,* 13854–13858. doi:10.1002/anie.201607493
106. Chen, B.; Cao, P.; Liao, Y.; Wang, M.; Liao, J. *Org. Lett.* **2018,** *20,* 1346–1349. doi:10.1021/acs.orglett.7b03860
107. Yang, Y. *Angew. Chem., Int. Ed.* **2016,** *55,* 345–349. doi:10.1002/anie.201508294
108. Wu, N.-Y.; Xu, X.-H.; Qing, F.-L. *ACS Catal.* **2019,** *9,* 5726–5731. doi:10.1021/acscatal.9b01530
109. Gan, X.-C.; Zhang, Q.; Jia, X.-S.; Yin, L. *Org. Lett.* **2018,** *20,* 1070–1073. doi:10.1021/acs.orglett.7b04039
110. Li, X.; Meng, F.; Torker, S.; Shi, Y.; Hoveyda, A. H. *Angew. Chem., Int. Ed.* **2016,** *55,* 9997–10002. doi:10.1002/anie.201605001
111. Jia, T.; He, Q.; Ruscoe, R. E.; Pulis, A. P.; Procter, D. J. *Angew. Chem., Int. Ed.* **2018,** *57,* 11305–11309. doi:10.1002/anie.201806169
112. Zhao, W.; Montgomery, J. *J. Am. Chem. Soc.* **2016,** *138,* 9763–9766. doi:10.1021/jacs.6b05216
113. Zhao, W.; Montgomery, J. *Angew. Chem., Int. Ed.* **2015,** *54,* 12683–12686. doi:10.1002/anie.201507303
114. Kim, H. K.; Mane, M. V.; Montgomery, J.; Baik, M.-H. *Chem. – Eur. J.* **2019,** *25,* 9456–9463. doi:10.1002/chem.201900673
115. Bergmann, A. M.; Dorn, S. K.; Smith, K. B.; Logan, K. M.; Brown, M. K. *Angew. Chem., Int. Ed.* **2019,** *58,* 1719–1723. doi:10.1002/anie.201812533
116. Semba, K.; Ohtagaki, Y.; Nakao, Y. *Org. Lett.* **2016,** *18,* 3956–3959. doi:10.1021/acs.orglett.6b01675
117. Logan, K. M.; Smith, K. B.; Brown, M. K. *Angew. Chem., Int. Ed.* **2015,** *54,* 5228–5231. doi:10.1002/anie.201500396
118. Logan, K. M.; Brown, M. K. *Angew. Chem., Int. Ed.* **2017,** *56,* 851–855. doi:10.1002/anie.201609844
119. Huang, Y.; Smith, K. B.; Brown, M. K. *Angew. Chem., Int. Ed.* **2017,** *56,* 13314–13318. doi:10.1002/anie.201707323
120. Smith, K. B.; Huang, Y.; Brown, M. K. *Angew. Chem., Int. Ed.* **2018,** *57,* 6146–6149. doi:10.1002/anie.201801139
121. Yang, Y.; Perry, I. B.; Buchwald, S. L. *J. Am. Chem. Soc.* **2016,** *138,* 9787–9790. doi:10.1021/jacs.6b06299
122. Smith, J. J.; Best, D.; Lam, H. W. *Chem. Commun.* **2016,** *52,* 3770–3772. doi:10.1039/c6cc00603e
123. Itoh, T.; Kanzaki, Y.; Shimizu, Y.; Kanai, M. *Angew. Chem., Int. Ed.* **2018,** *57,* 8265–8269. doi:10.1002/anie.201804117
124. Sakae, R.; Hirano, K.; Satoh, T.; Miura, M. *Angew. Chem.* **2015,** *127,* 623–627. doi:10.1002/ange.201409104
125. Iwadate, N.; Suginome, M. *J. Am. Chem. Soc.* **2010,** *132,* 2548–2549. doi:10.1021/ja1000642
126. Sakae, R.; Hirano, K.; Miura, M. *J. Am. Chem. Soc.* **2015,** *137,* 6460–6463. doi:10.1021/jacs.5b02775
127. Butcher, T. W.; McClain, E. J.; Hamilton, T. G.; Perrone, T. M.; Kroner, K. M.; Donohoe, G. C.; Akhmedov, N. G.; Petersen, J. L.; Popp, B. V. *Org. Lett.* **2016,** *18,* 6428–6431. doi:10.1021/acs.orglett.6b03326
128. Ito, H.; Yamanaka, H.; Tateiwa, J.-i.; Hosomi, A. *Tetrahedron Lett.* **2000,** *41,* 6821–6825. doi:10.1016/s0040-4039(00)01161-8
129. Ding, W.; Song, Q. *Org. Chem. Front.* **2016,** *3,* 14–18. doi:10.1039/c5qo00289c
130. Sole, C.; Fernández, E. *Chem. – Asian J.* **2009,** 1790–1793. doi:10.1002/asia.200900311
131. Molander, G. A.; McKee, S. A. *Org. Lett.* **2011,** *13,* 4684–4687. doi:10.1021/ol201900d
132. Molander, G. A.; Wisniewski, S. R.; Hosseini-Sarvari, M. *Adv. Synth. Catal.* **2013,** *355,* 3037–3057. doi:10.1002/adsc.201300640
133. Lauberteaux, J.; Crévisy, C.; Baslé, O.; de Figueiredo, R. M.; Mauduit, M.; Campagne, J.-M. *Org. Lett.* **2019,** *21,* 1872–1876. doi:10.1021/acs.orglett.9b00479
134. Laitar, D. S.; Tsui, E. Y.; Sadighi, J. P. *J. Am. Chem. Soc.* **2006,** *128,* 11036–11037. doi:10.1021/ja064019z
135. Kubota, K.; Yamamoto, E.; Ito, H. *J. Am. Chem. Soc.* **2015,** *137,* 420–424. doi:10.1021/ja511247z
136. Kubota, K.; Osaki, S.; Jin, M.; Ito, H. *Angew. Chem., Int. Ed.* **2017,** *56,* 6646–6650. doi:10.1002/anie.201702826
137. McIntosh, M. L.; Moore, C. M.; Clark, T. B. *Org. Lett.* **2010,** *12,* 1996–1999. doi:10.1021/ol100468f
138. Ishiyama, T.; Murata, M.; Miyaura, N. *J. Org. Chem.* **1995,** *60,* 7508–7510. doi:10.1021/jo00128a024
139. Yang, C.-T.; Zhang, Z.-Q.; Tajuddin, H.; Wu, C.-C.; Liang, J.; Liu, J.-H.; Fu, Y.; Czyzewska, M.; Steel, P. G.; Marder, T. B.; Liu, L. *Angew. Chem., Int. Ed.* **2012,** *51,* 528–532. doi:10.1002/anie.201106299
140. Akiyama, S.; Kubota, K.; Mikus, M. S.; Paioti, P. H. S.; Romiti, F.; Liu, Q.; Zhou, Y.; Hoveyda, A. H.; Ito, H. *Angew. Chem., Int. Ed.* **2019,** *58,* 1–6. doi:10.1002/anie.201983561
141. Ito, H.; Kubota, K. *Org. Lett.* **2012,** *14,* 890–893. doi:10.1021/ol203413w
142. Bose, S. K.; Brand, S.; Omoregie, H. O.; Haehnel, M.; Maier, J.; Bringmann, G.; Marder, T. B. *ACS Catal.* **2016,** *6,* 8332–8335. doi:10.1021/acscatal.6b02918
143. Iwamoto, H.; Endo, K.; Ozawa, Y.; Watanabe, Y.; Kubota, K.; Imamoto, T.; Ito, H. *Angew. Chem., Int. Ed.* **2019,** *58,* 11112–11117. doi:10.1002/anie.201906011
144. Wang, J.; Shang, M.; Lundberg, H.; Feu, K. S.; Hecker, S. J.; Qin, T.; Blackmond, D. G.; Baran, P. S. *ACS Catal.* **2018,** *8,* 9537–9542. doi:10.1021/acscatal.8b02928
145. Mao, L.; Szabó, K. J.; Marder, T. B. *Org. Lett.* **2017,** *19,* 1204–1207. doi:10.1021/acs.orglett.7b00256

License and Terms

BEILSTEIN JOURNAL OF ORGANIC CHEMISTRY

Copper catalysis with redox-active ligands

Agnideep Das[1], Yufeng Ren[2], Cheriehan Hessin[1] and Marine Desage-El Murr[*1]

Review

Open Access

Address:
[1]Université de Strasbourg, Institut de Chimie, UMR CNRS 7177, 67000 Strasbourg, France and [2]Sorbonne Université, Institut Parisien de Chimie Moléculaire, UMR CNRS 8232, 75005 Paris, France

Email:
Marine Desage-El Murr[*] - desageelmurr@unistra.fr

* Corresponding author

Keywords:
bioinspired catalysis; biomimetic copper complexes; cooperative catalysis; redox-active ligands; redox catalysis

Beilstein J. Org. Chem. **2020,** *16,* 858–870.
doi:10.3762/bjoc.16.77

Received: 20 January 2020
Accepted: 08 April 2020
Published: 24 April 2020

This article is part of the thematic issue "Copper-catalyzed reactions for organic synthesis".

Guest Editor: G. Evano

Abstract

Copper catalysis finds applications in various synthetic fields by utilizing the ability of copper to sustain mono- and bielectronic elementary steps. Further to the development of well-defined copper complexes with classical ligands such as phosphines and N-heterocyclic carbenes, a new and fast-expanding area of research is exploring the possibility of a complementing metal-centered reactivity with electronic participation by the coordination sphere. To achieve this electronic flexibility, redox-active ligands can be used to engage in a fruitful “electronic dialogue” with the metal center, and provide additional venues for electron transfer. This review aims to present the latest results in the area of copper-based cooperative catalysis with redox-active ligands.

Introduction

Interaction of earth-abundant metals, such as copper, with radical ligands is originally known from biological systems such as metalloenzymes [1]. Among the myriad of existing enzymes, galactose oxidase (GAO) is a copper-based enzyme performing the two-electron oxidation of galactose through a mechanism involving the metal and a neighboring tyrosine radical ligand for the shuttling of overall two protons and two electrons. This peculiar mechanism is enabled by transient storage of electronic density on the tyrosine ligands and perfectly illustrates the central role of ancillary pro-radical ligands in biological systems. Among other tasks, copper enzymes are known to be actively involved in electron transfer as exemplified by blue copper enzymes, which have captured the interest of chemists and biochemists. Copper can also cooperate with iron to perform activation of O_2 and nitrogen oxides (NO_x) in cytochrome c oxidases [2,3]. Inspired by the broad chemical repertoire of radical-ligand containing metalloenzymes, chemists have developed redox-active ligands as surrogates for the biologically occurring redox cofactors and this has translated into active developments in homogeneous catalysis [4]. The unique electronic interaction due to matching or inverted energy levels between metal and ligand leads to valence tautomerism [5-8], which paves the way for orchestrated electronic events occurring within the metal complex and influences the chemical reactivity of the complex. While the field of catalysis with redox-active ligands is itself a much broader area, we shall limit our discussion to copper catalysis with redox-active ligands and the present review aims at provid-

ing an overview of the relevant literature on this topic over the last three decades.

Review

Oxidation: C–O bond formation

The central role of copper intermediates in oxidation reactions in biological systems is very well documented [9]. It is therefore not surprising that this would be an area of choice for the development of bioinspired and/or redox-active copper complexes.

Inspired by the pioneering works by Stack [10], Wieghardt and Chaudhuri on GAO mimics [11-13], Safaei and Storr have reported Cu(II) complexes bearing a non-innocent amidophenolate type benzoxazole ligand which was fully characterized by X-ray crystallography and other spectroscopic techniques (Scheme 1) [14]. These complexes were found to perform the aerobic catalytic oxidation of alcohols into aldehydes, thus mimicking the reactivity of galactose oxidase. Complexes **1** and **2**, exhibiting a twisted tetracoordinated geometry, and a distorted square pyramidal geometry, respectively, were used in alcohol oxidation on a wide variety of mostly aromatic alcohols in the presence of base (Cs_2CO_3). The results suggested that **2** is more efficient than **1** and this reactivity difference could be attributed to an increased stabilization of the involved reactive catalytic intermediates by the electron-donating acetate ions present in complex **2**.

The same team later reported on another family of galactose oxidase mimics based on copper(II) complex **4** bearing a non-innocent iminophenol-iminopyridine hybrid ligand **3** that performed two-electron oxidations of primary alcohols to alde-

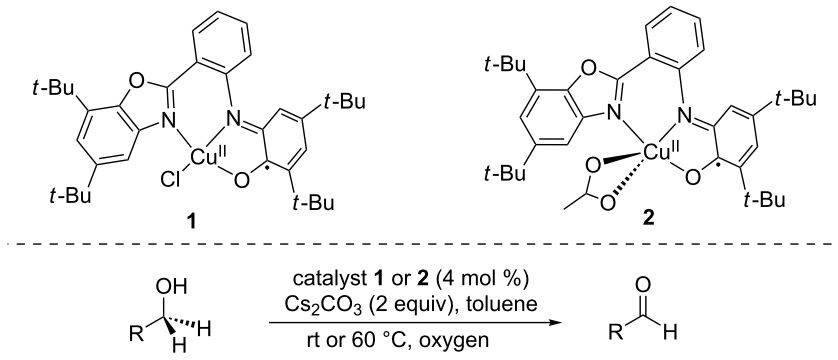

Scheme 1: Copper complexes with amidophenolate type benzoxazole ligands for alcohol oxidations.

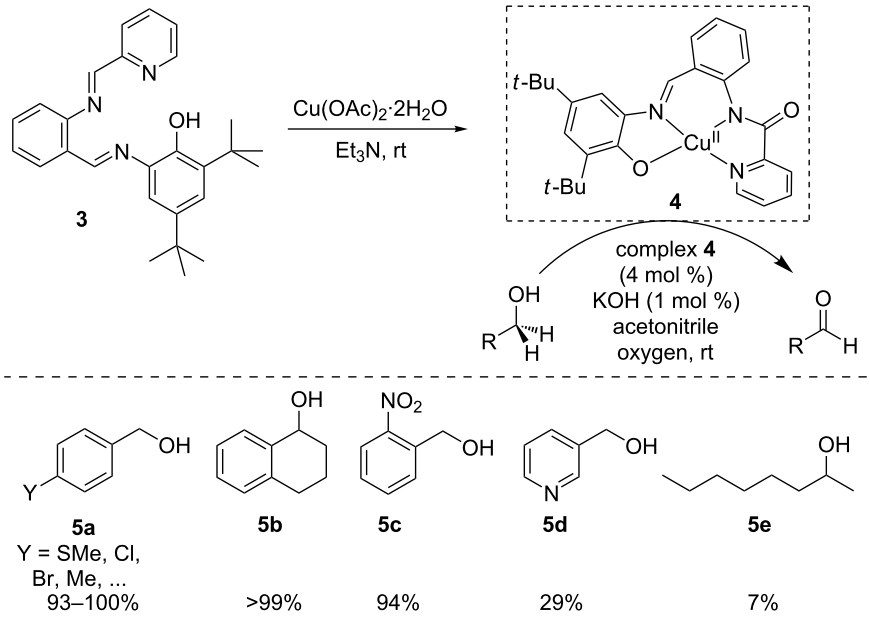

Scheme 2: Copper-catalyzed aerobic oxidation of alcohols and representative substrate scope.

hydes (Scheme 2) [15]. Catalyst **4** was fully characterized by combined EPR, cyclic voltammetry and electronic spectroscopic studies to reveal two quasi-reversible one-electron redox processes, including a ligand-centered oxidation generating a Cu^{II}-phenoxyl radical species, thus suggesting the electronic participation of the ligand in the redox processes. This catalyst is efficient in the oxidation of a large number of alcohols (**5a–e**) in the presence of base (KOH 1 mol %).

An interesting strategy aiming to explore the possibility of interfacing the redox-activity with H-bonding ability inside the ligand coordination sphere has been disclosed by Swart and Garcia-Bosch [16], and relies on the design and study of a new copper(II) complex. A family of *o*-phenylenediamido ligands was synthesized through the introduction of ureanyl groups, using a synthetic approach developed by Borovik [17,18] for the stabilization of metal–oxo and metal–hydroxo complexes via intramolecular H-bonding interactions. The resulting copper complexes were synthesized and single crystal X-ray diffraction analysis evidenced the existence of H-bonding inside the coordination sphere of **6** (Scheme 3). The authors reported that the influence of the geometry of the complex on the H-bonding interactions as well as the nature of this interaction greatly affected the chemical properties. They also reported that complexes that had higher oxidation potential and went through irreversible oxidation were not good catalysts for the oxidation

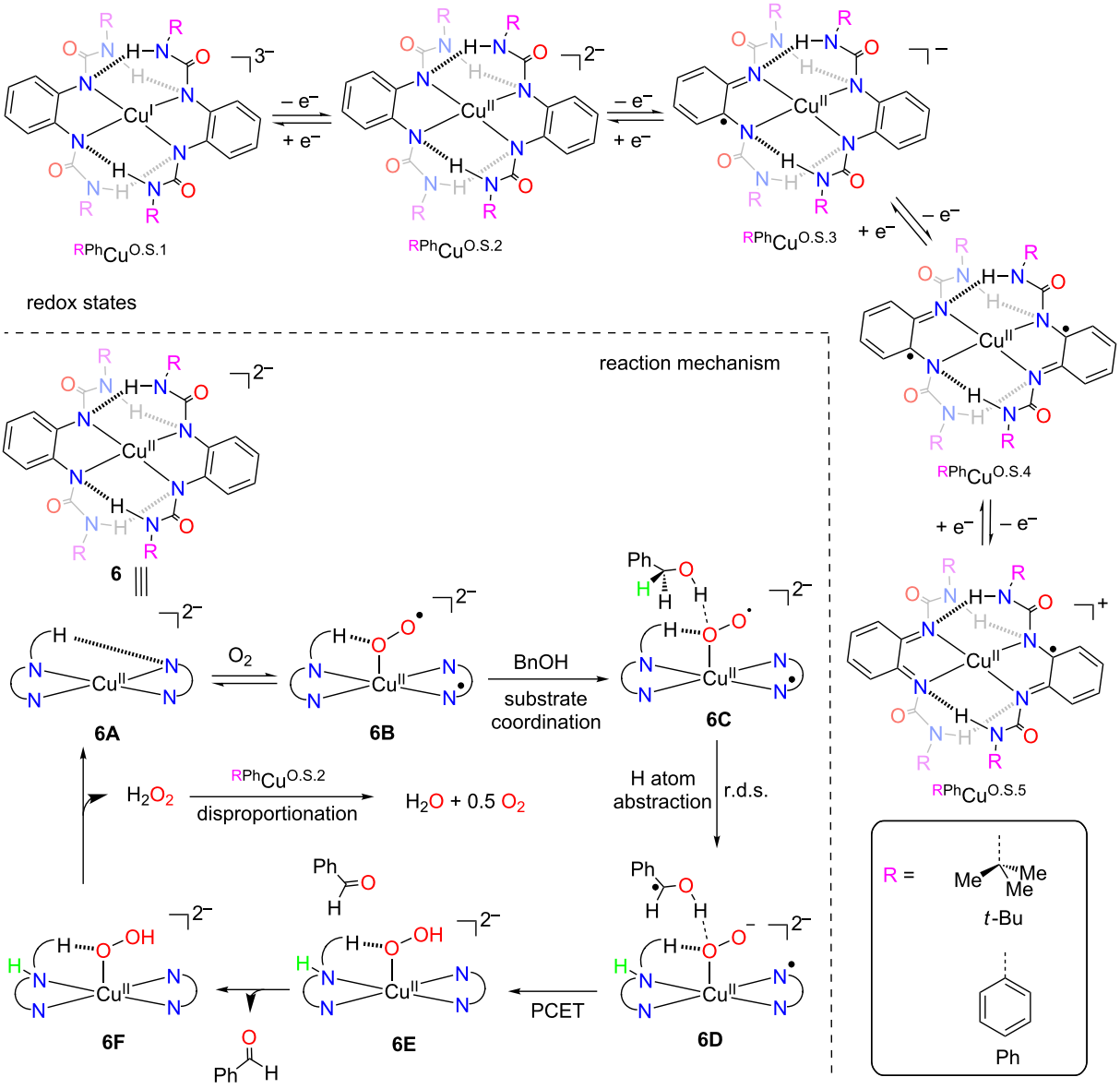

Scheme 3: Introduction of H-bonding network in the ligand coordination sphere.

of benzyl alcohol to benzaldehyde (0–30% yields, e.g., $^{PhPh}Cu^{O.S.2}$, O.S.*x* signifies oxidation state and *x* increases with the removal of electrons). On the other hand, complex $^{t\text{-}BuPh}Cu^{O.S.2}$, showing a reversible oxidation behavior very efficiently performs dehydrogenation of benzyl alcohol with low catalyst loading (0.1 mol %) and high turnover numbers (TONs up to 184). Besides the oxidation of benzyl alcohol to benzaldehyde, the authors also show that reaction with $^{t\text{-}BuPh}Cu^{O.S.2}$ (5 mol %) could be efficiently extended to other substrates containing weak C–H bonds and acidic O–H bonds such as diphenylmethanol (PhBzOH), benzoin, and cinnamyl alcohol. However, alcohols with stronger C–H bonds (cyclohexanol) and more basic O–H bonds (1-phenylethanol, MeBzOH) were either not oxidized at all, or in very low yields.

Relying on a combination of kinetic and computational studies, the authors propose a detailed mechanistic overview (Scheme 3) for the transformation. A proposed model mechanism involves reaction of Cu^{II} complex **6A** with dioxygen to generate a Cu^{II} superoxide intermediate **6B**. The electron needed to reduce O_2 to superoxide is provided by the redox-active ligand. Subsequent coordination of benzyl alcohol results in the formation of species **6C**, which undergoes a H-atom abstraction step to form **6D**, in which the H-atom is transferred from the secondary benzylic sp^3 carbon to the redox-active ligand, acting as a cooperative H-atom acceptor. Following a proton-coupled electron transfer (PCET) to generate **6E**, the oxidized product (benzaldehyde) is released and final elimination of H_2O_2 regenerates the active catalyst, thus closing the catalytic cycle. Interestingly, this catalytic behavior involving participation of the ligand framework to release electrons and store an H-atom is reminiscent of the galactose oxidase copper enzyme.

A recent investigation by Martins, Davidovich and co-workers reports on copper complexes of the redox-active Schiff-base isatin bearing various functional groups (Scheme 4) [19]. The main feature of these ligands is their ability to form four distinct and well-defined types of complexes depending on the reaction conditions (i.e., the number of equivalents of metal precursor, solvent, etc.). These complexes performed the oxidation of benzyl alcohol into benzaldehyde and the results suggested that the optimization of the ligand structures by the introduction of different substitutions leads to better catalytic efficiency. The redox behavior of the ligands and complexes was investigated through electrochemical studies and suggested to proceed via an electrochemical chemical event (EC) including reversible electrochemical and irreversible chemical steps. The authors also observed a diminished stability of the complexes upon reduc-

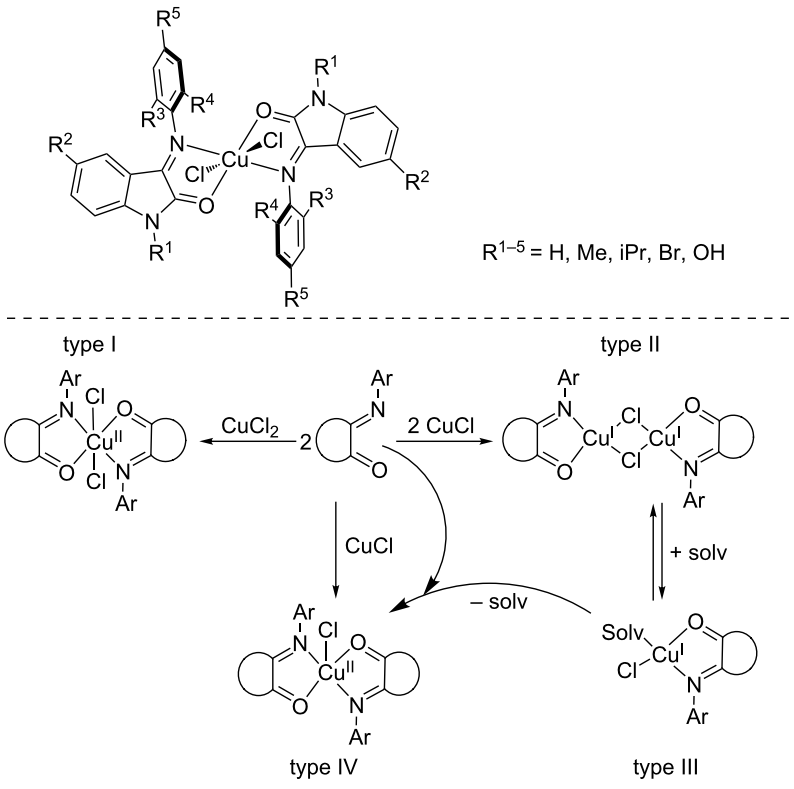

Scheme 4: Well-defined isatin copper complexes.

tion, and this low redox stability could be circumvented through ligand modification.

Phenol oxidation is ubiquitous in biological systems as demonstrated by the involvement of the copper enzymes tyrosinases (type III) in the melanogenesis process. The regioselectivity and reactivity of the oxidation of phenols are strongly dependent on the phenol substrate substitution pattern, and it is therefore difficult to develop general methods for this transformation. This substrate–control bias was successfully outmaneuvered by the development of a copper-based catalytic system operating under aerobic conditions and allowing selective access to benzoxepines and 2,2'-biphenols through catalyst control (Scheme 5, top) [20].

Extensive mechanistic studies evidenced a biomimetic pathway involving a key Cu^{II}-semiquinone intermediate in which the substrate becomes activated as a redox-active ligand (Scheme 5, bottom) [21]. This radical Cu^{II} species is the catalyst resting state and is accessed starting from a dinuclear side-on peroxodicopper(II) intermediate, thus closely mimicking copper tyrosinases [22,23]. Interestingly, further studies have focused on a

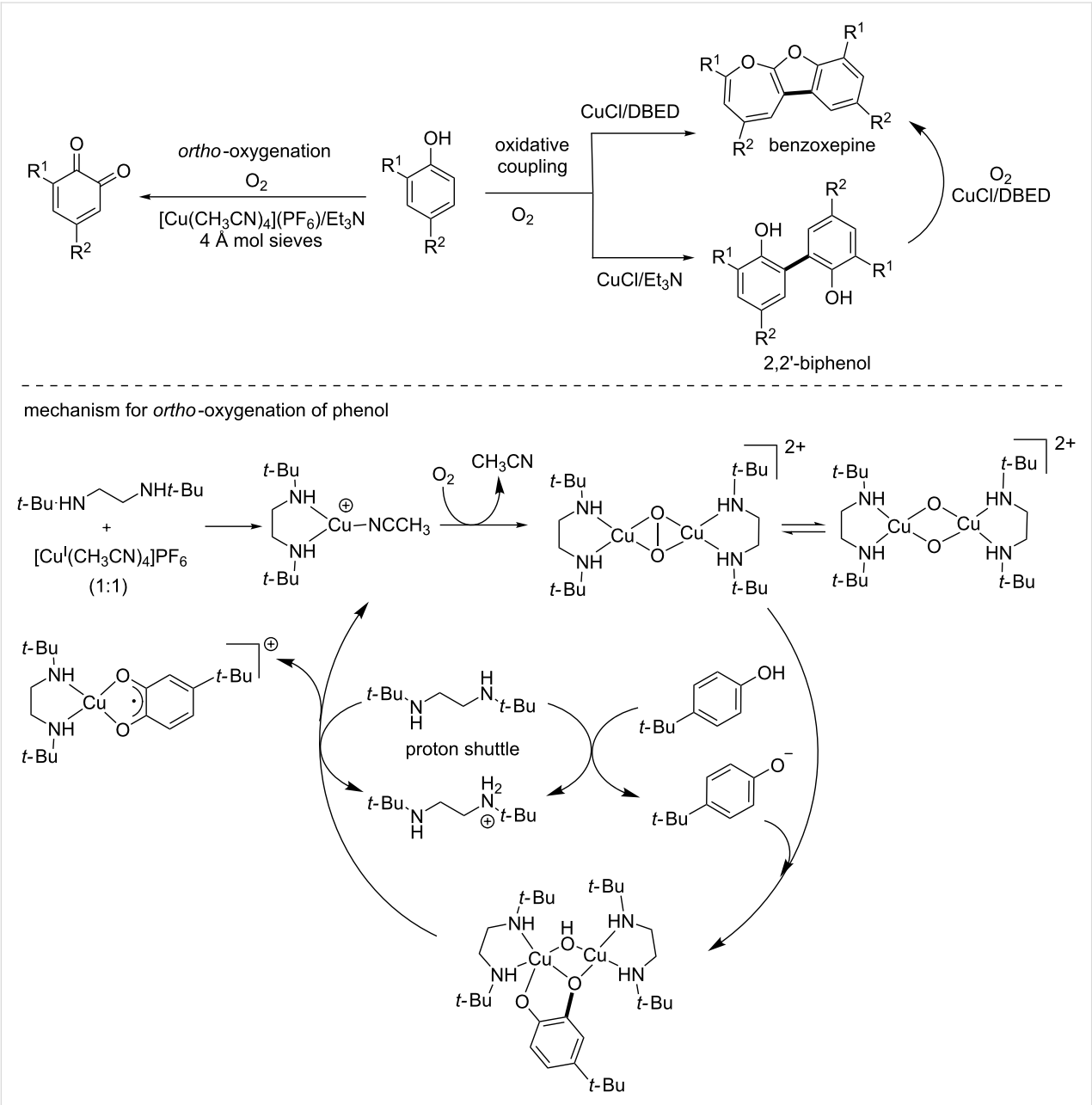

Scheme 5: Catalyst control in the biomimetic phenol *ortho*-oxidation.

closely related combination of copper salt, diamine (DBED: *N*,*N*'-di-*tert*-butylethylenediamine) for the oxidation of benzyl alcohol to benzaldehyde and shown that under aerobic conditions, the system leads to the formation of a nitroxyl radical on the DBED moiety [24]. This newly formed radical acts as a redox-active cocatalyst in the oxidation reaction, which has previously been reported with TEMPO (2,2,6,6-tetramethyl-1-piperidine *N*-oxyl) [25] and ABNO (9-azabicyclo[3.3.1]nonane *N*-oxyl) radicals [26]. Later reports enlarged the synthetic scope of this methodology and provided access to a wide range of synthetically useful building blocks such as substituted heterocycles, fluorinated phenols, ketones and 1,3-dienes (Scheme 6) [27].

C–C bond formation

Complexes of radical and redox-active ligands with transition metals are known to be able to promote radical reactions through single-electron transfer (SET) processes [28]. Expanding on the research area pioneered by Wieghardt and Chaudhuri [11-13] using well-defined copper complex **7**, originally reported as a GAO mimic [20-22], we showed that this ability could be extended to the catalytic generation of trifluoromethyl radicals (Scheme 7) [29]. The synthetic efficiency of complex **7** in trifluoromethylation was reported on a wide variety of substrates including silyl enol ethers, heteroaromatics and alkynes using an electrophilic CF_3^+ source (**8** or **9**), opening new opportunities to access pharmaceutically relevant trifluoromethylated products under mild reaction conditions. The ligand-based SET step involved the iminosemiquinone redox-active ligand which was oxidized to iminobenzoquinone.

The Canary group [30] reported a redox-reconfigurable copper catalyst that exhibits reversal of its helical chirality through redox stimuli (Scheme 8). Combining L-methionine and catalytic urea groups with two different copper salts as precursors affords both enantiomers Δ-**10** (from $CuClO_4$) and Λ-**10** from ($Cu(CH_3CN)_4PF_6$). UV–vis and circular dichroism spectroscopic studies evidence that the helical chirality exhibited by these two catalysts could be reversed by redox stimuli. These complexes could perform enantioselective Michael addition between diethyl malonate and nitrostyrene to afford only one of the two (*S*)-**11** and (*R*)-**11** enantiomers, depending on the redox state of the copper center. The reaction was run with a 5 mol % catalyst loading and a base (Et_3N) and was compatible with different solvents (THF, MeCN, CH_2Cl_2 and hexane). Acetonitrile gave the highest yield (55%) and ee (72%) of product

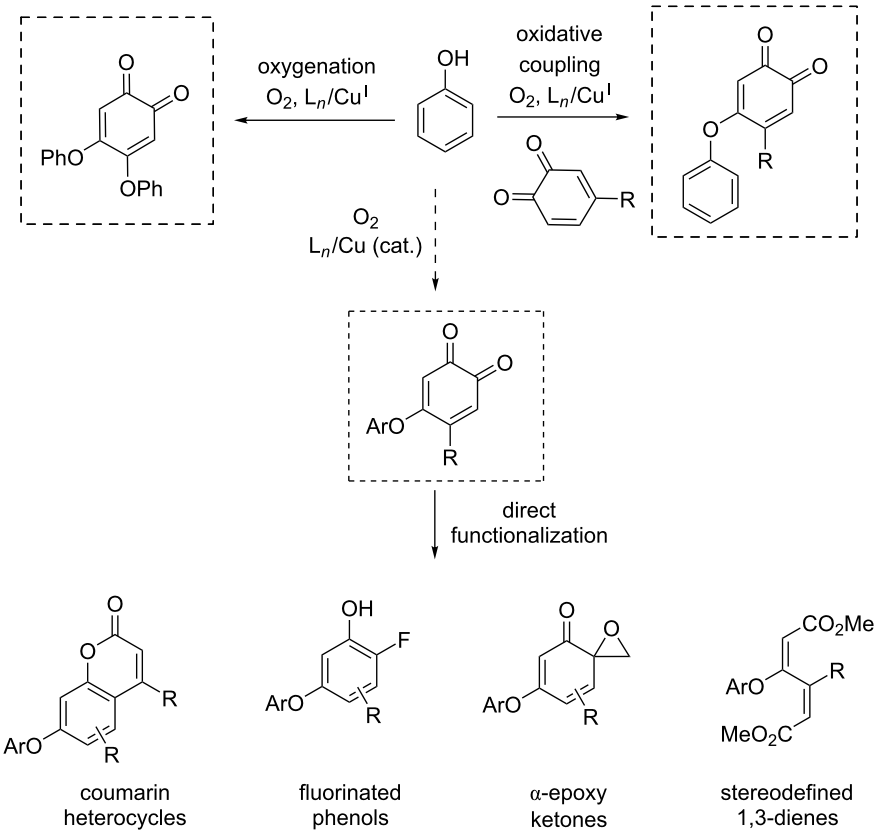

Scheme 6: Structural diversity accessible by direct functionalization.

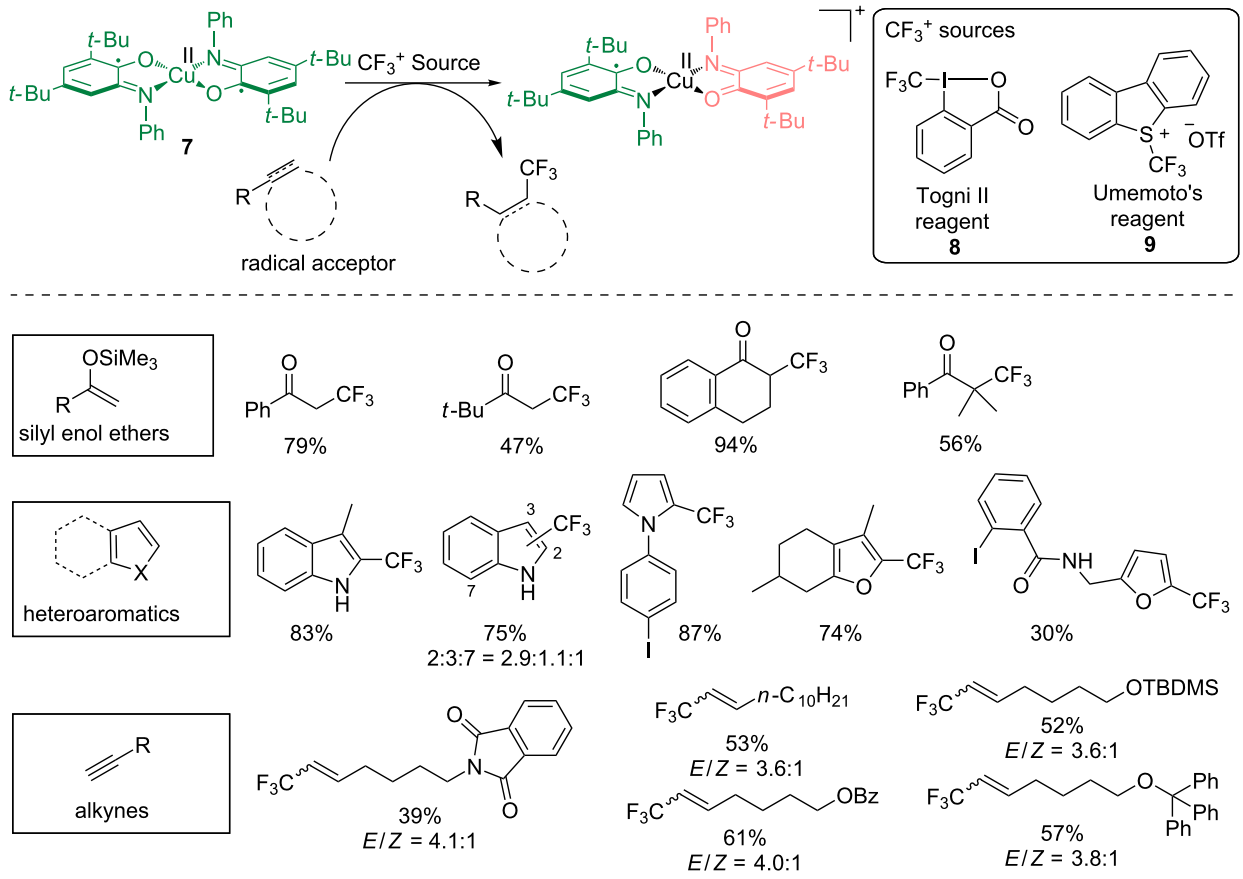

Scheme 7: Copper-catalyzed trifluoromethylation of heteroaromatics with redox-active iminosemiquinone ligands.

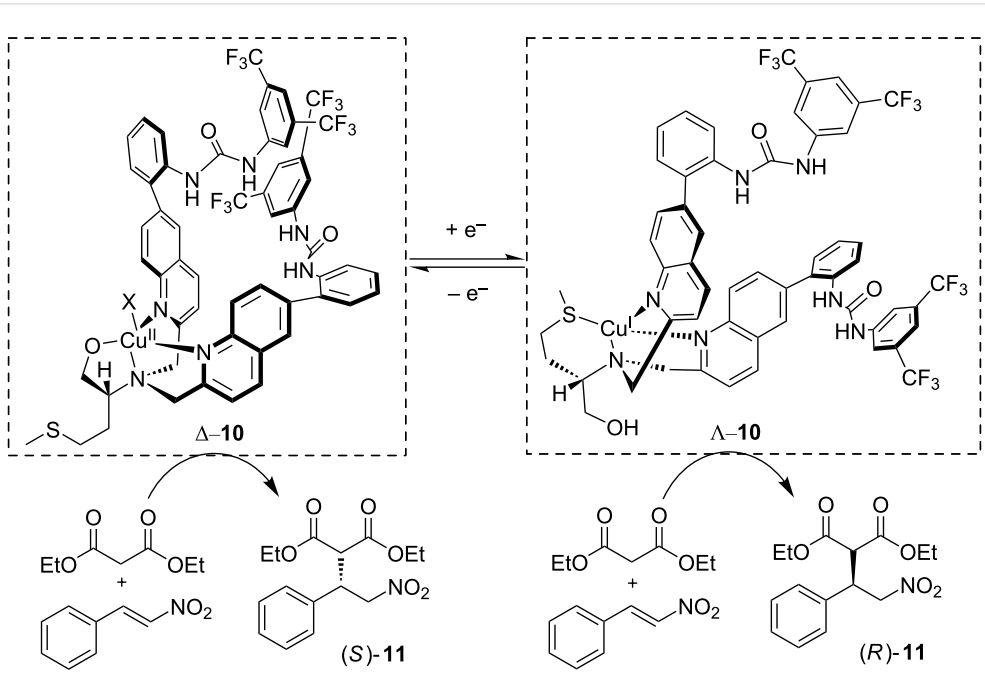

Scheme 8: Reversal of helical chirality upon redox stimuli and enantioselective Michael addition with a redox-reconfigurable copper catalyst.

(*S*)-**11** in presence of Λ-**10** as catalyst. While the free ligand is found to catalyze the reaction, the authors show that the templating effect of the copper ion is necessary to sustain enantioselectivity.

Himmel and co-workers have reported the use of copper(I) complexes bearing redox-active guanidine ligands **12** for catalytic aerobic homo- and cross-coupling of phenols with dioxygen as oxidation source (Scheme 9). This strategy allowed access to nonsymmetrical biphenols and the best results were obtained with dinuclear complex **13** incorporating two copper(I) centers. These specific quinidine ligands have the ability to supply electrons to the metal center thanks to their low oxidation potential and can shuttle up to two electrons to the copper centers. The specific geometry of this ligand also has an influence on the rate of electron transfer through a "structural harmonization" between the Cu^{II} and Cu^{I} redox states through an entatic state geometry [31,32]. According to the authors' findings, **13** initially reacts with dioxygen to generate an unstable bis-μ-oxo-complex intermediate **13*** which is the active species during the catalytic cycle for the C–C coupling. The coupling reaction follows a radical–anion mechanism due

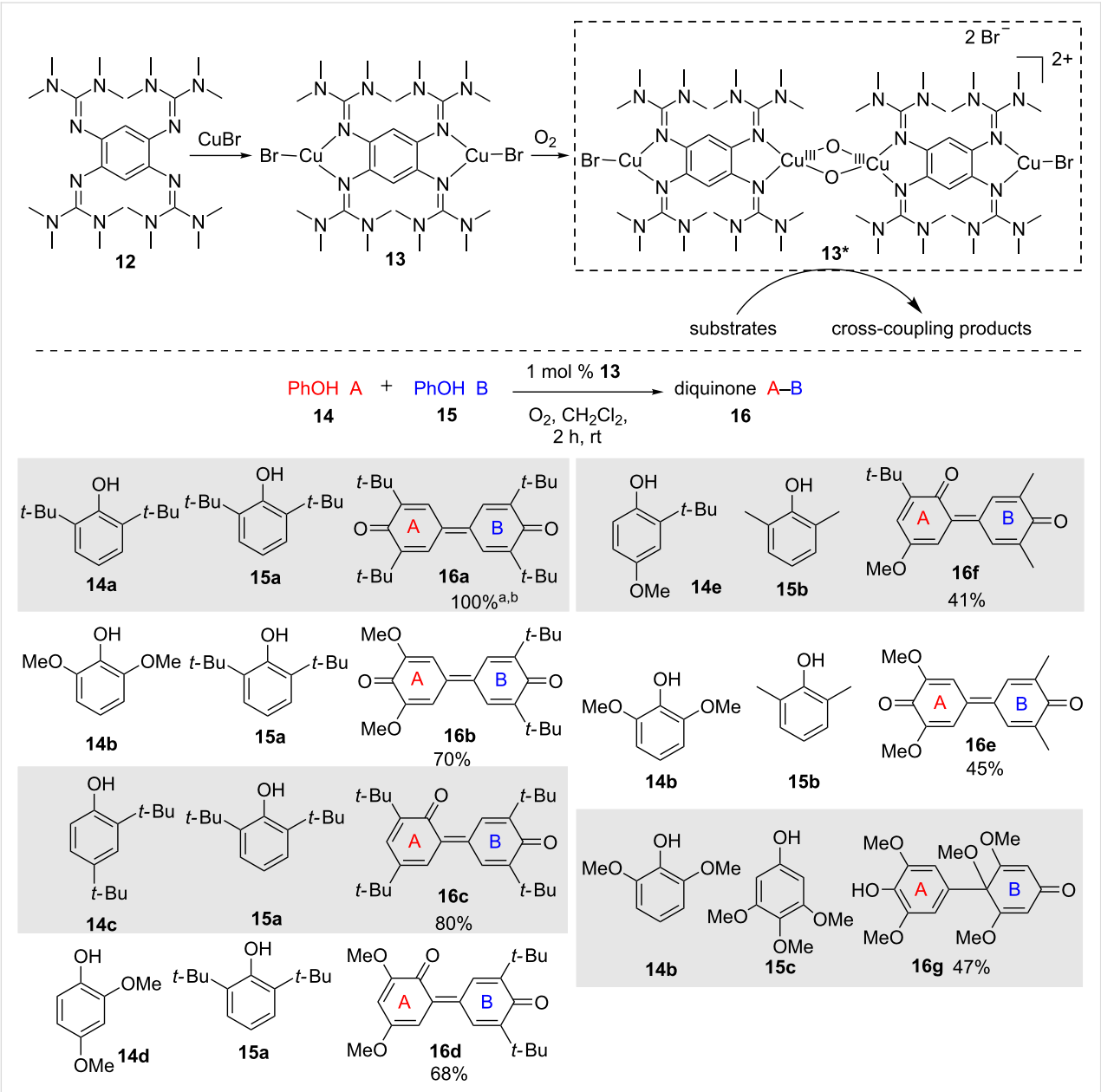

Scheme 9: Interaction of guanidine-copper catalyst with oxygen and representative coupling products. [a]4 mol % catalyst loading, [b]homo-coupling adduct.

to the presence of electron-donating ligand **12** and this is the key feature allowing preferential binding of the phenoxyl radicals for PCET. Products arising from homo- and heterocouplings were formed with high selectivity. Homo- and cross-coupling adducts **16a** and **16b–g** were obtained from the corresponding phenols (**14a–e** and **15a–c**) as shown in the bottom of Scheme 9 with high chemoselectivity.

C–N bond formation

While copper complexes are at the heart of oxidative biological networks, the introduction of nitrogen is a different matter. The Arnold group has elegantly shown that through iterative mutagenesis "directed evolution" enzymes can be coaxed to perform unnatural transformations such as C–N bond forming aziridination, which has no biological counterpart [33]. While the exact structure of the mutant metalloenzymatic active site was not characterized in detail, it might bear some resemblance to the original biological active site.

Building on their previously discussed phenol oxidation methodology (Scheme 5 and Scheme 6), Lumb and co-workers have targeted subsequent C–N bond formation to access oxindoles [34], and perform C–H functionalization through aerobic dearomatization of phenols [35]. These broad synthetic outcomes further led to a unified approach for the preparation of 1,2-oxy-aminoarenes by phenol–amine couplings (Scheme 10) [36].

We reported the formation of a C–N bond through copper-catalyzed aziridination with redox-active complex $Cu(SQ)_2$ **17** [37], originally developed as a GAO mimic. The reaction worked very efficiently under ambient conditions with *N*-tosyliminobenzyliodinane (PhINTs) as a nitrene source. The reaction mechanism was proposed to involve a transient mono-nitrene Cu^{II} intermediate **18** in equilibrium with a spectator bis-nitrene species **19** and proceeded through styrene **20** insertion, followed by ring closure and release of the aziridine. Interestingly, this otherwise classical mechanism is enabled by the accessibility of doublet and quadruplet states close in energy and this molecular spin catalysis is reminiscent of the multistate reactivity observed at the metal center, for example in heme enzymes [38,39]. A wide range of substrates could be converted including mono-substituted aziridines (**21a**, **21b** and **21j**), disubstituted aziridines (**21c–h** and **21l**,**m**), and more challenging scaffolds such as gem-disubstituted (**21k**) and trisubstituted (**21i** and **21n**,**o**) aziridines (Scheme 11). Furthermore, the reaction conditions are compatible with aldehyde, ester or ketone functions.

Metalloenzymes routinely rely on 3d metals and amino acid-derived coordination spheres to perform complex (multi)electronic transformations of paramount importance in atom transfer reactions and activation of small molecules. To do so, metalloenzymes have acquired many evolutionary reactivity-enhancing tools that enable efficient chemical processes. Among these tools, the entatic state model relies on the fact that

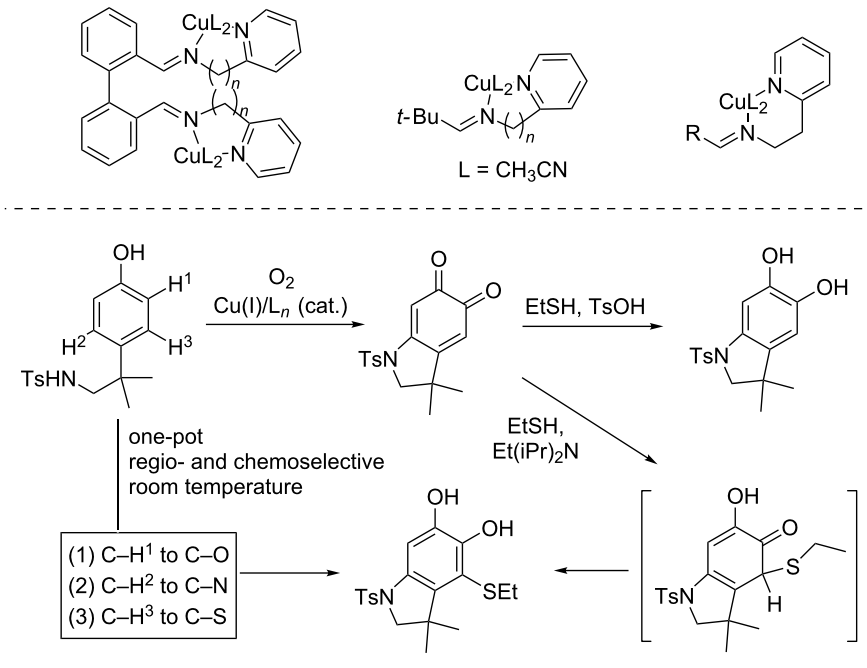

Scheme 10: Access to 1,2-oxy-aminoarenes by copper-catalyzed phenol–amine coupling.

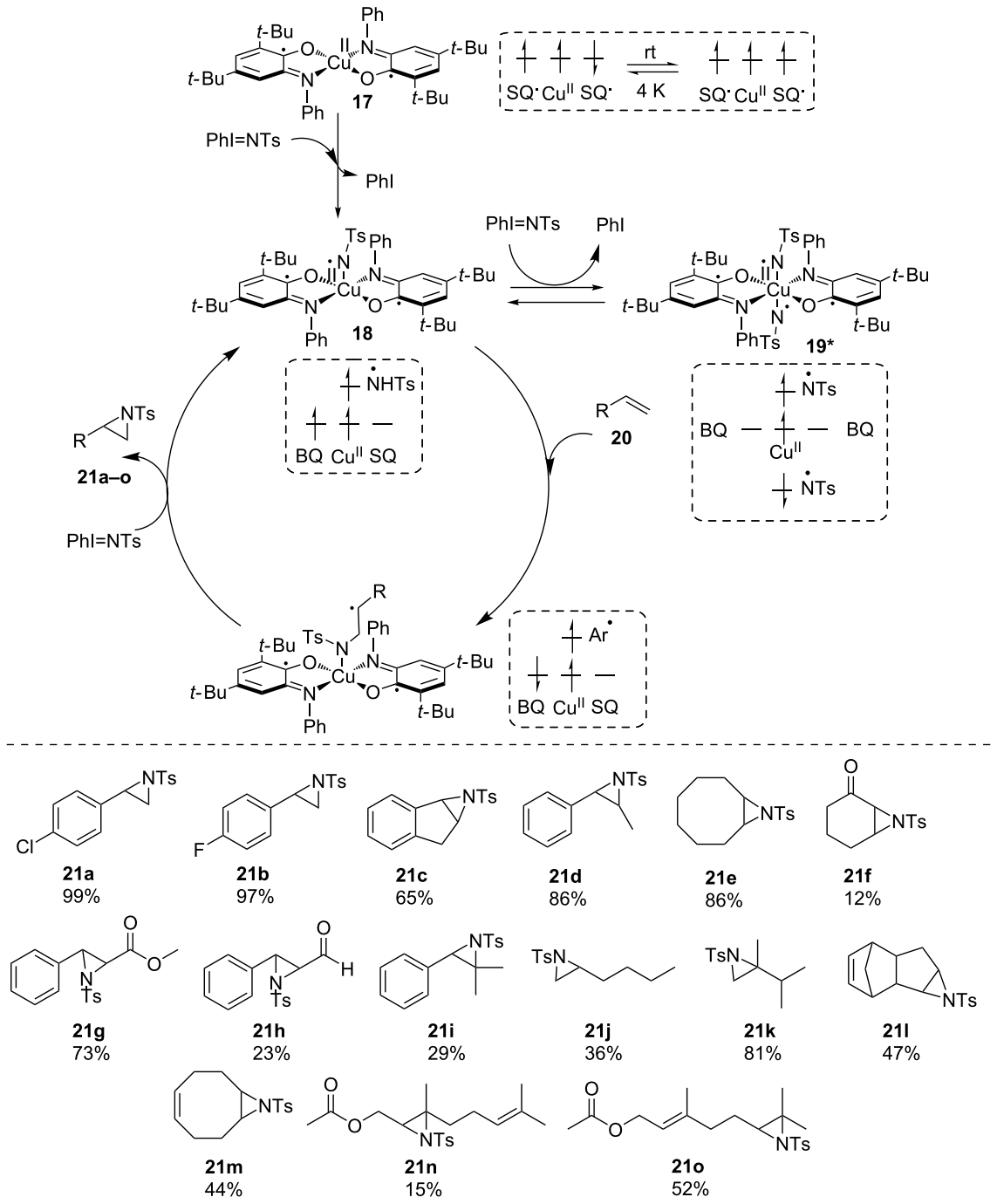

Scheme 11: Copper-catalyzed aziridination through molecular spin catalysis with redox-active iminosemiquinone ligands.

a strong steric distortion induced by ligands in the coordination sphere around a metal center produces an energized and highly reactive structure. Our recently published study revealed, that use of a highly-strained redox-active ligand facilitates a transfer of nitrogen- and carbon-containig group by copper complex **22** in as fast as two minutes, and therefore, it exhibits a strong increase in reactivity when compared to its unstrained analogue [40]. This example of a bioinspired small-molecule synthetic system combines two reactivity-enhancing features from metalloenzymes: entasis and redox cofactors. Strikingly, combination of these unique steric and electronic features results in a distorted pentacoordinated sphere exhibiting a newly occupied coordination site, as confirmed by single crystal X-ray diffraction analysis. This particular geometry results in enhanced catalytic reactivity and is clearly reminiscent of the entatic state model. The proposed mechanism (Scheme 12) involves the

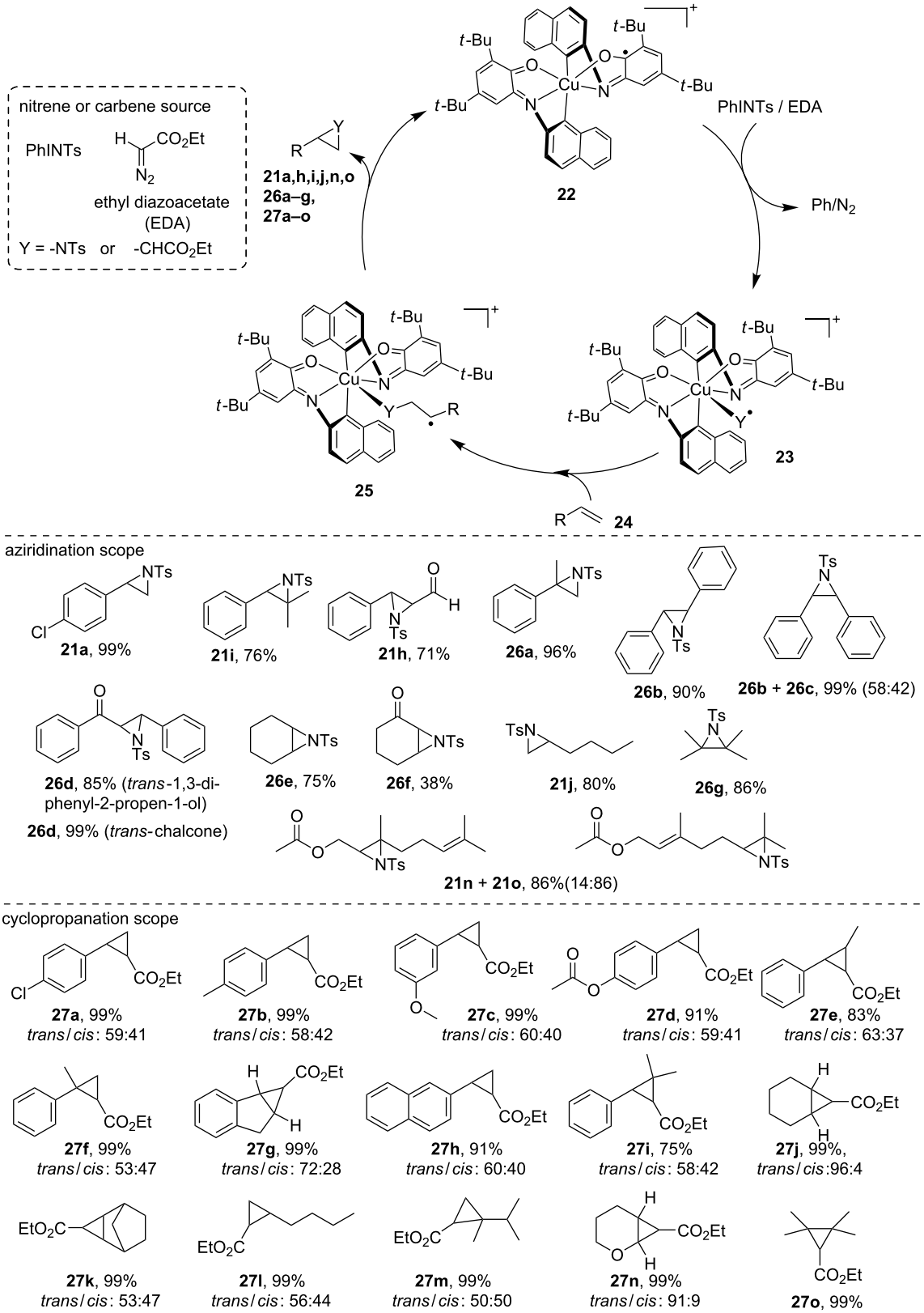

Scheme 12: Nitrogen-group and carbon-group transfer in copper-catalyzed aziridination and cyclopropanation through a strained redox-active ligand framework reminiscent of the entatic state model. Products are obtained as a mixture of *cis* and *trans* isomers.

insertion of a nitrene or carbene group to the copper complex **22** to form intermediate **23**. Subsequent alkene insertion yields species **25** and the group-transfer product (**21a**,**h–j**,**n**,**o**, **26a–g** and **27a–o**) is released upon ring-closure (Scheme 12). A wide range of substrates including diverse mono-, di-, and trisubstituted styrene derivatives (**21a**,**i**,**h**, **26a–d and 27a–i**) substrates as well as unactivated or deactivated tri- and tetrasubstituted scaffolds (**21j**,**n**,**o**, **26e–g** and **27j–o**) were efficiently converted.

Conclusion

The use of redox-active ligands opens new venues in copper catalysis by utilizing the efficient electronic interplay between the metal center, the redox-active ligand and the reaction substrate. While such an behavior is a cornerstone in enzymatic reactions, the wide opportunities offered by these bioinspired approaches are only emerging and should blossom in the near future. In order to assert this field as a true game-changer in copper catalysis, further work should aim at rationalizing the "redox dialogue" between the metal and the ligand, and provide a deeper understanding of the valence tautomerism at work in such systems in order to develop predictive tools for reactivity control [41]. Such knowledge is most likely to result in new advances in the fast-expanding field of redox catalysis.

Funding

This work has been supported through funding from the Université de Strasbourg, CNRS, IDEX Excellence Initiative (AD), Emergence Sorbonne Universités grant, Chinese Council CSC (YR), LabEx CSC (ANR-10-LABX-0026_CSC), Fondation pour la Recherche en Chimie (FRC, CH) and CNRS Mission for Interdisciplinarity. The authors gratefully acknowledge COST Action 27 CM1305 ECOSTBio (Explicit Control Over Spin-States in Technology and Biochemistry) and the FrenchBIC network.

ORCID® iDs

Agnideep Das - https://orcid.org/0000-0002-0672-3811
Yufeng Ren - https://orcid.org/0000-0002-5254-3360
Marine Desage-El Murr - https://orcid.org/0000-0001-5017-4496

References

1. Stubbe, J.; van der Donk, W. A. *Chem. Rev.* **1998,** *98,* 705–762. doi:10.1021/cr9400875
2. Wasser, I. M.; de Vries, S.; Moënne-Loccoz, P.; Schröder, I.; Karlin, K. D. *Chem. Rev.* **2002,** *102,* 1201–1234. doi:10.1021/cr0006627
3. Hematian, S.; Garcia-Bosch, I.; Karlin, K. D. *Acc. Chem. Res.* **2015,** *48,* 2462–2474. doi:10.1021/acs.accounts.5b00265
4. Chirik, P. J.; Wieghardt, K. *Science* **2010,** *327,* 794–795. doi:10.1126/science.1183281
5. Himmel, H.-J. *Inorg. Chim. Acta* **2018,** *481,* 56–68. doi:10.1016/j.ica.2017.07.069
6. Ye, S.; Sarkar, B.; Lissner, F.; Schleid, T.; van Slageren, J.; Fiedler, J.; Kaim, W. *Angew. Chem., Int. Ed.* **2005,** *44,* 2103–2106. doi:10.1002/anie.200462339
7. Kaim, W.; Wanner, M.; Knödler, A.; Záliš, S. *Inorg. Chim. Acta* **2002,** *337,* 163–172. doi:10.1016/s0020-1693(02)01081-2
8. Rall, J.; Kaim, W. *J. Chem. Soc., Faraday Trans.* **1994,** *90,* 2905–2908. doi:10.1039/ft9949002905
9. Que, L., Jr.; Tolman, W. B. *Nature* **2008,** *455,* 333–340. doi:10.1038/nature07371
10. Wang, Y.; DuBois, J. L.; Hedman, B.; Hodgson, K. O.; Stack, T. D. P. *Science* **1998,** *279,* 537–540. doi:10.1126/science.279.5350.537
11. Chaudhuri, P.; Hess, M.; Müller, J.; Hildenbrand, K.; Bill, E.; Weyhermüller, T.; Wieghardt, K. *J. Am. Chem. Soc.* **1999,** *121,* 9599–9610. doi:10.1021/ja991481t
12. Chaudhuri, P.; Verani, C. N.; Bill, E.; Bothe, E.; Weyhermüller, T.; Wieghardt, K. *J. Am. Chem. Soc.* **2001,** *123,* 2213–2223. doi:10.1021/ja003831d
13. Chaudhuri, P.; Hess, M.; Flörke, U.; Wieghardt, K. *Angew. Chem., Int. Ed.* **1998,** *37,* 2217–2220. doi:10.1002/(sici)1521-3773(19980904)37:16<2217::aid-anie2217>3.0.co;2-d
14. Balaghi, S. E.; Safaei, E.; Chiang, L.; Wong, E. W. Y.; Savard, D.; Clarke, R. M.; Storr, T. *Dalton Trans.* **2013,** *42,* 6829–6839. doi:10.1039/c3dt00004d
15. Alaji, Z.; Safaei, E.; Chiang, L.; Clarke, R. M.; Mu, C.; Storr, T. *Eur. J. Inorg. Chem.* **2014,** 6066–6074. doi:10.1002/ejic.201402687
16. Rajabimoghadam, K.; Darwish, Y.; Bashir, U.; Pitman, D.; Eichelberger, S.; Siegler, M. A.; Swart, M.; Garcia-Bosch, I. *J. Am. Chem. Soc.* **2018,** *140,* 16625–16634. doi:10.1021/jacs.8b08748
17. Cook, S. A.; Borovik, A. S. *Acc. Chem. Res.* **2015,** *48,* 2407–2414. doi:10.1021/acs.accounts.5b00212
18. Borovik, A. S. *Chem. Soc. Rev.* **2011,** *40,* 1870–1874. doi:10.1039/c0cs00165a
19. Smirnov, A. S.; Martins, L. M. D. R. S.; Nikolaev, D. N.; Manzhos, R. A.; Gurzhiy, V. V.; Krivenko, A. G.; Nikolaenko, K. O.; Belyakov, A. V.; Garabadzhiu, A. V.; Davidovich, P. B. *New J. Chem.* **2019,** *43,* 188–198. doi:10.1039/c8nj02718h
20. Esguerra, K. V. N.; Fall, Y.; Petitjean, L.; Lumb, J.-P. *J. Am. Chem. Soc.* **2014,** *136,* 7662–7668. doi:10.1021/ja501789x
21. Askari, M. S.; Esguerra, K. V. N.; Lumb, J.-P.; Ottenwaelder, X. *Inorg. Chem.* **2015,** *54,* 8665–8672. doi:10.1021/acs.inorgchem.5b01297
22. Mirica, L. M.; Vance, M.; Rudd, D. J.; Hedman, B.; Hodgson, K. O.; Solomon, E. I.; Stack, T. D. P. *Science* **2005,** *308,* 1890–1892. doi:10.1126/science.1112081
23. Mirica, L. M.; Rudd, D. J.; Vance, M. A.; Solomon, E. I.; Hodgson, K. O.; Hedman, B.; Stack, T. D. P. *J. Am. Chem. Soc.* **2006,** *128,* 2654–2665. doi:10.1021/ja056740v
24. McCann, S. D.; Lumb, J.-P.; Arndtsen, B. A.; Stahl, S. S. *ACS Cent. Sci.* **2017,** *3,* 314–321. doi:10.1021/acscentsci.7b00022
25. Hoover, J. M.; Stahl, S. S. *J. Am. Chem. Soc.* **2011,** *133,* 16901–16910. doi:10.1021/ja206230h
26. Walroth, R. C.; Miles, K. C.; Lukens, J. T.; MacMillan, S. N.; Stahl, S. S.; Lancaster, K. M. *J. Am. Chem. Soc.* **2017,** *139,* 13507–13517. doi:10.1021/jacs.7b07186
27. Huang, Z.; Lumb, J.-P. *Angew. Chem., Int. Ed.* **2016,** *55,* 11543–11547. doi:10.1002/anie.201606359
28. van der Vlugt, J. I. *Chem. – Eur. J.* **2019,** *25,* 2651–2662. doi:10.1002/chem.201802606

29. Jacquet, J.; Blanchard, S.; Derat, E.; Desage-El Murr, M.; Fensterbank, L. *Chem. Sci.* **2016,** *7,* 2030–2036. doi:10.1039/c5sc03636d
30. Mortezaei, S.; Catarineu, N. R.; Canary, J. W. *J. Am. Chem. Soc.* **2012,** *134,* 8054–8057. doi:10.1021/ja302283s
31. Schrempp, D. F.; Leingang, S.; Schnurr, M.; Kaifer, E.; Wadepohl, H.; Himmel, H.-J. *Chem. – Eur. J.* **2017,** *23,* 13607–13611. doi:10.1002/chem.201703611
32. Schön, F.; Kaifer, E.; Himmel, H.-J. *Chem. – Eur. J.* **2019,** *25,* 8279–8288. doi:10.1002/chem.201900583
33. Farwell, C. C.; Zhang, R. K.; McIntosh, J. A.; Hyster, T. K.; Arnold, F. H. *ACS Cent. Sci.* **2015,** *1,* 89–93. doi:10.1021/acscentsci.5b00056
34. Esguerra, K. V. N.; Fall, Y.; Lumb, J.-P. *Angew. Chem., Int. Ed.* **2014,** *53,* 5877–5881. doi:10.1002/anie.201311103
35. Huang, Z.; Askari, M. S.; Esguerra, K. V. N.; Dai, T.-Y.; Kwon, O.; Ottenwaelder, X.; Lumb, J.-P. *Chem. Sci.* **2016,** *7,* 358–369. doi:10.1039/c5sc02395e
36. Esguerra, K. V. N.; Xu, W.; Lumb, J.-P. *Chem* **2017,** *2,* 533–549. doi:10.1016/j.chempr.2017.03.003
37. Ren, Y.; Cheaib, K.; Jacquet, J.; Vezin, H.; Fensterbank, L.; Orio, M.; Blanchard, S.; Desage-El Murr, M. *Chem. – Eur. J.* **2018,** *24,* 5086–5090. doi:10.1002/chem.201705649
38. Hirao, H.; Kumar, D.; Thiel, W.; Shaik, S. *J. Am. Chem. Soc.* **2005,** *127,* 13007–13018. doi:10.1021/ja053847+
39. Usharani, D.; Wang, B.; Sharon, D. A.; Shaik, S. Principles and Prospects of Spin-States Reactivity in Chemistry and Bioinorganic Chemistry. In *Spin States in Biochemistry and Inorganic Chemistry: Influence on Structure and Reactivity;* Swart, M.; Costas, M., Eds.; John Wiley & Sons Ltd.: Chichester, UK, 2015; pp 131–156. doi:10.1002/9781118898277.ch7
40. Ren, Y.; Forté, J.; Cheaib, K.; Vanthuyne, N.; Fensterbank, L.; Vezin, H.; Orio, M.; Blanchard, S.; Desage-El Murr, M. *iScience* **2020,** *23,* 100955. doi:10.1016/j.isci.2020.100955
41. Ziesak, A.; Steuer, L.; Kaifer, E.; Wagner, N.; Beck, J.; Wadepohl, H.; Himmel, H.-J. *Dalton Trans.* **2018,** *47,* 9430–9441. doi:10.1039/c8dt01234b

License and Terms

BEILSTEIN JOURNAL OF ORGANIC CHEMISTRY

Copper-catalysed alkylation of heterocyclic acceptors with organometallic reagents

Yafei Guo and Syuzanna R. Harutyunyan*

Review

Open Access

Address:
Stratingh Institute for Chemistry, University of Groningen, Nijenborgh 4, 9747 AG, Groningen, The Netherlands

Email:
Syuzanna R. Harutyunyan* - s.harutyunyan@rug.nl

* Corresponding author

Keywords:
conjugate addition; copper catalysis; heterocyclic Michael acceptor; organometallics

Beilstein J. Org. Chem. **2020,** *16,* 1006–1021.
doi:10.3762/bjoc.16.90

Received: 13 January 2020
Accepted: 20 April 2020
Published: 14 May 2020

This article is part of the thematic issue "Copper-catalyzed reactions for organic synthesis".

Guest Editor: G. Evano

Abstract

Copper-catalysed asymmetric C–C bond-forming reactions using organometallic reagents have developed into a powerful tool for the synthesis of complex molecules with single or multiple stereogenic centres over the past decades. Among the various acceptors employed in such reactions, those with a heterocyclic core are of particular importance because of the frequent occurrence of heterocyclic scaffolds in the structures of chiral natural products and bioactive molecules. Hence, this review focuses on the progress made over the past 20 years for heterocyclic acceptors.

Introduction

The copper-catalysed asymmetric addition of organometallic reagents to various acceptors is a useful strategy for C–C bond-forming reactions [1-4]. These important transformations have been thoroughly developed in the last few decades and were widely used in the synthesis of chiral natural products and bioactive molecules [5-8]. The majority of these molecules has a crucial commonality, namely the presence of heterocyclic units containing nitrogen, oxygen, sulphur, or other heteroatoms. These units are also often responsible for the key bioactivities that such molecules exhibit [9-11]. This has motivated the development of various strategies that target the synthesis of chiral heterocyclic motives [12-14]. Among these, methodologies based on the copper-catalysed asymmetric addition of organometallics are especially valuable because of i) the compatibility between copper catalysts and heteroatoms present in the starting materials that often show inhibitory effects in combination with other metal-based catalysts, and ii) the availability and cost-efficiency of copper(I) salts and most organometallics.

This review aims to provide an overview on the copper-based catalytic systems that enable the direct application of hetero-

cyclic acceptors in highly enantioselective C–C bond-forming reactions with organometallics. The work highlighted in this minireview is divided into two sections, based on the position where the bond is formed. The first part focuses on acceptors in which the reacting unsaturated double bond is embedded into the heterocyclic ring, while the second part deals with acceptors in which the reacting unsaturated double bond is located outside of the heterocyclic unit (e.g., alkenyl-substituted heterocycles). The organometallics discussed in this minireview include organoaluminium, organozinc, organozirconium, organolithium, and Grignard reagents.

Review

Copper-catalysed C–C bond-forming reactions at the heterocycle

The direct synthesis of chiral heterocyclic molecules from pyridine, quinolone, or indole derivatives is advantageous due to the abundance of such building blocks. Unfortunately, establishing catalytic enantioselective methods for the synthesis of these compounds resulting in high yield and enantioselectivity has proven challenging. As a result, significant effort has been invested into copper-catalysed asymmetric conjugate addition reactions using organometallics.

In 2005, Feringa and co-workers reported on the copper-catalysed asymmetric conjugate addition (ACA) of dialkylzinc reagents to *N*-substituted 2,3-dehydro-4-piperidones **1** in order to access useful chiral piperidine derivatives (Scheme 1A) [15]. They found the catalytic system based on the chiral phosphoramidite **L1** and a copper salt to be the most efficient one to achieve an enantioselectivity of up to 96% ee.

Interestingly, piperidones with different carbamate protecting groups (Me, Et, Ph, tosyl, and Bn, respectively) were tolerated, and a high enantioselectivity could also be obtained with several other dialkylzinc reagents (e.g., iPr_2Zn and n-Bu_2Zn, respectively). Later, T. Shibata and K. Endo prepared the same product (**2c**) with a higher enantioselectivity (97% ee) by using the multinuclear phosphorus ligand catalyst **L2** [16]. Organoaluminium reagents are also commonly used organometallics in copper-catalysed ACA reactions. For example, in the work of Feringa and co-workers, the methylation reaction using Me_2Zn resulted in a low yield of 44% due to the difficult purification of the crude product [15]. However, the same authors showed later that the copper-catalysed ACA of Me_3Al to Boc-protected 4-piperidone can be used as a key step in the total synthesis of the natural product (+)-myrtine with 14% overall yield (Scheme 1B) [17]. For this application, the highest yield (73%) and enantioselectivity (96% ee) were obtained using the chiral ligand **L3** and a copper salt as the catalyst.

Despite the fact that examples of high yield and enantioselectivity have been reported for conjugate additions of both organoaluminium and organozinc reagents, these reagents also present major drawbacks, namely their commercial availability and atom efficiency, given that only one alkyl group is transferred from the organometallic reagent to the Michael acceptor. In contrast, Grignard reagents are very favourable organometallics in terms of both their availability and atom efficiency. On the other hand, Grignard reagents are significantly more reactive than organoaluminium and organozinc reagents, rendering the catalytic control of both the regio- and enantioselectivity in addition reactions challenging. Nevertheless, Harutyunyan and co-workers introduced the first general catalytic methodology to access a wide variety of chiral piperidones in 2019, using Grignard reagents (Scheme 1C) [18]. Therein, a new catalytic system based on the ligand **L4**/Cu complex promoted the addition of Grignard reagents to *N*-Cbz-pyridone and *N*-Cbz-2,3-dihydropyridone Michael acceptors with high enantioselectivity and yield. It is worth mentioning that in copper-catalysed additions of Grignard reagents to *N*-Cbz-pyridone, the use of a Lewis acid ($BF_3{\cdot}OEt_2$) together with the copper catalyst is essential for achieving a high yield as well as a high regio- and enantioselectivity (up to 99% ee).

Although organoaluminium, organozinc, and Grignard reagents were all successfully applied in the ACA of 2,3-dehydro-4-piperidones, an introduction of the vinyl group was not successful until 2012, when Alexakis and co-workers disclosed that vinylalanes could be used in the copper-catalysed ACA to *N*-substituted-2,3-dehydro-4-piperidones [19]. Optimisation studies revealed that the combination of the ligand **L5** and Cu(II) naphthenate constituted the most efficient catalytic system, allowing the synthesis of the corresponding products with good yield and enantiomeric purity (up to 83% yield and 97% ee). Furthermore, a large variety of vinylalanes was investigated, and the product **2l** was further derivatised into a chiral bicyclic structure (**5**, Scheme 2A). In addition, simple vinyl aluminium reagents and commercial alkylaluminium reagents were examined in this methodology, providing the corresponding products with a moderate yield but high enantioselectivity (Scheme 2B).

In 2009, Feringa and co-workers presented the first highly enantioselective 1,2-addition of dialkylzinc reagents to an *N*-acyl-4-methoxypyridinium salt using a copper/phosphoramidite catalytic system (Scheme 3) [20,21]. The authors highlighted that the *N*-acylpyridinium salts were unstable species and that their instability affected the regioselectivity of the dearomatisation process upon the nucleophilic addition of the organozinc reagents. To solve this problem, the intermediate of the *N*-acyl-4-methoxypyridinium salt must be formed in situ and added

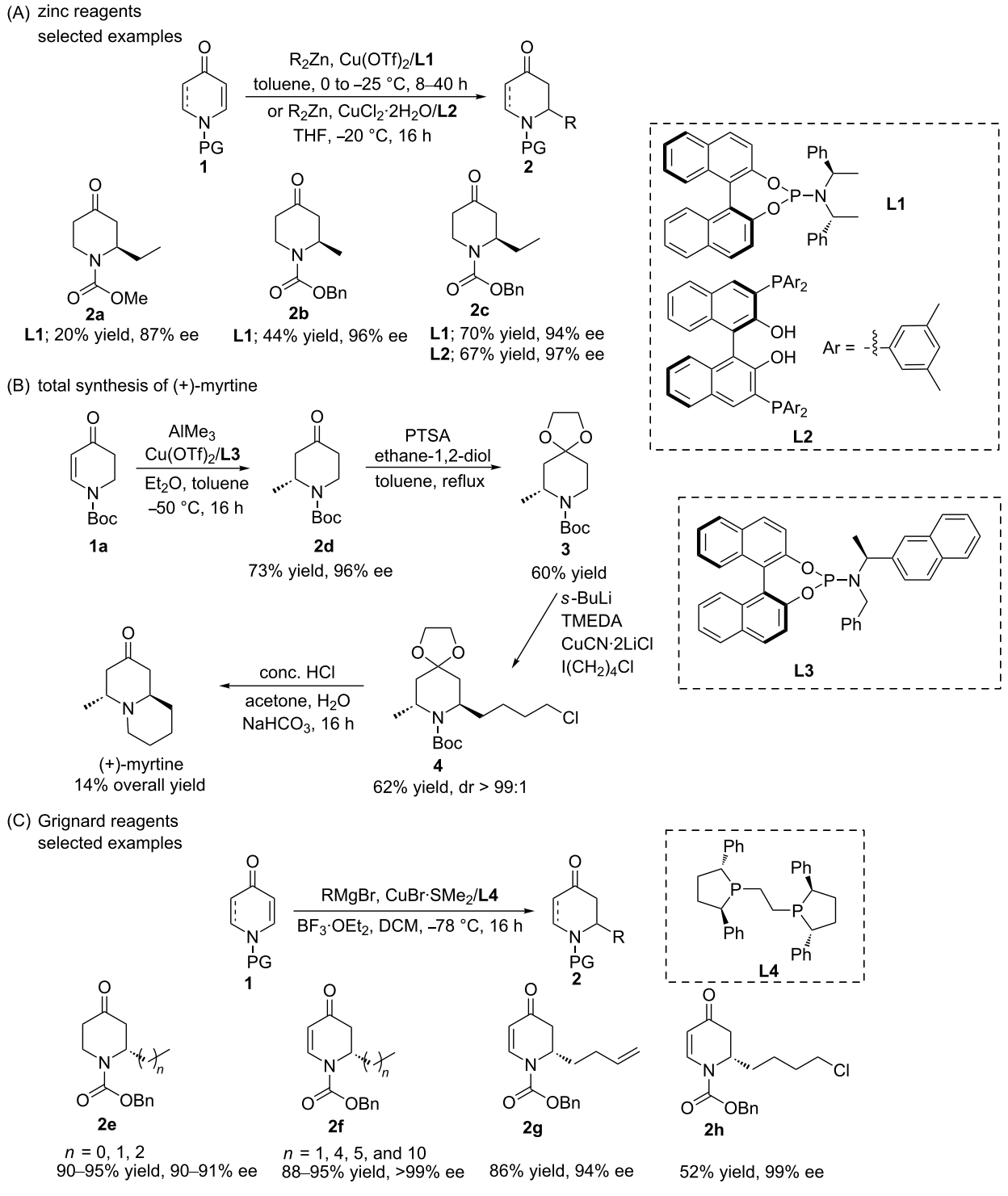

Scheme 1: Copper-catalysed ACA of organometallics to piperidones. A) addition of organozinc reagents; B) addition of organoaluminium reagent in the total synthesis of (+)-myrtine; C) addition of Grignard reagents.

slowly to the solution of the Cu(OTf)$_2$/**L6** complex and dialkylzinc reagent at −78 °C. Several dialkylzinc reagents were found to be effective as nucleophiles in this reaction, in most cases providing the products with a high enantioselectivity and a moderate yield. An exception was found with diisopropylzinc, for which only 56% ee could be obtained. The methodology was also successfully applied to the total synthesis of the natural alkaloid (*R*)-coniine.

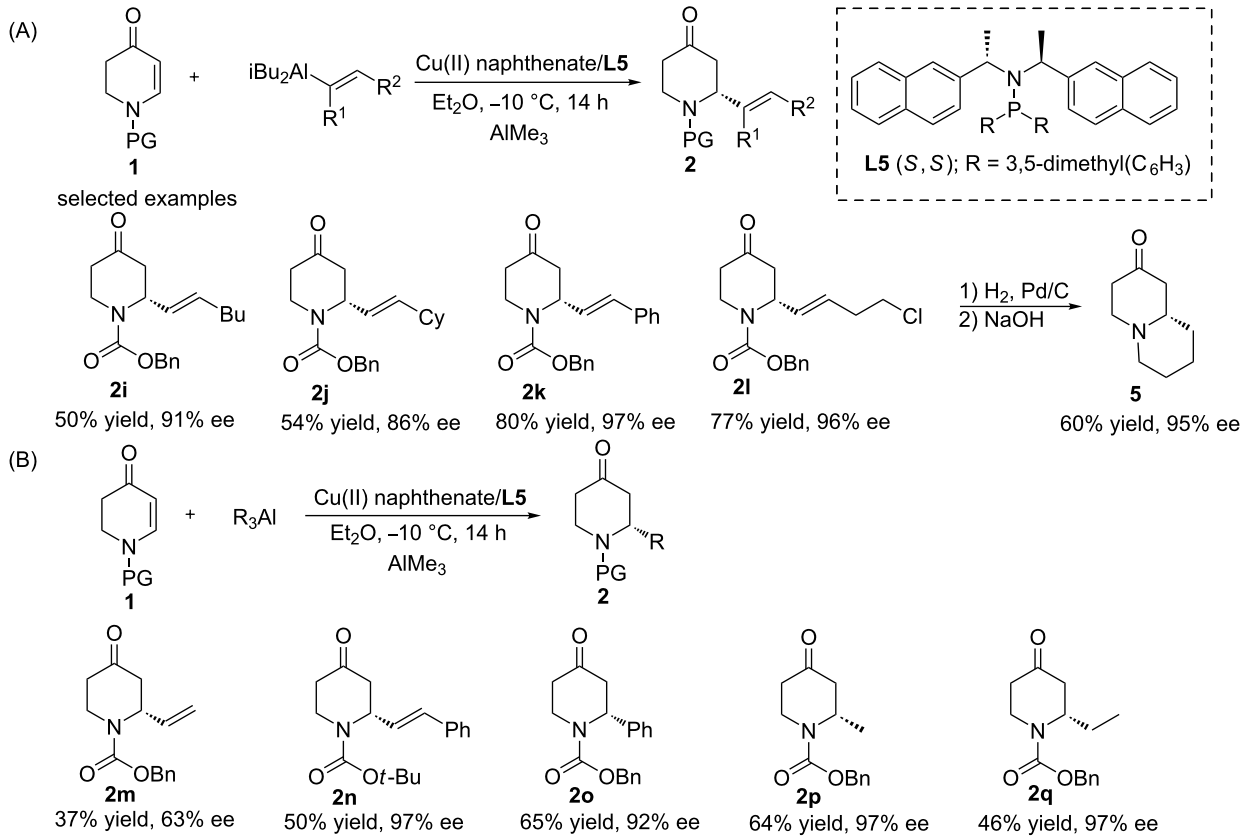

Scheme 2: Copper-catalysed ACA of alkenylalanes to N-substituted-2,3-dehydro-4-piperidones.

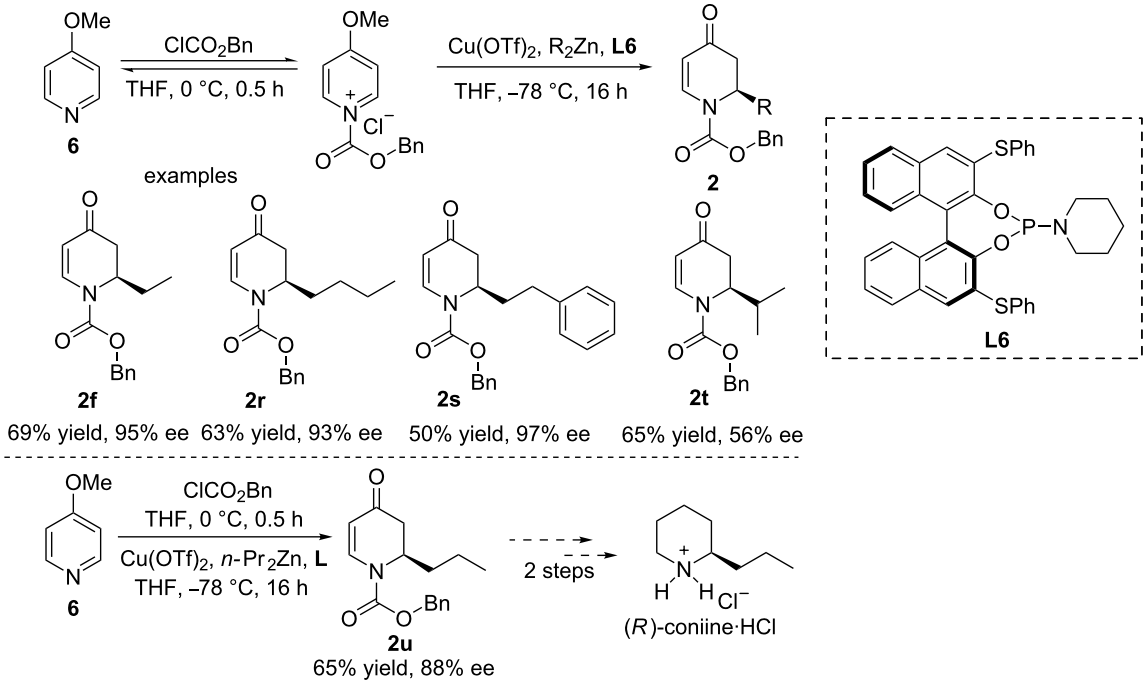

Scheme 3: Copper-catalysed asymmetric addition of dialkylzinc reagents to *N*-acyl-4-methoxypyridinium salts formed in situ.

Organozirconium compounds are another class of organometallic reagents that have been used widely in the synthesis of complex molecules. Recently, Fletcher and co-workers demonstrated the applicability of a hydrozirconation in the ACA reaction to non-heterocyclic conjugated substrates [22-26], while the Šebesta group was the first to report the copper-catalysed addition of organozirconium reagents to *N*-substituted 2,3-dehydro-4-piperidones (Scheme 4A) [27]. In the latter work, the organozirconium reagents were generated first in situ by the hydrozirconation of alkenes. Subsequently, the **L1**/Cu catalytic system was used to test different organozirconium reagents. The results showed that with *N*-substituted 2,3-dehydro-4-piperidones, several products could be obtained with an enantiomeric ratio of up to 92:8, but with yields not exceeding 22%. Interestingly, this methodology could also be applied to the lactams **7**, leading to the corresponding products with up to 81% yield and an enantiomeric ratio of up to 82:18 (Scheme 4B).

Oxygen-containing heterocyclic compounds are ubiquitous in natural products and medicines, with many of them being chiral. Copper-catalysed ACA reactions of organometallics have also been employed to synthesize such chiral oxygen-containing heterocyclic compounds. Feringa's group reported the highly regio- and enantioselective copper-catalysed direct conjugate addition of Grignard reagents to chromones and coumarins (Scheme 5) [28,29]. A variety of Grignard reagents, including linear and secondary alkylmagnesium reagents and various chromones and coumarins, were tolerated by the catalytic system, providing the products with a high yield and enantioselectivity. It was also demonstrated that the addition products could be used for further transformations in order to access various derivatives, such as **12** and **13**, derived from the trapping and Baeyer–Villiger oxidation of **11**, respectively, or compound **16**, obtained via the ring opening reaction of **15** with an amine (Scheme 5). Taking the enolate intermediate derived from the addition of EtMgBr to coumarin as an example, it was shown that upon the treatment with an amine, this enolate produced the final chiral amide product with a good yield (82%) and ee (96%).

While the methodology for the ACAs of Grignard reagents to chromones and coumarins has been established successfully, quinolones remained challenging substrates for such transformations until very recently. It was not until 2019 that this problem was solved, when the Harutyunyan group employed a cata-

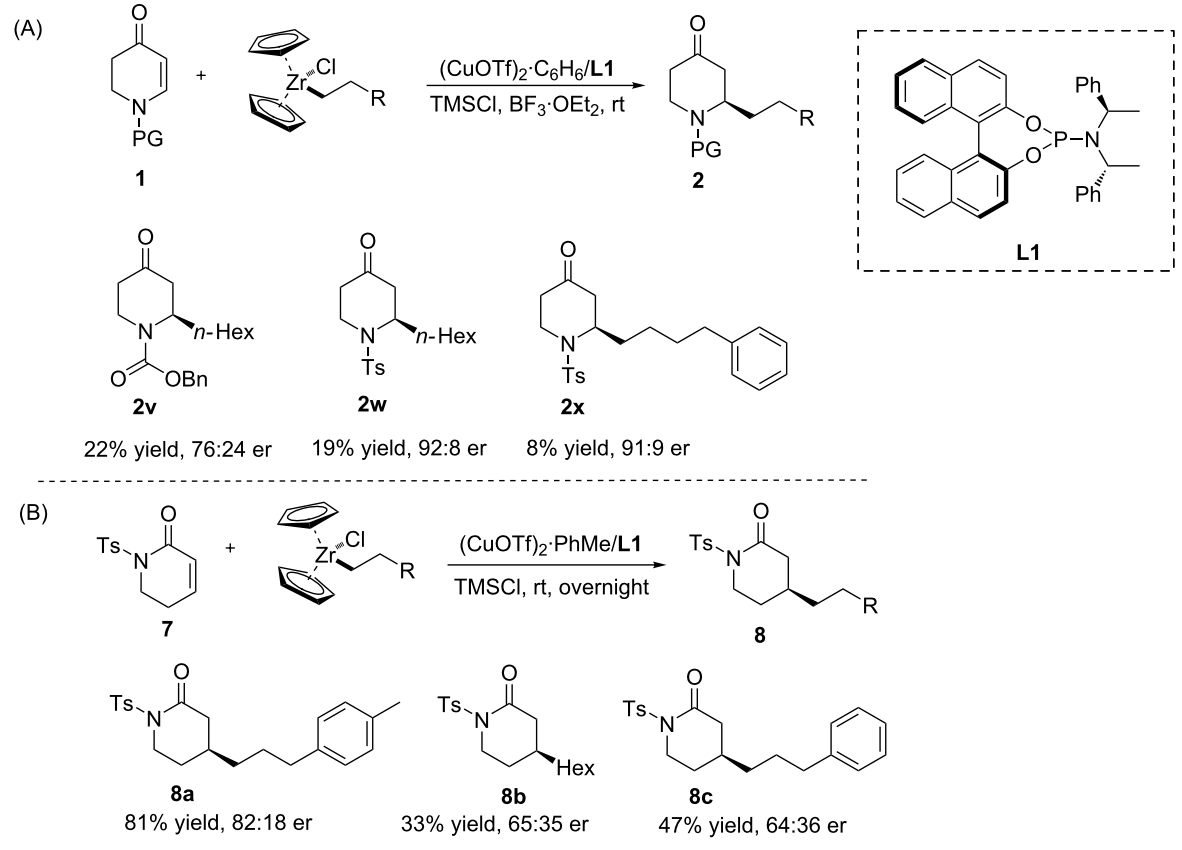

Scheme 4: Copper-catalysed ACA of organozirconium reagents to N-substituted 2,3-dehydro-4-piperidones and lactams.

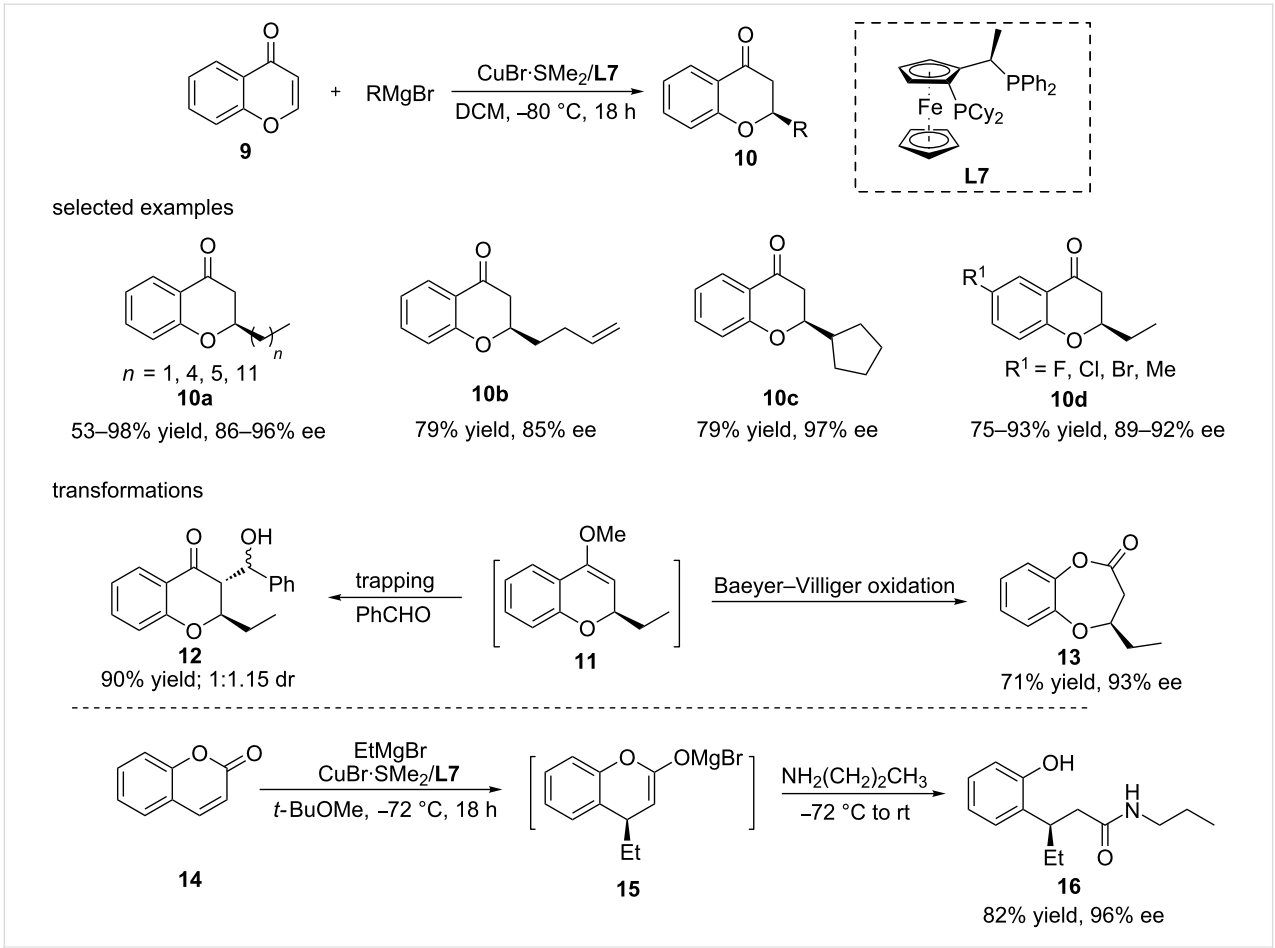

Scheme 5: Copper-catalysed ACA of Grignard reagents to chromones and coumarins and further derivatisation of the corresponding products.

lytic system based on **L4**/Cu, which efficiently catalysed the ACA of Grignard reagents to N-protected quinolones **17** at room temperature (Scheme 6) [18]. Initially, the methodology was developed for additions to *N*-Cbz-4-quinolone-based substrates, and the catalytic system was demonstrated to facilitate the addition of a wide variety of reagents, including linear, α-, β-, and γ-substituted, as well as aryl Grignard reagents. The subsequent broadening of the quinolone scope revealed that substrates bearing Me, Br, CF_3, ether, amide, and ester substituents, respectively, were also tolerated successfully. In addition, the catalytic system was applied to the synthesis of the natural product (+)-angustureine with an excellent outcome (92% yield, 97% ee) (Scheme 6A). When the method was applied to the ACA of Grignard reagents to N-substituted 2-quinolones, their lower reactivity led to a lower conversion. Performing the reaction in the presence of TMSBr resolved this and allowed the reaction to proceed for various Grignard reagents and substrates with an excellent enantioselectivity (Scheme 6B).

The copper-catalysed ACA of organometallics has also been applied to lactams, which are useful building blocks for synthetic chemistry. In 2004, Pineschi and co-workers successfully introduced the methodology of copper-catalysed ACAs of organoaluminium and organozinc reagents to lactams (Scheme 7A) [30]. They found that with a phenylcarbamate protecting group on the nitrogen atom, the addition of Et_2Zn and Me_3Al could be promoted by the **L1**/Cu catalytic system, leading to the corresponding alkylated products with 95% and 68% enantioselectivity, respectively. Furthermore, the intermediate formed upon this ACA could be trapped with acetaldehyde and allyl bromide or allyl acetate to form valuable compounds with high ee and dr values. Later, Harutyunyan's research group showed that also non-activated lactams with alkyl-protected groups could undergo ACA reactions with EtMgBr, with 93% ee (**22c**, Scheme 7A) [31]. The research group of Alexakis was able to push this chemistry further when they developed a new methodology that allowed to access the chiral lactams **26** with moderate yield and high enantioselectivity (up to 96% ee). Therein, the copper(II) naphthenate/**L5**-catalysed ACA of alkenylaluminium and alkylaluminium reagents to the β-substituted unsaturated conjugated lactams **25** was utilized (Scheme 7B) [32].

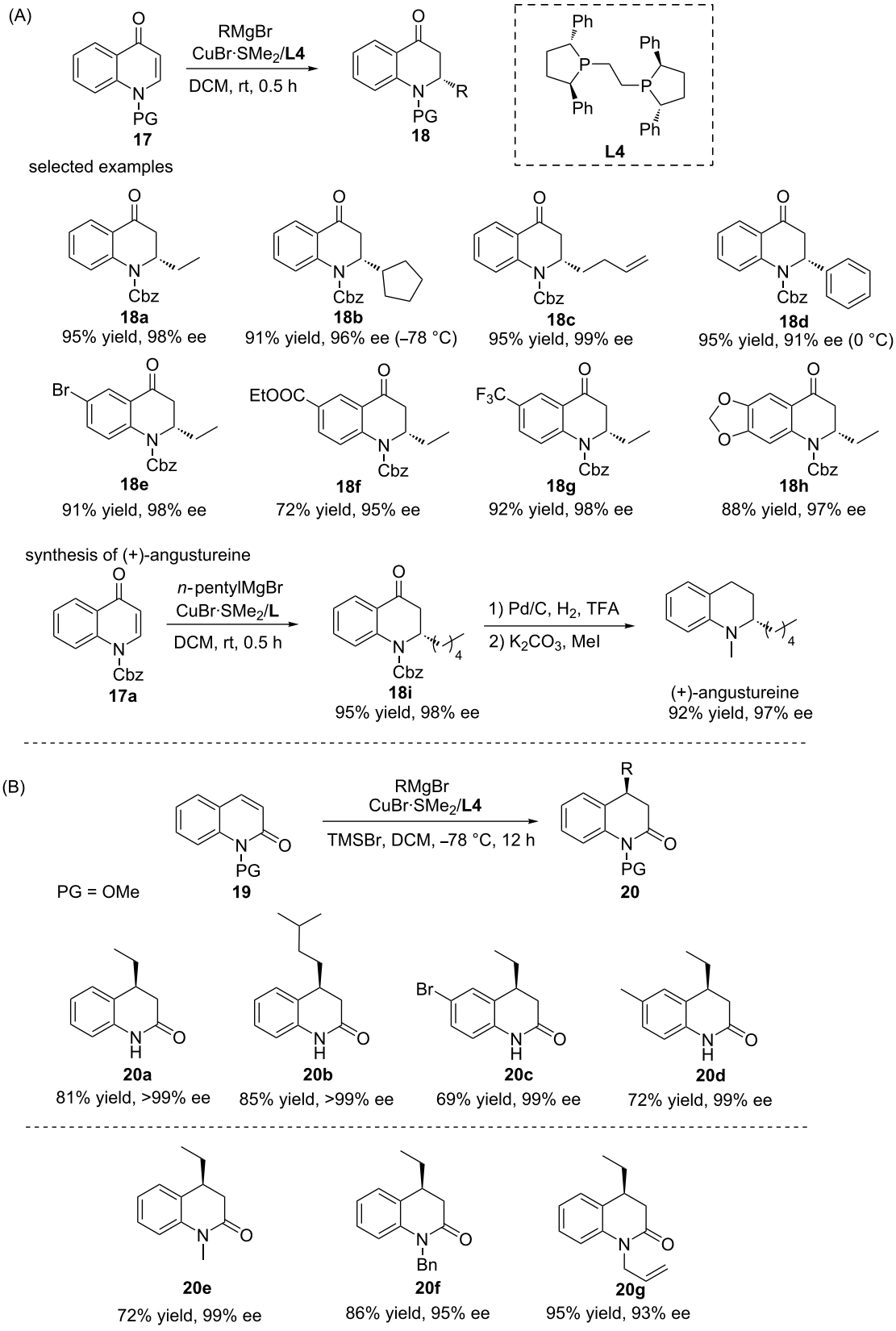

Scheme 6: Copper-catalysed ACA of Grignard reagents to N-protected quinolones.

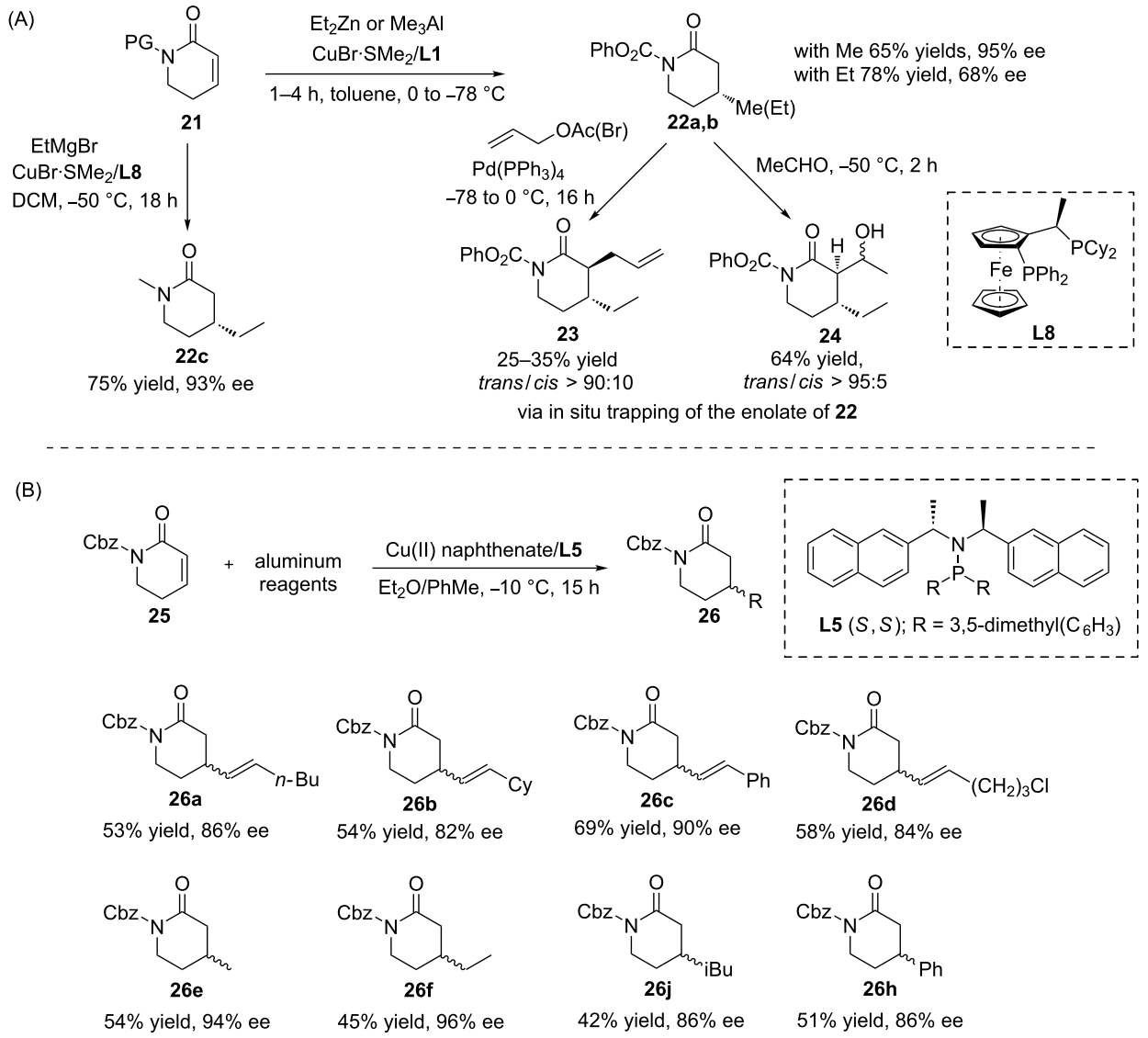

Scheme 7: Copper-catalysed ACAs of organometallics to conjugated unsaturated lactams.

Chiral lactones are yet another interesting class of heterocyclic substrates that have attracted great attention because of their usefulness in both organic synthesis and medicinal chemistry. The copper-catalysed ACA of organozinc reagents to 5,6-dihydro-2-pyranone is one of the best methods to obtain chiral lactones. During the past two decades, the research groups of Chan, Hoveyda (who applied an approach depending on the trapping by an aldehyde), Mauduit, and Wang reported a variety of methods employing the chiral ligands **L9**–**L13** that, in combination with copper, efficiently catalysed the ACA of diethylzinc to 5,6-dihydro-2-pyranone (Scheme 8), providing access to chiral β-substituted lactones with high enantioselectivity and conversion [33-37].

Although the copper-catalysed ACA of Et_2Zn to 5,6-dihydro-2-pyranone has been reported, the reactivity and commercial availability of the former renders the ACA of Grignard reagents a more attractive methodology. Feringa and co-workers were the first to report copper-catalysed ACAs of alkyl Grignard reagents to pyranones and 5,6-dihydro-2-pyranone (Scheme 9) [38]. In the presence of the Cu/**L7** catalytic system, several alkyl Grignard reagents underwent ACAs to form the chiral lactones with high enantioselectivity. Importantly, the authors showed how the conjugate addition products could be further derivatised to lead to versatile chiral building blocks, such as a β-alkyl-substituted aldehyde (66% yield, 94:6 er) or a β-bromo-γ-alkyl-substituted alcohol (71% yield, 93:7 er).

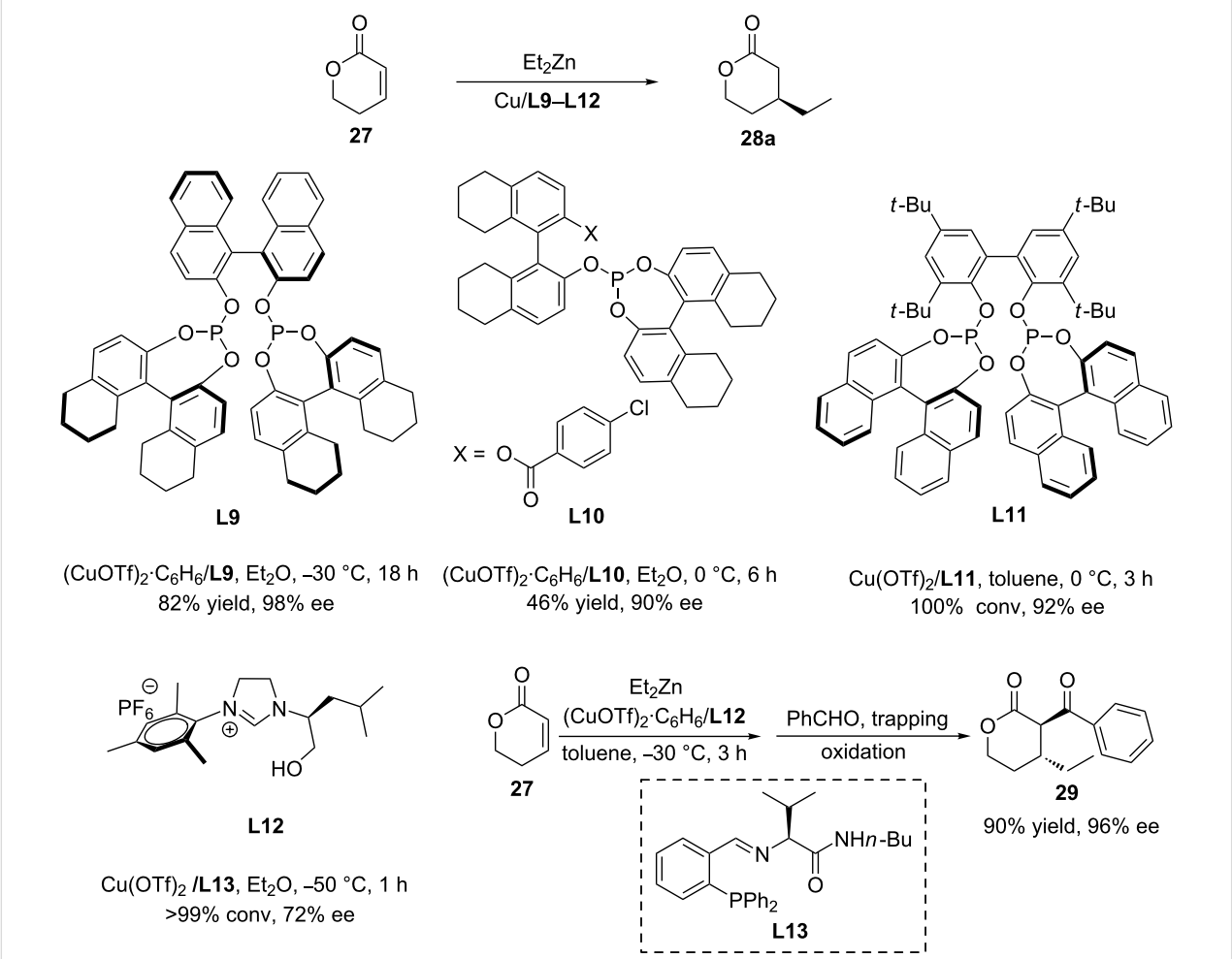

Scheme 8: Copper-catalysed ACA of Et_2Zn to 5,6-dihydro-2-pyranone.

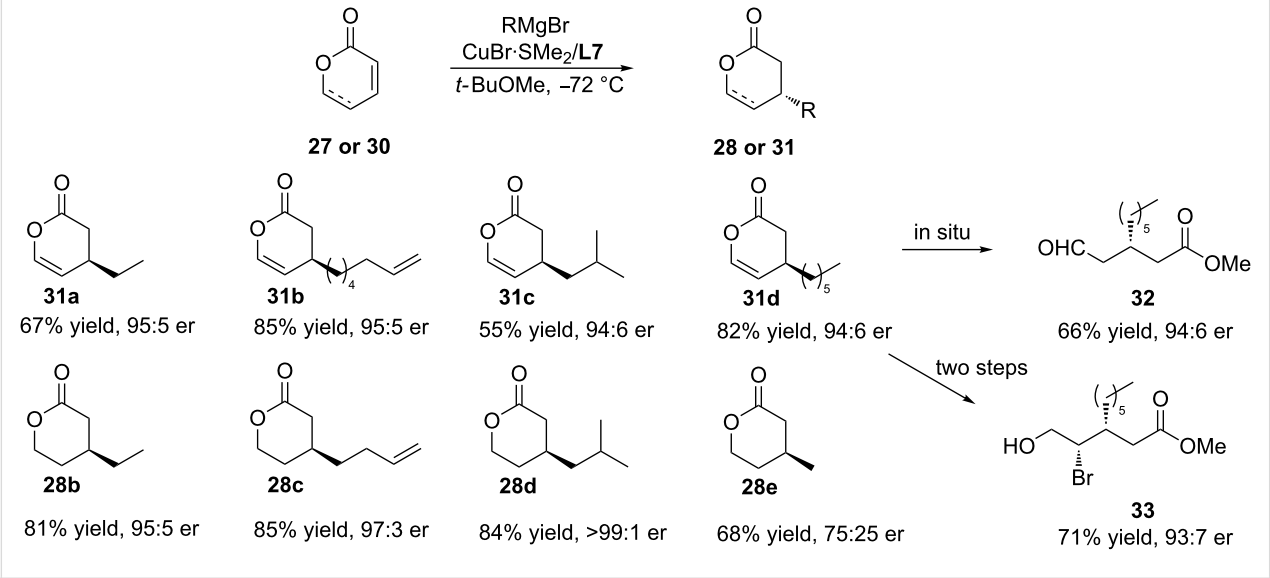

Scheme 9: Copper-catalysed ACA of Grignard reagents to pyranone and 5,6-dihydro-2-pyranone.

The asymmetric allylic alkylation (AAA) is a very useful method that allows the enantioselective formation of C–C bonds, and copper-catalysed AAAs using Grignard, organolithium, organoaluminium, and organozirconium reagents have been reported. In 2015, Fletcher and co-workers presented the copper-catalysed AAA of racemic 3,6-dihydro-2*H*-pyrans using alkylzirconocenes in the presence of the Cu/**L14** catalytic system (Scheme 10A) [39]. Several alkylzirconocenes were examined, resulting in the respective products with 45–93% ee and 20–33% yield. The same group also described the copper-catalysed desymmetrisation of heterocyclic meso compounds via the AAA reaction, once again using alkylzirconocenes as nucleophiles (Scheme 10B). In this reaction, two seven-membered heterocyclic bisphosphates (O- and N-containing, respectively,) underwent Cu/**L15**-catalysed AAAs and provided the corresponding chiral products with good yield and high enantioselectivity (92–93% ee) [40].

Ring opening reactions where carbon–carbon bonds are formed upon the addition of organometallics to heterocyclic acceptors, resulting in products that are not heterocyclic, provide an alternative strategy to generate important building blocks with two stereocentres, starting from heterocyclic substrates. The copper-catalysed ring opening of oxygen-bridged heterocyclic acceptors with trialkylaluminium reagents was explored by the group of Alexakis in 2009 (Scheme 11) [41]. Various chiral phosphoramidite ligands, in combination with a copper salt, were found to be efficient catalysts for this transformation, with the best results obtained with the ligand **L16**.

Feringa and co-workers elaborated the copper-catalysed ring opening reaction of oxabicyclic alkene substrates using organolithium reagents, finding excellent *anti* selectivities and enantioselectivity (Scheme 12) [42]. During the optimisation studies, they discovered that when the Lewis acid $BF_3{\cdot}OEt_2$ was employed in combination with the Cu/**L1** catalyst system, the *anti* diastereoisomer could be obtained with 97% enantioselectivity. In addition, this methodology tolerated *n*-BuLi, iBuLi, *n*-HexLi, and EtLi, providing a full conversion and high *anti* selectivity and enantioselectivity in all cases.

Alexakis and co-workers exploited the copper-catalysed asymmetric ring opening of polycyclic meso hydrazines with organoaluminium reagents (Scheme 13) [43]. This reaction fol-

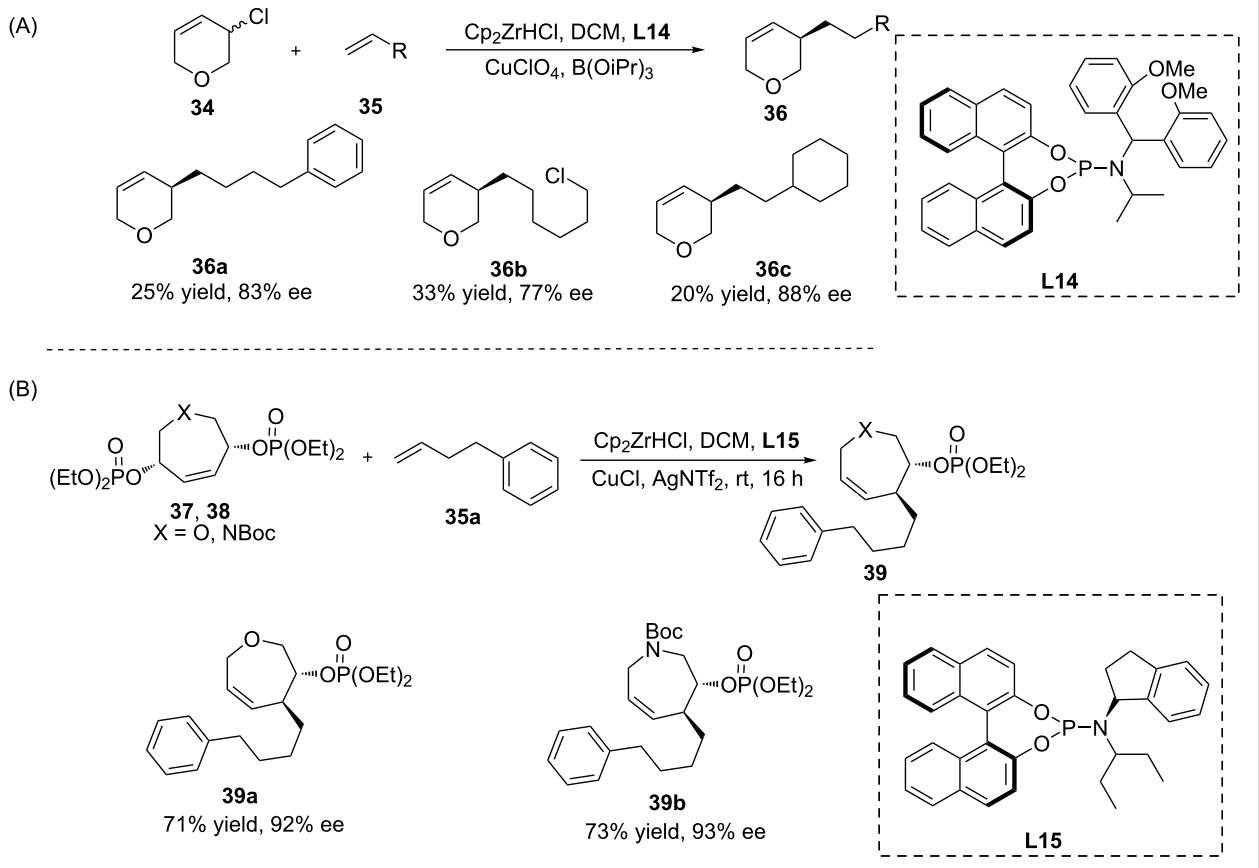

Scheme 10: Copper-catalysed AAA of an organozirconium reagent to heterocyclic acceptors.

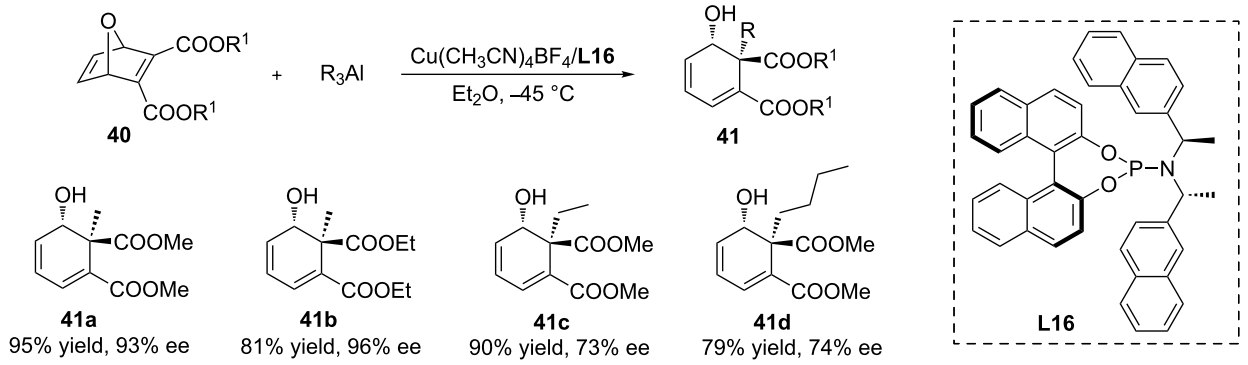

Scheme 11: Copper-catalysed ring opening of an oxygen-bridged substrate with trialkylaluminium reagents.

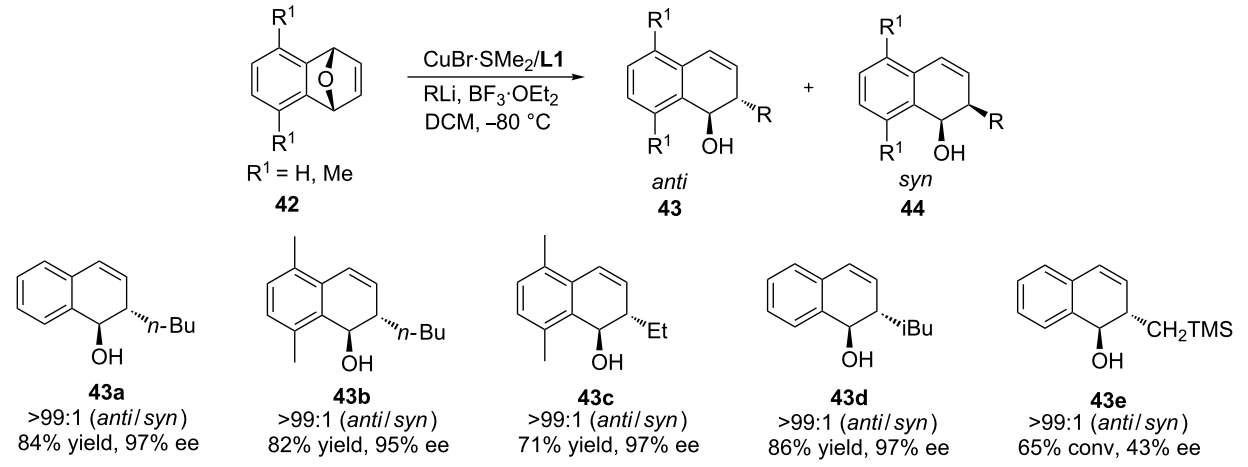

Scheme 12: Copper-catalysed ring opening of oxabicyclic substrates with organolithium reagents (selected examples).

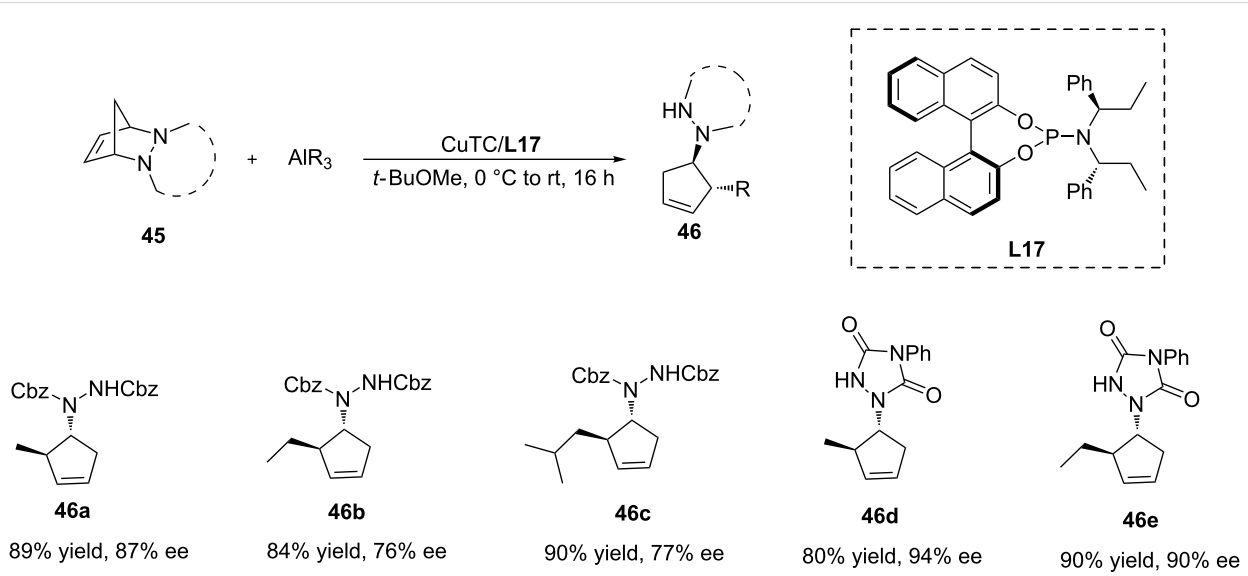

Scheme 13: Copper-catalysed ring opening of polycyclic meso hydrazines.

lowed a classical allylic substitution pathway. Interestingly, the organoaluminium reagents in this reaction did not only act as alkyl donors but could also activate the leaving group. After testing several kinds of phosphoramidite ligands with copper salts, the catalyst system **L17**/CuTc was selected for further studies. The solvent was found to play a crucial role in this reaction, with MTBE as the solvent of choice. Various organoaluminium reagents and protecting groups were examined, providing the products with good yield (up to 90%) and ee (up to 95%).

Copper-catalysed conjugate addition reactions to alkenyl-substituted heterocycles

Chiral heterocyclic aromatic compounds are crucial motifs in natural products and bioactive molecules, and in recent years, many strategies have been reported for their highly enantioselective synthesis. However, while catalytic asymmetric C–C bond formations by ACAs of organometallics is a routine procedure for additions to common Michael acceptors, such as enones and enoates, examples of catalytic asymmetric additions to N-heteroaromatic alkenyl compounds are less developed. This deficiency is largely due to the intrinsically low reactivity of alkenyl-substituted heterocycles towards nucleophilic addition compared to common Michael acceptors. A way to lift this barrier was introduced in 2016 by Harutyunyan and co-workers, who developed a general methodology for the direct and facile access to a variety of chiral heterocyclic aromatic compounds by the ACA of Grignard reagents to conjugated N-heteroaromatic alkenyl compounds (Scheme 14) [44]. The key of the presented method was the enhancement of the reactivity of the heteroaromatic alkenyl substrates by Lewis acid activation in combination with readily available and highly reactive Grignard reagents and a copper catalyst bound to a chiral diphosphine ligand. Using this methodology, various chiral heteroaromatic products were obtained with high enantioselectivity (up to 99% ee) and yield (up to 95%). Remarkably, both alkyl and aromatic Grignard reagents provided a high yield and enantioselectivity in this methodology. Furthermore, the

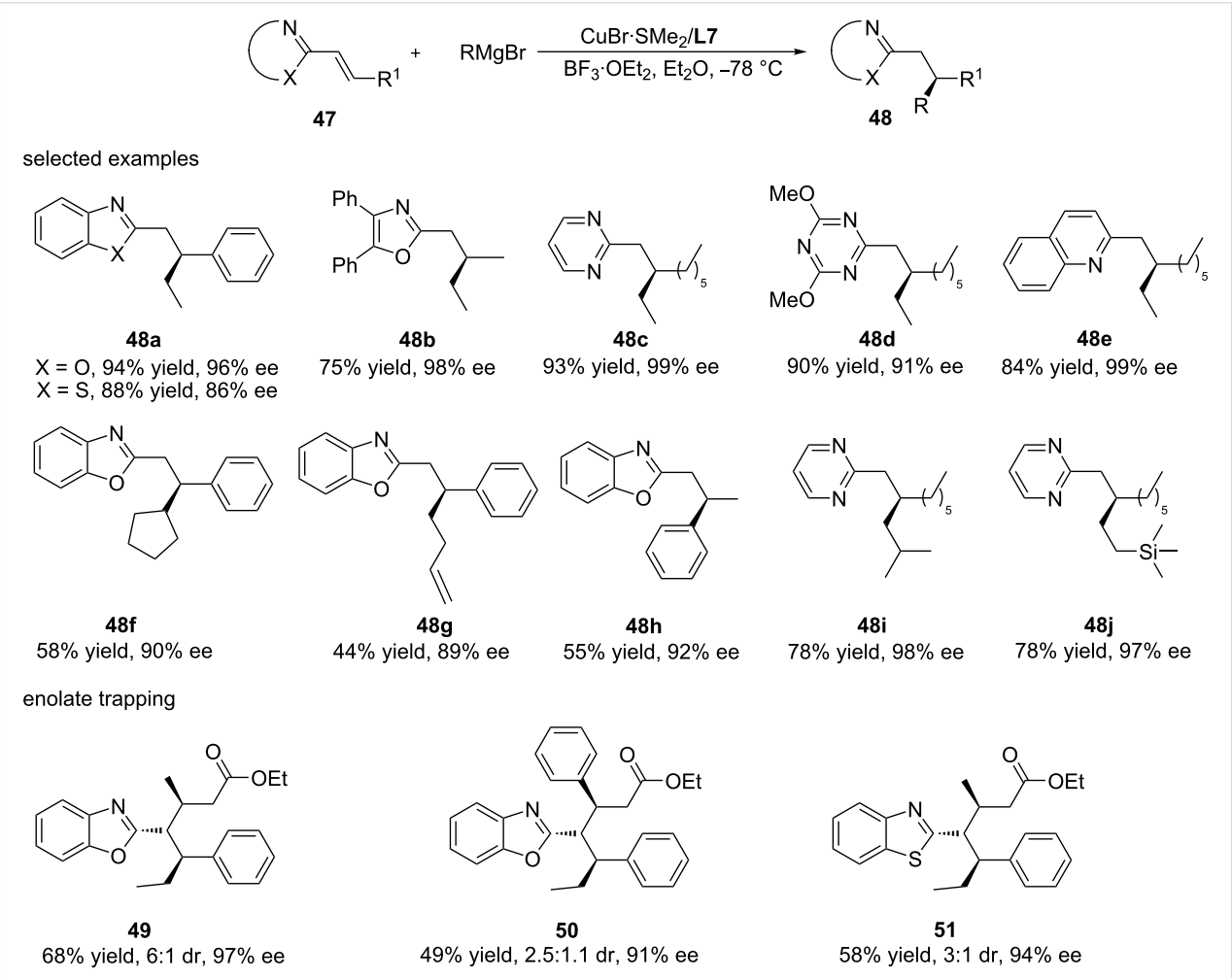

Scheme 14: Copper-catalysed ACA of Grignard reagents to alkenyl-substituted aromatic N-heterocycles.

same group reported a one-pot conjugate addition to alkenylheteroarenes with subsequent trapping of the resulting azaenolate with reactive Michael acceptors in a follow-up study [45].

While pyridines are among the most important classes of heterocyclic moieties that occur in many bioactive molecules, such as natural products, pharmaceuticals, and agrochemicals, the initial report by the Harutyunyan group did not include alkenylpyridines in the substrate scope. The reason for this was the markedly lower reactivity of alkenylpyridines towards nucleophilic addition as compared to other alkenylheteroarenes.

For the same reason, the synthesis of chiral pyridine derivatives has always been considered a challenge in organic chemistry research. In an attempt to overcome this reactivity issue, the same authors decided to use the trimethylsilyl-based Lewis acid TMSOTf in order to allow the covalent activation of the alkenylpyridine via pyridinium formation. This strategy turned out successful, and optimisation studies identified reaction conditions that allowed highly enantioselective ACAs of Grignard reagents to alkenylpyridines (Scheme 15) [46]. Using the optimised conditions (Cu/**L7**/TMSOTf), a large variety of pyridine-based chiral compounds was synthesized. Apart from allowing the introduction of different linear, branched, cyclic, and functionalised alkyl chains at the β-position of the alkenylpyridines, the catalytic system also showed a high functional group tolerance, and thus allowing straightforward chemical transformations of the addition products, including, for example, reductions, cycloadditions, and coupling reactions (Scheme 15B).

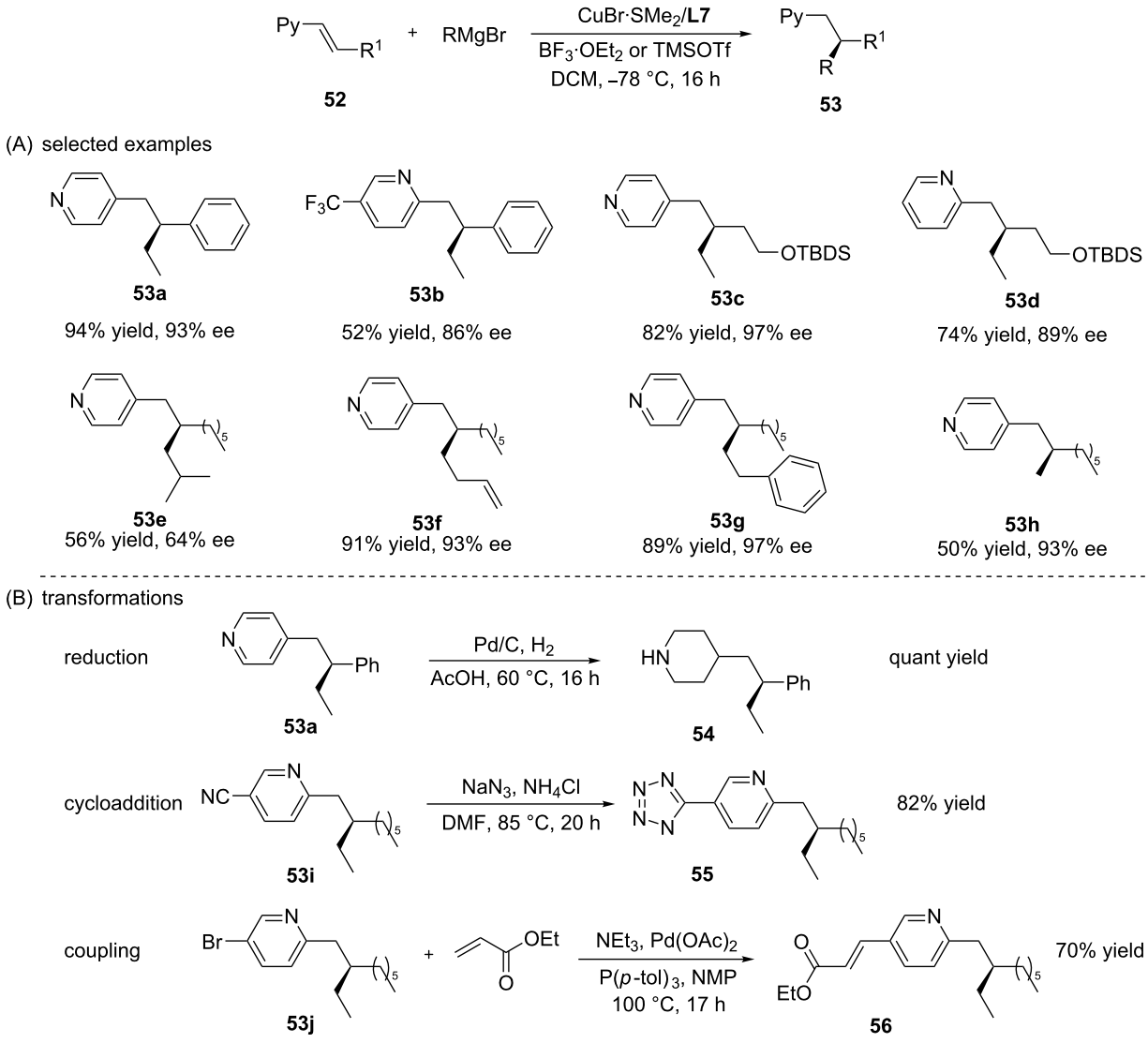

Scheme 15: Copper-catalysed ACA of Grignard reagents to β-substituted alkenylpyridines.

Meldrum's acid and its derivatives are versatile reagents in organic synthesis that can be transformed into a wide range of compounds. In 2006, the group of Fillion described the highly enantioselective synthesis of all-carbon benzylic quaternary stereocentres via a conjugate addition of dialkylzinc reagents to alkylidene Meldrum's acids, resulting in the ACA products with high enantiopurity (Scheme 16) [47-52]. Different kinds of Meldrum's acid derivatives were tolerated in this reaction, and the products could undergo various chemical transformations (Scheme 16A). Later on, this methodology was also demonstrated to enable the 1,6-addition of dialkylzinc reagents to functionalized alkylidene Meldrum's acids, providing the resulting products **60** with moderate yields (65%) and enantioselectivity (70% ee) (Scheme 16B).

Conclusion

The aim of this review was to give the reader an overview on the progress made over the past two decades in the field of copper-catalysed C–C bond-forming reactions between heterocyclic acceptors and organometallics. Many excellent methodologies have been reported to date, and the key to the success of these transformations lies in the capability of chiral copper catalysts to activate both the organometallics and heterocyclic acceptors for the reaction. The development of a wide variety of chiral ligands allowed an impressive scope of heterocycles to undergo reactions with organometallics. However, the current state of the field is certainly incomplete, and future developments in substrate and organometallics scope can be expected.

Funding

Financial support was received from the European Research Council (ERC Consolidator to S. R. H.; Grant No. 773264, LACOPAROM), the China Scholarship Council (CSC, to Y. G.), and the Netherlands Organisation for Scientific Research (NWO, Vici grant 491 724.017.003).

ORCID® iDs

Yafei Guo - https://orcid.org/0000-0001-8720-3887
Syuzanna R. Harutyunyan - https://orcid.org/0000-0003-2411-1250

References

1. Harutyunyan, S. R.; den Hartog, T.; Geurts, K.; Minnaard, A. J.; Feringa, B. L. *Chem. Rev.* **2008,** *108,* 2824–2852. doi:10.1021/cr068424k
2. Alexakis, A.; Bäckvall, J. E.; Krause, N.; Pamies, O.; Dieguez, M. *Chem. Rev.* **2008,** *108,* 2796–2823. doi:10.1021/cr0683515

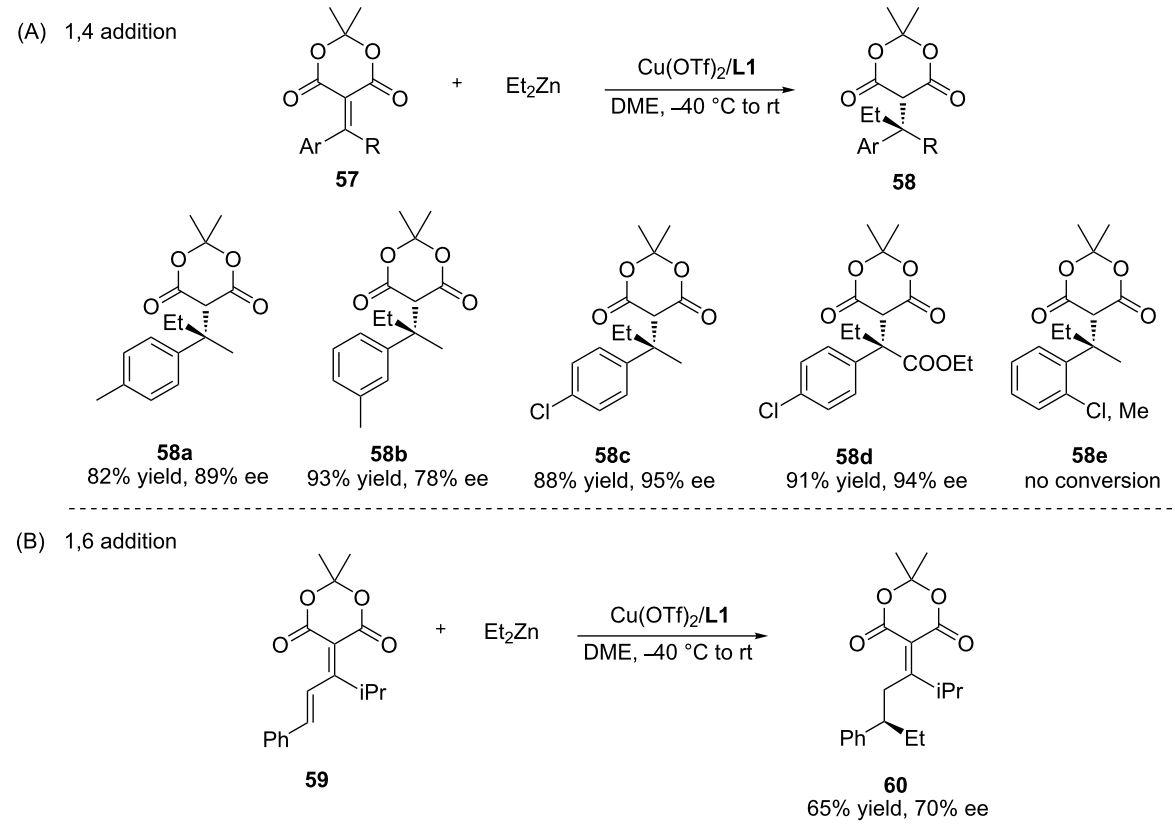

Scheme 16: Copper-catalysed ACA of organozinc reagents to alkylidene Meldrum's acids.

3. Jerphagnon, T.; Pizzuti, M. G.; Minnaard, A. J.; Feringa, B. L. *Chem. Soc. Rev.* **2009,** *38,* 1039–1075. doi:10.1039/b816853a
4. Schmid, T. E.; Drissi-Amraoui, S.; Crévisy, C.; Baslé, O.; Mauduit, M. *Beilstein J. Org. Chem.* **2015,** *11,* 2418–2434. doi:10.3762/bjoc.11.263
5. Bates, R. W.; Sridhar, S. *J. Org. Chem.* **2008,** *73,* 8104–8105. doi:10.1021/jo801433f
6. Brown, M. K.; Hoveyda, A. H. *J. Am. Chem. Soc.* **2008,** *130,* 12904–12906. doi:10.1021/ja8058414
7. Chin, Y.-J.; Wang, S.-Y.; Loh, T.-P. *Org. Lett.* **2009,** *11,* 3674–3676. doi:10.1021/ol901480s
8. Pereira, C. L.; Chen, Y.-H.; McDonald, F. E. *J. Am. Chem. Soc.* **2009,** *131,* 6066–6067. doi:10.1021/ja9009265
9. Rani, R.; Granchi, C. *Eur. J. Med. Chem.* **2015,** *97,* 505–524. doi:10.1016/j.ejmech.2014.11.031
10. Vinogradov, M. G.; Turova, O. V.; Zlotin, S. G. *Org. Biomol. Chem.* **2019,** *17,* 3670–3708. doi:10.1039/c8ob03034k
11. Sharma, V.; Kumar, P.; Pathak, D. *J. Heterocycl. Chem.* **2010,** *47,* 491–502. doi:10.1002/jhet.349
12. Chung, Y. K.; Fu, G. C. *Angew. Chem., Int. Ed.* **2009,** *48,* 2225–2227. doi:10.1002/anie.200805377
13. Fustero, S.; Moscardó, J.; Jiménez, D.; Pérez-Carrión, M. D.; Sánchez-Roselló, M.; del Pozo, C. *Chem. – Eur. J.* **2008,** *14,* 9868–9872. doi:10.1002/chem.200801480
14. Takahashi, K.; Midori, M.; Kawano, K.; Ishihara, J.; Hatakeyama, S. *Angew. Chem., Int. Ed.* **2008,** *47,* 6244–6246. doi:10.1002/anie.200801967
15. Šebesta, R.; Pizzuti, M. G.; Boersma, A. J.; Minnaard, A. J.; Feringa, B. L. *Chem. Commun.* **2005,** 1711–1713. doi:10.1039/b417727d
16. Endo, K.; Ogawa, M.; Shibata, T. *Angew. Chem., Int. Ed.* **2010,** *49,* 2410–2413. doi:10.1002/anie.200906839
17. Pizzuti, M. G.; Minnaard, A. J.; Feringa, B. L. *Org. Biomol. Chem.* **2008,** *6,* 3464–3466. doi:10.1039/b807575a
18. Guo, Y.; Harutyunyan, S. R. *Angew. Chem., Int. Ed.* **2019,** *58,* 12950–12954. doi:10.1002/anie.201906237
19. Müller, D.; Alexakis, A. *Org. Lett.* **2012,** *14,* 1842–1845. doi:10.1021/ol3004436
20. Fernández-Ibáñez, M. Á.; Maciá, B.; Pizzuti, M. G.; Minnaard, A. J.; Feringa, B. L. *Angew. Chem., Int. Ed.* **2009,** *48,* 9339–9341. doi:10.1002/anie.200904981
21. Alexakis, A.; Amiot, F. *Tetrahedron: Asymmetry* **2002,** *13,* 2117–2122. doi:10.1016/s0957-4166(02)00531-1
22. Rideau, E.; You, H.; Sidera, M.; Claridge, T. D. W.; Fletcher, S. P. *J. Am. Chem. Soc.* **2017,** *139,* 5614–5624. doi:10.1021/jacs.7b02440
23. Gao, Z.; Fletcher, S. P. *Chem. Sci.* **2017,** *8,* 641–646. doi:10.1039/c6sc02811j
24. Schäfer, P.; Sidera, M.; Palacin, T.; Fletcher, S. P. *Chem. Commun.* **2017,** *53,* 12499–12511. doi:10.1039/c7cc07151e
25. Ardkhean, R.; Roth, P. M. C.; Maksymowicz, R. M.; Curran, A.; Peng, Q.; Paton, R. S.; Fletcher, S. P. *ACS Catal.* **2017,** *7,* 6729–6737. doi:10.1021/acscatal.7b01453
26. Wang, J. Y. J.; Palacin, T.; Fletcher, S. P. *Org. Lett.* **2019,** *21,* 378–381. doi:10.1021/acs.orglett.8b03520
27. Némethová, I.; Bilka, S.; Šebesta, R. *J. Organomet. Chem.* **2018,** *856,* 100–108. doi:10.1016/j.jorganchem.2017.12.042
28. Vila, C.; Hornillos, V.; Fañanás-Mastral, M.; Feringa, B. L. *Chem. Commun.* **2013,** *49,* 5933–5935. doi:10.1039/c3cc43105c
29. Teichert, J. F.; Feringa, B. L. *Chem. Commun.* **2011,** *47,* 2679–2681. doi:10.1039/c0cc05160h
30. Pineschi, M.; Del Moro, F.; Gini, F.; Minnaard, A. J.; Feringa, B. L. *Chem. Commun.* **2004,** 1244–1245. doi:10.1039/b403793f
31. Rodríguez-Fernández, M.; Yan, X.; Collados, J. F.; White, P. B.; Harutyunyan, S. R. *J. Am. Chem. Soc.* **2017,** *139,* 14224–14231. doi:10.1021/jacs.7b07344
32. Cottet, P.; Müller, D.; Alexakis, A. *Org. Lett.* **2013,** *15,* 828–831. doi:10.1021/ol303505k
33. Liang, L.; Su, L.; Li, X.; Chan, A. S. C. *Tetrahedron Lett.* **2003,** *44,* 7217–7220. doi:10.1016/s0040-4039(03)01788-x
34. Tian, M.; Pang, Z.-b.; Li, H.-f.; Wang, L.-l. *Tetrahedron: Asymmetry* **2017,** *28,* 330–337. doi:10.1016/j.tetasy.2017.01.011
35. Yan, M.; Zhou, Z.-Y.; Chan, A. S. C. *Chem. Commun.* **2000,** 115–116. doi:10.1039/a908467c
36. Brown, M. K.; Degrado, S. J.; Hoveyda, A. H. *Angew. Chem., Int. Ed.* **2005,** *44,* 5306–5310. doi:10.1002/anie.200501251
37. Clavier, H.; Coutable, L.; Toupet, L.; Guillemin, J.-C.; Mauduit, M. *J. Organomet. Chem.* **2005,** *690,* 5237–5254. doi:10.1016/j.jorganchem.2005.04.027
38. Mao, B.; Fañanás-Mastral, M.; Feringa, B. L. *Org. Lett.* **2013,** *15,* 286–289. doi:10.1021/ol303141x
39. Rideau, E.; Fletcher, S. P. *Beilstein J. Org. Chem.* **2015,** *11,* 2435–2443. doi:10.3762/bjoc.11.264
40. Jacques, R.; Pullin, R. D. C.; Fletcher, S. P. *Nat. Commun.* **2019,** *10,* No. 21. doi:10.1038/s41467-018-07871-x
41. Ladjel, C.; Fuchs, N.; Zhao, J.; Bernardinelli, G.; Alexakis, A. *Eur. J. Org. Chem.* **2009,** 4949–4955. doi:10.1002/ejoc.200900662
42. Bos, P. H.; Rudolph, A.; Perez, M.; Fañanás-Mastral, M.; Harutyunyan, S. R.; Feringa, B. L. *Chem. Commun.* **2012,** *48,* 1748–1750. doi:10.1039/c2cc16855c
43. Palais, L.; Bournaud, C.; Micouin, L.; Alexakis, A. *Chem. – Eur. J.* **2010,** *16,* 2567–2573. doi:10.1002/chem.200902417
44. Jumde, R. P.; Lanza, F.; Veenstra, M. J.; Harutyunyan, S. R. *Science* **2016,** *352,* 433–437. doi:10.1126/science.aaf1983
45. Lanza, F.; Pérez, J. M.; Jumde, R. P.; Harutyunyan, S. R. *Synthesis* **2019,** *51,* 1253–1262. doi:10.1055/s-0037-1611657
46. Jumde, R. P.; Lanza, F.; Pellegrini, T.; Harutyunyan, S. R. *Nat. Commun.* **2017,** *8,* 2058. doi:10.1038/s41467-017-01966-7
47. Fillion, E.; Wilsily, A. *J. Am. Chem. Soc.* **2006,** *128,* 2774–2775. doi:10.1021/ja056692e
48. Dumas, A. M.; Fillion, E. *Acc. Chem. Res.* **2010,** *43,* 440–454. doi:10.1021/ar900229z
49. Wilsily, A.; Fillion, E. *J. Org. Chem.* **2009,** *74,* 8583–8594. doi:10.1021/jo901559d
50. Wilsily, A.; Fillion, E. *Org. Lett.* **2008,** *10,* 2801–2804. doi:10.1021/ol800923q
51. Fillion, E.; Wilsily, A.; Liao, E.-T. *Tetrahedron: Asymmetry* **2006,** *17,* 2957–2959. doi:10.1016/j.tetasy.2006.11.009
52. Wilsily, A.; Lou, T.; Fillion, E. *Synthesis* **2009,** 2066–2072. doi:10.1055/s-0029-1216845

BEILSTEIN JOURNAL OF ORGANIC CHEMISTRY

Copper-based fluorinated reagents for the synthesis of CF_2R-containing molecules (R ≠ F)

Louise Ruyet and Tatiana Besset*

Review

Open Access

Address:
Normandie Univ, INSA Rouen, UNIROUEN, CNRS, COBRA (UMR 6014), 76000 Rouen, France

Email:
Tatiana Besset* - tatiana.besset@insa-rouen.fr

* Corresponding author

Keywords:
copper; difluoromethylation; fluorinated reagents; fluorine chemistry; synthetic methodologies

Beilstein J. Org. Chem. **2020,** *16,* 1051–1065.
doi:10.3762/bjoc.16.92

Received: 19 March 2020
Accepted: 29 April 2020
Published: 18 May 2020

This article is part of the thematic issue "Copper-catalyzed reactions for organic synthesis".

Guest Editor: O. Riant

Abstract

Over the years, the development of new methodologies for the introduction of various fluorinated motifs has gained a significant interest due to the importance of fluorine-containing molecules in the pharmaceutical and agrochemical industries. In a world eager to eco-friendlier tools, the need for innovative methods has been growing. To address these two challenges, copper-based reagents were developed to introduce CF_2H, CF_2R_F, CF_2CH_3, $CF_2PO(OEt)_2$ and CF_2SO_2Ph motifs on a broad range of substrates. Copper-based fluorinated reagents have the advantage of being inexpensive and generally in situ generated or prepared in a few steps, which make them convenient to use. In this review, an overview of the recent advances made for the synthesis of fluorinated molecules using copper-based fluorinated reagents will be given.

Introduction

In a society in which fluorinated molecules are playing a pivotal role in pharmaceutical and agrochemical industries as well as in materials science [1-4], the quest for innovation in the organofluorine chemistry field is of high importance. In that context, the development of new strategies is an important driving force [5-14], offering efficient and original tools to introduce a fluorine atom or a fluorinated moiety of unique properties [15]. Despite the tremendous advances made in that field, key synthetic challenges remain to synthesize fluorinated scaffolds. Among the different developed strategies to ravel synthetic issues, the use of inexpensive and readily available copper-based fluorinated reagents appeared over the years as a powerful tool in various transformations for the introduction of fluorinated moieties. Such strategy has already demonstrated a significant synthetic value for the trifluoromethylation of various compounds [16-27]. In contrast, available reagents for the incorporation of a CF_2R (R = H, alkyl, R_F, FG; FG = functional group) moiety remain restricted, despite the potential of

these functionalized fluorinated moieties. In this review, the main contributions in the field of copper-based reagents for the introduction of CF_2H, CF_2FG, CF_2Me and CF_2R_F moieties over the last 5 years (period of 2014–2019) will be summarized. The design and the elaboration of either pre-formed or in situ-generated copper-based reagents was an efficient tool in several reactions. Note that only transformations involving the use of such copper-based reagents will be depicted and copper-catalyzed reactions are therefore beyond the scope of this review.

Review

Copper-based difluoromethylating reagents

In this section the key advances made to access copper-based difluoromethylating reagents are summarized. The CF_2H moiety [28-32], a well recognized alcohol and thiol bioisoster, is particularly attractive due to its unique features [33-36]. Besides, this residue is present in several bioactive compounds such as Deracoxib and Thiazopyr. In comparison with trifluoromethylcopper complexes, the difluoromethylcopper ones are less stable as demonstrated by the work of Burton in 2007 [37]. Investigations on the in situ synthesis of difluoromethylcopper from a difluoromethylcadmium source at low temperature and the study of its reactivity with various classes of compounds such as allylic halides, propargylic halides and tosylates, iodoalkynes and reactive alkyl halides were realized. It was established that $CuCF_2H$ readily decompose into 1,1,2,2-tetrafluoroethane and *cis*-difluoroethylene. From this pioneer work, attention was paid either to the design of new synthetic pathways for the synthesis of a well-defined copper-based reagent or to new tools for the in situ generation of an active $CuCF_2H$ species and its application in several transformations.

Pre-defined difluoromethylating reagents

In the quest for well-defined and isolable MCF_2H species, Sanford depicted for the first time in 2017 the synthesis and characterization of isolable difluoromethylcopper(I) complexes [38]. The latter were prepared in a two-step sequence starting from the corresponding (NHC)CuCl as precursors in the presence of NaO*t*-Bu followed by the addition of $TMSCF_2H$ (Scheme 1). The latter was prepared in a one step synthesis after reduction of the Ruppert–Prakash reagent with sodium borohydride [39]. The key of success was the use of bulky IPr and SIPr ligands to stabilize the organometallic species. Indeed, in the case of IPr as a ligand, the complex was stable in solution at room temperature for at least 24 hours. The reactivity of the complex was then studied in stoichiometric reactions with aryl iodides and iodonium salts. The difluoromethylation reaction was smoothly carried out at 90 °C with electron-rich and electron-poor aryl iodides. However, the reaction was more efficient with electron-poor aryl iodides (Scheme 1). It is important to highlight that, in the course of their study for the synthesis of a stable and isolable (NHC)$CuCF_2H$ complex and the study of its reactivity, Sanford and co-workers demonstrated the possibility to develop a catalytic version of the reaction through the in situ generation of the active (IPr)$CuCF_2H$, starting from (IPr)CuCl [38].

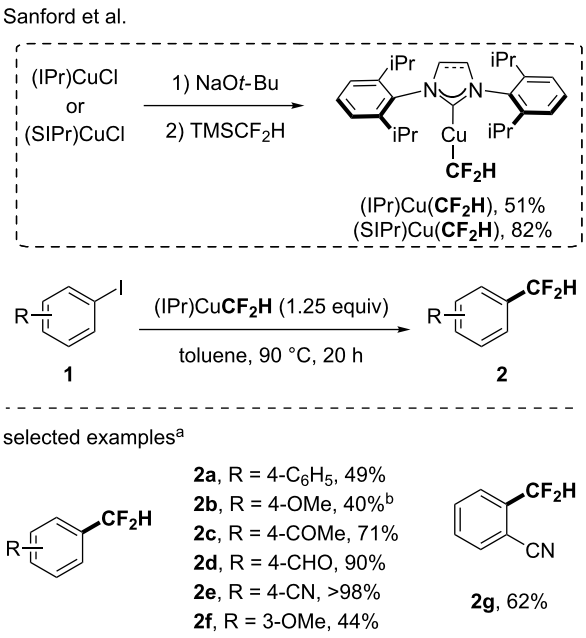

Scheme 1: Synthesis of the first isolable (NHC)$CuCF_2H$ complexes from $TMSCF_2H$ and their application for the synthesis of difluoromethylated arenes from aryl iodides. [a]Yields were determined by ^{19}F NMR with fluorobenzene as the internal standard. [b]Reaction carried out at 120 °C.

In situ-generated copper-based difluoromethylating reagents

Although the review focused on the 2014–2019 period, a brief overview of seminal major advances should be given. In 2012, Hartwig and co-worker studied the difluoromethylation reaction of aryl and vinyl iodides by a copper-mediated transformation using $TMSCF_2H$ as the fluorinated source [39]. In this work, $CuCF_2H$ was suggested as the active species to promote the expected transformation. They highlighted that the formation of a cuprate species: $Cu(CF_2H)_2^-$, favoured by the presence of an excess of $TMSCF_2H$, might act as a reservoir of the unstable and reactive $CuCF_2H$ species. Xu and Qing reported a similar strategy for the difluoromethylation of electron-poor (hetero)aryl iodides at room temperature, using only 2.4 equivalents of $TMSCF_2H$ [40]. Note that the use of a strong base (*t*-BuOK) and 1,10-phenanthroline as a ligand was crucial in their system. In 2012, Prakash also studied the in situ generation of $CuCF_2H$ from *n*-Bu_3SnCF_2H, the presence of DMF being the key to stabilize the $CuCF_2H$ intermediate [41] (Scheme 2).

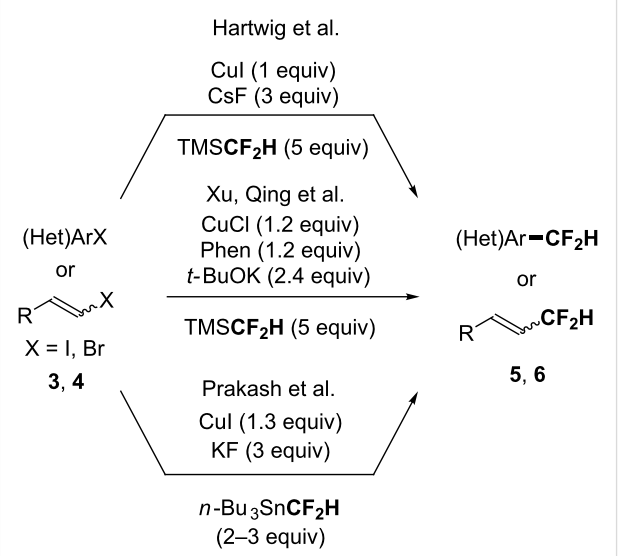

Scheme 2: Pioneer works for the in situ generation of $CuCF_2H$ from $TMSCF_2H$ and from n-Bu_3SnCF_2H. Phen = 1,10-phenanthroline.

From these seminal works, a handful of reports was then published by different research groups. In 2014, the group of Goossen astutely reported the in situ generation of the $CuCF_2H$ complex starting from $TMSCF_2H$, CuSCN and CsF as an activator in DMF. This approach was successfully applied in a Sandmeyer-type difluoromethylation reaction (Scheme 3) [42]. Starting from (hetero)aryldiazonium salts, a panel of difluoromethylated arenes and heteroarenes was obtained (26 examples, up to 84% yield). Note that the transformation was also carried out starting from 4-methoxyaniline followed by the in situ formation of the corresponding diazonium salt.

In the same vein, the authors used this in situ generation of a $CuCF_2H$ species to access high value-added difluoromethylthiolated molecules starting from organothiocyanates [43]. With this approach, they then developed a one pot, two-step sequence (generation of the organothiocyanates followed by the difluoromethylation step) for the functionalization of alkyl bromides, alkyl mesylates, aryldiazonium salts [43] as well as electron-rich arenes [44] (Scheme 4).

In 2015, the group of Qing investigated the oxidative difluoromethylation reaction of terminal alkynes with $TMSCF_2H$ via a copper-mediated reaction [45]. Using a stoichiometric amount of CuI, in the presence of t-BuOK and 9,10-phenanthraquinone, the functionalization of a panel of (hetero)aromatic and aliphatic terminal alkynes was achieved (Scheme 5). A good functional group tolerance was observed as alkynes bearing a cyano, ester, bromo or amino group among others were suitable substrates. Based on ^{19}F NMR studies, the authors suggested the following mechanism: first the in situ generation of a $CuCF_2H$ complex from $TMSCF_2H$ in equilibrium with the corresponding cuprate ($Cu(CF_2H)_2^-$) occurred followed by the reaction with terminal alkynes under basic conditions. The resulting organocopper derivative was then oxidized resulting in the formation of the desired products.

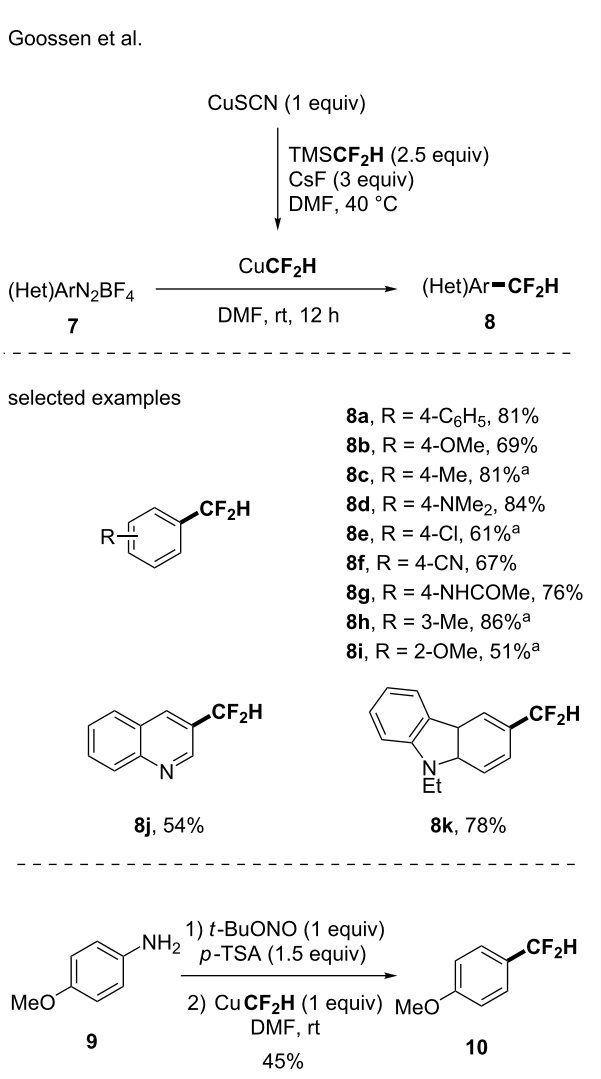

Scheme 3: A Sandmeyer-type difluoromethylation reaction via the in situ generation of $CuCF_2H$ from $TMSCF_2H$. [a] ^{19}F NMR yields determined using 2,2,2-trifluoroethanol as the internal standard.

Note that in 2018 the same group reported the copper-mediated oxidative difluoromethylation of heteroarenes under similar reaction conditions ($TMSCF_2H$, CuCN, 9,10-phenanthrenequinone, t-BuOK in NMP) [46]. Not only oxazoles (17 examples, up to 87% yield) were difluoromethylated but a variety of other heteroarenes turned out to be suitable such as pyridine, imidazole, benzo[d]thiazole, benzo[b]thiophene, benzo[d]oxazole, thiazole and thiophene derivatives (Scheme 6).

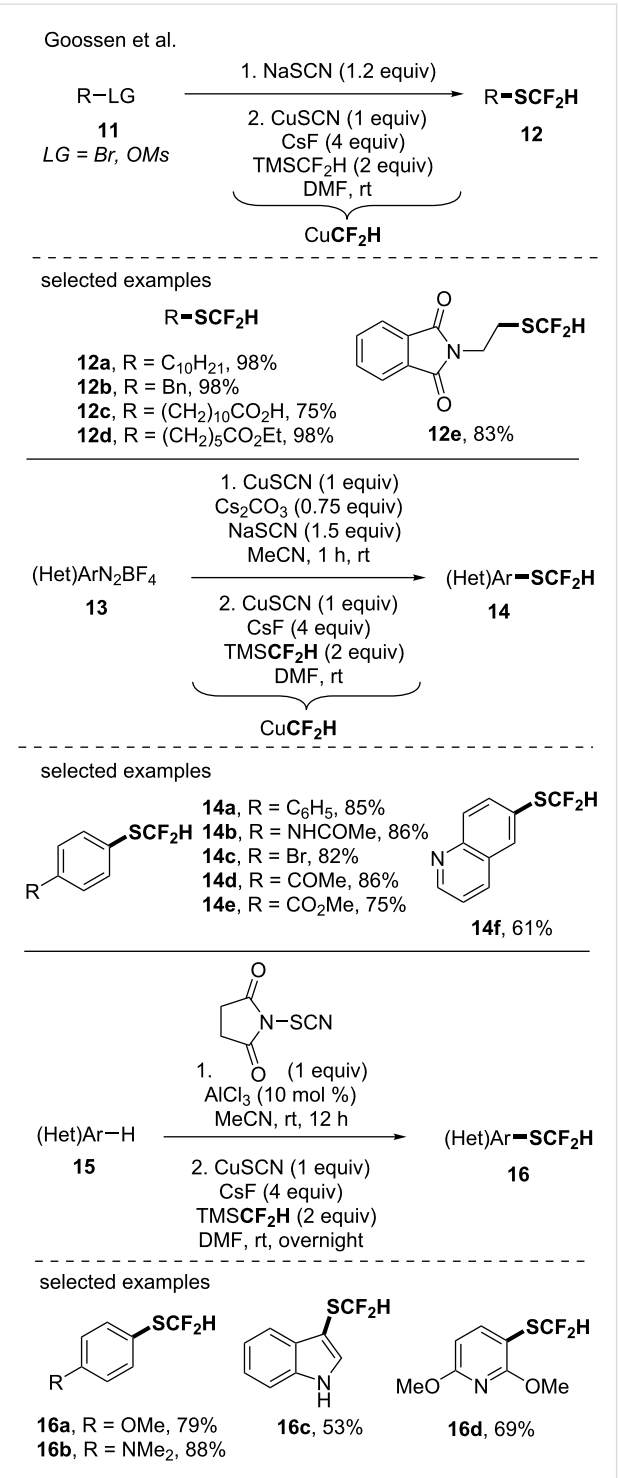

Scheme 4: A one pot, two-step sequence for the difluoromethylthiolation of various classes of compounds via the in situ generation of $CuCF_2H$ from $TMSCF_2H$.

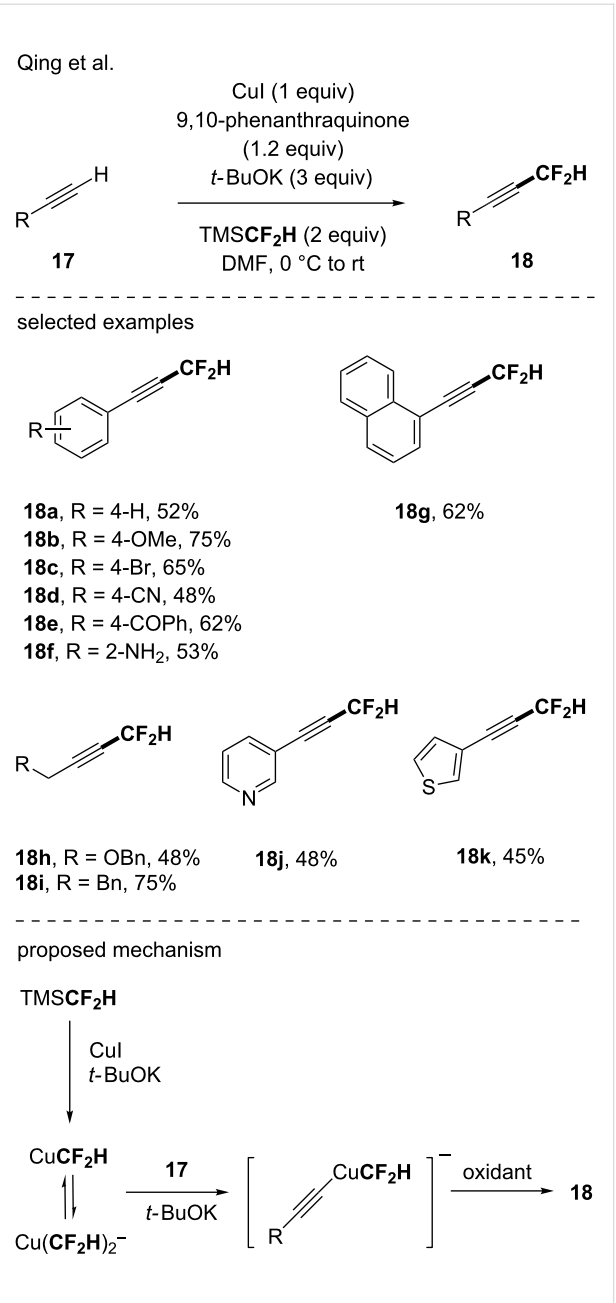

Scheme 5: A copper-mediated oxidative difluoromethylation of terminal alkynes via the in situ generation of a $CuCF_2H$ complex.

Copper-based CF_2FG-containing reagents

Besides the traditional CF_3 and CF_2H groups, a strong interest was devoted to other CF_2R groups (R = $PO(OEt)_2$, SO_2Ph and Me). In that aim, the development of copper-based reagents to introduce them onto molecules was studied over the last years and the major advances will be summarized in this section.

An in situ-generated copper-based $CF_2PO(OEt)_2$ reagent

As a bioisostere of the phosphonate group [47], a lot of attention was paid to the difluoromethylphosphonate residue as well as the development of efficient methodologies to introduce it onto molecules [48]. In that context, main contributions were made by the groups of Poisson and Goossen.

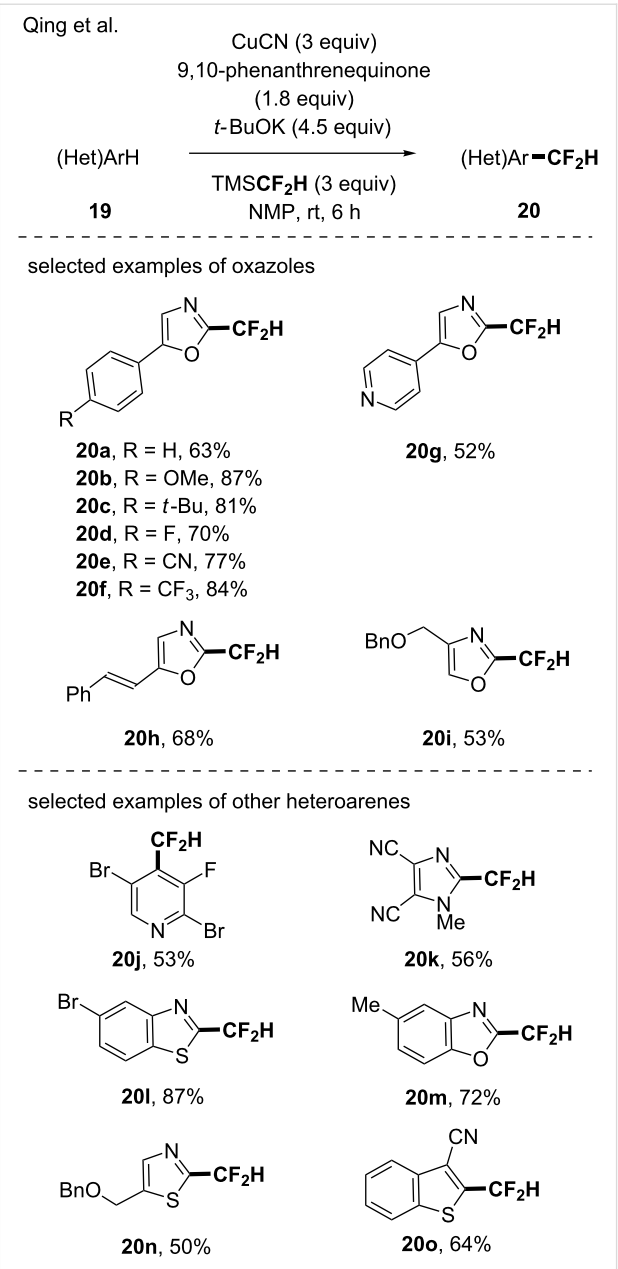

Scheme 6: A copper-mediated oxidative difluoromethylation of heteroarenes.

In the course of their study regarding the synthesis of difluoromethylphosphonate-containing molecules, Poisson and co-workers investigated the in situ generation of a $CuCF_2PO(OEt)_2$ species and its application to functionalize various classes of compounds [49-54]. The active species was prepared from $TMSCF_2PO(OEt)_2$, a copper salt and an activator. Note that the $TMSCF_2PO(OEt)_2$ was easily prepared from the commercially available $BrCF_2PO(OEt)_2$ and TMSCl under basic conditions [49]. The access to $CF_2PO(OEt)_2$-containing arenes was obtained after a Sandmeyer-type reaction (Scheme 7, reaction a) [49]. The reaction was efficient, al-

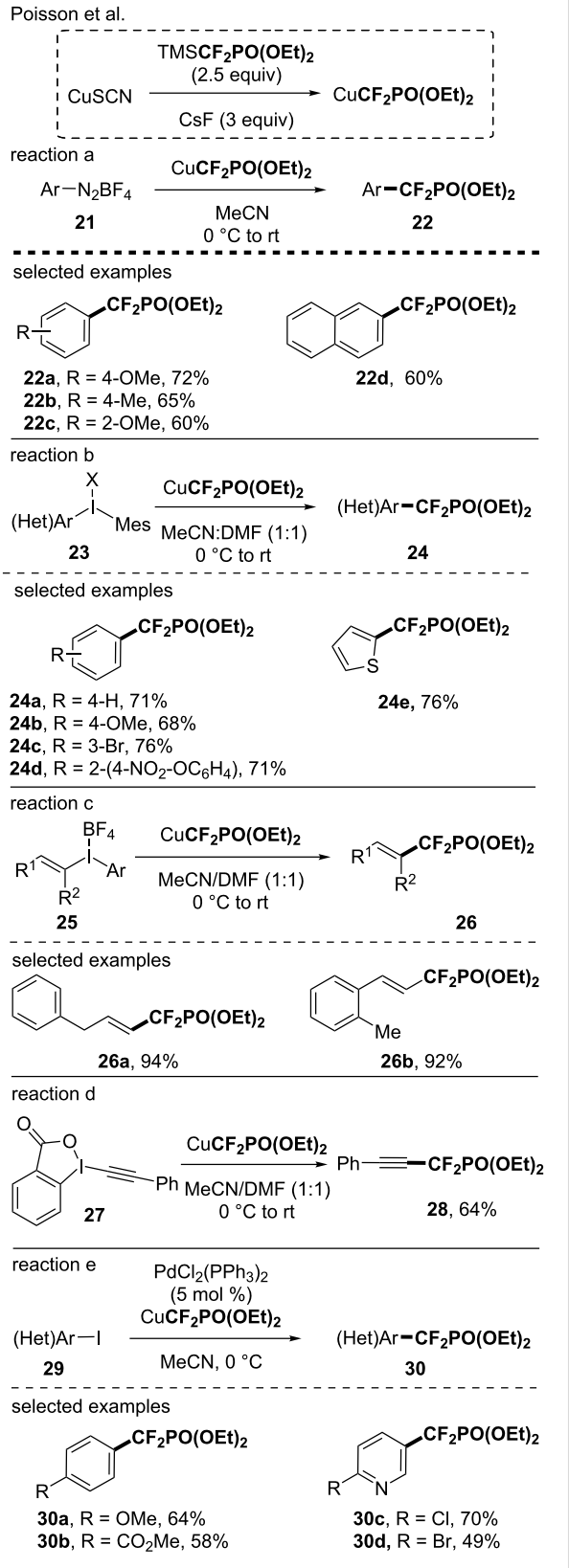

Scheme 7: Synthesis of difluoromethylphosphonate-containing molecules using the in situ-generated $CuCF_2PO(OEt)_2$ species.

though heteroaryl diazonium salts were reluctant in this reaction. To overcome these limitations, hypervalent iodinated species were used as substrates. The copper-mediated reaction with λ^3-iodanes demonstrated a large functional group tolerance and was efficiently applied to the synthesis of $CF_2PO(OEt)_2$-containing (hetero)arenes, alkenes and alkynes (Scheme 7, reactions b–d) [50]. Later on, the same group depicted the Pd-catalyzed introduction of the $CF_2PO(OEt)_2$ residue on (hetero)aryl iodides [51] by using an in situ-generated copper-based reagent (19 examples, up to 80% yield, Scheme 7e).

With a similar method and in the presence of 1,10-phenanthroline as a ligand, the functionalization of alkenyl halides (8 examples, up to 82% yield), allyl halides (7 examples, up to 99% yield) and benzyl bromides (6 examples, up to 87% yield) was investigated (Scheme 8) [52].

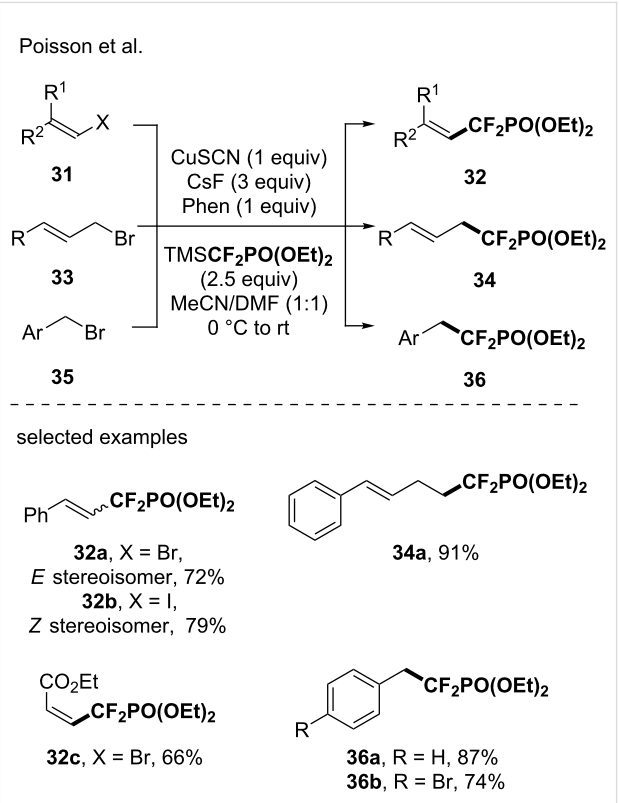

Scheme 8: Synthesis of difluoromethylphosphonate-containing molecules using in situ-generated $CuCF_2PO(OEt)_2$ species with 1,10-phenantroline as a ligand. Phen: 1,10-phenanthroline.

Finally, the Poisson's group developed a methodology for the Ullman cross-coupling reaction between the in situ-generated $CuCF_2PO(OEt)_2$ and aryl iodides containing a coordinating group (e.g., CO_2CH_3, $COCH_3$, NO_2), at the *ortho*-position of the halide [52]. This reaction broadened the portfolio of $CF_2PO(OEt)_2$-containing molecules leading to the corresponding compounds in good to excellent yields (Scheme 9). Note that the versatility of this methodology was further proved through its application to disulfides [52] with moderate to good yields.

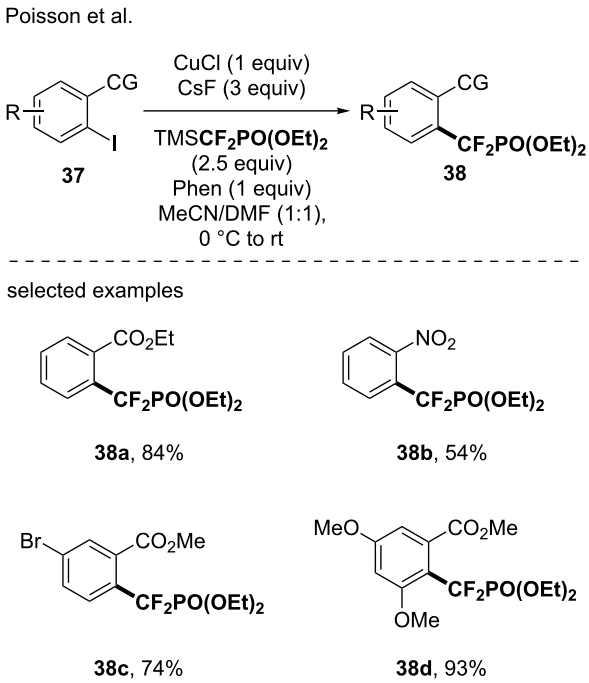

Scheme 9: Synthesis of difluoromethylphosphonate-containing molecules using in situ-generated $CuCF_2PO(OEt)_2$ species by an Ullman cross-coupling. CG = coordinating group.

Poisson and co-workers also reported the reaction of the $CuCF_2PO(OEt)_2$ reagent with α-diazocarbonyl derivatives. Depending on the copper salt used for the generation of the copper reagent, the reaction with α-diazocarbonyl derivatives provided either the α-fluorovinylphosphonate, in a stereoselective fashion, or the $SCF_2PO(OEt)_2$ derivatives [53]. In the same vein, the reaction of the $CuCF_2PO(OEt)_2$ species, generated from CuSCN, with α-bromoketones provided the α-$SCF_2PO(OEt)_2$-containing ketones [54] (Scheme 10).

In 2019, the group of Goossen developed an approach to access $SCF_2PO(OEt)_2$-containing arenes based on a Sandmeyer thiocyanation reaction followed by a Langlois-type nucleophilic substitution of the cyano group by the $CF_2PO(OEt)_2$ residue [55]. Several (diethylphosphono)difluoromethylthiolated products were obtained and this report further showcased the potential of using a copper-based reagent for the introduction of fluorinated moieties as this reaction involved the in situ generation of a suitable $CuCF_2PO(OEt)_2$ species (Scheme 11).

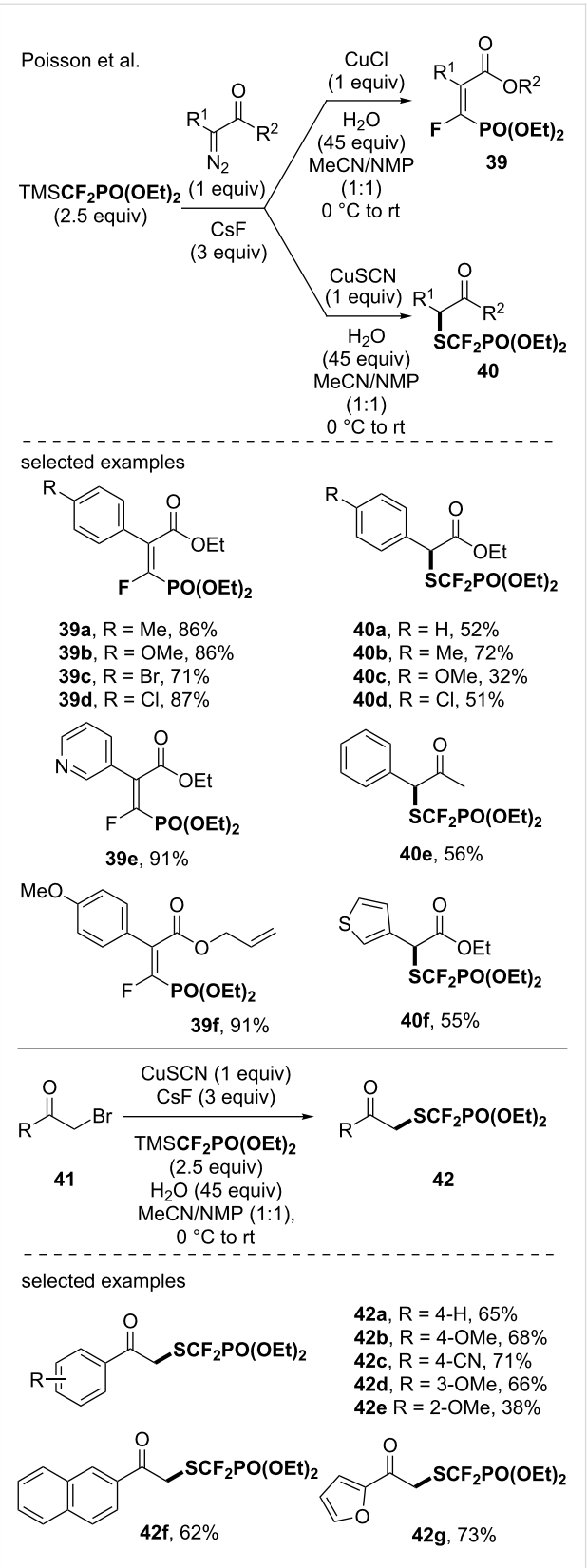

Scheme 10: Synthesis of (diethylphosphono)difluoromethylthiolated molecules using in situ-generated $CuCF_2PO(OEt)_2$ species. Phen: 1,10-phenanthroline.

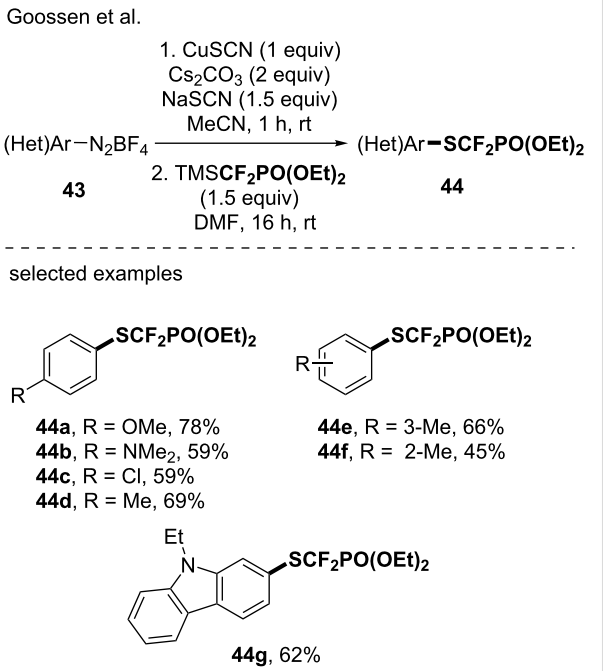

Scheme 11: Access to (diethylphosphono)difluoromethylthiolated molecules via the in situ generation of $CuCF_2PO(OEt)_2$ species.

An in situ-generated copper-based CF_2SO_2Ph reagent

As a long standing interest to the $PhSO_2CF_2$ moiety [56-60] thanks to its unique features, the group of Hu investigated the generation of the $PhSO_2CF_2Cu$ species from $PhSO_2CF_2TMS$, CuI and CsF in DMF [61] (Scheme 12). Note that $PhSO_2CF_2TMS$ was prepared from $PhSO_2CF_2Br$ after treatment with *n*-BuLi and TMSCl [61]. Due to its relatively low stability at room temperature, $PhSO_2CF_2Cu$ was in situ generated and applied to the (phenylsulfonyl)difluoromethylation reaction of propargyl chlorides and alkynyl halides, offering an access to the corresponding fluorinated allenes (6 examples) and alkynes (8 examples). In 2016, still interested by this versatile fluorinated moiety, the same authors demonstrated that the $PhSO_2CF_2Cu$ species might be prepared from difluoromethylphenylsulfone ($PhSO_2CF_2H$) and used it to functionalize an array of (hetero)aromatic boronic acids [62] (Scheme 12). The transformation showed a good functional group tolerance (aldehyde, CN, halogens). Note that the synthetic utility of the CF_2SO_2Ph group was further demonstrated by its conversion into the high value-added CF_2H moiety after treatment with Mg/AcOH/AcONa.

An in situ-generated copper-based CF_2CH_3 reagent

A strong interest was dedicated to the CF_2CH_3 residue, an important moiety in medicinal chemistry [63]. Among the different approaches developed to synthesize CF_2CH_3-containing

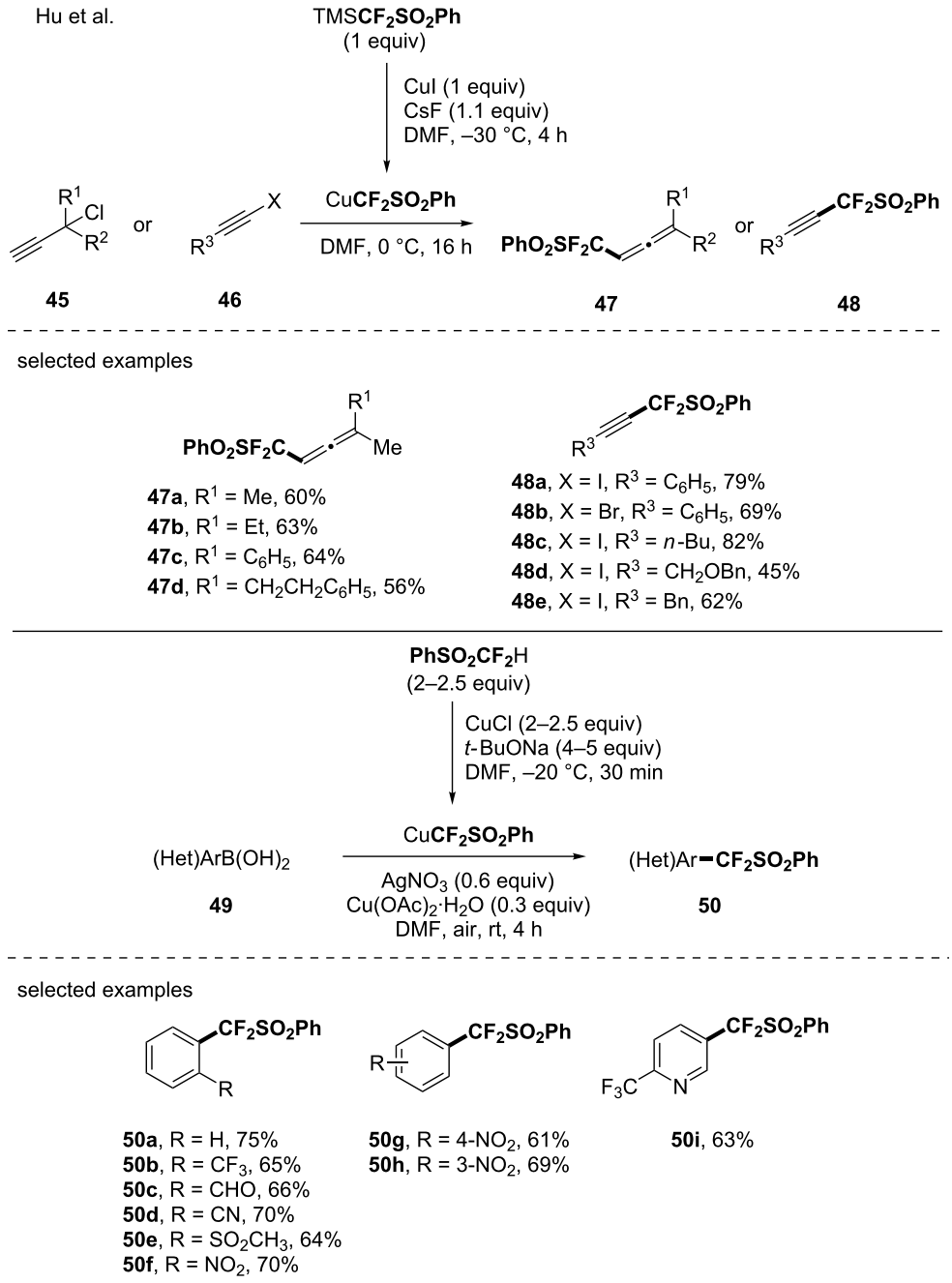

Scheme 12: Synthesis of (phenylsulfonyl)difluoromethyl-containing molecules via the in situ generation of $CuCF_2SO_2Ph$ species.

molecules, Wang, Hu and co-workers demonstrated the possibility to use 1,1-difluoroethylsilane ($TMSCF_2CH_3$) as a precursor for the in situ generation of the corresponding $CuCF_2CH_3$ species [64]. The synthetic utility of this copper-based reagent was illustrated through the 1,1-difluoroethylation of diaryliodonium salts, leading to the corresponding (1,1-difluoroethyl)arenes in moderate to high yields (Scheme 13). The transformation turned out to be functional group tolerant and even heteroaromatic compounds were functionalized.

Copper-based CF_2R_F reagents

Due to the importance of perfluorinated moieties [2] and since their synthesis could not be achieved from the fluorination of the corresponding alkyl chains like in case of perfluoroalkyl arenes, several research groups investigated the synthesis of CF_2R_F-containing molecules via the use of perfluoroalkyl copper species. Before 2014, key contributions were made by the groups of Kremlev, Tyrra [65], Hartwig [66,67] and Grushin [68] as briefly summarized below. These major advances paved

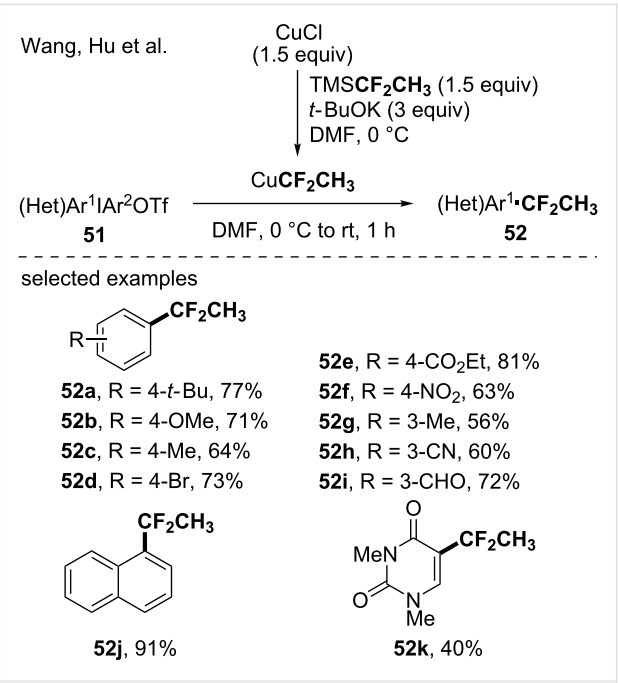

Scheme 13: Copper-mediated 1,1-difluoroethylation of diaryliodonium salts by using the in situ-generated $CuCF_2CH_3$ species.

the way towards the synthesis of important pentafluoroethylated and more generally perfluoroalkylated molecules. Kremlev, Tyrra and co-workers depicted the in situ generation of a $CuCF_2CF_3$ species by mixing $Zn(CF_3)Br{\cdot}2DMF$ and CuBr [65], and its application for the functionalization of (hetero)aryl halides (Scheme 14).

In the course of their studies to develop stable and well-defined copper reagents for perfluoroalkylation reactions [66], Hartwig developed in 2011 the $(Phen)CuCF_3$ and $(Phen)CuCF_2CF_2CF_3$ complexes from inexpensive reagents. Indeed, when mixing $(CuOt\text{-}Bu)_4$, 1,10-phenanthroline and the corresponding $TMSR_F$, the perfluoroalkyl copper complexes were isolated for the first time (Scheme 14, a). One year later, they demonstrated that these copper-based reagents ($(Phen)CuCF_2R_F$, R_F = F, CF_3 and CF_2CF_3) were efficient in a two-step sequence reaction (borylation/perfluoroalkylation) allowing the functionalization of either sterically hindered arenes or aryl bromides with the CF_2CF_3 and $CF_2CF_2CF_3$ moieties (Scheme 14, b) [67]. In 2013, the group of Grushin reported the synthesis, characterization and application of a copper-based pentafluoroethylating reagent (Scheme 14) [68]. Using the cost-efficient pentafluoroethane as

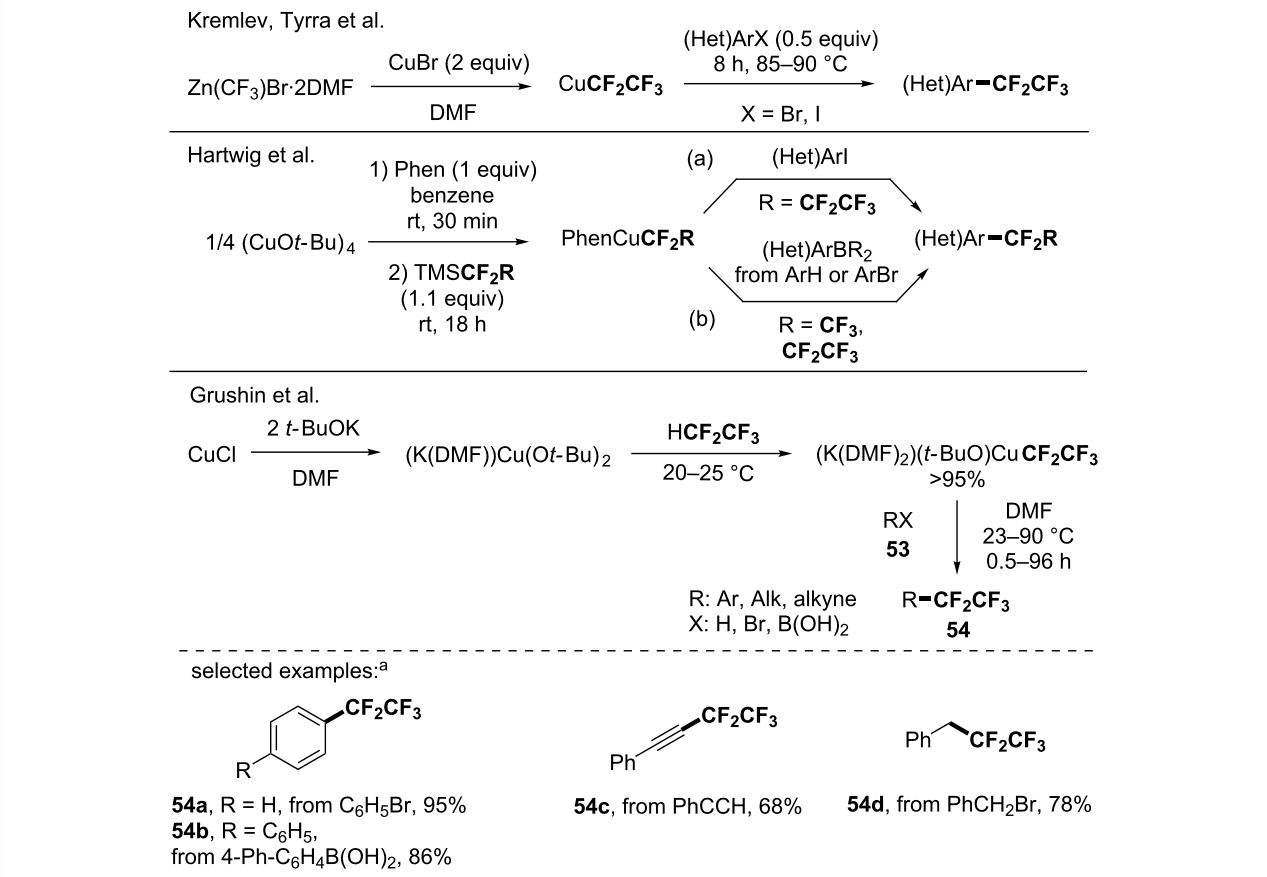

Scheme 14: Pioneer works for the pentafluoroethylation and heptafluoropropylation using a copper-based reagent. Phen = 1,10-phenanthroline.
[a] ^{19}F NMR yields determined using 1,3-bis(trifluoromethyl)benzene as the internal standard.

a precursor, the $(K(DMF)_2)(t\text{-BuO})Cu(CF_2CF_3)$ complex was prepared either from the pre-isolated $(K(DMF))Cu(Ot\text{-Bu})_2$ or in situ from CuCl, *t*-BuOK in DMF in a nearly quantitative yield. The copper reagent was used for the pentafluoroethylation of a panel of (hetero)aryl iodides and bromides (up to 99% ^{19}F NMR yield) and its synthetic utility was further demonstrated with the functionalization of different classes of compounds (benzyl and vinyl bromides, 4-biphenylboronic acid, phenylacetylene for instance).

From these pioneering reports of perfluoroalkylation (trifluoromethylation, pentafluoroethylation and heptafluoropropylation), several groups studied the synthesis and/or the application of copper-based reagents in various transformations as depicted in this section. This latter will be organized into two sub-sections depending if the CuR_F-reagent was well-defined or in situ generated.

Well-defined pentafluoroethylating reagents

In 2014, a report from Hartwig dealt with the copper-mediated perfluororalkyaltion of (hetero)aryl bromides using the previously developed $PhenCuR_F$ [69]. Although the trifluoromethylation reaction was mainly studied, the methodology was efficiently extended to the pentafluoroethylation of various heteroarenes such as pyridine, pyrimidine and quinolone derivatives, for instance, when the $PhenCuCF_2CF_3$ complex was used as the pentafluoroethyl source (24 examples, up to 99% ^{19}F NMR yield and up to 93% isolated yield, Scheme 15). Note that a complete mechanistic study was recently reported to explain the reactivity of this well-designed complex [70].

In 2015, Grushin reported the generation of four well-defined CuC_2F_5 complexes, namely $(Ph_3P)_2CuCF_2CF_3$, $(bpy)CuCF_2CF_3$, $(IPr^*)CuCF_2CF_3$ and $(Ph_3P)Cu(Phen)CF_2CF_3$. The reactivity of the latter was studied for the synthesis of pentafluoroethyl ketones from acyl chlorides [71]. Indeed, the pentafluoroethylation of a large panel of acyl chlorides (23 examples) was achieved illustrating the synthetic utility and the efficiency of the newly designed $(Ph_3P)Cu(phen)CF_2CF_3$ reagent (Scheme 16).

Huang and Weng and co-workers reported the synthesis of air-stable perfluorocarboxylatocopper(I) complexes and their use in the perfluoroalkylation of (hetero)aryl halides [72]. By mixing *t*-BuOCu, in situ generated from CuCl and *t*-BuONa, with 1,10-phenanthroline, followed by a reaction with perfluorocarboxylic acids, four $(Phen)_2Cu(O_2CCF_2R_F)$ complexes were synthesized (R_F = CF_3, CF_2CF_3, $CF_2CF_2CF_3$ and $CF_2CF_2CF_2CF_3$). The reaction was efficient (65 examples, up to 97% yield), showed a good functional group tolerance (i.e., cyano, ester, ketone) and even heteroarenes such as pyridine,

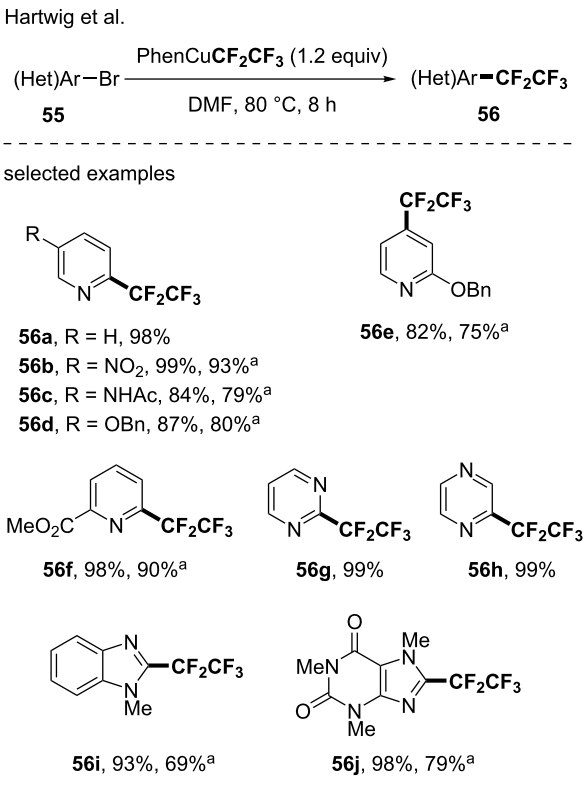

Scheme 15: Pentafluoroethylation of (hetero)aryl bromides using the $(Phen)CuCF_2CF_3$ complex. ^{19}F NMR yields were determined using 4-trifluoromethoxyanisole as the internal standard. [a]Isolated yields.

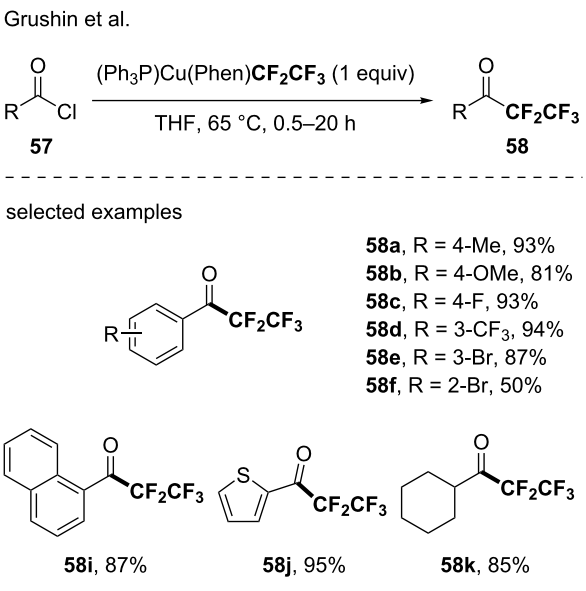

Scheme 16: Synthesis of pentafluoroethyl ketones using the $(Ph_3P)Cu(phen)CF_2CF_3$ reagent. ^{19}F NMR yields were given using 1,3-bis(trifluoromethyl)benzene as the internal standard.

quinoline and quinoxaline were functionalized with the four fluorinated moieties (Scheme 17).

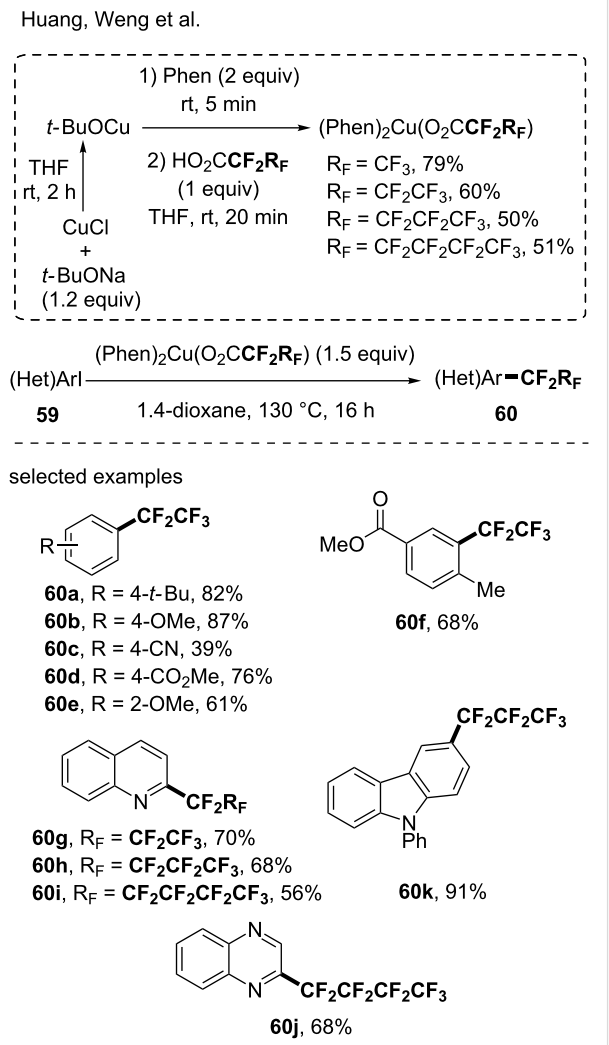

Scheme 17: Synthesis of $(Phen)_2Cu(O_2CCF_2RF)$ and functionalization of (hetero)aryl iodides.

In situ-generated copper-based pentafluoroethylating reagents

Several research groups investigated the generation of a $CuCF_2CF_3$ species from different fluorinated precursors offering various technological solutions.

In 2014, a study from Mikami reported the functionalization of a panel of (hetero)arylboronic acids (10 examples, up to 95% yield) and (hetero)aryl bromides (11 examples, up to 98% ^{19}F NMR yield) via the in situ generation of the suitable $CuCF_2CF_3$ from CuCl, KO*t*-Bu or NaO*t*-Bu and ethyl pentafluoropropionate [73]. Note that the methodology was also applied to the functionalization of a vinylboronic acid and a vinyl bromide (Scheme 18).

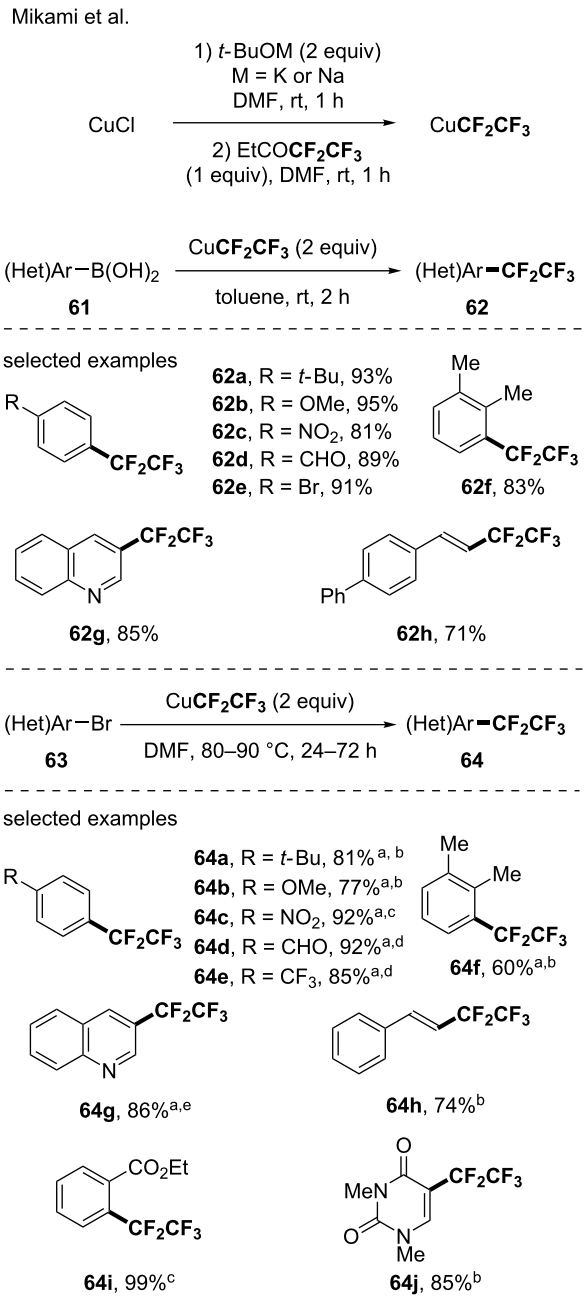

Scheme 18: Pentafluoroethylation of arylboronic acids and (hetero)aryl bromides via the in situ-generated $CuCF_2CF_3$ species from ethyl pentafluoropropionate and CuCl. [a]Yields were determined by ^{19}F NMR using benzotrifluoride (BTF) or trifluoromethoxybenzene as internal standards. [b]90 °C, 72 h. [c]80 °C, 24 h. [d]80 °C, 48 h. [e]90 °C, 48 h.

More recently, in the course of their investigation to generate a $CuCF_3$ reagent from a cyclic-protected hexafluoroacetone, an air-stable liquid trifluoromethylating reagent, and $KCu(OtBu)_2$, the group of Mikami showed that a CF_2CF_3 analog (Scheme 19) was prepared in a similar way and applied for the pentafluoroethylation of aromatic derivatives [74] (2 examples).

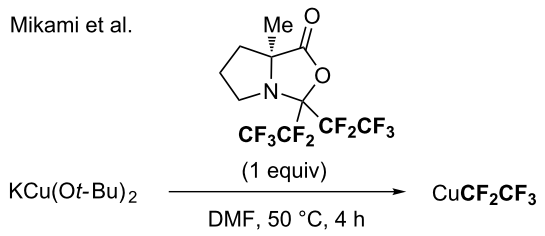

Scheme 19: In situ generation of $CuCF_2CF_3$ species from a cyclic-protected hexafluoroacetone and $KCu(Ot\text{-}Bu)_2$. ^{19}F NMR yields were determined using benzotrifluoride (BTF) as the internal standard.

In 2015, Grushin and co-workers further investigated the functionalization of vinyl halides with CuR_F reagents generated from inexpensive fluoroform ($R_F = CF_3$) and pentafluoroethane (CF_3CF_2H) [75]. Both trifluoromethylation and pentafluoethylation of vinyl bromides and iodides were efficiently achieved in high yields under mild reaction conditions. Noteworthy, the transformation turned out to be functional group tolerant and highly chemo- and stereroselective (Scheme 20).

The group of Hu studied the fluoroalkylation of aryl halides. Indeed, a copper(0)-mediated reductive cross-coupling reaction between the iodobenzene and various 2-bromo-1,1,2,2-tetrafluoroethyl derivatives (RCF_2CF_2Br) was developed presumably involving a RCF_2CF_2Cu species (Scheme 21) [76].

In 2015, Yagupolskii and co-workers investigated the synthesis of perfluoroalkylcopper reagents [77]. Depending on the reaction conditions they were able to access to perfluoroorganolithium copper species or perfluroalkylcopper derivatives from iodoperfluoroalkanes in reaction with either *n*-BuLi or copper powder, respectively (Scheme 22).

In 2017, the group of Hu offered an original synthetic route to the generation of the $PhenCuCF_2CF_3$ reagent [78]. Indeed, they demonstrated that the Ruppert–Prakash reagent was a suit-

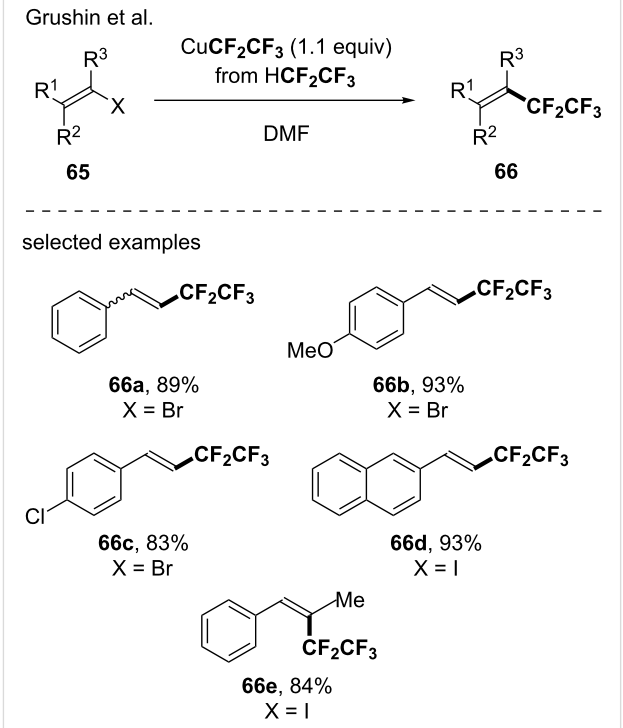

Scheme 20: Pentafluoroethylation of bromo- and iodoalkenes. Only examples of isolated compounds were depicted.

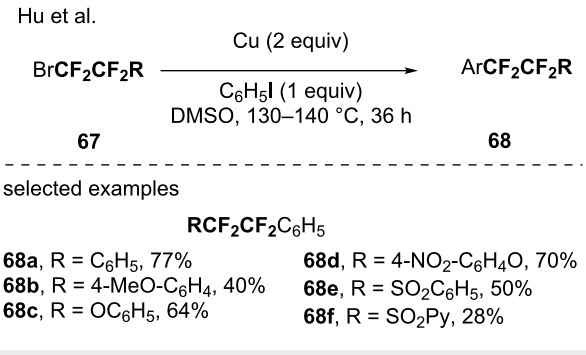

Scheme 21: Fluoroalkylation of aryl halides via a RCF_2CF_2Cu species.

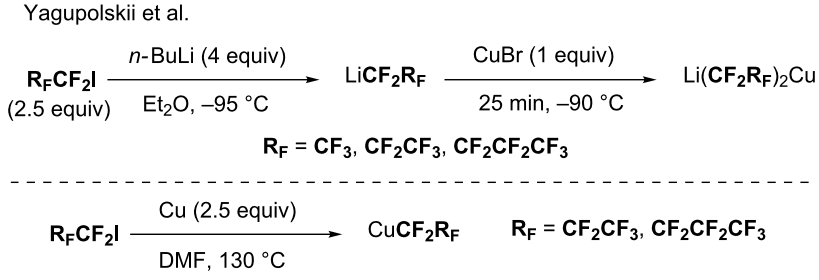

Scheme 22: Synthesis of perfluoroorganolithium copper species or perfluroalkylcopper derivatives from iodoperfluoroalkanes.

able source for the generation of tetrafluoroethylene in the presence of a catalytic amount of NaI. Then, the cupration of the tetrafluoroethylene led to the formation of the expected Phen-$CuCF_2CF_3$ reagent (Scheme 23). This constituted a complementary approach to the existing ones for its synthesis, as it avoided the use of $TMSCF_2CF_3$ or CF_3CF_2H. This copper-based reagent was then used for the pentafluoroethylation of iodoarenes [78]. The transformation was efficient and turned out to be functional group tolerant. The same group extended their protocol to the functionalization of aryldiazonium salts [79]. Very recently, a similar protocol was applied to the pentafluoroethylation of (hetero)aryl halides as well as alkenyl iodides derived from natural compounds (e.g., glycals, nucleosides and nucleobases) [80].

In 2018, Hu and co-workers reported a complementary approach for the pentafluoroethylation of aryl iodides using $TMSCF_3$ for the formation of $CuCF_2CF_3$ [81]. They suggested that in the presence of CuCl, KF and $TMSCF_3$, the corresponding $CuCF_3$ species will be formed and a subsequent homologation step involving a putative copper difluorocarbene will allow the formation of the $CuCF_2CF_3$ species. With this tool in hand, a panel of aryl iodides was functionalized (Scheme 24).

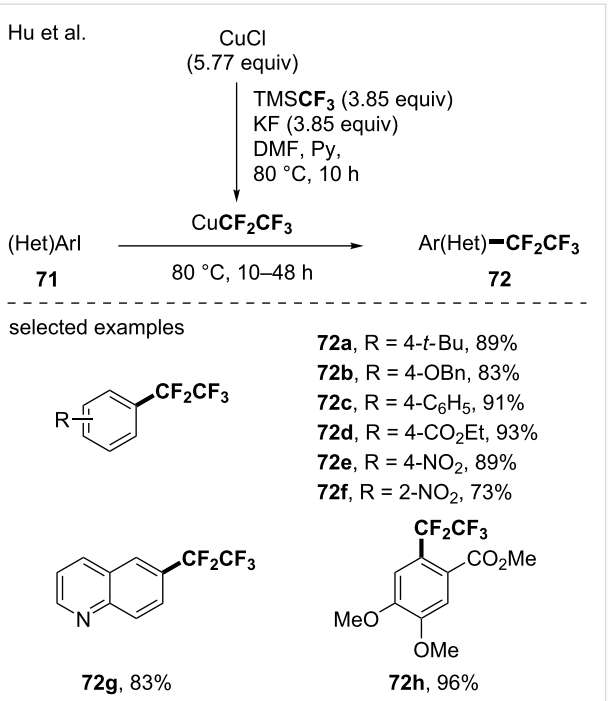

Scheme 24: Generation of a $CuCF_2CF_3$ reagent from $TMSCF_3$ and applications.

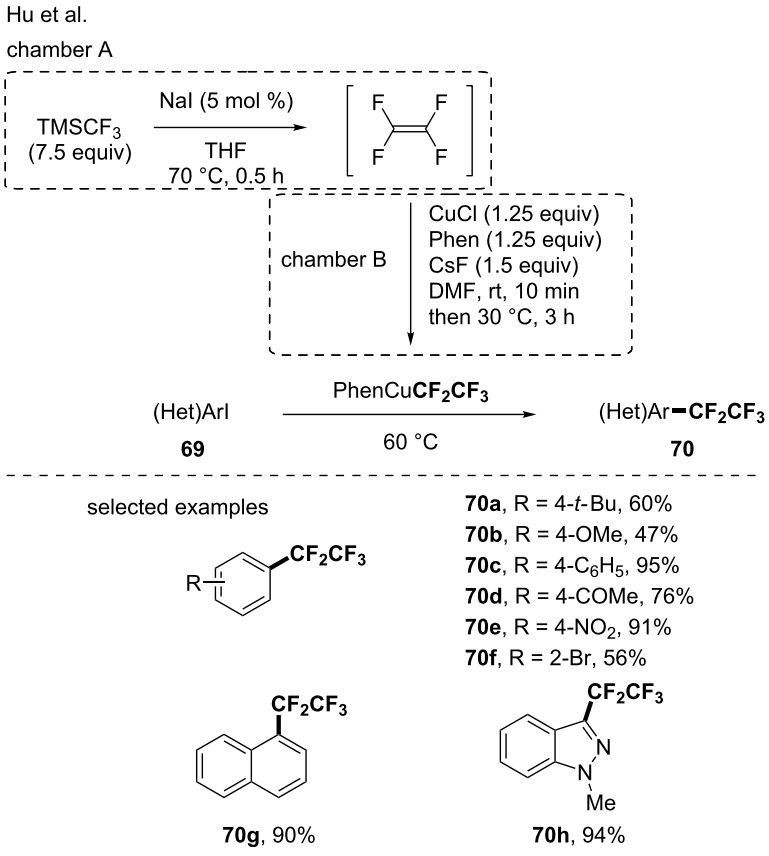

Scheme 23: Formation of the $PhenCuCF_2CF_3$ reagent by means of TFE and pentafluoroethylation of iodoarenes and aryldiazonium salts.

Conclusion

This review aims at providing an overview of the recent advances made since 2014 for the construction of CF_2R-containing molecules (R ≠ F) using versatile and efficient copper-based reagents. Groundbreaking advances were made in the synthesis of well-defined copper-based reagents and innovative strategies were developed to generate in situ CuR_f complexes from various precursors. Unprecedented transformations were successfully achieved using these copper-based reagents and these efficient synthetic tools opened new perspectives in the very active research field of organofluorine chemistry. Nevertheless, this field is still in its infancy and milestones towards copper-based difluoromethylating reagents are expected in the upcoming years.

Funding

This work was partially supported by Normandie Université (NU), the Région Normandie, the Centre National de la Recherche Scientifique (CNRS), Université de Rouen Normandie (URN), INSA Rouen Normandie, Labex SynOrg (ANR-11-LABX-0029) and Innovation Chimie Carnot (I2C). L.R. and T.B. thanks the European Research Council (ERC) under the European Union's Horizon 2020 research and innovation program (grant agreement no. 758710) and especially L.R. for a doctoral fellowship.

References

1. Wang, J.; Sánchez-Roselló, M.; Aceña, J. L.; del Pozo, C.; Sorochinsky, A. E.; Fustero, S.; Soloshonok, V. A.; Liu, H. *Chem. Rev.* **2014,** *114,* 2432–2506. doi:10.1021/cr4002879
2. Purser, S.; Moore, P. R.; Swallow, S.; Gouverneur, V. *Chem. Soc. Rev.* **2008,** *37,* 320–330. doi:10.1039/b610213c
3. Gillis, E. P.; Eastman, K. J.; Hill, M. D.; Donnelly, D. J.; Meanwell, N. A. *J. Med. Chem.* **2015,** *58,* 8315–8359. doi:10.1021/acs.jmedchem.5b00258
4. Ilardi, E. A.; Vitaku, E.; Njardarson, J. T. *J. Med. Chem.* **2014,** *57,* 2832–2842. doi:10.1021/jm401375q
5. Liang, T.; Neumann, C. N.; Ritter, T. *Angew. Chem., Int. Ed.* **2013,** *52,* 8214–8264. doi:10.1002/anie.201206566
6. Besset, T.; Poisson, T.; Pannecoucke, X. *Chem. – Eur. J.* **2014,** *20,* 16830–16845. doi:10.1002/chem.201404537
7. Ni, C.; Hu, J. *Chem. Soc. Rev.* **2016,** *45,* 5441–5454. doi:10.1039/c6cs00351f
8. Landelle, G.; Panossian, A.; Leroux, F. *Curr. Top. Med. Chem.* **2014,** *14,* 941–951. doi:10.2174/1568026614666140202210016
9. Besset, T.; Jubault, P.; Pannecoucke, X.; Poisson, T. *Org. Chem. Front.* **2016,** *3,* 1004–1010. doi:10.1039/c6qo00164e
10. Champagne, P. A.; Desroches, J.; Hamel, J.-D.; Vandamme, M.; Paquin, J.-F. *Chem. Rev.* **2015,** *115,* 9073–9174. doi:10.1021/cr500706a
11. Merino, E.; Nevado, C. *Chem. Soc. Rev.* **2014,** *43,* 6598–6608. doi:10.1039/c4cs00025k
12. Egami, H.; Sodeoka, M. *Angew. Chem., Int. Ed.* **2014,** *53,* 8294–8308. doi:10.1002/anie.201309260
13. Belhomme, M.-C.; Besset, T.; Poisson, T.; Pannecoucke, X. *Chem. – Eur. J.* **2015,** *21,* 12836–12865. doi:10.1002/chem.201501475
14. Song, H.-X.; Han, Q.-Y.; Zhao, C.-L.; Zhang, C.-P. *Green Chem.* **2018,** *20,* 1662–1731. doi:10.1039/c8gc00078f
15. O'Hagan, D. *Chem. Soc. Rev.* **2008,** *37,* 308–319. doi:10.1039/b711844a
16. Roy, S.; Gregg, B. T.; Gribble, G. W.; Le, V.-D.; Roy, S. *Tetrahedron* **2011,** *67,* 2161–2195. doi:10.1016/j.tet.2011.01.002
17. Jouvin, K.; Guissart, C.; Theunissen, C.; Evano, G. Emerging Areas in Copper-Mediated Trifluoromethylations: Catalytic and Oxidative Processes. In *Copper-Mediated Cross-Coupling Reactions;* Evano, G.; Blanchard, N., Eds.; John Wiley & Sons: Hoboken, NJ, USA, 2013; pp 515–530. doi:10.1002/9781118690659.ch14
18. Danoun, G.; Bayarmagnai, B.; Grünberg, M. F.; Gooßen, L. J. *Angew. Chem., Int. Ed.* **2013,** *52,* 7972–7975. doi:10.1002/anie.201304276
19. Grushin, V. V. *Chim. Oggi* **2014,** *32* (3), 81–88.
20. Liu, X.; Xu, C.; Wang, M.; Liu, Q. *Chem. Rev.* **2015,** *115,* 683–730. doi:10.1021/cr400473a
21. Morstein, J.; Hou, H.; Cheng, C.; Hartwig, J. F. *Angew. Chem., Int. Ed.* **2016,** *55,* 8054–8057. doi:10.1002/anie.201601163
22. Lin, X.; Hou, C.; Li, H.; Weng, Z. *Chem. – Eur. J.* **2016,** *22,* 2075–2084. doi:10.1002/chem.201504306
23. Zhang, C. *J. Chem. Sci.* **2017,** *129,* 1795–1805. doi:10.1007/s12039-017-1380-5
24. Kaplan, P. T.; Lloyd, J. A.; Chin, M. T.; Vicic, D. A. *Beilstein J. Org. Chem.* **2017,** *13,* 2297–2303. doi:10.3762/bjoc.13.225
25. Ye, Y.; Cheung, K. P. S.; He, L.; Tsui, G. C. *Org. Chem. Front.* **2018,** *5,* 1511–1515. doi:10.1039/c8qo00191j
26. Geri, J. B.; Wade Wolfe, M. M.; Szymczak, N. K. *Angew. Chem., Int. Ed.* **2018,** *57,* 1381–1385. doi:10.1002/anie.201711316
27. Li, G.-b.; Zhang, C.; Song, C.; Ma, Y.-d. *Beilstein J. Org. Chem.* **2018,** *14,* 155–181. doi:10.3762/bjoc.14.11
28. Landelle, G.; Panossian, A.; Pazenok, S.; Vors, J.-P.; Leroux, F. R. *Beilstein J. Org. Chem.* **2013,** *9,* 2476–2536. doi:10.3762/bjoc.9.287
29. Hu, J.; Zhang, W.; Wang, F. *Chem. Commun.* **2009,** 7465–7478. doi:10.1039/b916463d
30. Gao, B.; Ni, C.; Hu, J. *Chimia* **2014,** *68,* 414–418. doi:10.2533/chimia.2014.414
31. Rong, J.; Ni, C.; Hu, J. *Asian J. Org. Chem.* **2017,** *6,* 139–152. doi:10.1002/ajoc.201600509
32. Levi, N.; Amir, D.; Gershonov, E.; Zafrani, Y. *Synthesis* **2019,** *51,* 4549–4567. doi:10.1055/s-0039-1690027
33. Meanwell, N. A. *J. Med. Chem.* **2011,** *54,* 2529–2591. doi:10.1021/jm1013693
34. Kirk, K. L. *Org. Process Res. Dev.* **2008,** *12,* 305–321. doi:10.1021/op700134j
35. Graton, J.; Wang, Z.; Brossard, A.-M.; Gonçalves Monteiro, D.; Le Questel, J.-Y.; Linclau, B. *Angew. Chem., Int. Ed.* **2012,** *51,* 6176–6180. doi:10.1002/anie.201202059
36. Giuffredi, G. T.; Gouverneur, V.; Bernet, B. *Angew. Chem., Int. Ed.* **2013,** *52,* 10524–10528. doi:10.1002/anie.201303766
37. Burton, D. J.; Hartgraves, G. A. *J. Fluorine Chem.* **2007,** *128,* 1198–1215. doi:10.1016/j.jfluchem.2007.05.015
38. Bour, J. R.; Kariofillis, S. K.; Sanford, M. S. *Organometallics* **2017,** *36,* 1220–1223. doi:10.1021/acs.organomet.7b00025
39. Fier, P. S.; Hartwig, J. F. *J. Am. Chem. Soc.* **2012,** *134,* 5524–5527. doi:10.1021/ja301013h

40. Jiang, X.-L.; Chen, Z.-H.; Xu, X.-H.; Qing, F.-L. *Org. Chem. Front.* **2014,** *1,* 774–776. doi:10.1039/c4qo00153b
41. Prakash, G. K. S.; Ganesh, S. K.; Jones, J.-P.; Kulkarni, A.; Masood, K.; Swabeck, J. K.; Olah, G. A. *Angew. Chem., Int. Ed.* **2012,** *51,* 12090–12094. doi:10.1002/anie.201205850
42. Matheis, C.; Jouvin, K.; Goossen, L. J. *Org. Lett.* **2014,** *16,* 5984–5987. doi:10.1021/ol5030037
43. Bayarmagnai, B.; Matheis, C.; Jouvin, K.; Goossen, L. J. *Angew. Chem., Int. Ed.* **2015,** *54,* 5753–5756. doi:10.1002/anie.201500899
44. Jouvin, K.; Matheis, C.; Goossen, L. J. *Chem. – Eur. J.* **2015,** *21,* 14324–14327. doi:10.1002/chem.201502914
45. Zhu, S.-Q.; Xu, X.-H.; Qing, F.-L. *Org. Chem. Front.* **2015,** *2,* 1022–1025. doi:10.1039/c5qo00186b
46. Zhu, S.-Q.; Liu, Y.-L.; Li, H.; Xu, X.-H.; Qing, F.-L. *J. Am. Chem. Soc.* **2018,** *140,* 11613–11617. doi:10.1021/jacs.8b08135
47. Ivanova, M. V.; Bayle, A.; Besset, T.; Pannecoucke, X.; Poisson, T. *Chem. – Eur. J.* **2016,** *22,* 10284–10293. doi:10.1002/chem.201601310
48. Pannecoucke, X.; Poisson, T. *Synlett* **2016,** *27,* 2314–2326. doi:10.1055/s-0035-1562784
49. Bayle, A.; Cocaud, C.; Nicolas, C.; Martin, O. R.; Poisson, T.; Pannecoucke, X. *Eur. J. Org. Chem.* **2015,** 3787–3792. doi:10.1002/ejoc.201500373
50. Ivanova, M. V.; Bayle, A.; Besset, T.; Poisson, T.; Pannecoucke, X. *Angew. Chem., Int. Ed.* **2015,** *54,* 13406–13410. doi:10.1002/anie.201507130
51. Ivanova, M. V.; Besset, T.; Pannecoucke, X.; Poisson, T. *Synthesis* **2018,** *50,* 778–784. doi:10.1055/s-0036-1589140
52. Ivanova, M. V.; Bayle, A.; Besset, T.; Pannecoucke, X.; Poisson, T. *Chem. – Eur. J.* **2017,** *23,* 17318–17338. doi:10.1002/chem.201703542
53. Ivanova, M. V.; Bayle, A.; Besset, T.; Pannecoucke, X.; Poisson, T. *Angew. Chem., Int. Ed.* **2016,** *55,* 14141–14145. doi:10.1002/anie.201608294
54. Ivanova, M. V.; Bayle, A.; Besset, T.; Pannecoucke, X.; Poisson, T. *Eur. J. Org. Chem.* **2017,** 2475–2480. doi:10.1002/ejoc.201700182
55. Ou, Y.; Gooßen, L. J. *Asian J. Org. Chem.* **2019,** *8,* 650–653. doi:10.1002/ajoc.201800461
56. Prakash, G. K. S.; Hu, J. *Acc. Chem. Res.* **2007,** *40,* 921–930. doi:10.1021/ar700149s
57. Zhang, W.; Zhu, J.; Hu, J. *Tetrahedron Lett.* **2008,** *49,* 5006–5008. doi:10.1016/j.tetlet.2008.06.064
58. Hu, J. *J. Fluorine Chem.* **2009,** *130,* 1130–1139. doi:10.1016/j.jfluchem.2009.05.016
59. He, Z.; Luo, T.; Hu, M.; Cao, Y.; Hu, J. *Angew. Chem., Int. Ed.* **2012,** *51,* 3944–3947. doi:10.1002/anie.201200140
60. He, Z.; Hu, M.; Luo, T.; Li, L.; Hu, J. *Angew. Chem., Int. Ed.* **2012,** *51,* 11545–11547. doi:10.1002/anie.201206556
61. Zhu, J.; Wang, F.; Huang, W.; Zhao, Y.; Ye, W.; Hu, J. *Synlett* **2011,** 899–902. doi:10.1055/s-0030-1259676
62. Li, X.; Zhao, J.; Hu, M.; Chen, D.; Ni, C.; Wang, L.; Hu, J. *Chem. Commun.* **2016,** *52,* 3657–3660. doi:10.1039/c5cc10550a
63. Carbonnel, E.; Poisson, T.; Jubault, P.; Pannecoucke, X.; Besset, T. *Front. Chem. (Lausanne, Switz.)* **2019,** *7,* 111. doi:10.3389/fchem.2019.00111
64. Li, X.; Zhao, J.; Wang, Y.; Rong, J.; Hu, M.; Chen, D.; Xiao, P.; Ni, C.; Wang, L.; Hu, J. *Chem. – Asian J.* **2016,** *11,* 1789–1792. doi:10.1002/asia.201600577
65. Kremlev, M. M.; Tyrra, W.; Mushta, A. I.; Naumann, D.; Yagupolskii, Y. L. *J. Fluorine Chem.* **2010,** *131,* 212–216. doi:10.1016/j.jfluchem.2009.10.011
66. Morimoto, H.; Tsubogo, T.; Litvinas, N. D.; Hartwig, J. F. *Angew. Chem., Int. Ed.* **2011,** *50,* 3793–3798. doi:10.1002/anie.201100633
67. Litvinas, N. D.; Fier, P. S.; Hartwig, J. F. *Angew. Chem., Int. Ed.* **2012,** *51,* 536–539. doi:10.1002/anie.201106668
68. Lishchynskyi, A.; Grushin, V. V. *J. Am. Chem. Soc.* **2013,** *135,* 12584–12587. doi:10.1021/ja407017j
69. Mormino, M. G.; Fier, P. S.; Hartwig, J. F. *Org. Lett.* **2014,** *16,* 1744–1747. doi:10.1021/ol500422t
70. Kalkman, E. D.; Mormino, M. G.; Hartwig, J. F. *J. Am. Chem. Soc.* **2019,** *141,* 19458–19465. doi:10.1021/jacs.9b10540
71. Panferova, L. I.; Miloserdov, F. M.; Lishchynskyi, A.; Martínez Belmonte, M.; Benet-Buchholz, J.; Grushin, V. V. *Angew. Chem., Int. Ed.* **2015,** *54,* 5218–5222. doi:10.1002/anie.201500341
72. Huang, Y.; Ajitha, M. J.; Huang, K.-W.; Zhang, Z.; Weng, Z. *Dalton Trans.* **2016,** *45,* 8468–8474. doi:10.1039/c6dt00277c
73. Serizawa, H.; Aikawa, K.; Mikami, K. *Org. Lett.* **2014,** *16,* 3456–3459. doi:10.1021/ol501332g
74. Negishi, K.; Aikawa, K.; Mikami, K. *Eur. J. Org. Chem.* **2016,** 4099–4104. doi:10.1002/ejoc.201600711
75. Lishchynskyi, A.; Mazloomi, Z.; Grushin, V. V. *Synlett* **2015,** *26,* 45–50. doi:10.1055/s-0034-1379497
76. Zhu, J.; Ni, C.; Gao, B.; Hu, J. *J. Fluorine Chem.* **2015,** *171,* 139–147. doi:10.1016/j.jfluchem.2014.08.011
77. Kremlev, M. M.; Mushta, A. I.; Tyrra, W.; Yagupolskii, Y. L.; Naumann, D.; Schäfer, M. *Dalton Trans.* **2015,** *44,* 19693–19699. doi:10.1039/c5dt02925b
78. Li, L.; Ni, C.; Xie, Q.; Hu, M.; Wang, F.; Hu, J. *Angew. Chem., Int. Ed.* **2017,** *56,* 9971–9975. doi:10.1002/anie.201705734
79. Xing, B.; Li, L.; Ni, C.; Hu, J. *Chin. J. Chem.* **2019,** *37,* 1131–1136. doi:10.1002/cjoc.201900268
80. Mestre, J.; Castillón, S.; Boutureira, O. *J. Org. Chem.* **2019,** *84,* 15087–15097. doi:10.1021/acs.joc.9b02001
81. Xie, Q.; Li, L.; Zhu, Z.; Zhang, R.; Ni, C.; Hu, J. *Angew. Chem., Int. Ed.* **2018,** *57,* 13211–13215. doi:10.1002/anie.201807873

License and Terms